RS-8232-21 7/323
C-1
8524

CONTRACTOR REPORT

SAND89—7147
Unlimited Release
UC—721

Preliminary Geohydrologic Conceptual Model of the Los Medaños Region Near the Waste Isolation Pilot Plant for the Purpose of Performance Assessment

Kenneth F. Brinster
Science Applications International Corporation
2109 Air Park Road SE
Albuquerque, NM 87106

8232-2//071323
00000001 -

Prepared by
Sandia National Laboratories
Albuquerque, New Mexico 87185 Livermore, California 94550
for the United States Department of Energy
under Contract DE-AC04-76DP00789

Printed January 1991

Issued by Sandia National Laboratories, operated for the United States Department of Energy by Sandia Corporation.

NOTICE: This report was prepared as an account of work sponsored by an agency of the United States Government. Neither the United States Government nor any agency thereof, nor any of their employees, nor any of their contractors, subcontractors, or their employees, makes any warranty, express or implied, or assumes any legal liability or responsibility for the accuracy, completeness, or usefulness of any information, apparatus, product, or process disclosed, or represents that its use would not infringe privately owned rights. Reference herein to any specific commercial product, process, or service by trade name, trademark, manufacturer, or otherwise, does not necessarily constitute or imply its endorsement, recommendation, or favoring by the United States Government, any agency thereof or any of their contractors or subcontractors. The views and opinions expressed herein do not necessarily state or reflect those of the United States Government, any agency thereof or any of their contractors.

Printed in the United States of America. This report has been reproduced directly from the best available copy.

Available to DOE and DOE contractors from
Office of Scientific and Technical Information
PO Box 62
Oak Ridge, TN 37831

Prices available from (615) 576-8401, FTS 626-8401

Available to the public from
National Technical Information Service
US Department of Commerce
5285 Port Royal Rd
Springfield, VA 22161

NTIS price codes
Printed copy: A14
Microfiche copy: A01

SAND89-7147
Unlimited Release
Printed January 1991

Distribution
Category UC-721

PRELIMINARY GEOHYDROLOGIC CONCEPTUAL MODEL OF THE LOS MEDAÑOS REGION NEAR THE WASTE ISOLATION PILOT PLANT FOR THE PURPOSE OF PERFORMANCE ASSESSMENT*

Kenneth F. Brinster

Science Applications International Corporation
2109 Air Park Road SE
Albuquerque, NM 87106

ABSTRACT

This report describes a geohydrologic conceptual model of the northern Delaware Basin to be used in modeling three-dimensional, regional ground-water flow for assessing the performance of the Waste Isolation Pilot Plant (WIPP) in the Los Medaños region near Carlsbad, New Mexico. Geochemical and hydrological evidence indicates that flow is transient in the Rustler Formation and the Capitan aquifer in response to changing geologic, hydrologic, and climatic conditions. Before the Pleistocene, ground-water flow in the Rustler Formation was generally eastward, but uneven tilting of the Delaware Basin lowered the regional base level and formed fractures in the evaporitic sequence of rocks approximately parallel to the basin axis. Dissolution along the fractures, coupled with erosion, formed Nash Draw. Also, the drop in base level resulted in an increase in the carrying power of the Pecos River, which began incising the Capitan aquifer near Carlsbad, New Mexico. Erosion and downcutting released hydraulic pressure that caused a reversal in Rustler ground-water flow direction near the WIPP. Flow in the Rustler west of the WIPP is toward Nash Draw and eventually toward Malaga Bend; flow south of the WIPP is toward Malaga Bend.

---

*Work Performed Under Contract No. 75-8370 For Performance Assessment Division (6342), Sandia National Laboratories

RELATED WIPP PERFORMANCE ASSESSMENT DOCUMENTS

PUBLISHED

Bertram-Howery, S. G., and R. L. Hunter, eds. 1989. *Plans for Evaluation of the Waste Isolation Pilot Plant's Compliance with EPA Standards for Radioactive Waste Management and Disposal*. SAND88-2871. Albuquerque, NM: Sandia National Laboratories.

Bertram-Howery, S. G., and R. L. Hunter, eds. 1989. *Preliminary Plan for Disposal-System Characterization and Long-Term Performance Evaluation of the Waste Isolation Pilot Plant*. SAND89-0178. Albuquerque, NM: Sandia National Laboratories.

Bertram-Howery, S. G., and P. N. Swift. 1990. *Status Report: Potential for Long-Term Isolation by the Waste Isolation Pilot Plant Disposal System*. SAND90-0616. Albuquerque, NM: Sandia National Laboratories.

Bertram-Howery, S. G., M. G. Marietta, D. R. Anderson, K. F. Brinster, L. S. Gomez, R. V. Guzowski, and R. P. Rechard. 1989. *Draft Forecast of the Final Report for the Comparison to 40 CFR Part 191, Subpart B for the Waste Isolation Pilot Plant*. SAND88-1452. Albuquerque, NM: Sandia National Laboratories.

Bertram-Howery, S. G., M. G. Marietta, R. P. Rechard, P. N. Swift, D. R. Anderson, B. L. Baker, J. E. Bean, Jr., W. Beyeler, K. F. Brinster, R. V. Guzowski, J. C. Helton, R. D. McCurley, D. K. Rudeen, J. D. Schreiber, and P. Vaughn. 1990. *Preliminary Comparison with 40 CFR Part 191, Subpart B for the Waste Isolation Pilot Plant, December 1990*. SAND90-2347. Albuquerque, NM: Sandia National Laboratories.

Guzowski, R. V. 1990. *Preliminary Identification of Scenarios That May Affect the Escape and Transport of Radionuclides From the Waste Isolation Pilot Plant, Southeastern New Mexico*. SAND89-7149. Albuquerque, NM: Sandia National Laboratories.

Hunter, R. L. 1989. *Events and Processes for Constructing Scenarios for the Release of Transuranic Waste from the Waste Isolation Pilot Plant, Southeastern New Mexico*. SAND89-2546. Albuquerque, NM: Sandia National Laboratories.

Marietta, M. G., S. G. Bertram-Howery, D. R. Anderson, K. F. Brinster, R. V. Guzowski, H. J. Iuzzolino, and R. P. Rechard. 1989. *Performance Assessment Methodology Demonstration: Methodology Development for Evaluating Compliance with EPA 40 CFR 191, Subpart B, for the Waste Isolation Pilot Plant*. SAND89-2027. Albuquerque, NM: Sandia National Laboratories.

Rechard, R. P. 1989. *Review and Discussion of Code Linkage and Data Flow in Nuclear Waste Compliance Assessments*. SAND87-2833. Albuquerque, NM: Sandia National Laboratories.

Rechard, R. P., H. J. Iuzzolino, J. S. Rath, R. D. McCurley, and D. K. Rudeen. 1989. *User's Manual for CAMCON: Compliance Assessment Methodology Controller.* SAND88-1496. Albuquerque, NM: Sandia National Laboratories.

Rechard, R. P., H. J. Iuzzolino, and J. S. Sandha. 1990. *Data Used in Preliminary Performance Assessment of the Waste Isolation Pilot Plant (1990).* SAND89-2408. Albuquerque, NM: Sandia National Laboratories.

Rechard, R. P., W. Beyeler, R. D. McCurley, D. K. Rudeen, J. E. Bean, and J. D. Schreiber. 1990. *Parameter Sensitivity Studies of Selected Components of the Waste Isolation Pilot Plant Repository/Shaft System.* SAND89-2030. Albuquerque, NM: Sandia National Laboratories.

Rechard, R. P., P. J. Roache, R. L. Blaine, A. P. Gilkey, and D. K. Rudeen. 1991. *Quality Assurance Procedures for Computer Software Supporting Performance Assessments of the Waste Isolation Pilot Plant.* SAND90-1240. Albuquerque, NM: Sandia National Laboratories.

Tierney, M. S. 1990. *Constructing Probability Distributions of Uncertain Variables in the Models of the Performance of the Waste Isolation Pilot Plant.* SAND90-2510. Albuquerque, NM: Sandia National Laboratories.

IN PREPARATION

Berglund, J., and M. G. Marietta. *A Computational Model for the Direct Removal of Repository Material by Drilling.* SAND90-2977. Albuquerque, NM: Sandia National Laboratories.

Guzowski, R. V. *Evaluation of Applicability of Probability Techniques to Determining the Probability of Occurrence of Potentially Disruptive Intrusive Events at the Waste Isolation Pilot Plant.* SAND90-7100. Albuquerque, NM: Sandia National Laboratories.

Helton, J. C. *Sensitivity Analysis Techniques and Results for Performance Assessment of the Waste Isolation Pilot Plant.* SAND90-7103. Albuquerque, NM: Sandia National Laboratories.

Hora, S., D. Scott, and K. Trauth. *Expert Judgment on Inadvertent Human Intrusion into the Waste Isolation Pilot Plant.* SAND90-3063. Albuquerque, NM: Sandia National Laboratories.

Marietta, M. G., D. R. Anderson, D. Scott, and P. N. Swift. *Review of Parameter Sensitivity Studies for the Waste Isolation Pilot Plant.* SAND89-2028. Albuquerque, NM: Sandia National Laboratories.

Marietta, M. G., P. N. Swift, B. L. Baker, K. F. Brinster, and P. J. Roache. *Parameter and Boundary Conditions Sensitivity Studies Related to Climate Variability and Scenario Screening for the Waste Isolation Pilot Plant.* SAND89-2029. Albuquerque, NM: Sandia National Laboratories.

Marietta, M. G., R. P. Rechard, P. N. Swift, and others. *Preliminary Probabilistic Safety Assessment of the Waste Isolation Pilot Plant.* SAND90-2718. Albuquerque, NM: Sandia National Laboratories.

Rechard, R. P. *CAMCON Architectural Overview and Program Reference Manual.* SAND90-1984. Albuquerque, NM: Sandia National Laboratories.

Rechard, R. P., A. P. Gilkey, D. K. Rudeen, J. S. Rath, W. Beyeler, R. Blaine, H. J. Iuzzolino, and R. D. McCurley. *User's Reference Manual for CAMCON: Compliance Assessment Methodology Controller Version 3.0.* SAND90-1983. Albuquerque, NM: Sandia National Laboratories.

Roache, P. J., R. Blaine, and B. L. Baker. *SECO 2.1 User's Manual.* SAND90-7096. Albuquerque, NM: Sandia National Laboratories.

Tierney, M. S. *Combining Scenarios in a Calculation of the Overall Probability Distribution of Cumulative Releases of Radioactivity from the Waste Isolation Pilot Plant, Southeastern New Mexico.* SAND90-0838. Albuquerque, NM: Sandia National Laboratories.

ACKNOWLEDGMENTS

This report would not have been possible without the help and suggestions from the technical reviewers: Peter Davies (6344), Dave Borns (6233), Sharla Bertram-Howery (6342), Mel Marietta (6342), and Bob Guzowski (SAIC), and the editorial assistance of Marilyn Gruebel, John Stikar, and Chris Northrop of Tech Reps, Inc., who remained cheerful throughout the many revisions. I would also like to thank Steve Lambert, Dave Borns, Rick Beauheim, and Peter Davies for taking the time from their work to discuss with me the many aspects of geology, geomorphology, and hydrology of the Los Medaños region.

PREFACE

The Performance Assessment team for the Waste Isolation Pilot Plant (WIPP) comprises staff of the Performance Assessment Division of Sandia National Laboratories (SNL) and other specialists who generally are contractors to SNL. This report documents a preliminary geohydrologic conceptual model for the region near the WIPP and is written by Kenneth F. Brinster, a contractor to the Performance Assessment Division. This report has completed SNL peer review and SNL management review and is an official SNL Sandia (SAND) report.

CONTENTS

EXECUTIVE SUMMARY ES-1

I. INTRODUCTION I-1

Purpose I-2
Location I-3
Method of Study I-5

II. REGIONAL GEOLOGY II-1

Geologic History of the Delaware Basin II-1
Stratigraphy of the Pennsylvanian Rocks II-5
Morrowan Series II-5
Desmoinesian Series II-5
Missourian Series II-7
Virgilian Series II-7
Stratigraphy of the Permian Rocks II-7
Wolfcampian Series II-7
Leonardian Series II-7
Guadalupian Series II-8
Capitan Limestone II-8
Delaware Mountain Group II-12
Ochoan Series II-14
Castile Formation II-17
Salado Formation II-17
Rustler Formation II-19
Dewey Lake Red Beds II-36
Stratigraphy of the Mesozoic Rocks II-43
Stratigraphy of the Cenozoic Rocks II-48

III. REGIONAL GEOMORPHOLOGY III-1

Natural Occurrence and Removal of Evaporites in the Study Area III-1
Evidence of Dissolution III-2
Mechanisms of Dissolution III-4
Dissolution Features III-9
Nash Draw III-9
Breccia Chimneys III-10
Discussion of the Geologic History of Erosion and Dissolution in the Study Area III-13

IV. REGIONAL HYDROLOGY IV-1

Surface Water IV-1
Precipitation IV-2
Rivers, Lakes, and Springs IV-2
Ground Water IV-7
Capitan Limestone Aquifer IV-8
Hydraulic Conductivity and Permeability IV-8
Porosity IV-12
Potentiometric Surface IV-12
Fluid Density IV-12

Bell Canyon Hydrostratigraphic Unit IV-15
Hydraulic Conductivity IV-15
Porosity IV-17
Potentiometric Surface IV-17
Recharge and Discharge IV-19
Hydraulic Gradient IV-19
Castile Formation IV-21
Salado Formation IV-22
Rustler Formation IV-27
Aquitard Units of the Rustler Formation IV-27
Rustler-Salado Contact Residuum Hydrostratigraphic Unit IV-29
Hydraulic Conductivity IV-31
Porosity IV-31
Potentiometric Surface IV-31
Storativity IV-35
Fluid Density IV-35
Recharge and Discharge IV-35
Culebra Dolomite (Rustler Formation) Hydrostratigraphic Unit IV-41
Hydraulic Conductivity IV-42
Porosity IV-48
Potentiometric Surface IV-48
Storativity IV-50
Fluid Density IV-50
Recharge and Discharge IV-50
Multipad Aquifer Tests in the Culebra Dolomite Member IV-55
Magenta Dolomite (Rustler Formation) Hydrostratigraphic Unit IV-68
Hydraulic Conductivity and Permeability IV-68
Porosity IV-70
Storativity IV-70
Potentiometric Surface IV-70
Fluid Density IV-70
Recharge and Discharge IV-74
Vertical Flow in the Rustler Formation IV-74
Supra-Rustler Rocks IV-82
Dewey Lake Red Beds (Supra-Rustler) IV-82
Dockum Group IV-83
Cenozoic Rocks IV-84

V. GEOCHEMICAL STUDIES V-1

VI. BOUNDARY CONDITIONS IN THE NORTHERN DELAWARE BASIN VI-1

Initial Conditions VI-2
Three-Dimensional Boundary and Initial Conditions VI-4
Estimation and Distribution of Hydrologic Properties VI-10

VII. SUMMARY VII-1

REFERENCES R-1

APPENDIX A: Principles of Hydrology A-1

APPENDIX B: Geohydrologic Data Bases B-1

GLOSSARY G-1

NOMENCLATURE N-1

FIGURES

Figure		Page
I-1	Location of the Study Area in the Delaware Basin	I-4
I-2	Index Map Showing Study Area and Model Boundaries in the Los Medaños Region	I-6
I-3	Index Map Showing Well Locations Used for Geologic Information in the Los Medaños Region	I-8
II-1	Los Medaños Geologic Column	II-2
II-2	Isopach Map of the Capitan Limestone, Showing Possible Submarine Canyons	II-6
II-3	Capitan Reef and Associated Shelfward and Basinward Units	II-9
II-4	Portion of a Longitudinal Cross Section of the Capitan Limestone along the Northern Edge of the Delaware Basin from A to A', as Shown in Figure II-2	II-11
II-5	Basinward Units of the Delaware Mountain Group	II-13
II-6	Orientation of Sandstone Stringers in the Bell Canyon Formation of the Delaware Mountain Group	II-15
II-7	Generalized Structure Contours on Top of the Lamar Shale (Informal Unit) of the Bell Canyon Formation (Delaware Mountain Group) in the Delaware Basin	II-16
II-8	Generalized Distribution of the Castile and Salado Formations in the Delaware Basin, with Emphasis on Distribution of Halites	II-18
II-9	Structure Contours on Top of the Salado Formation	II-20
II-10	General Stratigraphic Column Showing the Five Members of the Rustler Formation	II-22
II-11	Cross Section from A to A' of Figure I-2, Showing Rustler Formation Stratigraphy	II-23
II-12	Histograms Showing Thicknesses of Rustler Formation and the Unnamed Lower and Culebra Dolomite Members	II-25
II-13	Generalized Geologic Map of Nash Draw with Overburden Removed	II-26
II-14	Longitudinal Cross Section along Nash Draw from A to A' of Figure II-13	II-27
II-15	Isopach Map of the Unnamed Lower Member	II-28
II-16	Distribution of Halite in the Rustler Formation	II-29
II-17	Structure Contours on Top of the Unnamed Lower Member	II-30

Figure		Page
II-18	Isopach Map of the Culebra Dolomite Member	II-32
II-19	Structure Contours on Top of the Culebra Dolomite Member	II-33
II-20	Isopach Map of the Tamarisk Member	II-34
II-21	Histograms Showing Thicknesses of the Tamarisk, Magenta Dolomite, and Forty-niner Members	II-35
II-22	Structure Contours on Top of the Tamarisk Member	II-37
II-23	Isopach Map of the Magenta Member	II-38
II-24	Structure Contours on Top of the Magenta Member	II-39
II-25	Isopach Map of the Forty-niner Member	II-40
II-26	Structure Contours on Top of the Forty-niner Member	II-41
II-27	Isopach Map of the Dewey Lake Red Beds	II-42
II-28	Structure Contours on Top of the Dewey Lake Red Beds	II-44
II-29	Structure Contours on Top of Lower Dockum Group	II-45
II-30	Isopach Map of Lower Dockum Group in the Study Area	II-46
II-31	Isopach Map of the Supra-Rustler Rocks	II-47
III-1	Columnar Cross Section across the WIPP, Showing Lithologic Correlations of Rustler Formation Units	III-3
IV-1	Precipitation Contours in and near the Study Area	IV-3
IV-2	Surface Drainage in and near the Study Area	IV-6
IV-3	Pre-development and Post-development Potentiometric Surfaces for Permian Hydrostratigraphic Units in Eddy and Lea Counties, New Mexico	IV-13
IV-4	Diagrammatic Maps Depicting the Evolution of Ground-water Regions in Permian-age Guadalupian Strata in Southeastern New Mexico and Western Texas	IV-14
IV-5	Potentiometric Surface of the Hydrologic Unit in the Upper Part of the Bell Canyon in the Study Area	IV-18
IV-6	Comparisons of Models Proposed for Ground-water Movement in the Guadalupian Rocks of the Delaware Basin	IV-20
IV-7	Variation in Measured Permeability with Increasing Test-Interval Depth	IV-25
IV-8	Approximate Areal Extent of the "Brine Aquifer" in the Study Area	IV-30
IV-9	Contour Plot of the Log Hydraulic Conductivities of the Ruster-Salado Contact Residuum in the Study Area	IV-33

Figure		Page
IV-10	Adjusted Potentiometric Surface of the Rustler-Salado Contact Residuum in the Study Area	IV-34
IV-11	Adjusted Potentiometric Surface of the Rustler-Salado Contact Residuum in the Study Area (Pecos River heads included)	IV-36
IV-12	Contour Map of Brine Density in the Rustler-Salado Contact Residuum in the Study Area	IV-37
IV-13	Cross Section Illustrating the Relationship of Flowing Wells to Recharge and Discharge Areas	IV-39
IV-14	Location Map of the WIPP Test Wells in the Study Area	IV-43
IV-15	Contour Map of Log Hydraulic Conductivity of the Culebra Dolomite Member in the Study Area	IV-46
IV-16	Adjusted Potentiometric Surface of the Culebra Dolomite Member in the Study Area	IV-49
IV-17	Adjusted Potentiometric Surface of the Culebra Dolomite Member of the Rustler Formation in the Study Area (Pecos River heads included)	IV-51
IV-18	Contour Map of Brine Density in the Culebra Dolomite Member in the Study Area	IV-52
IV-19	Plot Showing Change in Transmissivity in Observation Wells Surrounding H-3	IV-60
IV-20	Plot Showing Change in Transmissivity in Observation Wells Surrounding WIPP-13	IV-62
IV-21	Drawdown of Observation Wells near and over the WIPP during the WIPP-13 Pump Test, Showing Homogeneity of the Culebra in that Region	IV-65
IV-22	Contour Plot of Drawdown at End of H-11 Multipad Test (all wells)	IV-67
IV-23	Contour Plot of Drawdown at End of H-11 Multipad Test (wells H-15, H-3b2, and DOE-1 not included)	IV-67
IV-24	Contour Map of Log Hydraulic Conductivities of the Magenta Dolomite Member in the Study Area	IV-71
IV-25	Adjusted Potentiometric Surface of the Magenta Dolomite Member of the Rustler Formation in the Study Area	IV-72
IV-26	Contour Map of Brine Density in the Magenta Dolomite Member in the Study Area	IV-73
IV-27	Comparisons Between Wells H-1, H-2, H-3 and H-4, Showing Potentials for Vertical Flow in the Rustler Formation	IV-75

Figure		Page
IV-28	Comparisons Between Wells H-5, H-6, H-7, and H-8, Showing Potentials for Vertical Flow in the Rustler Formation	IV-76
IV-29	Comparisons Between Wells H-9, H-10, P-14, and P-15, Showing Potentials for Vertical Flow in the Rustler Formation	IV-77
IV-30	Comparisons Between Wells P-17, WIPP-25, WIPP-26, and WIPP-27, Showing Potentials for Vertical Flow in the Rustler Formation	IV-78
IV-31	Comparisons Between Wells WIPP-28, WIPP-29, and WIPP-30, Showing Potentials for Vertical Flow in the Rustler Formation	IV-79
V-1	Hydrochemical Facies in the Culebra Dolomite	V-4
VI-1	Regional Ground-water Flow in the Rustler-Salado Contact at the Base of the Rustler Formation	VI-6
VI-2	Regional Ground-water Flow in the Culebra Dolomite Member of the Rustler Formation	VI-7
VI-3	Regional Ground-water Flow in the Magenta Dolomite Member of the Rustler Formation	VI-8

TABLES

Table		Page
II-1	Major Stratigraphic and Time Divisions, Southeastern New Mexico	II-4
II-2	Thicknesses (m) of the Rustler Formation and Each Member	II-21
III-1	Summary of Dissolution Mechanisms in the Los Medaños Region	III-5
IV-1	Stream Discharge at Gaging Stations between Carlsbad and Malaga Bend, New Mexico	IV-5
IV-2	Minimum and Maximum Annual Ground-water Discharge to the Pecos River	IV-8
IV-3	Hydraulic Characteristics of the Capitan Aquifer	IV-9
IV-4	Summary of Bell Canyon Test Results	IV-16
IV-5	Summary of Hydraulic Conductivities and Formation Pressures Interpreted from the Testing of the Boreholes in the Waste-Handling Shaft	IV-26
IV-6	Summary of Hydraulic Parameters of the Rustler-Salado Contact Residuum from Selected Test Holes in the Study Area	IV-32
IV-7	Culebra Dolomite Geohydrologic Data Base	IV-44
IV-8	Summary of Multipad Well Responses for H-3 Multipad Test	IV-56
IV-9	Summary of Multipad Well Responses for WIPP-13 Multipad Test	IV-57
IV-10	Summary of Multipad Well Responses for H-11 Multipad Test	IV-58
IV-11	Results of Correlations of Pump Test Results	IV-64
IV-12	Magenta Dolomite Geohydrologic Data Base	IV-69
IV-13	Comparison of Methods for Determining Vertical Flow Potential in the Rustler Formation	IV-81
V-1	Recent Geochemical Studies in the Study Area	V-2

EXECUTIVE SUMMARY

This report summarizes the geohydrology of the Los Medaños region east of Carlsbad, New Mexico, for the purpose of developing a preliminary geohydrological conceptual model of the northern Delaware Basin to determine potential contaminant-transport pathways in the hydrostratigraphic units for the purpose of assessing the performance of the Waste Isolation Pilot Plant (WIPP). This report presents regional geologic and hydrologic data in preliminary form for the Bell Canyon Formation, Capitan aquifer, Castile Formation, Salado Formation, Rustler Formation hydrostratigraphic units, Dewey Lake Red Beds, Dockum Group, Cenozoic rocks, and alluvium. It also formulates, for the first time, a possible explanation of the origin of the present Los Medaños regional ground-water flow and then shows how the conceptual model can be used to establish regional boundary conditions and initial conditions for modeling three-dimensional regional ground-water flow.

The Los Medaños region is in the north-central part of the Delaware Basin in the southern Pecos Valley section of the Great Plains Physiographic Province, which lies between the high plains of West Texas and the Guadalupe Mountains in southeastern New Mexico. The Study Area covers an area 34 km by 40 km and extends from the Pecos River in southern Eddy County eastward into Lea County and southward from just inside the Delaware Basin edge to about 20 km north of the New Mexico-Texas state line and consists of Nash Draw in the west and The Dunes in the east.

The lowest hydrostratigraphic units and oldest units to crop out in the northern Delaware Basin are the Capitan Limestone (reef unit) and the Bell Canyon Formation (basinal unit). In southeastern New Mexico, the Capitan is exposed in an uplifted portion forming the Guadalupe Mountains southwest of Carlsbad and is overlapped by younger rocks northeast and east of Carlsbad. The massive Capitan ranges in thickness from 76 to 230 m and averages about 120 m. Hydraulic conductivity ranges from 8×10^{-6} to 9×10^{-5} m/s and averages about 2×10^{-5} m/s. Effective porosity, which is enhanced by dissolution and fracturing of the limestone, is about 0.08. Ground water flows from the Guadalupe recharge area northward around the periphery of the Delaware Basin, eastward into the back reef rocks (shelf aquifer), and then into Texas. Ground-water flow direction is influenced locally by the Pecos River and by large withdrawals as a result of drilling activity. Fluid density ranges from 1.000 to 1.115 g/cm^3.

The Bell Canyon, which crops out southwest of Carlsbad just north of the New Mexico-Texas state line, is the fore-reef equivalent of the Capitan Limestone and interfingers with the Capitan at the basin margins. The upper part of the Bell Canyon is composed of informally named sandstone and shale members, which are, in ascending order, the Hays sandstone, Olds sandstone, Ford shale, Ramsey sandstone, and the Lamar limestone. The upper siltstones and shales contain elongated sandstone stringers that were deposited by density currents moving from the reef basinward along the bottom. Ground water occurs in the upper portion of this unit. The vertical potential of the fresh-water equivalent heads of this unit is upward, which has led to the speculation that the Bell Canyon waters have been, in the past, involved with dissolution of the Castile Formation, causing collapse features that can be seen at the surface. However, some workers believe the Castile does not have the extensive fracture network necessary to provide pathways upward to the halites and back down to the Bell Canyon. The Bell Canyon will not be included in the numerical modeling because of the poor hydraulic connection to the upper hydrostratigraphic units and because the upward vertical potential is not sufficient to push water saturated with respect to halite into the upper hydrostratigraphic units.

Near the end of Bell Canyon deposition, circulation within the Delaware Basin became more constricted, resulting in a thick sequence of organic layers alternating with siltstone laminations that change in character upward from organically layered calcite to calcite-layered anhydrite. This thick sequence forms the lower Castile Formation, which then grades upward into the anhydrite-layered halite of the upper Castile Formation and the thick halite of the Salado Formation. The Salado is of particular interest because it is the host rock for the WIPP.

The Castile and Salado Formations are present everywhere in the Study Area but are dissolved and eroded away southwest of the Study Area in Texas. In New Mexico, north of the WIPP, the Castile is about 360 m thick and thickens southward across the WIPP, where it is about 470 m thick. At the southern edge of the Study Area, the Castile is about 500 m thick. Throughout the Study Area, the Salado is about 600 m of thick, bedded salt rhythmically interbedded with anhydrite, polyhalite, and some glauberite and thin mudstones. The structure of the Salado consists of a series of low anticlines and shallow synclines with axes dipping southeastward. In the northeastern part of the Study Area the Salado surface dips steeply northeastward. Unlike the Castile, the Salado Formation overlaps the reef structure, with some thinning over the reef, and is present outside of the basin, extending eastward and northward for many kilometers into West Texas and the Texas Panhandle.

Conservative estimates of the hydraulic conductivity of the Castile yield a range of about one nanodarcy (1.0×10^{-14} m/s) to about 0.1 microdarcy (1.0×10^{-12} m/s). Porosity of the anhydrite is about 0.001.

In the Study Area, where the Salado is intact, ground-water circulation is minimal because, as is the nature of the highly plastic salt deposits, the Salado lacks primary porosity and open fractures. Permeability of the Salado is very low but measurable, averaging about 0.05 microdarcies and ranging from 9 nanodarcies to 25 microdarcies throughout the formation. The Salado has an estimated effective porosity of 0.001. Formation pressure varies from hydrostatic to near lithostatic and, although the formation may be saturated, the low effective porosity allows for very little ground-water movement.

The Salado Formation is conformably overlain by the Rustler Formation, which is the youngest unit of the Ochoan evaporite series. The composition of the Rustler Formation is about 40 percent anhydrite, 30 percent halite, 20 percent siltstone and sandstone, and 10 percent anhydritic dolomite. The Rustler consists of five members, which are, in ascending order, the unnamed lower member, the Culebra Dolomite Member, the Tamarisk Member, the Magenta Dolomite Member, and the Forty-niner Member. Ground-water occurrence in the Rustler is mostly restricted to the Rustler-Salado residuum at the base of the unnamed lower member and the dolomite units, with some flow in a thin siltstone in the unnamed lower member and in a thin claystone of the Forty-niner.

Data from the intervening units—the unnamed lower member, the Tamarisk Member and the Forty-niner Member—are restricted to wells H-14 and H-16. These aquitard units are considered isotropic and homogeneous, with a very low permeability throughout the Study Area. The estimated hydraulic conductivities of the three units are, in ascending order, 1×10^{-10} m/s, 1×10^{-12} m/s, and 1×10^{-9} m/s. The Tamarisk was too impermeable to test, and the value of 10^{-12} m/s is an estimate. The porosity of the aquitards is about 0.3.

The Rustler-Salado residuum, or "brine aquifer," occurs above the halite of the Salado Formation at the Rustler contact as a post-Rustler-Formation dissolution residue in and near Nash Draw and as a post-Salado/pre-Rustler dissolution residue in the WIPP vicinity. The residuum has a range of thickness from 3 m to 30 m and a mean thickness of about 8 m. More recent information shows a range of 2.4 m in test hole P-14 to 33 m in test hole WIPP-29. Hydraulic conductivity ranges from about 10^{-12} to 10^{-6} m/s. The hydraulic conductivities for Nash Draw are higher by several orders of magnitude than the values east of the draw and range from 10^{-8} to 10^{-6} m/s. Eastward, the range is from 10^{-12} to 10^{-9} m/s. Near Malaga Bend, the

hydraulic conductivity is around 6 x 10^{-4} m/s. Effective porosity estimates for the brine aquifer range from 0.15 to 0.33, with an average effective porosity of 0.2. Fluid density of the water in the residuum ranges from 1.048 to 1.24 g/cm^3.

More is known about the hydrologic properties of the Culebra Dolomite Member than any other unit in the study area. The thickness of the Culebra near the WIPP ranges in thickness from 4.8 m to 11.0 m. The hydraulic conductivities range from 10^{-10} m/s to 10^{-4} m/s. Porosity of the Culebra ranges from 0.07 to 0.30 and averages about 0.16. The quality of Culebra Dolomite waters is marginal, and use is restricted to stock watering. Fluid density of the Culebra water ranges from 1.007 to 1.171 g/cm^3.

The hydraulic conductivity of the Magenta Dolomite Member ranges from 10^{-10} to 10^{-5} m/s. No porosity measurements have been done on the Magenta, but a porosity of 0.20 is estimated for the dolomite, which is slightly high for intact dolomite but may be close to an average porosity of dolomite that has undergone some fracturing and/or dissolution. Water density varies from 1.004 to 1.171 gm/cm^3.

The hydraulic conductivity of the Supra-Rustler rocks, assuming saturation, is assumed to be 10^{-11} m/s, similar to the hydraulic conductivity of the Forty-niner Member. The estimated porosity falls in the range of fine-grained sandstone: 20 percent. Water density is assumed to be similar to that of the Magenta waters.

Geochemical and hydrological evidence indicates that ground-water flow in the Los Medaños region through the Rustler Formation and Capitan aquifer may be under transient conditions, not under steady-state conditions, in response to changing geology, hydrology, and climate. Before the Pleistocene, the ground-water flow direction in the Capitan aquifer was eastward around the periphery of the basin, and basinal flow was eastward through the Rustler Formation and Bell Canyon Formation and then ultimately into Texas. Uneven tilting of the Delaware Basin formed fractures in the brittle evaporitic rocks parallel to the basin axis, and, combined with the lowering of the regional base level, an episode of dissolution and erosion began forming Nash Draw. Coincident with the tectonic activity, precipitation increased in the region that, in turn, increased recharge to the Capitan in the Guadalupe Mountains area. The vertical potential of the Capitan near what is now the Eddy-Lea county line forced water upward into fractured rocks, dissolving the evaporites over the reef and forming conduits (breccia chimneys) that are still evident over the Capitan along the axis of Nash Draw.

The drop in base level and increase in precipitation increased the carrying power of the Pecos River, which began incising the Capitan Limestone near Carlsbad. The down cutting of the Pecos River into the Capitan, coupled with the Nash Draw dissolution/erosion, released the eastward regional hydraulic pressure in the basinal units and the northern part of the Capitan. Breccia chimney formation above the Capitan along the Nash Draw axis ceased, and ground water in the Rustler Formation in the north-central Delaware Basin east of Nash Draw changed direction and began to flow toward the draw and ultimately to the Pecos River.

The hydraulic head of the Capitan aquifer exerts pressure vertically upward on the northern rim of the Delaware Basin under the almost impermeable Salado Formation. The Salado prevents Capitan water from moving upward except where the Salado anhydrites and halites have undergone weakening caused by deformation from extension fracturing or by compression. The Salado exhibits thinning above the Capitan in areas where surface depression features are now forming (San Simon Swale and San Simon Sink) and in areas where deep dissolution features have filled with Cenozoic sediments (from Winkler County, Texas, into southern Lea County, New Mexico). In some of the breccia chimneys, which are up to 300 m in diameter, fluids undersaturated with respect to halite may have removed all or almost all of the halite.

In the lower part of Nash Draw near the Pecos River, the Rustler Formation ground water is under water-table conditions. In this region, the Rustler is represented by the unnamed lower member, which has been affected by dissolution of the upper Salado and by a high degree of dissolution of its own evaporites. The Culebra Dolomite Member, where present in lower Nash Draw, has also been affected by the dissolution of the upper Salado and the unnamed lower member. All the dissolution has resulted in a poorly consolidated unit, with horizontal flow toward the Pecos River. Below the river, flow is vertical toward the river.

In the upper part of Nash Draw, the Rustler ground water is only partially confined, and ground-water flow is southwest down the axis of the draw toward the Pecos River. Along the rim of Nash Draw, flow from the Magenta Dolomite is downward through the poorly consolidated, karstic Tamarisk Member into the Culebra and then toward the water-table aquifer near the Pecos River.

East of Nash Draw, the Rustler hydrostratigraphic units are completely confined, and very little ground water flows vertically through the low-permeability aquitard units. Flow in the confined Magenta Dolomite Member is west toward Nash Draw, and as previously mentioned, then downward into and perhaps through the Tamarisk Member, either directly into Nash Draw where the Tamarisk is present or into the Culebra.

Flow in the confined Culebra Dolomite Member is apparently south-southwest across the WIPP and then toward the water-table aquifer in lower Nash Draw. In some areas, particularly south of the WIPP where the ground-water gradient is low and where the Culebra dips gently east, ground-water flow direction may be affected by the variable density of the Culebra waters.

Ground water, when found in the units above the Rustler Formation, is under water-table conditions over the WIPP, but whether the condition prevails east of the WIPP or where the change would occur is uncertain.

Future modeling studies will determine the sensitivity of the regional system to variable density effects, the sensitivity of regional ground-water flow to Capitan pressure to determine under what conditions flow in the upper hydrostratigraphic units will be affected in the vicinity of the WIPP, and the sensitivity to leakage from units above the Rustler Formation (and within the Rustler) on the Rustler hydrostratigraphic units.

I. INTRODUCTION

The Waste Isolation Pilot Plant (WIPP) near Carlsbad, New Mexico, is planned as the first mined geologic repository for transuranic (TRU) wastes generated by defense programs of the United States Department of Energy (DOE). The purpose of the WIPP is to demonstrate that a safe facility for handling, storage, and disposal of TRU waste is feasible. The WIPP Project will assess compliance with the requirements of the United States Environmental Protection Agency's (EPA) Standard, *Environmental Radiation Protection Standards for the Management and Disposal of Spent Nuclear Fuel, High-Level and Transuranic Radioactive Wastes* (40 CFR Part 191). Assessing compliance with the long-term performance criteria of Subpart B of the Standard is a cornerstone for successfully implementing a DOE TRU-waste disposal system.

Subpart B of the Standard defines "performance assessment" as an analysis that identifies the processes and events that might affect the disposal system, examines the effects of these processes and events on the performance of the disposal system, and estimates the cumulative releases of radionuclides, considering the associated uncertainties, caused by all significant processes and events (U.S. EPA, 1975). Modeling of regional and local ground-water flow is the basis for calculating radionuclide transport, an integral part of assessing the performance of the disposal system. Site characterization defines the local conceptual model and the present flow fields, synthesizes observational data into flow and material-property fields that help explain and reproduce the data, and establishes confidence in the understanding of the geology, hydrology, and geochemistry of the WIPP. Performance assessment will use this conceptual model and the present flow field as initial conditions from which simulations of the system are run far into the future (10,000 years) to perform the consequence and uncertainty analyses required by the Standard (SNL, 1990).

The objective of regional hydrologic modeling is to establish and maintain a credible conceptual model that simulates the hydrology of the region for the preliminary and final consequence analyses. The objective of local hydrologic modeling is to establish and maintain a credible ground-water flow model of the local hydrology for preliminary and final consequence analyses (SNL, 1990).

The evaporite deposits in southeastern New Mexico were chosen as a potential repository for TRU wastes because the bedded salt has several characteristics that make it a suitable geologic medium for storage of radioactive waste. The Salado Formation fulfills the basic criteria for a repository as listed below (from Powers and others, 1978):

Geologic Criteria: The geology (topography, lithology, thickness, and structure) shall provide suitable assurances that the repository shall not be breached by natural phenomena as long as the waste is hazardous to man.

Hydrologic Criteria: The hydrology of the site shall not allow a possible breach of the repository by dissolution of the evaporites, thereby releasing waste that poses a threat to man.

Tectonic Criteria: The site shall be suitably stable, and no geologic activity shall occur to breach the repository as long as the stored waste is hazardous to man.

Physico-chemical Criteria: The geologic medium must not react with the waste material and must not pose a threat to man.

Purpose

The primary objectives of this report are the following:

To compile a regional geologic and hydrologic data base for the Los Medaños region, where the WIPP is located. Previous studies in the area have concentrated on specific aspects of geology and hydrology; this report combines the efforts of many workers into a single report.

To present a regional conceptual geohydrological model for the Los Medaños region so that computer simulations in three dimensions of ground-water flow and transport can be developed.

These activities will help in the evaluation of performance of the WIPP. A clear understanding of a ground-water flow system requires a knowledge of the geology of the region to be studied, the location and state of the ground water within the system, the nature of the boundaries of the region containing the ground water, the behavior of the system under natural or unstressed conditions, and the behavior of the system under stressed conditions. This report examines the relationship of the confined and unconfined ground-water systems in the vicinity of the WIPP, the nature and occurrence of recharge to the system, the relationship of the unsaturated zones and perched zones, anomalous water-level rises in some of the observation wells, regional ground-water flow, and the relationship of the Capitan aquifer and the Bell Canyon Formation to regional flow. The geohydrology of the Bell Canyon is briefly discussed as part of the regional flow system but will not be included in the regional modeling. The Bell Canyon is of interest because it may have an upward gradient sufficient to move water undersaturated with respect to halite upward into the Culebra Dolomite Member of the Rustler Formation. The Capitan aquifer is discussed because it is the primary source of ground water in southeastern New Mexico and has had an influence on flow in the Los Medaños region. Data are taken from published reports and are used to develop the

overall conceptual model. This report complements Lappin (1988) and reviews the geologic history, stratigraphy, basic concepts of geohydrology, and geohydrology of the Los Medaños region.

This report will partly satisfy issue 1.3 of the Preliminary Plan for the Disposal System (Bertram-Howery and Hunter, 1989), which is the behavior characterization and performance modeling of the controlled area.

Performance assessment as applied here has three parts:

a) Identifying and screening scenarios that may have an effect on the repository;

b) Selecting or developing computer codes for simulating the scenarios selected, which involves 1) collecting and compiling data into a conceptual physical model of the region, 2) developing probabilistic and statistical techniques for determining parameter uncertainty and sensitivity, and 3) developing methods of linking the various codes in order to analyze performance; and

c) Assessing compliance with regulatory standards.

The preliminary identification of suitable scenarios has been completed (Guzowski, 1990). This report will be used to give direction to the development of a computer model of the Los Medaños region, and the scenarios will be incorporated into the model to determine the radionuclide releases associated with each scenario.

Location

The Los Medaños Regional-Model Study Area (hereafter called the Study Area) is located in the north-central part of the Delaware Basin in the southern Pecos Valley section of the Great Plains Physiographic Province. This area lies between the high plains of West Texas and the Guadalupe Mountains in southeastern New Mexico (Figure I-1). The Study Area covers approximately 1600 km^2 and extends from the Pecos River in southern Eddy County eastward into Lea County and southward from just inside the Delaware Basin edge to about 20 km north of the New Mexico-Texas state line.

The Study Area, which is located on the northern edge of the Chihuahuan Desert, has an arid to semiarid climate because of the low rainfall (about 0.3 m/yr) (Hunter, 1985). The area has hot summers and mild winters.

The Study Area consists of two geomorphological parts, both of which are distinctly different geologically and hydrologically. The western part is

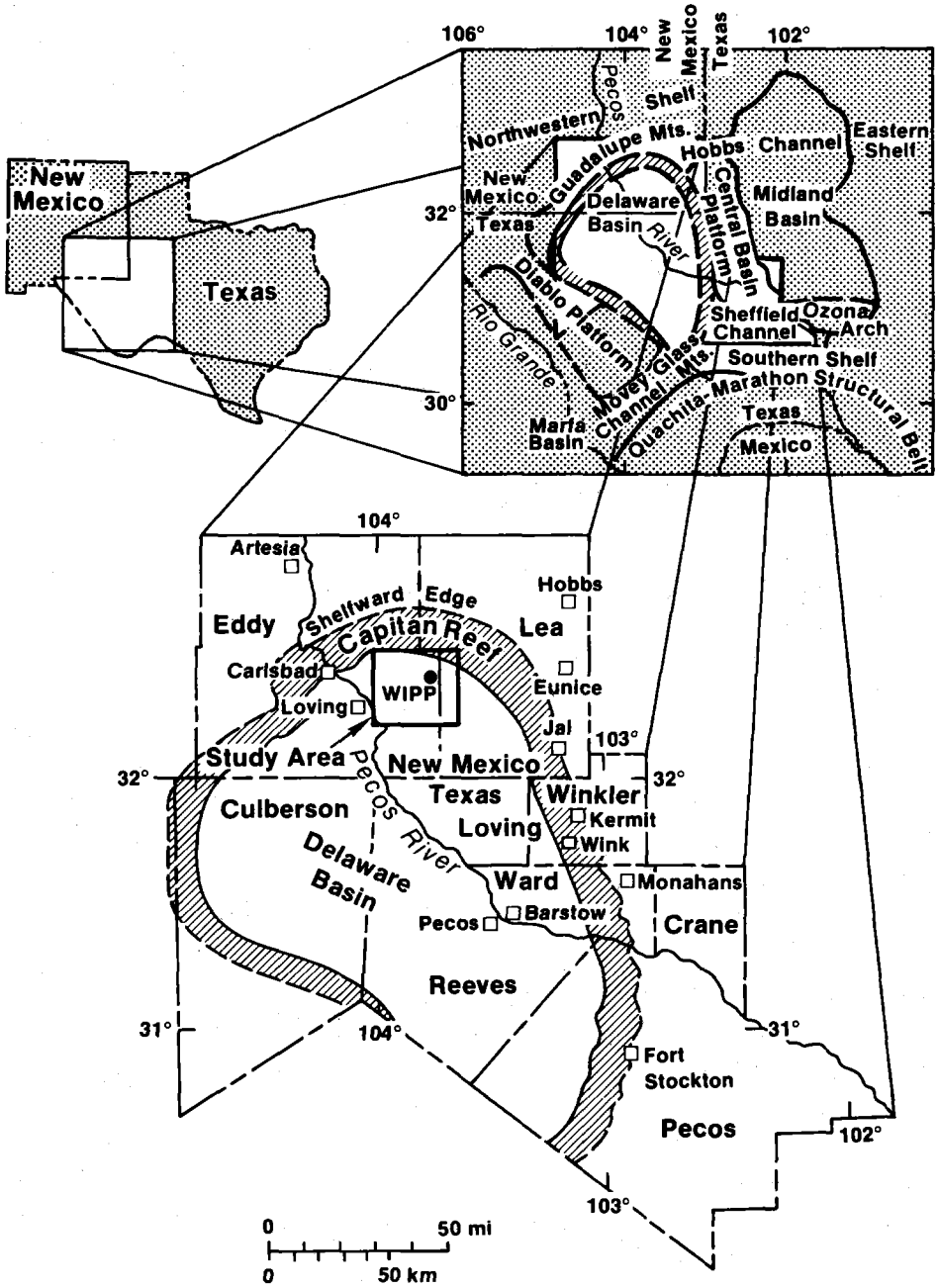

Figure I-1. Location of the Study Area in the Delaware Basin (modified from Richey and others, 1985).

dominated by Nash Draw, a broad, shallow topographic depression with no external surface drainage (Figure I-2). Nash Draw extends nearly 35 km from the Pecos River east of Malaga, New Mexico, almost due north to the Maroon Cliffs area and is bounded on the east by Livingston Ridge and on the west by Quahada Ridge. The eastern part of the Study Area is a region of gently rolling hills sloping upward to the northeast across the WIPP from Livingston Ridge on the eastern boundary of Nash Draw to a low ridge called "The Divide." The elevation of the Study Area ranges from 900 m at Malaga Bend to 1100 m near the Eddy-Lea county line.

Method of Study

The data presented in this survey are compiled from many sources. Since the Geological Characterization Report (GCR) (Powers and others, 1978) for the WIPP was published, many reports have been released concerning the geology and hydrology of the WIPP and WIPP vicinity. To date, most of the data collected in the WIPP vicinity are concerned with the Culebra Dolomite Member of the Rustler Formation because it is the most hydraulically conductive hydrostratigraphic unit that provides likely potential pathways for material released from a breached repository to reach the accessible environment 5 km from the WIPP. Performance assessment requires that all potential hydrostratigraphic units be considered, including the Delaware Mountain Group and deeper units, the Capitan aquifer, the Rustler-Salado contact residuum, the Culebra Dolomite and Magenta Dolomite Members of the Rustler Formation, the Dewey Lake Red Beds, the Lower Dockum Group (Santa Rosa Sandstone), and the alluvial aquifers.

Hydrologic and geologic data were compiled from Sandia National Laboratories (SNL) Hydrology Program reports, U.S. Geological Survey (USGS) reports, SNL contractor reports, private consultant reports for various government agencies, driller's logs, and well logs. A discussion of terms used in this report is presented in Appendix A. The data are presented in tables and figures and in Appendix B of this report.

Hydrologic data pertaining to the Rustler Formation hydrostratigraphic units at and near the WIPP were obtained from tests on wells and groups of wells. The designation H is used for hydro-pad wells (groups of 3 or more wells completed in the Rustler Formation). An alphabetical designation of a, b, or c (such as H-2a) denotes the horizon of completion, starting from Magenta (a), Culebra (b), or the Rustler-Salado contact residuum (c). The WIPP (for example, WIPP-25) designation is for wells in or near Nash Draw that were used for dissolution and subsidence investigations. P-wells (P-14) are potash resource evaluation wells that have been reworked for WIPP investigations.

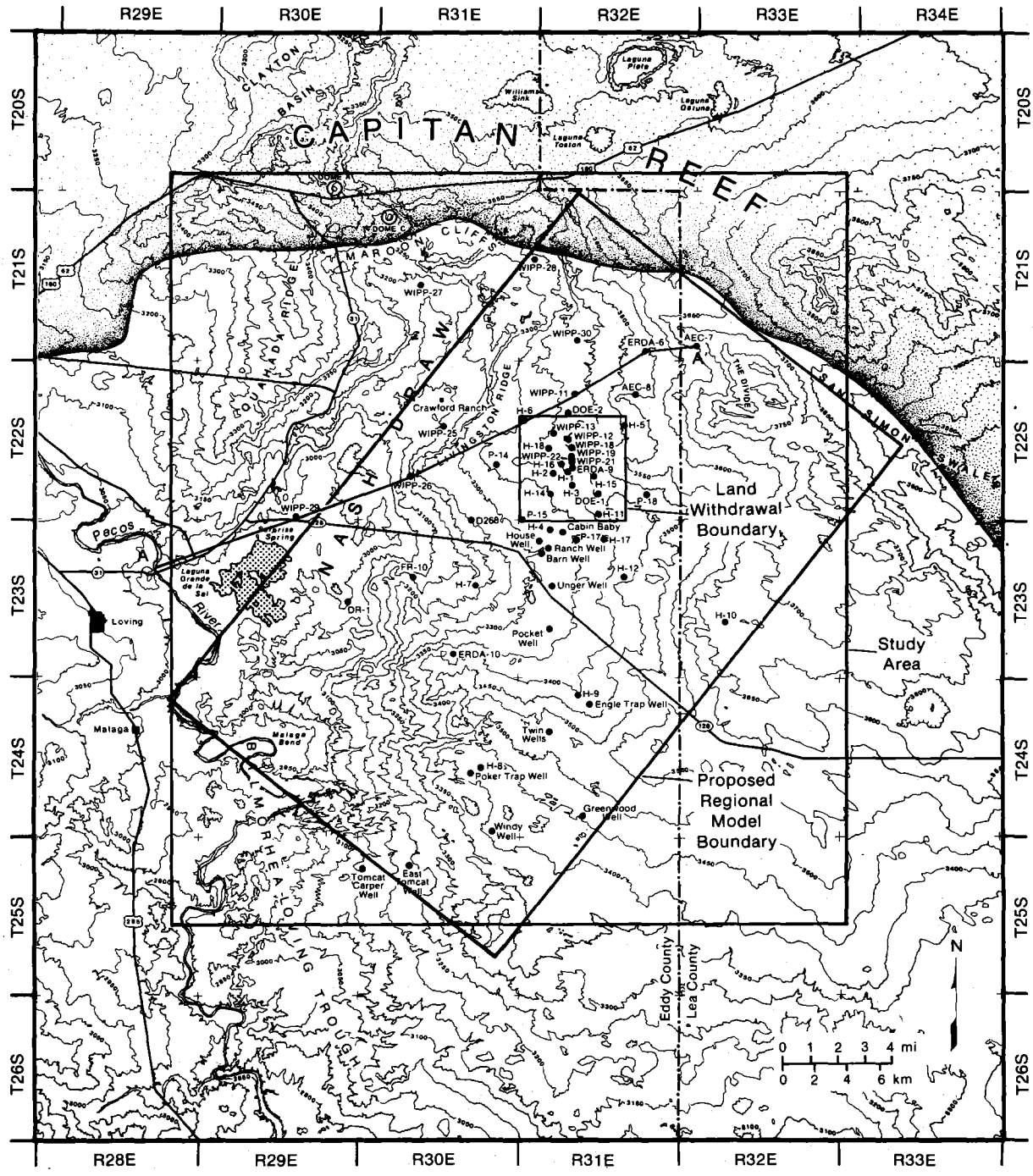

TRI-6342-612-0

Figure I-2. Index Map Showing Study Area and Model Boundaries in the Los Medaños Region (modified from LaVenue and others, 1988).

Other wells from which data were obtained are from previous investigations in the area, such as AEC-7, AEC-8, and ERDH-10, which were used for Bell Canyon Formation testing, and from wells used for domestic or ranching purposes.

Contour maps show hydrologic properties such as hydraulic conductivity and water levels. The isopleths of hydraulic conductivities are the logarithms of the value; the water levels are converted to fresh-water values and contoured. Structure (formation surface) contour maps and isopachous (thickness) maps present geologic data. As an expediency, the maps are computer generated using Surfer® from Golden Software, Inc. (1987).[1] Computer-generated maps are adequate for most of the data presentation, but in some cases, such as in areas with a low density of data points, the contour generation results in uneven (sawtooth) contours or in a "bull's-eye" pattern. Special algorithms in the contour package smooth these contours. This smoothing affects the hydrologic parameter maps more than it affects the computer-generated contour maps. For instance, the water-density maps are generated from data around the WIPP, but as the contours are extrapolated toward the Study Area boundary, the lines become erratic. Gradients in this report are presented as decimal fractions with units of m/m.

Geologic data are from SNL reports (Bachman, 1987; Borns, 1983, 1985, 1987a,b; Borns and Shaffer, 1985; Borns and others, 1983), USGS reports (Richey, 1987, 1989; Mercer, 1983; Mercer and Orr and others, 1977, 1979), and driller's logs. Hydrologic data are from SNL and USGS reports (Beauheim and others, 1983a,b; Beauheim, 1986, 1987a,b,c; Mercer, 1987; Mercer and others, 1987; Stormont and others, 1987; Peterson and others, 1987; Saulnier and others, 1987; Saulnier and Avis, 1988; Haug and others, 1987; LaVenue and others, 1988; Lappin, 1988; Richey and others, 1987; Mercer, 1983). Rock and water properties are from Haug and others (1987) and LaVenue and others (1988).

Geomorphology, physiography, and stratigraphy of the region in the vicinity of the WIPP have been thoroughly discussed in many reports (Powers and others, 1978; Mercer, 1983; Bachman, 1973, 1974, 1980, 1984, and 1987; Snyder, 1985; and Lappin, 1988). The reader is referred to these reports for a more detailed discussion of these subjects. Hydrologic data for the Culebra Dolomite Member were obtained from USGS and SNL reports for wells shown in Figure I-2. Figure I-3 shows the density of wells used for geologic data. The data are presented in Tables B-1 through B-6 of Appendix B.

---

[1] The use of a brand name in this report is for identification only and does not imply endorsement of specific products by Sandia National Laboratories.

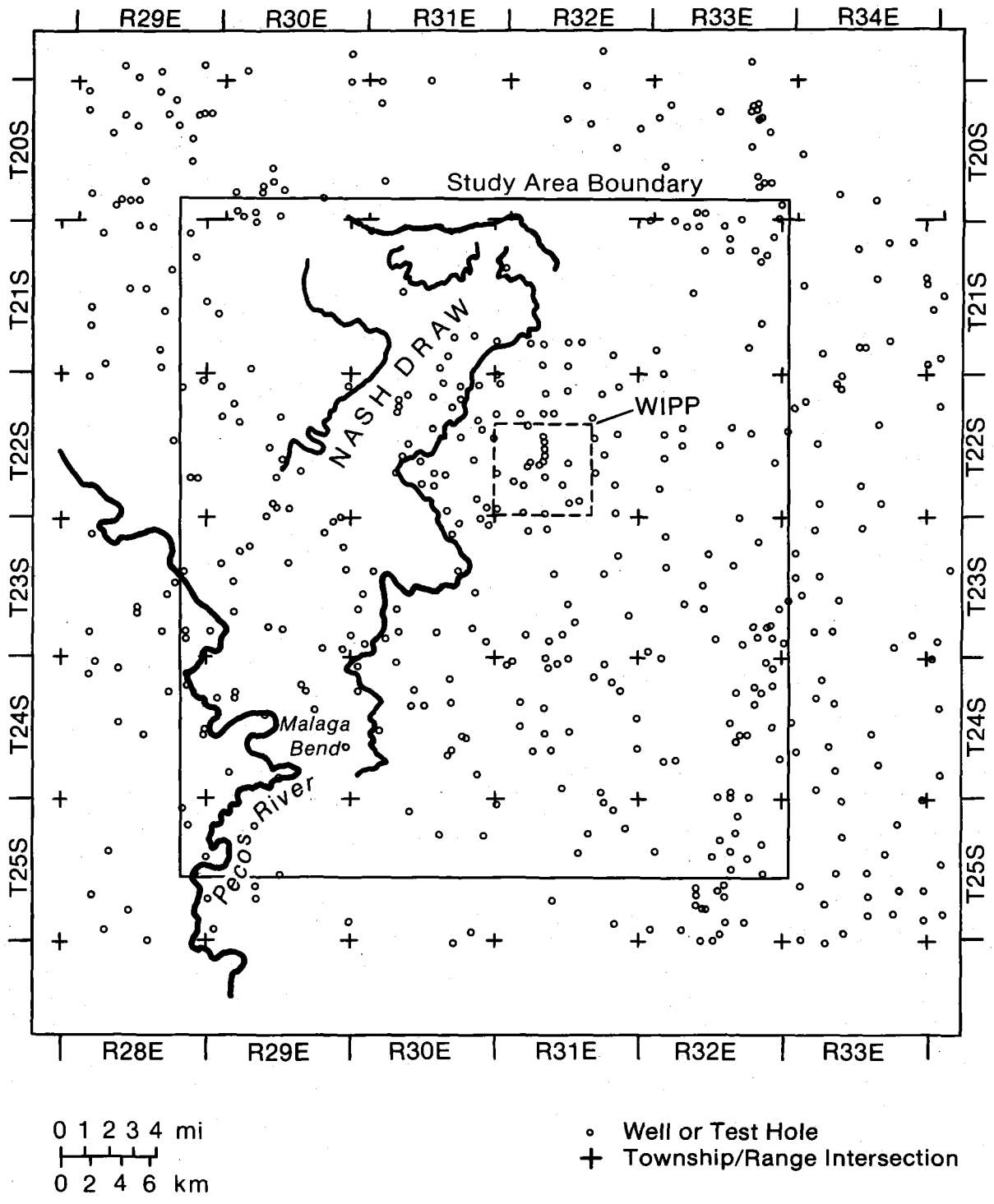

Figure I-3. Index Map Showing Well Locations Used for Geologic Information in the Los Medaños Region.

II. REGIONAL GEOLOGY

A dominant geologic feature in southeastern New Mexico and western Texas is the Permian Basin, which is comprised of a sequence of rocks that have a classic limestone to sandstone facies relationship, that is, a gradual change is represented in the rocks. The following brief description of the formation of the Permian Basin and, subsequently, the Midland and Delaware Basins, is taken from Powers and others, (1978), Cheeseman (1978), Williamson (1978), Hiss (1975), Hills (1984), Harms and Williamson (1988), and Ward and others, (1986). The reader is also referred to the Los Medaños Geologic Column (Figure II-1) for the following discussion.

Geologic History of the Delaware Basin

The Delaware Basin extends from just north of Carlsbad, New Mexico, into Texas west of Fort Stockton (Figure I-1). The elongated, confined depression, one-fourth of which is in New Mexico, covers an area of over 33,000 km^2 and is filled to depths as great as 7300 m with Phanerozoic rocks (Hills, 1984).

The precursor of the Permian Basin, the Tobasa Basin, began forming as a broad, low depression in Ordovician time when transgressing seas began accumulating clastic and carbonate sediments. After a long period of accumulation and subsidence, the basin began separating into the Delaware and Midland Basins when the area now called the Central Platform uplifted during Pennsylvanian time.

During the Early Permian, the subsiding basin, which was delineated by a reef complex, began subsiding at a faster rate, and clastics to the south and reef deposits to the north formed the Wolfcampian rocks (Cheeseman, 1978). Leonardian-time rock units consisting of thick shelf and marginal dolomites (San Andreas Dolomite and Victorio Peak Dolomite, respectively) and a thick basinal limestone (Bone Spring Limestone) comprise the basal units for the shelfward Artesia Group; the marginal reef units and the clastic basinal Delaware Mountain Group of Guadalupian time (Figure II-1) form the Capitan Reef and Delaware Basin.

Ochoan time is represented by the Castile Formation, which is confined to the basin by the reef; the Salado Formation, which extends over the reef margin and shelf rocks; the Rustler Formation; and the Dewey Lake Red Beds. A period of erosion and deposition, now apparent in the present-day Study Area, occurred at the end of Ochoan time, which corresponds to the end of Permian time. The only Triassic rocks present are of the Dockum Group. The

EXPLANATION

LITHOLOGIC SYMBOLS

- Sandstone
- Mudstone; siltstone; silty and sandy shale.
- Shale
- Limestone
- Dolomite
- Cherty limestone and dolomite
- Shaly limestone
- Anhydrite (or gypsum)
- Interlaminated anhydrite-calcite
- Halite (rock salt)
- Granitic rocks

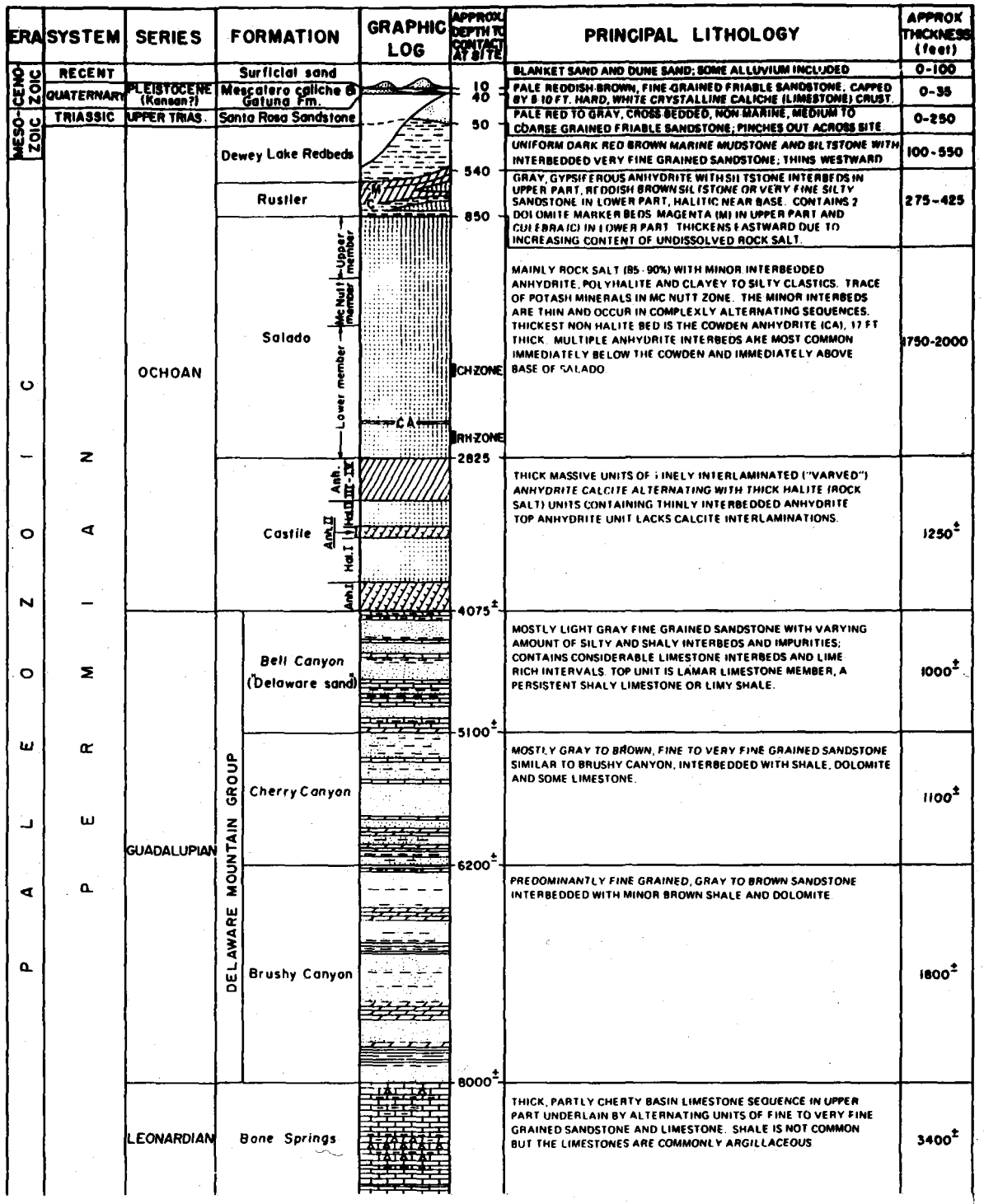

ERA	SYSTEM	SERIES	FORMATION	APPROX. DEPTH TO CONTACT AT SITE	PRINCIPAL LITHOLOGY	APPROX THICKNESS (feet)
CENOZOIC	RECENT		Surficial sand		BLANKET SAND AND DUNE SAND; SOME ALLUVIUM INCLUDED	0-100
CENOZOIC	QUATERNARY	PLEISTOCENE (Kansan?)	Mescalero caliche & Gatuna Fm.	10 40	PALE REDDISH-BROWN, FINE-GRAINED FRIABLE SANDSTONE, CAPPED BY 5-10 FT. HARD, WHITE CRYSTALLINE CALICHE (LIMESTONE) CRUST.	0-35
MESOZOIC	TRIASSIC	UPPER TRIAS.	Santa Rosa Sandstone	50	PALE RED TO GRAY, CROSS BEDDED, NON MARINE, MEDIUM TO COARSE GRAINED FRIABLE SANDSTONE; PINCHES OUT ACROSS SITE	0-250
			Dewey Lake Redbeds	540	UNIFORM DARK RED BROWN MARINE MUDSTONE AND SILTSTONE WITH INTERBEDDED VERY FINE GRAINED SANDSTONE; THINS WESTWARD	100-550
			Rustler	850	GRAY, GYPSIFEROUS ANHYDRITE WITH SILTSTONE INTERBEDS IN UPPER PART, REDDISH BROWN SILTSTONE OR VERY FINE SILTY SANDSTONE IN LOWER PART, HALITIC NEAR BASE. CONTAINS 2 DOLOMITE MARKER BEDS MAGENTA (M) IN UPPER PART AND CULEBRA (C) IN LOWER PART. THICKENS EASTWARD DUE TO INCREASING CONTENT OF UNDISSOLVED ROCK SALT.	275-425
PALEOZOIC	PERMIAN	OCHOAN	Salado — Upper member / Mc Nutt member / Lower member	CH ZONE RH ZONE	MAINLY ROCK SALT (85-90%) WITH MINOR INTERBEDDED ANHYDRITE, POLYHALITE AND CLAYEY TO SILTY CLASTICS. TRACE OF POTASH MINERALS IN MC NUTT ZONE. THE MINOR INTERBEDS ARE THIN AND OCCUR IN COMPLEXLY ALTERNATING SEQUENCES. THICKEST NON HALITE BED IS THE COWDEN ANHYDRITE (CA), 17 FT THICK. MULTIPLE ANHYDRITE INTERBEDS ARE MOST COMMON IMMEDIATELY BELOW THE COWDEN AND IMMEDIATELY ABOVE BASE OF SALADO.	1750-2000
			Castile — Anh. III-XX / Anh. II / Hal. I / Anh. I	2825 4075±	THICK MASSIVE UNITS OF FINELY INTERLAMINATED ("VARVED") ANHYDRITE-CALCITE ALTERNATING WITH THICK HALITE (ROCK SALT) UNITS CONTAINING THINLY INTERBEDDED ANHYDRITE. TOP ANHYDRITE UNIT LACKS CALCITE INTERLAMINATIONS.	1250±
		GUADALUPIAN	DELAWARE MOUNTAIN GROUP — Bell Canyon (Delaware sand)	5100±	MOSTLY LIGHT GRAY FINE GRAINED SANDSTONE WITH VARYING AMOUNT OF SILTY AND SHALY INTERBEDS AND IMPURITIES; CONTAINS CONSIDERABLE LIMESTONE INTERBEDS AND LIME RICH INTERVALS. TOP UNIT IS LAMAR LIMESTONE MEMBER, A PERSISTENT SHALY LIMESTONE OR LIMY SHALE.	1000±
			DELAWARE MOUNTAIN GROUP — Cherry Canyon	6200±	MOSTLY GRAY TO BROWN, FINE TO VERY FINE GRAINED SANDSTONE SIMILAR TO BRUSHY CANYON, INTERBEDDED WITH SHALE, DOLOMITE AND SOME LIMESTONE.	1100±
			DELAWARE MOUNTAIN GROUP — Brushy Canyon	8000±	PREDOMINANTLY FINE GRAINED, GRAY TO BROWN SANDSTONE INTERBEDDED WITH MINOR BROWN SHALE AND DOLOMITE.	1800±
		LEONARDIAN	Bone Springs		THICK, PARTLY CHERTY BASIN LIMESTONE SEQUENCE IN UPPER PART UNDERLAIN BY ALTERNATING UNITS OF FINE TO VERY FINE GRAINED SANDSTONE AND LIMESTONE. SHALE IS NOT COMMON BUT THE LIMESTONES ARE COMMONLY ARGILLACEOUS.	3400±

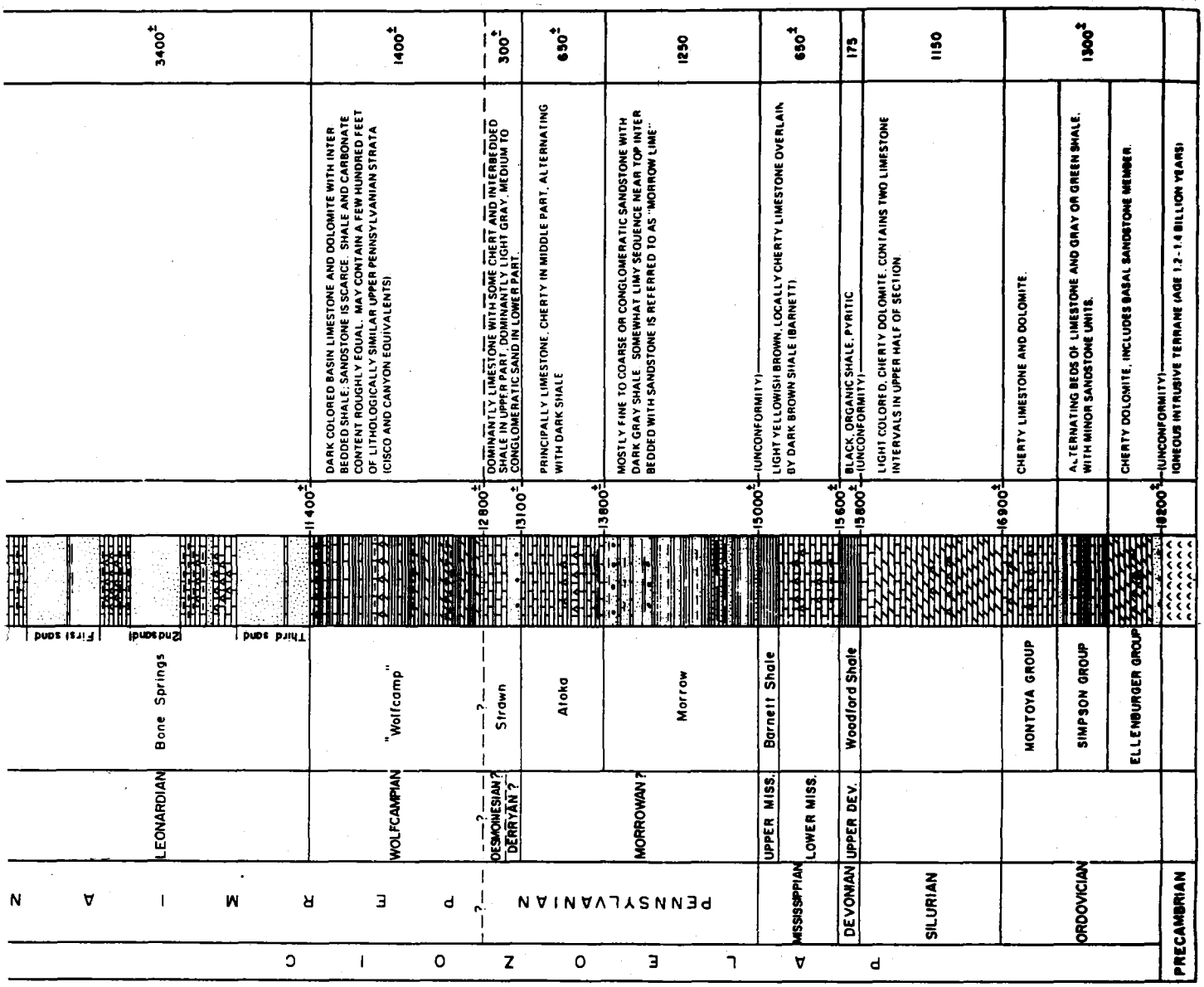

Figure II-1. Los Medaños Geologic Column (from Powers and others, 1978).

Jurassic is not represented in this area, and the Cretaceous is almost completely missing. The Tertiary is represented only by the Ogallala Formation. The Quaternary is represented by the Gatuña Formation, the informally named Mescalero caliche, and dune sands. The stratigraphic units and the relative times that the rock units were formed are given in Table II-1. Figure II-1, a geologic column at the WIPP, illustrates the major stratigraphic divisions, relative ages, and lithologies of the units.

TABLE II-1. MAJOR STRATIGRAPHIC AND TIME DIVISIONS, SOUTHEASTERN NEW MEXICO

Era	System	Series	Formation	Age Estimate (yr)
Cenozoic	Quaternary	Holocene	Windblown sand	
		Pleistocene	Mescalero Caliche	~500,000
			Gatuña Formation	~600,000+
	Tertiary	Pliocene	Ogallala Formation	5 million
		Miocene		25 million
		Oligocene	Absent Southeastern New Mexico	
		Eocene		
		Paleocene		65 million
Mesozoic	Cretaceous	Upper (Late)	Absent Southeastern New Mexico	
		Lower (Early)	Detritus preserved	144 million
	Jurassic		Absent Southeastern New Mexico	208 million
	Triassic	Upper (Late)	Dockum Group	
		Lower	Absent Southeastern New Mexico	245 million
Paleozoic	Permian	Ochoan	Dewey Lake Red Beds Rustler Formation Salado Formation Castile Formation	
		Guadalupian	Capitan Limestone and Bell Canyon Formation	
		Leonardian	Bone Springs	
		Wolfcampian	Wolfcamp	275 million

Source: Modified from Bachman, 1987

Minimal tectonic activity has occurred in the region except for a slow eastward tilting in the eastern part of the basin caused by faulting that began in late Pennsylvanian time and continued through the Permian (Hayes, 1964; Williamson, 1978; Hills, 1984). Late-Tertiary faulting formed the Guadalupe and Delaware Mountains along the western edge of the basin. Evidence of volcanic activity in the area consists of a lamprophyre dike of medium-gray to grayish-black, fine-grained porphyritic material. The dike is northeast trending and occurs 16 km northwest of the WIPP at its closest point (Figure 2-5 in Powers and others, 1978). Figure II-2 in this report shows the trace of the dike.

Stratigraphy of the Pennsylvanian Rocks

The oldest rocks in the Delaware Basin discussed in this report are of Pennsylvanian age (Figure II-1). Pennsylvanian rocks are of particular interest to performance assessment because they are a potential source of natural gas or fluids that may be under sufficient pressure to reach the repository level (see "Formation Pressure" in Appendix A). The total thickness of these Pennsylvanian rocks ranges from 500 to 800 m in southern Lea County (Nicholson and Clebsch, 1961). In the northern Delaware Basin, the Pennsylvanian rocks are about 760 m thick.

MORROWAN SERIES

The basal Morrowan Series, deposited in a transgressive, fluvial-deltaic environment, possesses variations in cementation and depositional patterns that create stratigraphic traps for hydrocarbons (James, 1985). The Morrowan Series consists of about 350 m of fine- to coarse-grained conglomeratic sandstone. Also present is a dark shale that grades into a limey sequence near the top.

The Morrow Formation grades conformably into the Atoka Formation, which consists primarily of about 110 m of limestone alternating with shale (Figure II-1) (Nicholson and Clebsch, 1961; Powers and others, 1978; Hills, 1984; James, 1985).

DESMOINESIAN SERIES

The Strawn Formation represents the Upper Pennsylvanian rocks in the basin (Figure II-1). The Strawn Formation consists of about 70 m of dark brown, cherty limestones (James, 1985; Hills, 1984) with some sandstone beds (Powers and others, 1978).

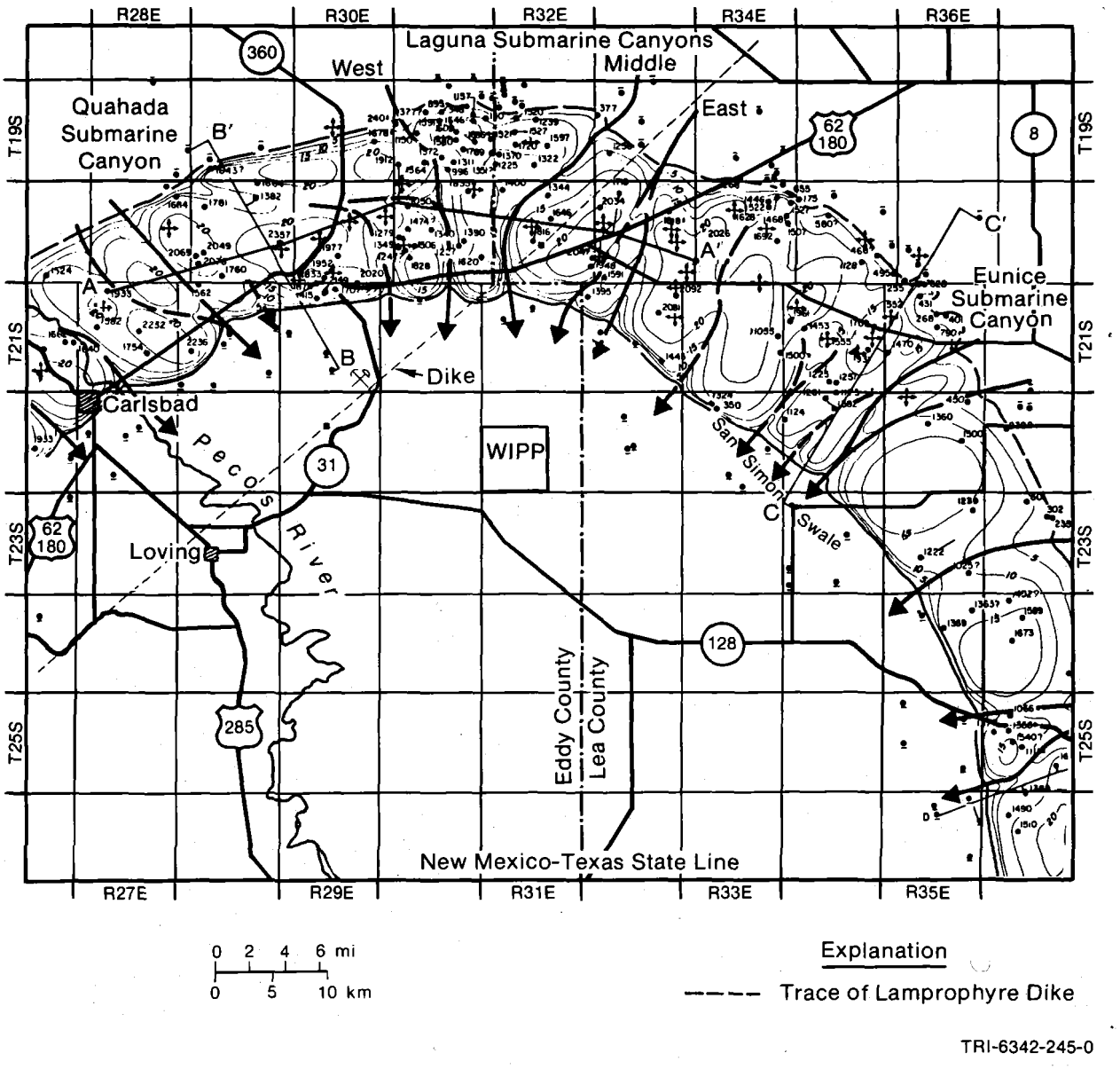

Figure II-2. Isopach Map of the Capitan Limestone, Showing Possible Submarine Canyons (Hiss, 1975).

MISSOURIAN SERIES

These rocks consist of about 400 m of dark shales and limestones, sandstone, and some chert (Powers and others, 1978).

VIRGILIAN SERIES

In the Delaware Basin, this series consists of about 300 m of brown to tan, fine-grained sandstone, black to brown shale, and light-colored sandstone (Powers and others, 1978).

Stratigraphy of the Permian Rocks

Lithologic delineation of the Upper Pennsylvanian rocks from the Permian rocks is difficult because of differential rates of deposition on the Pennsylvanian surface and differential rates of subsidence throughout the Permian Basin. In the Delaware Basin, the boundary is determined by an interpretation based on fusulinids (Hayes, 1964; Powers and others, 1978). Table II-1 gives the bounding ages of the systems from the Permian to the present.

The Permian rocks are divided into the following series: Wolfcampian, Leonardian, Guadalupian, and Ochoan. In New Mexico, Wolfcampian, Leonardian, and early Guadalupian rocks are described from drillhole cores, while late Guadalupian and Ochoan rocks are described from outcrops. Descriptions of outcrops in Texas (Hayes, 1964) provide additional data on all Permian rocks.

WOLFCAMPIAN SERIES

In the northern part of the Delaware Basin, the Early Permian, Wolfcampian rocks unconformably overlie the Pennsylvanian rocks. The rocks consist primarily of limestones and dolomites with some thick shales and are unlike the stratigraphically equivalent rocks in the Glass Mountains, which are mainly limestone (Hayes, 1964; Powers and others, 1978; Hills, 1984). West of the Study Area between the Pecos River and Guadalupe Mountains, the Wolfcampian Series is about 550 m thick in the subsurface and consists of gray, black, and brown shale with some interbeds of fine-crystalline, brownish limestone (Hayes, 1964; Nicholson and Clebsch, 1961).

LEONARDIAN SERIES

Continued deposition of fine-grained, clastic sediments in the middle Permian formed the Leonardian rocks. These porous and permeable sandstones are interfingered with less permeable and porous, thin black limestones, and the

series is as much as 900 m thick in the central basin (Hayes, 1964; Nicholson and Clebsch, 1961; Hills, 1984; Powers and others, 1978).

GUADALUPIAN SERIES

The oldest rocks of interest in the development of a geohydrologic conceptual model for the Delaware Basin are the upper units of the Guadalupian Delaware Mountain Group and its time equivalents: the Capitan Limestone and the Artesia Group (Figure II-3). Leonardian Series and older rocks will be considered as sources of fluid under pressure only if further examination of well data shows that deep reservoirs are important (see Chapter VI).

The Capitan Reef and the associated rocks represent a classical example of facies change. Ward and others (1986) divided the complex into seven parts. Beginning from the basin and going shelfward, the facies are the following:

Deep water basin (Delaware Mountain Group)
Reef talus (Capitan Reef)
Reef (Capitan Reef)
Carbonate sand flats (Artesia Group)
Carbonate barrier islands (Artesia Group)
Lagoonal structures (Artesia Group)
Coastal playas and sabkhas (supratidal salt flats) (Artesia Group)

The development of the current conceptual model will include only the first three facies listed above. The shelf facies are outside the scope of this report but are presumed to have some influence on the hydrology of the Capitan Reef. Although aquifers are present in the Artesia Group, the contact of the units with the Capitan Reef is gradational (Hiss, 1975).

Capitan Limestone

The Guadalupian Capitan Reef is an arcuate structure that almost completely surrounds the Delaware Basin. In New Mexico, the reef is exposed in an uplifted portion that forms the Guadalupe Mountains southwest of Carlsbad and is overlapped by Ochoan evaporites northeast and east of Carlsbad. The Capitan limestone disconformably overlies the Goat Seep Dolomite and is equivalent to the basinal Bell Canyon Formation described below. The top of the limestone is eroded in the Guadalupe Mountains but remains intact where it is covered. Hayes (1964) divided the reef into two parts, a massive member and a breccia member, that correspond to the reef and the talus facies, respectively. He interpreted the massive member to be biogenic in origin but only sparsely fossiliferous because of dissolution and recrystallization. The massive member ranges in thickness from 76 to 230 m and averages about 120 m

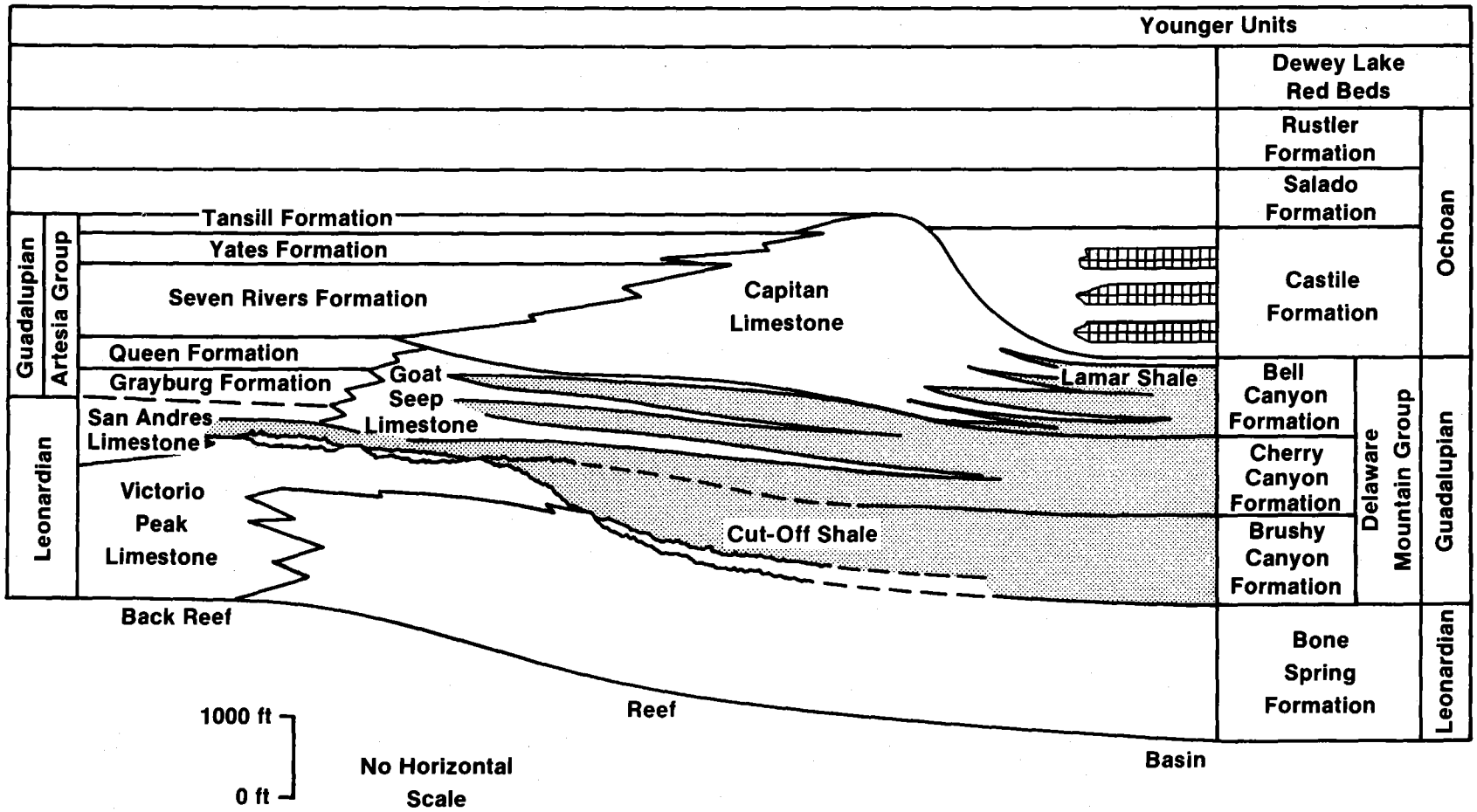

TRI-6342-119-0

Figure II-3. Capitan Reef and Associated Shelfward and Basinward Units (modified from Mercer, 1983).

thick. The reef in outcrop is a light-gray, massive limestone overlying steeply dipping fore-reef talus of bedded, blocky limestone rubble (Ward and others, 1986). The matrix porosity in the reef is low because of biogenic cementation, but where dissolution and fracturing have occurred, permeability is greatly enhanced. This is also true for the upper talus facies, but in the lower part of the talus, dolomitization, silicification, and compaction have decreased porosity and permeability (Ward and others, 1986; Hayes, 1964; Hiss, 1975; Hills, 1984). The relationship of porosity and permeability to the hydrology are discussed further in "Principles of Hydrology" (Appendix A).

The carbonate breccia of the talus front grades basinward into the sandstone of the Bell Canyon Formation by interfingering. The youngest limestone at the reef front may grade into the Castile Formation (Hayes, 1964). Hayes estimates that the maximum vertical thickness of the breccia across the inclined beds, without regard to dip, may be as much as 534 m, averaging about 381 m. He puts the total thickness of the Capitan Limestone at about 610 m. In Eddy County, the Capitan averages about 450 m thick and ranges from 50 to 720 m, and in Lea County, 21 km northeast of Carlsbad in T20S, R29E, the unit has an average thickness of about 400 m, with a range from 50 to 640 m (Hiss, 1975). At all locations, the Capitan Limestone progrades (builds) basinward.

Isopach maps, structure contour maps, and cross sections of the Capitan Limestone show depressions across the surface and a scalloped pattern along the basinward edge. Maps and a longitudinal cross section of the Capitan Limestone (Figures II-2 and II-4) from Hiss (1975) illustrate these characteristics. Figure II-2 shows that the Capitan thickness undulates and creates the scalloped appearance along the basinward edge. Figure II-4, a longitudinal cross section parallel to the reef edge, shows that the surface of the reef undulates up and down. These surface depressions in the reef were formed when storm-generated density currents (gravity-induced currents caused by density difference in fluids) flushed sediment from the evaporitic back-reef lagoons and, using the silt- and sand-laden water, abraded channels into the reef (Hiss, 1975; Williamson, 1978). Williamson's postulation (1978) is that some low-density turbidity currents (currents with material in suspension) were responsible, but the features associated with these currents are not evident. Harms and Williamson's (1988) conclusion is that dense shelf water spilling through the channels in the carbonate banks and flowing down the reef face and out into the basin formed the channels. The dense flows cut channels, and less dense flows spread out over the basin floor, covering the bottom with fine-grained materials. This deposition resulted in facies changes within the basin that show vertical variation in sediment grain size and texture (see also "Bell Canyon Hydrostratigraphic Unit" in Chapter IV).

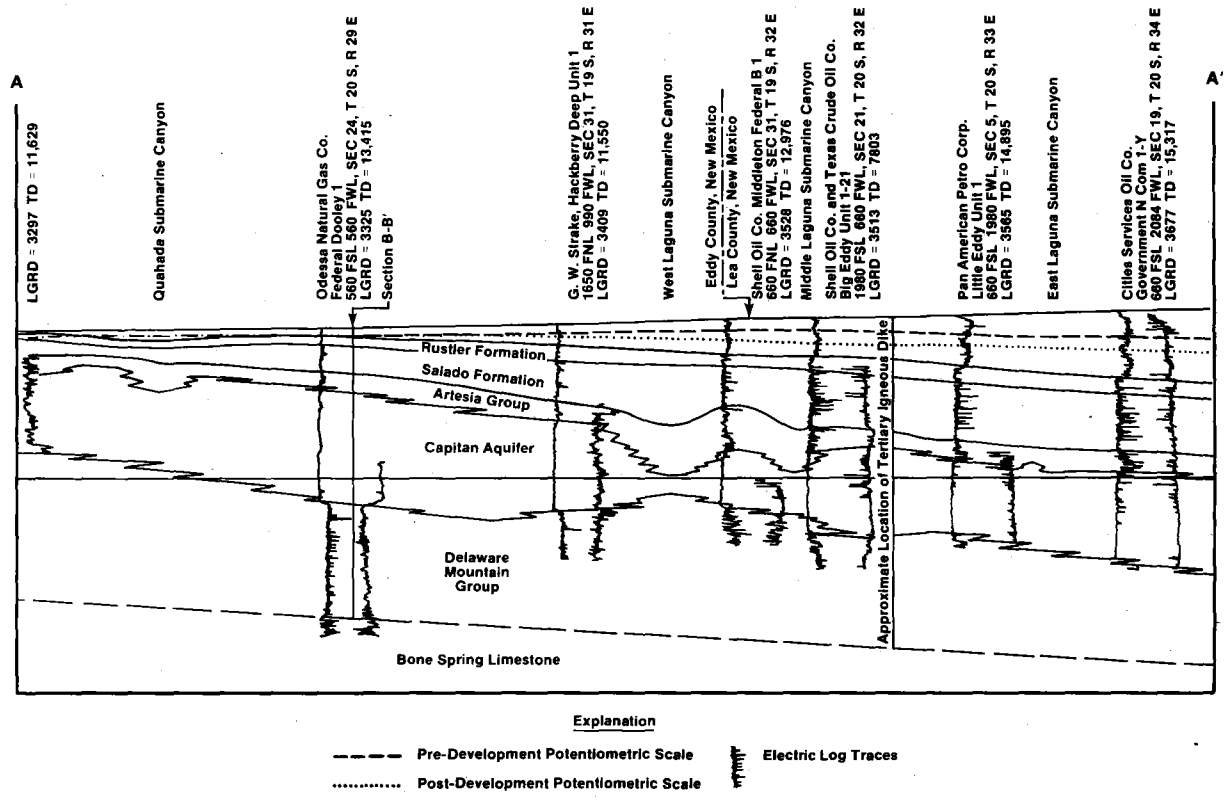

Figure II-4. Portion of a Longitudinal Cross Section of the Capitan Limestone along the Northern Edge of the Delaware Basin from A to A' (Hiss, 1975), as Shown in Figure II-2.

The reef canyons in the Capitan aquifer are important hydrologically because the transmissivities of the channel fill are less than those of the reef carbonates, thus restricting ground-water flow. The following description of the Bell Canyon Formation of the Delaware Mountain Group and Appendix A further discuss the relationship and importance of the sandstone channels to regional ground-water flow.

Delaware Mountain Group

The Guadalupian Delaware Mountain Group consists of three siliciclastic units. In ascending order they are the Brushy Canyon, Cherry Canyon, and Bell Canyon Formations. The Bell Canyon is almost completely restricted within the basin, but the Cherry Canyon has been noted north and west of the reef (Hiss, 1975). The Brushy Canyon Formation consists of a basal unit of about 50 m of dark gray to black shale and shaly sandstone interbedded with limestone and sandstone and is overlain by about 300 m of resistant, lenticular, coarse-grained sandstone beds. The Brushy Canyon overlaps the Bone Spring limestone and has no time equivalent in the basin and margin (Hayes, 1964). The Brushy Canyon is conformably overlain by the Cherry Canyon Formation, which consists of about 300 m of fine-grained sandstone with some limestone members. The Brushy Canyon and Cherry Canyon do not crop out in the Study Area but are exposed just south of the Guadalupe Mountains in Texas. The only outcrops of the Delaware Mountain Group in New Mexico are Bell Canyon rocks to the southwest of Carlsbad, just north of the New Mexico-Texas state line (Hayes, 1964).

The Bell Canyon Formation conformably overlies the Cherry Canyon Formation and is about 210 m thick in outcrop to about 260 m thick in the subsurface (Hayes, 1964). The Bell Canyon consists of thinly bedded, fine-grained sandstones and coarse-grained siltstones with less than five percent gray to black limestone, dolomites, and conglomerates, and virtually no clay (Williamson, 1978; Mercer, 1983; Harms and Williamson, 1988). The upper part of the Bell Canyon in the WIPP area was divided into six informal units based on the studies of cores from test holes ERDA-10, AEC-7, and AEC-8 (Figure II-5) (Mercer, 1983). The Ramsey sandstone is the thickest sandstone unit in the upper Bell Canyon Formation and has had the greatest amount of data recorded because of its importance as an oil and gas producer in some parts of the basin. The Ramsey is separated from the younger Castile Formation by the thin (10 m) Lamar limestone and the very thin (3 m) Trap shale. A marker bed called the Ford shale separates the Ramsey from older units (Olds and Hays sandstones).

As previously mentioned, the Bell Canyon Formation is time equivalent to the Capitan Reef. The unit interfingers with the reef and dips out into the deep

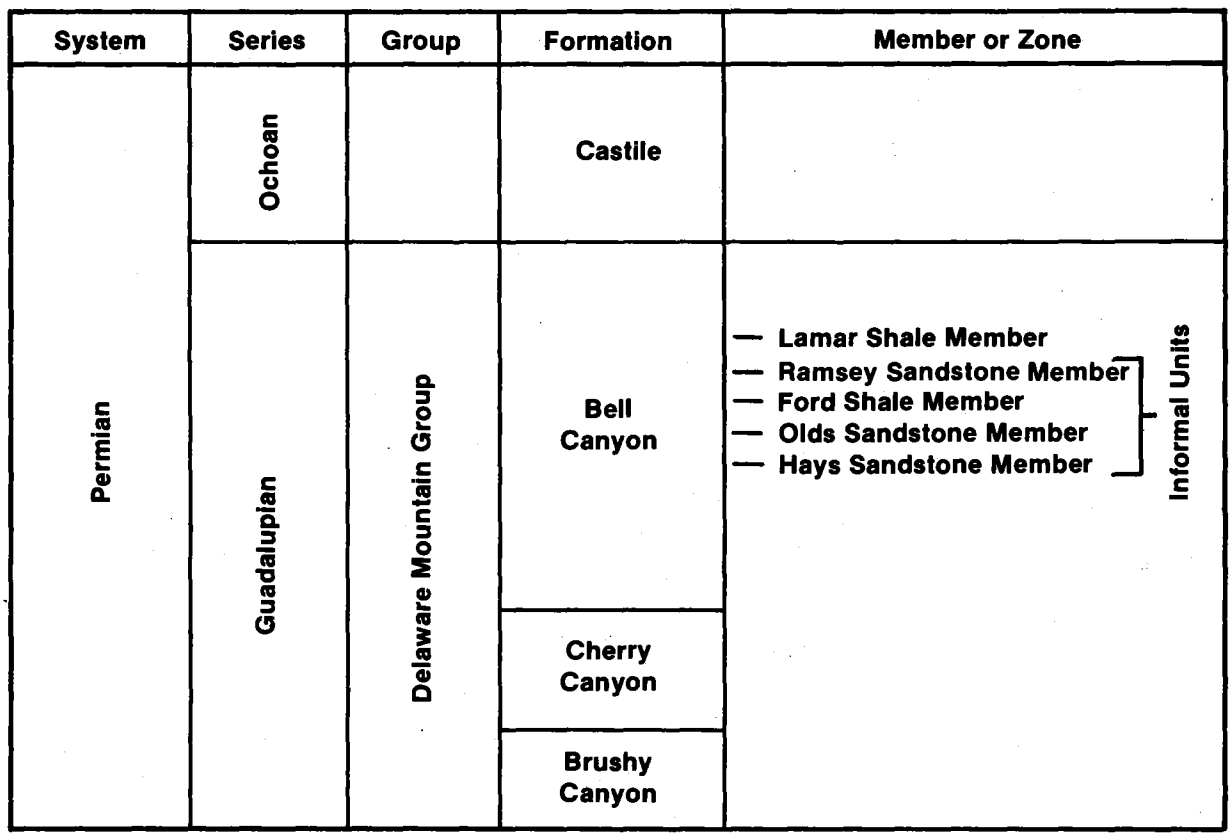

TRI-6342-122-0

Figure II-5. Basinward Units of the Delaware Mountain Group (not to scale) (modified from Mercer, 1983).

basin. Evidence for the deep depositional environment is the presence of deep-water sponges (Cys, 1978).

Nearly all sandstones in the Bell Canyon Formation are restricted to long, sinuous channels, with siltstones comprising the interchannel material (Williamson, 1978; Harms and Williamson, 1988). The channel sands are the remnants of the density currents and possible turbidity currents discussed in a previous section on the Capitan Limestone. A regional isolith map shows the general southwest direction of the density flows in Eddy and Lea Counties, New Mexico (Figure II-6). Not shown are the broad distal portions of the channels that form as the currents reach the basin center. The overall structure of the Bell Canyon Formation (Figure II-7) shows a steady structural gradient dipping easterly (about one degree) through Eddy County. The formation occurs at a depth of about 1200 m in the vicinity of the WIPP.

OCHOAN SERIES

The Ochoan Series is the last series of Permian age in the Study Area. The Ochoan consists of, in ascending order, the Castile Formation, the Salado Formation, the Rustler Formation, and the Dewey Lake Red Beds. The Castile and Salado Formations are mostly anhydrite and halite; the Rustler Formation is a mixture of shales (claystone, mudstone, and siltstone), anhydrite, halite, and dolomite; and the Dewey Lake Red Beds consist of sandstones, siltstones, and shales. All units are present over the WIPP, but west of the WIPP from Nash Draw to the Guadalupe Mountains, some or nearly all of the formations may have been removed by erosion. At Nash Draw, the Dewey Lake Red Beds and part of the Rustler Formation have been removed by erosion. West of the draw at Quahada Ridge, the Dewey Lake Red Beds may or may not be present. To the southwest only the Castile Formation is present, and near the Texas-New Mexico state line, the Castile Formation is missing, and Bell Canyon rocks crop out.

Near the end of the Bell Canyon deposition, circulation within the Delaware Basin became more constricted, resulting in a sequence of organic layers alternating with siltstone laminations that changes in character upward from organically layered calcite to calcite-layered anhydrite. This thick sequence forms the lower Castile Formation, which then grades into the anhydrite-layered halite of the upper Castile Formation and the thick halite of the Salado Formation (Anderson and others, 1972). Speculation by Anderson and others (1972) is that the laminations persist to a "basal limestone breccia, probably of the Rustler Formation, that rests on the lower part of the Salado Formation." A sequence of 260,000 varves was measured and had a composite thickness of 447 m. The varves are correlative over a distance of 113 km across the Delaware Basin (Anderson and others, 1972).

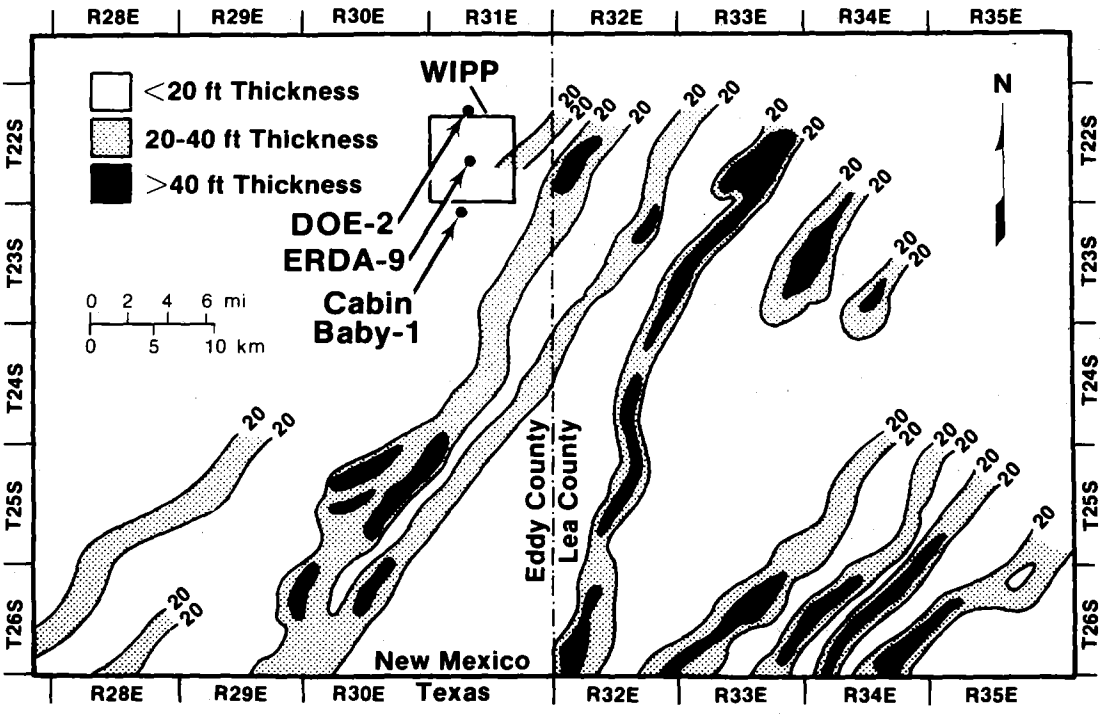

TRI-6334-65-1

Figure II-6. Orientation of Sandstone Stringers in the Bell Canyon Formation of the Delaware Mountain Group (Lappin, 1988).

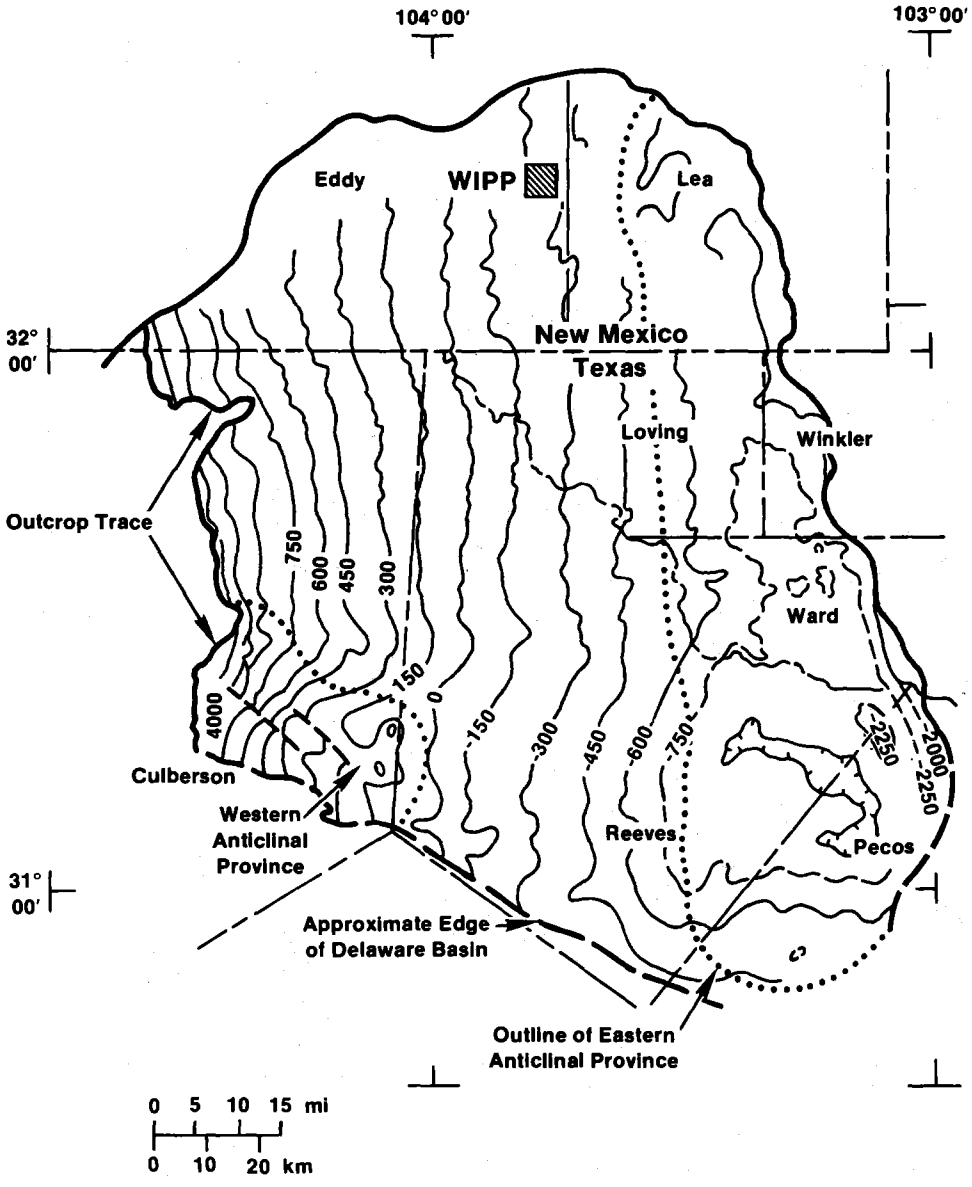

Figure II-7. Generalized Structure Contours on Top of the Lamar Shale (Informal Unit) of the Bell Canyon Formation (Delaware Mountain Group) in the Delaware Basin (Mercer, 1983).

Castile Formation

The Castile Formation conformably overlies the Bell Canyon Formation and consists of seven lithologic members, which include four anhydrite members intercalated with three halite members. In the vicinity of the WIPP, there are three anhydrite and two halite layers. The Capitan Limestone reef completely contains the Castile Formation in the Delaware Basin, and the formation is not present beneath the reef or in the back reef. The formation is present everywhere in the Study Area but is eroded away southwest of the Study Area in the western lobe of the Delaware Basin (Figure II-8). In Loving County, Texas, where the section is complete, the Castile Formation is 640 m thick. In New Mexico north of the WIPP, the Castile Formation is about 360 m thick and thickens southward across the WIPP, where it is about 470 m thick. At the southern edge of the Study Area, the Castile Formation is about 500 m thick.

The Bell Canyon-Castile contact is of particular interest because of the change of environments from deep basinal to evaporitic. A study by Cys (1978) of a core from a well just south of the Texas-New Mexico state line showed the change as transitional but rapid. In the span of one meter, the rocks change from laminated siltstone and shale to siltstone and limestone to anhydrite and limestone. Cys's conclusion (1978) was that the fauna present indicate deposition in deep rather than shallow water. The constriction of channels that had previously allowed free circulation in the basin probably caused the depositional environment to change from open marine to evaporitic. Sedimentation and reef growth rather than diastrophism probably caused the constriction of the channels in the southern segment of the reef (Adams, 1944).

Exploratory coring of the WIPP at ERDA-6 indicated that flowage of the halite in the Castile Formation occurred locally during mid-Cenozoic time and formed anticlines parallel to the strike of the underlying Bell Canyon Formation (Anderson and Powers, 1978).

Salado Formation

As originally defined, the Castile Formation included a halite-rich upper section and an anhydrite-rich lower section (Richardson, 1904, cited in Mercer, 1983). The Castile Formation was later divided into two formations; the lower anhydrite was called the Castile Formation, and the upper halite section was called the Salado Formation (Lang, 1938). The upper unit is of particular interest because it is the host rock for the WIPP. Bachman's conclusion (1984) was that the Salado Formation in the northern Delaware Basin conformably overlies and interfingers with the Castile Formation, whereas some

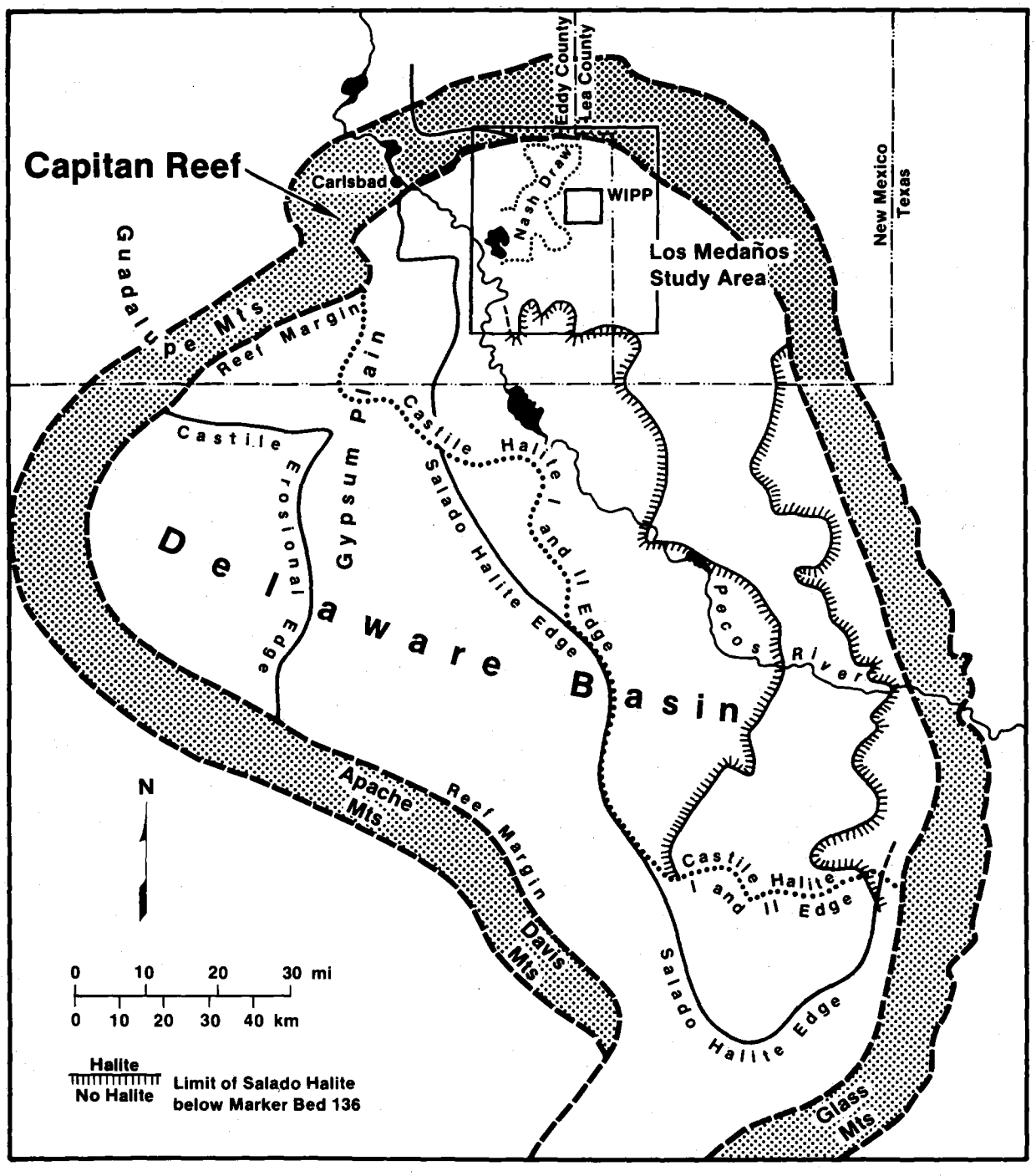

TRI-6342-237-1

Figure II-8. Generalized Distribution of the Castile and Salado Formations in the Delaware Basin, with Emphasis on Distribution of Halites (Lappin, 1988).

earlier workers had concluded that the contact was an angular unconformity (Adams, 1944).

The Salado Formation is present throughout the Study Area but is absent west of the Study Area (Figure II-8). Because the Salado Formation is extremely soluble, there are no intact Salado Formation outcrops. Dissolution breccias consisting mostly of gypsum and clay are all that remain. Throughout the Study Area, the Salado is about 600 m thick and consists of salt rhythmically interbedded with anhydrite, polyhalite, some glauberite, and some thin mudstones (Jones, 1975; Borns, 1985; Mercer, 1983, 1987). The Salado Formation is divided, using borehole data, into three informal members by economic importance, even though the lithologies are similar (Jones, 1974). The following are the three members as described by Jones (1978):

> The lower member is 296 to 354 m of mostly halite with lesser amounts of anhydrite, polyhalite, and glauberite, and has some layers of fine clastic sediments. The rock colors grade upward from light gray at the bottom of the unit to red. This unit will be the host rock for the repository.
>
> The middle member, the McNutt Potash Zone, is 106 to 126 m of a reddish-orange and brown halite with deposits of sylvite and langbeinite from which potassium salts are mined. The unit is bounded at the bottom by a thin anhydrite layer and at the top by a thin, silty sandstone unit called the Vaca Triste Sandstone.
>
> The upper unit is 136 to 161 m of reddish-orange to brown halite interbedded with polyhalite, anhydrite, and sandstone.

A structure map of the surface of the Salado Formation constructed using the data in Appendix B shows a series of low anticlines and shallow synclines with axes dipping southeastward (Figure II-9). In the northeastern part of the Study Area, the Salado Formation surface dips steeply northeastward. In the western part of the Study Area, the Salado Formation has an irregular surface caused by dissolution. Unlike the Castile Formation, the Salado Formation overlaps the Capitan Reef and is present outside of the reef area, extending eastward into West Texas and northward into the Texas Panhandle.

Rustler Formation

The Salado Formation is conformably overlain by the Rustler Formation, which is the youngest unit of the Ochoan evaporite series. The Rustler Formation is of particular interest because it includes hydrostratigraphic units that may provide potential pathways for radionuclides to the accessible environment.

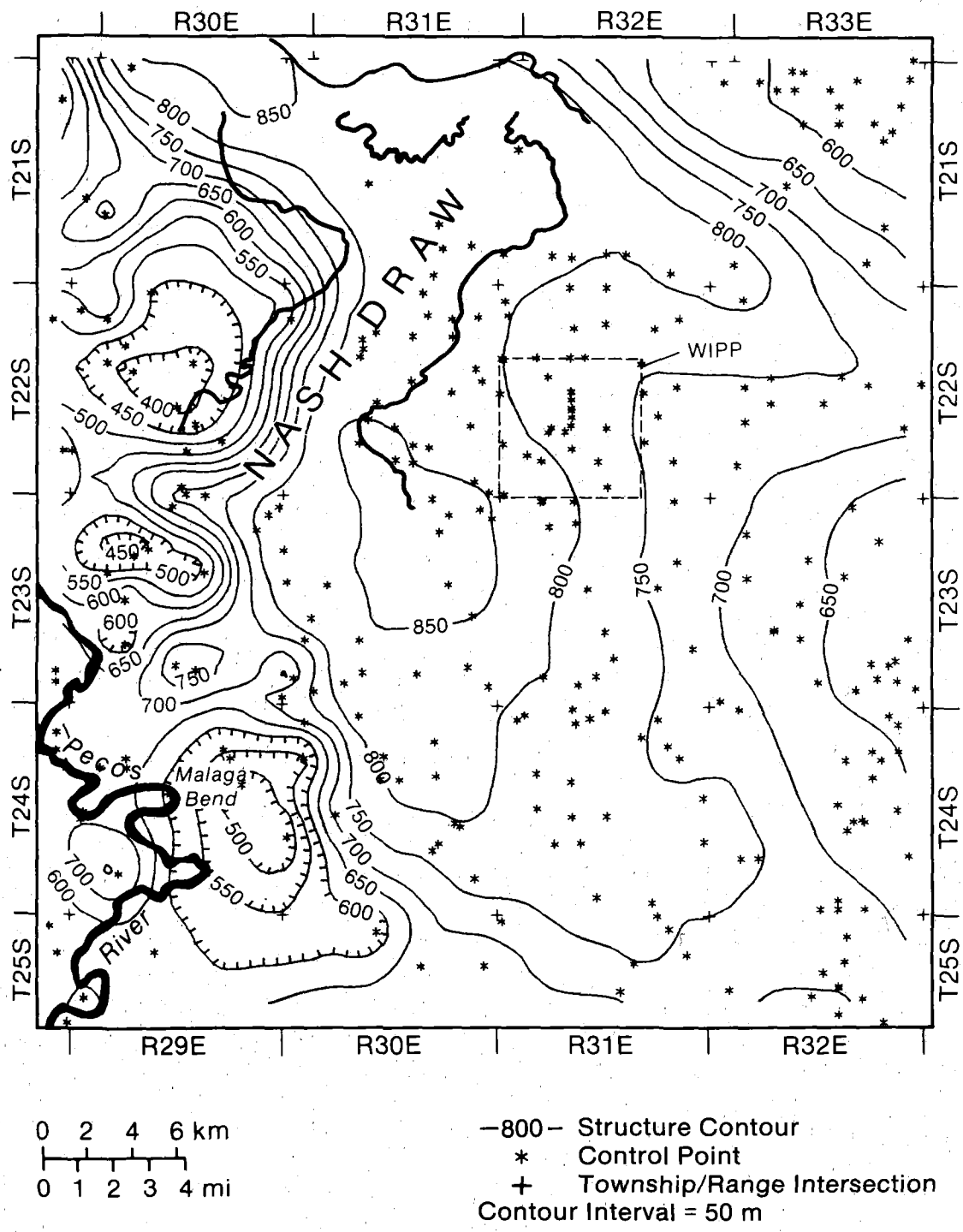

Figure II-9. Structure Contours on Top of the Salado Formation.

The Rustler Formation is composed of about 40 percent anhydrite (or gypsum), 30 percent halite, 20 percent siltstone and sandstone, and 10 percent anhydritic dolomite (Lambert, 1983). Vine's division (1963) of the Rustler Formation delineated four formally named members and a lower unnamed member (Figure II-10) on the basis of lithologies of units that crop out west of the WIPP along the eastern edge of Nash Draw. The five units described by Vine (1963) and Mercer (1983) are, in ascending order, as follows:

Unnamed lower member
Culebra Dolomite Member
Tamarisk Member
Magenta Dolomite Member
Forty-niner Member

A cross section from the Pecos River northeast of Loving, New Mexico, across Nash Draw to the east-northeast shows that the Rustler Formation is relatively flat under Nash Draw but then dips to the east until approximately over the repository (south of H-6), where it begins to rise (Figure II-11). The Rustler has a fairly uniform thickness, but the Dewey Lake Red Beds increase in thickness eastward. The presence of younger units is also noted as the section goes eastward. The low area to the left of WIPP-29 is just north of Laguna Grande de la Sal (Figure I-2).

The Rustler Formation in the Study Area ranges in thickness from 8.5 m where dissolution and erosion have occurred, to 216 m thick east of the WIPP and has a mean thickness of 109.4 m (Table II-2). The dolomitic members range from 3 to 13.7 m, and the non-dolomitic members range from about 3 to 162 m. Table II-2 shows a small standard deviation for the members, especially the Culebra and Magenta Dolomites, which indicates small spread or variability. (If the numbers are spread out, the standard deviation tends to be large.) The Rustler Formation has a normally distributed composite-thickness range

TABLE II-2. THICKNESSES (m) OF THE RUSTLER FORMATION AND EACH MEMBER

Name	Number of Wells	Min	Max	Mean	Standard Deviation
Rustler Formation	545	8.5	216.4	109.4	25.4
Forty-niner Member	513	5.5	35.1	19.8	3.3
Magenta Dolomite Member	513	3.0	11.2	6.5	1.2
Tamarisk Member	513	7.6	84.4	39.5	15.0
Culebra Dolomite Member	513	3.0	13.7	7.5	1.4
Unnamed lower member	513	2.8	162.1	39.1	11.7

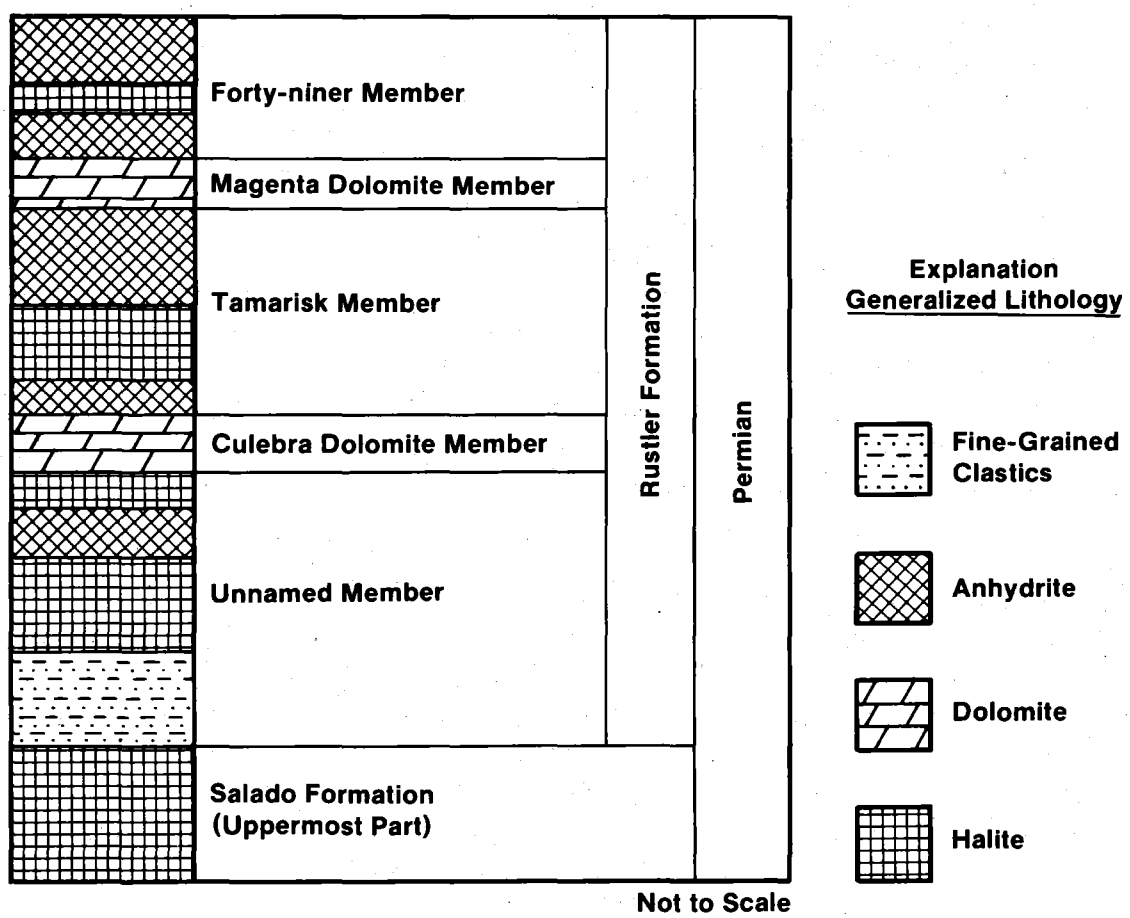

Figure II-10. General Stratigraphic Column Showing the Five Members of the Rustler Formation (Mercer, 1983).

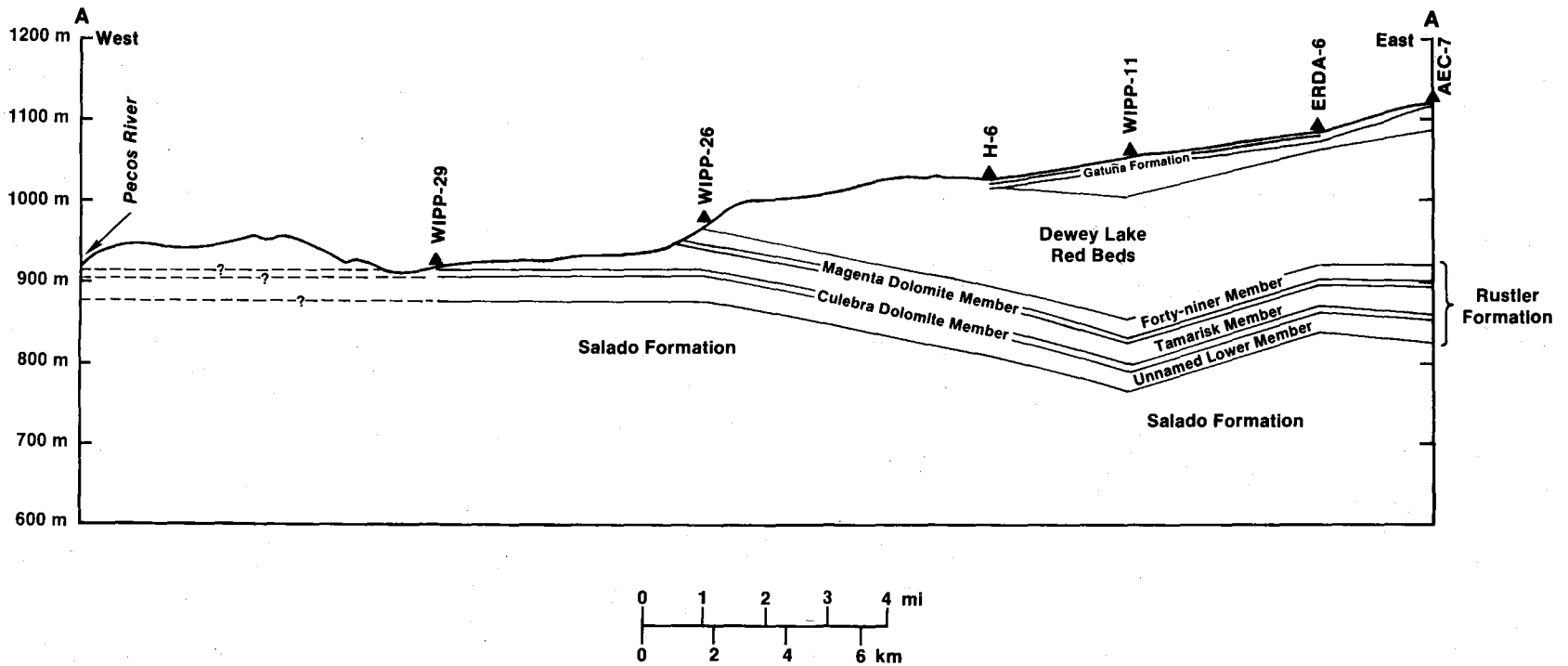

Figure II-11. Cross Section from A to A' of Figure I-2, Showing Rustler Formation Stratigraphy.

(Figure II-12a). Knowing that a sample distribution is normally distributed allows a more exact probability distribution function for a variable, which is useful in performance assessment modeling (see Chapter VI). Also, comparison of the composite thickness of the Rustler to the Rustler thickness in individual wells may be useful in determining the areal distribution of halite or degree of dissolution. All the Rustler Formation members are present over the WIPP.

Dissolution of the evaporites in the nondolomitic members caused collapse features in Nash Draw, resulting in exposures of Dewey Lake Red Beds and of the upper four Rustler Formation members. Figure II-13 is a generalized geologic map of the Nash Draw area with the overburden stripped away. The map was drawn from well data and a geologic map of the Nash Draw Quadrangle by Vine (1963). Figure II-14 is a cross section parallel to the axis of the draw with the surface topography included, which gives a sense of the layered aspect of the rocks.

The unnamed lower member has a mean thickness of about 40 m and is about 36 m thick at the WIPP (Table II-2). A histogram of the frequency of thickness shows a normal distribution with a cluster around 40 m (Figure II-12b). An isopach map of the unit shows a fairly uniform thickness across the Study Area, with a slight thickening to the east (Figure II-15). This thickening can also be seen in a cross section of the Study Area (Figure II-11). The unnamed lower member is composed mostly of fine-grained, silty sandstones and siltstones interbedded with anhydrite (gypsum at Nash Draw) in the western part of the Study Area but becomes thicker with increasing amounts of halite in the eastern part of the Study Area (Vine, 1963; Mercer, 1983).

The presence of the halite is somewhat correlative to a decrease in hydraulic conductivity of the member in the eastern part of the Study Area and is discussed in Appendix A. Halite in the unnamed lower member extends farthest westward over the WIPP but is absent north and south of the WIPP at a topographic low, the so-called "Nash Draw Reentrant" (Figure II-16) (Beauheim, 1987b). Halite is present in the other two clastic units above the lower member but does not extend as far west over the WIPP (Snyder, 1985).

A structure contour map of the unnamed lower member, which is very close to the surface in the southwestern part of the Study Area (Figure II-17), is similar to the Salado Formation structure map (Figure II-9). The southeast-plunging anticline north of the WIPP shown on the Salado Formation structure contour map is also present in the unnamed unit.

A dissolution residuum at the base of the unnamed lower member resulted from dissolution of the upper Salado Formation or the upper Salado and lower

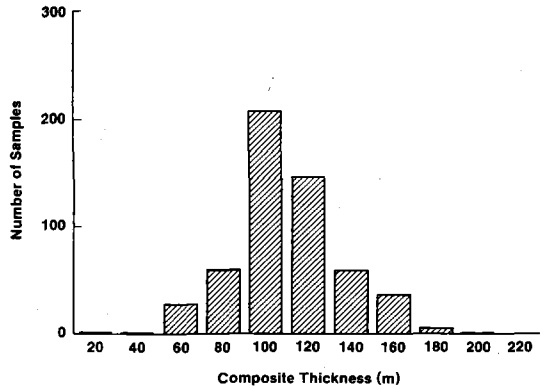

a. Rustler Formation

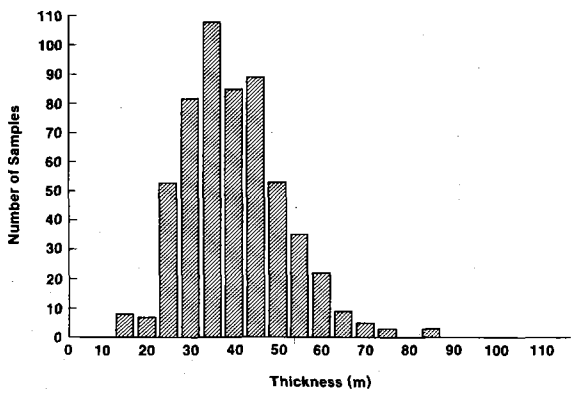

b. Unnamed Lower Member

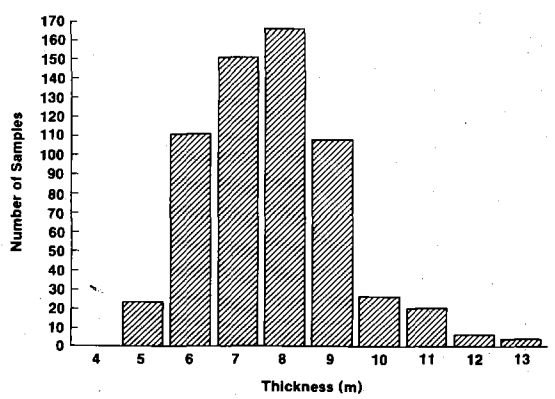

c. Culebra Dolomite Member

TRI-6342-137-0

Figure II-12. Histograms Showing Thicknesses of the Rustler Formation and the Unnamed Lower and Culebra Dolomite Members.

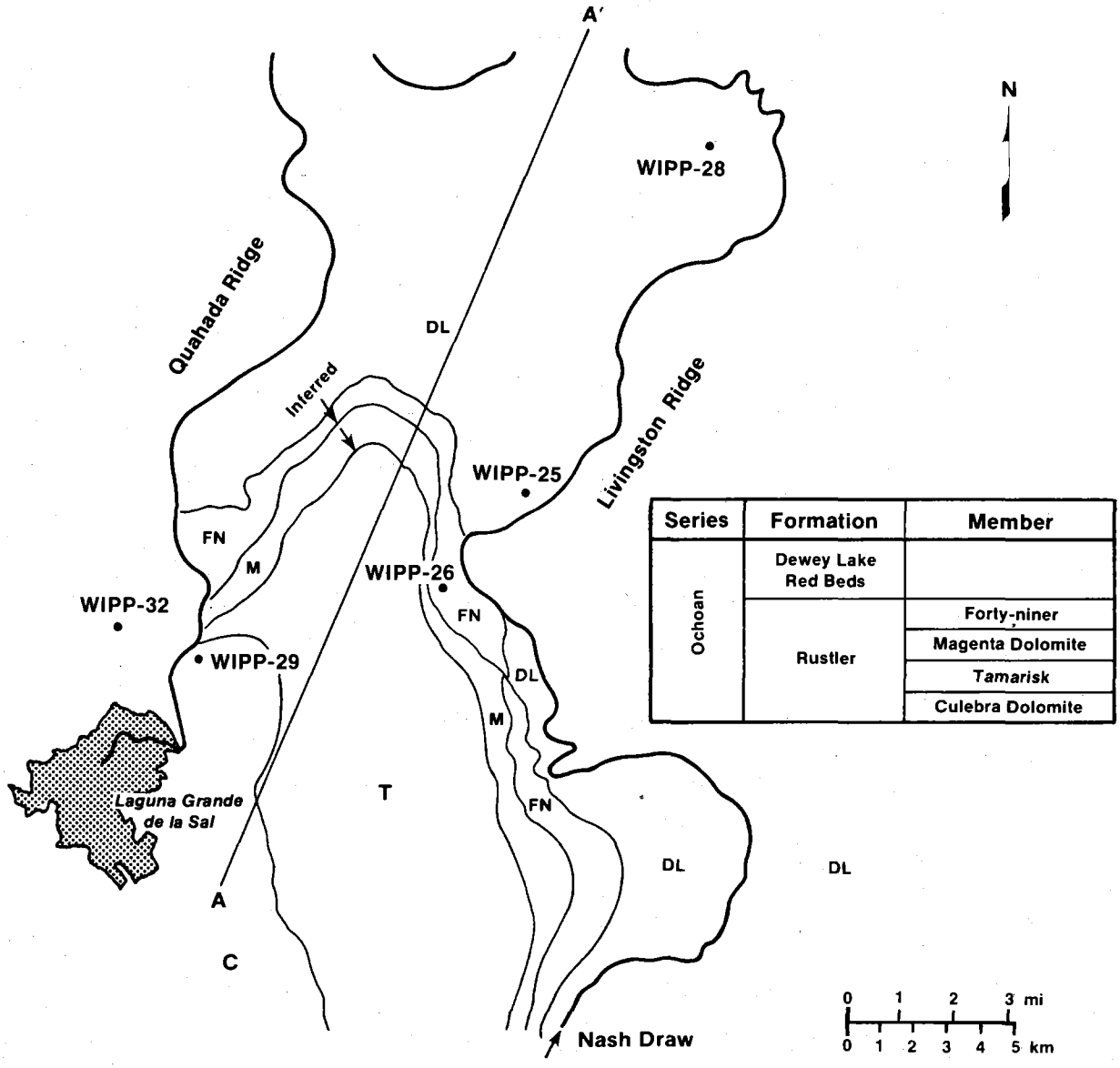

Figure II-13. Generalized Geologic Map of Nash Draw with Overburden Removed (geology from 7½' Quadrangle [Vine, 1963]).

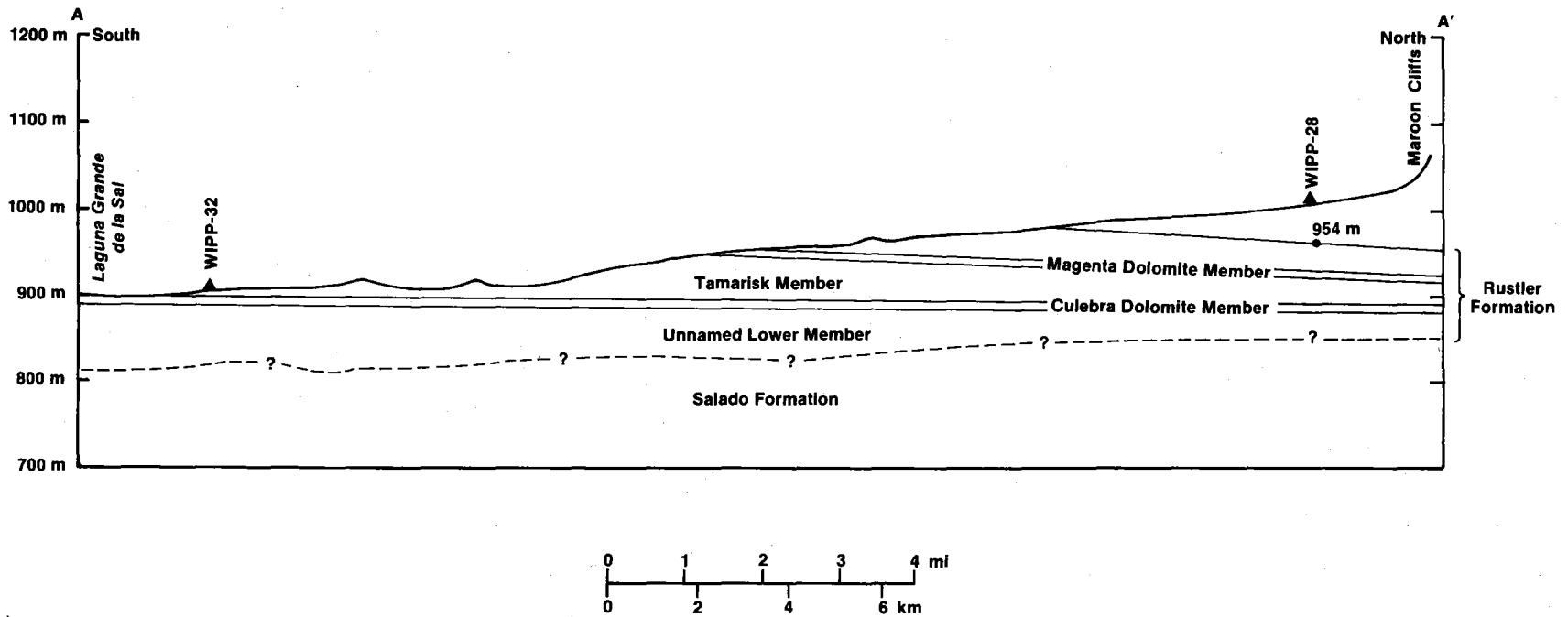

Figure II-14. Longitudinal Cross Section along Nash Draw from A to A' of Figure II-13 (geology from 7½' Quadrangle [Vine, 1963]).

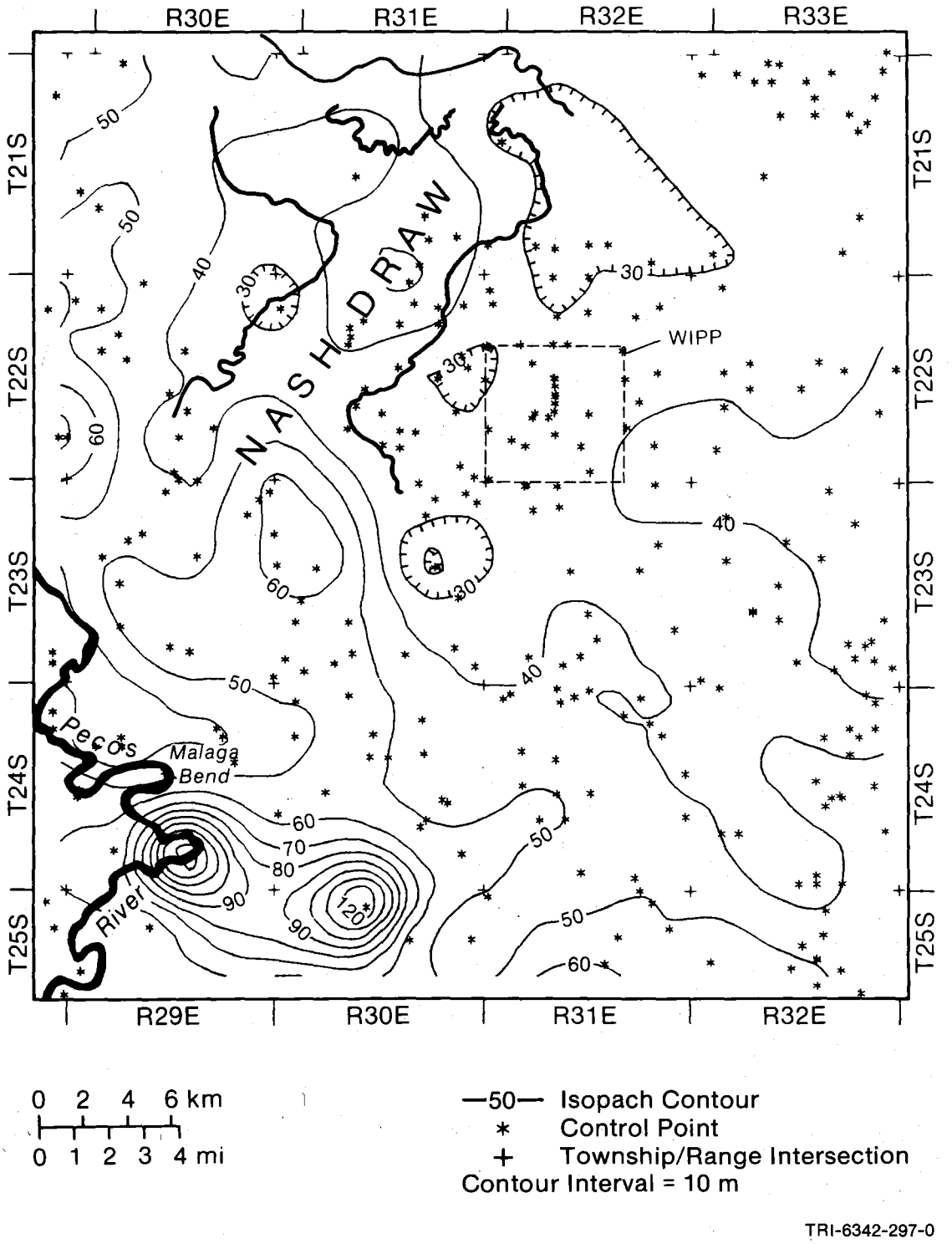

Figure II-15. Isopach Map of the Unnamed Lower Member.

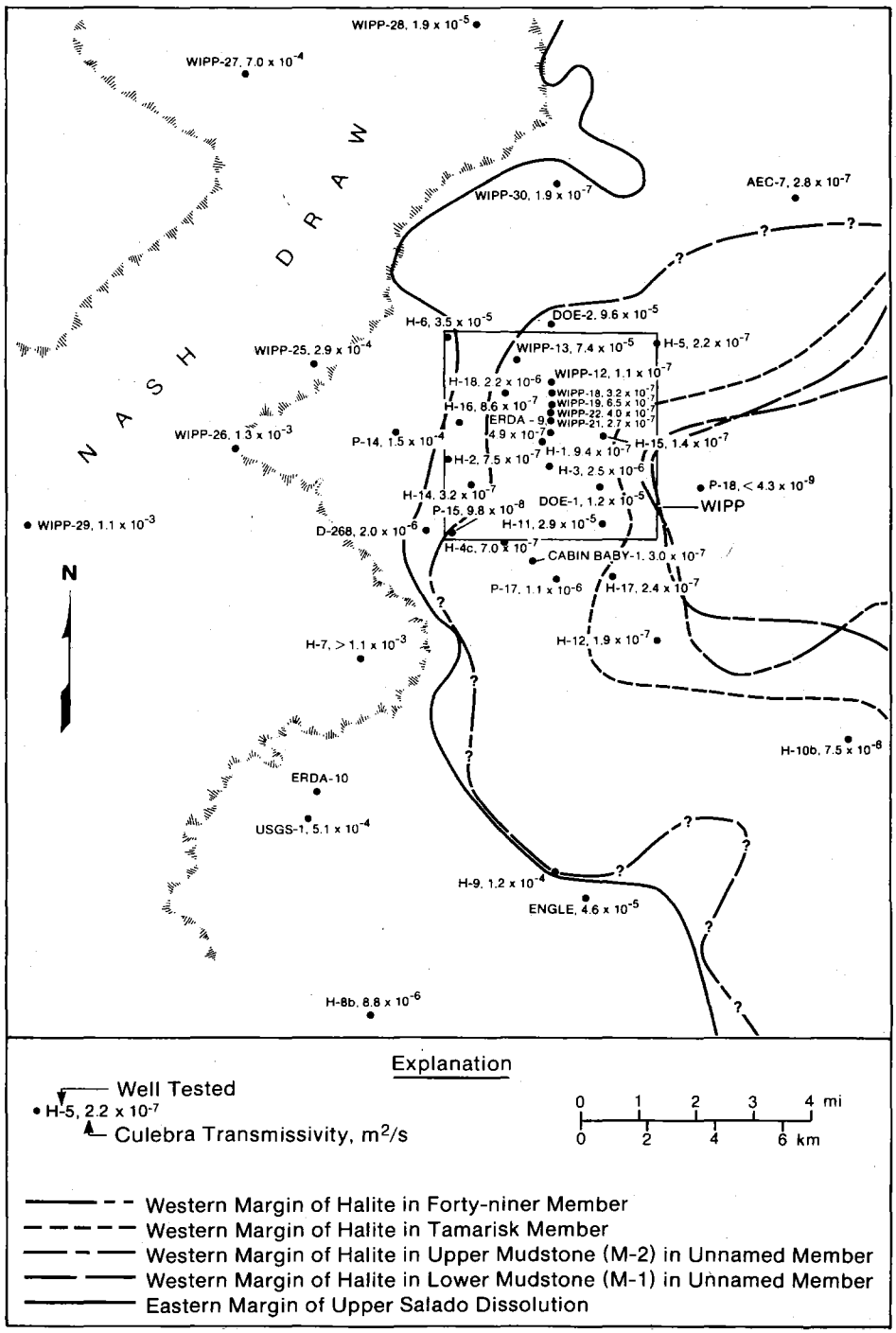

TRI-6330-94-2

Figure II-16. Distribution of Halite in the Rustler Formation (Beauheim, 1987b).

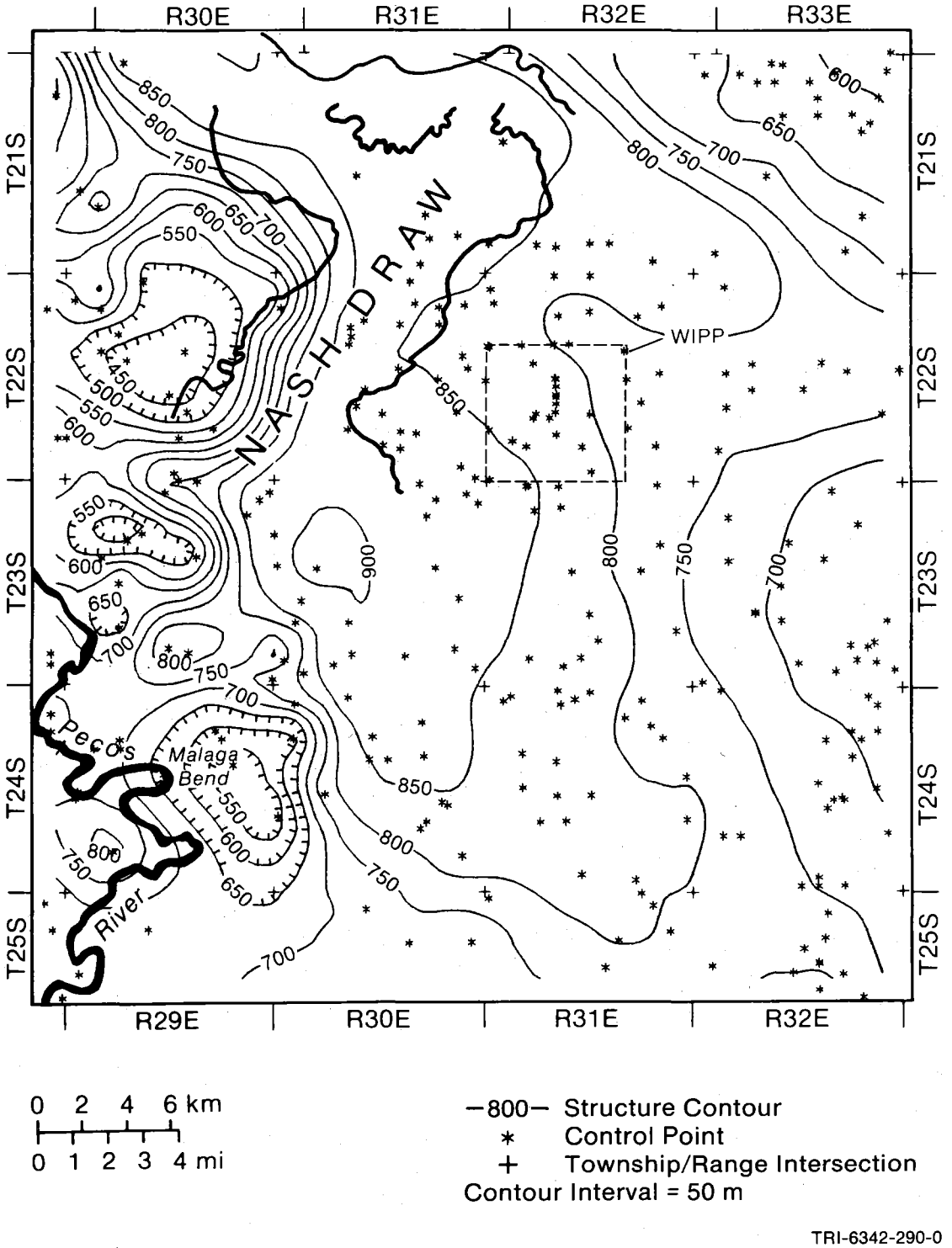

Figure II-17. Structure Contours on Top of the Unnamed Lower Member.

unnamed member. In the vicinity of Nash Draw, the residuum is an unstructured, distinctive gray residue of gypsum, clay, and sandstone that grades eastward and intertongues with the clayey halite of the unnamed lower member. The dissolution was demonstrated by Mercer (1983) to have been post-Rustler on the basis of the brecciation present. In the vicinity of the WIPP, the residuum was observed in the shafts and shows evidence of channeling and filling, fossils, and bioturbation. This would indicate the dissolution occurred before Rustler deposition by water that was fresher than the lagoonal water that formed the Salado (Holt and Powers, 1988). This residuum ranges in thickness from 3 m to about 20 m and averages about 8 m in the vicinity of Nash Draw (Mercer, 1983).

The Culebra Dolomite Member of the Rustler Formation is microcrystalline grayish dolomite or dolomitic limestone with solution cavities (Vine, 1963) containing some gypsum and anhydrite filling (Holt and Powers, 1988). The Culebra Dolomite, where present, ranges in thickness from 3 to 13.7 m and has a mean thickness of about 7.5 m (Table II-2). A histogram of the frequency of thickness in the Culebra Dolomite shows a normal distribution with a cluster around 8 m (Figure II-12c). An isopach map of the Culebra Dolomite (Figure II-18) shows a nearly uniform thickness throughout the Study Area. The Culebra Dolomite dips gently to the southeast with a gradient of 0.01 (about 0.50) south of the WIPP and relatively steeply to the northeast with a gradient of 0.03 (about 1.70) north of the WIPP (Figure II-19). In the western and southwestern parts of the Study Area, the Culebra Dolomite thickness is erratic because of extensive weathering and removal of evaporites. Outcrops of the Culebra Dolomite occur in the southern part of Nash Draw north of Laguna Grande de la Sal and along the Pecos River.

A structure contour map of the top of the Culebra Dolomite Member shows a shallow syncline at the northeast corner of the WIPP, with an associated anticline farther to the northeast (Figure II-19). Southwest of the WIPP between wells H-8 and H-9 is a small anticline with an amplitude of about 40 m.

The Tamarisk Member, where present, ranges in thickness from 8 to 84 m in southeast New Mexico, with a mean thickness of 39.5 m in the Study Area, and is about 36 m thick at the WIPP (Table II-2). The Tamarisk Member consists of mostly anhydrite interbedded with thin layers of claystone and siltstone. Halite is also present just east of the WIPP (Figure II-16) where the Rustler is intact. The member crops out along the southwestern side of Nash Draw. An isopach map (Figure II-20) of the member reveals a thickening in the east-central, southeastern, and southwestern parts of the Study Area and to the west of Nash Draw. A histogram (Figure II-21a) of the frequency of thickness shows a cluster below the mean; a calculation of the mean shows a large

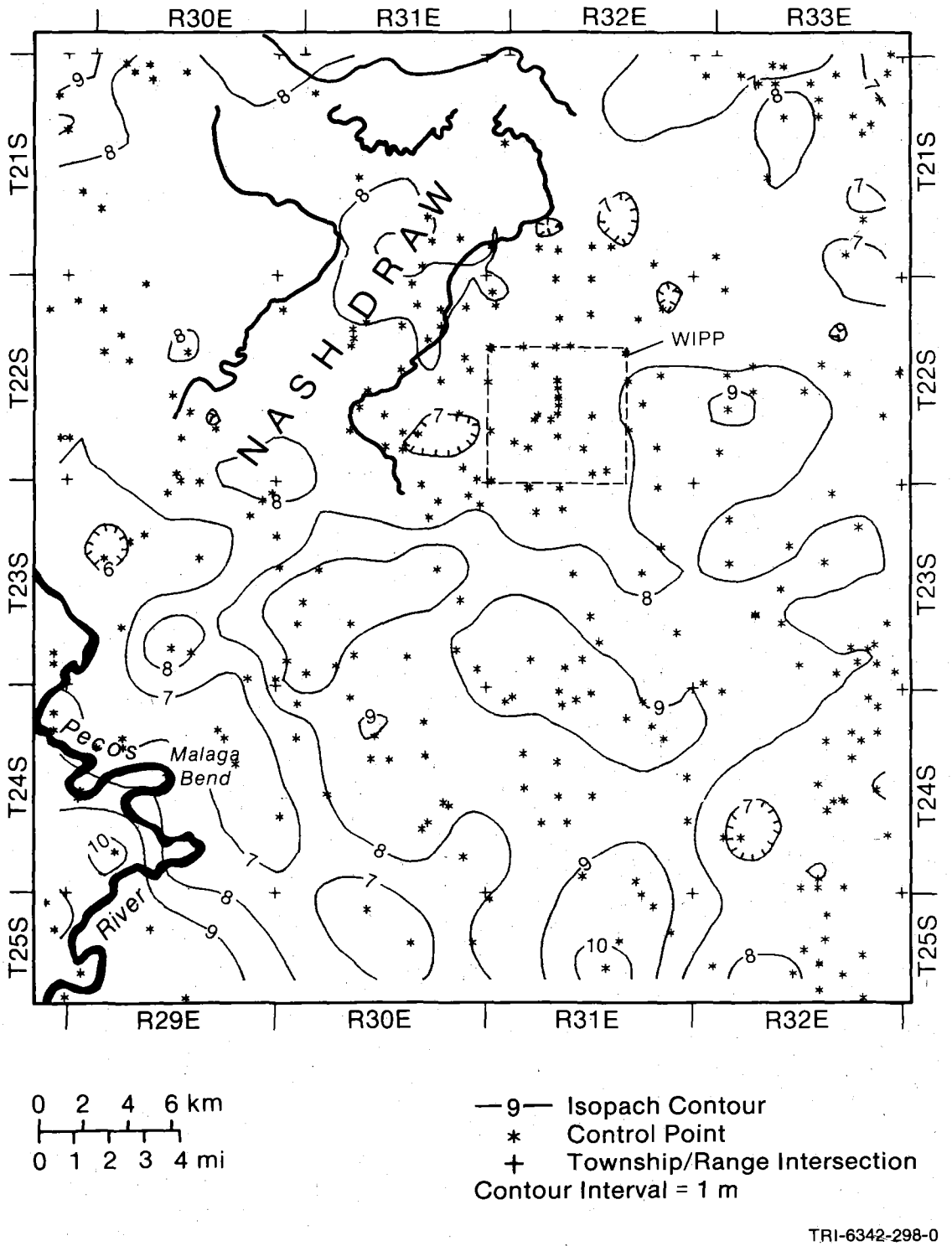

Figure II-18. Isopach Map of the Culebra Dolomite Member.

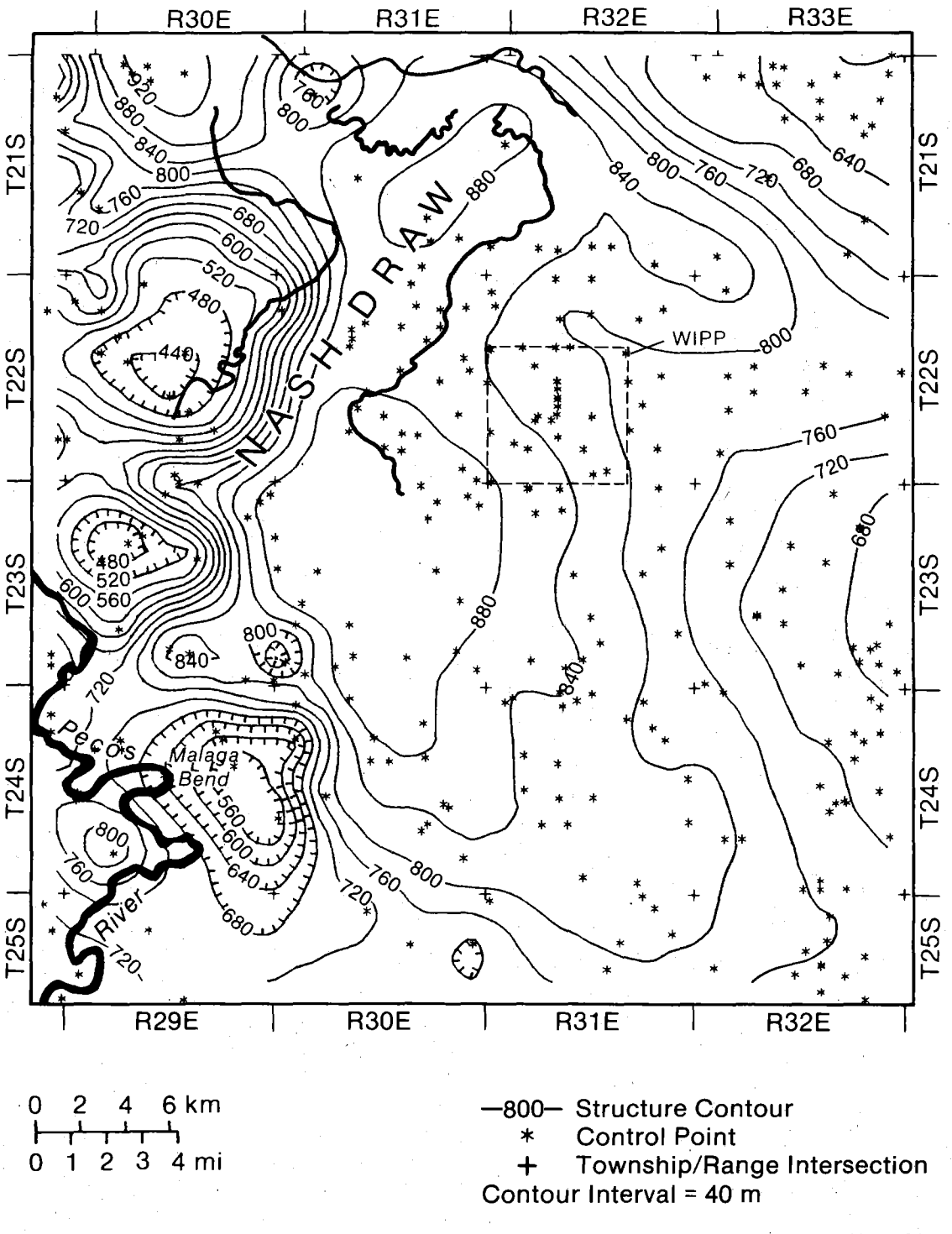

Figure II-19. Structure Contours on Top of the Culebra Dolomite Member.

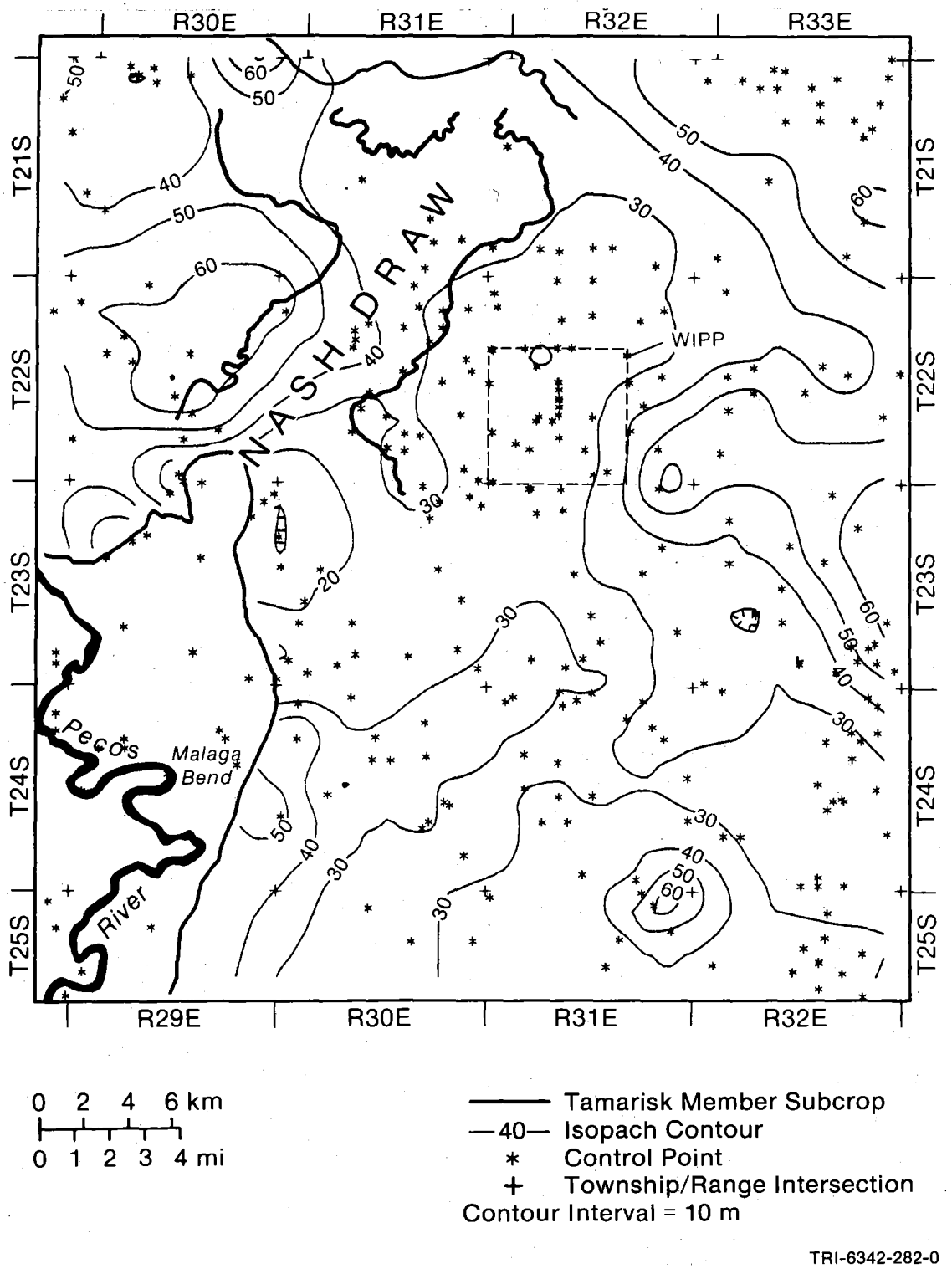

Figure II-20. Isopach Map of the Tamarisk Member.

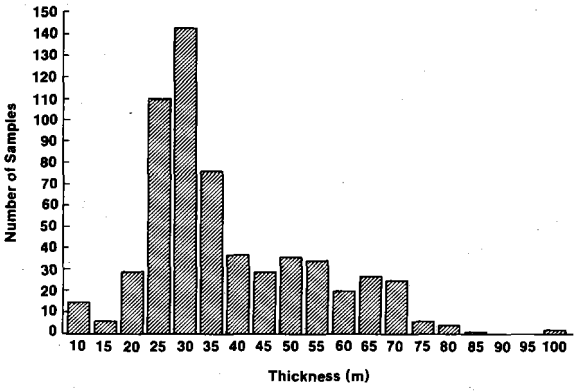

a. Tamarisk Member

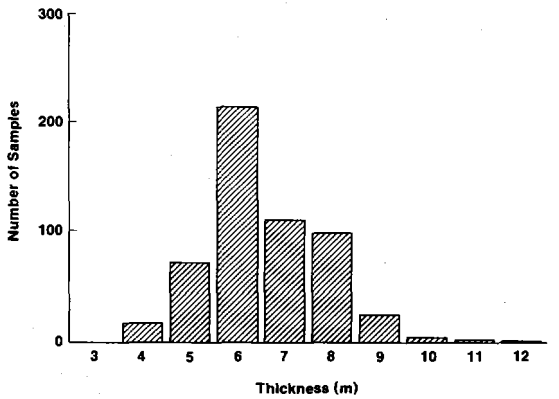

b. Magenta Dolomite Member

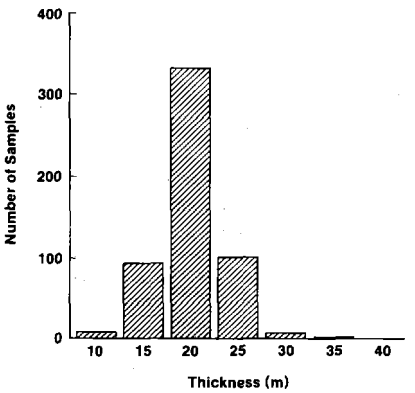

c. Forty-niner Member

TRI-6342-139-0

Figure II-21. Histograms Showing Thicknesses of the Tamarisk, Magenta Dolomite, and Forty-niner Members.

standard deviation, which indicates a large variability in thickness that could be the result of extensive dissolution of the Tamarisk evaporites near Nash Draw. East of the WIPP, the Tamarisk increases in thickness, which corresponds to the presence of halite (Figure 5 in Mercer, 1983). The structure contour map of the surface of the Tamarisk Member (Figure II-22) is consistent with the unnamed lower member and Culebra Dolomite Member structure contour maps (Figures II-17 and II-19), which show a series of associated parallel anticlines and synclines in the northeast portion of the Study Area with axes oriented northwest to southeast.

The Magenta Dolomite Member of the Rustler Formation is a very fine-grained, greenish-gray dolomite with reddish-purple layers and ranges in thickness from 3 to 11 m, with a mean thickness of 6 m (Table II-2). The Magenta Dolomite is about 6.5 m thick at the WIPP. A histogram indicates a small variability in thickness (Figure II-21b), with a normal distribution of the available data. An isopach map (Figure II-23) of the WIPP area reveals a slight thickening in the central part of the Study Area and a thinning to the southeast and east. The Magenta Dolomite crops out along most of southern Nash Draw and has structural features similar to those of the underlying units (Figure II-24).

The uppermost member of the Rustler Formation, the Forty-niner Member, consists of anhydrite interbedded with a layer of siltstone, with halite present in the eastern part of the Study Area. The unit ranges in thickness from 5.5 to 35 m and has a mean thickness of 20 m (Figure II-21c). At the WIPP, the unit is about 20 m thick. An isopach map (Figure II-25) of the unit indicates a relatively uniform thickening east of the WIPP across the Study Area. The structure is consistent with the lower units (Figure II-26).

Dewey Lake Red Beds

Present in the Study Area are several rock units younger than the Ochoan Rustler Formation. These units may not be of hydrologic importance because they are not extensive aquifers, and some units are unsaturated throughout most of the Study Area. Overlying the Rustler Formation are the youngest Ochoan rocks, the Dewey Lake Red Beds. Although the contact has been described as an unconformity with a slight discordance (Jones, 1975), the more common interpretation is that the rocks lie conformably on the Rustler Formation (Bachman, 1987; Vine, 1963). The Dewey Lake Red Beds (Pierce Canyon Red Beds of Vine, 1963) consist of alternating layers of reddish-brown, fine-grained sandstones and siltstones cemented with calcite and gypsum. Bedding may be structureless, or cross-bedding, ripple marks, and mud cracks may be present. In the Study Area, the Dewey Lake Red Beds are absent in Nash Draw but range up to about 60 m thick west of Nash Draw and to over 200 m thick east of the WIPP (Figure II-27). Also, east of the WIPP the unit has a nearly

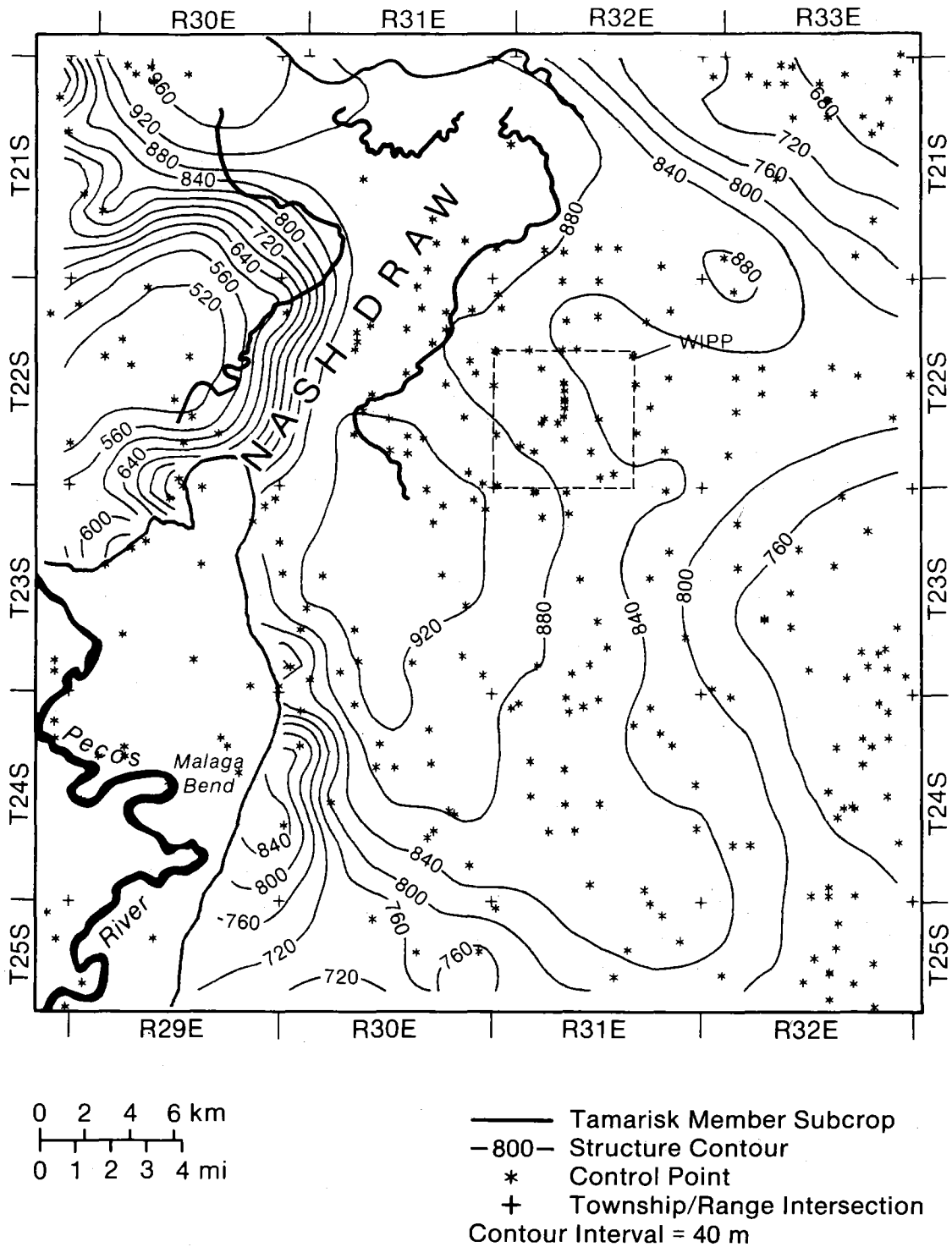

Figure II-22. Structure Contours on Top of the Tamarisk Member.

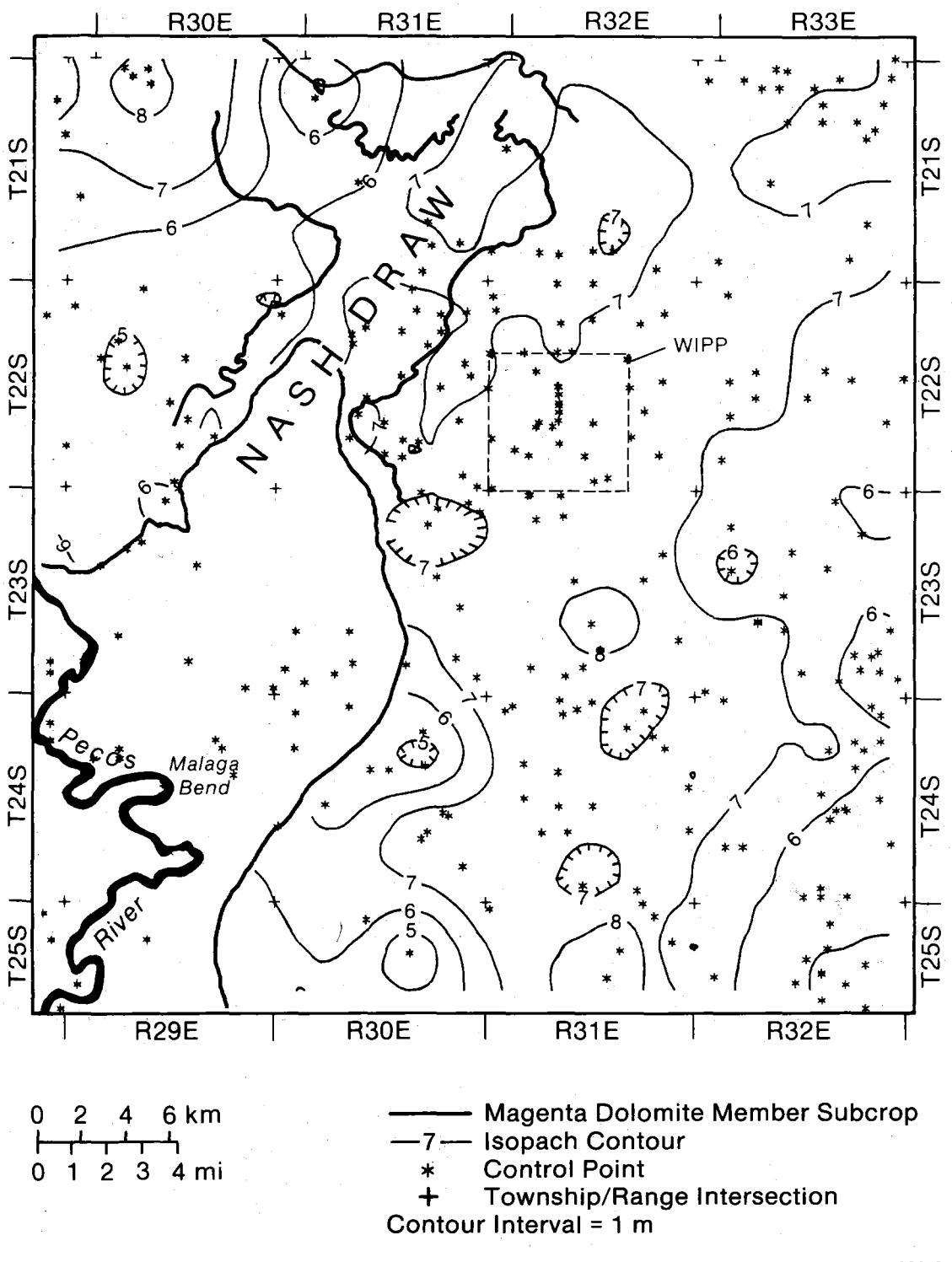

Figure II-23. Isopach Map of the Magenta Member.

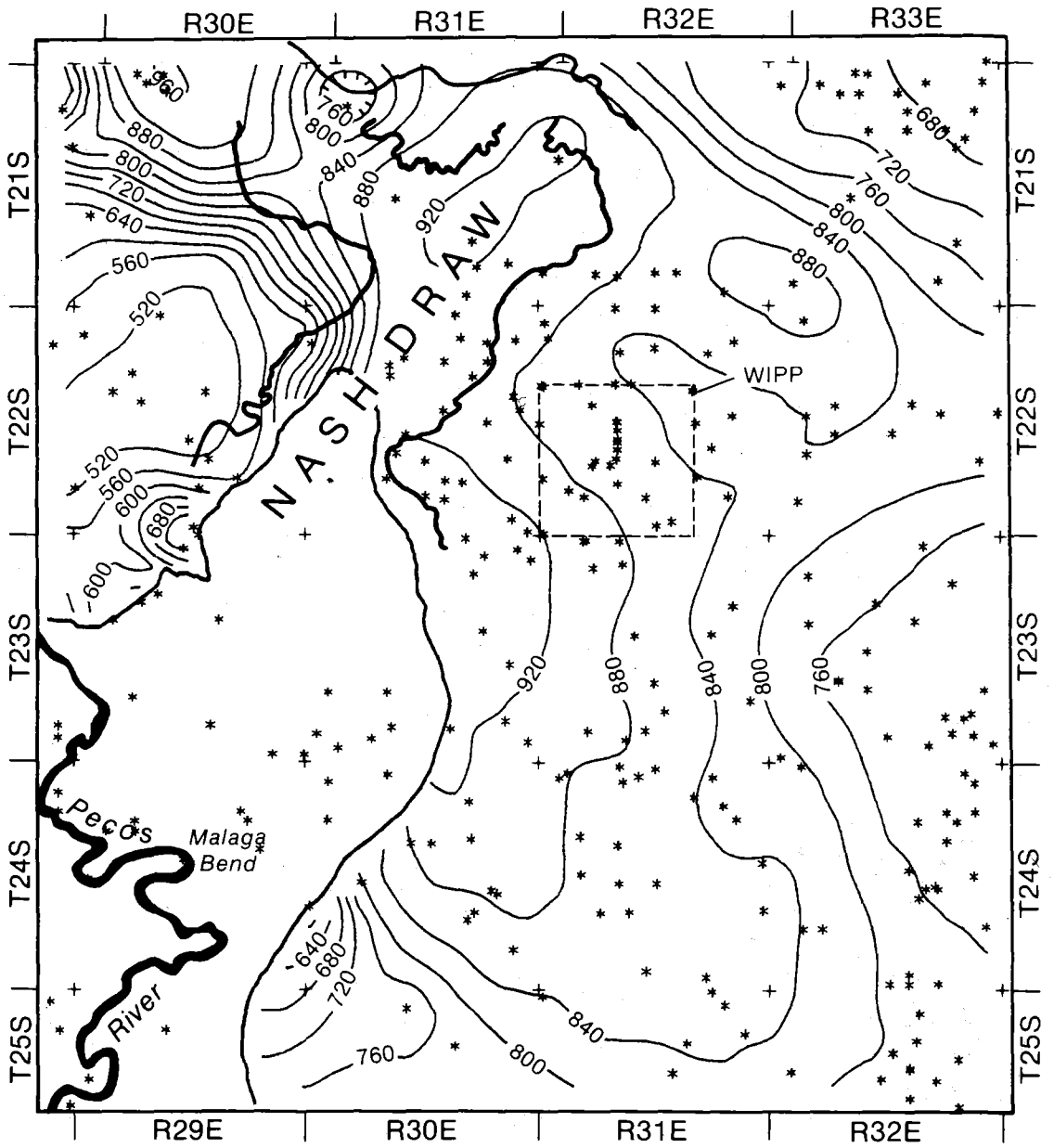

Figure II-24. Structure Contours on Top of the Magenta Member.

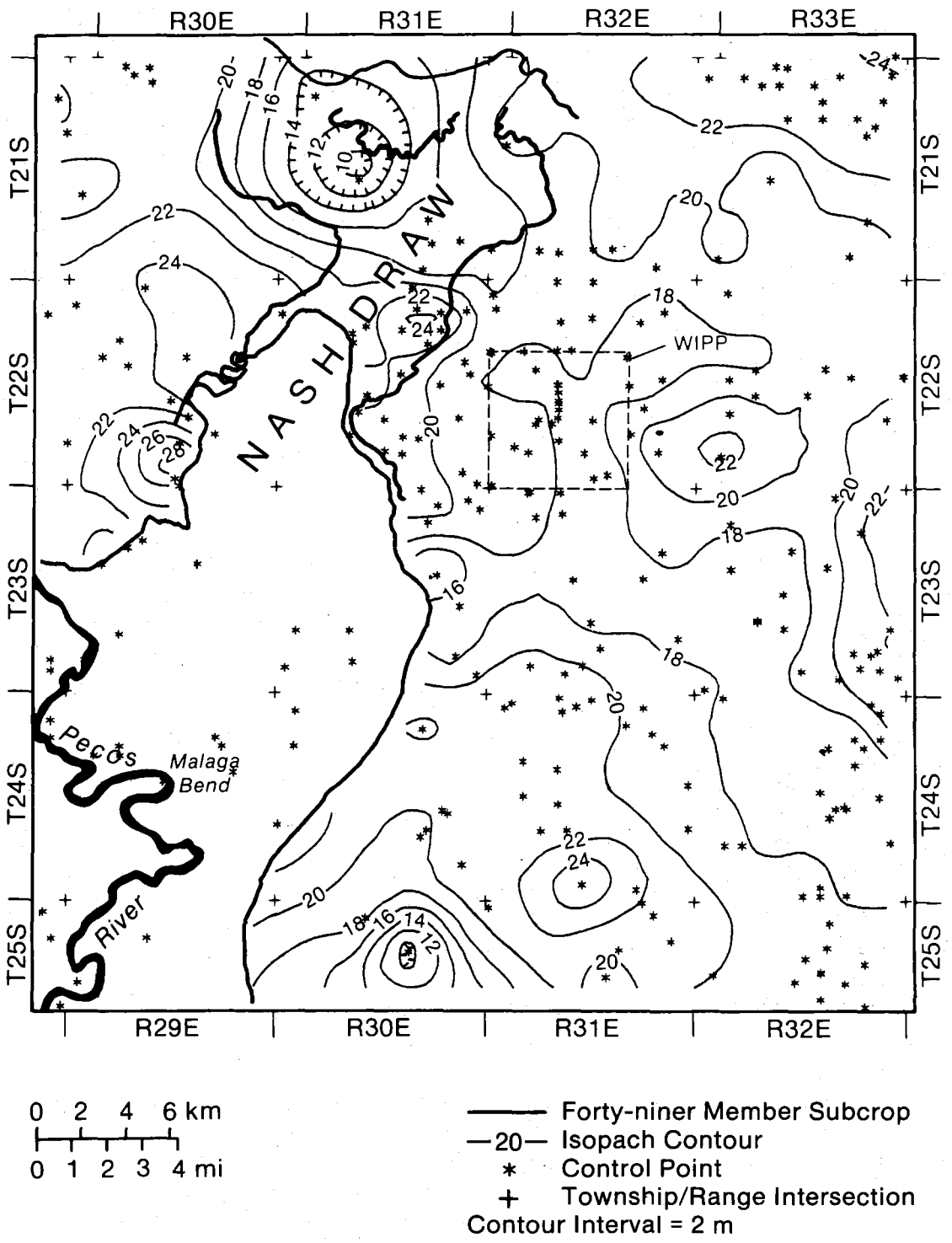

Figure II-25. Isopach Map of the Forty-niner Member.

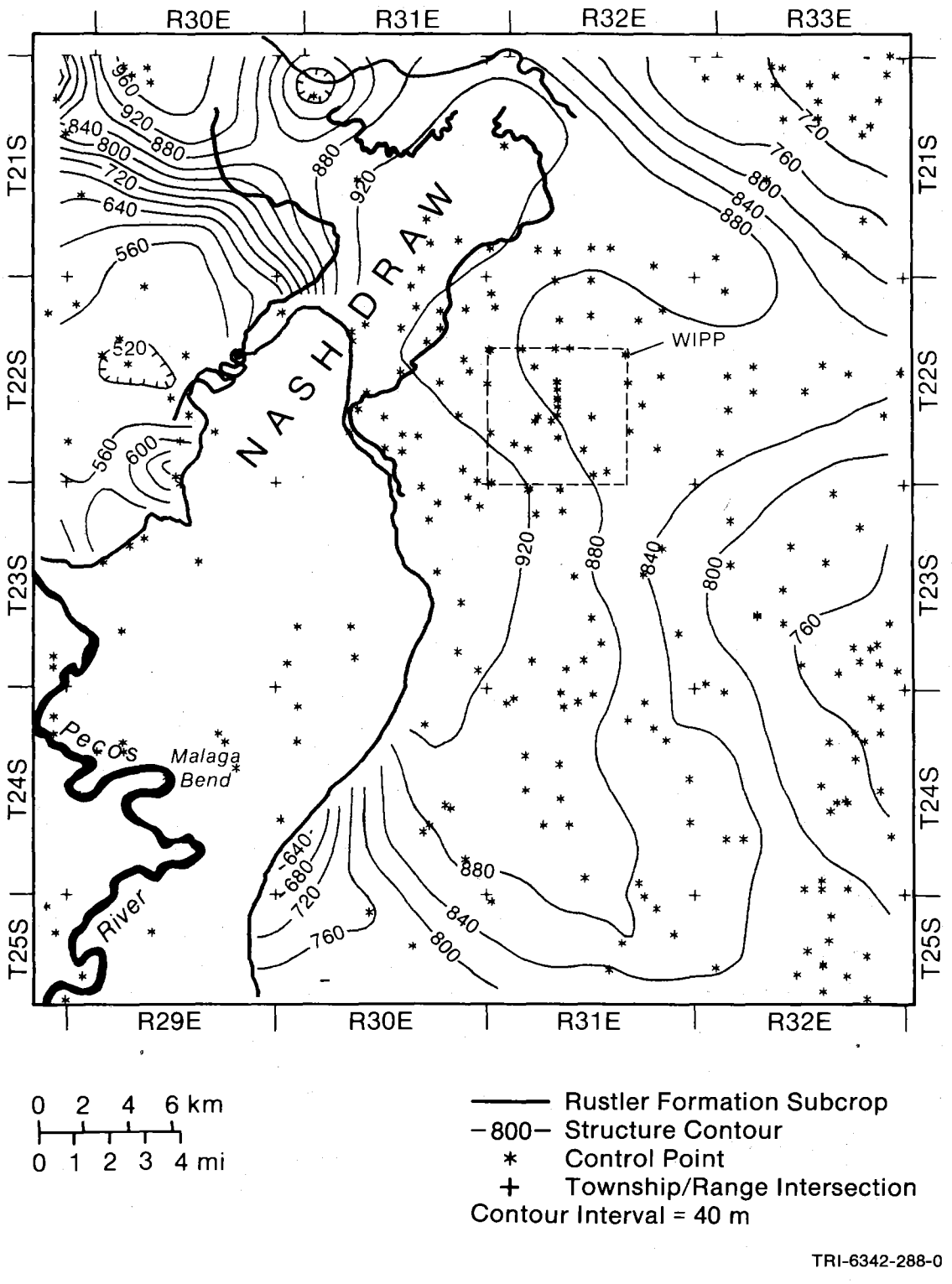

Figure II-26. Structure Contours on Top of the Forty-niner Member.

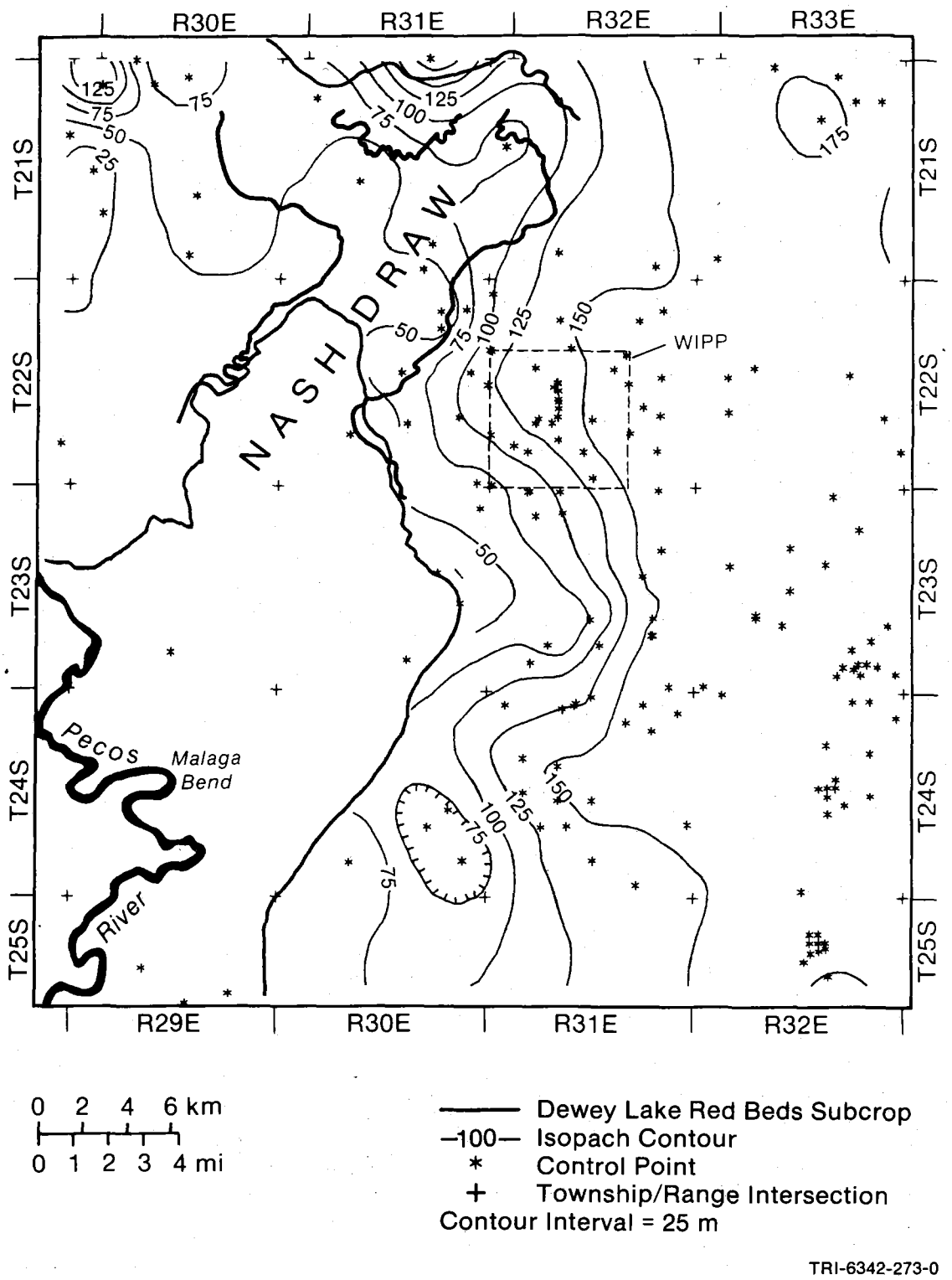

Figure II-27. Isopach Map of the Dewey Lake Red Beds.

uniform thickness (about 150 m). Structure contours of the surface of the Dewey Lake Red Beds show it to be relatively flat except to the northeast and southeast, where the unit dips sharply (Figure II-28).

Stratigraphy of the Mesozoic Rocks

The Dewey Lake Red Beds are unconformably overlain by Mesozoic rocks of the Triassic called, in this report, the undifferentiated Dockum Group (Figure II-29). In a paper describing geological conditions during Dockum time, McGowan and others (1979) showed how the arid conditions of the late Permian gradually gave way to more humid conditions in early Triassic time. Braided stream deposits, alluvial fans, deltas, and lake deposits present in the lower Dockum rocks of southeastern New Mexico and West Texas record this change. The Triassic rocks in southeastern New Mexico have been identified as the Chinle Formation and the Santa Rosa Formation (Mercer, 1983), which are names extended from the Four Corners area in northwestern New Mexico (Chinle Formation) and the Santa Rosa area in east central New Mexico. As pointed out by Bachman (1980), this terminology is probably not correct because of "intricate facies changes and interfingering of lithologic" units over the area. The Dockum Group crops out in the Study Area in the Maroon Cliffs area where Clayton Basin joins Nash Draw and in the Laguna Plata area northeast of the draw (Figure I-2) (Bachman, 1980; Vine, 1963; and a personal communication with G. O. Bachman in 1989). Figure II-30 is an isopach map of the lower Dockum Group constructed by subtracting the total thickness of the Dewey Lake Red Beds, the Cenozoic rocks, and alluvium from the total thickness of the post-Rustler rocks (Figure II-31). Where present, the lower Dockum is reported to range from 23 m at Nash Draw to more than 460 m in Lea County, New Mexico (Bachman, 1980; McGowan and others, 1979). A comparison of the lower Dockum with the Dewey Lake Red Beds (Bachman, 1980, Table 2) showed that whereas the Dewey Lake is made of well-sorted, well-rounded, fine-grained, evenly bedded quartz sand, the lower Dockum is composed of poorly sorted, angular, coarse-grained to conglomeratic, thickly bedded material interfingering with shales.

A major unconformity exists between the Triassic lower Dockum and the Cenozoic rocks in the Study Area. No rocks represent Jurassic or Cretaceous time east of the Pecos River. Either the rocks were never deposited or were eroded before Cenozoic rocks were deposited. Some Cretaceous outliers were reported west of the Pecos River, and some Cretaceous detritus were noted in sinks in the Castile Formation near White's City in Eddy County (Bachman, 1980).

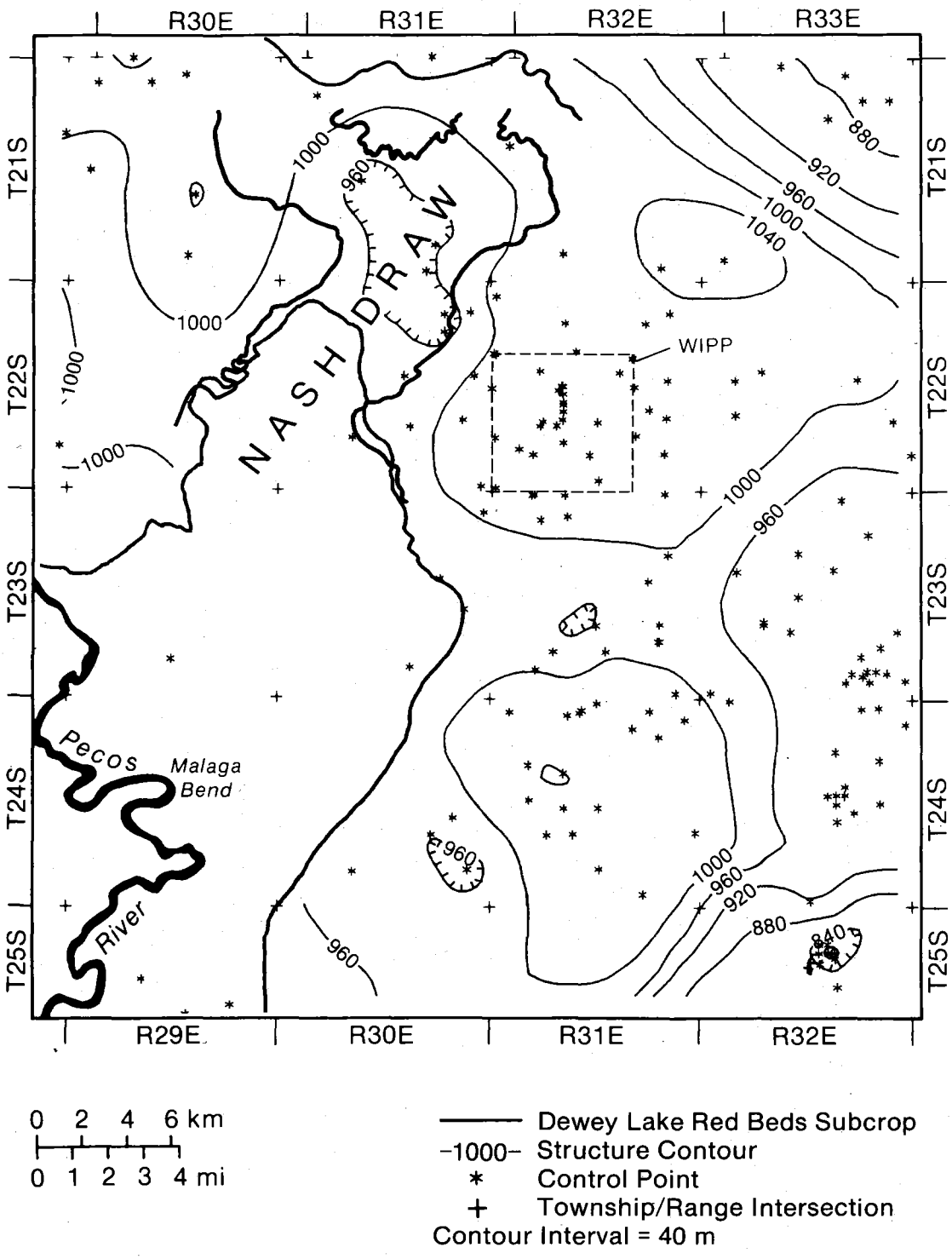

Figure II-28. Structure Contours on Top of the Dewey Lake Red Beds.

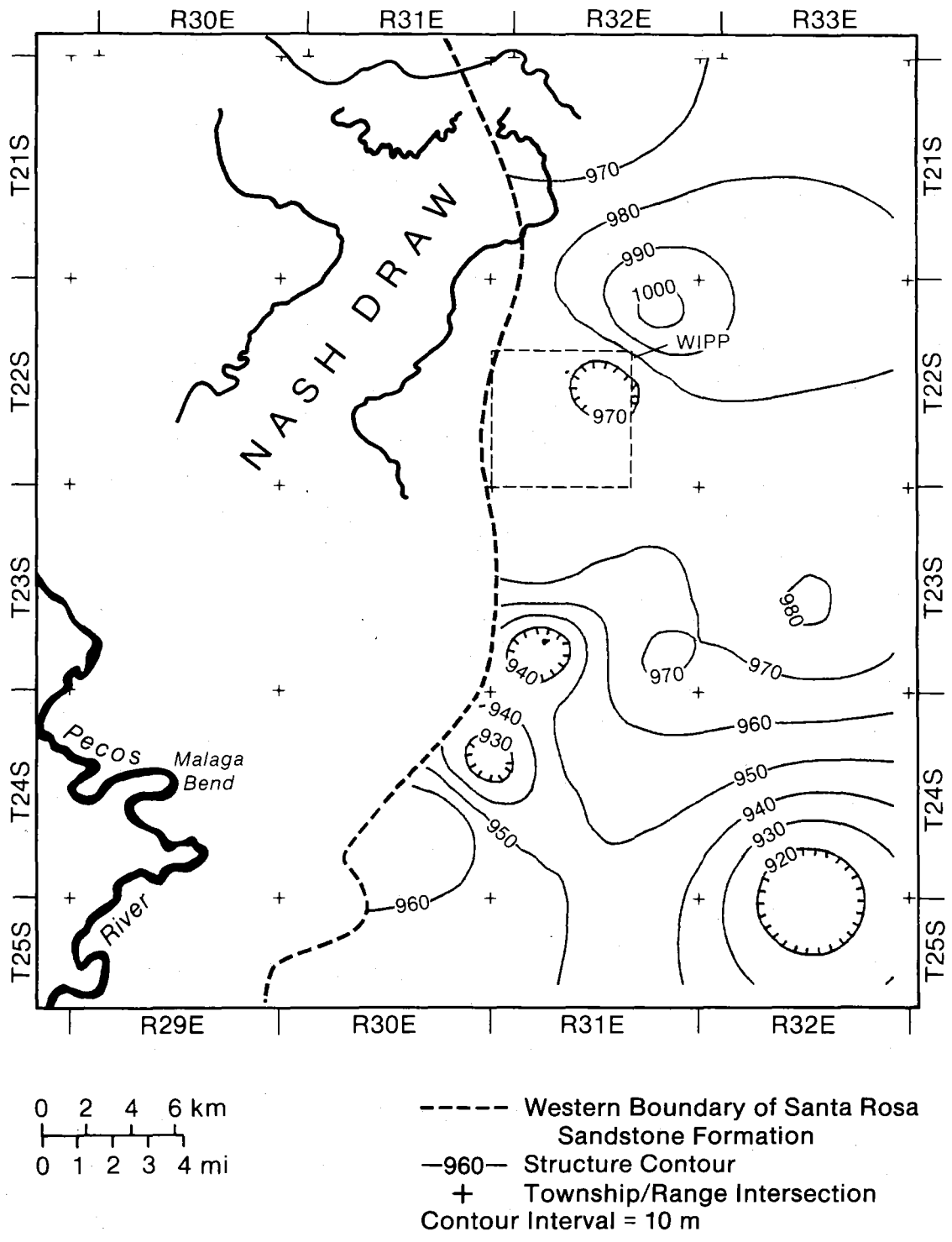

Figure II-29. Structure Contours on Top of Lower Dockum Group (modified from Cooper and Glanzman, 1971).

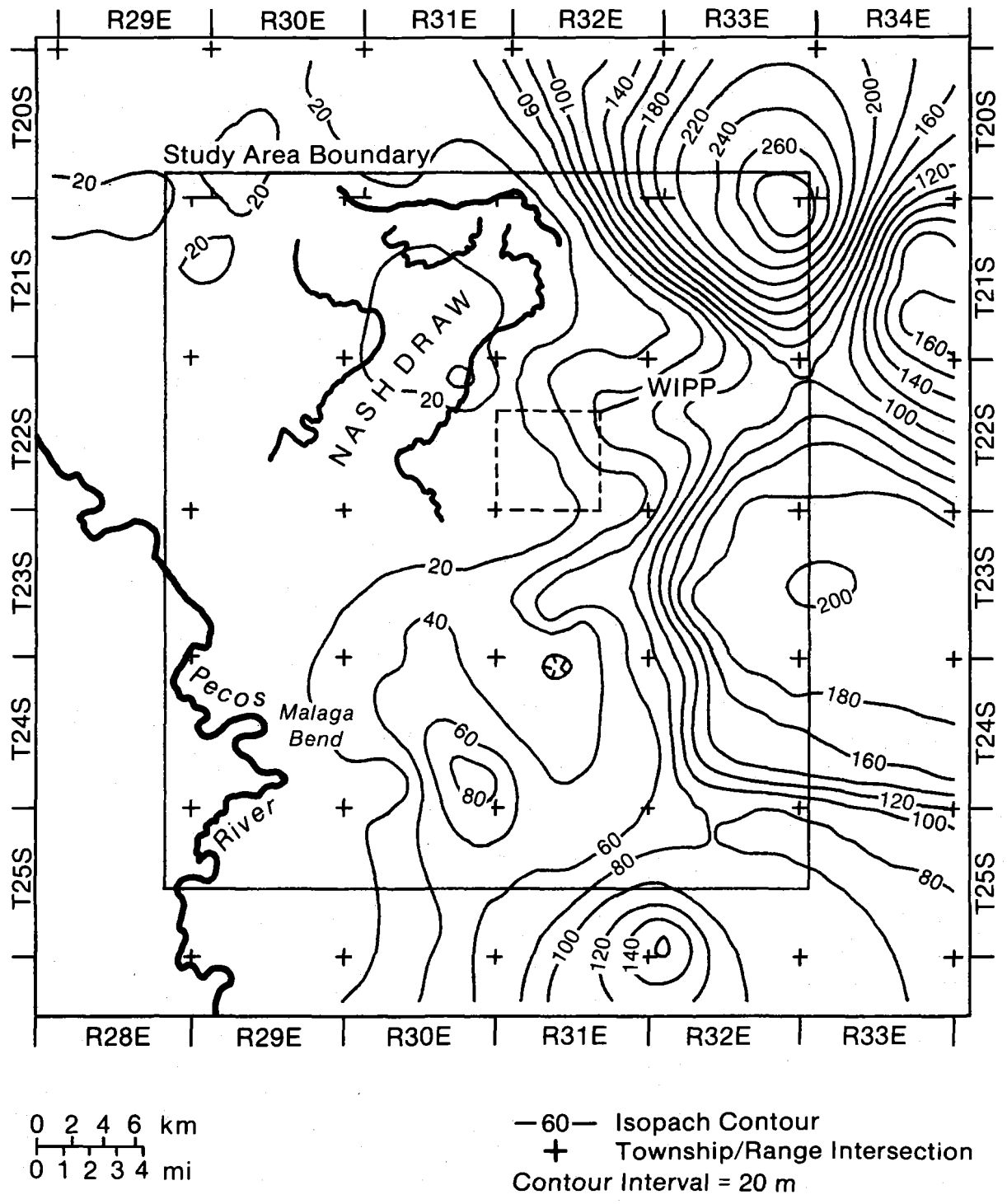

Figure II-30. Isopach Map of Lower Dockum Group in the Study Area.

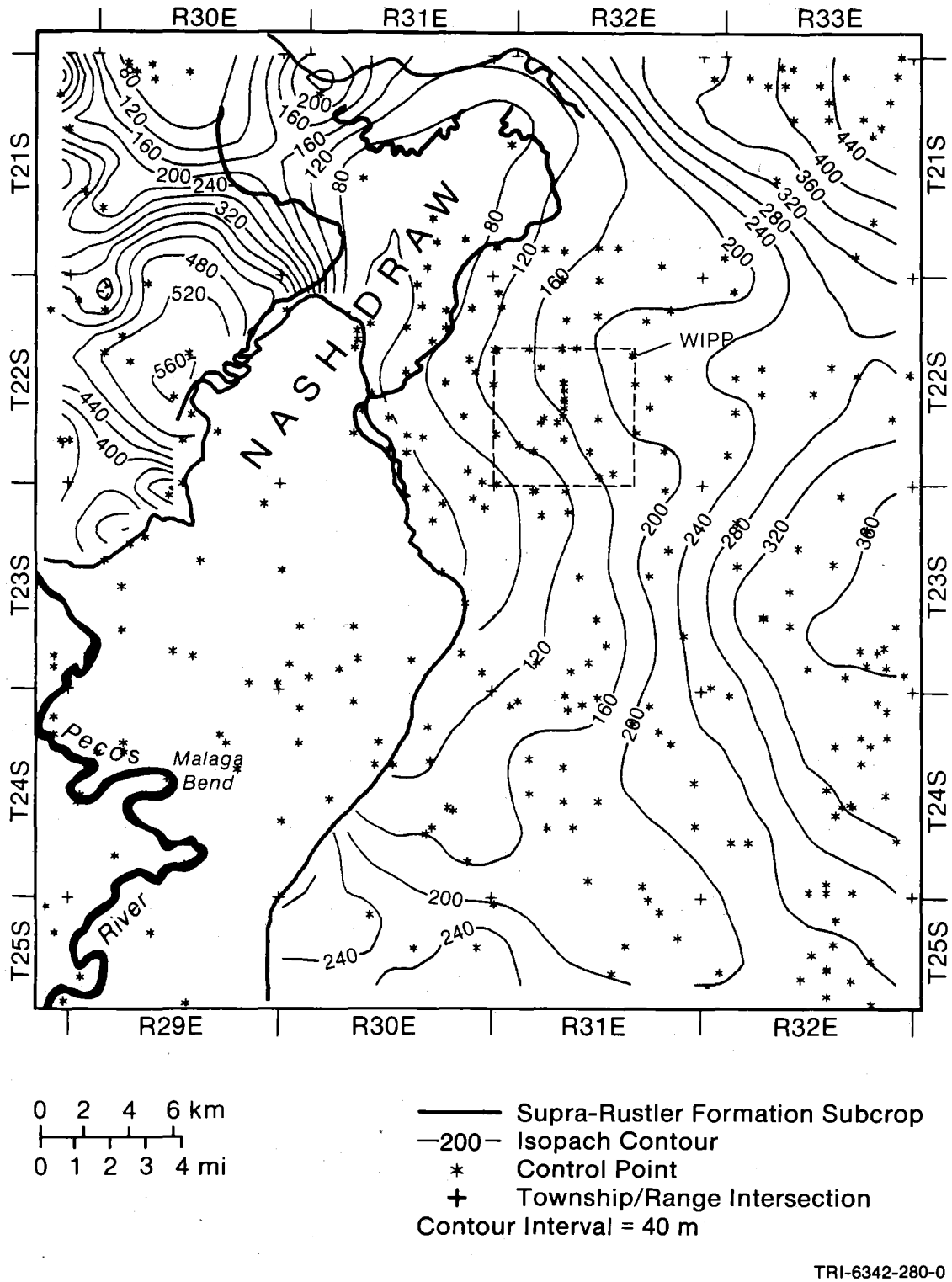

Figure II-31. Isopach Map of the Supra-Rustler Rocks.

Stratigraphy of the Cenozoic Rocks

As previously mentioned, a long depositional hiatus occurred from Triassic time to the Late Tertiary. Overlying the Mesozoic rocks in Eddy and Lea Counties are the Upper Tertiary, Quaternary, and Holocene units. The Miocene-Pliocene Ogallala Formation represents the Tertiary, the Gatuña Formation and the informally named Mescalero caliche represent the Quaternary, and soils represent the Holocene.

The Miocene-Pliocene Ogallala Formation is only represented west of San Simon Swale at The Divide (Figure I-2) and is very thin. The unit is composed of well-sorted, wind-blown sand derived from the Rocky Mountains and is capped by a caliche layer correlative to the Mescalero caliche (Bachman, 1980, 1984). The middle-Pleistocene Gatuña Formation consists of sandstone, siltstone, and conglomerate and occurs as a discontinuous floodplain deposit in channels and depressions (Bachman, 1980, 1984; Mercer, 1983). East of Nash Draw, a 600,000-year-old volcanic ash derived from the Yellowstone region caps the Gatuña Formation (Bachman, 1984).

The informally named Mescalero caliche is a well-cemented, calcareous paleosol formed about 510,000 years ago and is overlain by the sandy, argillaceous Berino paleosol, which began to form about 350,000 years ago (Mercer, 1983; Bachman, 1984).

Recent deposits of alluvium are restricted to the area near the Pecos River north of Malaga Bend, in San Simon Swale, and as fill in a solution depression south of the Study Area. Localized accumulations of alluvium and stabilized dunes are also present over most of the area.

Where present, the Supra-Rustler units range in thickness from 4 m in the western part of the Study Area to 536 m at the eastern margin of the Study Area. An isopach map of the units shows that the rocks thicken to the east, forming a uniform wedge of overburden in the Study Area (Figure II-31). The surface map of the area, taken from a topographic map, shows a fairly gentle rise to the east (see Figure I-2).

III. REGIONAL GEOMORPHOLOGY

In the Study Area, regional karst topography is of particular geomorphological significance. The term karst is usually applied to regions where dissolution of dolomite and/or limestone resulted in collapse of the surface, forming a unique topography. In the Study Area, however, the term is applied to features formed by dissolution of evaporites such as halite and anhydrite as well as carbonates. The formation of the karst topography in Eddy and Lea Counties is thoroughly discussed by Bachman (1973, 1974, 1980, 1981, 1984, 1985, and 1987). This regional study considers only karst features of regional magnitude such as Nash Draw, San Simon Sink, breccia chimneys, and large dissolution depressions.

Natural Occurrence and Removal of Evaporites in the Study Area

This examination and discussion is presented to familiarize the reader with previous work and to present these studies in the context of performance assessment. The geomorphological features seen in southeastern New Mexico were formed by large amounts of water moving through a system of soluble rocks. Studying the occurrence of evaporites and the cause, rate, and extent of evaporite dissolution is necessary for evaluating the integrity of the geologic media in which the repository is constructed and in the rocks above and below the repository horizon. Removal by dissolution of material under a competent unit may result in fracturing, depending on the properties of the unit and rate of removal. A brittle rock may settle slowly and not fracture; that is, it behaves as a ductile unit. If the unit is let down at a rate that results in fracturing, the hydrologic properties of the previously competent rock are profoundly affected by changing its porosity, permeability, and hydraulic conductivity. Rock units that are dissolved are not completely removed; an insoluble residue remains that also has properties unlike the original rock.

Occurrence and dissolution of Ochoan evaporites has been extensively examined and discussed by Anderson and others (1972, 1978), Anderson (1978, 1981), Lambert (1983), Bachman (1980, 1981, 1984, and 1987), Gustavson and others (1980), Snyder (1985), Snyder and Gard (1982), Lowenstein (1987), Holt and Powers (1988), and Lappin (1988). A summary of this body of work follows, and the reader should refer to the studies mentioned for elaboration.

EVIDENCE OF DISSOLUTION

Evidence of dissolution in southeastern New Mexico can be demonstrated along several lines. Salts are highly concentrated in the Pecos River near Malaga Bend due to the influx of dissolved material from lower Nash Draw. The high concentration of dissolved salts in the Pecos River indicates dissolution of evaporites is occurring (Hunter, 1985; Bachman, 1987). Although what precise fraction of dissolved solids in the Pecos River is due to dissolution of rocks and what fraction is due to man's activities (potash mining and brine pits from hydrocarbon exploration) is not known, most dissolved solids in the river result from dissolution of rocks at the top of the underlying evaporite section.

Dissolution residues are found in drill cores and outcrops and are represented by gypsum, siltstones, and clay in stratigraphic intervals that are normally evaporites. In some cases, abrupt thinning or absences of rock units due to missing evaporite sequences can be seen in logs of closely spaced wells. Wells over the Capitan Reef north of Nash Draw and east of the WIPP show thinning of the Salado Formation (Adams, 1944; Maley and Huffington, 1953; Hiss, 1975; and Anderson, 1978).

Along Nash Draw at WIPP-32, where the Rustler Formation evaporites are exposed, the more dissolution-resistant dolomites of the Magenta Dolomite and Culebra Dolomite Members are separated by only a few meters (<10 m) of material due to dissolution of the Tamarisk Member, which is normally about 30 m thick. Snyder (1985) summarized dissolution in the Rustler Formation:

> As one progresses westward across the WIPP site there is both a progressive dissolution of halite and a gradual hydration of anhydrite to gypsum [Figure III-1]. Seemingly, halite from the uppermost member, the Forty-niner, is removed first, followed by removal of halite from the middle Tamarisk Member, and then finally from the unnamed lower member. The intervening dolomite members are not directly affected by these processes, but as halite is removed from below each of them, the dolomites settle and fracture and transmit ground water more readily. At some stage in the removal of halite, possibly when the dissolution reaches a point where the anhydrites settle and crack allowing ground water to flow through them, the anhydrites begin hydrating to gypsum. This process tends to thicken the formation even though halite is being removed. The mutual interaction between these two processes results in an erratic thickening and thinning of the Rustler Formation as seen on the [Rustler Formation] isopach maps.

This dissolution results from subterranean movement of water because the missing material has not been replaced by surficial material.

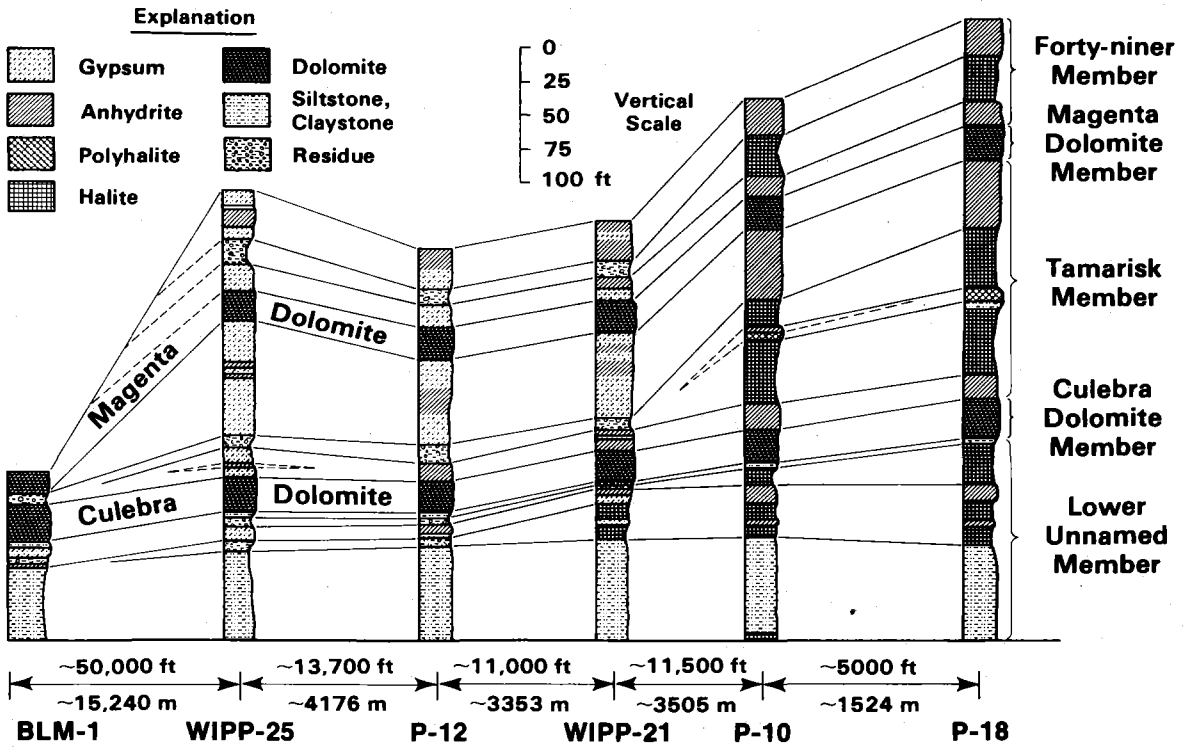

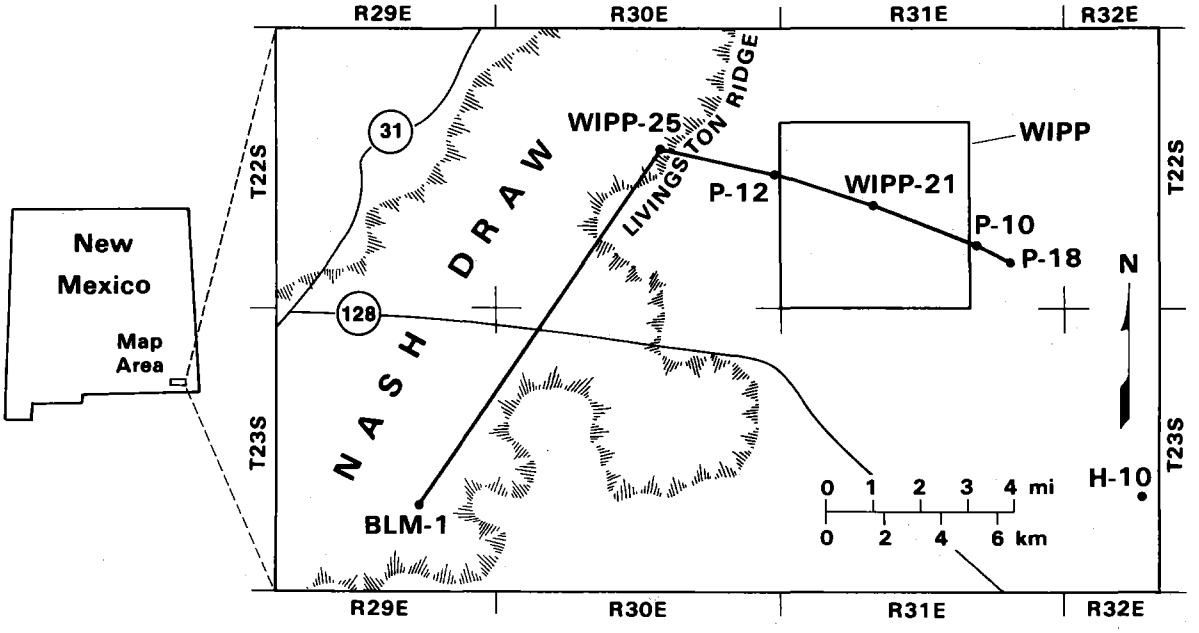

TRI-6342-243-0

Figure III-1. Columnar Cross Section across the WIPP, Showing Lithologic Correlations of Rustler Formation Units (modified from Snyder, 1985).

MECHANISMS OF DISSOLUTION

As ground water moves through the saturated zone, it reacts with the rocks it contacts and begins dissolving them. Dissolution occurs until the water reaches equilibrium or until no soluble rocks remain.

If conditions are such that the saturated water is carried away, unsaturated water moves in and continues dissolving the rocks. In areas such as southeast New Mexico, where the rocks are highly soluble, dissolution occurs rapidly in the halite and less rapidly in the somewhat less soluble gypsum and anhydrite.

Four models have been proposed for mechanisms of dissolution: brine density flow, "solution and fill," phreatic, and stratabound (Bachman, 1980, 1981, 1985, and 1987; Lambert, 1983; Anderson and others, 1972; and Anderson 1978, 1981).

For a dissolution model to operate, five factors must be present: a trigger, a path, continuity, a source, and a sink (Lambert, 1983). The trigger for dissolution is an event that changes the relationships among geologic structure, stratigraphy, and hydrology that previously protected an evaporite unit. A path (permeable zone) is needed and must be maintained for unsaturated fluid to contact the perturbed unit and carry away the saturated fluid. The perturbed unit must have some extent (continuity in any direction), or dissolution will soon terminate. Dissolution requires a continuous source of unsaturated fluid and a place for the saturated fluid to go (sink). A discussion of the five dissolution factors for the proposed models follows.

All four dissolution models have been postulated to occur in the Study Area (Table III-1). Solution and fill occurs when fresh water (source) permeates fractures in evaporites (trigger), dissolves the material (path), and carries the solution away (sink). The resulting large voids cause a collapse of the overburden, forming a sinkhole. Subsequent degradation by erosion and slumping of the sinkhole walls creates debris that then fills the hole. Coalescing sinkholes and slumping walls helped to form Nash Draw.

Phreatic dissolution occurs in brittle rocks such as limestones in the vadose or phreatic zone when water (source) enters fractures (trigger), moves along the fractures (path), and is carried off in old dissolution channels (sink) (Lambert, 1983). Carlsbad Caverns and San Simon Sink are examples of this type of dissolution. According to Vine (1963), Hills A and C (Figure I-6) are domal karst features formed by catastrophic sinkholes filling with Gatuña

TABLE III-1. SUMMARY OF DISSOLUTION MECHANISMS IN THE LOS MEDAÑOS REGION

	Solution and Fill	Phreatic	Brine Density Flow	Stratabound
Trigger	Delaware Basin tilting	Fractures	Evaporite is exposed to fluid from below, possibly through fractures	Delaware Basin tilting (solution and fill can be triggering mechanisms)
Path	Rock-atmosphere interface	Either the triggering fracture or another fracture	Bedding plane or vertical fractures	Anhydrite interbeds
Rock Continuity Laterally or Vertically	Amount of exposure of soluble rock (gypsum)	Large pure limestone body of rock	Solution has to move downgradient	Beds of halite
Source	Shallow infiltration of rainfall (meteoric water is the source for all the models) (Lambert, 1983)	Meteoric water	Surface water (meteoric water) or water undersaturated with respect to NaCl	Meteoric water or water undersaturated with respect to NaCl
Sink	Governed by surface and shallow subsurface patterns of drainage	Dissolution channels	Aquifer to carry away brine	Through local "lows" in potential level such as Balmorhea-Loving Trough
Examples in New Mexico	Nash Draw Gypsum Plain Clayton Basin	Brittle rocks such as limestone - Carlsbad Caverns - San Simon Sink, Vine's Domes (Lambert, 1983)	Dissolution of Castile in Delaware Basin (Anderson and Kirkland, 1980)	Nash Draw and probably the Cenozoic gravel-filled depressions

Formation sediments, with the surrounding evaporites subsequently dissolving away, leaving a dome. According to Lambert (1983), these features are analogous to San Simon Sink and Carlsbad Caverns.

How surface water (source) (if, indeed, the source is surface water) gets into conduits such as a bedding plane (path) and moves downgradient to the Bell Canyon Formation (sink) is not well understood. Lambert (1983) concludes that this model is flawed because the Bell Canyon waters are not adequately saline or of the right composition to account for the large amount of dissolution in the overlying evaporites. Lambert also bases his conclusion on evidence that the ground water in the Bell Canyon may be stagnant (see also "Recharge and Discharge" of the "Bell Canyon Hydrostratigraphic Unit" in Chapter IV). This latter conclusion does not account for the direct evidence of ground-water movement in the Bell Canyon (Davies, 1984).

Hubbert (1953) showed that the gravitational theory of oil entrapment in which oil or gas in rocks moves vertically from regions of high energy to low energy and becomes entrapped in structures such as anticlines is only a special case of hydrocarbon entrapment and is associated with hydrostatic conditions. Hubbert then showed that water under hydrodynamic conditions, flowing nonvertically, will cause oil and gas to occur in traps that do not necessarily coincide and may even be so divergent that the oil trap may not be capable of holding gas and the gas trap may not be capable of holding oil. These accumulations occur in monoclines and structural features such as those in the Bell Canyon, thus indicating hydrodynamic conditions and the possibility of a potential sink.

Brine density flow might be the triggering or sink agent for the fourth model, stratabound dissolution. Tilting of the Delaware Basin exposed the evaporites by erosion and triggered the mechanism. Meteoric (rain) water then moved along the fractures in anhydrite (path) and dissolved halite, which collapsed, increasing permeability. Lambert has difficulty proving a sink for stratabound dissolution, but he proposes that the solution moved downgradient through the rocks with newly enhanced permeability to an area of low hydraulic potential such as a filled depression, the Balmorhea-Loving Trough, or possibly San Simon Swale. These subsidence features may have up to 600 m of Cenozoic fill and may be efficient sinks for the disposal of brine (Maley and Huffington, 1953; Lambert, 1983).

Brine density flow was proposed as a mechanism to explain dissolution residues in the Castile Formation that were found in drill cores in the western part of the Delaware Basin and correlated to appropriate stratigraphic horizons in the eastern Delaware Basin. Some workers feel that the presence of these dissolution residues indicates that some, if not all, of the salt beds

extended to the western margin of the basin (Anderson, 1978; Anderson and others, 1972, 1978).

Anderson (1978) estimates that 50 percent of the original Delaware Basin halite has been dissolved and concludes that, if surface or near surface salt were removed by surface or near-surface drainage, the amount of halite removed would decrease linearly with depth. This relationship may not be the case. The lower Salado Formation in the central basin, Anderson (1978) estimates, has only 30 percent of its original volume, which is attributed to a deep dissolution wedge moving along a somewhat more permeable layer formed between the Castile and Salado Formations during a hiatus in deposition after Castile time. Anderson's (1978) model involves the following steps:

Uplifting and tilting of the Delaware Basin,

Exposure and erosion of basinal units at the western edge,

Movement of ground water down dip and hydrocarbons up dip, then into fractured anhydrite,

Replacement of anhydrite fracture walls with biogenic calcite derived from bacterial cultures,

Movement of ground water through large fractures coming into contact with halite,

Dissolution of halite, forming large chambers in lower salt, and

Collapse of the rocks over the chambers.

This model, then, requires the movement of undersaturated water (source) to the halite along bedding planes (path) and removal of saturated water through permeable rocks identified as the upper Delaware Mountain Group (sink) in some cases, or as the Capitan aquifer. The source of water in the western part of the basin is meteoric and in the eastern part of the basin is the Capitan aquifer.

Dissolution of halite in the central basin resulted in a large depression in the Poker Lake-Big Sink area of southern Eddy County. Bachman (1980) disagreed with part of the Anderson hypothesis in that the Bell Canyon in the upper Delaware Mountain Group is not transmissive enough to quickly remove all the brine that would be generated by the brine density flow mechanism. Bachman (in Chaturvedi, 1980) contends that blanket dissolution as proposed in the Anderson model has not been observed, that dissolution on the western edge occurred when the Castile Formation was near sea level before Cretaceous time, and that the absence of halite in the Castile was not due to deep-seated dissolution but that halite was never present because the occurrence of halite

is a facies relationship. This absence also means that the interformational breccias at the western edge of the basin are probably not correlative to halite in the eastern basin.

Davies (1983, 1984, 1987) thoroughly discusses dissolution in southeast New Mexico and concludes that no single mechanism can account for what has been observed in the basin. North of the WIPP, in the SE¼ of T22N, R31E, the lower Salado Formation thins, causing what seemingly is a depression in the lower Salado or upper Castile. Griswold (1977) postulated that the anomalously thinned halite (referred to as the FC-92 depression) may have been the result of a breccia pipe, dissolution of limestone in the upper Bell Canyon Formation, or dissolution of halite in the Salado or Castile Formation. Powers and others (1978) did not include the data that shows the anomaly and concluded that it was "not significant to WIPP."

Davies (1983) confirmed the presence of the anomaly and found the following:

> Physical analyses of salt deformation processes suggest that this structural depression formed as the result of ductile subsidence in response to the localized removal of salt at some lower horizon. Processes capable of removing salt include dissolution of lower Castile salt, dissolution of lower Salado salt, and depletion of Castile salt by gravity driven flow. Deep boreholes in the northern WIPP area and elsewhere in the basin reveal geologic features that are characteristic of each of these processes. Consideration of complex structures in these areas leads to the conclusion that there are potentially significant interrelationships between individual processes and that more than one process may be active in a given area. For example, lower Castile salt dissolution may play a critical role in triggering the gravity foundering process by creating local increases in the deviatoric stress at the quasi-stable Anhydrite II and III density inversions and by causing the influx of a small amount of intergranular saturated brine, thereby decreasing the strength of the salt. Another example of process interrelationships is the potentially important role of lower Castile salt dissolution and gravity foundering in creating vertical and horizontal hydrologic pathways, thereby facilitating lower Salado dissolution.
>
> At the Salado depression in the northern WIPP site, there is insufficient data in the Castile and lower Salado to delineate which processes have been active and what process interrelationships exist. Therefore, either additional subsurface data should be gathered in the lower Salado and Castile, or safety analyses of the WIPP facility should explicitly encompass all possible processes, or both.

The so called "disturbed zone" (Borns and others, 1983) was examined more closely after Davies' (1983) proposal, and a drill hole was sited within the

depression. The depression was confirmed, but "contrary to several hypotheses, halite layers were thicker in the lower part of the Salado, not thinner as a result of any removal of halite." However, in the Castile, the upper anhydrite was found to be "anomalously thick" and "strongly deformed," and the halite was "significantly thinner than usually encountered" (Mercer and others, 1987). The depression was interpreted to be the result of gravity-driven Castile deformation, not deep-seated dissolution, because no dissolution residue or breccia was found in the core.

DISSOLUTION FEATURES

Examination of dissolution features in evaporites in the Delaware Basin is important with respect to performance assessment of the WIPP. This section discusses the formation of Nash Draw, dissolution depressions, and breccia chimneys (also termed breccia pipes) in the vicinity of the WIPP.

The effect of deep-seated dissolution at or near the WIPP has been examined by Anderson (1978), Anderson and Kirkland (1980), Snyder and Gard (1982), Davies (1983, 1984, 1989), and Spiegler (1982). This section gives a brief review of their work and discusses the possible effects of breccia chimneys on groundwater flow in the Study Area.

Nash Draw

Nash Draw is the largest surface expression of evaporite dissolution in southeast New Mexico. It is a large, open feature of coalesced solution cavities formed by dissolution of evaporites in the shallow subsurface. As the surface subsides, the walls of the dissolution cavities cave in, forming a debris-filled "valley." The process is known as solution and fill and is discussed in the next section of this chapter, "Discussion of the Geologic History of Erosion and Dissolution in the Study Area. Vine's (1963) description of Nash Draw is as follows:

> Topography and surface structure conform in some areas with the configuration of the underlying solution surface at the top of the massive salt in the Salado Formation; however, locally there is an inverse correspondence. Many circular karst features 1/10 to 1/2 mile [150 m - 800 m in diameter] are in the area. Some of these features are structural domes, but they contain a core of tilted or brecciated rock.

A much larger but not as obvious feature is south of Nash Draw just beyond the Study Area. This feature is a relic consisting of a series of coalesced, lens-shaped solution troughs formed by an ancestral Pecos River (Bachman, 1984) (Figure I-2). Up to 550 m of debris from sedimentary rocks, ranging in age from Triassic to Holocene, fill the trough (Hiss, 1975). The series of

troughs extending from Balmorhea, Texas, northward to just south of Loving, New Mexico, had been collectively termed the Balmorhea-Pecos-Loving Trough by Hiss (1975) but was later shortened to Balmorhea-Loving Trough (Bachman, 1984). A second trough extends from Belding, Texas, northward to San Simon Swale and is parallel with and coincidental to the Capitan Reef (Figure I-2). The next section of this chapter discusses the origin of these features and of Nash Draw. Other geomorphologic features (also in Figure I-2) large enough to note are the following:

San Simon Sink east of the WIPP, which covers about 1.3 km^2 and is surrounded by San Simon Swale, which covers an area of about 300 km^2. Either deep dissolution (Anderson, 1978, 1981) or the collapse of a phreatic cavity in the Capitan Limestone formed the swale (Lambert, 1983);

Poker Lake, a sink west of Malaga Bend in the southwestern part of the Study Area;

Big Sink, which was probably formed by the collapsed leading edge of an eastward advancing dissolution front (Anderson, 1981); and

Wink Sink, a sink probably formed by dissolution around a plugged and abandoned well by ground water from the Capitan aquifer.

Breccia Chimneys

Breccia chimneys in the WIPP vicinity (called Domes in Figure I-2) were originally of interest because formation of these features over or in proximity to a repository may be detrimental. Generally, the features are not likely to form in the WIPP vicinity due to the WIPP's distance from a good source of fluids (Capitan aquifer). Breccia pipes, though, may have some effect on ground-water flow in the Rustler Formation. Whether a perturbation to ground-water flow of the magnitude that would be likely from the catastrophic formation of a breccia chimney 300 m across would affect Rustler flow over the repository and, also, whether breccia chimneys may affect regional recharge and discharge has not yet been determined.

Breccia chimneys were first recognized as being unique positive geomorphological features by Vine (1960, 1963). The features were described as dome-like, composed of brecciated sedimentary rocks, and draped by a caliche layer that dips away from the center of the dome. The features are cylindrical (up to 245 m in diameter) and extend nearly vertically through one or more formations (Vine, 1960; Bachman, 1980). Gustavson and others (1980) discuss chimneys in the Anadarko and Palo Duro Basins in the Texas Panhandle region on the Texas-Oklahoma border. The chimneys in the Anadarko Basin are in upper Permian rocks and were probably formed in the Late Cretaceous because the chimneys are filled with breccia from Late Cretaceous rocks. In the Palo

Duro Basin, Gustavson and others located many breccia chimneys in Late Permian exposures. The chimneys are filled with Triassic, Tertiary, and Quaternary sediments and range up to 300 m in diameter. The chimneys occur in areas of paleodissolution or where dissolution is presently taking place.

Hill A has been described in detail by Vine (1960), Bachman (1980), and Snyder and Gard (1982). It is a low hill located about 30 km east of Carlsbad, New Mexico (Sec. 35, T20S, R30E). The hill is about 12 to 15 m high and is 370 m in diameter. A shallow basin with an intermittent lake draining to the west has been eroded in the center. The basin is surrounded by Dewey Lake Red Beds, Dockum Group, and Mescalero caliche, in ascending order, that dip about 15 degrees away from the center.

The brecciated core is about 245 m in diameter and is surrounded by a circular or "ring" fault that leaves the Permian and Triassic rocks inside the ring higher than the corresponding units outside the fault. The core consists of lithified debris up to 4 or 5 m in diameter that has undergone repeated dissolution and recementation. Drillhole WIPP-31 penetrated the chimney to 258 m and did not encounter any Salado Formation halite, although hydrocarbon wells outside the periphery of the chimney penetrated over 300 m of salt. The Triassic and Permian rocks near the surface dip away from the chimney because near-surface dissolution of Rustler Formation salt and the upper Salado by an eastward-migrating dissolution wedge has lowered the rocks surrounding the pipe (which were already devoid of halite). Because the once flat-lying Mescalero caliche, which began forming about 510,000 years ago, is now dipping away from the center of the hill, the eastward-moving dissolution wedge can be dated. Bachman (1980) dates the wedge movement past the hill at less than 400,000 years ago. Snyder and Gard (1982) outline the following order of formation of the chimney:

1. Deposition of rocks as young as Triassic Dockum Group.

2. Cavity formation in the Capitan Limestone by circulating ground water.

3. Collapse of the Yates and Tansill Formations into cavity.

4. Support by the Fletcher Anhydrite that kept further upward collapse from occurring for some time.

5. Eventual collapse of the Fletcher and downdropping of Salado and younger units. This stage probably consisted of some massive and some fragmental downdropping.

6. Continual dissolution of Salado and Rustler halites in the pipe, possibly from downward-moving water. Mud and small rock fragments in the pipe continually carried or dropped downward during this stage.

7. Formation of Mescalero caliche across nearly horizontal surface.

8. Removal of all Rustler halite and some upper halite from the Salado from around the pipe by a dissolution front, causing near-surface beds to dip away from pipe.

Hill B is similar to Hill A but does not have the ring fracture system (Bachman, 1980). Hill C is 3 km southeast of Hill A. It rises about 30 m above the surrounding terrain and is 350 m across. Geologically, it resembles Hill A in that it is draped by Mescalero caliche overlying Gatuña and brecciated Triassic rocks (Snyder and Gard, 1982).

A unique opportunity for subsurface study of a chimney occurred in 1975 when mining operations encountered the Hill C chimney 366 m below ground surface. Davies (1984) did a thorough study of the underground exposure of the chimney at Hill C. This study showed that this chimney was probably formed by a slow incremental process of downward displacement of between 103 to 168 m, based on a large block of anhydrite that could only have come from marker beds 103 or 109 in the Salado Formation, whereas fragments of dolomite from the Magenta Dolomite and Culebra Dolomite Members of the Rustler Formation were found 274 to 366 m below their normal horizon. Drillhole WIPP-16 in Hill C shows possible displacement of up to 210 m, indicating nonuniform movement within the chimney.

Further evidence of noncatastrophic formation of Hill C's chimney is the lack of jumbled rocks as was encountered in WIPP-31 at Hill A. WIPP-16 penetrated the rocks in recognizable stratigraphic order but about 189 m below normal (Snyder and Gard 1982).

In WIPP-31, all halite of the Rustler Formation and most halite of the Salado Formation is missing. In WIPP-16, halite is missing only from the Forty-niner and Tamarisk Members but was cored from below the Culebra Dolomite Member (Snyder and Gard, 1982). Examination of clasts and matrix indicates movement, however, of fluids though the chimney during or following subsidence. Davies (1984) analyzed matrix clays using X-ray diffraction and showed a higher ratio of clay to halite in the breccia than in the average Salado halite, thus indicating dissolution of halite. Halite clasts have rounded edges, and halite has recrystallized in fractures, indicating fluid has moved through the breccia since subsidence. Another indicator of fluid movement in the chimney is the presence of oil from the Yates Formation in small quantities at crystal boundaries in the matrix clays and in the transition zone adjacent to the chimney. The oil is seen in both WIPP-16 and WIPP-31 as well as in the mine

drifts near Hill C's chimney (Davies 1984; Snyder and Gard, 1982). Davies (1984) concludes that, because most of the halite clasts have not undergone recrystallization and because of the large amount of soluble clasts still present, the fluid moving through the rocks was either close to saturation with respect to halite and sulfates or was not of sufficient quantity. Some evidence indicates that movement has occurred in Hill C's chimney since Mescalero time, which may be due to structural readjustment or to mining (Davies 1984).

Snyder and Gard (1982) estimated that, at time of formation of the breccia pipe, the Dockum Group and Dewey Lake Red Beds had a composite thickness of more than twice the present day thickness (about 145 m in nearby wells). Also, core from drillhole WIPP-16 contained no voids and had a filling consisting of clay- and silt-size material, presumably from surface material washing into the chimney and from disintegrating collapse material.

There is other evidence that water may have at one time been moving upward from lower units, and Nicholson and Clebsch (1961) cite the Laguna Plata, Gatuña, Toston, and Tonton about 20 km north of the WIPP; Bell Lake about 30 km southwest of the WIPP; and other depressions that have gypsum dunes, indicating the hydraulic head in pre-Tertiary rocks was much higher than it is today.

Other potential pathways for fluid movement are degraded and abandoned deep wells. Wink Sink in Texas near the New Mexico border is located above the Capitan aquifer and is manifested at the surface by a 25-m-deep sinkhole that is circular in shape and has a diameter of 110 m. The sink is believed to be the result of dissolution of salt at a depth of from 400 m to 670 m by circulation of ground water from the Capitan that was facilitated by the presence of a plugged and abandoned well (Davies, 1984).

Discussion of the Geologic History of Erosion and Dissolution in the Study Area

An understanding of geologic processes such as erosion and dissolution requires an understanding of stratigraphy, lithologic relationships, how hydrologic pressures control dissolution rates, and how structural pressures control subsidence. A geologic history of the dissolution in the Study Area has been summarized by Bachman (1984) as follows:

> The region of southeastern New Mexico was uplifted at the close of Permian time. It was above sea level throughout Triassic and Jurassic times. During the Early Cretaceous the region was again below sea level.... At the close of Cretaceous the entire region

> was lifted above the sea level again.... [T]he region has been above sea level for a minimum of 154 million years and below sea level for less than 71 million years since the end of the Permian.

Although dissolution can occur when units are below base level, erosion and dissolution of stratigraphic units in the Study Area occurred principally while the units were above base level. During Triassic time, when the Study Area was above sea level, climatic conditions were relatively more humid than during the arid Permian time. Easterly flowing streams from the highlands (Sacramento Mountains) west of Eddy County carried sediments into the Delaware Basin and deposited a wedge of Triassic sediment that thickens toward the basin depocenter east of the Study Area. The western edge of the sediment wedge is almost coincidental to the present-day Pecos River (McGowan and others, 1979). Permian-Triassic rock relationships in the western part of the basin indicate that the upper Rustler Formation was eroded before or during the Triassic deposition. Bachman's (1984) observation was that ancient evidence of dissolution (>60 mya) is not as obvious as the karst features formed during Cenozoic and Holocene times and pointed out the following:

> [T]he association of other rock types [Permian, Triassic, and Jurassic] with Cretaceous deposits indicates the depth of erosion before Cretaceous time. These rock associations indicate the following stratigraphic relationship along the western edge of the Delaware Basin in New Mexico:
>
> 1. Rocks above the Culebra Dolomite were partially removed in the vicinity of the modern Pecos River before Cretaceous time.
>
> 2. The Salado Formation was removed completely in a belt along the western margin of the basin in New Mexico before Cretaceous time allowing the Culebra Formation to rest on the Castile Formation.

IV. REGIONAL HYDROLOGY

Data requirements for solving the three-dimensional flow equations presented in Appendix A are separated into two main groups: surface water and ground water. Sources and sinks (recharge and discharge) for each group are considered and discussed together. The "Surface Water" section of this chapter discusses the relationship of the Pecos River, Surprise Spring, and the Laguna Grande de la Sal to the hydrology of the Study Area.

In the "Ground Water" section, the Bell Canyon Formation, the Capitan Limestone/Rustler-Salado contact residuum, and the Culebra Dolomite and Magenta Dolomite Members of the Rustler Formation are presented as separate transmissive hydrologic units. The Castile Formation is discussed because of its potential as a high-pressure brine source in a scenario that examines the breaching of high-pressure fluid pockets by exploratory drilling in the vicinity of the WIPP. The Salado Formation is discussed as the host rock for the repository. The unnamed lower member, Tamarisk Member, and Forty-niner Member of the Rustler Formation are discussed as aquitards. The units above the Rustler Formation are treated as playing a role in recharge events. To summarize, this chapter discusses ground-water movement in the northern Delaware Basin.

Surface Water

A discussion of the hydrology of the Study Area requires understanding the interrelationships of the complex surface-/ground-water system as it exists in an arid environment. Constructing a water budget of the Study Area does this best. Basic data requirements of this phase of the Los Medaños model development are the following:

Inflow and outflow rates of the Pecos River, its tributaries, and the lakes in the model area;

Precipitation rates;

Withdrawal rates (consumption) from both the surface waters and ground waters;

Surface and subsurface storage; and

Inflow rates from upper ground-water basins and outflow rates to lower ground-water basins.

A water budget for the Study Area was developed by Hunter (1985), and the salient points pertinent to a ground-water model have been included here. Hunter's study presents the principles used to determine recharge and discharge and are not reiterated in this report.

PRECIPITATION

The average annual rainfall over the Study Area is about 0.3 m (12-in contour in Figure IV-1). In the Study Area, most of the precipitation becomes runoff or evaporates. In southeastern New Mexico, the evaporation from a Class A pan is 2.8 m/yr (Powers and others, 1978), with 1.85 m/yr from May to October. Of the small amount of precipitation that does infiltrate, about 90 percent undergoes evapotranspiration. Of the remaining 10 percent, any water going through the topsoil must then percolate through a tight Mescalero caliche layer that is ubiquitous throughout the Study Area except in Nash Draw. Recharge to the regional system from rainfall is considered negligible in this study but warrants attention for performance-assessment purposes. Geohydrology Associates, Inc. (1978a, 1978b) reported a range of recharge from 8 to 23 mm/yr.

RIVERS, LAKES, AND SPRINGS

The Pecos River drainage system is the primary surface water feature in southeastern New Mexico. The river, which is part of the Rio Grande Basin, flows southeastward in New Mexico, approximately parallel to the axis of the Delaware Basin in Eddy County, and drains into the Rio Grande in West Texas. In the vicinity of the WIPP, the drainage system consists of small ephemeral streams and draws in addition to the Pecos River and drains an area of about 50,000 km^2. The Pecos River, which is about 20 km from the southwest boundary of the WIPP, flows diagonally across the southwest corner of the Study Area at the lowest elevation of the Study Area.

Understanding the evolution of the role of the Pecos River drainage system is fundamental to the conceptual model of ground-water flow in the Study Area. The following is a description of the Ancestral Pecos River (Bachman, 1984, terminology).

The Ancestral Pecos River drained the area south of Carlsbad from the late Tertiary to the early Pleistocene, following a course that was about 20 km east of its present course south of Loving, New Mexico, and was responsible for the karst features in southeastern Eddy County (Bachman, 1984).

The stream was of higher energy than today as evidenced by the size and amount of material in the stream and the distance that the material was carried. The

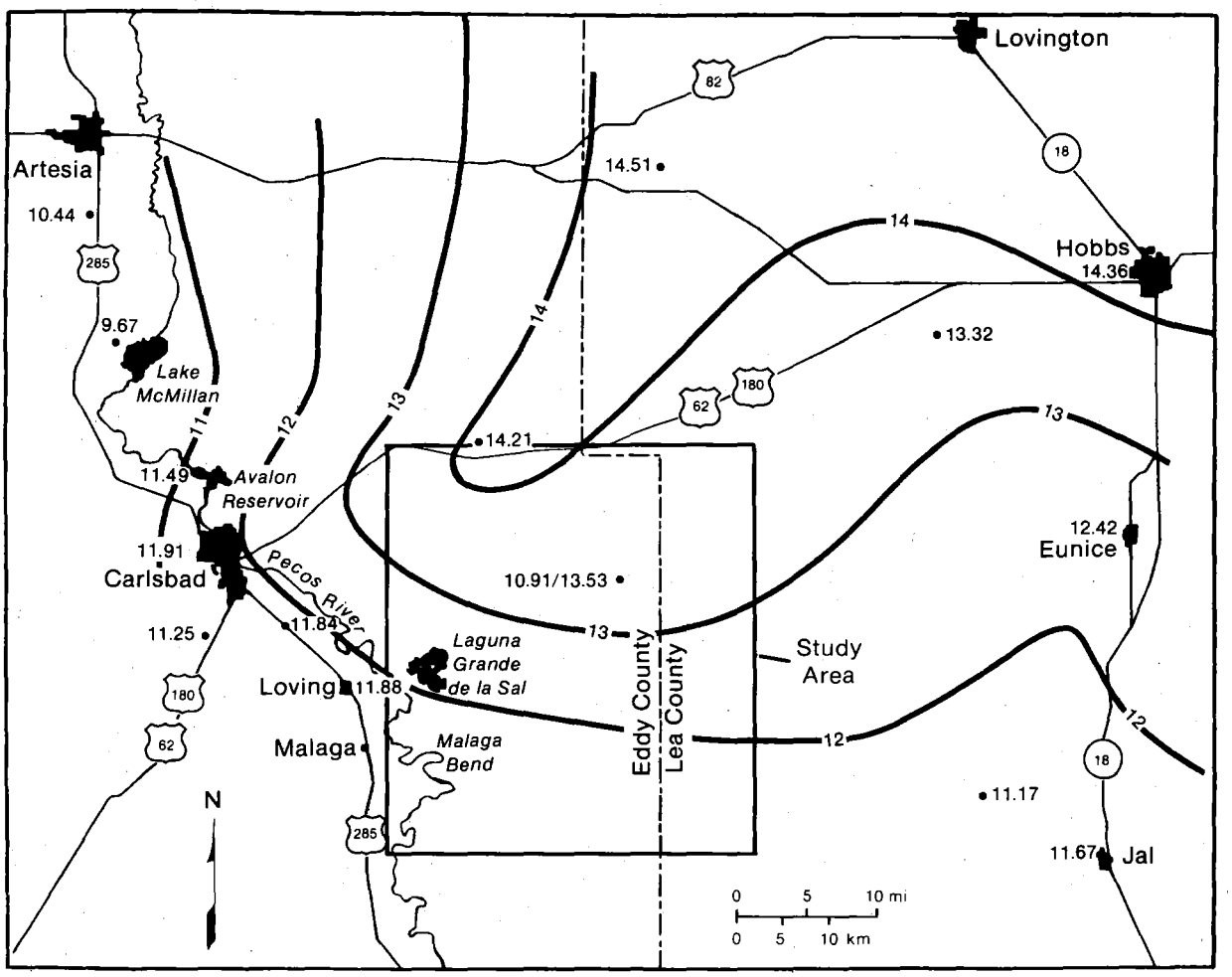

TRI-6342-123-0

Figure IV-1. Precipitation Contours (in inches) in and near the Study Area (Hunter, 1985).

sediment includes medium-to-coarse (up to 7 cm), well-sorted, light-gray and reddish-brown sand and pebbles derived from the Capitan and Sacramento Mountains 160 km to the northwest of Carlsbad. The accumulated sediments may be up to 6.5 m thick (Bachman 1984, 1987; Maley and Huffington, 1953, plate 1).

The sediments accumulated in sinks formed by Pecos River water, which is unsaturated with respect to halite, that dissolved the underlying evaporites. The water percolated to the top of a relatively impermeable anhydrite at the top of the Castile Formation and moved downward in the fractured western edge of the basin, where it perched and moved laterally. The Castile Formation halites (I, II, and III) below the protective anhydrite are intact, but the Salado Formation halite above the Castile Formation is dissolved down to Marker Bed 137, thus lowering overlying strata (Bachman, 1984). Maley and Huffington (1953) point out, "In general, in areas of maximum salt thickness, the Rustler [F]ormation is structurally high and thickness of fill is at a minimum. Conversely, areas of minimum salt thickness are overlain by structurally low Rustler and the thickest deposits of fill." Maley and Huffington also point out that structural lows may be caused by tectonism but believe the lows are the result of dissolution of evaporites. Wells correlated from west to east across southern Eddy County into Lea County show that evaporites are absent in the central part of the Ancestral Pecos River drainage system but are present east of the trough in Lea County (Figure 7 in Bachman, 1984; see also the discussion of the work by Anderson and others, 1978, and Anderson, 1978, in the previous section.)

In the middle Pleistocene, the Ancestral Pecos River eroded headward across the Capitan Reef near Carlsbad and pirated a stream that flowed eastward into Texas. Subsequently, the stream migrated westward, where it is now entrenched in karst features such as sinks and collapsed caves that form abnormally straight reaches (along fractures), pseudo-oxbows, and pseudo-cutoff meanders as seen at Malaga Bend (Bachman, 1984, 1987).

Elevation of Pleistocene sediments indicates that the river gradient during Mescalero time when the caliche was formed is about the same as today (1 m/km). The caliche can be used as a marker, and although it was not formed as a horizontal plane, it can be used to ascertain the relative position of the ancient sediments. The caliche layer in the ancient sediments in the Carlsbad area is about 40 m below the caliche layer in the Phantom Banks sediments, which is downgradient, indicating that subsidence has occurred from Carlsbad to Pierce Canyon near Malaga Bend (Bachman, 1984). Bachman believes the entrenchment of the Pecos River precludes further extensive dissolution of evaporites in the Pierce Canyon area, presumably because the river is at a lower elevation than the floor of the canyon.

Data (Table IV-1) from four USGS gaging stations (Figure IV-2) south of Carlsbad show the average discharge and the extremes for the period of record. The Pecos is a gaining stream between Carlsbad and Malaga Bend. Gains from municipal discharge, return flow from irrigation, and water from potash spoil ponds were coupled with diversion losses and evaporative losses that resulted in a calculated gain in 1980 of 0.24 m^3/s between stations 4052 and 4065 and a calculated gain of 0.12 m^3/s between stations 4065 and 4070 (Hunter, 1985). The gains south of Carlsbad were attributed mostly to ground water discharging to the river (Hunter, 1985).

TABLE IV-1. STREAM DISCHARGE AT GAGING STATIONS BETWEEN CARLSBAD AND MALAGA BEND, NEW MEXICO

Station No.	Location and Period of Record	Average Discharge (m^3/s)	Extremes (m^3/s)
4040	Below Avalon Dam (1951-1984)	0.86	0-2550
4052	Below Dark Canyon (1970 to 1984)	1.32	0-800
4055	Black River above Malaga Bend (1948 to 1984)	0.37	0.02-2110
4065	Pecos River near Malaga Bend (1938 to 1984)	4.75	0.01-3398
4070	Pecos River at Pierce Canyon (1939 to 1941 and 1952 to 1984)	3.68	0.02-1841
4075	Pecos River 0.2 mi downstream from Red Bluff Draw (1938-1984)	4.62	0.01-3144

Source: USGS, 1985

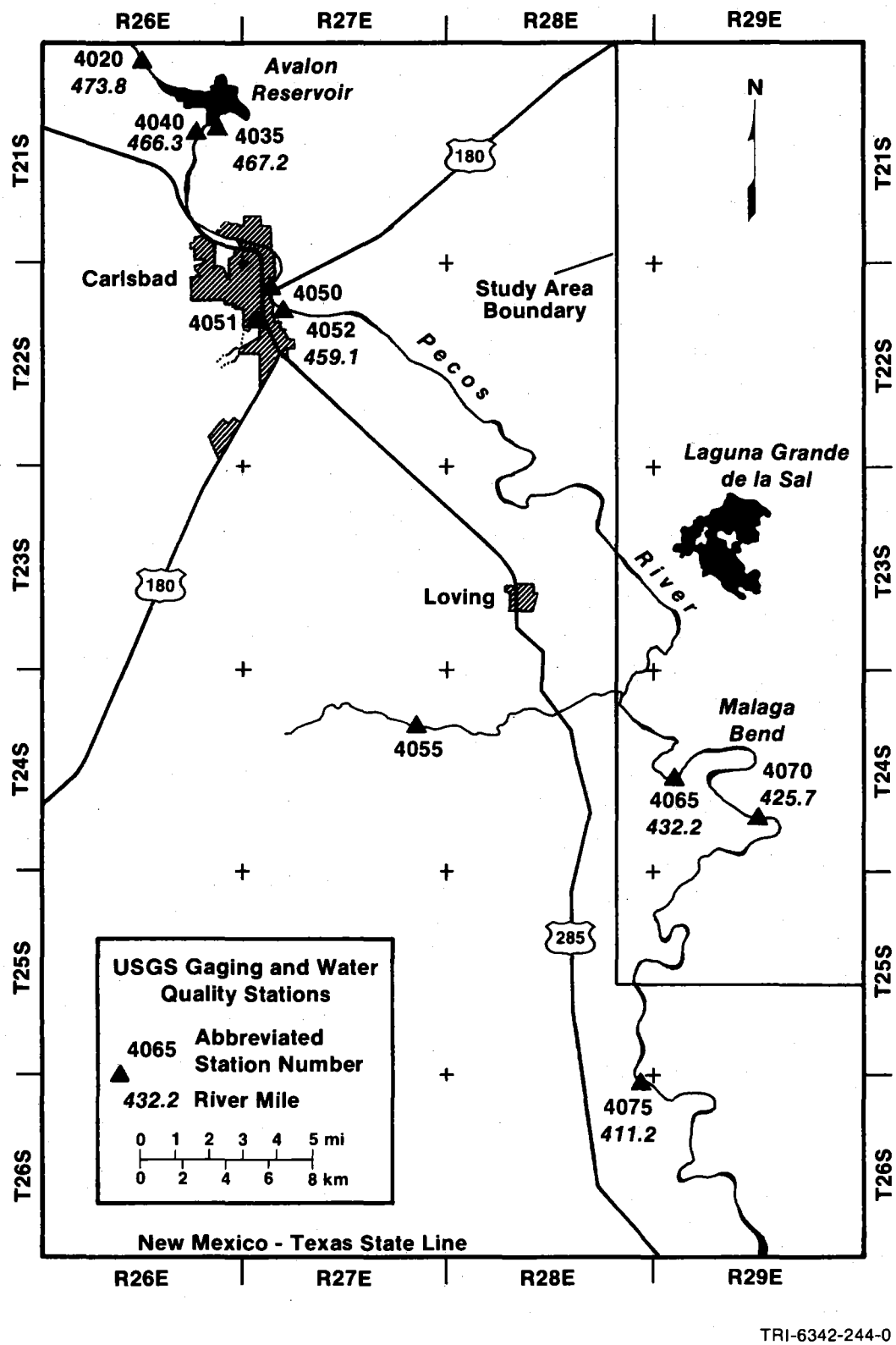

Figure IV-2. Surface Drainage in and near the Study Area (Hunter, 1985).

The minimum and maximum ground-water discharge to the Pecos River in and near the Study Area from just north of Carlsbad at Lake Avalon to south of Malaga Bend is given in Table IV-2. The maximum and minimum gains to the Pecos River in the Study Area for 1982 are 0.9 and 0.09 m^3/s, which yields an uncertainty of an order of magnitude. Both the east and west sides of the river are considered to contribute equally to ground water. The average net gain for the reach from station 4052 to station 4075 is 3.35 m^3/s or 0.04 $m^3/s/km$ (Hunter, 1985).

North of Malaga Bend and west of the southwestern corner of the WIPP in Nash Draw are several broad shallow lakes that cover an area of about 16 km^2. The largest lake, Laguna Grande de la Sal, has existed for years, but since 1942, smaller, intermittent lakes in closed depressions north of Laguna Grande de la Sal have formed as a result of potash mining, effluence, and oil-well brine discharge in the area (Hunter, 1985). In addition to the effluence, which has also caused Laguna Grande de la Sal to grow, the lakes formed from the collection of precipitation, surface drainage, and ground-water discharge from springs and seeps. After examination of hydraulic-head data from the Culebra Dolomite and the Rustler-Salado contact residuum, and after chemical analyses of the lake water, the Culebra Dolomite waters, and the Rustler-Salado contact residuum waters, Mercer's (1983) determination was that no direct contact exists between the lakes and the lower units of the Rustler. An additional conclusion was that the ground-water source for the lake was the Tamarisk Member of the Rustler Formation. Hunter's (1985) estimate was that the rate of discharge from the ground water to the lakes in the area is 0.67 m^3/s. Some workers have concluded that very little, if any, of the water from these lakes makes it to the Pecos River (Robinson and Lang, 1938; Lambert, 1983).

The only spring of importance in the Study Area is Surprise Spring at the northern edge of Laguna Grande de la Sal. In 1942, the spring discharged at a rate of less than 0.01 m^3/s, but this rate has since declined (Lambert, 1987; Hunter, 1985). Lambert's (1987) study concurred with Mercer's (1983), which stated that no hydraulic connection exists between the underlying Culebra Dolomite and the spring and that Surprise Spring is discharging from the Tamarisk Member. Although Quaternary spring deposits have formed from evaporation of ground water that drained from the surface through fractures in Rustler Formation gypsum and emerged along the boundary of Nash Draw, no springs are active at this time (Bachman, 1981).

Ground Water

This section discusses the occurrence and movement of ground water in the vicinity of the WIPP and hydrologic properties of the hydrostratigraphic units. The properties necessary to develop a conceptual geohydrologic model

TABLE IV-2. MINIMUM AND MAXIMUM ANNUAL GROUND-WATER DISCHARGE TO THE PECOS RIVER

Pairs of Stations	Minimum Discharge (m^3/s)	Maximum Discharge (m^3/s)	Length of Reach (km)
4040-4052	0	0.29	11.6
4052-4065	0.02	0.24	43.3
4065-4070	0.01	0.12	10.5
4070-4075	0.03	0.27	14.5

Source: Modified from Hunter, 1985

will be discussed for each hydrostratigraphic unit, and each unit will be presented in ascending order from the deepest to the surface.

CAPITAN LIMESTONE AQUIFER

The Capitan Limestone aquifer is a part of the Permian-age Guadalupian aquifer system in southeastern New Mexico that consists of the shelf aquifer (San Andreas Limestone), the Capitan Reef aquifer, and the basinal aquifer (Delaware Mountain Group). Hydrologically, the shelf system is poorly connected to the reef system. The hydraulic conductivity of the shelf is about the same as for the Capitan but several orders of magnitude lower for the basinal aquifer (Hiss, 1973, 1975, 1980). Although the shelf system is important hydrologically in the region, it will not be considered separately but rather as a part of the Capitan. The Bell Canyon will be considered separately from the Capitan aquifer.

Hydraulic Conductivity and Permeability

The Capitan aquifer is a very productive unit in southeast New Mexico and is used as a water supply for the city of Carlsbad, New Mexico, but hydrologic data are scarce. Aquifer tests on six Capitan aquifer wells yielded calculated hydraulic conductivities ranging from 8×10^{-6} to 9×10^{-5} m/s (Table IV-3). An average hydraulic conductivity for the Capitan aquifer east of Carlsbad is 1.7×10^{-5} m/s. Hydraulic conductivity of the reef at the submarine canyons is about an order of magnitude lower than at the intercanyon nodes (Hiss, 1975) because of the fine materials that collected in the low areas. The igneous dike, noted earlier in "Geologic History of the Delaware Basin" in Chapter II, does not have any apparent effect on the hydraulic conductivity of the Capitan because wells on either side of the dike show that ground-water flow is not restricted (Hiss, 1975).

TABLE IV-3. HYDRAULIC CHARACTERISTICS OF THE CAPITAN AQUIFER

Location of Wells	Aquifer	Date of Completion of Test	Interval Tested Depth in ft (m), Below Land Surface or Other Reference Datum		Hydraulic Conductivity Determined from Interval Tested		Remarks
			Top	Bottom	ft/day	m/day (m/s)	
1993 ft (607 m) FEL[1] and 3060 ft (934 m) FNL[2], Sec. 5, T21S, R27E, Eddy County, NM	Capitan	8-12-69	1007 (306.7) 1024 (312.1) 1042 (317.6) 1059 (322.8) 1167 (355.7)	1014 (309.1) 1025 (312.4) 1044 (318.2) 1060 (323.1) 1170 (356.6)	2.4	0.73 (8×10^{-6})	Recovery test. Effects measured in pumped well. Well produced through 14 ft (4 m) net of perforations in casing. Well was acidized with 6,000 gal (22.7 m^3) of 15 percent hydrochloric acid. Well was swabbed at an estimated 85 gpm (463 m^3/d) for 3 1/3 hr prior to shut-in for test. Recovery measured for 140 hr.
1650 ft (503 m) FNL[2] and 1650 ft (503 m) FWL[3], Sec. 30, T21S, R28E, Eddy County, NM	Capitan	8-9-61	640 (195.1)	1060 (323.1)	16	4.98 (6×10^{-5})	Recovery test. Effects measured in pumped well. Well produced through open-hole completion. Aquifer was not treated with acid. Water produced with air lift at estimated rate of 100 gpm (545 m^3/d) for four hr. Recovery period of only 28 min. Driller reported lost circulation zone during penetration of Capitan Limestone. A similar hydraulic conductivity was estimated from specific capacity.
1650 ft (503 m) FSL[4] and 330 ft (101 m) FWL[3], Sec. 24, T21S, R34E, Lea County, NM	Capitan	1-14-65	3547 (1081.1)	5020 (1530.1)		0.92 (1×10^{-5})	Hydraulic conductivity estimated from specific capacity of well. Specific capacity was determined after well pumped at rate of approximately 240 gpm (1,308 m^3/d) over a period of about 207 hr. Well produced from open-hole completion after acidizing with 15,000 gal (57 m^3) of 15 percent hydrochloric acid.

1. From east line.
2. From north line.
3. From west line.
4. From south line.

Source: Modified from Hiss, 1975

TABLE IV-3. HYDRAULIC CHARACTERISTICS OF THE CAPITAN AQUIFER (continued)

Location of Wells	Aquifer	Date of Completion of Test	Interval Tested Depth in ft (m), Below Land Surface or Other Reference Datum		Hydraulic Conductivity Determined from Interval Tested		Remarks
			Top	Bottom	ft/day	m/day (m/s)	
1650 ft (503 m) FWL[3] and 660 ft (201 m) FNL[2], Sec. 14, T21S, R35E, Lea County, NM	Capitan	7-8-62	4178 (1273.5)	4663 (1421.3)	1.7	0.52 (6×10^{-6})	Hydraulic conductivity estimated from specific capacity of well. Specific capacity was determined after well pumped at rate of approximately 270 gpm (1472 m^3/d) over a period of about 90 hr. Well produced from open-hole completion.
1650 ft (503 m) FWL[3] and 660 ft (201 m) FWL[3], Sec. 14, T21S, R35E, Lea County, NM	Capitan	10-15-66	4178 (1273.5)	4663 (1421.3)	3.5	1.07 (1×10^{-5})	Drawdown test. Effects measured in pumped well. Well pumped only 28 min before equipment failure. Open-hole completion. Aquifer treated with 5000 gal (19 m^3) of 15 percent hydrochloric acid on March 3, 1965. Periodic cleaning of "silt" from borehole required to maintain 660 ft (201 m) FNL[2], production.
1650 ft (503 m) FWL[3] and 660 ft (201 m) FWL[3], Sec. 14, T21S, R35E, Lea County, NM	Capitan	12-14-66	4178 (1273.5)	4663 (1421.3)	1.9	0.58 (7×10^{-6})	Drawdown test. Effects measured in pumped well. Well pumped for approximately 26 hr. Average discharge rate of 328 gpm (1788 m^3/d) during test.
1650 ft (503 m) FWL[3] and 660 ft (201 m) FWL[3], Sec. 14, T21S, R35E, Lea County, NM	Capitan	12-15-66	4178 (1273.5)	4663 (1421.3)	1.4	0.43 (5×10^{-6})	Recovery test. Effects measured in production well. Well recovery measured for approximately four hr.
1313 ft (400 m) FSL[4] and 1327 ft (404 m) FWL[3], Sec. 4, T24S, R36E, Lea County, NM	Capitan	2-28-68	3875 (1181.1)	4500 (1371.6)	24	7.32 (8×10^{-5})	Drawdown test. Effects measured in pumped well. Well produced through open-hole completion. Well pumped at rate of 550 gpm (2998 m^3/d) for 10 hr after being shut in for more than 24 hr. Open-hole completion without acid treatment. Driller reported two lost circulation zones while drilling through the Capitan Limestone.

2. From north line.
3. From west line.
4. From south line.

Source: Modified from Hiss, 1975

TABLE IV-3. HYDRAULIC CHARACTERISTICS OF THE CAPITAN AQUIFER (concluded)

Location of Wells	Aquifer	Date of Completion of Test	Interval Tested Depth in ft (m), Below Land Surface or Other Reference Datum		Hydraulic Conductivity Determined from Interval Tested		Remarks
			Top	Bottom	ft/day	m/day (m/s)	
1650 ft (503 m) FWL[3] and 660 ft (201 m) FWL[3], Sec. 14, T21S, R35E, Lea County, NM	Capitan	2-28-68	3875 (1181.1)	4500 (1371.6)	25	7.62 (9×10^{-5})	Hydraulic conductivity estimated from specific capacity of well as determined during drawdown test above.
1313 ft (400 m) FSL[4] and 1310 ft (399 m) FWL[3], Sec. 16, T24S, R36E, Lea County, NM	Capitan	10-4-67	3955 (1205.5)	4500 (1371.6)	4.4	1.34 (2×10^{-5})	Hydraulic conductivity estimated from specific capacity of well. Specific capacity was determined after well pumped approximately 47 hr at rate of 504 gpm (2747 m^3/d). Well was not treated with acid. Driller reported that tools dropped from 2 to 6 ft (0.6 to 1.8 m) several times while drilling in Capitan Limestone. Lower 200 ft (61 m) of hole caved in after rotary tools were removed. Sand pump and boiler was used to remove rock fragments. The largest pieces recovered were 2 to 3 in (5 to 8 cm) in diameter. Open-hole completion.

3. From west line.
4. From south line.

Source: Modified from Hiss, 1975

Porosity

Dissolution and redeposition of the limestone by circulating ground water has changed the porosity of the Capitan aquifer. The average effective porosity of limestone in Eddy and Lea Counties ranges from 0.04 to 0.11 and averages about 0.08, with some locally very high-porosity zones such as at Carlsbad Caverns and in poorly cemented algal limey grainstones on the fore-reef edge (Hiss, 1975).

Potentiometric Surface

Two figures presented in Hiss (1980) show a pre-development potentiometric surface and a post-development potentiometric surface for the shelf, reef, and basin aquifers in Eddy and Lea Counties (Figure IV-3). During the latter part of the Cenozoic Era, several factors influenced flow in the region and also disrupted the potentiometric surface.

The five factors described by Hiss (1980) are tectonics; geomorphology; transmissivities in these aquifers; change in recharge rates; and exploitation of ground water and petroleum. As shown by Hiss (1980), flow in the region after uplift of the Guadalupe and Glass Mountains and before development of the Pecos River was to the east-southeast under a low regional gradient (Figure IV-4a). Recharge occurred in the uplands, and ground water in the aquifer moved northeast from the Guadalupes around the reef and joined with northward-flowing water from the Glass Mountains. The water then moved eastward out of the reef into Texas via the San Andreas Limestone, eventually discharging to streams draining to the Gulf of Mexico. A second big change came when the headward-eroding Pecos River finally incised the Capitan aquifer and became a discharge point for the Capitan (Figure IV-4b). Flow east of the incision reversed direction so that flow was toward the river. Recharge from the Glass Mountains continued northward into New Mexico and discharged eastward into Texas. A third important influence on flow in the Capitan is the withdrawal for the past 60 years of ground water and petroleum in the region east of the Pecos River (Figure IV-4c). The amount of flow into the Pecos River from the Capitan east of the incision has decreased substantially as has flow eastward into Texas (Hiss, 1980).

Fluid Density

The average specific gravity of the Capitan aquifer water is about 1.04, with ranges from 1.000 to 1.115. The high values (1.115) in southeastern New Mexico are near the Eddy-Lea county line in Sec. 31, T19S, R31E and near the Texas-New Mexico border. The waters get progressively more saline east of Carlsbad (Hiss, 1973). The regions of high salinity indicate active

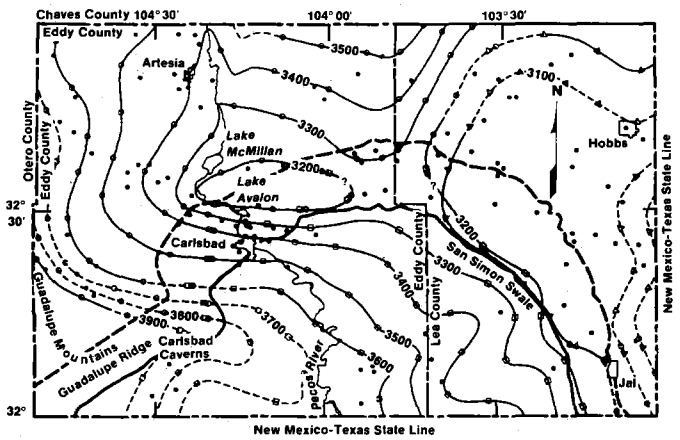

a. Pre-development

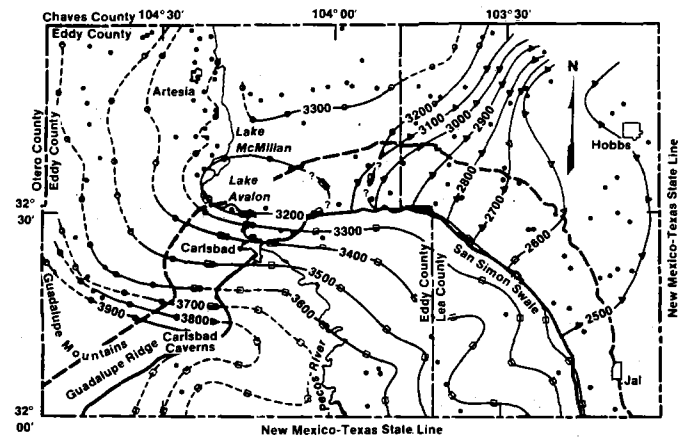

The potentiometric surface is extremely low over oil fields on the Artesia-Vacuum arch wherever the hydraulic communication of the reservoir with the Capitan aquifer is poor.

The potentiometric surface is extremely low over oil fields on the Central Basin platform wherever the hydraulic communication of the oil reservoir with the Capitan aquifer is poor.

b. Post-development

Explanation

- Well penetrating sediments of Permian Ochoan, Guadalupian, or Leonardian age
- Position of Capitan aquifer
- Approximate position of extreme shelfward edge
- Basinal edge
- Head measured in shelf aquifer system where the hydraulic communication with the Capitan aquifer is relatively poor
- Head measured in the Capitan aquifer and shelf aquifer system where the hydraulic communication between the two aquifers is relatively good
- Head measured in basin aquifer system where the hydraulic communication with the Capitan aquifer is relatively poor

Contour of head, in feet above sea-level datum, for formations of Permian Ochoan, Guadalupian, or Leonardian age. Values of head are expressed as water with specific gravity of 1.00. Contours are dashed wherever data are sparse or of doubtful reliability.

The contours express a generalized regional head considered to be representative for basin and shelf aquifers during the period 1960 to 1970. Similarly, contours in the Capitan aquifer are an interpretation of the head representative for the latter part of 1972.

TRI-6342-312-0

Figure IV-3. Pre-development and Post-development Potentiometric Surfaces for Permian Hydrostratigraphic Units in Eddy and Lea Counties, New Mexico (Hiss, 1980).

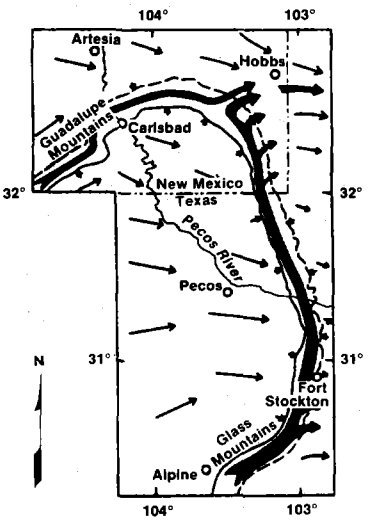

a. Regimen principally controlled by regional tectonics prior to development of Pecos River.

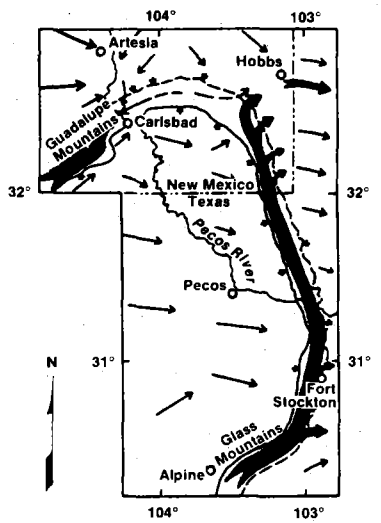

b. Regimen influenced by erosion of Pecos River at Carlsbad downward into hydraulic communication with the Capitan aquifer.

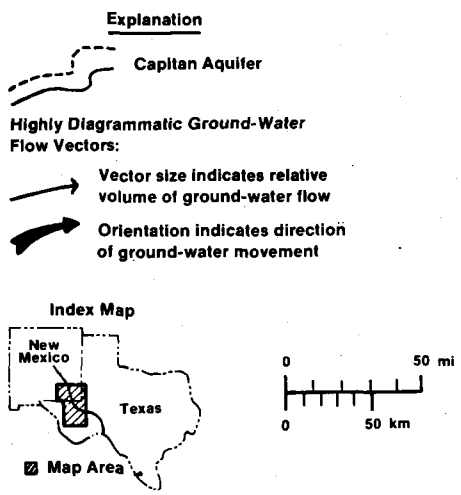

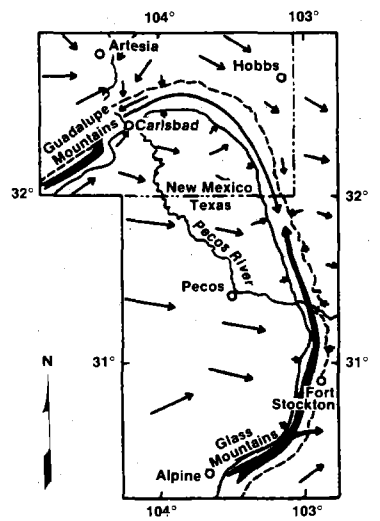

c. Regimen influenced by both communication with the Pecos River at Carlsbad and the exploitation of ground water and petroleum resources.

TRI-6342-126-0

Figure IV-4. Diagrammatic Maps Depicting the Evolution of Ground-water Regions in Permian-age Guadalupian Strata in Southeastern New Mexico and Western Texas (Hiss, 1980).

dissolution of salt, and, in areas where the Castile and Salado Formations are anomalously thin, the Capitan aquifer water is now less saline (Hiss, 1975). Also, increased salinity may be the result of ground-water flow from the Bell Canyon (see "Recharge and Discharge" in the following section).

BELL CANYON HYDROSTRATIGRAPHIC UNIT

The deepest hydrostratigraphic unit below the evaporite sequence of interest to performance assessment in the Study Area is the Bell Canyon Formation at the top of the Delaware Mountain Group. Two reasons for the interest are listed by Lappin (1988):

> The Bell Canyon may be a source for fluids that could dissolve overlying Castile and Salado Formations evaporites.
>
> The direction of fluid flow from the permeable zones in the Bell Canyon must be determined in case a drill stem that penetrates the WIPP may also penetrate the channel sands.

Horizontal hydraulic conductivity of the siltstones and shales controls flow into and out of the Bell Canyon. The upper part of this hydrostratigraphic unit, as mentioned in Chapter II, consists of tightly cemented siltstones and shales surrounding clean, poorly cemented sandstone stringers that are of special interest because of the fluids (oil, gas, or water) they may contain (Williamson, 1978).

Hydraulic Conductivity

As reported by Hiss (1975), an average hydraulic conductivity of 0.0049 m/d (6×10^{-8} m/s) is based on about 4,500 core samples taken from wells indicated as "Delaware Mountain wells" in Eddy and Lea Counties in New Mexico and Ward and Winkler Counties in Texas. His report also gave values of hydraulic conductivity from other workers that ranged from 1×10^{-7} to 2×10^{-7} m/s.

Data compiled from Bell Canyon wells in 100 oil fields in the Delaware Basin indicate an overall range of permeabilities of 0.1 md to 197 md, with a geometric mean of 7.7 md; permeabilities range from 18 md to 45 md in the northern part of the Delaware Basin, with no preferred direction of permeability (Williamson, 1978). (1 md is approximately equal to a hydraulic conductivity of 10^{-8} m/s; therefore, 7.7 md is about 8×10^{-8} m/s, which is close to Hiss's average.)

Table IV-4 presents the test results from two wells that penetrate the Bell Canyon in the vicinity of the WIPP. The hydraulic conductivities (K) for the

TABLE IV-4. SUMMARY OF BELL CANYON TEST RESULTS

Zone	Depth[a] (ft)	Test	k (md)	K (ft/day)	K (m/s)	P_{ext} (psia)[b]
DOE-2[c]						
Ramsey	4138-4180[d]	FBU[e]	8.4×10^{-2}	1.9×10^{-4}	6.7×10^{-10}	
		SBU[f]	8.8×10^{-2}	2.0×10^{-4}	7.0×10^{-10}	
		Slug	9.4×10^{-2}	2.1×10^{-4}	7.4×10^{-10}	
Olds	4177-4218[g]	FBU	0.10	2.3×10^{-4}	8.1×10^{-10}	
		SBU	9.8×10^{-2}	2.2×10^{-4}	7.8×10^{-10}	
		Slug	0.11	2.5×10^{-4}	8.8×10^{-10}	
Hays	4220-4325[h]	FBU	2.4	5.6×10^{-3}	2.0×10^{-8}	
		SBU	2.3	5.3×10^{-3}	1.9×10^{-8}	
		Slug	2.4	5.5×10^{-3}	1.9×10^{-8}	
Cabin Baby-1[i]						
Hays	4178.0-4298.6	DST-4178/FBU	0.57	1.3×10^{-3}	4.6×10^{-9}	1894[j]
		/SFL[k]	1.7	3.9×10^{-3}	1.4×10^{-8}	NA
		/SBU	0.71	1.7×10^{-3}	6.0×10^{-9}	1891[j]
		/SLUG	0.94	2.2×10^{-3}	7.8×10^{-9}	NA
Olds	4138.5-4170.9	DST-4138/FBU	2.2×10^{-2}	4.5×10^{-5}	1.6×10^{-10}	1945[l]
		/SFL	6.7×10^{-2}	1.4×10^{-4}	4.9×10^{-10}	NA
		/SBU	3.5×10^{-2}	7.2×10^{-5}	2.5×10^{-10}	1921[l]
		/SLUG	8.2×10^{-2}	1.7×10^{-4}	6.0×10^{-10}	NA
Ramsey	4100.5-4132.9	DST-4100/FBU	2.3×10^{-2}	4.7×10^{-5}	1.7×10^{-10}	1927[m]
		/SFL	8.2×10^{-2}	1.7×10^{-4}	6.0×10^{-10}	NA
		/SBU	2.9×10^{-2}	6.0×10^{-5}	2.1×10^{-10}	1903[m]
		/SLUG	8.7×10^{-2}	1.8×10^{-4}	6.4×10^{-10}	NA
Lamar	4044.2-4097.4	DST-4044/FBU	6.0×10^{-4}	1.0×10^{-6}	3.5×10^{-12}	1897[n]

a All depths are relative to kelly bushing
b psig≈psia - 10.6 psi
c Beauheim, 1986
d Effective thickness 4144-4172 ft
e First build-up period
f Second build-up period
g Effective thickness 4187-4217 ft
h Effective thickness 4255-4325 ft
i Beauheim and others, 1983b
j Pressures measured at depth 4165.4 feet
k Second flow period
l Pressures measured at depth 4125.9 feet
m Pressures measured at depth 4087.9 feet
n Pressures measured at depth 4031.6 feet

three upper, more permeable layers range from 2 x 10^{-10} m/s in the Ramsey to 2 x 10^{-8} m/s in the Hays. The uppermost Lamar shale has a hydraulic conductivity that is less than the "sands" by more than an order of magnitude. The Ramsey and Olds members (the so-called "upper sand") in Cabin Baby-1 and DOE-2 wells were absent, and siltstone replaced the channel sands; that is, the wells were probably drilled between the channels (Lappin, 1988).

Earlier tests on three other holes in the vicinity of the WIPP (AEC-7, AEC-8, and ERDA-10) (Mercer and Orr, 1979) yielded hydraulic conductivity and transmissivity data (Mercer, 1983) several orders of magnitude different than the Cabin Baby-1 and DOE-2 results (Table IV-4). The discrepancy exists because the tested units are incorrectly identified and because the data from the tests were probably not interpreted correctly (personal communication with R. L. Beauheim of Sandia National Laboratories in 1988). Any comparisons should be made with care until the data from the AEC-7, AEC-8, and ERDA-10 drill-stem tests have been reevaluated.

Porosity

Porosity ranges from 13.1 to 28.2 percent, with a mean of 21.9 percent, were reported by Williamson (1978) for 100 oil fields analyzed. An average of 15.6 percent for the 4,500 "Delaware Mountain wells" was reported by Hiss (1975), and ranges of porosity of 17.9 to 21.0 percent were reported by Hogan and Sipes (in Hiss, 1975). Williamson (1978) stated that no correlation existed between permeability and porosity, which probably results from authigenic clays (clays generated in situ) in the sands. A comparison of Bell Canyon Formation permeabilities versus porosities from oil well data from Eddy and Lea Counties showed a poor correlation.

Potentiometric Surface

In some previous studies, workers (Hiss, 1975; Mercer and Orr, 1979) reported the sandstones as probably being continuous, but Mercer and Orr (1979) indicated that two sandstone stringers in well AEC-8 that are 5 m apart with water of similar density had a head difference of about 17 m. This head discrepancy seems to indicate that the two sands are not hydraulically connected, but later water level measurements in 1983 show a head difference of less than 5 m (Richey, 1987).

A composite potentiometric map of the upper Bell Canyon units was constructed by Mercer (1983) using corrected head data from Hiss (1975) and data collected between 1975 and 1983 (Figure IV-5). Because the data may be from separate channel sands, interpretation of the data as a single hydraulically connected unit should be made cautiously.

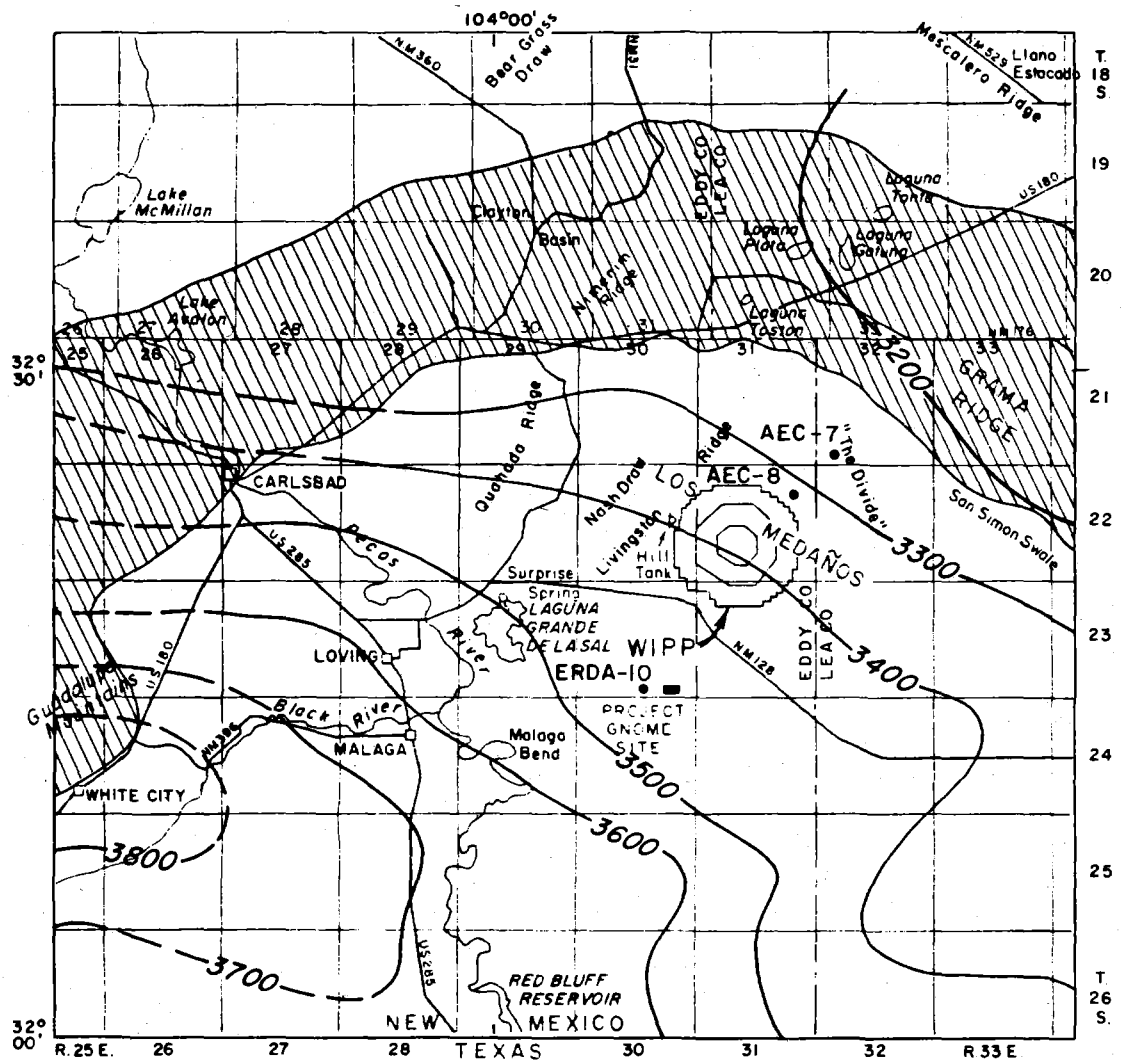

Figure IV-5. Potentiometric Surface of the Hydrologic Unit in the Upper Part of the Bell Canyon in the Study Area (Mercer, 1983).

Recharge and Discharge

Using potentiometric maps, Hiss (1975) determined that ground water flows from the Bell Canyon into the Capitan Reef. Mercer's (1983) potentiometric map (Figure IV-5) implies that recharge into the Bell Canyon by precipitation occurs near the western margin of the Delaware Basin where surface exposures of the formation exist and that discharge occurs to the east into the reef.

Lambert (1983) examined the chemistry of the Bell Canyon hydrostratigraphic unit and the Capitan aquifer waters and reached these conclusions:

> Recharge or discharge involvement of the Bell Canyon with the Capitan aquifer does not occur.
>
> Flow is not connected in the Bell Canyon.
>
> Active recharge of the Bell Canyon by meteoric water does not occur.

These conclusions require a model of ground-water flow that differs from those of Hiss (1975) and Mercer (1983). Figure IV-6 illustrates the differences between Hiss's (1975) and Lambert's (1983) models. Hiss's model (Figure IV-6a) implies ground-water movement from the Bell Canyon Formation into the Capitan. Lambert's model (Figure IV-6b) shows that ground-water flow into the Capitan is from the shelfward side only and that no flow comes from the Bell Canyon (a basin aquifer). Thus, Lambert concludes that no ground-water flow system exists in the Bell Canyon because of poor horizontal connection and that it is a stagnant system. However, as pointed out in Chapter III, direct evidence for ground-water movement indicates that the Bell Canyon is not necessarily stagnant. Oil trapped in Bell Canyon rocks where permeability and porosity changes occur indicates hydrodynamic conditions, not static conditions. Therefore, because ground-water flow does exist in the Bell Canyon, Hiss's model holds, and flow is into the Capitan.

Hydraulic Gradient

Assuming the possibility of horizontal connections, the horizontal hydraulic gradient for the Bell Canyon ranges from 0.05 (3°) to 0.07 (4°) eastward along the structural dip (Williamson, 1978; Mercer, 1983). Calculation of the head gradient from Mercer's (1983) potentiometric surface map (Figure IV-5) gives a slightly smaller gradient of 0.004 (2.3°).

The vertical fluid potential difference of Bell Canyon Formation water and Culebra Dolomite Member water is of particular interest. If a deep drill hole breached the WIPP repository and hydraulically connected the two units with the repository, the direction of fluid flow must be known. The original

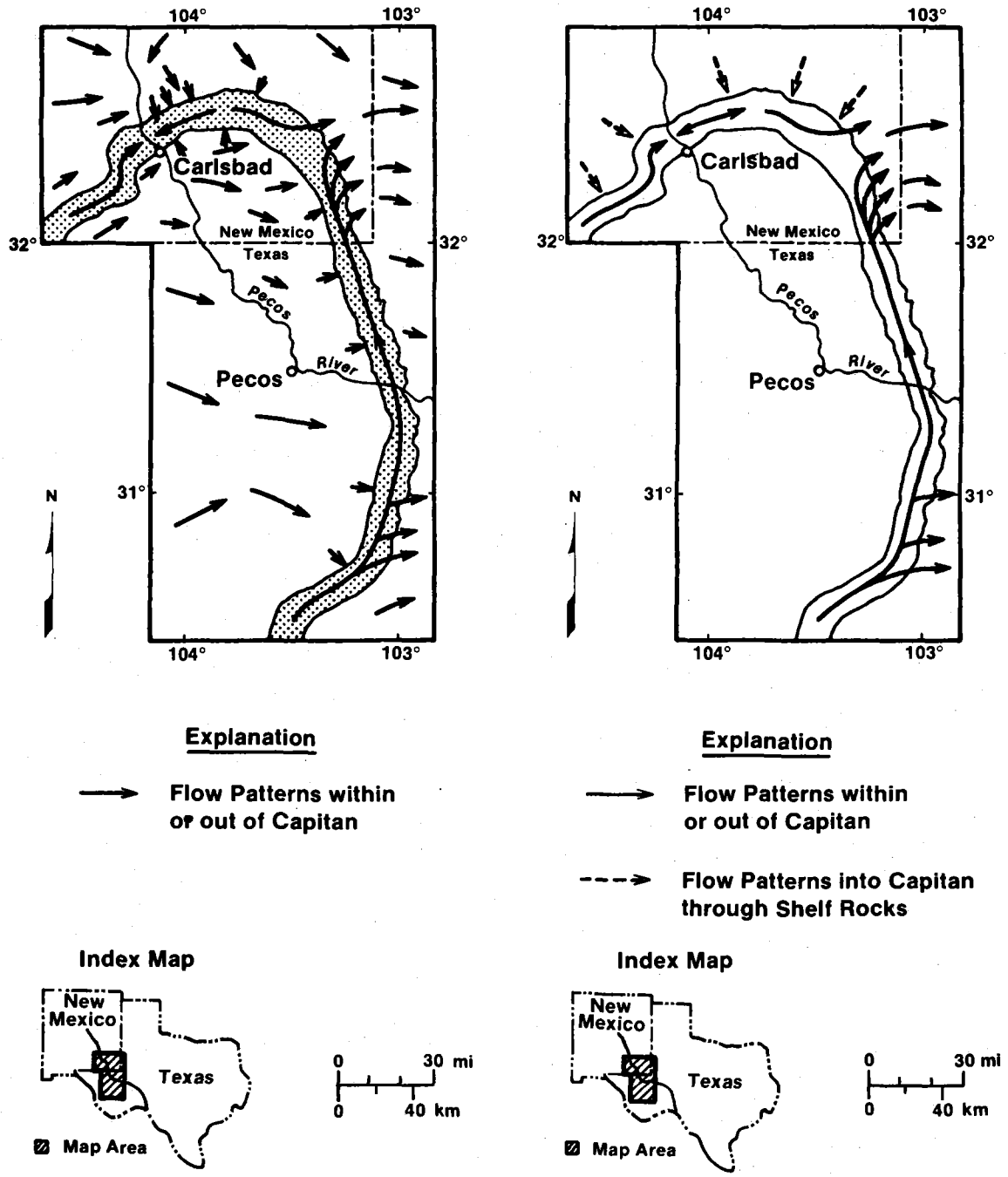

a. Hiss's 1975 Model.

b. Lambert's 1983 Model.

TRI-6342-125-0

Figure IV-6. Comparisons of Models Proposed for Ground-water Movement in the Guadalupian Rocks of the Delaware Basin. Arrows do not indicate relative magnitude, but only the direction of ground-water flow (modified from Lambert, 1983).

examination of the fresh-water equivalent heads of the Bell Canyon and the Culebra Dolomite Member (1020 and 920 m [3,335 and 3,008 ft] respectively) (U.S. DOE, 1980) indicates an upward hydraulic gradient if the Bell Canyon and Culebra Dolomite were connected by a borehole. Lappin (1988) examined recent Bell Canyon aquifer test results from test wells DOE-2 and Cabin Baby-1 and made some basic assumptions about the interconnected units. The first assumption was that, if a connection were to occur, Bell Canyon water would be much denser than the Culebra Dolomite water. Bell Canyon water at AEC-7 was reported to have a density of 1.2 g/cm^3 (Christensen and Peterson, 1981), meaning that Bell Canyon water standing in an open hole would not reach the Culebra Dolomite. The second assumption was that drilling would cause the fluids in the hole to have equal densities because of local dissolution of halite in the Salado Formation. The third assumption was that fluid potentials would affect the Salado Formation. The fourth, and last, assumption was that entrainment of waste from a possible breach of a repository panel could cause possible density changes. All things considered, if the Bell Canyon is connected to the Culebra Dolomite by an open well, vertical flow will be downward from the Culebra Dolomite to the Bell Canyon (Lappin, 1988), and the fresh-water heads do not provide a meaningful measure of vertical flow potential. Because of the poor hydraulic connection to the upper hydrostratigraphic units, the Bell Canyon will not be considered as part of the regional flow system.

CASTILE FORMATION

The Castile Formation is of interest because of its proximity to the Bell Canyon Formation and because of the occurrence of isolated pressurized brine reservoirs that some workers, particularly Anderson (1978), consider a source of water that may cause extensive dissolution of the Castile and Salado Formations.

Hydrologic data from the Castile Formation are scarce. Data for the Castile Formation are from the "brine reservoirs" in fractured anhydrite that the DOE encountered in exploratory drilling at ERDA-6 and WIPP-12 and at 13 of about 100 exploratory petroleum wells (U.S. DOE, 1982) and from drill stem tests (DSTs) in the Castile from test holes AEC-7, AEC-8, and ERDA-10 (Mercer, 1983).

Hydrologic and geochemical data indicate that the brine pockets are hydraulically isolated and contain stagnant pockets of fluid (Lambert and Mercer, 1978; Lappin, 1988). The origin of the fluids within the Castile Formation is probably interstitial entrapment of connate water after deposition, conversion by dehydration of the original gypsum to anhydrite (Popielak and others, 1983), and/or movement by meteoric waters from the

Capitan aquifer into the fractured anhydrites (Lappin, 1988). Water with high amounts of dissolved solids also occurs in the fractured, weathered portions of the Castile Formation at the western margins of the Delaware Basin far outside of the Study Area. In the Study Area, the Castile Formation is considered to be intact with no regional flow system.

Primary effective porosity (porosity of interconnected voids in the unfractured matrix through which fluid can flow) was measured on cores of anhydrite from WIPP-12 and ERDA-6 and ranged from 0.002 at a depth of 916 m (2,995 ft) at WIPP-12 to 0.016 at a depth of 792 m (2,590 ft) at ERDA-6; geophysical logs yielded secondary porosity (fracture porosity) measurements, and calculations gave a range of 0.001 to 0.01 (Popielak and others, 1983).

Hydraulic conductivities of the Castile Formation obtained from DSTs of the Castile Formation are less than the sensitivity of the testing apparatus (Mercer and Orr, 1977; Mercer, 1983; Mercer, 1987). A conservative estimate by Mercer (1983) of the hydraulic conductivity of the Castile Formation based on the sensitivity of the testing instruments would be about one nanodarcy (1.0×10^{-14} m/s). Mercer's (1987) estimate was less than 0.1 microdarcy (1.0×10^{-12} m/s).

SALADO FORMATION

As in the Castile Formation, ground-water occurrence in the Salado Formation is restricted to areas in the Delaware Basin where extensive dissolution of the halite has occurred and only a breccia remains. In the Study Area, where the Salado Formation is intact, circulation of ground water is minimal or non-existent because, as is the nature of the highly plastic salt deposits, primary porosity and open fractures are lacking (Mercer, 1983). Mercer's (1987) analysis is as follows:

> Investigations to date of the Salado Formation at the WIPP site do not indicate an active, circulating, ground-water system. Small pockets of nitrogen-rich gas and brine under pressure have been encountered, however, during drilling operations and in nearby potash mining activities. An active ground-water system is defined here as one that is now active and one in that ground water moves along a flow system (be it along fractures or through an interconnected intergranular porosity under a hydraulic gradient) from areas of recharge to areas of discharge. That system is a dynamic and not a static one. Even though the salt may have a regional hydrostatic pressure gradient, as evidenced by testing or may be saturated with fluid, the limiting low permeability probably would result in an imperceptible rate of fluid movement in conventional hydrologic considerations. The permeability of the competent halite is so low that the halite can be considered to provide isolation of the waste during the required life of the facility (10,000

> years) provided the very low permeability is not disrupted by a breach of the facility. This does not, however, preclude the possibility for local fluid movement in response to deformation or a response to WIPP facility excavation or borehole stress concentration relief. Also, if there were continuous interconnection between the cavities of nitrogen-rich gas or brine, this interconnection could provide a potential pathway for radionuclides to migrate should the WIPP facility be breached.

Permeability of the Salado Formation is very low but measurable (Mercer, 1983, 1987). The average permeability of rock salt at lithostatic pressure stated by Powers and others (1978) is 0.05 microdarcies. DSTs in seven wells in the Salado Formation by Mercer (1987) and in the walls of the WIPP by Stormont and others (1987) also indicate measurable permeabilities in this formation. Tables of the DSTs reported by Mercer and others (1987) and Mercer (1987) show a range of permeability from 9 nanodarcies to 25 microdarcies throughout the Salado Formation. All testing assumed a porosity of 0.001.

The DSTs were summarized by Mercer (1987) as follows:

> [I]t appears that the bulk permeability of most of the test intervals in the Salado Formation is less than 0.1 microdarcy, the sensitivity limit of the test system. Other drill-stem tests in the Salado would indicate that the bulk permeability of the competent halite may approach 25 microdarcies.

The well head pressures of wells completed in the Salado Formation vary, but in some wells the hydraulic heads are higher than the hydraulic heads in aquifers in the overlying Rustler Formation. No measurable buildup of pressure was found at the surface at wells DOE-2 and AEC-7 as was found at some potash wells and Cabin Baby-1, WIPP-12, and WIPP-13 (Mercer, 1987). Cabin Baby-1, WIPP-12, and WIPP-13 had extrapolated surface pressures between lithostatic and hydrostatic pressures that were, however, rapidly depleted, with very little fluid produced.

The above-mentioned, surface-based attempts of DSTs on the Salado interval to determine hydraulic properties were examined by Beauheim and Saulnier (in prep.) and were found unreliable. Their evaluation is summarized as follows:

> In Wells AEC-7 and AEC-8, no interpretable results were obtained because no flows were observed, although pressures increased in tests that were only one hour or less in length.
>
> In examination of ten ERDA-9 tests of the Salado interval, no flow was observed during the DST, no buildup data were fitted to type curves, and time matches were used incorrectly to estimate permeabilities.

Estimates of Cabin Baby-1 were determined to be poorly defendable upper bounds because recovery responses for earlier tests (pre-1983) were superimposed on 1983 DSTs.

Interpretation of two DSTs from DOE-2 overestimated permeabilities because of a poor fit to type curves.

WIPP-12 tests were not designed to determine permeabilities.

Beauheim and Saulnier concluded that surface-based tests are unreliable or inconclusive at best because of the extended period required to test a unit of such low permeability as exists in the Salado Formation.

The WIPP repository itself provides an environment for in situ testing of the halite of the Salado Formation. Gas-flow measurements in the wall of the repository gave a calculated permeability of 1 to 10 nanodarcies (Stormont and others, 1987). Higher permeabilities (in the microdarcy range) are the result of disturbance of the salt, and the lower measurements are probably more indicative of the undisturbed salt and anhydrites. Figure IV-7, from Peterson and others (1985), illustrates that gas permeability may be inversely related to test-interval depth and could also be related to presence of brine in pores. The permeability range is from nanodarcies to microdarcies. All testing assumed a porosity of 0.001. Borns and Stormont (1988) calculated the free water content around the WIPP excavations to be from 0.5 percent to 1.0 percent by weight (approximately 1 percent to 2 percent by volume) to between 2.0 percent to 3.0 percent by weight (approximately 4 percent to 6 percent by volume) at several meters depth.

The depth of disturbance has not been determined. Flow tests were conducted in the halite with gas; brine was then injected, and the halite was retested with gas (Peterson and others, 1987). The gas was initially injected at a pressure of 2.1 MPa, and the permeability was calculated. The halite was then injected with brine. After the brine injection, an attempt to inject gas at about 3.5 MPa failed, but brine began to flow into the borehole. In a personal communication with J. C. Stormont of Sandia National Laboratories in 1988, he concluded that the halite had become unsaturated before the gas flow test was conducted and that measurements of the disturbed-rock permeability were made. The brine injection then resaturated the halite, reconnected the enlarged disturbed pores, and aided brine flow from the undisturbed halite to the borehole. Stormont also suggested that future coring should be done with overcoring to preserve fracturing in order to determine the extent of the halite disturbance.

Pulse injection tests using a multipacker test tool were conducted in the Salado Formation at the 259.1-m (850-ft) and 402.3-m (1320-ft) intervals of

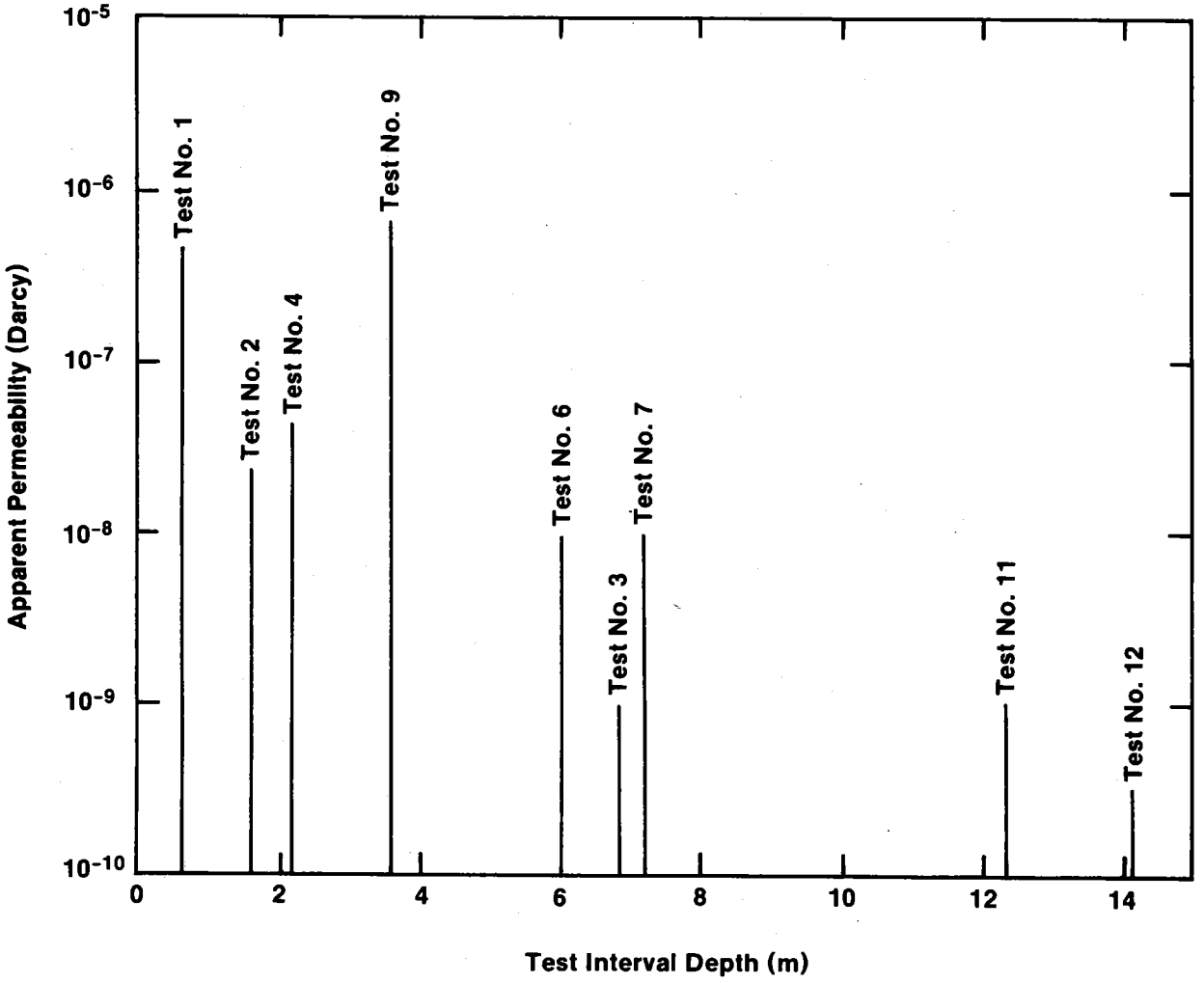

TRI-6342-128-0

Figure IV-7. Variation in Measured Gas Permeability with Increasing Test-Interval Depth (Peterson and others, 1985).

the waste-handling shaft above the WIPP repository and have yielded more reliable results. Table IV-5 is a summary from Saulnier and Avis (1988). Hydraulic conductivities ranged from 3 x 10^{-14} m/s to 1 x 10^{-13} m/s (permeabilities of 3 x 10^{-21} m^2 to 1 x 10^{-20} m^2).

Bredehoeft (1988) assumed Darcian flow in the salt to estimate brine inflow based on the following observations:

Fifty-four boreholes in the floor and ceiling of the repository produce fluids.

Salt efflorescences occur throughout the mine.

Experimental heater holes produce fluids.

Complete boreholes in the evaporites produce brine.

Permeability is measurable in the Salado Formation (about 10 nanodarcies).

His conclusions were that the Salado Formation is not "dry" but is a saturated, permeable medium and that once the repository is closed, brine will flow into the repository at a rate of 0.01 ℓ/day/m of tunnel. Nowak and others (1988), using properties similar to properties used by Bredehoeft,

TABLE IV-5. SUMMARY OF HYDRAULIC CONDUCTIVITIES AND FORMATION PRESSURES INTERPRETED FROM THE TESTING OF THE BOREHOLES IN THE WASTE-HANDLING SHAFT

Borehole	Lithology	Test Zone	Depth Interval from Shaft Wall (ft)	Test Period	Hydraulic Conductivity (m/s)	Apparent Formation Pressure (psig)	Apparent Formation Pressure (PA)
W850W	Halite	1	18.6-26.0	07-30/08-03/87	1.0 E-13	40	2.76 x 10^5
		2	12.3-15.9	08/2-3/87	1.0 E-13	40	2.76 x 10^5
		3	5.4-9.5	07-31/08-3/87	Not Analyzable		
W850SE	Halite	1	23.2-36.0	08/19-24/87	3.0 E-14	50	3.45 x 10^5
		2	16.8-20.5	08/21-24/87	3.0 E-14	45	3.10 x 10^5
		3	10.0-14.1	08/22-24/87	2.0 E-14	90	6.21 x 10^5
W1320E	Polyhalite/	1	18.6-41.8	08/11-17/87	2.0 E-14	550	3.79 x 10^6
	Anhydrite/	2	12.3-15.9	08/14-17/87	3.0 E-14	450	3.10 x 10^6
	Halite	3	5.4-9.5	08/15-17/87	3.0 E-14	100	6.90 x 10^5

Source: Saulnier and Avis, 1988

calculated a brine accumulation in the range of 4 to 43 m^3 (141 to 1,518 ft^3) per 100 yr. Nowak and others set an upper bound at a rate of 0.013 ℓ/day/m of tunnel, similar to Bredehoeft's calculation.

In summary, the Castile and Salado Formations have very low permeabilities and effective porosities. Measured permeabilities vary from the nanodarcy range to 25 microdarcies (now believed to be invalid), and porosities are on the order of 0.001 to slightly higher. Salado Formation pressure varies from less than or almost hydrostatic in the vicinity of the WIPP to about 11 MPa (lithostatic is about 14.8 MPa at repository level). Although the formations may be saturated, the low effective porosity allows for very little ground-water movement. Although the degree of saturation is not known, for performance assessment calculations the Salado Formation is assumed to be completely saturated, with brine that has a density of about 1.22 g/ℓ.

RUSTLER FORMATION

Ground-water flow in the Rustler Formation is restricted mostly to the Rustler-Salado contact residuum and the Culebra Dolomite and Magenta Dolomite Members. Appropriately, the discussion of the hydrology in the Rustler Formation is restricted to these three hydrostratigraphic units. The intervening units considered as the aquitards are the unnamed lower member, the Tamarisk Member, and the Forty-niner Member (even though at some locations, a thin claystone in the Forty-niner has a transmissivity as high as that of the Magenta [Beauheim, 1987b]). Data from these units are restricted to wells H-14 and H-16.

Three scales of testing have been performed in WIPP characterization studies:

> Near-field tests such as slug tests and bailer tests where a measured amount of water is injected or withdrawn and the rate of recovery is measured, yielding a transmissivity value for a small effective radius (meters scale).
>
> Hydropad tests where one well on a hydropad is pumped and the other wells on that hydropad are used to observe drawdown and recovery rates, yielding values on a scale of several tens of meters.
>
> Multipad tests where a well on one hydropad is pumped and the drawdown and recovery rates are observed up to hundreds and, in some cases, thousands of meters away.

AQUITARD UNITS OF THE RUSTLER FORMATION

Only one DST of the unnamed lower member, at H-16, has been performed to date. The test was conducted in a siltstone unit to determine the transmissivity and

hydraulic head for calculations of potential vertical leakage and leakage into the shaft (Beauheim, 1987b). Beauheim's (1987b) calculated transmissivities were 2.9×10^{-10} and 2.4×10^{-10} m^2/s for the first and second buildup periods, respectively, of the DST. Simulations of a single-porosity medium used the first transmissivity and a skin factor of -0.4 and assumed a porosity of 0.3, a system compressibility of 1.0×10^{-5}, and a viscosity of 1.0 cp. The simulations showed an excellent fit to the data curve for the first buildup, indicating a static formation pressure of 1.47×10^6 Pa. A second simulation requiring a slightly lower transmissivity to indicate well damage yielded a pressure of 1.44×10^6 Pa. From these results, Beauheim's (1987b) estimated pressure for the claystone unit tested was 1.58×10^6 Pa at an elevation of 793 m.

Tests in three horizontal boreholes in the waste-handling shaft at the WIPP yielded very low hydraulic conductivities for the unnamed lower member. The tests on a silty mudstone at 238.3 m (782 ft) below ground surface (BGS) and on a silty claystone measured in two directions at 245.4 m (805 ft) BGS had hydraulic conductivities ranging from 6×10^{-15} m/s to 1×10^{-13} m/s (Saulnier and Avis, 1988).

Attempts were made to test a 2.4-m (8-ft) sequence of the Tamarisk Member, which consists of claystone, mudstone, and siltstone overlain and underlain by anhydrite in wells H-14 and H-16. The tests were conducted to obtain the hydraulic head and transmissivity of the member to determine potential directions of vertical flow (Beauheim, 1987b). According to Beauheim (1987b), H-14 had no static formation pressure, and well H-16 had a static formation pressure of less than 1.30×10^6 Pa at 208 m (680 ft) below the surface (831 m above mean sea level). Permeability of the Tamarisk Member was too low to yield transmissivity values in both wells at the time scale of a few days, but according to Beauheim's (1987b) estimates, the transmissivity of the claystone sequence was one or more orders of magnitude below the values calculated for the unnamed lower member.

The Forty-niner Member was also tested in wells H-14 and H-16 to determine whether leakage from the Dewey Lake Red Beds is recharging the Magenta Dolomite and Culebra Dolomite Members and, therefore, reaching the shafts at the WIPP, and to obtain data for cross-sectional and three-dimensional flow modeling of the site. The tests were conducted on a clay unit in well H-14 and on a claystone in well H-16. Two DSTs and a slug test in H-14 yielded a mean transmissivity of about 4×10^{-9} m^2/s and a formation pressure of 71 psig. Two DSTs, a slug test, and a pulse test of H-16 yielded a mean transmissivity of 2×10^{-10} m^2/s and a formation pressure of 117.2 psig.

In Nash Draw, the aquitard units, where present, have increased hydraulic conductivities due to erosion, dissolution, and karstification. In lower Nash Draw, the unnamed lower member and Culebra Dolomite have a good hydraulic connection and may be considered as one hydrostratigraphic unit under water table conditions. Porosity of the saturated zone in lower Nash Draw ranges from 0.12 to 0.30, and the hydraulic conductivity ranges from 10^{-7} to 10^{-5} m/s (Geohydrology Associates, Inc., 1979).

In summary, the unnamed lower member, Tamarisk Member, and Forty-niner Member are aquitard units of low permeability throughout the Study Area. Horizontal hydraulic conductivity in the unnamed lower member is slightly higher than the vertical conductivity because of the siltstone sandwiched between hydraulically tighter anhydrite/gypsum sections. Horizontal conductivity of the Forty-niner Member is also higher than the vertical conductivity for the same reason. The claystone/mudstone/siltstone section of the Tamarisk has a conductivity too low to measure, and for modeling purposes, the Tamarisk can probably be considered as an isotropic, homogeneous unit. Beauheim (1987b) used a porosity of 0.3 for the claystone calculations. Anhydrite and halite porosity is much lower, about 0.01 or less. The estimated hydraulic conductivities calculated from the transmissivities of the three hydraulically tight units are, in ascending order, 1×10^{-10} m/s, 1×10^{-12} m/s, and 1×10^{-9} m/s. The Tamarisk Member was too tight to test, and the value of 1×10^{-12} m/s is an estimate.

RUSTLER-SALADO CONTACT RESIDUUM HYDROSTRATIGRAPHIC UNIT

The Rustler-Salado contact residuum or "brine aquifer" in the vicinity of Nash Draw occurs as a dissolution residue above the halite of the Salado Formation at the Rustler Formation contact (Robinson and Lang, 1938; Mercer and Orr, 1977; Mercer, 1983). According to Lang (1938, in Robinson and Lang, 1938), "...the structural conditions that caused the development of Nash Draw might also control the position of a body of salt water beneath it in the basal Rustler." Subsequent drilling and testing have confirmed Lang's (1938) conjecture to some extent (Figure IV-8), but evidence pointed out by Mercer (1983) indicates that in wells P-14 and H-7, the brine aquifer extends farther east than first reported. Estimates by Robinson and Lang (1938) were that the elongated aquifer thickens northward and has a range of thickness from 3 to 30 m and a mean thickness of about 8 m. More recent information (Lappin and others, 1989) shows a range of 2.4 m in test hole P-14 to 36 m in test hole H-16.

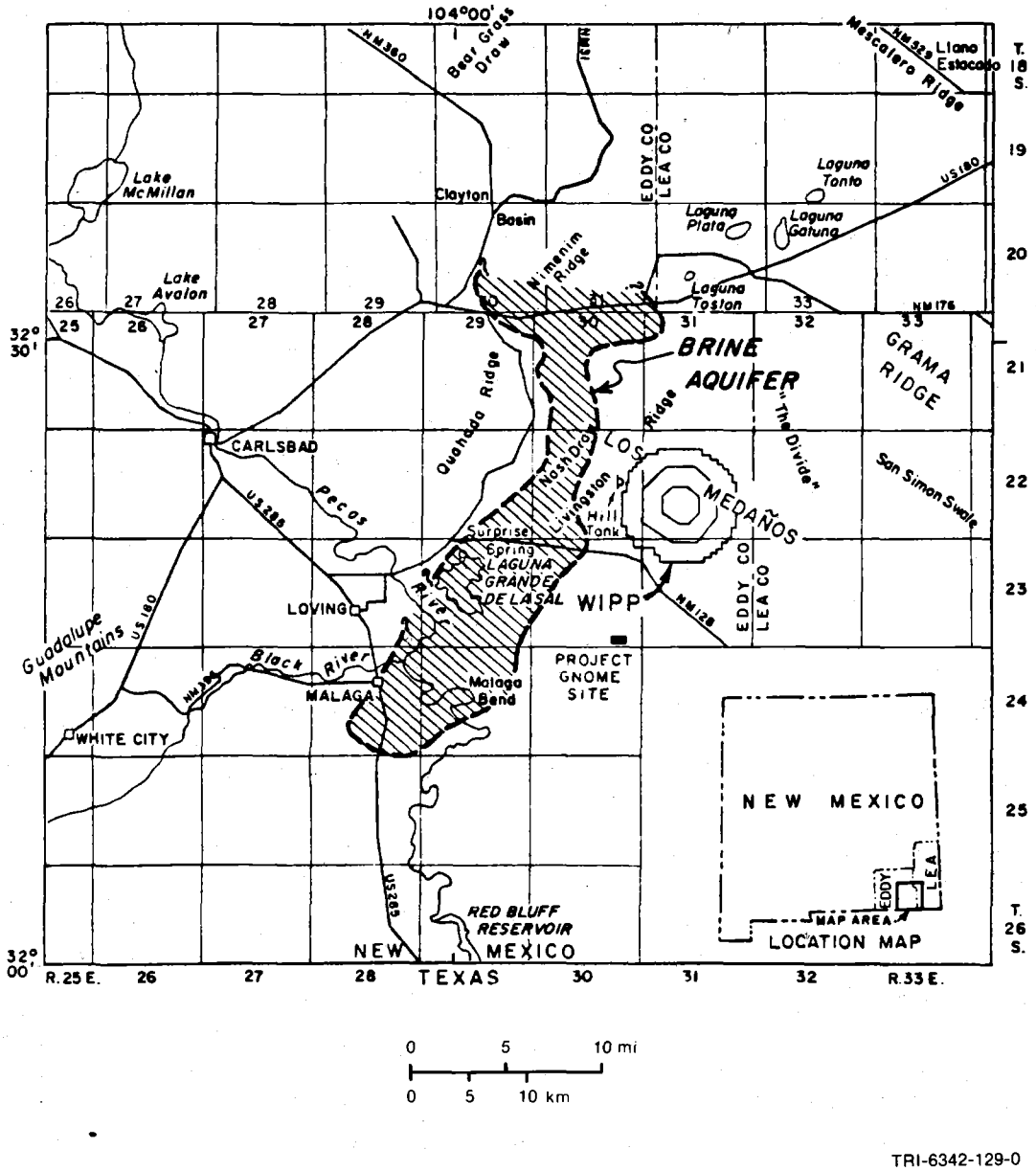

TRI-6342-129-0

Figure IV-8. Approximate Areal Extent of the "Brine Aquifer" in the Study Area (Mercer, 1983).

Hydraulic Conductivity

Hydraulic conductivity data pertaining to the Study Area are concentrated in and around the WIPP with the exception of a few data points near Malaga Bend. In the discussion of hydraulic conductivity (K) of the Rustler Formation hydrostratigraphic units, where more data are available, the logs of K are used because hydraulic conductivity is assumed to be log-normally distributed (Freeze, 1975). A thorough discussion of transmissivity and hydraulic conductivity data from the WIPP is given in the "Culebra Dolomite (Rustler Formation) Hydrostratigraphic Unit" discussion in this chapter and in Appendix A. The range of the logs of the hydraulic conductivities (Table IV-6) is from -12 to -6 (10^{-12} to 10^{-6} m/s), with a mean of the logs of -9.4. The log hydraulic conductivities for Nash Draw are higher by several orders of magnitude than are the values east of the draw (Figure IV-9). Nash Draw log hydraulic conductivities range from -8 to -6 (10^{-8} to 10^{-6} m/s). Eastward, the range is from -12 to -9 (10^{-12} to 10^{-9} m/s). Near Malaga Bend, the log hydraulic conductivity was reported by Hale and others (1954) and Havens and Wilkins (1979) to be around -3.2 (6×10^{-4} m/s). The contour plot of the log hydraulic conductivities measured in the brine aquifer indicates that the aquifer becomes tighter east of Nash Draw (Figure IV-9).

Porosity

Effective porosity estimates for the brine aquifer range from 0.15 to 0.33 (Hale and Clebsch, 1958; Robinson and Lang, 1938; Geohydrology Associates, Inc., 1979; Mercer, 1983). An average effective porosity of 0.2 was used in previous work (Hale and Clebsch, 1958, and Mercer, 1983) and is used in this study.

Potentiometric Surface

A contour map of the potentiometric surface adjusted to fresh-water density illustrates the decrease in hydraulic conductivity east of Nash Draw (Figure IV-10). Fresh-water heads are estimated using available water density data and are only as good as the data. The water density was measured at the time the water level was measured, and the degree of mixing of waters in the well bore is not known (see also "Fluid Density" and "Potentiometric Surfaces and Ground-Water Flow" in Appendix A for a discussion of the use of fresh-water heads and potentiometric surfaces and their relationship with water density). At the WIPP, where the hydraulic conductivity is low, the potentiometric surface is steep. West of the WIPP, where the hydraulic conductivity is several orders of magnitude higher, the surface is flatter. The gradient in Nash Draw is 0.002, and the gradient at the WIPP is 0.007. If

TABLE IV-6. SUMMARY OF HYDRAULIC PARAMETERS OF THE RUSTLER-SALADO CONTACT RESIDUUM FROM SELECTED TEST HOLES IN THE STUDY AREA

Hydropad Name	Transmissivity[a] (m^2/s)	Hydraulic Conductivity (m/s)	Log Hydraulic Conductivity	Water Level (m)	Water Density (g/cm^3)	Residuum Thickness Tested[b] (m)	Storativity	Halite[c]
H-1	3×10^{-10}	4×10^{-11}	-10.4	--	--	7	--	2
H-10	9×10^{-11}	5×10^{-12}	-11.2	--	--	17	--	2
H-2	1×10^{-10}	6×10^{-12}	-11.2	951	1.225	16	--	2
H-3	3×10^{-10}	4×10^{-11}	-10.4	--	--	7	1.0×10^{-4}	2
H-4	6×10^{-10}	4×10^{-11}	-10.4	905	1.215	15	1.0×10^{-4}	2
H-5	3×10^{-11}	2×10^{-12}	-11.7	--	--	16	1.0×10^{-3}	2
H-6	3×10^{-9}	2×10^{-10}	-9.6	915	1.21	13	1.0×10^{-6}	0
H-7	8×10^{-7}	4×10^{-8}	-7.3	904	1.048	19	--	0
H-8	3×10^{-9}	1×10^{-10}	-9.9	918	1.129	22	--	1
H-9	2×10^{-10}	2×10^{-11}	-10.7	--	--	10	--	1
P-14	5×10^{-8}	7×10^{-9}	-8.1	917	1.126	7	--	1
P-15	4×10^{-10}	4×10^{-11}	-10.4	924	1.16	9	--	2
P-17	2×10^{-10}	3×10^{-11}	-10.5	926	1.193	7	1.0×10^{-4}	2
P-18	3×10^{-11}	4×10^{-12}	-11.4	--	--	7	1.0×10^{-5}	4
WIPP-25	5×10^{-6}	6×10^{-7}	-6.3	917	1.093	9	1.0×10^{-3}	0
WIPP-26	4×10^{-7}	1×10^{-8}	-7.9	910	1.189	31	--	0
WIPP-27	2×10^{-10}	2×10^{-11}	-10.7	930	1.207	10	--	0
WIPP-28	9×10^{-7}	7×10^{-8}	-7.2	941	1.152	13	--	0
WIPP-29	9×10^{-6}	9×10^{-7}	-6.0	911	1.129	10	--	1
WIPP-30	2×10^{-7}	3×10^{-8}	-7.5	978	1.204	7	1.0×10^{-4}	1
H-16[b]	2×10^{-10}	5×10^{-12}	-11.3	--	--	36	--	1

[a] Mercer, 1983
[b] Lappin and others, 1989
[c] Presence of halite in well (Beauheim, 1987b)
- 0 West of upper Salado dissolution front
- 1 Salado present
- 2 Halite in unnamed lower member
- 3 Halite in unnamed lower member and Tamarisk Member
- 4 Halite in unnamed lower member, Tamarisk Member, and Forty-niner Member

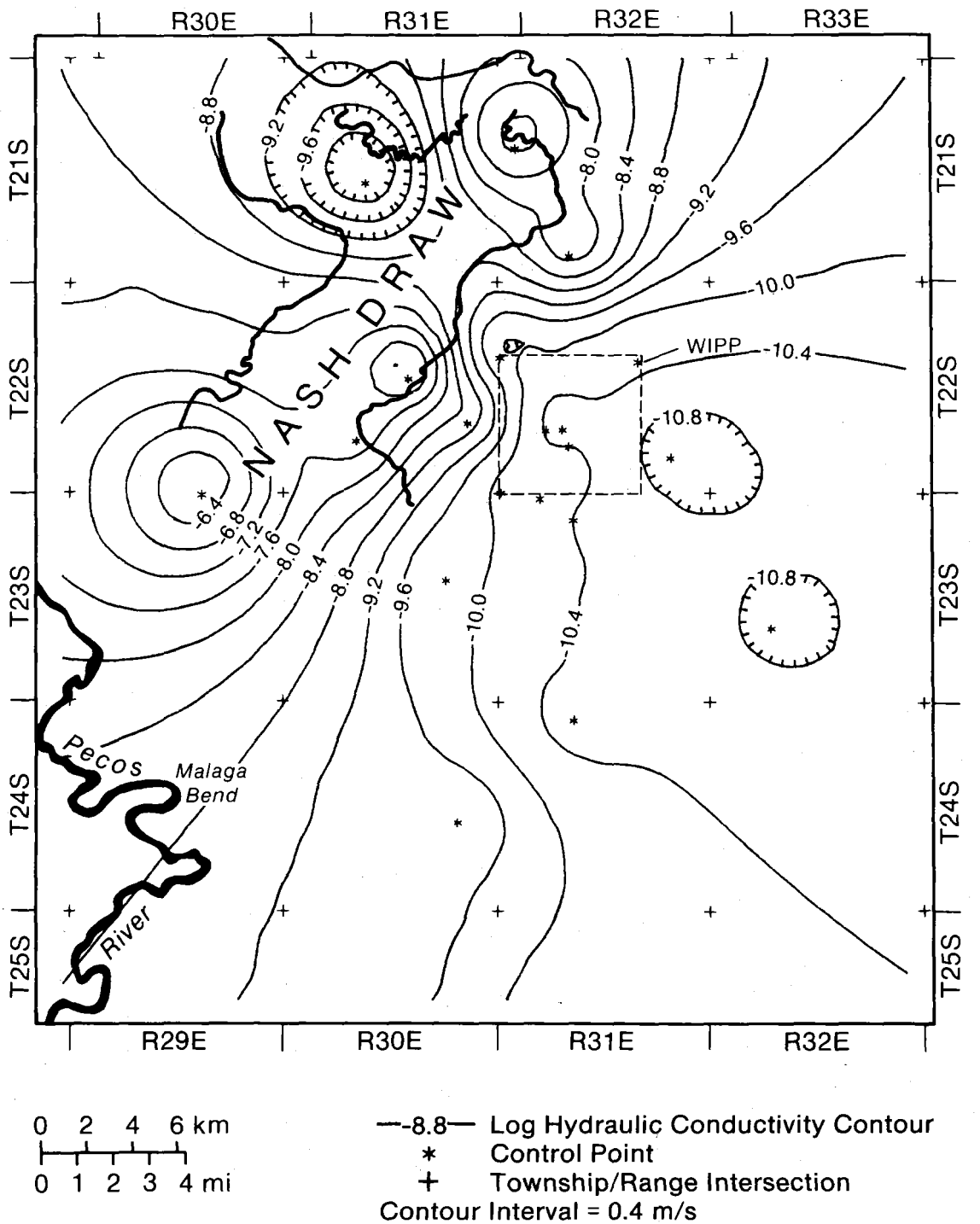

Figure IV-9. Contour Plot of the Log Hydraulic Conductivities of the Rustler-Salado Contact Residuum in the Study Area.

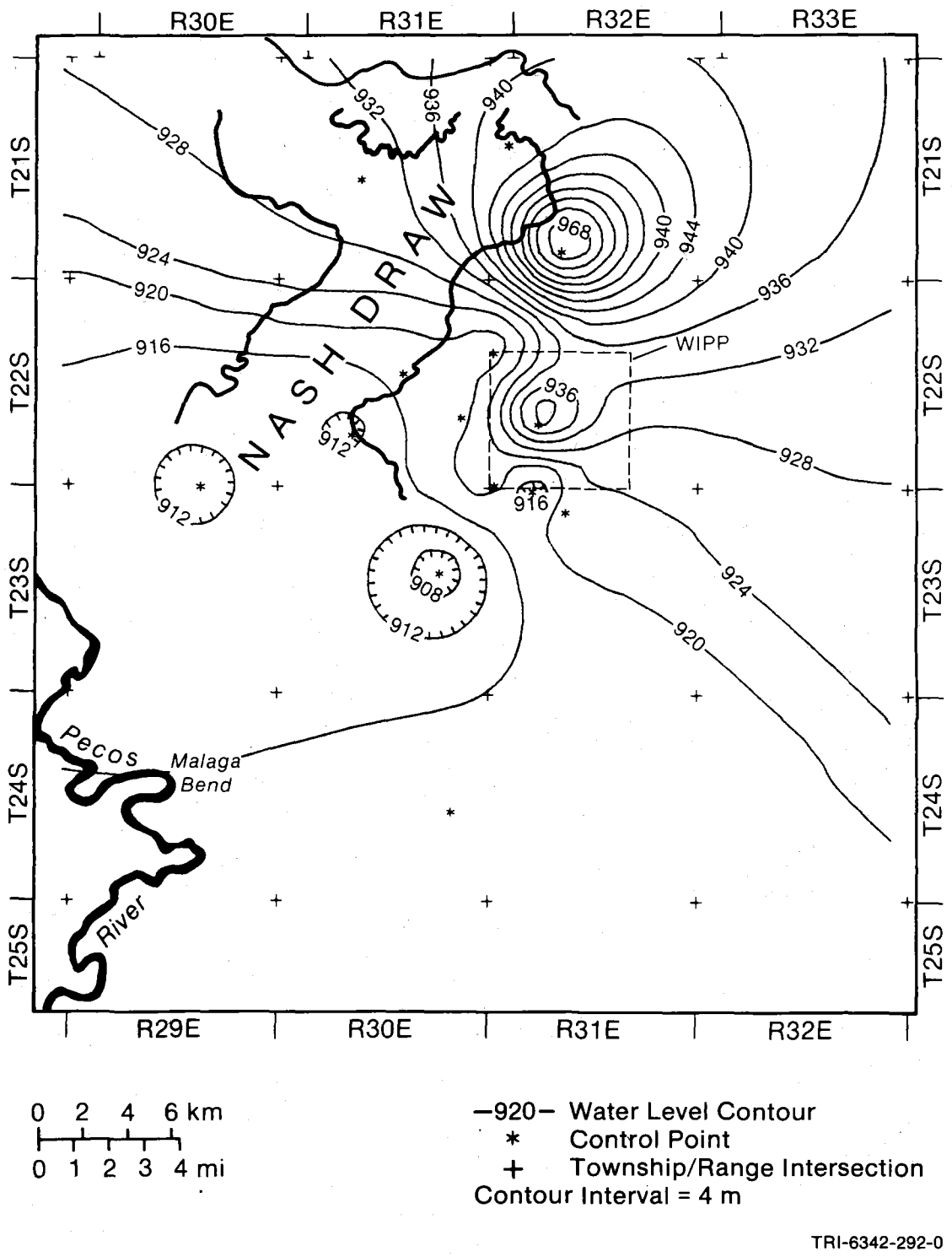

Figure IV-10. Adjusted Potentiometric Surface of the Rustler-Salado Contact Residuum in the Study Area.

the aquifer in the vicinity of the Pecos River is assumed to be a water-table aquifer with connection to the river, flow will be toward the river (Figure IV-11).

Storativity

Although storativity (storage coefficient) is not needed in steady-state model simulations, it is discussed here and used in transient modeling efforts. Most confined aquifers have a storativity that ranges from 10^{-5} to 10^{-3} (Lohman, 1972). The only measurements that are available from the brine aquifer are in Mercer (1983), and they all fall within this range except for well H-6c, which has a value of 10^{-6} (Table IV-6).

Fluid Density

The waters from the Rustler-Salado contact residuum are classified as brines containing mostly sulfates and chlorides of calcium, magnesium, sodium, and potassium. Sodium and chloride are the major constituents (Mercer, 1983) and are the highest concentration of dissolved solids in the WIPP area. The lowest density water (1.048 g/cm^3) is at well H-7c and has a concentration of dissolved solids of 79,800 mg/ℓ. The highest density water (1.25 g/cm^3), which has a concentration in excess of 450,000 mg/ℓ, is at test hole H-2c (Table IV-6). A contour map based on available data (albeit sparse) illustrates how the density of brine in the Rustler-Salado contact residuum waters vary (Figure IV-12). The contour map does not indicate it, but generally the brine becomes more concentrated as it moves toward the southwest and becomes nearly saturated in the lower region of Nash Draw near the Pecos River (Lang, 1938; Mercer, 1983).

Recharge and Discharge

Recharge to and discharge from the brine aquifer at Laguna Grande de la Sal and the relationship of Surprise Spring to the lake was first investigated by Robinson and Lang (1938) and later by Hale and others (1954) and Mercer (1983). Robinson and Lang (1938) and Mercer (1983) believed that the lake is not hydraulically connected to the brine aquifer. Observations showed that the waters from wells in units under the lake had a lower chloride content than the lake water and that wells near the lake that penetrated lower units were flowing. According to Theis and Sayre (1942, cited in Mercer, 1983), water levels in the lake are "high in winter and low in summer, whereas the hydraulic head in the brine aquifer is high in the irrigation season and low between seasons." The confined lower aquifer theory is invoked by Mercer on the basis of a flowing potash test well in the Culebra Dolomite 1 km north of Laguna Grande de la Sal. In addition, the WIPP-29 waters are higher in sodium

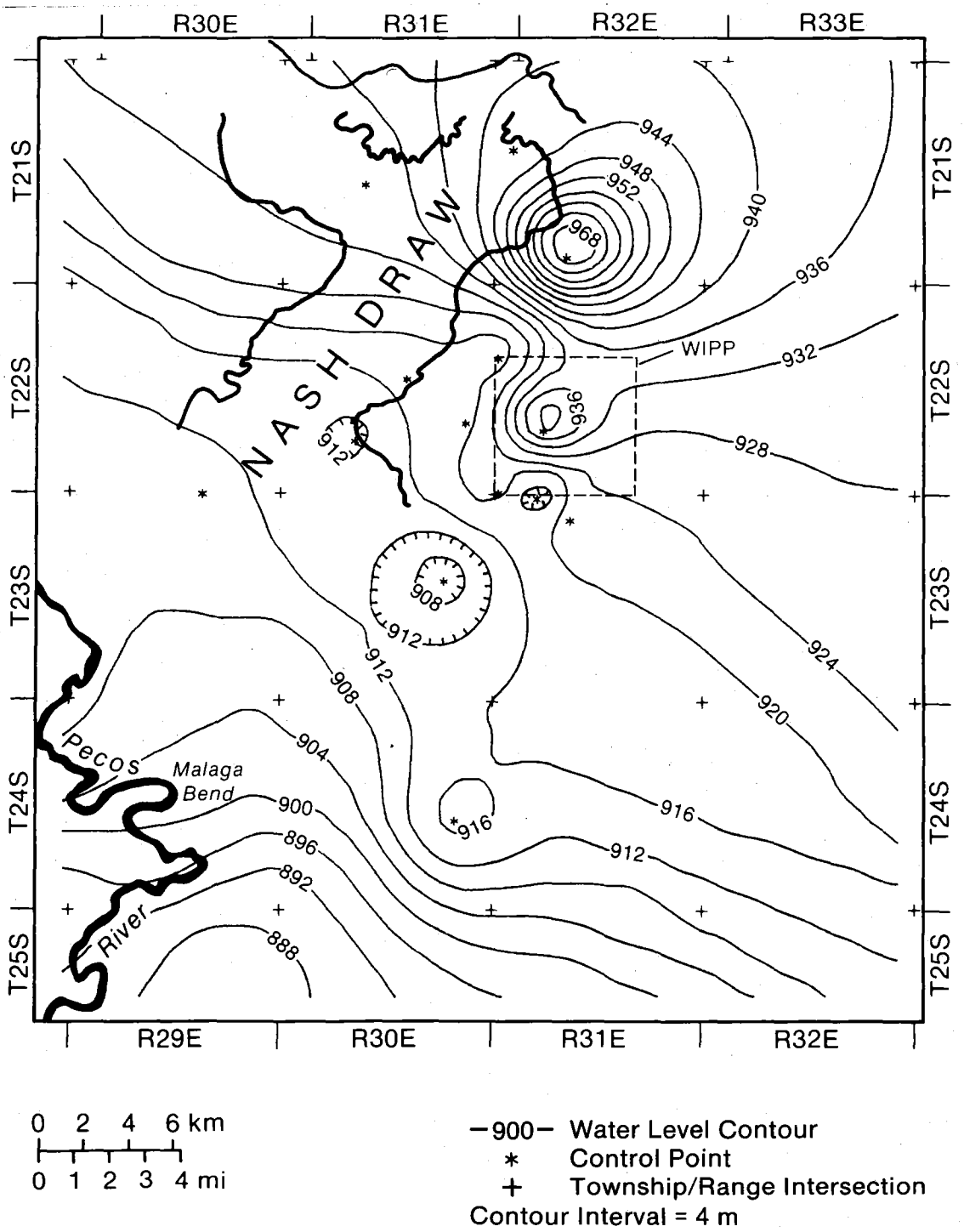

Figure IV-11. Adjusted Potentiometric Surface of the Rustler-Salado Contact Residuum in the Study Area (Pecos River heads included).

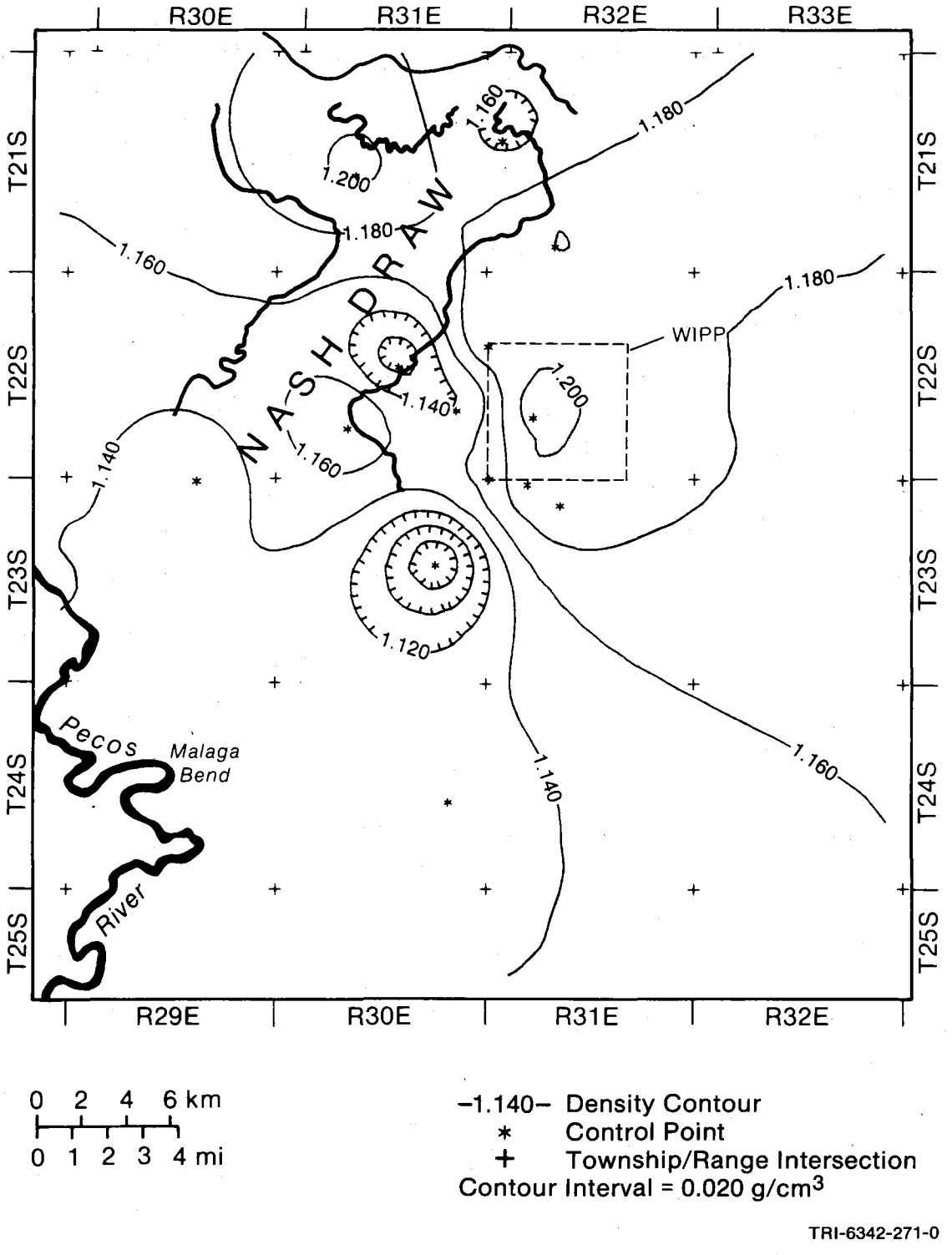

Figure IV-12. Contour Map of Brine Density in the Rustler-Salado Contact Residuum in the Study Area.

and chloride than the waters from Surprise Spring, indicating a different source (Mercer, 1983).

These observations do not necessarily mean that no connection to lower aquifers exists. If the lake is a discharge area for the lower units, the low chloride content and different water chemistry would be masked by evaporation or by the influx of surface runoff or near-surface flow from gypsiferous members of the Rustler Formation such as from Surprise Spring at the north end of the lake, which probably gets its water from the Tamarisk Member (Mercer, 1983).

The conclusion that the underlying units are confined assumes horizontal flow for the Culebra Dolomite and the brine aquifer. Horizontal flow in confined aquifers means flow lines are normal to vertical equipotential lines when viewed in cross section. In regions where water-table conditions exist (such as southern Nash Draw where the Tamarisk and Culebra Dolomite Members and the unnamed lower member are hydraulically connected), recharge and discharge result in equipotential lines that are not vertical but parallel to recharge and discharge surfaces (Figure IV-13). If the lake is a discharge point, the flow lines across the equipotential lines would show upward flow in the vicinity of discharge. If the point of a drill stem intersects an equipotential line, water will rise up the drill stem to the potentiometric level (Figure IV-13, well A). If the potentiometric level is higher than ground surface, a flowing well will result (Figure IV-13, well C). If a well penetrates at a point where flow is horizontal, the potentiometric lines are vertical (Figure IV-13, well B), and the water level in the well will be at the water-table level. Therefore, flowing wells do not necessarily mean that the water-bearing unit is confined. If the lake is a discharge point, the water level will rise in the winter when the pan evaporation rate is lowest. During the irrigation season, water will infiltrate and cause the water level in the underlying units to rise. In a personal communication with M. D. Siegel of Sandia National Laboratories in 1988, he stated that the high concentration of sodium and chloride at WIPP-29 is the result of flow from potash spoils north of the well. Discharge is also presently occurring at the southern end of Nash Draw into the Pecos River above Malaga Bend (Hale and others, 1954; Kunkler, 1980).

An analysis of fluid density effects on ground-water flow by Davies (1989) showed that, even though horizontal flow is driven by equivalent fresh-water head gradients, density-related gravity forces must be taken into account for a vertical component of flow. Davies (1989) examined density-related gravity effects by expanding the gravity term in Darcy's equation and concluded that the relative magnitude, not the absolute magnitude, of the density-related error term determines whether the density-related gravity effects will be

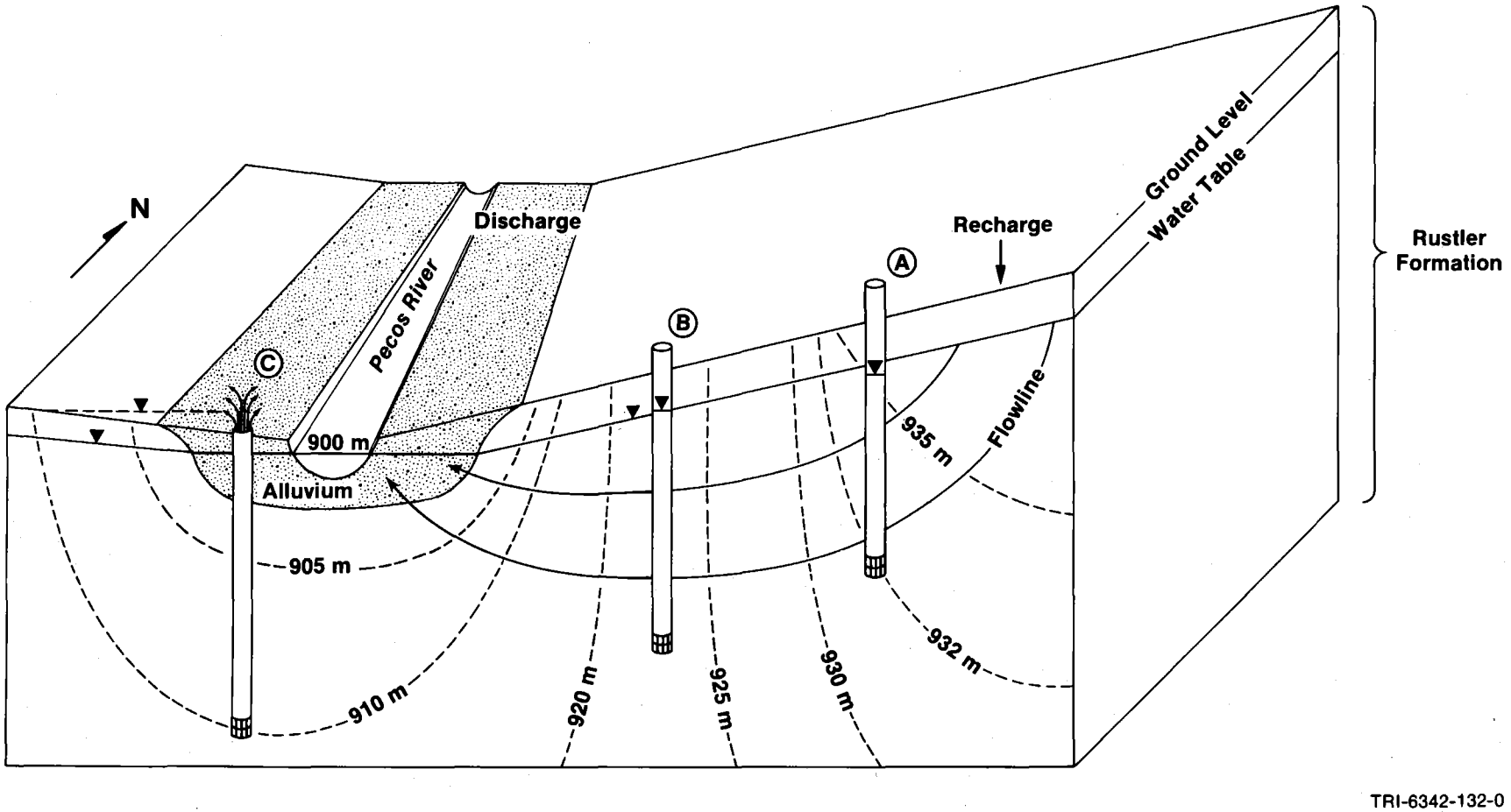

Figure IV-13. Cross Section Illustrating the Relationship of Flowing Wells to Recharge and Discharge Areas.

significant in any given situation. Davies (1989) examined ground-water flow in the Culebra Dolomite in the vicinity of the WIPP and found that in an area where the Culebra Dolomite is relatively flat-lying, density-related gravity effects are important. Davies (1989) showed in a comparison of fresh-water head simulations with variable density simulations that errors of up to 170 degrees in flow direction and up to almost a factor of 10 in velocity could be produced. Davies' (1989) work provides a way for ground-water modelers to predict whether natural or man-made density variations should be considered when defining ground-water flow in a region (see also "Fluid Density" in Appendix A).

The potentiometric-surface map of the fresh-water equivalent hydraulic heads indicates recharge east of the WIPP and discharge south-southwest to the river (Figure IV-10). According to Robinson and Lang (1938) and Lang (1938), the gradient of the potentiometric surface of the brine aquifer is toward the south, thus indicating recharge from the north in fractured rock near Bear Grass Draw (T18S, R30E) (Bachman, 1984). Mercer's (1983) study puts recharge at Clayton Basin and upper Nash Draw. A map of the regional structure (Figure 17 in Hiss, 1975) of the top of the Rustler Formation illustrates that the formation crops outs in the northwestern part of the area (Bear Grass Draw) and has a general dip south-southeastward. According to Mercer (1983), not enough data is available to indicate whether recharge is occurring in this region, but a possible source of recharge may be through fractures from the upper dolomitic units, the Culebra Dolomite, and the Magenta Dolomite Member, or from below the Capitan aquifer.

A third mode of recharge may be from units below the Rustler Formation where Capitan waters under the Salado Formation have moved up, via dissolution channels through the Salado, into the Rustler and through fractures in the anhydrites to the south, forming Nash Draw and Clayton Basin. A possible sequence of events is as follows:

1. Ground-water flow in the flat-lying basin in pre-Pleistocene time was generally eastward at a relatively low gradient (Hiss, 1980; see also "Capitan Limestone Aquifer" in this chapter).

2. In late Pliocene or early Pleistocene time, the Guadalupe Mountains were uplifted in the western part of the basin.

3. The uneven uplifting of the Delaware Basin resulted in tensional fracturing of the brittle reef rock of the Capitan, shelfward rocks, and the anhydrites in the Rustler Formation in what is now the vicinity of Clayton Basin and Nash Draw (a possible hinge area).

4. Water from the Capitan aquifer, which had sufficient head, moved upward and dissolved part of the Salado Formation over the reef.

5. Features such as breccia chimneys formed, resulting in a connection of the Rustler to the Capitan (see also the discussion of "Breccia Chimneys" as "Dissolution Features" in Chapter III).

6. Waters from the shelfward rocks and the Capitan, in conjunction with meteoric water from the surface, dissolved halite in the Rustler and moved south, down dip through the fractured lower Rustler anhydrites toward Malaga Bend of the Pecos River and possibly the Balmorhea-Loving Trough.

7. The Pecos River breached the Capitan, thus relieving upward pressure in the vicinity of the features.

Examination of a topographic map with a 15-m (50-ft) contour interval (Figure I-2) reveals a topographic low extending from the northwest lobe of Nash Draw (T21S, R30E) toward Clayton Basin across the Capitan Reef area. Breccia pipes in Hills A, B, and C are within this low. If the northeast lobe of Nash Draw is extended in the direction of its trend, it intercepts an area of sinks (Laguna Gatuña and Laguna Plata). Also, where the northwest extension of Nash Draw crosses the reef area, the Rustler and Salado Formations become thinner due to dissolution. The so-called dissolution front has passed through this part of the region (Anderson, 1978), resulting in lowering of rocks surrounding the breccia pipes (Davies, 1984). The surface of the Rustler is somewhat uneven in the region of Clayton Basin (Figure 17 in Hiss, 1975), probably due to the hydration of anhydrite to gypsum, resulting in an increase in Rustler Formation volume.

Some local recharge occurs in the brine aquifer in the vicinity of Malaga Bend. According to Hale and others (1954), an almost immediate water level rise occurred in a brine-aquifer observation well after a heavy rainstorm. Good hydraulic connection, possibly a sinkhole, from the surface through the lower Rustler Formation to the brine aquifer may exist in the vicinity of Malaga Bend (Hale and others, 1954). Immediate response to rainfall may also indicate that water-table conditions exist.

CULEBRA DOLOMITE (RUSTLER FORMATION) HYDROSTRATIGRAPHIC UNIT

More is known about the hydraulic properties of the Culebra Dolomite Member than about any other unit in the Study Area. The following discussion of hydrologic properties is a summary of work by Mercer and Orr (1977, 1979), Mercer (1983), Beauheim (1987b), and LaVenue and others (1988). A comprehensive Culebra Dolomite Member data base from the workers mentioned above has been compiled by LaVenue and others (1988), and these data are condensed and compiled in tables in their report.

Prior to Beauheim (1987b), transmissivity data were presented by Mercer (1983) for 20 locations around the WIPP. Eighteen new locations were tested since 1983 (Beauheim, 1987b):

The 15 new locations and 7 new transmissivity estimates for 7 previously tested locations presented in Beauheim (1987b).

Work at DOE-2 (Beauheim, 1986).

Work at H-11 (Saulnier, 1987).

Work at WIPP-13 (Beauheim, 1987b).

Figure IV-14 shows the locations of the tested wells in the Culebra Dolomite Member. Eighty percent of the 38 data points lie within a 10-km (6.2 mi) radius of the center of the WIPP, and 60 percent of these points are within the WIPP boundary.

Hydraulic Conductivity

The log hydraulic conductivities presented in Table IV-7 were calculated by LaVenue and others (1988) from mean transmissivities measured at each hydropad (well cluster) and divided by the thickness of the Culebra Dolomite tested at each hydropad (Beauheim, 1987b). The thickness of the Culebra Dolomite near the WIPP ranges from 4.8 to 11.0 m. A histogram of the log hydraulic conductivities shows a range from -10 to -4 (10^{-10} to 10^{-4} m/s), with a log normal mean of -6.4. The range and geometric mean of the hydraulic conductivity may be biased because, as previously mentioned, most of the data have a small spatial distribution. As more data are collected and analyzed on a regional scale, this distribution may change. A contour map of the log hydraulic conductivities (Figure IV-15) shows the variation in the calculated hydraulic conductivities across the Study Area. The hydraulic conductivities show a steady decrease from west to east, with higher conductivities north and south of the WIPP at the "Nash Draw reentrants." The reentrants show up on the topographic map of the area as surficial lows and are probably caused by dissolution of evaporitic units below the Dewey Lake Red Beds. The lows also roughly correspond to the dissolution indentations shown on the map of distribution of halite in the Rustler Formation (Figure II-16). How far east the trend of low conductivity holds is not known. According to Hiss (1973), a well (South Wilson Deep Unit #2) over the Capitan aquifer has a total Rustler Formation thickness of about 70 m, indicating that dissolution may be occurring east of the WIPP in San Simon Swale. In well P-18, the Culebra Dolomite Member has a very low hydraulic conductivity, but examination of the drilling, perforation, and reperforation record indicates that this well may be a poor well to use to establish a trend. The well was originally used to

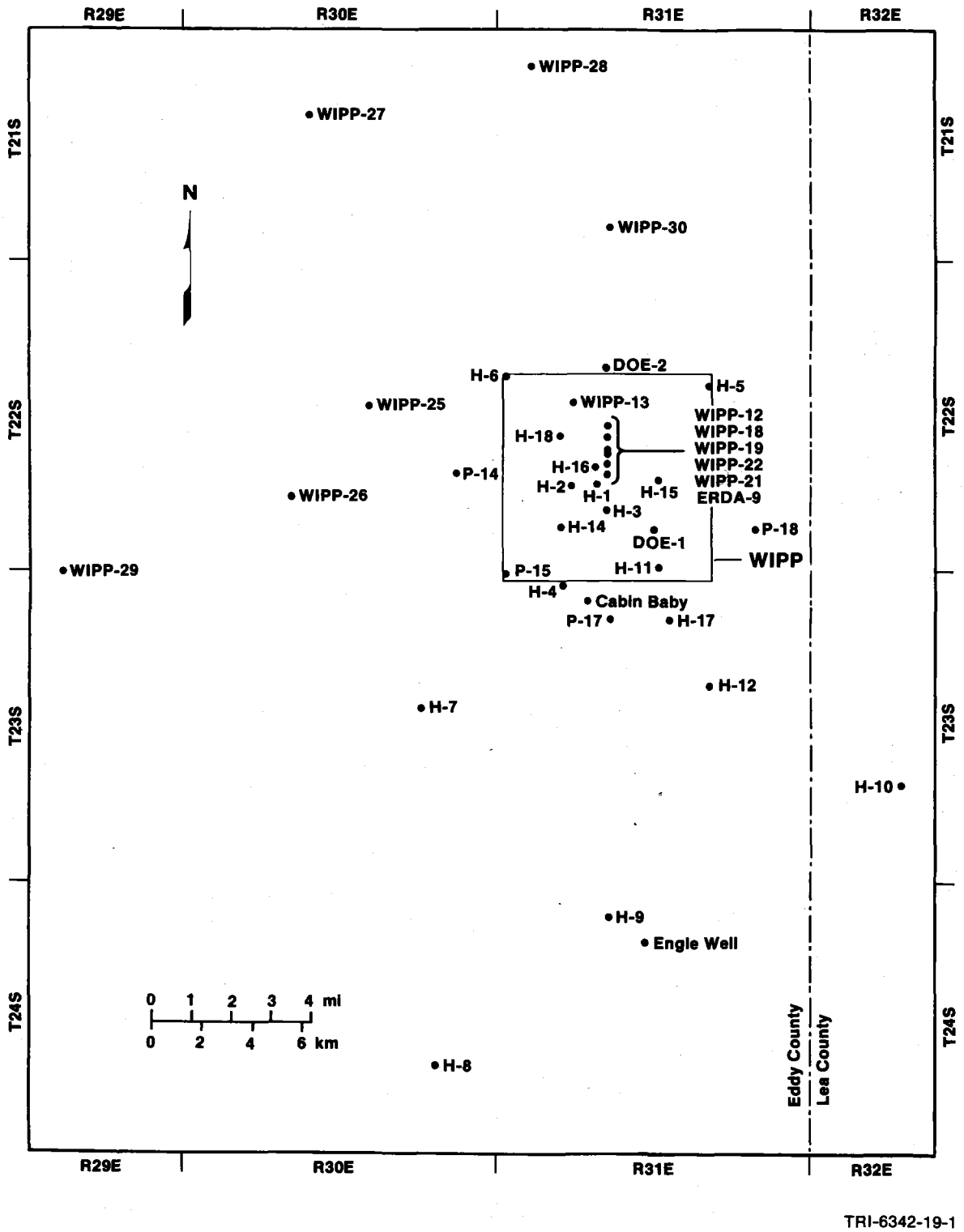

Figure IV-14. Location Map of the WIPP Test Wells in the Study Area (Beauheim 1987b).

TABLE IV-7. CULEBRA DOLOMITE GEOHYDROLOGIC DATA BASE

Well Name	Transmissivity[a] (m^2/s)	Hydraulic Conductivity (m/s)	Log Hydraulic Conductivity	Water Level[a] (m)	Water Density[a] (g/cm^3)	Culebra Thickness[a] (m)	Storativity[a]	Halite[b]
CABIN								
BABY-1	3×10^{-7}	4×10^{-8}	-7.4	911.2	--	7.9	--	2
DOE-1	1×10^{-5}	2×10^{-6}	-5.8	915	1.088	7	--	2
DOE-2	1×10^{-4}	1×10^{-5}	-4.8	935.4	1.041	6.7	--	2
ENGLE	5×10^{-5}	7×10^{-6}	-5.2	--	1.001	6.7	--	1
ERDA-9	5×10^{-7}	7×10^{-8}	-7.1	--	--	7	--	2
H-1	8×10^{-7}	1×10^{-7}	-7.0	921.6	1.022	7	1.0×10^{-4}	2
H-10	8×10^{-8}	8×10^{-9}	-8.1	920.8	1.047	9.4	1.0×10^{-4}	2
H-11	3×10^{-5}	4×10^{-6}	-5.4	912.5	1.078	7.6	--	2
H-12	2×10^{-7}	2×10^{-8}	-7.6	913.5	1.093	8.2	--	4
H-14	3×10^{-7}	4×10^{-8}	-7.4	915	1.008	8.2	--	2
H-15	1×10^{-7}	2×10^{-8}	-7.7	918	1.153	6.7	--	2
H-16	8×10^{-7}	1×10^{-7}	-7.0	--	--	7.6	--	2
H-17	2×10^{-7}	3×10^{-8}	-7.6	917.5	1.103	7.8	--	3
H-2	6×10^{-7}	9×10^{-8}	-7.0	923.5	1.009	6.1	1.0×10^{-9}	2
H-3	3×10^{-6}	3×10^{-7}	-6.5	917.1	1.036	7.3	--	2
H-4	1×10^{-6}	1×10^{-7}	-6.9	913.3	1.016	7.7	1.0×10^{-9}	2
H-5	2×10^{-7}	2×10^{-8}	-7.8	933.5	1.102	7.2	1.0×10^{-5}	2
H-6	8×10^{-5}	1×10^{-5}	-4.9	932.3	1.039	7	--	0
H-7	1×10^{-3}	1×10^{-4}	-4.0	912.6	1.001	11.3	--	0
H-8	9×10^{-6}	1×10^{-6}	-6.0	911.8	1	7.9	--	1
H-9	2×10^{-4}	2×10^{-5}	-4.7	907	1.001	9.1	--	1
P-14	2×10^{-4}	3×10^{-5}	-4.5	927	1.017	6.7	--	1
P-15	9×10^{-8}	1×10^{-8}	-7.9	916.4	1.015	6.7	1.0×10^{-4}	2
P-17	1×10^{-6}	2×10^{-7}	-6.7	912.6	1.061	7.6	1.0×10^{-6}	2
P-18	2×10^{-9}	2×10^{-10}	-9.7	--	--	8.8	--	4
USGS-1	6×10^{-4}	7×10^{-5}	-4.1	909	--	7.8	--	0

[a] LaVenue and others, 1988

[b] Presence of halite (Beauheim, 1987b)

0 West of upper Salado dissolution limit
1 Upper Salado present (No halite in Rustler)
2 Halite in unnamed lower member
3 Halite in unnamed lower member and Tamarisk Member
4 Halite in unnamed lower member, Tamarisk Member, and Forty-niner Member

TABLE IV-7. CULEBRA DOLOMITE GEOHYDROLOGIC DATA BASE (concluded)

Well Name	Transmissivity[a] (m^2/s)	Hydraulic Conductivity (m/s)	Log Hydraulic Conductivity	Water Level[a] (m)	Water Density[a] (g/cm^3)	Culebra Thickness[a] (m)	Storativity[a]	Halite[b]
WIPP-12	3×10^{-8}	4×10^{-9}	-8.4	932.2	--	7.6	--	2
WIPP-13	8×10^{-5}	1×10^{-5}	-5.0	934	1.043	7	--	2
WIPP-18	3×10^{-7}	5×10^{-8}	-7.3	930	--	6.7	--	2
WIPP-19	7×10^{-7}	1×10^{-7}	-7.0	--	--	6.4	--	2
WIPP-21	3×10^{-7}	4×10^{-8}	-7.4	--	--	7.3	--	2
WIPP-22	4×10^{-7}	6×10^{-8}	-7.2	--	--	6.7	--	2
WIPP-25	3×10^{-4}	4×10^{-5}	-4.4	931	1.008	7.7	--	0
WIPP-26	1×10^{-3}	2×10^{-4}	-3.7	917.5	1.012	7	--	0
WIPP-27	7×10^{-4}	9×10^{-5}	-4.1	937.5	--	7.9	--	0
WIPP-28	2×10^{-5}	3×10^{-6}	-5.6	938.1	1.032	7.9	--	0
WIPP-29	1×10^{-3}	1×10^{-4}	-4.0	905.4	--	9.1	--	1
WIPP-30	3×10^{-7}	5×10^{-8}	-7.3	934.7	1.041	7	1.0×10^{-4}	1

[a] LaVenue and others, 1988

[b] Presence of halite (Beauheim, 1987b)

0 West of upper Salado dissolution limit
1 Upper Salado present (No halite in Rustler)
2 Halite in unnamed lower member
3 Halite in unnamed lower member and Tamarisk Member
4 Halite in unnamed lower member, Tamarisk Member, and Forty-niner Member

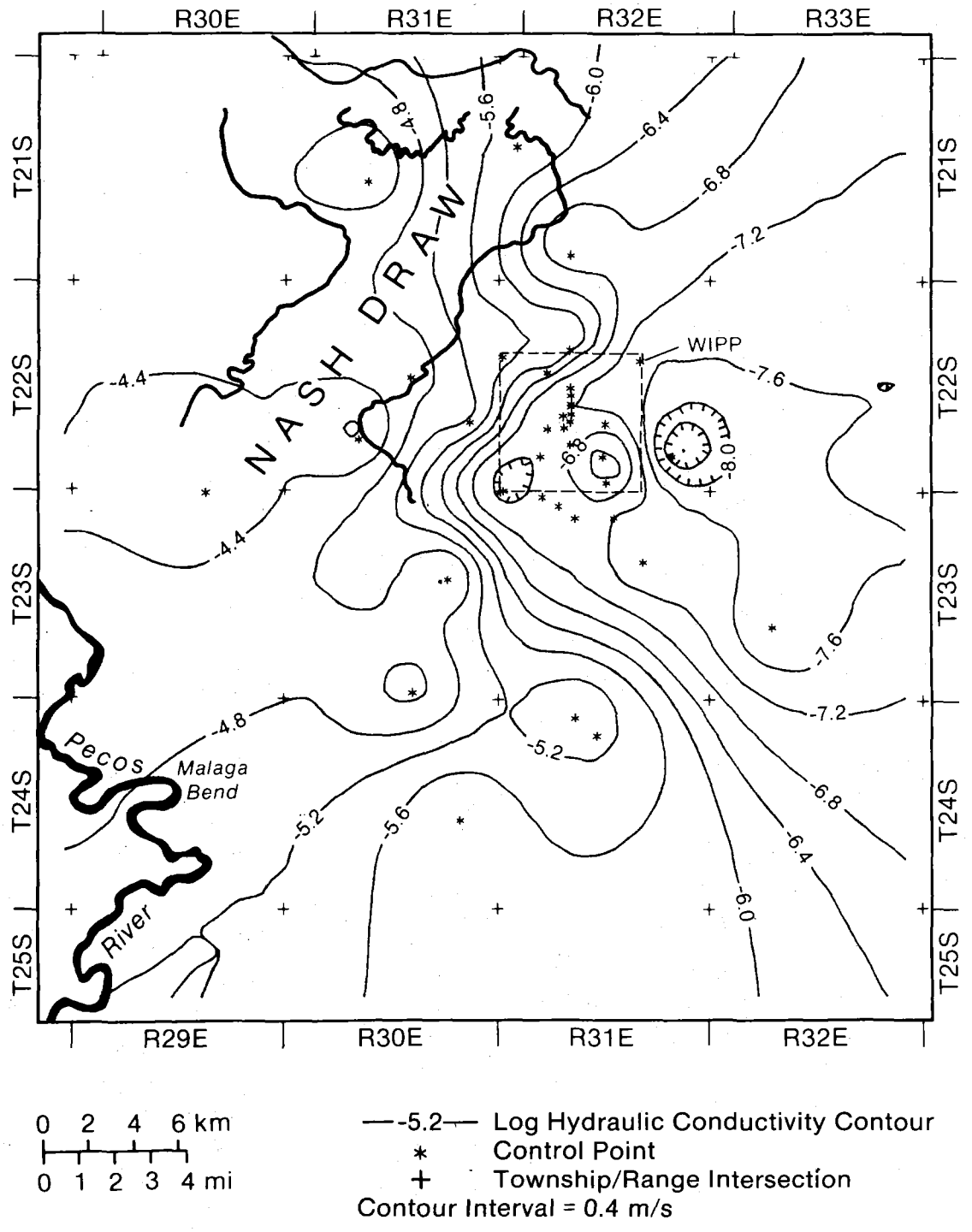

Figure IV-15. Contour Map of Log Hydraulic Conductivity of the Culebra Dolomite Member in the Study Area.

log the Salado Formation and was later perforated at the Culebra Dolomite and tested.

Post-depositional dissolution of salt in the Rustler Formation (Snyder, 1985), removal of overburden (Holt and Powers, 1988), or possibly a combination of both caused the variation in hydraulic conductivity. Eastward from Nash Draw, the Rustler Formation thickens as a result of the increase of halite in the nondolomitic members (Mercer, 1983; Mercer and Orr, 1977). Drilling cores from east and south of the WIPP where the Rustler Formation is thicker do not show the evidence of dissolution that is seen west of the WIPP toward Nash Draw where the Rustler Formation is thinner (Mercer, 1983; Snyder, 1985). Although a map from Beauheim (1987b) shows a "smooth" transition of the solution front from west to east, the isopach maps of the Rustler Formation Members (Figures II-15, II-18, II-20, II-23, and II-25) illustrate that the thickness is somewhat erratic in the vicinity of the WIPP.

A dissolution model proposed by Snyder (1985) explains the erratic thickening and thinning of the Rustler Formation. Dissolution of halite begins in the Forty-niner Member and continues through the Tamarisk Member into the unnamed lower member. As a result of the dissolution of the nondolomitic members, fracturing caused by settling enhances the permeability of the dolomite members. The anhydrites also settle, which causes permeability enhancement that allows ground water from the dolomites to flow through and hydrate the anhydrite, forming gypsum. The altered anhydrite swells, causing more fracturing, and the cycle continues, removing the more soluble gypsum until all soluble material is removed, leaving only a meter or so of residue between the dolomites, as seen near Nash Draw (Bachman, 1981; Vine, 1963).

The Holt-Powers model (Holt and Powers, 1988) explains the absence of halite in the Rustler Formation dolomites from a sedimentological approach. A detailed description of their evidence and conclusions is in their report and is only briefly summarized here. According to this model, the absence of halite is the result of syndepositional dissolution rather than post-Rustler dissolution. The depocenter for the Delaware Basin at Rustler time was east and south of the WIPP. As sediment was deposited in the basin, freshening events or stagnation at the margins changed the salinity of the water. The freshening events or stagnation of the lagoonal waters was a result of a change in base level of the water table caused by tectonic events, precipitation, or drought and resulted in a cycle of dissolution of salt at the margins and deposition of salt basinward. Post-Rustler removal of overburden enhanced the permeability of the dolomites and caused horizontal fracturing. In a personal communication with R. M. Holt of Science Applications International Corporation, Albuquerque, NM, in 1988, he indicated

that further studies are being proposed to determine the orientation of fracturing in the dolomites and to verify the proposed model.

Beauheim (1987b) compares the Snyder and Holt-Powers models using new information that was not available to Snyder (1985). He shows that well H-18, located east of the halite boundary (Figure II-16), has a low transmissivity consistent with the Snyder model, but WIPP-30, which has no halite, also has a low transmissivity. Wells DOE-1 and H-11 east of H-18 have relatively high transmissivities. The Holt-Powers model supports the low transmissivity of the Culebra Dolomite at WIPP-30, but this model cannot explain the high transmissivities of DOE-1 and H-11.

A preliminary statistical analysis of covariance shows a rough negative correlation ($r = -0.7$) between overburden and transmissivity. A cluster of low-transmissivity data points occurs where the overburden is thick, and a cluster of high-transmissivity data points occurs where the overburden is thin or nearly absent. Statistical analyses, such as covariance analysis, will be used to determine, for performance-assessment purposes, whether hydraulic conductivity can be inferred in areas where data are scarce by utilizing information about the presence or absence of halite and the thickness of overburden.

Porosity

A global porosity value of 0.20 for the single-porosity conceptual model and for the matrix porosity of the dual-porosity conceptual model was used by Haug and others (1987). A porosity of 0.20 was believed representative of porosities ranging from 0.07 to 0.30 that were obtained from laboratory analyses of 2.54-cm (1-in) plugs taken from core samples. Two blocks of dolomite taken from depths of 154 and 157 m during the access shaft excavation for the Atomic Energy Commission's (now U.S. DOE) Project Gnome (Figure IV-8) had total porosities of 0.144 and 0.137 and effective porosities of 0.078 and 0.111, respectively (Cooper and Glanzman, 1971).

More recently, 79 helium porosity determinations of core samples from the Culebra Dolomite yielded an arithmetic mean of 0.153, with a distribution skewed toward lower porosity values. Twenty-one pairs of helium porosity determinations, where each pair was separated approximately 5 cm (2 in) vertically, varied from 0.050 to 0.093 (Kelley and Saulnier, 1990).

Potentiometric Surface

Figure IV-16 is an adjusted potentiometric surface map of the Culebra Dolomite Member constructed from water-level data compiled in LaVenue and others, 1988.

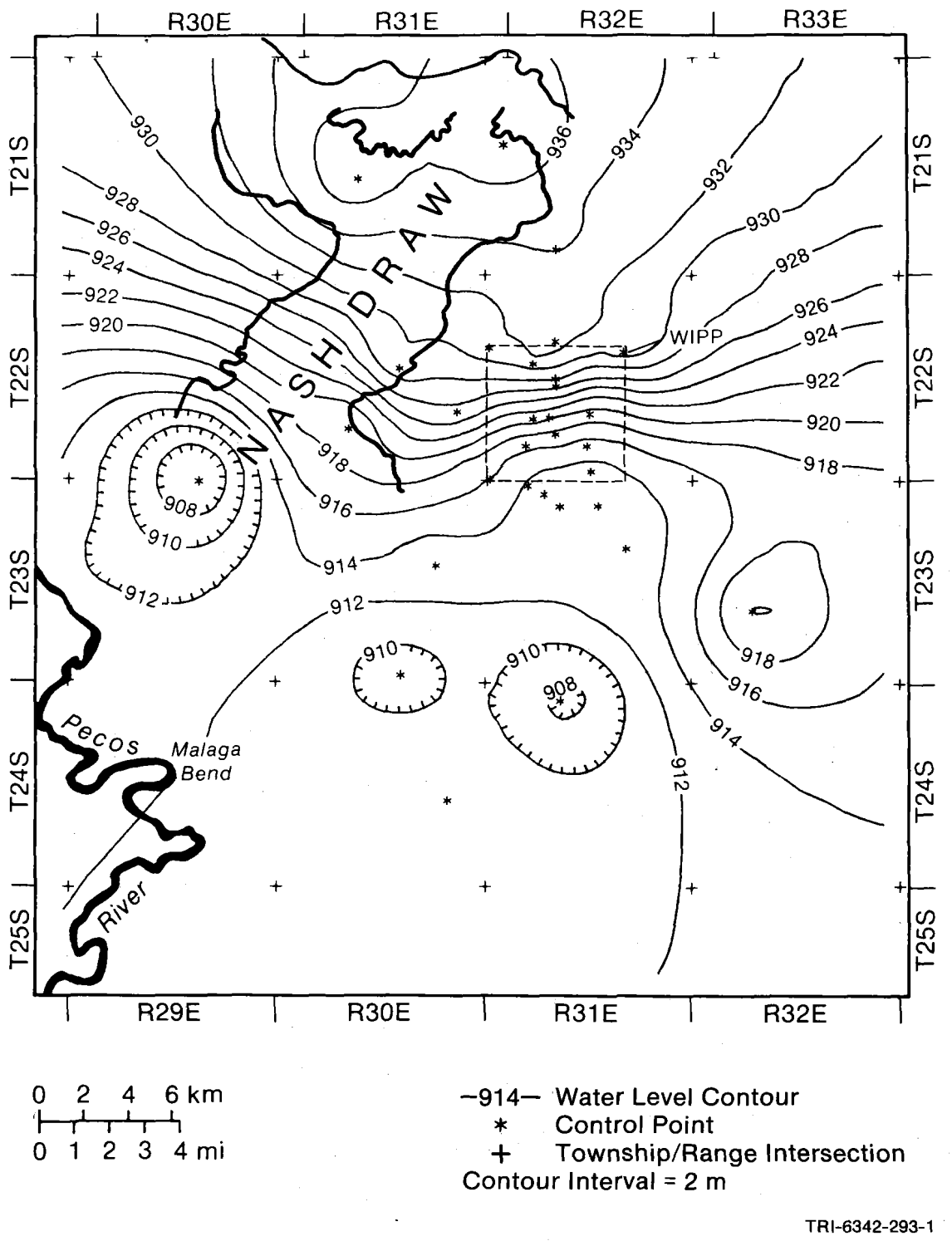

Figure IV-16. Adjusted Potentiometric Surface of the Culebra Dolomite Member in the Study Area.

Flow west of the WIPP is northeast to southwest, and the flow lines are roughly parallel to the axis of Nash Draw. Northeast and east of the WIPP, the data are insufficient, and inference of the potentiometric surface is difficult. A few data points are south of the WIPP, and flow is inferred to be southward. Flow in the Culebra Dolomite roughly follows Nash Draw because of the higher transmissivity of the dolomite in this area. The gradient in the upper Nash Draw area (0.003) is steeper where the Culebra Dolomite has more overburden. In the lower Nash Draw area near Malaga Bend, where the Culebra Dolomite is near the surface, the gradient is flatter (0.001). Figure IV-17 illustrates the effects of the Pecos River, assuming that a water-table aquifer exists near the river that results in a flow pattern going directly to the river at Malaga Bend (see also "Rustler Salado Contact Residuum Hydrostratigraphic Unit" in this chapter for a discussion of variable density effects and their impact on flow).

Storativity

Storage values presented by Mercer (1983) range from 10^{-9} to 10^{-4}. A value of 10^{-9} means that very little fluid is released from storage. The storage coefficient for most confined aquifers ranges from 10^{-5} to 10^{-3}.

Fluid Density

The quality of Culebra Dolomite Member waters is marginal, and use of this water is restricted mostly to stock watering, with very little used for domestic purposes. Total dissolved solids (TDS) range from 3,200 to 420,000 mg/ℓ at test holes H-8b and P-18, respectively. Test hole WIPP-29 has a high TDS (>230,000), which is attributed by M. D. Siegel of Sandia National Laboratories in a personal communication in 1989 to potash mine effluent. Brine concentrations for the Culebra Dolomite (Table IV-7) are compiled from Haug and others (1987) and LaVenue and others (1988). The data were plotted on a base map of the Study Area (Figure IV-16). The brine densities vary from very low (0.001 g/cm^3) at hydropad H-8 to almost a saturated density brine at WIPP-29. The value for WIPP-29 will not be used when inferring densities at the boundaries because of the possible effects of effluent from potash mines. Figure IV-18 shows an increase in water density across the WIPP from west to east. There is no potable water (<10,000 TDS) within 5 km (3.1 mi) of the WIPP disposal panels.

Recharge and Discharge

The potentiometric-surface map of the adjusted Culebra Dolomite heads (Figure IV-17) indicates recharge from the north, possibly at Bear Grass Draw where the Rustler Formation is near the surface and at Clayton Basin where

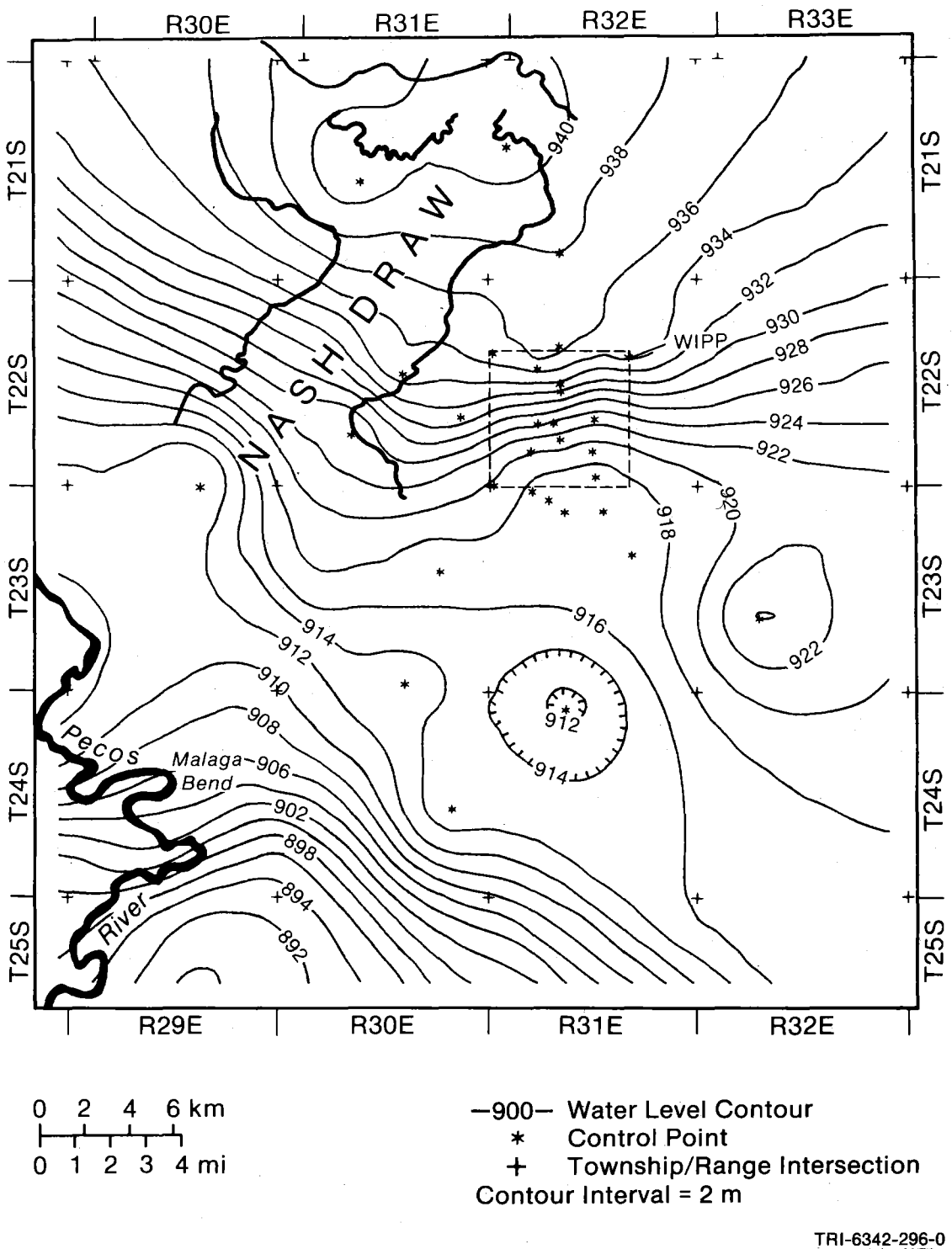

Figure IV-17. Adjusted Potentiometric Surface of the Culebra Dolomite Member of the Rustler Formation in the Study Area (Pecos River heads included).

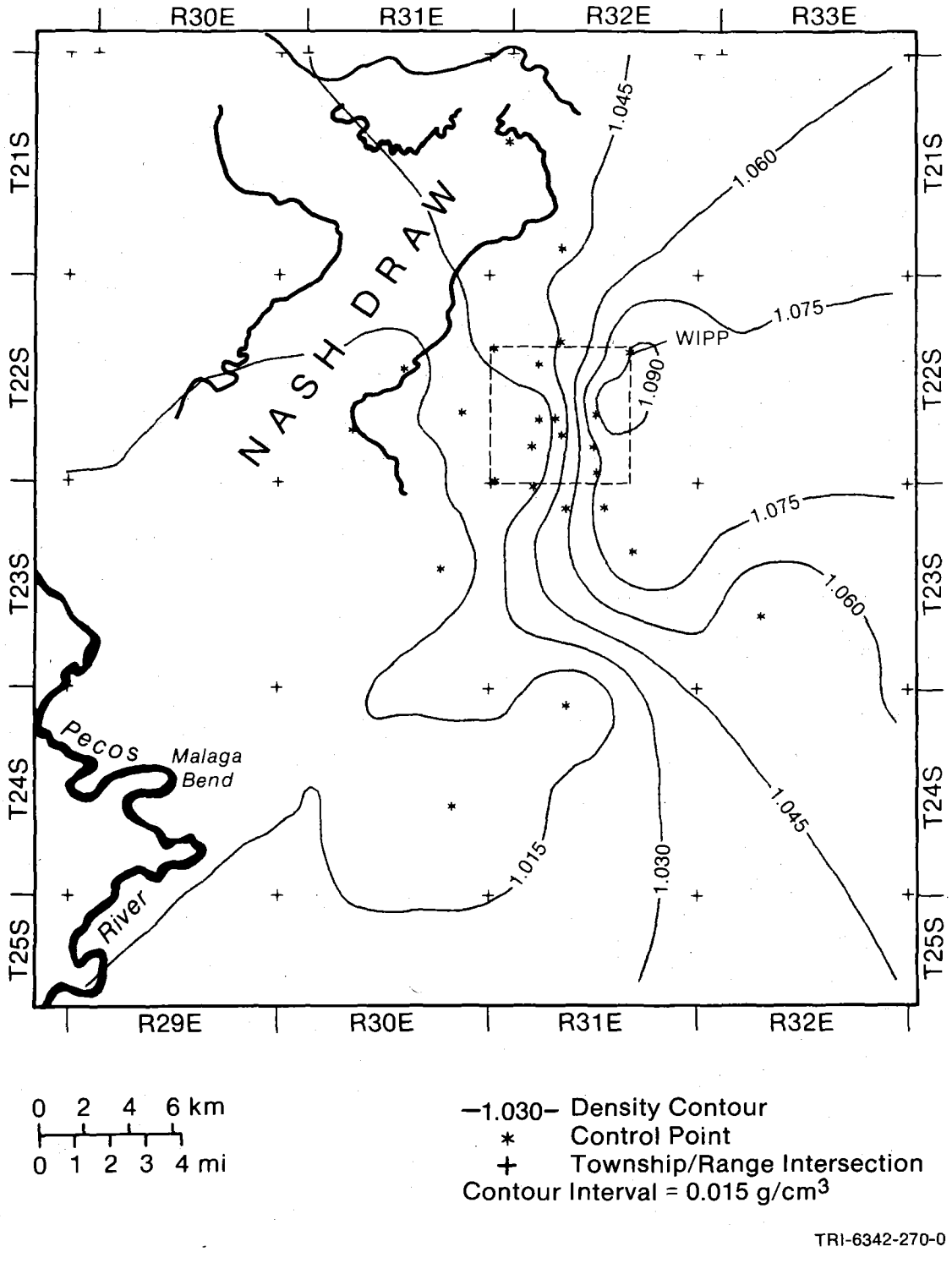

Figure IV-18. Contour Map of Brine Density in the Culebra Dolomite Member in the Study Area.

karst activity has disrupted the Culebra Dolomite (Mercer, 1983). Recharge from below the Culebra Dolomite requires water to pass through what is assumed to be very hydraulically tight material, but as was demonstrated in the Rustler-Salado residuum (see "Recharge and Discharge" of the "Rustler-Salado Contact Residuum Hydrostratigraphic Unit" in this chapter), recharge could enter the Rustler hydrostratigraphic units via dissolution features from above such as karst features or from below through collapse features above the reef area.

Recharge to the Culebra Dolomite may also occur east of the WIPP as a result of leakage from the Magenta Dolomite Member through the Tamarisk Member. Although the dolomite, anhydrite, and clays in the Magenta and Tamarisk have low storativities and transmissivities, large amounts of water can move downward to the Culebra, where gradients permit, through the thousands of square meters of surface that overlie the Culebra. If the Tamarisk anhydrites are fractured, even more water may leak downward.

Geochemical data suggest regional flow in the Culebra Dolomite may be complicated. According to Lambert and Carter (1987), examinations of uranium concentrations and uranium-234/uranium-238 activity ratios indicate that flow may originally have been from west to east instead of mostly from the east toward the west and south as currently. Activity-ratio values increase from Nash Draw eastward, which would be typical of flow in that direction in a reducing environment, but this direction is at variance with present-day flow. According to Lambert and Carter (1987), the Rustler Formation ground water is "now draining from high potentiometric level, low-permeability areas near the WIPP, without appreciable recharge." This drainage suggests the Rustler Formation is not at steady state and that recharge occurred at Nash Draw 10,000 to 30,000 yr ago under much wetter conditions (Lambert and Carter, 1987; Lambert and Harvey, 1987; Lambert, 1987).

Lambert and Harvey (1987) believe recharge through the overburden from direct infiltration of precipitation seems highly unlikely under present-day conditions. A comparison by Lambert and Harvey of recharge data from two modern basins similar to the Delaware Basin led them to state that "...we have little hope of determining definitive values for recharge to the confined Rustler at the WIPP site."

A recharge event that affected well responses was noted at observation wells by Beauheim (1989) during a multipad pump test at the H-11 hydropad. Recharge had no effect on simulation results for a WIPP-13 multipad pump test, although equally good curve fits were obtained with the presence of recharge (Beauheim, 1987a). The over-recovery of wells DOE-1, H3b2, and H-15 at the end of the H-11 pump test was explained, in part, as recovery from stresses to the system

that had preceded the H-11 test. At wells H-4b, H-12, H-17, P-15, P-17, and Cabin Baby-1, the recovery water level was higher than the pretest water levels (Beauheim, 1989). In addition, anomalous water-level rises were noted in the wells at the H-9 hydropad, 10.9 km (6.7 mi) south of H-11 (Beauheim, 1989), and at wells H-8 and P-18 (Beauheim, 1990). The water-level rise at well P-18 was attributed, by Beauheim, to very slow pressure equilibration with the Culebra. The Beauheim memo (1990) points out the following:

> Based on the rises observed at H-9 and H-8b, both clearly outside the area of influence of the H-11 multipad test, [he] believe[s] that the fact that many of the water level rises did not become evident until the recovery period from the H-11 test is merely a coincidence, and does not imply a causal relationship. Instead, the drawdowns associated with the H-11 test probably delayed our observation of the rising water levels. Historically high water levels observed at wells DOE-1, H-7b1, H-11b2, H-14, and H-15 may be related to the other water-level rises, or may be simply normal recoveries from multiple pumping episodes. Water-level rises at P-18 and WIPP-27 are clearly not related to the anomalous rises observed south of the WIPP site.

Beauheim (1989) gives three potential scenarios to account for the anomalous water-level rises:

> A decrease in discharge from Culebra if a drain on the system were stopped (considered unlikely).
>
> Injection of fluid into the Culebra either inadvertently through a leaky casing or as a loss of drilling fluid.
>
> Changes in the mechanical stress field resulting in a change in fracture permeability which would, in turn, cause a damming effect increasing upgradient heads.

A fourth explanation not considered by Beauheim (1989) is the possibility of local recharge to the Rustler Formation via dissolution features in proximity to wells H-8b and H-9b. Well H-8b is only about 200 m from a closed depression of approximately 40,000 m^2 that has an ephemeral lake in it and about 3 km from Poker Lake and Poker Tank. Well H-9b is also in an area of dissolution features and about 5 km northeast of Poker Tank. Both wells are in the southern Nash Draw reentrant, which corresponds to the area of complete halite dissolution from the Rustler (Figure II-16). Hydrographs of the two wells show increases in water level beginning about one year after two periods of increased average rainfall from 1981-1982 and 1985-1988 (Webb, 1990). Because of the short duration of the records and the distance from the rainfall recording station near Carlsbad to Wells H-8b and H-9b, Webb felt that caution should be exercised in using these records. Also, testing in 1983 caused a lowering of water levels that interfered with recovery of H-9, but since that time the well has shown a steady increase in water level,

surpassing the pretest levels. Because wells in karstic evaporites in southern Nash Draw have exhibited water-level increases after periods of recharge (see "Recharge and Discharge" of the "Rustler-Salado Contact Residuum Hydrostratigraphic Unit" in this chapter), a similiar mechanism could cause water-level rises in other regions where dissolution has occurred. The 1989 rainfall average was less than in 1988 in the region. If the rise was indeed caused by an increase in rainfall, observations will indicate whether a decline in water levels follows the recent decline in rainfall.

Discharge in the Study Area is to the west-southwest, either into the Pecos River at Malaga Bend or into the Balmorhea-Loving Trough, or into both. Because of the salinity increase of the Pecos River at Malaga Bend and because the river appears to be gaining there, this area has been described as a discharge area for the region (Hale and others, 1954; Hale and Clebsch, 1958; Havens and Wilkins, 1979; Mercer, 1983). However, the increase in salinity may only be due to local discharge of the "brine aquifer" and not because of regional drainage. Discharge may be toward the Balmorhea-Loving Trough and, at this time, rates of discharge from the region may only be estimated using flow-modeling techniques.

Figure IV-17 is a computer-generated, potentiometric-surface map of the Culebra Dolomite with the Pecos River heads included. The map illustrates how the potentiometric surface changes in lower Nash Draw if the river is connected hydraulically to the Culebra Dolomite. Conceptually, this connection may be the case because the lower part of Nash Draw is composed of karstified Tamarisk Member, Culebra Dolomite, and, very likely, the unnamed lower member. Above Malaga Bend, the contour lines are roughly parallel to the river, indicating discharge to the river, but below the bend, the contour lines are perpendicular to the river, which could be construed as discharge to the trough area to the south.

Multipad Aquifer Tests in the Culebra Dolomite Member

Three multipad tests have been reported in the Culebra Dolomite Member since 1986. The tests were conducted at H-3, WIPP-13, and H-11 multipads. The H-3 pump test had 7 observation wells that yielded results; WIPP-13 pump test had 18 observation wells, with 15 yielding results; and the H-11 multipad pump test had 14 observation wells, with 10 wells showing drawdowns and 7 wells away from the H-11 multipad yielding data that could be used for response interpretations. Tables IV-8, IV-9, and IV-10 summarize the results of the H-3, WIPP-13, and H-11 pump tests, respectively, as reported by Beauheim (1987a, 1987c, 1989).

TABLE IV-8. SUMMARY OF MULTIPAD WELL RESPONSES FOR H-3 MULTIPAD TEST

For the Flowpath Between H-3 and Well	Unmodified Data[a] Apparent T^c (ft^2/day)	(m^2/s)	Apparent S^d	Modified Data[b] T^c (ft^2/day)	(m^2/s)	S^d	Drawdown Compared	Time First Drawdown Observed (h)	Time Pump On Until Maximum Drawdown Observed (h)	Drawdown at End of Pumping Period (ft)	(m)	Maximum Drawdown (ft)	(m)	Distance from H-3 (ft)	(m)	Direction (Degrees)
H-1	0.83	8.9×10^{-7}	3.9×10^{-5}	0.46	4.9×10^{-7}	2.7×10^{-5}	1.3 ft/15 day	488	2911	9.1	2.8	23.8	7.2	2675	813	N19°W
H-2b2	2.5	2.7×10^{-6}	4.5×10^{-5}	1.2	1.3×10^{-6}	3.0×10^{-5}	0.57 ft/15 day	433	2881	3.4	1.0	8.6	2.6	4165	1267	N54°W
H-11b1	13	1.4×10^{-5}	6.6×10^{-6}	6.8	7.3×10^{-6}	7.4×10^{-6}	0.425 ft/15 day	79	1539	8.9	2.7	9.2	2.8	7950	2418	S42°E
DOE-1	9.2	9.9×10^{-6}	9.2×10^{-6}	5.5	5.9×10^{-6}	1.0×10^{-5}	0.27 psi/15 day	57	1536	13.7	4.2	14.2	4.3	5270	1603	S68°E
WIPP-19	2.9	3.1×10^{-6}	2.9×10^{-5}	NA		NA	None	1207	3343	0.9	0.3	6.0	1.8	6150	1870	N2°E
WIPP-21	1.1	1.2×10^{-6}	9.0×10^{-6}	NA		NA	None	437	2166	20	6.1	31.8	9.7	4715	1434	N3°E
WIPP-22	1.6	1.7×10^{-6}	1.7×10^{-5}	NA		NA	None	990	2215	3.5	1.1	10.6	3.2	5705	1735	N2°E

[a] But fit data w/no modification
[b] Includes linear compensation for pre-test trends
[c] Transmissivity
[d] Storativity

Source: Modified from Beauheim, 1987a

TABLE IV-9. SUMMARY OF MULTIPAD WELL RESPONSES FOR WIPP-13 MULTIPAD TEST

For the Flowpath Between WIPP-13 and Well	Transmissivity (ft^2/day)	Transmissivity (m^2/s)	Storativity	Time First Drawdown Observed (h)	Time Pump On Until Maximum Drawdown Observed (h)	Drawdown at End of Pumping Period (ft)	Drawdown at End of Pumping Period (m)	Maximum Drawdown (psi)	Maximum Drawdown (ft)	Maximum Drawdown (m)	Distance from WIPP-13 (ft)	Distance from WIPP-13 (m)	Direction (Degrees)
WIPP-12	7.9	8.4×10^{-6}	3.6×10^{-5}	74	1050	24.0	7.3	11.9	27.5	8.4	4210	1280	S55°E
WIPP-18	23	2.5×10^{-5}	4.0×10^{-5}	74	950	17.6	5.4	9.3	19.5	5.9	4990	1517	S45°E
WIPP-19	24	2.6×10^{-5}	4.0×10^{-5}	102	1050	12.0	3.6	7.2	14.7	4.5	5980	1819	S37°E
WIPP-21	22	2.4×10^{-5}	5.3×10^{-5}	133	1260	3.3	1.0	3.6	8.3	2.5	7270	2211	S29°E
WIPP-22	19	2.0×10^{-5}	4.7×10^{-5}	102	1150	10.3	3.1	5.7	11.5	3.5	6340	1928	S34°E
WIPP-25	650	6.7×10^{-4}	6.4×10^{-5}	76	890	0.7	0.2	0.3	0.7	0.2	20550	6249	S88°W
WIPP-30	28	3.0×10^{-5}	5.6×10^{-6}	61	100	9.0	2.7	4.9	10.6	3.2	18330	5574	N12°E
H-1	20	2.2×10^{-5}	1.3×10^{-4}	600	2950	0	0	1.1	2.5	0.8	8780	2670	S16°E
H-2b2	16	1.7×10^{-5}	7.3×10^{-4}	445	1850	0.5	0.2	1.4	3.2	1.0	8520	2591	S 0°W
H-3b2	--	--	--	--	--	--	--	--	--	--	11490	3494	S17°E
H-5b	--	--	--	--	--	--	--	--	--	--	13980	4251	N83°E
H-6a	71	7.6×10^{-5}	8.2×10^{-5}	8	869	17.0	5.2	7.7	17.1	5.2	7190	2186	N20°W
H-6b	69	7.4×10^{-5}	7.9×10^{-6}	8	869	17.4	5.3	7.9	17.5	5.3	7180	2183	N20°W
H-15	--	--	--	--	--	--	--	--	--	--	11740	3570	S48°E
DOE-2	57	6.1×10^{-5}	5.1×10^{-6}	1	865	38.2	11.6	17.3	38.4	11.7	4840	1472	N45°E
P-14	265	2.8×10^{-4}	5.2×10^{-5}	71	920	1.7	0.5	0.8	1.8	0.5	13870	4218	S58°W
ERDH-9	22	2.4×10^{-5}	5.4×10^{-5}	550	1260	0.6	0.2	2.0	4.4	1.3	8260	2512	S24°E
Ex. Shaft	28	3.0×10^{-5}	5.5×10^{-5}	400	1200	6.1	1.9	3	7.0	2.1	7920	2408	S26°E

Source: Modified from Beauheim, 1987a

TABLE IV-10. SUMMARY OF MULTIPAD WELL RESPONSES FOR H-11 MULTIPAD TEST

For the Flowpath Between H-11 and Well	Transmissivity (ft^2/day)	Transmissivity (m^2/s)	Storativity	Time First Drawdown Observed (h)	Time Pump On Until Maximum Drawdown Observed (h)	Drawdown at End of Pumping Period (ft)	Drawdown at End of Pumping Period (m)	Maximum Drawdown (ft)	Maximum Drawdown (m)	Distance from H-11 (ft)	Distance from H-11 (m)	Direction (Degrees)
DOE1	8.6	9.2×10^{-6}	2.3×10^{-6}	2	1513	33.4	10.16	33.4	10.16	3970	1207	N6.4°W
H3b2	9.2[a]	9.9×10^{-6}	1.1×10^{-5}	72	1704	12.2	3.71	12.6	3.83	7940	2415	N42.5°W
H4b	--	--	--	432	1560	0.9	0.27	0.9	0.27	9960	3029	S78°W
H-12	--	--	--	792	2112	0.3	0.09	0.5	0.15	13259	4032	S24°E
H-14	6.0	6.5×10^{-6}	3.7×10^{-5}	864	5232	0.4	0.12	2.0	0.61	10640	3236	N67.5°W
H-15	7.1	7.6×10^{-6}	4.7×10^{-6}	72	1608	14.9	4.53	15.3	4.65	8960	2725	N0.3°W
H-17	13	1.4×10^{-5}	1.8×10^{-5}	48	1560	8.2	2.49	8.3	2.52	5440	1654	S12.6°E
P-15	--	--	--	792	2280	0.1	0.03	0.4	0.12	15530	4723	S86.3°W
P-17	21	2.3×10^{-5}	4.7×10^{-5}	240	1752	2.7	0.82	2.9	0.88	7180	2183	S40.8°W
CB-1	13	1.4×10^{-5}	6.5×10^{-5}	648	2112	1.1	0.33	1.6	0.49	7910	2405	S63.7°W

[a] Median

Source: Modified from Beauheim, 1989

Pump test H-3 had 3 objectives:

Conceptualize flow around H-3 hydropad.

Quantify the hydraulic properties of the Culebra Dolomite around H-3 hydropad.

Quantify the hydraulic properties of the Culebra between H-3 and the observation wells.

Interpretations of results around the hydropad that satisfy the first two objectives indicate that the Culebra Dolomite is a dual-porosity medium with unrestricted interporosity flow and total system transmissivities calculated from two separate tests of 3.1 X 10^{-6} m^2/sec (2.9 ft^2/day) and 1.7 x 10^{-6} m^2/s (1.6 ft^2/day) (Table IV-8) (Beauheim 1987a).

Beauheim (1987a) reports that meeting the third objective

> ...was complicated by the effects of an apparent increase in groundwater leakage from the Culebra into the Waste-Handling Shaft on the data from wells near that shaft, and by water-level/pressure trends already existing at many of the observation wells when the multipad test began. Between H-3 and wells DOE-1 and H-11 to the southeast, the average apparent Culebra transmissivity is between 5.5 and 13 ft^2/day, and the apparent storativity is between 6.6 X 10^{-6} and 1.0 X 10^{-5}. The rapid responses observed at DOE-1 and H-11 during the multipad test, and the associated relatively high transmissivities, indicate a preferential hydraulic connection, probably related to fractures, between H-3 and the southeast portion of the WIPP site.
>
> Between H-3 and wells H-1 and H-2 to the north-northwest, the apparent transmissivity is between 0.46 and 2.5 ft^2/day, and the apparent storativity is between 2.7 X 10^{-5} and 4.5 X 10^{-5}. If the possible shaft-leakage effects are ignored, the apparent transmissivity between H-3 and wells WIPP-19, 21, and 22 to the north is between 1.1 and 2.9 ft^2/day, and the apparent storativity is between 9.0 X 10^{-6} and 2.9 X 10^{-5}. If shaft leakage did, as is believed, affect the responses observed at WIPP-19, 21, and 22, then the transmissivity values listed above are not representative. The wells to the north of H-3 are not so well connected hydraulically to H-3 as are DOE-1 and H-11, and provided no indications that groundwater flow was occurring primarily through fractures.

The conclusion of a preferred direction of transmissivity was tested using a plot of transmissivity against distance (Figure IV-19). The direction of the observation well from the pumping well was converted to total degrees as one rotates around the pumping well (that is, a well (DOE-2) that is S68°E would be 180°-68°, or 112°). Therefore, 0° and 360° are north of H-3. Inspection of the plot shows that wells H-11b1 and DOE-1 increase in transmissivity

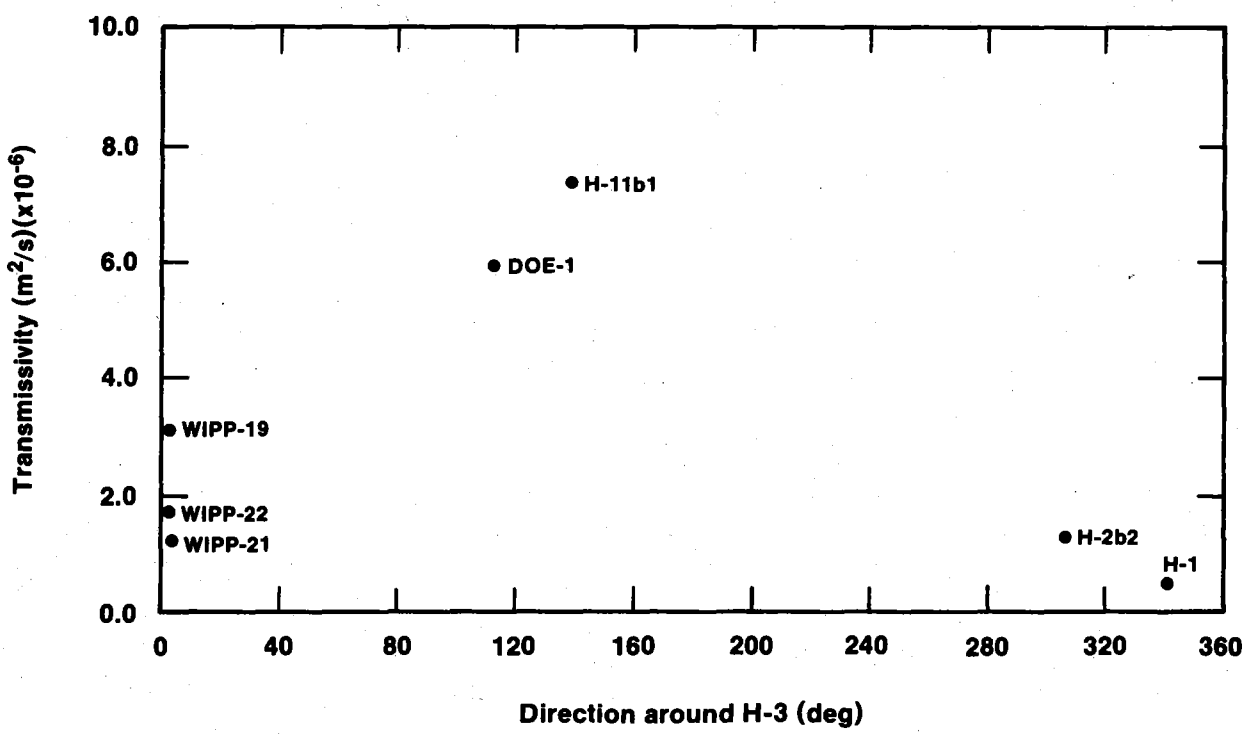

Figure IV-19. Plot Showing Change in Transmissivity in Observation Wells Surrounding H-3.

southeast (112° to 138°), and the remaining wells show a decrease to the north (300° to 360° and 10° to 20°). These observations were also tested by correlating maximum drawdown to the inverse of the square of the distance from the pumping well to each observation well. This correlation yielded a correlation coefficient for all the wells (n=7) of r = 0.49, showing a low correlation of drawdown to inverse distance, which may indicate a preferred direction. If the WIPP wells (WIPP-19, 21, and 22) are dropped from the correlation to test the hypothesis by Beauheim that the leakage into the waste handling shaft was interfering, the correlation coefficient increases to 0.87, indicating that the shaft effects may have influenced the results of the calculation. The high correlation also shows the region is fairly homogeneous northwest to southeast through H-3 because the inverse of the square of the distance is changing at a rate similar to drawdown. This changing rate is completely at variance with the ranked data, though, indicating no correlation at all (r = 0.40), which means that in the H-3 region a direction may be preferred, but more data are needed to verify Beauheim's (1987a) conclusions about a preferred direction of transmissivity.

The WIPP-13 multipad test northwest of the WIPP was intended to complement the H-3 test with similar objectives and to provide measurable responses over the WIPP. Table IV-9 is a summary of the results of the test. Beauheim (1987c) concluded the following:

> The Culebra is a fractured, double-porosity system around WIPP-13, H-6, and DOE-2, with relatively high transmissivity (~70 ft^2/day) and relatively low storativity (5 X 10^{-6} to 8 X 10^{-6}). This system appears to extend further to the north toward WIPP-30, although WIPP-30 itself lies in a lower transmissivity zone. The apparent transmissivity between WIPP-13 and observation wells toward the center of the WIPP site to the south and east, where fracturing in the Culebra decreases, decreases to 16 to 28 ft^2/day, and apparent storativity increases to 3.6 X 10^{-5} to 5.5 X 10^{-5}. To the west toward Nash Draw, the apparent transmissivity increases to 265 to 650 ft^2/day, reflecting increased fracturing in that direction, while the apparent storativity increases to 5.2 X 10^{-5} to 6.4 X 10^{-5}.
>
> The analyses of the responses measured at observation wells to the WIPP-13 multipad pumping test provide a qualitative conceptualization of three distinct domains within a heterogeneous portion of the Culebra north of the center of the WIPP site. This conceptualization is being refined by using numerical-modeling techniques to simulate the WIPP-13 multipad test and other tests at the WIPP site in an attempt to define the distribution of hydraulic properties that will reproduce the responses observed.

Again, the conclusions were tested using the techniques in the discussion of well H-3. Figure IV-20 shows that wells P-14 and WIPP-25 have a high

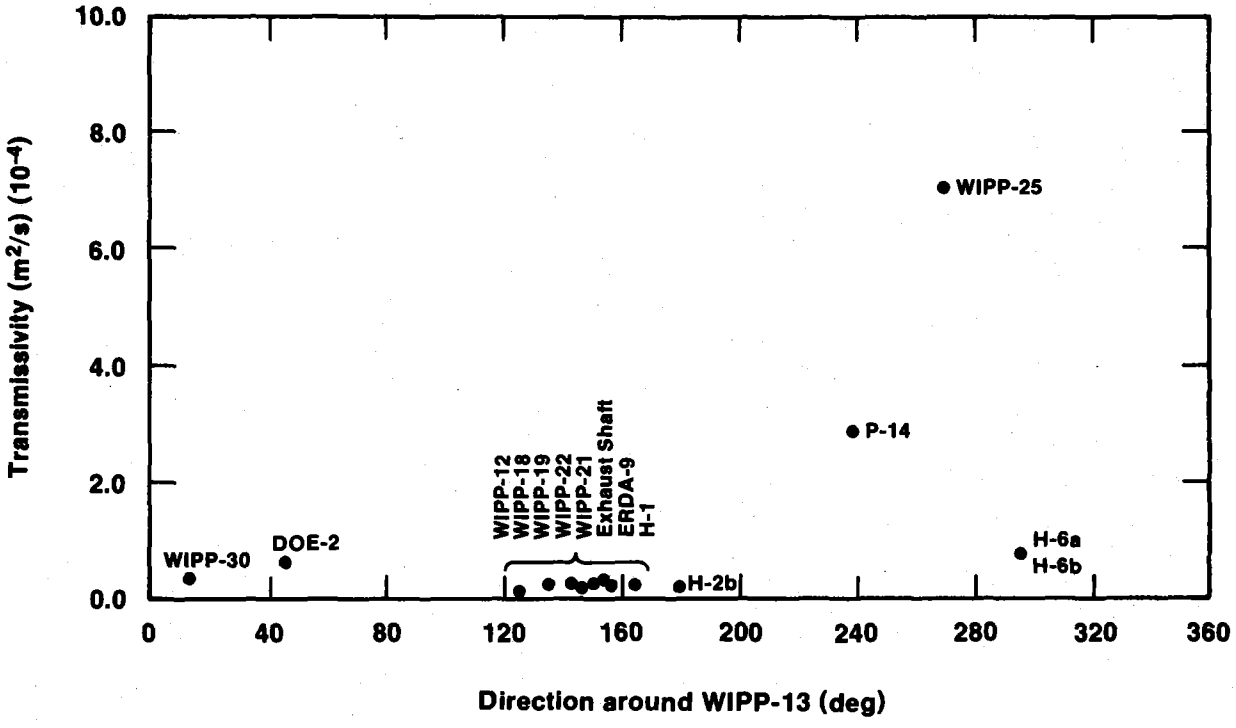

Figure IV-20. Plot Showing Change in Transmissivity in Observation Wells Surrounding WIPP-13.

transmissivity west (WIPP-23) and southwest of the pumping well. The other wells are clustered near the bottom of the plot, south-southeast of WIPP-13. The wells at 295° are wells H-6a and H-6b. Correlation of drawdown to the inverse of the square of the distance shows a very good raw correlation ($r = 0.83$). The ranked correlation is also very good ($r = 0.89$) (Table IV-11, WIPP-13a), indicating that homogeneity of the system may exist. More data are needed to support Beauheim's (1987c) conclusion of heterogeneity. If only the wells north of the WIPP are used in the correlation, the results yield values of $r = 0.98$, indicating homogeneity over the WIPP southeast of well WIPP-13.

The selection of these wells also provides a way of correlating direction and distance with drawdown because the wells are oriented in almost a straight line north to south and are oblique to WIPP-13. This orientation means that the distance increases as the direction increases (from 125° to 165°). Figure IV-21 shows that drawdown decreases as the direction changes and distance increases.

In addition to the three objectives listed for well H-3, a fourth objective for the H-11 multipad test included an attempt to determine how the heterogeneities within the test area are distributed. The results of the H-11 multipad test provided the following information (Beauheim, 1987c):

> The Culebra is a fractured, double-porosity system at H-11 with a transmissivity between 27 and 43 ft^2/day and a storativity between 3.4 X 10^{-5} and 1.5 X 10^{-4}. Drawdown during the multipad test appeared to be largely concentrated to the north and south of H-11; wells to the east and west showed relatively low-magnitude responses. The rapid and high-magnitude responses observed at DOE-1, H-3b2, and H-15 during the multipad test are believed to reflect the presence of a fracture network extending to the north from H-11. Numerical simulations indicate that the fracture network also extends south of H-11, but no wells are currently situated within it.
>
> Double-porosity hydraulic behavior was observed at DOE-1 during the multipad test, and at both DOE-1 and H-3b2 during other pumping tests performed at those locations. The fractures appear to continue past DOE-1 to the north toward H-15, although H-15 itself lies in a lower transmissivity, apparently single-porosity zone. Apparent transmissivities in the region north of H-11 range from 7.1 to 9.0 ft^2/day and apparent storativities range from 2.4 X 10^{-6} to 8.4 X 10^{-6}. Apparent transmissivities between H-11 and observation wells to the west, southwest, and southeast, where fracturing in the Culebra decreases and single-porosity hydraulic behavior is observed, range from 6.0 to 21.0 ft^2/day and apparent storativities range from 1.8 X 10^{-5} to 6.5 X 10^{-5}. Interpretation of the responses to the multipad test observed at the western and southern wells was complicated by an anomalous and widespread rise in water levels of unknown origin.

TABLE IV-11. RESULTS OF CORRELATIONS OF PUMP TEST RESULTS

Pump Test	Correlation	Data Used	n	r (Raw Data)	r (Ranked Data)
H-3	Maximum Drawdown vs. Inverse of Distance Squared	All maximum drawdown data	7	0.49	0.50
H-3	Maximum Drawdown vs. Inverse of Distance Squared	All drawdown data except 3 WIPP wells	4	0.87	0.40
WIPP-13a	Maximum Drawdown vs. Inverse of Distance Squared	All data	15	0.83	0.89
WIPP-13b	Maximum Drawdown vs. Inverse of Distance Squared	Wells W-12, W-18, W-19, W-21, W-22, H-1, H-28, E-9 and E Shaft	9	0.98	1.00
H-11a	Maximum Drawdown vs. Inverse of Distance Squared	All observation well data	10	0.85	0.75
H-11b	Maximum Drawdown vs. Inverse of Distance Squared	All observation well data except H-15, DOE-1 and H-3b2	7	0.95	0.89
H-11c	Drawdown at time pump off	Same as H-11a	10	0.85	0.81
H-11d	Drawdown at time pump off	Same as H-11b	7	0.96	1.00

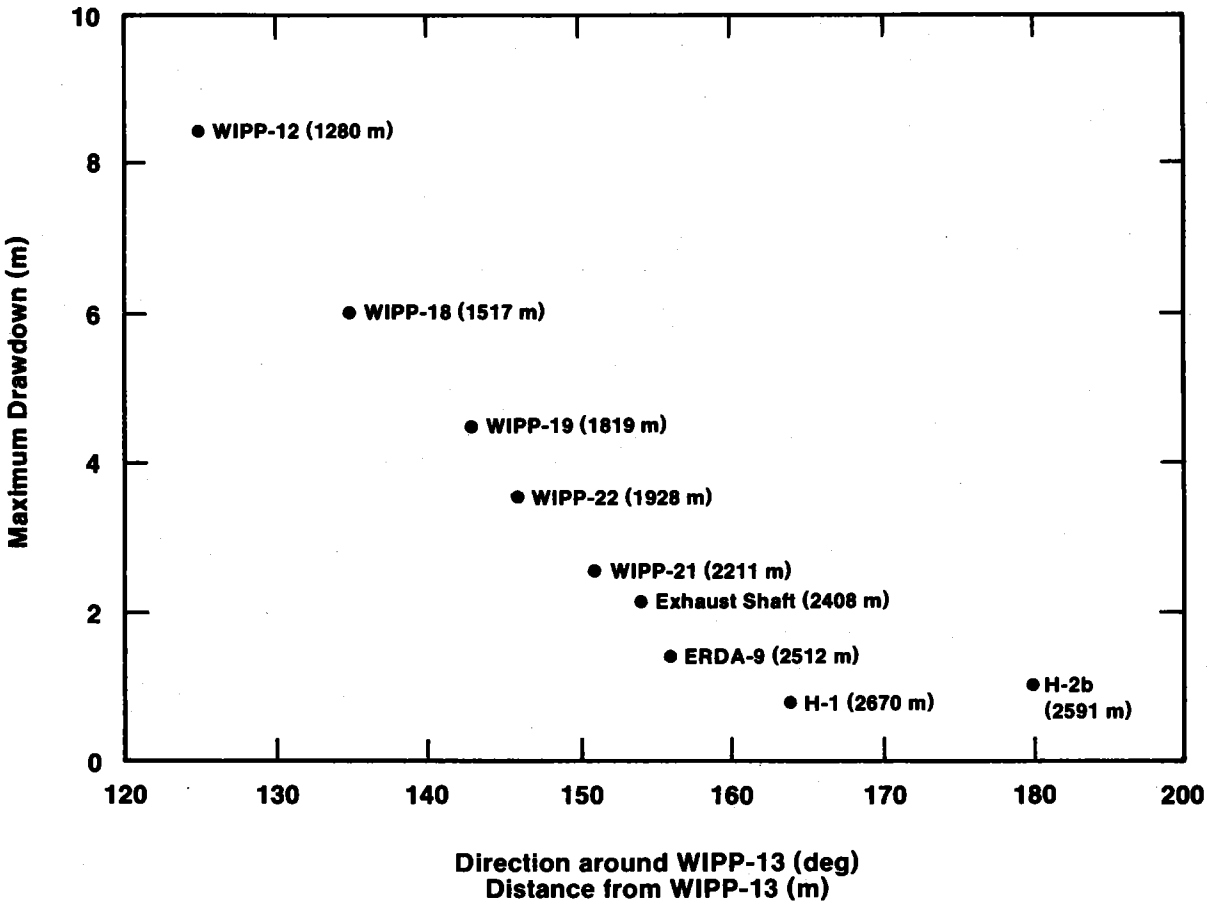

TRI-6342-627-0

Figure IV-21. Drawdown of Observation Wells near and over the WIPP during the WIPP-13 Pump Test, Showing Homogeneity of the Culebra in that Region. (Note: The increase in degrees also correlates to the inverse in distance.)

> Thus, the analyses of the responses measured at observation wells to the H-11 multipad pumping test are consistent with a conceptualization of two distinct domains within a heterogeneous portion of the Culebra south of the center of the WIPP site: a fractured region having low storativity extending to the north and south from H-11, and a relatively unfractured region west, southwest, and southeast of H-11 having higher storativity. This conceptualization is being refined using numerical-modeling techniques to simulate the H-11 multipad test and other tests at the WIPP site, in an attempt to define a distribution of hydraulic properties that will reproduce the responses observed.

Well P-18, northeast of H-11, did not respond to the test. This lack of response may be due to Culebra Dolomite properties or to the poor completion and/or poor perforations in the well casing. For this reason, its lack of response was ignored.

Correlation of the maximum drawdown and the inverse of the square of the distance yields a coefficient of 0.85 (0.86 if P-18 is included) for the raw data, but r = 0.75 (0.78 if P-18 is included) for the rank correlation (Table IV-11). The correlation was also done on drawdown data at the time the pumping was stopped, yielding r for the raw data of 0.85, but r = 0.81 for the ranked data. These correlations tested the hypothesis that the wells north of H-11 (wells H-15, H-3b2, and DOE-1) have drawdowns indicating an elongate zone of high transmissivity that might indicate fractures. A correlation excluding the northern wells was made. The results were r = 0.96 for the raw data and r = 1.00 for the ranked data, indicating homogeneity to the west, south, and southeast.

Beauheim (1989, Figure 5-24) presented a plot of drawdown contours at the end of the well multipad test that was, presumably, hand-drawn. The contours showed an elongate structure that was interpreted as indicative of fractures. Figure IV-22 is a contour plot of drawdowns (in original units) for the H-11 multipad test, and Figure IV-23 is a contour plot without wells H-3b2, H-15, and DOE-1. The plot in Figure IV-22 is slightly elongated to the north, which may be due to lack of data north and east of H-11 and not to a possible fracture zone. The very nearly concentric contours southwest and west in Figure IV-23 show homogeneity in that direction. The bulge in the 3-m contour is caused by the lack of data between wells H-12 and P-17. If well P-18 were included in the plots, the slight bulge to the northeast would be dampened.

The multipad tests do not necessarily indicate zones of preferential flow (heterogeneity). The linear responses to pumping indicate homogeneity south and west of H-11 and south and east of WIPP-13, but this homogeneity may only be a function of observation well location, that is, the response was recorded only because the well was there. Seven of the ten observation wells used for

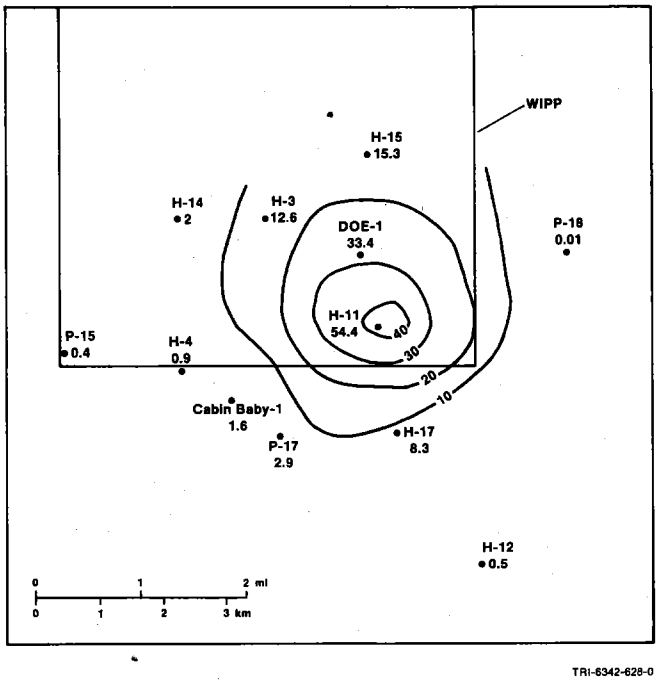

Figure IV-22. Contour Plot of Drawdown at End of H-11 Multipad Test (all wells).

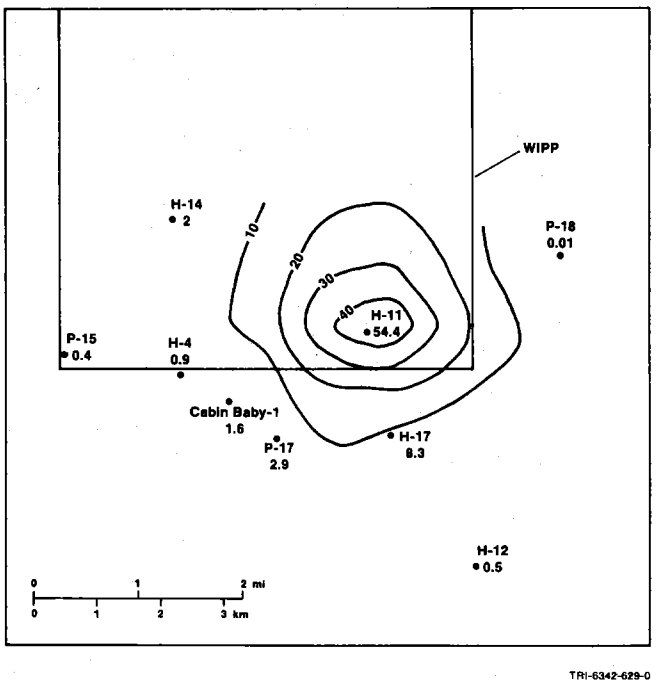

Figure IV-23. Contour Plot of Drawdown at End of H-11 Multipad Test (wells H-15, H-3b2, and DOE-1 not included).

the H-11 test are south (two wells) and west (five wells), and the other three wells are north of H-11. Nine of the 15 wells that responded to the WIPP-13 test are south or east of the pumping well. One well is northeast of WIPP-13 (DOE-2), three wells are north (both H-6 wells and WIPP-30), one well is almost due west (WIPP-25), and one well is southwest (P-14). Considering the high correlation of the inverse of the square of the distance to drawdown for these wells ($r = 0.89$), more pump tests with a better distribution of observation wells may be needed before a conclusion about amount and directions of heterogeneity can be made. Also, a single-porosity concept for regional-scale, ground-water flow modeling will be adequate.

MAGENTA DOLOMITE (RUSTLER FORMATION) HYDROSTRATIGRAPHIC UNIT

The Magenta Dolomite Member of the Rustler Formation is the third hydrostratigraphic unit of importance. It is a persistent dolomitic unit with thin laminae of anhydrite and produces water from a thin, silty dolomite, along bedding planes of rock units, and along fractures (Mercer, 1983). The unit, like the Culebra Dolomite Member, is present locally at the WIPP, but unlike the Culebra Dolomite Member is absent in the southern part of Nash Draw. Aquifer yield is low and, consequently, the member is of little interest to hydrologists, as reflected by the amount of data available. Twelve wells were tested and reported in Mercer (1983), and two additional wells were tested later (Beauheim, 1987b) (Table IV-12). The Magenta Dolomite Member is unsaturated at outcrops along Nash Draw, and in some places the Magenta Dolomite is almost in contact with the Culebra Dolomite, separated only by a few meters of dissolution residue (see the preceding section on the "Culebra Dolomite (Rustler Formation) Hydrostratigraphic Unit").

Hydraulic Conductivity and Permeability

Only 15 values of transmissivity have been measured from the Magenta Dolomite Member (Table IV-12) and have a small spatial distribution as stated previously in the section "Culebra Dolomite (Rustler Formation) Hydrostratigraphic Unit." The log transmissivity ranges over five orders of magnitude from -8.4 to -3.4, with a mean log transmissivity of -8.0. The Magenta has a mean formation thickness of 7.6 m (25 ft) and a range from 5.8 to 9.4 m (19 to 30 ft). The log hydraulic conductivities for the Magenta Dolomite have a range from -9.3 to -4.3, with a mean log hydraulic conductivity of -7.8. The largest transmissivity tested (4.0×10^{-4} m^2/s) was at WIPP-25 at the edge of Nash Draw west of the WIPP, and the lowest transmissivity tested (6.5×10^{-9} m^2/s) was at test hole H-8 (Table IV-12). Examination of a core of WIPP-28 revealed bedding-plane partings and fractures filled with gypsum (Mercer, 1983).

TABLE IV-12. MAGENTA DOLOMITE GEOHYDROLOGIC DATA BASE

Hydropad Name	Transmissivity (m^2/s)	Hydraulic Conductivity (m/s)	Log Hydraulic Conductivity	Water Level[a] (m)	Water Density (g/cm^3)	Magenta Thickness	Storativity	Halite[b]
H-1	5×10^{-8}	7×10^{-9}	-8.2	962.6	1.021	7.9	--	2
H-10	1×10^{-8}	2×10^{-9}	-8.8	980.8	1.171	7.3	1×10^{-3}	2
H-14	6×10^{-9}	8×10^{-10}	-9.1	<966[c]	1.2	7.3	--	2
H-16	3×10^{-8}	4×10^{-9}	-8.4	950[c]	1.2	7.9	--	2
H-2	1×10^{-8}	1×10^{-9}	-8.9	959.5	1.012	8.5	1×10^{-4}	2
H-3	1×10^{-7}	1×10^{-8}	-7.8	961.6	1.01	7.6	1×10^{-5}	2
H-4	6×10^{-8}	8×10^{-9}	-8.1	959.2	1.017	7.7	1×10^{-6}	2
H-5	1×10^{-7}	2×10^{-8}	-7.8	964.7	1.008	7.2	1×10^{-5}	2
H-6	3×10^{-7}	5×10^{-8}	-7.3	932.4	1.007	6.3	1×10^{-5}	0
H-8	6×10^{-9}	1×10^{-9}	-9.0	923.2	1.008	6.7	--	1
H-9	1×10^{-6}	1×10^{-7}	-6.9	952.2	1.006	9.4	1×10^{-9}	1
WIPP-25	4×10^{-4}	5×10^{-5}	-4.3	931.2	1.01	7.9	--	0
WIPP-27	5×10^{-5}	1×10^{-5}	-5.0	940	1.078	5.5	--	0
WIPP-28	d	5×10^{-10}	-9.3	959.8	1.048	7.9	--	0
WIPP-30	4×10^{-9}	5×10^{-10}	-9.2	953[c]	1.01	8.0	--	2
DOE-2[c]	1×10^{-9}	1×10^{-10}	-9.8	<970	1.18	7.0	--	2

[a] Mercer, 1983

[b] Presence of halite (Beauheim, 1987b)
- 0 No halite present
- 1 Salado present
- 2 Halite in unnamed lower member
- 3 Halite in unnamed lower member and Tamarisk Member
- 4 Halite in unnamed lower member, Tamarisk Member, and Forty-niner Member

[c] Lappin and others, 1989

[d] Low or unsaturated

Source: Modified from Mercer, 1983, and Beauheim, 1987b

A contour map of the Magenta Dolomite Member's log hydraulic conductivities (Figure IV-24) illustrates a decrease in conductivity from west to east, with slight indentations of the contours north and south of the WIPP at the "Nash-Draw reentrants" mentioned previously in the "Culebra Dolomite (Rustler Formation) Hydrostratigraphic Unit" discussion. A preliminary statistical analysis shows a poor correlation (r = -5.0) of overburden thickness to hydraulic conductivity. The poor correlation may be due to the way the material surrounding the Magenta Dolomite has been dissolved and the subsequent deposition of gypsum in parting planes and fractures.

Porosity

No porosity measurements have been made on the Magenta Dolomite, but a porosity of 0.20 has been estimated (after Beauheim, 1987b) for the dolomite, which is slightly high for intact dolomite (Davis and DeWeist, 1966) but may be close to an average porosity for a dolomite that has been affected by the karstification that has occurred above and below.

Storativity

Storage coefficients for the Magenta Dolomite range from 10^{-9} to 10^{-3} (Table IV-12).

Potentiometric Surface

The contours of the potentiometric-surface map (Figure IV-25) representing fresh-water equivalent heads indicate that flow is southwest at a gradient of 0.003 in the northeastern part of Nash Draw. Across the WIPP, flow is almost westward at a gradient of 0.004. Because the Magenta Dolomite is absent in the southwestern part of the draw and no springs are along the rim of the draw, the ground water probably flows into lower units through fractures. The undulating potentiometric surface follows the topographic surface north and south of the WIPP and outlines the north and south inlet.

Fluid Density

Water density varies from 1.004 g/cm^3 (only slightly saline) at test hole H-9a on hydropad H-9 in the southern part of the Study Area to 1.171 g/cm^3 at test hole H-10a southeast of the WIPP (Figure IV-26). According to Mercer (1983), the water-quality distribution was not as well defined as the Culebra Dolomite distribution but was, nevertheless, distinguishable and reflected the degree of dissolution of the underlying halite.

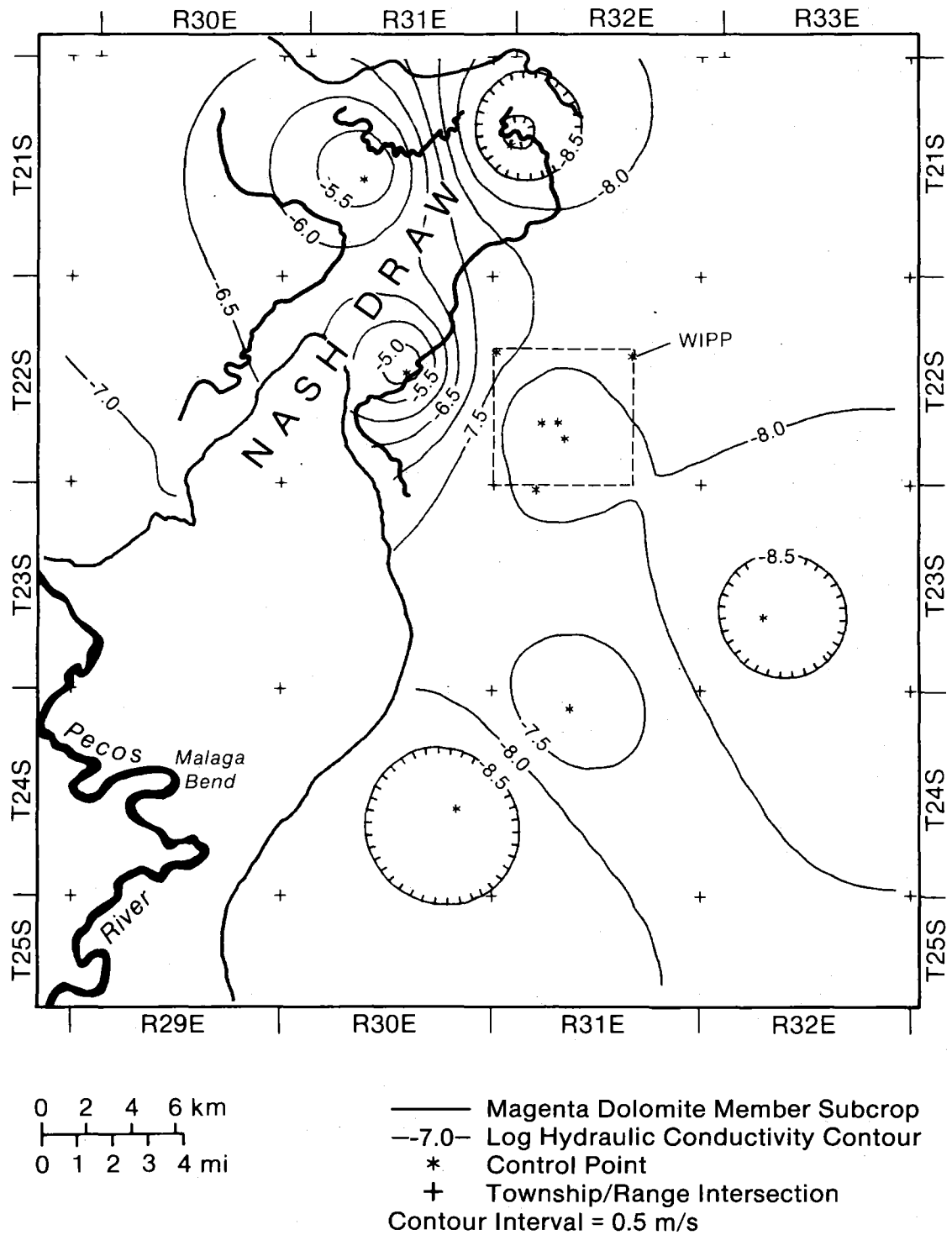

Figure IV-24. Contour Map of Log Hydraulic Conductivities of the Magenta Dolomite Member in the Study Area.

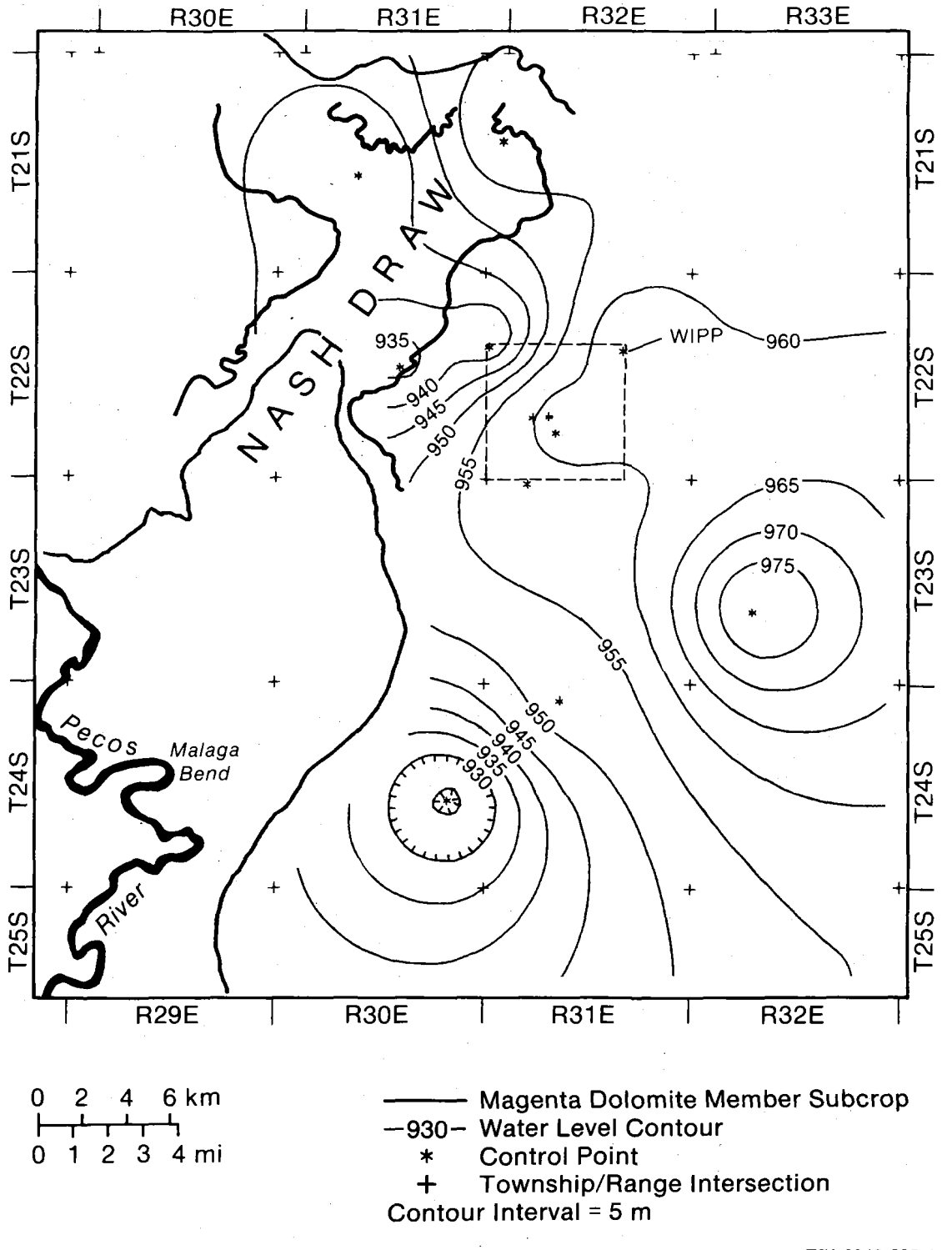

Figure IV-25. Adjusted Potentiometric Surface of the Magenta Dolomite Member of the Rustler Formation in the Study Area.

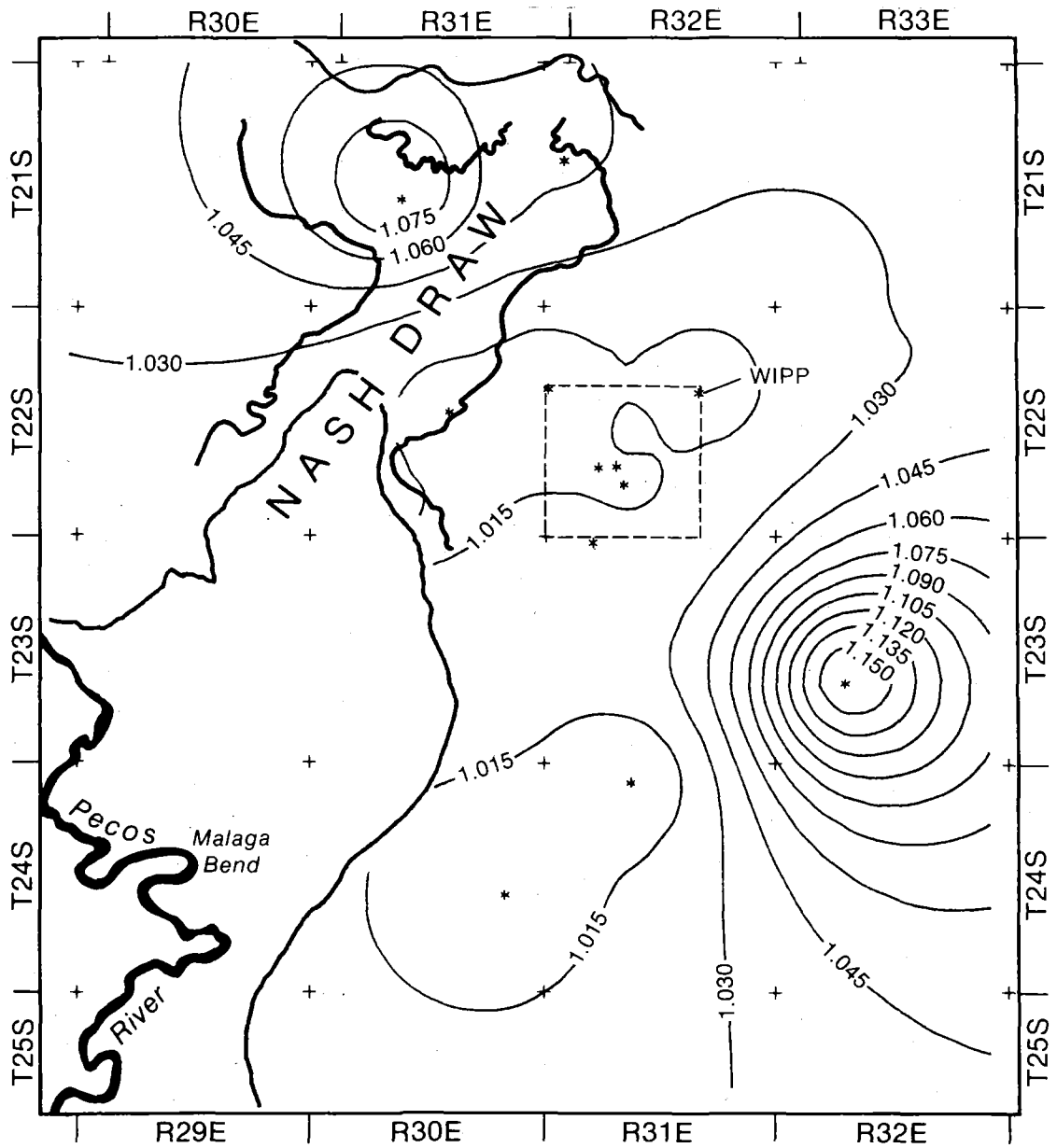

Figure IV-26. Contour Map of Brine Density in the Magenta Dolomite Member in the Study Area.

Recharge and Discharge

The potentiometric map indicates that recharge to the Magenta Dolomite probably occurs to the north, possibly in Clayton Basin, or farther north at Bear Grass Draw where the Rustler Formation crops out (Mercer, 1983). Mercer (1983) speculated that the apparent recharge to the east of the WIPP is an artifact of the variable water-density corrections. Recharge could also result from breccia pipes north and east of the WIPP that connect the Capitan to the Magenta Dolomite (see "Recharge and Discharge" in "Rustler-Salado Contact Residuum Hydrostratigraphic Unit" in this chapter).

Discharge is probably into the lower units, the Tamarisk Member and the Culebra Dolomite Member. The upper Forty-niner unit may also be a sink but does not supply a mechanism for upward flow in the vicinity of Nash Draw (Mercer, 1983). Flow direction in the Magenta Dolomite Member in upper Nash Draw is similar to Culebra Dolomite Member flow and is ultimately southward, either toward Malaga Bend or the Balmorhea-Loving Trough.

VERTICAL FLOW IN THE RUSTLER FORMATION

Figures IV-27 to IV-31 present a method for examining the potential for vertical flow in the Rustler Formation by using water-level data from Mercer (1983). The left-hand plot of Well H-1 (Figure IV-27a) shows formation elevation versus hydraulic head, with the stratigraphic layers and the elevation of the actual measured heads and fresh-water heads drawn. The right-hand side of each pair shows the actual head of each well as measured. The slope of the line connecting the heads in the left-hand plot indicates the direction of the vertical gradient. A line sloping downward to the left indicates a downward gradient (Figure IV-27a), a vertical slope indicates no gradient (such as between the Magenta Dolomite and Culebra Dolomite in well H-6, Figure IV-28b), and a line sloping downward to the right indicates an upward vertical gradient, as in well WIPP-30 (Figure IV-31c).

This visual method incorporated the density of the fluids from each well as reported by Mercer (1983), which were converted to fresh-water heads and then superimposed on the tandem plots. This method ignores the density term in Darcy's law and has a potential for producing misleading results if the plots are used to quantify flow, but the method is useful in determining potential direction of flow. Holt and others (in prep.) calculated a pressure-depth gradient from calculated static pressures at mid-formation for hydrostratigraphic units where more recent water-density data were known (Richey, 1987). The calculated pressure-depth gradient was converted to the equivalent fluid density that corresponds to the fluid density of an equilibrated system. The hypothetical fluid was then compared to the actual

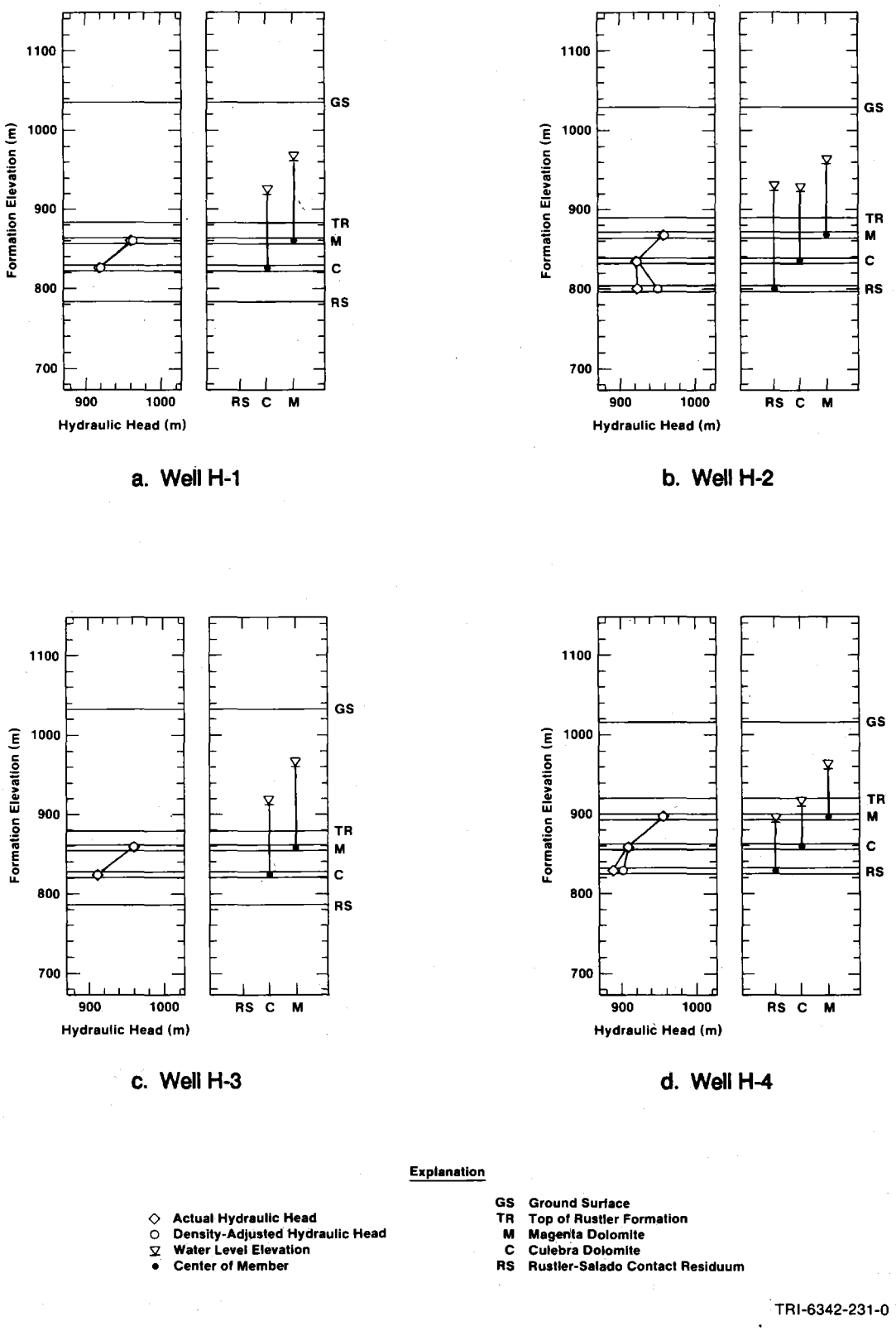

Figure IV-27. Comparisons Between Wells H-1, H-2, H-3, and H-4, Showing Potentials for Vertical Flow in the Rustler Formation (data from Mercer, 1983).

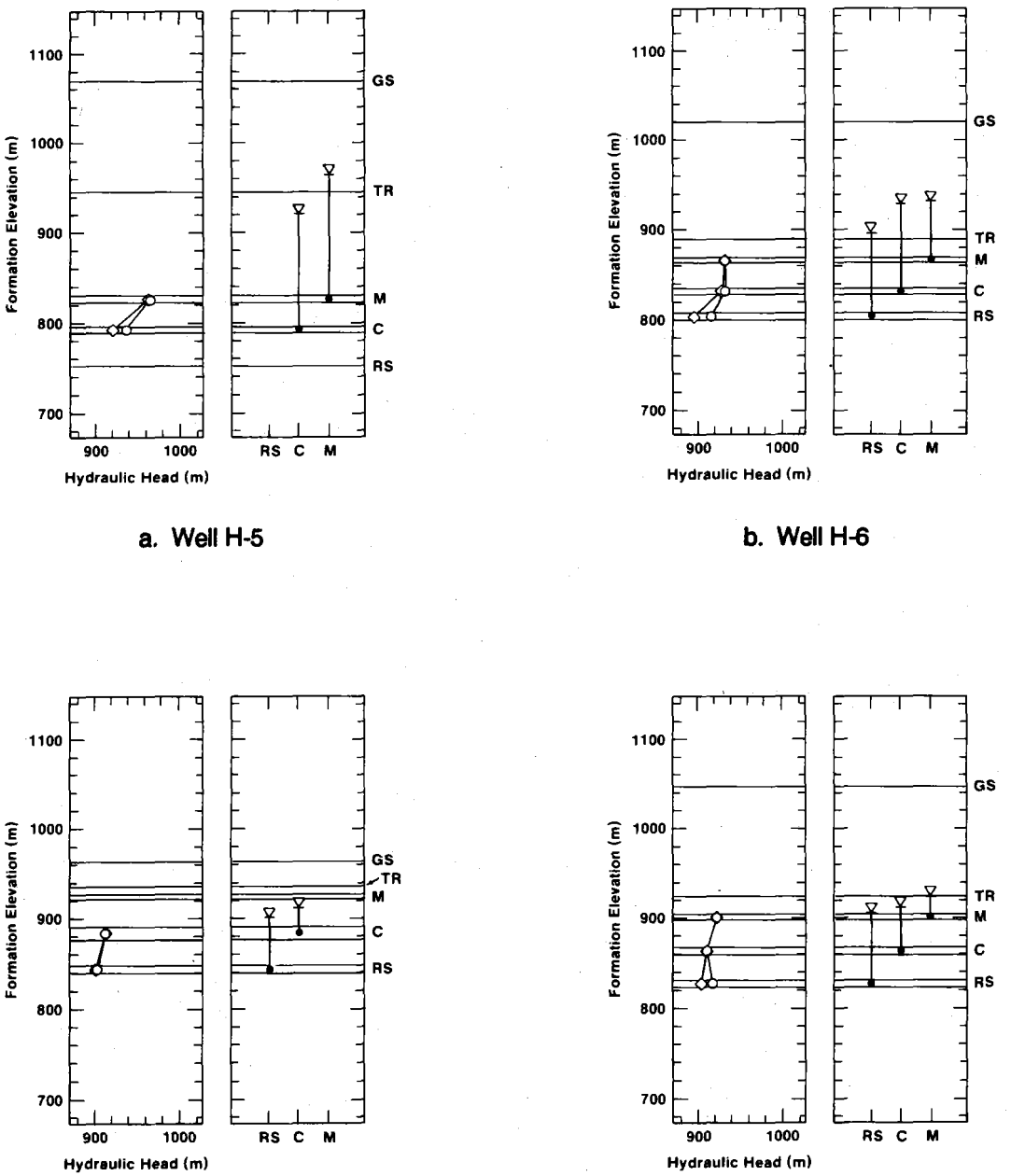

Figure IV-28. Comparisons Between Wells H-5, H-6, H-7, and H-8, Showing Potentials for Vertical Flow in the Rustler Formation (data from Mercer, 1983).

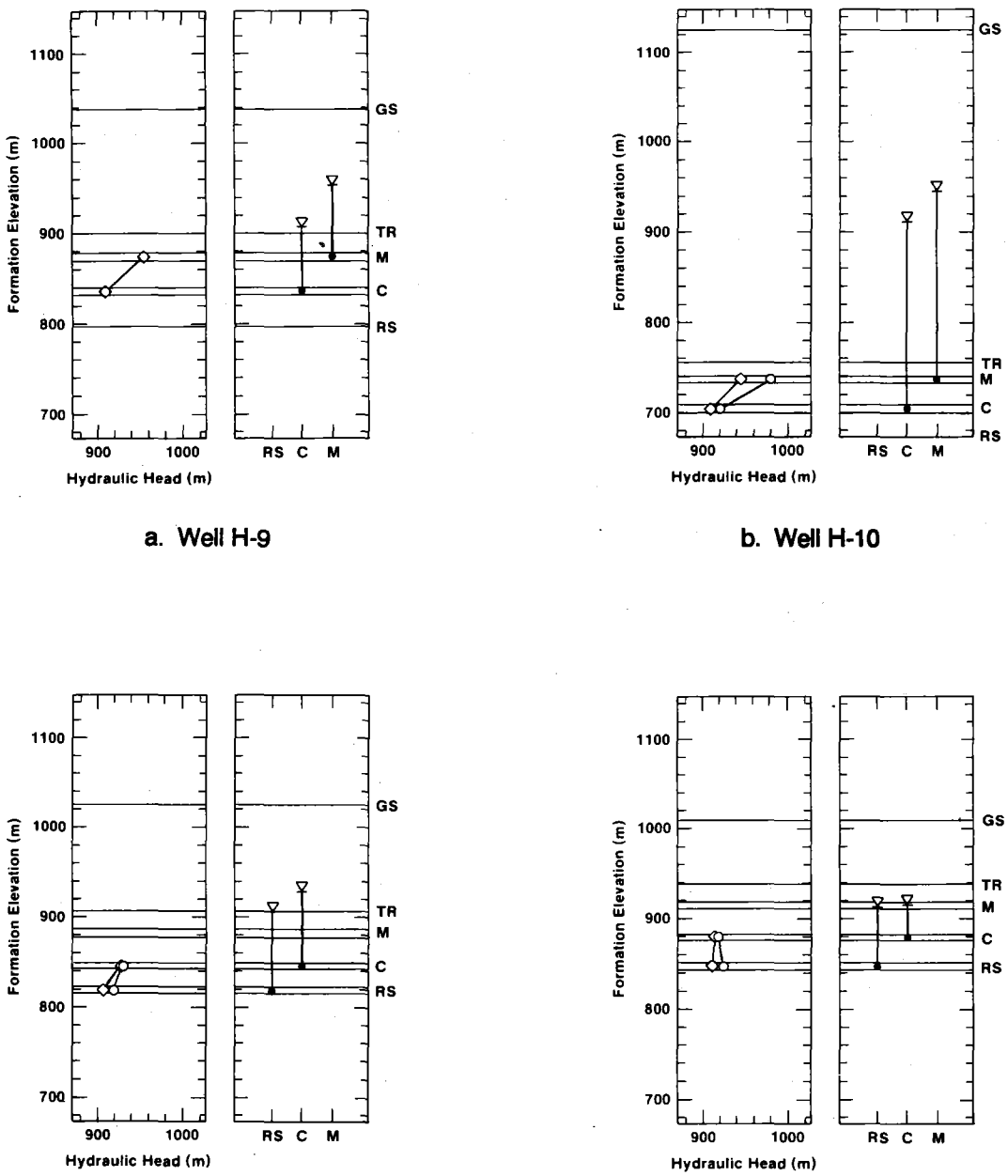

Figure IV-29. Comparisons Between Wells H-9, H-10, P-14, and P-15, Showing Potentials for Vertical Flow in the Rustler Formation (data from Mercer, 1983).

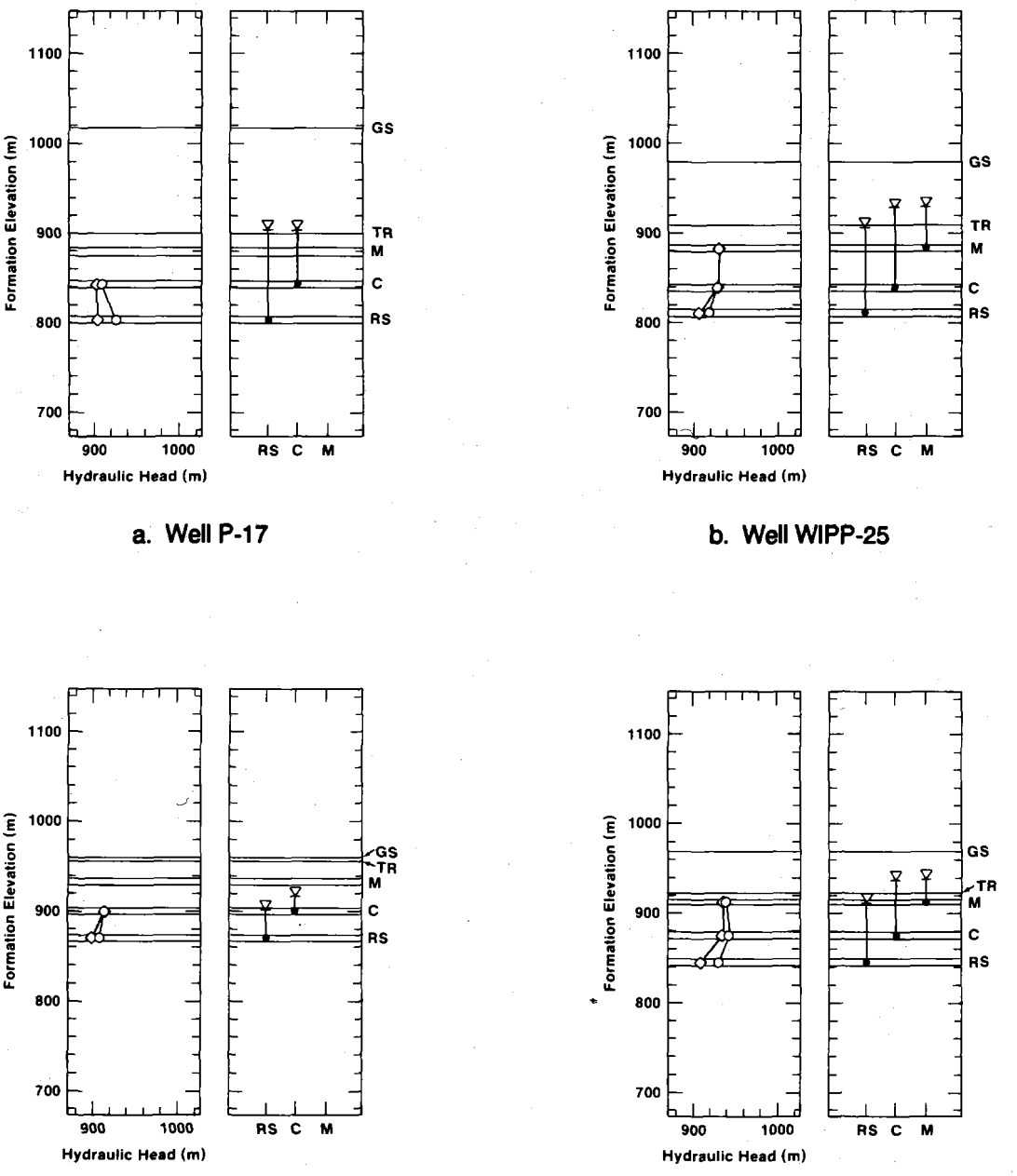

Figure IV-30. Comparisons Between Wells P-17, WIPP-25, WIPP-26, and WIPP-27, Showing Potentials for Vertical Flow in the Rustler Formation (data from Mercer, 1983).

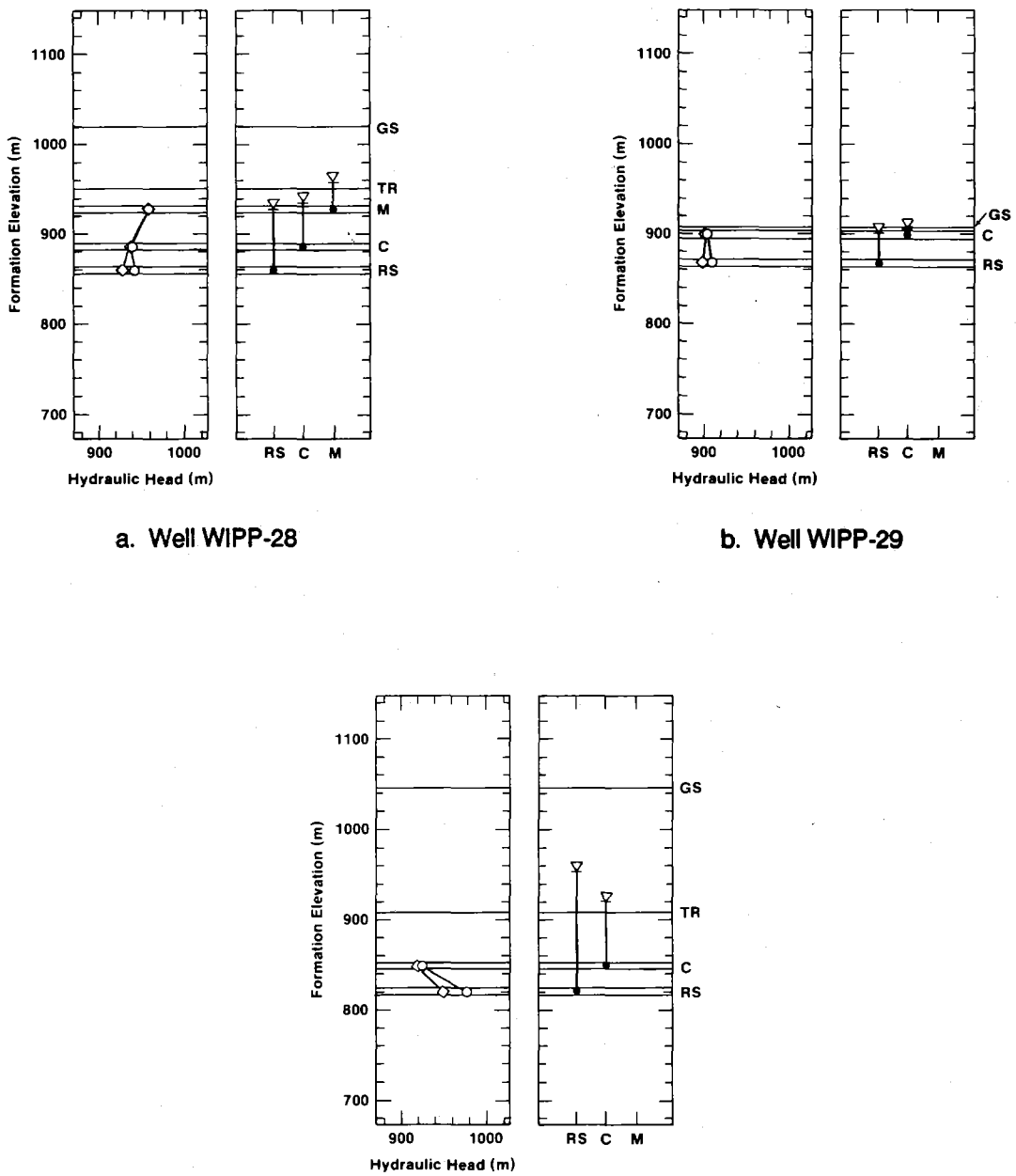

Figure IV-31. Comparisons Between Wells WIPP-28, WIPP-29, and WIPP-30, Showing Potentials for Vertical Flow in the Rustler Formation (data from Mercer, 1983).

fluid densities. If the density is lower than both, flow in the system is downward, and conversely, if the hypothetical fluid density is more than the actual densities, then flow is upward. If the hypothetical fluid density is intermediate or equal to the actual fluid densities, no flow occurs. Table IV-13 compares the Holt and others results with the results from the visual inspection of the plots in Figures IV-27 to IV-31.

In wells H-2 (Figure IV-27b), P-15 (Figure IV-29d), P-17 (Figure IV-30a), and possibly WIPP-29 (Figure IV-31b), the heads indicate an upward gradient. Wells H-2 and P-17 correspond to the results of Holt and others (in prep.), but wells WIPP-28 and WIPP-29 are listed as indeterminate. Wells H-3 (Figure IV-27c), H-4 (Figure IV-27d), H-6 (Figure IV-28b), H-7 (Figure IV-28c), P-14 (Figure IV-29c), WIPP-25 (Figure IV-30b), WIPP-26 (Figure IV-30c), and WIPP-27 (Figure IV-30d) show a downward gradient. Wells H-6, H-7, WIPP-25, and WIPP-26 are all listed by Holt and others (in prep.) as having the same gradient direction, and well P-14 is listed as indeterminate. WIPP-30 (Figure IV-31c) shows a strong upward gradient, but the same well has a downward gradient using the method of Holt and others (in prep.). This difference is due to the significant difference in densities used in the two methods (1.072 gm/cm^3 and 1.204 gm/cm^3 for the Culebra and Rustler-Salado residuum, respectively, for this report's calculations, and 1.018 gm/cm^3 and 1.202 gm/cm^3 for the Culebra and Rustler-Salado residuum, respectively, for the calculations of Holt and others (in prep.)). Well H-8 (Figure IV-28d) is indeterminate and should not be used to infer a direction of flow at that site. The method of illustrating direction of flow potential of fresh-water heads and actual measured heads presented here is adequate, but a more rigorous method is required when quantitative information is needed.

Vertical flow potential in wells H-2 and P-17 is upward from the Rustler-Salado contact residuum to the Culebra Dolomite Member and downward from the Magenta Dolomite Member to the Culebra Dolomite. These wells are in the region (Region 2 in Table IV-13) where dissolution of halite has occurred in the Tamarisk Member and the Forty-niner Member but not in the unnamed lower member. This vertical gradient toward the Culebra Dolomite is due to increase in vertical permeability in the upper aquitards, allowing leakage from the tighter Magenta Dolomite downward through the Tamarisk. In this region, the Culebra Dolomite is underpressured due to its relatively higher transmissivity, allowing flow to the southwest. The unnamed lower member has a low hydraulic conductivity due to the lack of dissolution of the lower Rustler Formation halites that prevents the brine aquifer from equilibrating. In wells where the vertical flow directions are indeterminate between the Rustler-Salado contact and the Culebra Dolomite (H-8, WIPP-28, and WIPP-29), dissolution of all Rustler halite has taken place, allowing better vertical connection (well P-15 is very close to the boundary of total halite

TABLE IV-13. COMPARISON OF METHODS FOR DETERMINING VERTICAL FLOW POTENTIAL IN THE RUSTLER FORMATION

	This Report		Holt and others (in prep.)		
	R-S-C[a]	C-M[b]	RS-C[a]	C-M[b]	Halite[c]
H-1		D		D	2
H-2	U	D	U	D	2
H-3		D		D	2
H-4	D	D		D	2
H-5		D		D	2
H-6	D	I	D	I	0
H-7	D	*	D	*	0
H-8	I	D	I	D	1
H-9		D		D	1
H-10		D		D	2
P-14	D	D	I		1
P-15	I				2
P-17	U		U		2
W-25	D	D(?) almost no flow (vertical)	D(?)	D(?)	0
W-26	D	*	D(?)	*	0
W-27	D	U(?) almost no flow (vertical)		D(?)	0
W-28	I	D	I	D	0
W-29	I	D	I		1
W-30	U		D	D	1
DOE2				D	2
H-14				D	2
H-16			U	D	1

a Rustler-Salado contact residuum
b Culebra-Magenta
c Presence of halite
- 0 Wells west of upper Salado dissolution front
- 1 Upper Salado present (no halite in Rustler)
- 2 Halite in unnamed lower member; absent in Tamarisk and Forty-Niner
- 3 Halite in unnamed lower member and Tamarisk; absent in Forty-Niner
- 4 Halite in unnamed lower member and in Forty-Niner

* Magenta Dry

U Upward
D Downward
I Indeterminate

dissolution in the Rustler), which results in an equilibrated flow system, that is, no vertical flow. Flow in wells H-6, H-8, P-15, WIPP-28, and WIPP-29 between the Magenta Dolomite and the Culebra Dolomite is downward to the underpressured Culebra. Flow is from the Culebra to the Rustler-Salado in wells H-6, H-7, P-14, WIPP-25, WIPP-26, and WIPP-27, and from the Magenta to the Culebra in wells H-1 to H-5, H-8 to H-10, P-14, and possibly WIPP-25. All wells with downward flow are from the Magenta to the Culebra in dissolution regions 0, 1, or 2 where the Tamarisk halite and Forty-niner halite have been dissolved.

SUPRA-RUSTLER ROCKS

Occurrence of ground water in the units above the Rustler Formation will be considered as though the Supra-Rustler rocks were one hydrostratigraphic unit in the same manner that Davies (1989) assumed one continuous unit above the Rustler Formation. This assumption is supported by very little evidence, though, of continuous hydraulic connection between the overlying Triassic sandstones and surficial Cenozoic and Holocene alluvial deposits with the fine-grained Dewey Lake Red Beds, the youngest Ochoan unit, but will, nevertheless, be made.

DEWEY LAKE RED BEDS (SUPRA-RUSTLER)

Drilling in the Dewey Lake Red Beds has not identified any continuous saturated zone, but some localized zones of relatively high permeability were identified because of the loss of drilling fluids at DOE-2 and H-3d (Mercer, 1983; Beauheim, 1987a). Some thin, lenticular, perched and semiperched sands were identified in the upper Dewey Lake Red Beds at wells H-1, H-2, and H-3 (Mercer and Orr, 1979; Mercer, 1983). Attempts were made to test moist Dewey Lake Red Bed sands at H-2c (Mercer, 1983) and the lower Dewey Lake Red Beds at DOE-2 and H-14 (Beauheim, 1986; Beauheim, 1987b). The H-2c test was halted after five hours because very little water was detected. The DOE-2 test was terminated after one hour because the very low inflow rate (<1 mℓ/min) would require a long time to reach steady-state, and the wait was deemed impractical (Beauheim, 1986). The H-14 test was terminated because the low permeability of the unit (one or more order(s) of magnitude less than the unnamed lower member) was responsible for an extremely slow buildup rate (Beauheim, 1987b).

The only Dewey Lake Red Bed wells producing sufficient water for livestock are the James Ranch wells, Fairview well, and Pocket well (Cooper and Glanzman, 1971). Completions were reported in the Triassic undifferentiated Dockum Group. According to Mercer (1983), however, the wells were completed in the Dewey Lake Red Beds, but he presented no rationale for the terminology. Examinations by Lambert and Harvey (1987) of the chemistry of samples taken

from the wells and of geologic maps constructed by Bachman (1980) show that no Triassic rocks are present at the locations of these wells and that the wells are probably completed in the Dewey Lake Red Beds.

Hydrologic properties of the Dewey Lake Red Beds are difficult to determine because of the lack of long-term hydraulic tests. The hydraulic conductivity of the Dewey Lake Red Beds, assuming saturation, is probably 1×10^{-8} m/s, similar to the hydraulic conductivity of fine-grained sandstone and siltstone (Mercer, 1983; Davies, 1989). The porosity is estimated in the range of fine-grained sandstone at 20 percent. Storativity is estimated to be 10^{-4}. Water density is similar to the Magenta Dolomite Member of the Rustler Formation.

Water percolating downward through fractures to bedding planes and fine-grained lenticular sandstones recharges the Dewey Lake Red Beds locally, and the water then discharges to lower zones (Mercer, 1983). The nature of the lenticular sands restricts lateral movement of ground water.

DOCKUM GROUP

Upper Triassic Dockum Group rocks occur in eastern Eddy County and extend east into Lea County. The undifferentiated Dockum Group (Tocovas, Santa Rosa, and Chinle in Mercer, 1983, and Richey and others, 1985) is the chief source of water for domestic and stock use in eastern Eddy County and western Lea County (Nicholson and Clebsch, 1961; Richey and others, 1985).

Data from only three aquifer tests performed on the Dockum Group rocks in Winkler County, Texas, to the south of the Study Area (Richey and others, 1985), provide an estimate (in the loosest sense) of the range of transmissivities, hydraulic conductivities, and storage coefficients. Transmissivities from these tests range over one order of magnitude from 3.8×10^{-4} to 3.4×10^{-3} (log transmissivity ranges from -3.4 to -2.5, with a mean log transmissivity of -2.9). Only two hydraulic conductivities were calculated, and they have a narrower range: 3.3×10^{-5} to 3.8×10^{-5} m/s. Two measured storativities were 1×10^{-4} to 3×10^{-4}. Porosities were not measured, but the sandstones probably range from 0.05 to 0.30.

Calculated log transmissivities for four aquifer and slug tests in Triassic rocks (Geohydrology Associates, Inc., 1979) ranged from -4 to -6, with a log mean of -5.5. In the same report, calculated log hydraulic conductivities ranged from -6 to -7, with a mean log hydraulic conductivity of -6.3. The report estimated a porosity of 0.30 for the Triassic rocks in the vicinity of the Study Area.

Recharge to the Triassic rocks is from precipitation on overlying sand dunes, precipitation on outcrops, and leakage from the overlying Ogallala east of San Simon Swale and from alluvium.

CENOZOIC ROCKS

Although occurrence of Cenozoic alluvium in the vicinity of the WIPP is sporadic, the material is of particular interest because of the role that the depression in which the very thick alluvium (up to 300 m [981 ft] in the southern part of Eddy County and up to almost 600 m [1,962 ft] in Texas) lies may play as the ultimate regional base level (sink) for regional ground-water flow. In the region other than around the WIPP, the alluvium is the primary source of water for domestic use, municipal use, stock watering, and industry (Richey and others, 1985). In the Study Area, the thickness of this material ranges from absent to about 50 m (163.5 ft) (see also "Regional Geomorphology," Chapter III in this report).

The mostly unconsolidated and semiconsolidated rocks are predominantly dry in the vicinity of the WIPP except for some localized perched zones (Mercer, 1983). The Cenozoic aquifers along the Pecos River are unconfined and under water-table conditions.

In the vicinity of the WIPP, packer-permeability tests for building foundations indicated a range of hydraulic conductivities for the dry material from 1×10^{-8} to 1×10^{-5} m/s (Mercer, 1983). Aquifer tests in the saturated alluvium along the river and south of the Study Area indicate a log hydraulic conductivity ranging from -5 to -3 (Geohydrology Associates, Inc., 1979; Richey and others, 1985). Only one aquifer test has been conducted in the alluvium for the WIPP, and that was on the previously drilled Carper well southwest of the WIPP (Beauheim, 1987b). The Carper well test indicated a transmissivity of 5.9×10^{-5} m^2/s and a hydraulic conductivity of 1.6×10^{-6} m/s for the 37 m tested. The calculated rate of movement through the alluvium ranges from 0.3 m/s in the fine-grained, evaporite-cemented sediments to 30 m/s in the fractured or conglomeratic sediments (Hale and Clebsch, 1958).

In New Mexico, precipitation, the adjacent Guadalupian reef complex units near Carlsbad, the adjacent Permian hydrostratigraphic units at Malaga Bend, ephemeral streams, and irrigation water from the Pecos River recharge the alluvial aquifers. Discharge from the alluvium occurs at Malaga Bend and by phreatophytes drawing water out of the relatively shallow alluvial aquifer near the river.

V. GEOCHEMICAL STUDIES

A summary of site-characterization studies by Lappin (1988) discusses four aspects of geochemical studies done in the Rustler Formation and younger rocks. The summary covers the status of geochemical studies of major and minor solutes, discusses an expansion of interpretation of results from geochemical studies, examines the length of time ground waters may have been isolated from contact with atmospherically derived components, and discusses fluid flow direction and rates in the Culebra Dolomite. Table V-1 summarizes recent geochemical work in and near the WIPP.

Solute distribution in the Culebra Dolomite Member in the Study Area was examined by Ramey (1985) and Siegel and others (1990). Three distinct Culebra-Dolomite water types were identified by Ramey (1985). A division by Siegel and others (1990) put the ground waters into four types roughly along the same lines as Ramey (1985) but added a zone along western Nash Draw (Figure V-1). The four hydrochemical facies identified by Siegel and others (1990) are the following:

Zone A - This zone is coincidental with the low hydraulic conductivity zone and the occurrence of halite in the Rustler Formation east of the WIPP. The Culebra Dolomite waters are sodium chloride brines.

Zone B - This zone contains the freshest water in the Culebra Dolomite and is south of the WIPP.

Zone C - This zone has water of variable composition and is between Zone A and Zone B and in the eastern part of Nash Draw.

Zone D - This zone is a high salinity zone and occurs in western Nash Draw.

Overlaying the zonation maps of Siegel and others (1990) and Ramey (1985) with a potentiometric map of the Culebra Dolomite or with the results of preliminary numerical simulations of ground-water flow (LaVenue and others, 1988) shows that present flow is not in a direction consistent with the water composition. Flow is from high to low salinity, that is, the water is apparently becoming fresher. This flow direction is not possible unless recharge from rain or from flow from other hydrostratigraphic units is freshening the water.

TABLE V-1. RECENT GEOCHEMICAL STUDIES IN THE STUDY AREA

Researcher	Method of Study	Unit(s) Studied	Results	Conclusions
Lambert and Robinson (1984)	Physiochemical tests on three zones in six wells in Nash Draw	Rustler Formation	pH, Eh, specific conductance, specific gravity (SG); major and minor inorganic solutes oxygen-18/oxygen-16 and deuterium/hydrogen activity ratios (A.R.), uranium-234/uranium-238 A.R.	Radiocarbon results difficult to interpret, need long observation time; need reliable sampling techniques
Ramey (1985)	Water chemistry of 20 test holes	Rustler Formation	Rustler-Salado contact (R-S) - waters almost halite saturated. Culebra Dolomite - has large chemical variation. Magenta Dolomite - Na and Cl are major ions	R-S results shown dissolution limit Flow direction inconsistent with chemistry, three zones of water types - water under-saturated with respect to halite. Low permeability of Magenta Dolomite inhibits flow; may have two distinct water types but conclusion may be premature
Chapman (1986)	Analysis of Lambert and Harvey (1987) data. Data compared to Roswell Basin. Obtain isotopic composition of precipitation, surface water and ground water	Culebra Dolomite	Roswell waters were dated showing origin and are the same as water from Rustler Formation. Carlsbad Cavern water isotopically the same as surface water	Isotopic composition not characteristic of recently recharged meteoric water. Nash Draw waters could be derived from evaporation of Rustler Formation ground water. WIPP-29 and Surprise Spring are enriched by evaporation. Steady-state conditions exist
Lambert (1987)	Radiocarbon dating with hydrogen-3 and chlorine-36	Rustler Formation ground water	All but six dates were negative (-1000 to -7000 yr) because of overadjustment of model for contamination caused by dilution and isotopic exchange with rock	Three ages from Rustler Formation and one from Dewey Lakes Red Beds gave age >10,000 and Lambert puts age of recharge of 13,000 yr ago - no advantage of further pursuit
Lambert and Carter (1987)	Uranium disequilibrium studies - Uranium concentration ([U]) and uranium-234/ uranium-238 A.R.	Culebra Dolomite	A. R.'s decrease westward in a reducing environment with a steady increase in [U]	Flow direction here changed - area of high potential and low permeability is draining
Siegel and others (1990)	Solute geochemistry major - solute analysis	Culebra Dolomite	Four hydrochemical facies based on salinity show modern flow not consistent with salinity	Culebra Dolomite flow is transient

TABLE V-1. RECENT GEOCHEMICAL STUDIES IN THE STUDY AREA (concluded)

Researchers	Method of Study	Unit(s) Studied	Results	Conclusions
Bodine and others (1988)	Normative salt assemblage Rustler Formation water	Rustler Formation	Four end-member fluid composition: 1. Primitive diagenetic brine 2. Alkali-bearing CO_3 waters produced during recharge 3. Sulfate-rich water dissolving anhydrite/gyp 4. Variable saline anhy-gyp-halite	P-18 has high proportion of primitive diagenetic brine Vertical recharge northwest and south of the WIPP
Siegel and others (1990)	Saturation indices and factor analysis	Culebra Dolomite	Same as 1 above and consistent trends in major (Ca, Mg, Na, K, Cl, SO_4) and (Br, I, Sr) categories	Samples are all from a single chemical population. Solutes are added to water by dissolution of halite, gyp/anhy carbonate. No mechanistic or mineralogical delineation between facies in (1) identified
Myers and others (1988)	Reduction-oxidation potentials	Culebra Dolomite	Zone B redox potential ranges from +330 to +630 or higher, western part of Zone similar. Zones A and C less oxidizing > +330 (see Figure 4.3.6 in Lappin, 1988)	Regional variation in oxidation potential. Reducing northeast and oxidizing southwest
Siegel and others (1990)	Mineralogic	Culebra Dolomite	Wells H-7d and H-10 85% dolomite with minor amounts of gypsum, calcite, and clay, fracture and usage lined with secondary clay and gypsum upper part of WIPP-29 in calcite some pyrite, magnesite, and quartz	Vertically and laterally heterogenous fluids do not reflect presence or absence of halite
Lambert and Harvey (1987)	Stable isotope	Meteoric water at Carlsbad Caverns compared with waters in past Rustler Formation rocks	Not all water falls in with cavern water and Dewey Lake waters	Dewey Lake (DL) at James Road well-made recharge; Fairview Pocket in DL does not get moderate recharge
Lambert and Harvey (1987)	Stable isotope	Culebra and Magenta Dolomites waters	There was no overlap of data from meteoric water and Culebra/ Magenta Dolomites water	Magenta/Culebra waters do not reflect modern meteoric recharge, no significant recharge at WIPP. Magenta/Culebra waters were recharged under different conditions. WIPP-29 and Surprise Spring are not Rustler Formation discharge points

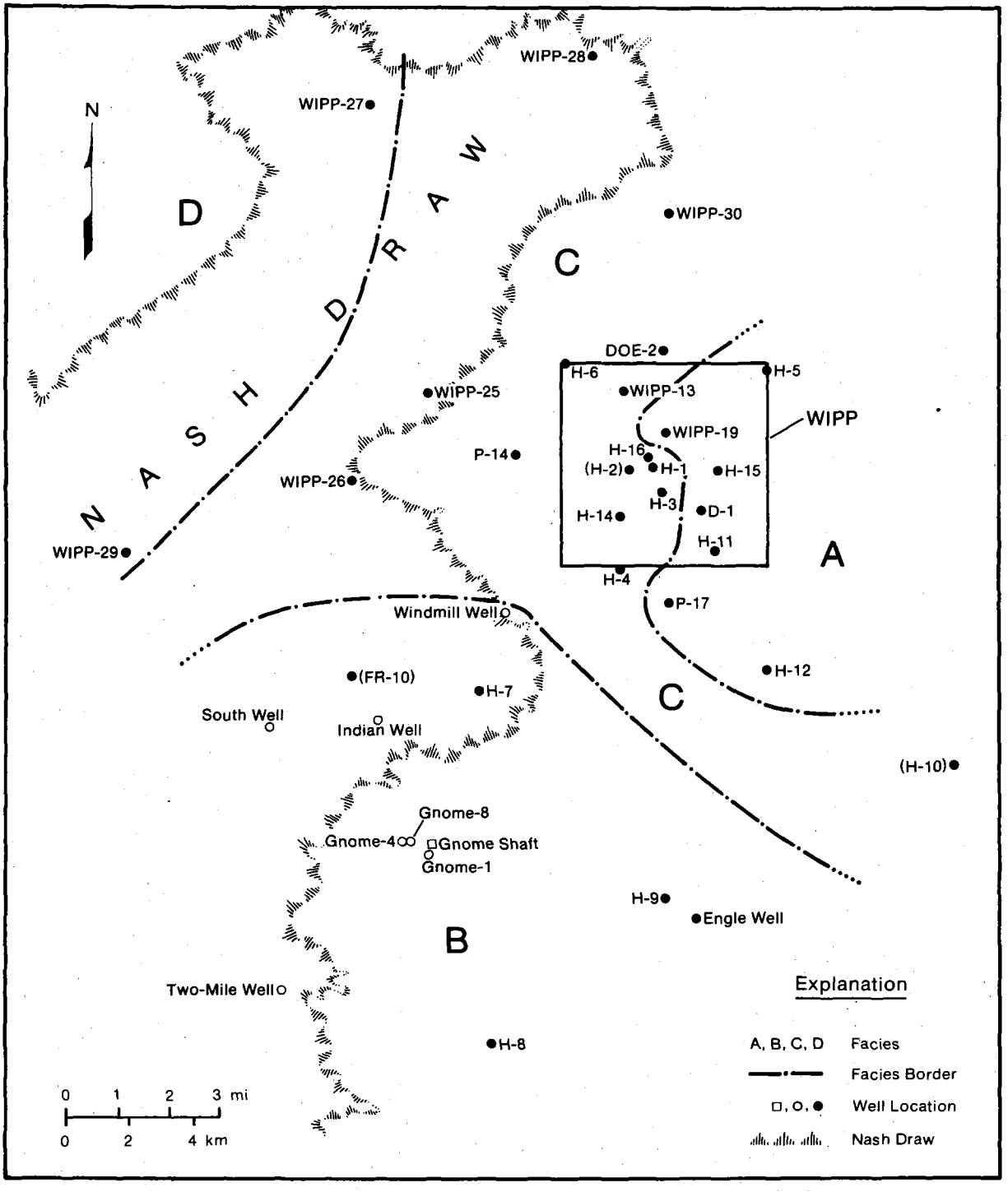

TRI-6331-78-0

Figure V-1. Hydrochemical Facies in the Culebra Dolomite (from Siegel and others, 1990).

Examination of the possibility of direct meteoric recharge to the Culebra Dolomite was done by Chapman (1986), Lambert and Harvey (1987), and Lambert (1987). Although using data from Lambert and Harvey (1987), Chapman's (1986) report gave results and interpretations that were not consistent with Lambert and Harvey's (1987) results. The differences occurred mainly in interpreting the relationships among Rustler Formation waters, waters from the unconfined Capitan aquifer, and modern precipitation. Chapman's conclusion was that evaporation of Rustler waters could form Surprise Spring waters, implying good hydraulic connection of the Rustler Formation to the surface water at the northern shore of Laguna Grande de la Sal, and that steady-state conditions exist in the Study Area. However, according to Lambert and Harvey (1987), Surprise Spring waters do not fall in the group of waters that are demonstrably meteoric, and the spring waters cannot be from the Rustler Formation. They also show that Magenta Dolomite and Culebra Dolomite waters do not reflect direct modern meteoric recharge at the WIPP and that the system is transient, with the system responding to a cessation of recharge occurring 10,000 to 30,000 yr ago, that is, the direction of flow has changed.

Radiocarbon dating was attempted in the Study Area, but results were somewhat inconclusive. A study by Lambert (1987) of the feasibility of applying radiocarbon and radiochloride dating techniques to samples from four hydrostratigraphic units at 16 localities found that, because of susceptibility of the components to contamination, further "dating" should not be pursued. Potash mine effluents (such as those found at WIPP-29) and organic material drilling fluids aided by the karstic porosity and the low to moderate permeabilities in Nash Draw, had contaminated the samples. Four acceptable results from widely separated localities within the Study Area yielded dates >10,000 yr, indicating that water of this age may have been widespread (see Lappin [1988] for a synopsis of Lambert's [1987] report).

Ground water can be "dated" by using changes in the ratio of uranium-234/uranium-238 and uranium concentration (U) along a flow path in a confined hydrostratigraphic unit under reducing conditions (Myers and others, 1988). Changes in uranium-234/uranium-238 activity ratios (A.R.) showed "that times required to achieve the observed [Culebra Dolomite] ground-water A.R. values indicate that the Rustler [Formation] hydrology at and near the WIPP is not at steady state on a time scale of approximately 10,000 to 30,000 years...." The general flow directions can be demonstrated to be "...eastward during a recharge interval at 10,000 to 30,000 years before present ... [and] westward for some time after the cessation of recharge..." (Lambert and Carter, 1987).

As demonstrated by the solute, isotopic, and radiochemistry studies, the prevailing condition at the WIPP is a transient hydrologic system over a time scale on the order of thousands of years. Current ground-water flow has changed significantly from the direction of flow 10,000 to 30,000 yr ago.

VI. BOUNDARY CONDITIONS IN THE NORTHERN DELAWARE BASIN

Another primary purpose of this report is to describe ground-water flow as accurately as possible because accurate simulation of ground-water flow requires an accurate description of boundary and/or initial conditions. A typical steady-state flow system consists of ground water flowing through a body of rock bounded by a surface, with average flow and water levels maintained under natural conditions at a mean level by either continuous or intermittent inflow and outflow (Franke and others, 1984). Because geologic, geochemical, and indirectly, hydrologic evidence indicates that the ground-water conditions in the Study Area are not steady state, a time-dependent (transient) solution of a boundary value problem is required for long-term simulations. This requirement means initial conditions in the Study Area must be specified.

In the Los Medaños transient-flow system, water levels will change with time, not only in response to human-induced stresses but also in response to natural flow associated with climate change. A poor description of boundary and initial conditions will result in a poor solution of a problem. An ideal, well-posed problem requires knowledge of conditions for an entire given domain. Relative to the long-term stresses in the Study Area, this knowledge is not possible. However, whenever possible, aquifer models should include physical or hydrologic boundaries. When this inclusion is impossible, such as at Los Medaños where the regional aquifer is much larger than the Study Area to be modeled, the model boundaries will be nebulous. In such a situation, the boundaries must be placed far enough away from the area of interest to have as negligible an effect as possible on the area modeled. If the Study Area is indeed in a transient state, the initial conditions can be obtained from a steady-state simulation of the flow system. This method requires calibration of the model by adjustment of hydrologic parameters until simulated heads correspond to the actual measured heads. The simulated heads are then used as initial conditions for transient-state model simulations because the heads are consistent with the hydraulic parameters. An accurate solution cannot be obtained if field-measured heads are used as initial conditions because the model would reflect a lack of correspondence caused by model adjustments to the head values between the initial heads and hydraulic parameters (Franke and others, 1984).

Properly posing a steady-state flow problem requires several conditions. Internal boundary conditions must be known exactly, external boundary positions and type must be known exactly, hydrologic variables such as sources, sinks, and flux must be known at all locations, and variables such as transmissivity, leakage, and storage must be known for all hydrostratigraphic units. In addition, if a transient solution is required, as may be the case

in the Study Area, initial conditions must be known. Because all of the conditions listed above cannot be met everywhere for any properly posed ground-water flow problem, the problem is commonly simplified to construct a tractable model and avoid serious error. If the effects of simplification are known, the model uncertainties can be evaluated.

Flows in all three Rustler hydrostratigraphic layers, where present, are generally in the same direction along the model boundaries, with some notable exceptions. Flows in Nash Draw in the residuum and in the Culebra Dolomite Member are parallel to the axis of the draw, but in part of the Magenta Dolomite Member, flow is normal to the axis. This flow direction is attributed to lowering of regional water levels, allowing a longer time for the upper unit to drain. A second point of concern is that flow along the northern boundary in the Magenta Dolomite is southwest into the system, but in the lower units, flow at this boundary is still in the direction of regional flow, to the east-southeast. Conceptually, this flow direction causes no problems, but in a numerical simulation, it can cause abnormal and artificial vertical flow near the region of the fixed boundary conditions. This problem will have to be considered when the simulations are made by adjusting the boundary conditions in the upper unit so that they will be more consistent with those of the lower units.

Initial Conditions

Establishing initial conditions for transient flow will require the analyst to determine adequate parameters to represent the paleohydrology of the region. A typical modeling problem usually involves a flux through porous media that have constant hydrologic parameters throughout the time simulated. The transient state of modeling involves variation of fluxes by adding storage properties and sources and/or sinks, with the geohydrologic parameters remaining constant. In the Los Medaños region, the geohydrologic properties have been changing through dissolution and re-precipitation of evaporite minerals, that is, the hydrologic parameters are transient as well as the fluxes. In pre-Nash Draw time, flow was to the east but was disrupted by the development of the draw, thus removing the very rocks that had developed enough porosity to allow flow. The down-cutting of the Pecos River, coupled with Nash Draw development, has caused a partial reversal of gradient in the upper units (Rustler-Salado contact residuum, Rustler Formation, and younger rocks), with flow now moving west-southwest.

Cross-sectional modeling by Davies (1989) used a simple two-dimensional ground-water flow code by Trescott and others (1976) for the numerical simulation to test the hypothesis of transient conditions existing in the Study Area. The model was a simple, physically based concept of the flow

system as it drains through time following an initially recharged state that corresponded to the last glacial-pluvial period. The primary objective was to examine drainage rates, with a secondary objective of examining vertical ground-water flow relationships.

The simulation by Davies (1989) extended from the center of Nash Draw eastward across the WIPP to about 12 km east of "the WIPP site" (Davies' [1989] terminology). In that study, hydraulic conductivity for the Culebra Dolomite ranged from 10^{-8} m/s east of the WIPP to 10^{-4} m/s in Nash Draw. For the Magenta Dolomite, the hydraulic conductivity ranged from 10^{-5} m/s east of the WIPP to 10^{-5} m/s in Nash Draw. The Forty-niner and Tamarisk Members and the unnamed lower member were assigned a range from 10^{-11} to 10^{-7} m/s, and the fine-grained Dewey Lake Red Beds were assigned a hydraulic conductivity value of 10^{-8} m/s. A specific yield for the Culebra Dolomite of 20 and a specific storage of 10^{-4} m^{-1} were used.

Because the evidence cited above indicates that the ground-water conditions in the Study Area are not at steady state, a time-dependent (transient) solution of a boundary value problem is required, and the initial conditions must be specified. In this transient-flow system, water levels change with time, not only in response to a human stress but also in response to long-term transients caused by climate change. A standard modeling technique is to put boundary conditions into a ground-water flow code and run it to steady state, thus realizing a potentiometric surface that can be used for starting a transient solution by applying a stress, such as a well, to that surface. Davies (1989) used boundary conditions that consisted of a water table at the top of the cross section, a no-flow boundary at the bottom coincident with the top of the Salado Formation, a no-flow boundary on the eastern edges, and a no-flow boundary at the axis of Nash Draw. Specified-head nodes were used at Nash Draw near the land surface to simulate discharge. Initial conditions were hydraulic heads representative of the end of the last glacial-pluvial period, which was assumed to be a fully charged system with a potentiometric profile reflecting the surface topography and a vertical hydrostatic head distribution.

Haug and others (1987) modeled an area surrounding the WIPP and did not incorporate the regional geologic or hydrologic boundaries that precluded the use of no-flow boundaries. The lateral boundaries were characterized by long-term mean formation pressures and long-term formation-water densities. Initially, the upper and lower boundaries were characterized as low permeability units with no flow into the Culebra Dolomite but were later changed by implementing vertical flux into the Culebra. LaVenue and others (1988), using a larger modeling domain than the Haug and others (1987) model, represented the eastern boundary as a no-flow boundary because of the low transmissivity and low flow. The northern, western, and southern boundaries

were represented by prescribed pressure and prescribed water densities. In a later study (LaVenue and others, 1990), the eastern boundary was eventually assigned formation pressures during the steady-state simulation in order to improve agreement with calculated and observed heads.

The Davies (1989) base case used initial conditions, boundary conditions, and hydrologic parameters. The simulation was for a 20,000-yr period, and the water-table configurations for time steps of 1000, 4000, 10,000, and 20,000 yr for a steady state were calculated. Drawdown occurred in the zone near Nash Draw, where the rock composition and physical properties change (transition zone), and a large amount of water still remained in storage in the Dewey Lake Red Beds after 20,000 yr. Flow was toward Nash Draw, with flow in the upper Supra-Rustler sandstone going downward to the Magenta Dolomite in the transition zone, where the Forty-niner Member becomes more conductive, and then to the Culebra Dolomite through the Tamarisk Member. The Culebra Dolomite finally discharges to lower Nash Draw. Comparing the variation sensitivity of the hydraulic conductivity's spatial distribution in the aquitard units to the original distribution of hydraulic conductivity indicates that most of the discharge to the Culebra Dolomite occurs on the eastern side of Nash Draw in the transition zone.

As shown by Davies (1989), steady-state models used for water-level prediction over extended periods of time introduce uncertainty into the calculations, and the transients may be important in calculating long-term behavior.

Three-Dimensional Boundary and Initial Conditions

Establishing boundary and initial conditions for a three-dimensional simulation of ground-water flow in the northern Delaware Basin is complicated by the complex geology, hydrology, and geomorphological processes in the region.

A classical method of choosing boundary conditions for flow problems is to pick boundaries that can be represented by identifiable natural ground-water or surface-water features such as rivers, lakes, divides, impermeable surfaces, or a water table. Three obvious hydrological features represented at ground surface are the Pecos River, Laguna Grande de la Sal, and Nash Draw. A fourth, not so obvious, regional feature is the Capitan aquifer. The other boundaries are not as straightforward and must be assigned conditions that require judgment of the analyst.

The lowest hydrostratigraphic unit in the Study Area that will be used in a three-dimensional simulation of ground-water flow is the Rustler-Salado contact residuum at the base of the Rustler Formation. Lower

hydrostratigraphic units, those below the Castile, are probably not important hydrologically to flow above the Salado Formation, as evidenced by the apparent underpressuring in the Delaware Mountain Group (see "Formation Pressure" in Appendix A) and because of the 1000 m of low permeability halite and anhydrite. The Salado Formation is a no-flow boundary in the Delaware Basin. At the basin perimeter, the degree of separation of the lower hydrostratigraphic units (Capitan aquifer) from the Rustler is not as well defined, and the Capitan may be a source of recharge to the upper units. In a steady-state case in which the Capitan is included as a source or sink, the aquifer will be a constant-head (pressure) boundary. Sensitivity of the ground-water flow field will be determined by varying the location of the constant-head nodes at the model edge and the permeability of the intervening geologic units.

Ground-water flow in the three hydrostratigraphic units of the Rustler Formation is presented in Figures VI-1 to VI-3, which show the adjusted potentiometric surfaces presented in Chapter IV in the discussion of the Rustler Formation hydrostratigraphic units, with flow lines and possible model boundaries added. The flow lines are perpendicular to the potentiometric lines, which indicates isotropy of the units. Isotropy may not be the case, but for a preliminary analysis, the units will be assumed to be isotropic.

Enough data will probably never be compiled to verify, once and for all, the existence of anisotropy in all hydrostratigraphic units over the region. Anisotropy tests on wells H-4, H-5, and H-6 yielded a calculated ratio of major to minor axis values for transmissivity across the WIPP, ranging from 1:2.3 to 1:2.7 oriented northwest-southeast (Barr and others, 1983).

An assumption of isotropy also ignores density-related gravity effects on flow that would alter the flow direction across the potentiometric lines. Davies (1989) shows that density effects are insignificant in the vicinity of the WIPP and that the equivalent fresh-water head concept can be used. South of the WIPP, however, the density-related flow component is important, and simulation of ground-water flow in this area must be done using variable-density computer codes or analytic techniques that are appropriate for density-related flow analysis. Davies also demonstrates, using mostly estimated data, that near Malaga Bend and northeast of the WIPP may be additional areas of concern.

Other previous modeling studies incorporating variable-density effects were conducted by Haug and others (1987), LaVenue and others (1988), and LaVenue and others (1990). Haug and others (1987) incorporated three fixed-density zones in a two-dimensional Culebra Dolomite model and concluded that vertical fluxes into the Culebra Dolomite from above and below influenced the hydrology of the system and resulted in discrepancies between observed and calculated

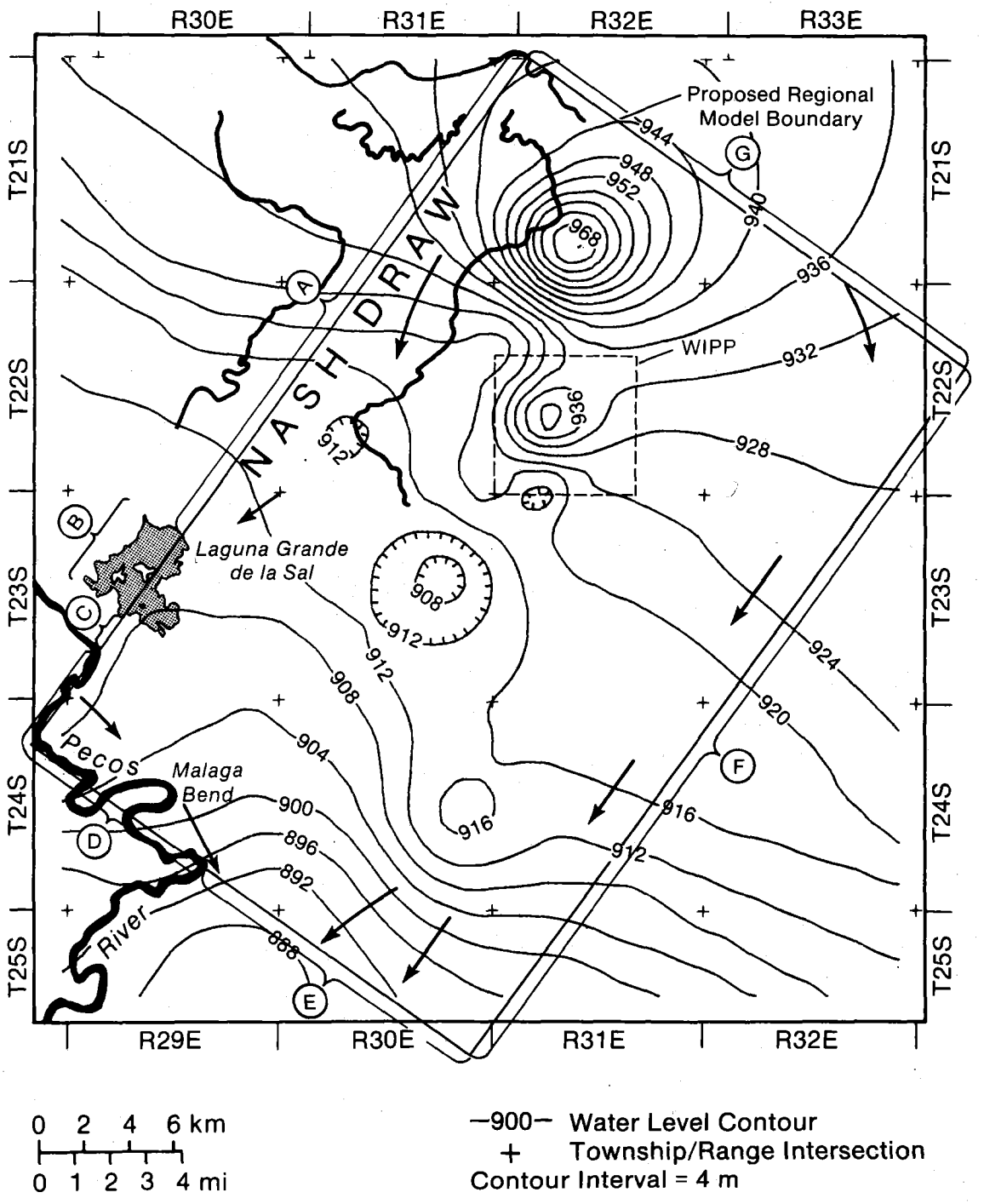

Figure VI-1. Regional Ground-water Flow in the Rustler-Salado Contact Residuum at the Base of the Rustler Formation. See Figure IV-11 for control points.

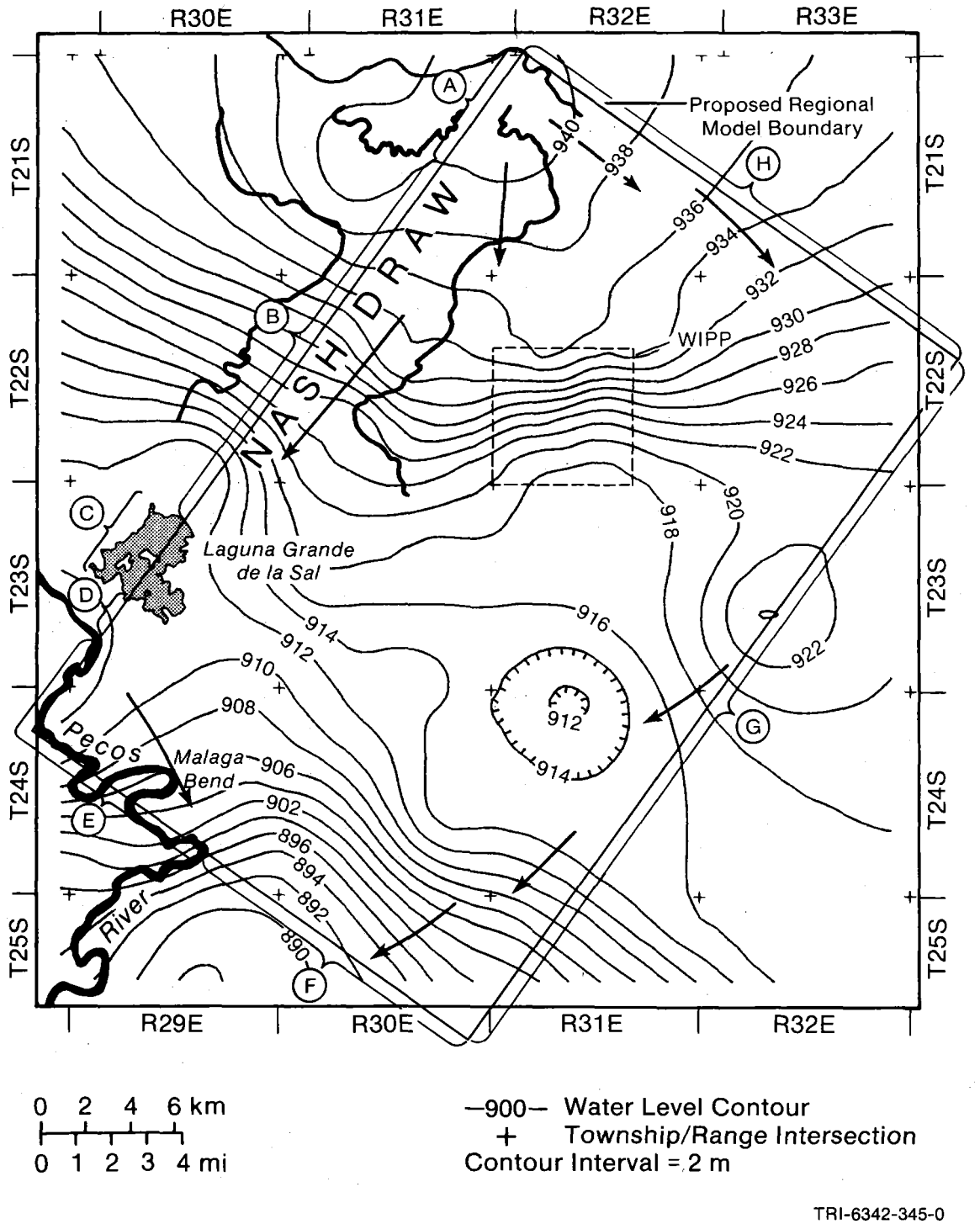

Figure VI-2. Regional Ground-water Flow in the Culebra Dolomite Member of the Rustler Formation. See Figure IV-17 for control points.

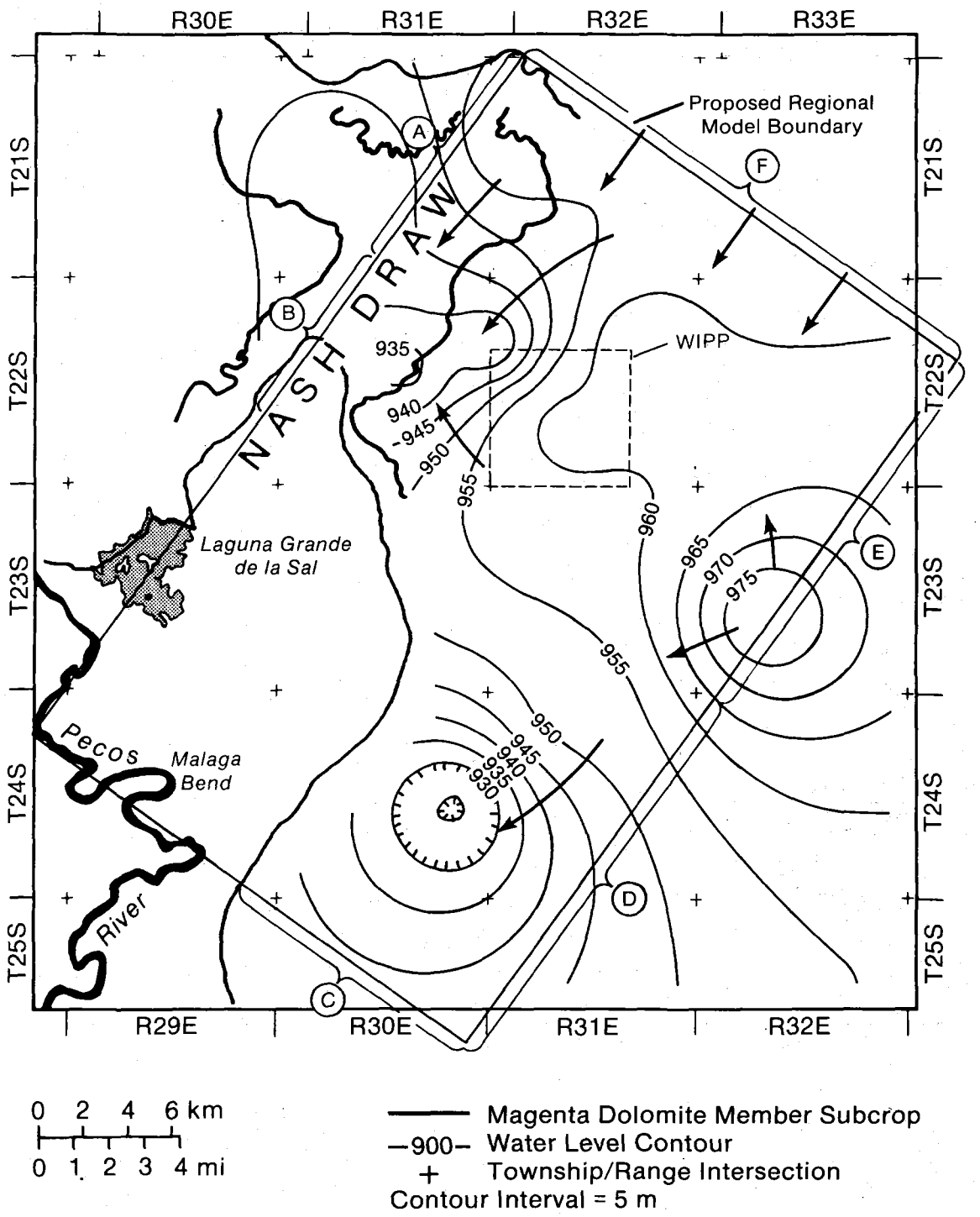

Figure VI-3. Regional Ground-water Flow in the Magenta Dolomite Member of the Rustler Formation. See Figure IV-25 for control points.

density distributions. They also noted that the model was moderately sensitive to vertical fluxes and very sensitive to vertical fluxes with respect to fluid density. LaVenue and others (1988) and LaVenue and others (1990) estimated Culebra Dolomite fluid density for each grid block of a two-dimensional model (an extension of the Haug and others [1987] model study) that "allowed inclusion of the observed density distribution and the effects that variable density has on the present day flow field."

Examination of the flow lines of the Rustler-Salado contact residuum shows that ground-water flow in Nash Draw is parallel to its axis, with no flow across the draw (Figure VI-1, A). The upper (northern) part of Nash Draw is a special type of no-flow boundary called a stream-surface boundary or a streamline, and no flow goes across Nash Draw. The head changes downgradient (down the draw to the south) and is called a specified-head boundary.

The hydrostratigraphic units in lower Nash Draw, from Laguna Grande de la Sal to Malaga Bend, are probably hydraulically connected because of dissolution of the upper Salado Formation and the halites in the Rustler Formation (see also discussion of "Recharge and Discharge" of the "Rustler-Salado Contact Residuum Hydrostratigraphic Unit" in Chapter IV). It is unclear what units are present in this area, and drillers' logs refer to the water-producing zones as "Rustler" (see Table B-5 in Appendix B, and Table 1 in Davies, 1989). If the assumption is made of good vertical connection in this area, then a constant-head boundary exists at the lower end of Nash Draw at the surface of the lake, Laguna Grande de la Sal (Figure VI-1, B). Between the Laguna and the Pecos River at Malaga Bend (Figure VI-1, C), where water-table conditions exist, the boundary is a free-surface boundary. An air/water interface is also present at the lake. This surface is not fixed and will be most affected by recharge such as precipitation. (A further complication may exist in this region—stratification may occur because of extreme differences in fluid density of the ground water.)

The region along the Pecos River in the southwestern corner of the model region (Figure IV-1, D) is similar to upper Nash Draw. Flow is parallel to the river, and the river is a stream-surface boundary decreasing in head as it flows southeastward. The lower right-hand side of the model region (Figure VI-1, E) is a constant-flux boundary; that is, flow is toward this boundary and out of the model domain toward the Balmorhea-Loving Trough. The southeastern side of the model (Figure VI-1, F) is a no-flow boundary similar to Nash Draw and the Pecos River.

The northeastern boundary (Figure VI-1, G), is an area with a constant flux into the model. A lack of data distorts the equipotentiometric lines in this region. Fluxes into the region will have to be determined through sensitivity studies.

Boundary conditions in the Culebra Dolomite Member hydrostratigraphic unit (Figure VI-2) are the most diverse because of the large amount of data for this unit near the WIPP. Sections B, E, G, and H (Figure VI-2) are streamline boundaries with flow parallel to each boundary. Section A is a flux boundary with ground water moving into the model. Section C is a constant-head boundary at Laguna Grande de la Sal. Section F is a constant-flux boundary with flow outward. Section D is a free-surface boundary where water-table conditions exist.

The absence of part of the Magenta Dolomite at the lower end of Nash Draw and near the Pecos River (Figure VI-3) complicates ground-water flow in the unit. At Section A (Figure VI-3) in the upper part of Nash Draw where the Magenta Dolomite is present, flow is southward along the draw's axis, forming a streamline boundary. Along the lower part of the draw (Section B), flow is toward the edge of the draw. Springs are evident in this region, but at present no flow comes out of the Magenta Dolomite to the draw. Flow is probably from the Magenta Dolomite Member, downward through the weathered Tamarisk Member, and into the Culebra Dolomite. At Section C (Figure VI-3), flow is toward the alluvium in the region of the Balmorhea-Loving Trough. Section D has flow parallel to the boundary. Sections E and F may be recharge areas with a constant flux into the model. The data here are not good, and the uncertainty about the boundary is high.

Estimation and Distribution of Hydrologic Properties

"The weakest link in the use of deterministic mathematical models of ground water flow lies in the scarcity of available data for hydrogeologic parameters" (Freeze, 1972). Parameter estimation for this study is no exception to this rule. Although geohydrologic properties for this modeling effort were taken from numerous geologic and hydrologic reports prepared by the U.S. Geological Survey, SNL, New Mexico and Texas state agencies, and independent consulting firms, most data pertain to the Culebra Dolomite Member.

Knowing the ranges and types of distributions of specific parameters will enable the modeler to determine the sensitivity of the model and the most important parameters. In an analysis of three aquifer properties—transmissivity, hydraulic conductivity, and storage coefficient—Hoeksema and Kitanidis (1985) obtained results that indicated that the properties, with very few exceptions, are lognormally distributed. The results of Hoeksema and Kitanidis' work are the basis for the assumptions of the distributions used in this study. Porosity is assumed to be normally distributed, in accordance with Freeze's (1975) work.

VII. SUMMARY

The Study Area is located in the north-central part of the Delaware Basin in the southern part of the Pecos Valley section of the Great Plains Physiographic Province. This area lies between the high plains of West Texas and the Guadalupe and Sacramento Mountains in southeast New Mexico. The Study Area is 34 km by 40 km and extends from the Pecos River in southern Eddy County eastward into Lea County and southward from just inside the Delaware Basin edge to about 20 km north of the New Mexico-Texas state line. Two primary features of the Study Area are Nash Draw in the western part and The Dunes in the eastern part.

Tectonic, geomorphological, and man-induced geologic processes have impacted regional ground-water flow in the northern Delaware Basin.

Tectonic processes caused a major late Pliocene or early Pleistocene uplift outside the Study Area that exposed the Capitan Reef and formed the eastern Guadalupe Mountains southwest of Carlsbad and the Glass Mountains near Fort Stockton, Texas. Before the uplifting, regional ground-water flow in the shelf and basin aquifers was generally eastward at a gentle gradient toward Texas. Flow within the reef was northward from the Guadalupe Mountains around the northern rim of the Delaware Basin and then eastward into the shelf aquifer south of Hobbs. Flow from the Glass Mountains was first northward and then eastward into the shelf aquifer, where it joined the Guadalupe Mountains water. The uplifting created faults and fractures in the reef that have allowed infiltration into the Capitan Reef, making the two exposures of limestone at the Guadalupe and Glass Mountains the major recharge areas. Another result of the uplifting is a major monoclinal structure dipping eastward from the Guadalupe Mountains across the basin.

The uplifts along the western margin of the basin caused an increase in surface elevation relative to the regional base level. Consequently, geomorphological processes had a major effect on the developments of the Pecos River and Nash Draw in early- to mid-Pleistocene time. The lower part of the ancestral Pecos River developed in the Delaware Basin in the wetter climate of early- to mid-Pleistocene time. This part of the ancestral Pecos River began eroding headward across the Capitan aquifer, pirating the northern part of the ancestral Pecos River that was flowing east-southeast between Clovis and Portales, New Mexico, into Texas. The additional water, combined with the apparent lowering of base level, caused an increase in energy that facilitated downcutting of the river into the reef. The hydraulic head of the reef, which was above that of the river, resulted in the aquifer discharging to the river. The two sources of additional water made the ancestral Pecos River a high-energy stream, allowing it to carry a much larger bed load and forming the

Gatuña Formation downstream in localized low-energy areas such as above what is now Nash Draw.

The discharge from the Capitan aquifer to the ancestral Pecos River lowered the hydraulic head in the Capitan aquifer near Carlsbad. This lowering caused a reversal of flow east of Carlsbad that formed a ground-water divide in the vicinity of the Eddy-Lea County line. Flow in the basinal and shelf aquifers was still eastward.

To the east of the river, as a result of dissolution along what is presumably a zone of fracturing caused by the uplifting of the Guadalupe Mountains, Nash Draw began forming. No definitive evidence has yet been presented to substantiate a fracture zone, but Nash Draw is the result not of erosion but of extensive dissolution of evaporites in the Rustler and upper Salado by water undersaturated with respect to halite and anhydrite. The source of the water was from overlying saturated units (Dewey Lake Red Beds), from the Rustler Formation, or from below (Capitan aquifer) via breccia chimneys (see Chapter III) located along the axis of the Clayton Basin-Nash Draw dissolution troughs. The fluid then moved downgradient along the axis of Nash Draw through fractures (not by surficial paths) toward the ancestral Pecos River or Balmorhea-Loving Trough. Eventually, the Pecos River migrated to its present position and became incised. As the Pleistocene progressed and the climate became drier and as a result of lowering the Capitan heads, the river lost much of its energy and became the sluggish river it is today. Presently, with the exception of storm events, the Pecos River is only capable of carrying dissolved material and has a very small bed load.

The downcutting action of the Pecos River and dissolution of Nash Draw caused the Rustler Formation rocks to begin draining locally through springs into the draw and downward through dissolution fractures along the draw. This drainage allowed more dissolution to occur even after the climate became drier. For example, in well H-7 the Magenta Dolomite is dry because of drainage to lower units. Continuous draining and dissolution have formed the so-called reentrants at both the headward end and at the lower part of Nash Draw that can be seen as topographic lows north and south of the WIPP (Figure I-2).

The third process to affect the regional ground-water flow results from human activity in the region. Between the Delaware and Midland Basins, withdrawal of ground water from the Capitan aquifer and the oil fields east of the Capitan on the Central Basin Platform has caused a drop in hydraulic head of about 50 m in the vicinity of the Eddy-Lea county line. This drop resulted in lowering of the ground-water divide and local changes in flow direction, especially the local flow direction over the shelf out of New Mexico into Texas.

The Guadalupian hydrostratigraphic units of interest in the Delaware Basin are the Bell Canyon Formation (basinal unit) and the Capitan Limestone (reef unit). This study does not consider the back reef units. The massive Capitan Limestone ranges in thickness from 76 to 230 m and averages 120 m. Hydraulic conductivity ranges from 8×10^{-6} to 9×10^{-5} m/s and averages about 2×10^{-5} m/s. Effective porosity, which is enhanced by dissolution and fracturing of the limestone, is about 0.08. Ground water flows from the Guadalupe Mountain recharge area eastward around the periphery of the Delaware Basin, into the shelf aquifer toward Texas. The Pecos River and large withdrawals as a result of drilling activity locally influence ground-water flow direction. Fluid density ranges from 1.000 to 1.115 g/cm^3 and averages about 1.04 g/cm^3.

The lowest basinal hydrostratigraphic unit and oldest unit to crop out in the northern Delaware Basin, the Bell Canyon, is the fore-reef equivalent of the Capitan Limestone and interfingers with the Capitan at the basin margins. Informally named sandstone and shale members (in ascending order the Hays sandstone, Olds sandstone, Ford shale, Ramsey sandstone, and Lamar limestone) compose the upper part of the Bell Canyon. The upper siltstones and shales contain elongated sandstone stringers deposited by density currents moving along the bottom basinward from the reef. Ground water occurs in the upper portion of this unit. The vertical potential of the fresh-water equivalent heads of this unit is upward, leading to the speculation that in the past the Bell Canyon waters have aided dissolution of the Castile Formation, causing collapse features that can be seen at the surface. The Castile, however, does not have the extensive fracture network needed to provide pathways upward to the halites and back down to the Bell Canyon. The numerical modeling will not include the Bell Canyon because of the poor hydraulic connection to the upper hydrostratigraphic units and because the Bell Canyon lacks potential for upward vertical flow.

Near the end of Bell Canyon deposition, circulation within the Delaware Basin became more constricted, resulting in a thick sequence of organic layers alternating with siltstone laminations that change in character upward from organically layered calcite to calcite-layered anhydrite. This thick sequence forms the lower Castile Formation, which then grades upward into the anhydrite-layered halite of the upper Castile Formation and the thick halite of the Salado Formation. The Salado Formation is particularly interesting because it is the host rock for the WIPP.

The Castile and Salado Formations are present everywhere in the Study Area but are eroded away southwest of the Study Area and in part of Texas. In New Mexico north of the WIPP, the Castile Formation is about 360 m thick and thickens southward across the WIPP, where it is about 470 m thick. At the southern edge of the Study Area, the Castile Formation is about 500 m thick.

Throughout the Study Area, the Salado Formation is about 600 m of salt rhythmically interbedded with anhydrite, polyhalite, glauberite, and some thin mudstones. The Salado Formation structure is a series of low anticlines and shallow synclines with axes dipping southeastward. In the northeastern part of the Study Area, the Salado Formation surface dips steeply northeastward. Unlike the Castile Formation, the Salado Formation overlaps the reef structure and is present outside of the reef area. It extends eastward for many kilometers into West Texas and the Texas Panhandle.

Conservative estimates of the hydraulic conductivity of the Castile Formation yield a range of about one nanodarcy (1.0×10^{-14} m/s) to about 0.1 microdarcy (1.0×10^{-12} m/s). Porosity of the anhydrite is about 0.001.

In the Study Area where the Salado Formation is intact, circulation of ground water is minimal because (as is the nature of highly plastic salt deposits) the Salado lacks primary porosity and open fractures. Measured permeability of the Salado Formation is very low and averages, at lithostatic pressure, about 0.05 microdarcies, with a range from 9 to 25 microdarcies throughout the formation. This average may be high because improved testing methods have given lower results, even for the marker beds. All of the tests assumed a porosity of 0.001. Porosity of the Salado around the WIPP is about 0.01 to 0.02 and goes up to about 0.06 at several meters depth. Formation pressure varies from hydrostatic to lithostatic, and although the formation may be saturated, the low effective porosity allows for very little ground-water movement.

The Salado Formation is conformably overlain by the Rustler Formation, which is the youngest unit of the Ochoan evaporite series. The composition of the Rustler Formation is about 40 percent anhydrite, 30 percent halite, 20 percent siltstone and sandstone, and 10 percent anhydritic dolomite. Ground water occurs only in the Rustler-Salado contact residuum and the dolomite units (the Culebra and Magenta Members). Data from the intervening units, the unnamed lower member, the Tamarisk Member, the Forty-niner claystone, and the Forty-niner Member, are restricted to wells H-14 and H-16. The aquitard units, the unnamed lower member, the Tamarisk Member, and the Forty-niner Member, will be considered isotropic and homogeneous aquitards of very low permeability throughout the Study Area. The estimated hydraulic conductivities of the three hydraulically impermeable units are, in ascending order, 1×10^{-10} m/s, 1×10^{-12} m/s, and 1×10^{-9} m/s. The Tamarisk Member was too impermeable to test, and the value of 1×10^{-12} m/s is an estimate. The porosity of the aquitards will be considered to be 0.3.

The Rustler-Salado contact residuum or "brine aquifer" occurs as a dissolution residue above the halite of the Salado Formation at the Rustler contact and

has a range of thickness from 3 to 30 m and a mean thickness of about 8 m. More recent information shows a range of 2.4 m in test hole P-14 to 33 m in test hole WIPP-29. Log hydraulic conductivity ranges from -12 to -6, with a lognormal mean of -9.4. The log hydraulic conductivities for Nash Draw are higher by several orders of magnitude than the values east of the draw and range from -8 to -6. Eastward, the range is from -12 to -9. Near Malaga Bend the log hydraulic conductivity is around -3.2. Effective porosity estimates for the brine aquifer range from 0.15 to 0.33, and an average effective porosity of 0.2 has been assumed.

More is known about the hydrologic properties of the Culebra Dolomite Member than about any other unit in the Study Area. The log transmissivity for the region ranges from -8.7 to -2.9 and has a mean of -5.5 in the vicinity of the WIPP. The thickness of the Culebra Dolomite near the WIPP ranges from 4.8 to 11.0 m. The log hydraulic conductivities range from -9.7 to -3.7, with a mean of -6.4. A global porosity value of 0.20 has been used for the single-porosity conceptualization and for the matrix porosity of the dual-porosity conceptualization because 0.20 probably best represents porosities ranging from 0.07 to 0.30.

The log transmissivity for the Magenta Dolomite Member of the Rustler Formation ranges over five orders of magnitude from -8.4 to -3.4, with a mean log transmissivity of -8.0. The log hydraulic conductivity ranges from -9.3 to -4.3, with a mean log hydraulic conductivity of -7.8. No porosity measurements have been made on the Magenta Dolomite, but a porosity of 0.20 is assumed for the dolomite, which is slightly high for intact dolomite but may be close to an average porosity of dolomite that has undergone some dissolution. Water density varies from 1.004 g/cm^3 (only slightly saline) at test hole H-9a in the southern part of the Study Area to 1.171 g/cm^3 at test hole H-10a southeast of the WIPP.

The hydraulic conductivity of the Supra-Rustler rocks, assuming saturation, varies from 10^{-8} m/s, similar to the hydraulic conductivity of the Forty-niner Member, to about 10^{-4} m/s in the alluvium. The porosity is assumed to fall in the range of fine-grained sandstone at 20 percent. Storativity is assumed to be 10^{-4}. Water density is assumed to be similar to that of the Magenta Dolomite.

East of the WIPP, dissolution is occurring at San Simon Sink and San Simon Swale. What has occurred in other areas such as Nash Draw is probably now taking place in the swale area. Water that is carrying gypsum is moving upward to the ground surface and evaporating, thus forming gypsum dunes that are evident at the perimeter of the swale. The only source of gypsum is anhydrite, which is present in Rustler or older rocks. In this area, the

Salado and Rustler Formations thin, presumably due to dissolution, which will enhance permeability. How far west the permeability is enhanced is not known because no WIPP wells are between the WIPP and the swale. If a connection exists between the Capitan aquifer and units above the Salado Formation, the swale area could be a recharge area for the Rustler Formation. Examination of a potentiometric map (post-development) of the Capitan shows Capitan heads above the Rustler Formation elevation. Other evidence that water has been moving upward is in dissolution features that contain dunes of gypsum that could only have come from below from pre-existing rocks.

Both pre- and post-development potentiometric-surface maps for the Capitan show that the potentiometric surface has dropped nearly one half the way to the top of the Rustler Formation in about 50 yr of development. At this rate, the potentiometric surface may drop below the Culebra Dolomite north of the WIPP at the Eddy-Lea county line, increasing downward vertical movement of water and forming a hydrologic divide between the Capitan and the WIPP in the near geologic future. East of the WIPP at San Simon Swale, the Capitan heads will never drop below the Rustler Formation, but a drop in heads will reverse the gradient between the swale and the WIPP.

North of the WIPP, the continued lowering of the hydraulic head has affected flow locally, but a continued lowering of hydraulic head in the reef and shelf aquifers will result in a regional downward movement of water from upper hydrostratigraphic units into the reef and shelf aquifers via structures similar to San Simon Sink (provided such pathways exist north of the WIPP). Further withdrawal from the reef and shelf aquifers will form a downward vertical gradient in the areas where the Dockum Group and alluvial material are saturated. This gradient may prove to be unimportant in the short term because of the low hydraulic conductivity of the Permian hydrostratigraphic units and Permian aquitards, but for the long time span required in performance assessment, the possibility of downward movement and its effect should be investigated.

Other potential pathways for fluid movement are degraded and abandoned deep wells. Wink Sink in Texas near the New Mexico border is located above the Capitan aquifer and is manifested at the surface by a 25-m-deep sinkhole that is circular in shape and has a diameter of 110 m. The sink is believed to be the result of dissolution of salt at a depth of from 400 m to 670 m by circulation of ground water from the Capitan that was facilitated by the presence of a plugged and abandoned well (Davies, 1984).

The potentiometric surface for the Delaware Mountain Group has not responded to the extensive withdrawals from the upper units because it is separated from the Rustler Formation by hydraulically tight anhydrite and halite in the

vicinity of the WIPP. The potential for upward vertical ground-water flow through a borehole to the Culebra, a potential pathway for radionuclides if the repository were breached, is nonexistent near the WIPP because in situ fluid density prevents Bell Canyon fluid from reaching the Culebra. For this reason, the Bell Canyon is not incorporated in the regional flow model.

REFERENCES

Adams, J. E. 1944. "Upper Permian Ochoan Series of Delaware Basin, West Texas and Southeast New Mexico." *American Association of Petroleum Geologists Bulletin* vol. 28, no. 11: 1596-1625.

Anderson, R. Y. 1978. "Deep Dissolution of Salt, Northern Delaware Basin, New Mexico." Unpublished report to Sandia National Laboratories, January, 1978.

Anderson, R. Y. 1981. *Deep-Seated Salt Dissolution in the Delaware Basin, Texas and New Mexico.* New Mexico Geologic Society Special Publication No. 10. 133-145.

Anderson, R. Y. and D. W. Kirkland. 1980. "Dissolution of Salt Deposits by Brine Density Flow." *Geology* 8: 66-69.

Anderson, R. Y., W. E. Dean, Jr., D. W. Kirkland, and H. I. Snider. 1972. "Permian Castile Varved Evaporite Sequence, West Texas and New Mexico." *Geological Society of America Bulletin* 83: 59-86.

Anderson, R. Y., K. K. Kietzke, and D. J. Rhodes. 1978. "Development of Dissolution Breccias, Northern Delaware Basin, New Mexico and Texas" in *Geology and Mineral Deposits of Ochoan Rocks in Delaware Basin and Adjacent Areas.* New Mexico Bureau of Mines and Mineral Resources Circular 159. Socorro, NM: New Mexico Bureau of Mines and Mineral Resources. 47-52.

Bachman, G. O. 1973. *Surficial Features and Late Cenozoic History in Southeastern New Mexico.* U.S. Geological Survey Open-File Report 4339-8. Albuquerque, NM: U.S. Geological Survey.

Bachman, G. O. 1974. *Geologic Processes and Cenozoic History Related to Salt Dissolution in Southeastern New Mexico.* U.S. Geological Survey Open-File Report 74-194. Denver, CO: U.S. Geological Survey.

Bachman, G. O. 1980. *Regional Geology and Cenozoic History of the Pecos Region, Southeastern New Mexico.* U.S. Geological Survey Open-File Report D-77-946. Albuquerque, NM: U.S. Geological Survey.

Bachman, G. O. 1981. *Geology of Nash Draw, Eddy County, New Mexico.* U.S. Geological Survey Open-File Report 81-31. Albuquerque, NM: U.S. Geological Survey.

Bachman, G. O. 1984. *Regional Geology of Ochoan Evaporites, Northern Part of Delaware Basin.* New Mexico Bureau of Mines and Mineral Resources Circular 184. Socorro NM: New Mexico Bureau of Mines and Mineral Resource.

Bachman, G. O. 1985. Assessment of Near Surface Dissolution at and near the Waste Isolation Pilot Plant (WIPP), Southeastern, New Mexico.

Bachman, G. O. 1987. *Karst in Evaporites in Southeastern New Mexico.* SAND86-7078. Albuquerque, NM: Sandia National Laboratories.

Barr, G. E., W. B. Miller, and D. D. Gonzalez. 1983. *Interior Report on the Modeling of the Regional Hydraulics of the Rustler Formation.* SAND83-0391. Albuquerque, NM: Sandia National Laboratories.

Beauheim, R. L. 1986. *Hydraulic-Test Results for Well DOE-2 at the Waste Isolation Pilot Plant (WIPP) Site.* SAND86-1364. Albuquerque, NM: Sandia National Laboratories.

Beauheim, R. L. 1987a. *Analysis of Pumping Tests of the Culebra Dolomite Conducted at the H-3 Hydropad at the Waste Isolation Pilot Plant (WIPP) Site.* SAND86-2311. Albuquerque, NM: Sandia National Laboratories.

Beauheim, R. L. 1987b. *Interpretations of Single-Well Hydraulic Tests Conducted at and near the Waste Isolation Pilot Plant (WIPP) Site, 1983-1987.* SAND87-0039. Albuquerque, NM: Sandia National Laboratories.

Beauheim, R. L. 1987c. *Interpretation of the WIPP-13 Multipad Pumping Test of the Culebra Dolomite at the Waste Isolation Pilot Plant (WIPP) Site.* SAND87-2456. Albuquerque, NM: Sandia National Laboratories.

Beauheim, R. L. 1989. *Interpretation of H-11b4 Hydraulic Tests and the H-11 Multipad Pumping Test of the Culebra Dolomite at the Waste Isolation Pilot Plant (WIPP) Site.* SAND89-0536. Albuquerque, NM: Sandia National Laboratories.

Beauheim, R. L. 1990. "Anomalous Culebra Water Levels around the WIPP Site," memorandum to distribution (January 5). Albuquerque, NM: Sandia National Laboratories.

Beauheim, R. L., S. R. Black, C. L. Christensen, T. O. Hunter, I. Jarolimek, A. K. Kuhn, S. J. Lambert, R. F. McKinney, D. Meyer, J. B. Murray, R. S. Newton, D. W. Powers, C. L. Stein, D. E. Stephenson, B. R. Sullivan, M. J. Timmer, and W. D. Weart. 1983a. *Results of Site Validation Experiments, Waste Isolation Pilot Plant (WIPP) Project, Southeastern New Mexico.* TME-3177, vols. I and II. Albuquerque, NM: U.S. Department of Energy.

Beauheim, R. L., B. W. Hassinger, and J. A. Klaiber. 1983b. *Basic Data Report for Borehole Cabin Baby-1 Deepening and Hydrologic Testing, Waste Isolation Pilot Plant (WIPP) Project, Southeastern New Mexico.* WTSD-TME-020. Albuquerque, NM: U.S. Department of Energy.

Bertram-Howery, S. G., and R. L. Hunter. 1989. *Plans for Evaluation of the Waste Isolation Pilot Plant's Compliance with EPA Standards of Radioactive Waste Management and Disposal.* SAND88-2871. Albuquerque, NM: Sandia National Laboratories.

Bodine, M. W. Jr., B. F. Jones, and S. J. Lambert. 1988. "Normative Analysis of Groundwaters from the Rustler Formation." Eds. M. D. Siegel, S. J. Lambert, and K. L. Robinson. *Hydrogeochemical Studies of the Rustler Formation and Related Rocks in the WIPP Area, Southeastern New Mexico*. SAND88-0196. Albuquerque, NM: Sandia National Laboratories.

Borns, D. J. 1983. *Petrographic Study of Evaporite Deformation near the Waste Isolation Pilot Plant (WIPP)*. SAND83-0166. Albuquerque, NM: Sandia National Laboratories.

Borns, D. J. 1985. *Marker Bed 139: A Study of Drillcore from a Systematic Array*. SAND85-0023. Albuquerque, NM: Sandia National Laboratories.

Borns, D. J. 1987a. *The Geologic Structures Observed in Drillhole DOE-2 and Their Possible Origins: Waste Isolation Pilot Plant*. SAND86-1495. Albuquerque, NM: Sandia National Laboratories.

Borns, D. J. 1987b. *Rates of Evaporite Deformation: The Role of Pressure Solution*. SAND85-1599. Albuquerque, NM: Sandia National Laboratories.

Borns, D. J. and S. E. Shaffer. 1985. *Regional Well-Log Correlation in the New Mexico Portion of the Delaware Basin*. SAND83-1798. Albuquerque, NM: Sandia National Laboratories.

Borns, D. J., and J. C. Stormont. 1988. *An Interim Report on Excavation Effect Studies at the Waste Isolation Pilot Plant: The Delineation of the Disturbed Rock Zone*. SAND87-1375. Albuquerque, NM: Sandia National Laboratories.

Borns, D. J., L. J. Barrows, D. W. Powers, and R. P. Snyder. 1983. *Deformation of Evaporites near the Waste Isolation Pilot Plant (WIPP) Site*. SAND82-1069. Albuquerque, NM: Sandia National Laboratories.

Bredehoeft, J. D. 1988. "Will Salt Repositories Be Dry?" *EOS Transaction* vol. 69, no. 9: 121-136. Washington, DC: American Geophysical Union.

Chapman, J. B. 1986. *Stable Isotopes in Southeastern New Mexico Groundwater: Implications for Dating Recharge in the WIPP Area*. EEG-35. Santa Fe, NM: New Mexico Environmental Evaluation Group.

Chaturvedi, Lokesh. 1980. *WIPP Site and Vicinity Geological Field Trip*. EEG-7. Environmental Evaluation Group, Environmental Improvement Division, Health and Environment Department, State of New Mexico.

Cheeseman, R. J. 1978. *Geology and Oil/Potash Resources of Delaware Basin, Eddy and Lea Counties, New Mexico*. New Mexico Bureau of Mines and Mineral Resources Circular 159. Socorro, NM: New Mexico Bureau of Mines and Mineral Resources. 7-14.

Christensen, C. L., and E. W. Peterson. 1981. *The Bell Canyon Test Summary Report*. SAND80-1375. Albuquerque, NM: Sandia National Laboratories.

Cooper, J. B., and V. M. Glanzman. 1971. "Geohydrology of Project GNOME Site, Eddy County, New Mexico." *Hydrology of Nuclear Test Sites*. U.S. Geological Survey Professional Paper 712-A. Washington, DC: U.S. Geological Survey.

Cys, J. M. 1978. *Transitional Nature and Significance of the Castile-Bell Canyon Contact*. New Mexico Bureau of Mines and Mineral Resources Circular 159. Socorro, NM: New Mexico Bureau of Mines and Mineral Resources. 53-56.

Davies, P. B. 1983. "Assessing the Potential for Deep-Seated Salt Dissolution and Subsidence at the Waste Isolation Pilot Plant (WIPP)." Unpublished manuscript presented at the State of New Mexico Environmental Evaluation Group Conference, *WIPP Site Suitability for Radioactive Waste Disposal*, Carlsbad, NM, May 12-13, 1983.

Davies, P. B. 1984. "Deep-Seated Dissolution and Subsidence in Bedded Salt Deposits." Ph.D dissertation. Dept. of Applied Earth Sciences, Stanford University.

Davies, P. B. 1987. "Modeling Areal, Variable Density, Ground-Water Flow Using Equivalent Freshwater Head--Analysis of Potentially Significant Errors." *Proceedings of NWWA Conference on Solving Ground Water Problems with Models*, Denver, Colorado, February 10-12, 1987.

Davies, P. B. 1989. *Variable-Density Ground-Water Flow and Paleohydrology in the Waste Isolation Pilot Plant (WIPP) Region Southeastern New Mexico*. U.S. Geological Survey Open-File Report 88-490. Albuquerque, NM: U.S. Geological Survey/Water Resources Division.

Davis, S. N., and R. J. M. Deweist. 1966. *Hydrogeology*. New York: John Wiley and Sons, Inc.

Franke, O. L., T. E. Reilly, and G. O. Bennett. 1984. *Definition of Boundary and Initial Conditions in the Analysis of Saturated Ground-water Flow Systems - An Introduction*. U.S. Geological Survey Open-File Report 84-458. Washington, DC: U.S. Geological Survey.

Freeze, R. A. 1972. "Regionalization of Hydrologic Parameters for Use in Mathematical Models of Groundwater Flow." *Proceedings International Geological Congress, Twenty-Fourth Session*, Montreal, Canada.

Freeze, R. A. 1975. "A Stochastic Conceptual Analysis of One-Dimensional Groundwater Flow in Non-Uniform Homogeneous Media." *Water Resources Research* 11: 725-741.

Geohydrology Associates, Inc. 1978a. *Ground-Water Study Related to Proposed Expansion of Potash Mining Near Carlsbad, New Mexico*. Denver, CO: Bureau of Land Management.

Geohydrology Associates, Inc. 1978b. *Collection of Hydrologic Data Eastside Roswell Range EIS Area, New Mexico*. Denver, CO: Bureau of Land Management.

Geohydrology Associates, Inc. 1979. *Water Resources Study of the Carlsbad Potash Area, New Mexico*. Denver, CO: Bureau of Land Management.

Griswold, G. B. 1977. *Site Selection and Evaluation, Los Medaños, New Mexico*. SAND77-0946. Albuquerque, NM: Sandia National Laboratories.

Gustavson, T. C., R. J. Finely, and K. A. McGillis. 1980. *Regional Dissolution of Permian Salt in the Anadarko, Dalhart, and Palo Duro Basins of the Texas Panhandle*. Austin, TX: University of Texas.

Guzowski, R. V. 1990. *Preliminary Identification of Scenarios That May Affect the Escape and Transport of Radionuclides from the Waste Isolation Pilot Plant, Southeastern New Mexico*. SAND89-7149. Albuquerque, NM: Sandia National Laboratories.

Hale, W. E., and A. Clebsch, Jr. 1958. *Preliminary Appraisal of Ground-water conditions in Southeastern Eddy County and Southwestern Lea County, New Mexico*. U.S. Geological Survey Trace Elements Memorandum Report 1045. Washington, DC: U.S. Geological Survey.

Hale, W. E., L. S. Hughes, and E. R. Cox. 1954. *Possible Improvement of Quality of Water of the Pecos River by Diversion of Brine at Malaga Bend, Eddy County, New Mexico*. Carlsbad, NM: Pecos River Commission.

Harms, J. C., and C. R. Williamson. 1988. "Deep-water Density Current Deposits of Delaware Mountain Group (Permian), Delaware Basin, Texas and New Mexico." *American Association of Petroleum Geologists Bulletin* vol. 72, no. 3: 299-317.

Haug, A., V. A. Kelly, A. M. LaVenue, and J. F. Pickens. 1987. *Modeling of Groundwater Flow in the Culebra Dolomite at the Waste Isolation Pilot Plant (WIPP) Site: Interim Report*. SAND86-7167. Albuquerque, NM: Sandia National Laboratories.

Havens, J. S., and D. W. Wilkins. 1979. *Experimental Salinity Alleviation at Malaga Bend of the Pecos River, Eddy County, New Mexico*. U.S. Geological Survey Water Resources Division Report 80-4. Albuquerque, NM: U.S. Geological Survey/Water Resources Division and the Pecos River Commission.

Hayes, P. T. 1964. *Geology of the Guadalupe Mountains, New Mexico*. Geological Survey Professional Paper No. 446. Washington, DC: U.S. Geological Survey.

Hills, J. M. 1984. "Sedimentation, Tectonism, and Hydrocarbon Generation in Delaware Basin, West Texas and Southeastern New Mexico." *American Association of Petroleum Geologist Bulletin* 68: 250-267.

Hiss, W. L. 1973. "Capitan Aquifer Observation Well Network, Carlsbad to Jal." Technical Report 38. *New Mexico State Engineer.* Santa Fe, NM.

Hiss, W. L. 1975. "Stratigraphy and Ground-water Hydrology of the Capitan Aquifer, Southeastern New Mexico and Western Texas." Ph.D. dissertation. University of Colorado, Boulder.

Hiss, W. L. 1980. "Movement of Ground Water in Permian Guadalupian Aquifer Systems Southeastern New Mexico and Western Texas." *New Mexico Geological Society Guidebook, 31st Field Conference in Trans-Pecos Region.*

Hoeksema, R. J., and P. K. Kitannidis. 1985. "Analysis of the Spatial Structure of Properties of Selected Aquifers." *Water Resources Research* vol. 21, no. 4: 563-572.

Holt, R. M. 1988. Personal Communication to K. Brinster, Science Applications International Corporation, Albuquerque, NM. [Name of Memo]

Holt, R. M., and D. W. Powers. 1988. *Facies Variability and Post-Depositional Alteration within the Rustler Formation in the Vicinity of the Waste Isolation Pilot Plant, Southeastern New Mexico.* DOE/WIPP-88-004. Carlsbad, NM: U.S. Department of Energy.

Holt, R. M., D. W. Powers, R. L. Beauheim, and M. E. Crawley. 199_. SAND89-0862. Albuquerque, NM: Sandia National Laboratories. In preparation.

Hubbert, M. K. 1953. "Entrapment of Petroleum under Hydrodynamic Conditions." *American Association of Petroleum Geologist Bulletin* vol. 37, no. 8: 1954-2026.

Hunter, R. L. 1985. *A Regional Water Balance for the Waste Isolation Pilot Plant (WIPP) Site and Surrounding Area.* SAND84-2233. Albuquerque, NM: Sandia National Laboratories.

James, A. D. 1985. "Producing Characteristics and Depositional Environments of Lower Pennsylvanian Reservoirs, Parkway-Empire South Area, Eddy County, New Mexico." *American Association of Petroleum Geologist Bulletin* vol. 69, no. 7: 1043-1063.

Jones, C. L. 1974. *Salt Deposits of the Mescalero Plains Area, Chaves County, New Mexico.* OFR 74-190. U.S. Geological Survey.

Jones, C. L. 1975. *Potash Resources in Part of Los Medaños Area of Eddy and Lea Counties, New Mexico.* U.S. Geological Survey Open-File Report 75-507. Denver, CO: U.S. Geological Survey.

Jones, C. L. 1978. *Test Drilling for Potash Resources: Waste Isolation Pilot Plant Site, Eddy County, New Mexico.* U.S. Geological Survey Open-File Report 78-592. Washington, DC: U.S. Geological Survey.

Kelley, V. A., and G. J. Saulnier, Jr. 1990. *Core Analysis from the Culebra Dolomite at the Waste Isolation Pilot Plant.* SAND90-7011. Albuquerque, NM: Sandia National Laboratories.

Kunkler, J. L. 1980. *Evaluation of the Malaga Bend Salinity Alleviation Project Eddy County, New Mexico.* U.S. Geological Survey Open-File Report 80-1111. Albuquerque, NM: U. S. Geological Survey/Water Resources Division and the Pecos River Commission.

Lambert, S. J. 1983. *Dissolution of Evaporites in and around the Delaware Basin, Southeastern New Mexico and West Texas.* SAND82-0461. Albuquerque, NM: Sandia National Laboratories.

Lambert, S. J. 1987. *Feasibility Study: Applicability to Geochronologic Methods Involving Radiocarbon and Other Nuclides to the Groundwater Hydrology of the Rustler Formation.* SAND86-1054. Albuquerque, NM: Sandia National Laboratories.

Lambert, S. J., and J. A. Carter. 1987. *Uranium-Isotope Systematics in Groundwaters of the Rustler Formation, Northern Delaware Basin, Southeastern New Mexico.* SAND87-0388. Albuquerque, NM: Sandia National Laboratories.

Lambert, S. J., and D. M. Harvey. 1987. *Stable-Isotope Geochemistry of Groundwaters in the Delaware Basin of Southeastern New Mexico.* SAND87-0138. Albuquerque, NM: Sandia National Laboratories.

Lambert, S. J., and J. W. Mercer. 1978. *Hydrologic Investigation of the Los Medaños Area, Southeastern New Mexico, 1977.* SAND77-1401. Albuquerque, NM: Sandia National Laboratories.

Lambert, S. J., and K. L. Robinson. 1984. *Field Geochemical Studies of Groundwaters in Nash Draw, Southeastern New Mexico.* SAND83-1122. Albuquerque, NM: Sandia National Laboratories.

Lang, W. B. 1938. "Geology of the Pecos River between Laguna Grande de la Sal and Pierce Canyon, in 12th and 13th Biannual Reports." *New Mexico State Engineer.* Santa Fe, NM. 80-86.

Lappin, A. R. 1988. *Summary of Site Characterization Studies Conducted from 1983 through 1987 at the Waste Isolation Pilot Plant (WIPP) Site, Southeastern New Mexico.* SAND88-0157. Albuquerque, NM: Sandia National Laboratories.

Lappin, A. R., R. L. Hunter, D. P. Garber, P. B. Davies, eds. 1989. *Systems Analysis Long-Term Radionuclide Transport and Dose Assessments, Waste Isolation Pilot Plant (WIPP), Southeastern New Mexico; March 1989.* SAND89-0462. Albuquerque, NM: Sandia National Laboratories.

LaVenue, A. M., A. Haug, and V. A. Kelley. 1988. *Numerical Simulation of Groundwater Flow in the Culebra Dolomite at the Waste Isolation Pilot Plant (WIPP) Site; Second Interim Report.* SAND88-7002. Albuquerque, NM: Sandia National Laboratories.

LaVenue, A. M., T. L. Cauffman, and J. F. Pickens. 1990. *Ground-Water Flow Modeling of the Culebra Dolomite, Volume 1: Model Calibration.* SAND89-7068/1. Albuquerque, NM: Sandia National Laboratories.

Lohman, S. W. 1972. *Ground-water Hydraulics.* U.S. Geological Survey Professional Paper No. 708. Washington, DC: U.S. Geological Survey.

Lowenstein, T. K. 1987. *Post-Burial Alteration of the Permian Rustler-Formation Evaporites, WIPP Site, New Mexico: Textural Stratigraphic and Chemical Evidence.* EEG-36 DOE/AL/10752-366. Santa Fe, NM: New Mexico Environmental Evaluation Group.

McGowan, J. H., G. E. Granata, and S. J. Seni. 1979. *Depositional Framework of the Lower Dockum Group (Triassic).* Report of Investigation No. 97. Austin, TX: University of Texas.

Maley, V. C., and R. M. Huffington. 1953. "Cenozoic Fill and Evaporite Solution in the Delaware Basin, Texas and New Mexico." *Geologic Society of America Bulletin* vol. 64, no. 5: 539-546.

Mercer, J. W. 1983. *Geohydrology of the Proposed Waste Isolation Pilot Plant Site, Los Medaños Area, Southeastern New Mexico.* U.S. Geological Survey Water Resources Investigations Report 83-4016. Albuquerque, NM: U.S. Geological Survey.

Mercer, J. W. 1987. *Compilation of Hydrologic Data from Drilling the Salado and Castile Formations near the Waste Isolation Pilot Plant (WIPP) Site in Southeastern New Mexico.* SAND86-0954. Albuquerque, NM: Sandia National Laboratories.

Mercer, J. W. and B. R. Orr. 1977. *Review and Analysis of Hydrogeologic Conditions near the Site of a Nuclear-Waste Repository, Eddy and Lea Counties, New Mexico.* U.S. Geological Survey Open-File Report 77-123. Albuquerque, NM: U.S. Geological Survey.

Mercer, J. W. and B. R. Orr. 1979. *Interim Data Report on the Geohydrology of the Proposed Waste Isolation Pilot Plant Site, Southeast New Mexico.* U.S. Geological Survey Water Resources Investigations Report 79-78. Albuquerque, NM: U.S. Geological Survey.

Mercer, J. W. and R. L. Beauheim, R. P. Snyder, and G. M. Fairer. 1987. *Basic Data Report for Drilling and Hydrologic Testing of Drillhole DOE-2 at the Waste Isolation Pilot Plant (WIPP) Site.* SAND86-0611. Albuquerque, NM: Sandia National Laboratories.

Myers, J., P. Jones and P. Drez. 1988. "The Redox State of the Culebra Member of the Rustler Formation." *Hydrogeochemical Studies of the Rustler Formation and Related Rocks in the WIPP Area, Southeastern New Mexico.* Eds. M. D. Seigel, S. J. Lambert, and K. L. Robinson. SAND88-0196. Albuquerque, NM: Sandia National Laboratories.

Nicholson, A. Jr., and A. Clebsch, Jr. 1961. *Geology and Ground-water Conditions in Southern Lea County, New Mexico*. Ground-water Report No. 6. Socorro, NM: New Mexico Bureau of Mines and and Mineral Resources.

Nowak, E. J., D. F. McTigue, and R. Beraun. 1988. *Brine Inflow to WIPP Disposal Rooms: Data, Modeling, and Assessment*. SAND88-0112. Albuquerque, NM: Sandia National Laboratories.

Peterson, E. W., P. Lagus, J. Brown, K. Lie. 1985. *WIPP Horizon In Situ Permeability Measurements Final Report*. SAND85-7166. Albuquerque, NM: Sandia National Laboratories.

Peterson, E. W., P. Lagus, and K. Lie. 1987. *WIPP Horizon Free Field Fluid Transport Characteristics*. SAND87-7164. Albuquerque, NM: Sandia National Laboratories.

Popielak, R. S., R. L. Beauheim, S. R. Black, W. E. Coons, C. T. Ellingson, and R. L. Olsen. 1983. *Brine Reservoirs in the Castile Formation, Waste Isolation Pilot Plant, Southeastern New Mexico*. TME-3153. Albuquerque, NM: U.S. Department of Energy.

Powers, D. W., S. J. Lambert, S. E. Shaffer, L. R. Hill, and W. D. Weart, eds. 1978. *Geological Characterization Report, Waste Isolation Pilot Plant (WIPP) Site, Southeastern New Mexico*. SAND78-1596. Albuquerque, NM: Sandia National Laboratories.

Ramey, D. S. 1985. *Chemistry of Rustler Fluids*. EEG-31. Santa Fe, NM: New Mexico Environmental Evaluation Group.

Richey, S. F. 1987. *Water Level Data from Wells in the Vicinity of the Waste Isolation Pilot Plant, Southeastern New Mexico*. U.S. Geological Survey Open-File Report 87-120. Washington, DC: U.S. Geological Survey.

Richey, S. F. 1989. *Geologic and Hydrologic Data for the Rustler Formation near the Waste Isolation Pilot Plant, Southeastern New Mexico*. U.S. Geological Survey Open-File Report 89-32. Washington, DC: U.S. Geological Survey.

Richey, S. F., J. G. Wells, and K. T. Stephens. 1985. *Geohydrology of the Delaware Basin and Vicinity, Texas and New Mexico*. U.S. Geological Survey Water Resources Investigations Report 84-4077. Washington, DC: U.S. Geological Survey.

Robinson, T. W., and W. B. Lang. 1938. "Geology and Ground-Water Condition of the Pecos River Valley in the Vicinity of Laguna Grande de la Sal, New Mexico, in 12th and 13th Biannual Reports." *New Mexico State Engineer*. Santa Fe, NM. 77-100.

Sandia National Laboratories. 1990. *Waste Isolation Pilot Plant Program Plan for FY90*. Albuquerque, NM: Sandia National Laboratories.

Saulnier, G. J. Jr. 1987. *Analysis of Pumping Test of the Culebra Dolomite Conducted at the H-11 Hydropad at the Waste Isolation Pilot Plant (WIPP) Site.* SAND87-7001. Albuquerque, NM: Sandia National Laboratories.

Saulnier, G. J. Jr., and J. D. Avis. 1988. *Interpretation of Hydraulic Tests Conducted in the Waste-Handling Shaft at the Waste Isolation Pilot Plant (WIPP) Site.* SAND87-7001. Albuquerque, NM: Sandia National Laboratories.

Saulnier, G. J. Jr., G. A. Freeze, and W. A. Stensrud. 1987. *WIPP Hydrology Program, Waste Isolation Pilot Plant, Southeastern New Mexico, Hydrologic Data Report No. 4.* SAND86-7166. Albuquerque, NM: Sandia National Laboratories.

Siegel, M. D., S. J. Lambert, and K. L. Robinson, eds. 1990. *Hydrogeochemical Studies of the Rustler Formation and Related Rocks in the WIPP Area, Southeastern New Mexico.* SAND88-0196. Albuquerque, NM: Sandia National Laboratories.

Snyder, R. P. 1985. *Dissolution of Halite and Gypsum, and Hydration of Anhydrite to Gypsum, Rustler Formation, in the Vicinity of the Waste Isolation Pilot Plant, Southeastern New Mexico.* U.S. Geological Survey Open-File Report 85-229. Washington, DC: U.S. Geological Survey.

Snyder, R. P., and L. M. Gard. 1982. *Evaluation of Breccia Pipes in Southeastern New Mexico and their Relation to the Waste Isolation Pilot Plant (WIPP) Site.* OFR 82-968. U.S. Geological Survey for the U.S. Department of Energy (Interagency Agreement E (29-2)-3627).

Spiegler, P. 1982. *Analysis of Potential Formation of a Breccia Chimney Beneath the WIPP Repository.* EEG-13. Environmental Evaluation Group, Environmental Improvement Division, Health and Environment Department, State of New Mexico.

Stormont, J. C., E. W. Peterson, and P. L. Lagus. 1987. *Summary of and Observation about WIPP Facility Horizon Flow Measurements through 1986.* SAND87-1076. Albuquerque, NM: Sandia National Laboratories.

Trescott, P. C., G. F. Pinder, and S. P. Larson. 1976. *Finite Difference Model for Aquifer Simulation in Two Dimensions with Results of Numerical Experiments.* U.S. Geological Survey Techniques of Water-Resources Investigation. Washington, DC: U.S. Geological Survey.

U.S. DOE (Department of Energy). 1980. *Final Environmental Impact Statement, Waste Isolation Pilot Plant.* DOE/TIS-0026. Washington, DC: U.S. Department of Energy.

U.S. DOE (Department of Energy). 1982. *Brine Reservoirs in the Castile Formation, Waste Isolation Pilot Plant (WIPP) Project, Southeastern New Mexico.* Albuquerque, NM: U.S. Department of Energy.

U.S. EPA (U.S. Environmental Protection Agency). 1985. *Environmental Standards for the Management and Disposal of Spent Nuclear Fuel, High-Level and Transuranic Radioactive Waste; Final Rule*. 40 CFR Part 191. *Federal Register* 50: 38066-38089.

USGS (U.S. Geological Survey). 1982. *Water Resources Data, New Mexico, Water Year 1981*. U.S. Geological Survey Water Data Report NM-81-1. Washington, DC: U.S. Geological Survey.

USGS (U.S. Geological Survey). 1985. *Water Resources Data, New Mexico, Water Year 1984*. Water Data Report NM-84-1. U.S. Geological Survey.

Vine, J. D. 1960. "Recent Domal Structures in Southeastern New Mexico." *American Association of Petroleum Geologists Bulletin* vol. 44, no. 12: 1903-1911.

Vine, J. D. 1963. *Surface Geology of the Nash Draw Quadrangle, Eddy County, New Mexico*. U.S. Geological Survey Bulletin 1141-B.

Ward, R. F., C. G., St. C. Kendall, and P. M. Harris. 1986. "Upper Permian (Guadalupian) Facies and Their Association with Hydrocarbons — Permian Basin, West Texas and New Mexico." *American Association of Petroleum Geologist Bulletin* vol. 70, no. 3: 239-262.

Webb, S. W. 1990. "Water-level Rise Investigation—Rainfall and SWIFT Simulation Results," memorandum to E. D. Gorham (May 14). Albuquerque, NM: Sandia National Laboratories.

Williamson, C. R. 1978. "Depositional Processes, Diagenesis and Reservoir Properties of Permian Deep-Sea Sandstones, Bell Canyon Formation, Texas-New Mexico." Ph.D. dissertation. Austin, TX: University of Texas.

APPENDIX A:
PRINCIPLES OF HYDROLOGY

APPENDIX A
TABLE OF CONTENTS

HYDROLOGIC CYCLE A-5
HYDROLOGIC PROPERTIES A-6
- Porosity A-6
- Permeability A-7
- Hydraulic Conductivity A-8
- Transmissivity A-8
- Specific Storage, Storage Coefficient, and Specific Yield A-9
- Determination of Transmissivity and Storativity A-10
- Fluid Density A-11
- Formation Pressure A-12
- Potentiometric Surfaces and Ground-water Flow A-15
- Darcy's Law A-21
- Three-Dimensional Flow Equations A-22
- Ground-water Velocity and Travel Time A-26

REFERENCES A-27

FIGURES

Figure — Page

A-1. Relationship of Pressure Head, Environmental Head, and Pressure A-16
A-2. Water Level Map of Study Area A-18
A-3. Results of the Variable Density Flow Analysis A-20
A-4. Concept of Flow through a Control Volume of a Porous Medium A-24
A-5. Flow In the X-Axis Direction A-24

TABLES

Table — Page

A-1. Relationship of Permeability and Hydraulic Conductivity A-9

APPENDIX A:
PRINCIPLES OF HYDROLOGY

This appendix is presented as a basis for making assumptions required to evaluate performance of the WIPP. Terminology used in reference to hydrology and mathematical modeling of flow and transport throughout this report is discussed and defined in this section. Further elaboration on the terms used in this report can be found in hydrology textbooks, specifically, Freeze and Cherry (1979) and Lohman (1972). Definitions found in these sources typify common usage and are used freely throughout the report.

Hydrologic Cycle

In nature, water is transferred from the atmosphere to the land and back to the atmosphere in a process called the hydrologic cycle. Two primary mechanisms for this cycle are precipitation and evaporation. Precipitation occurs as rain or snow that may evaporate immediately, sometimes even before it reaches the ground. Once the water is on the ground, it may evaporate, or it may infiltrate the soil, where it may be taken up by plants and incorporated into the plants' cells or given off by transpiration. The processes of evaporation and transpiration are collectively called evapotranspiration. If the precipitation is of large enough quantity and is not completely lost through evapotranspiration, it will either become runoff or infiltrate farther into the soil and eventually become part of the ground water. The runoff may flow to surface reservoirs (oceans or lakes) where it will ultimately return to the atmosphere by evaporation.

At any time throughout the cycle, ground water may become surface water, and surface water may become part of the ground water. Consequently, the ground water and surface water are in constant motion trying to attain equilibrium. At some point, the amount of input will equal the amount of output, and the system is then called steady state. If at some time a change alters the cycle, such as extensive withdrawal of water from the system or addition of water to the system either naturally or by man's activities, the system will go into a transient state. If the perturbation to the system becomes constant, the system will again reach steady state but at a new level.

If all the pores in a given volume of rock are filled with a fluid, the rock is saturated. If a layer of rock or a group of layers of rock is completely saturated and yields its water readily and in amounts large enough to make withdrawal worthwhile, it is called an aquifer. In the report, the term "hydrostratigraphic units" describes units that are not aquifers in the

strictest sense of the word, but are units that have water in them and may have some potential as flow paths for radionuclides. If the surface of the water in saturated rock is at atmospheric pressure, the water is said to be under water-table conditions. If the upper surface of the saturated zone is a relatively impermeable material, the aquifer is said to be confined, and the confining, less permeable beds are called aquitards. The term aquiclude is also used to describe a unit that is saturated but will not yield water under ordinary hydraulic gradients (Freeze and Cherry, 1979).

Hydrologic Properties

POROSITY

The upper part of the earth's crust is made up of rocks consisting of both consolidated and unconsolidated material that must possess two important rock properties, porosity and permeability, in order for water to flow. Porosity (n) is defined quantitatively as the ratio of free space (voids, pores, pore spaces, interstices) to total volume of rock or, simply stated, as the percentage of the total rock volume occupied by voids. Rocks may possess either primary porosity or secondary porosity. Primary porosity is the porosity the rock possesses by virtue of its origin, such as the interstices that are formed between grains when sands or gravels are deposited or voids are made from gas bubbles in molten rock that hardens. Secondary porosity is formed by activities such as jointing, faulting, cracking, or dissolution of the matrix after the rocks are deposited. A third term associated with porosity is effective porosity, which is the volume percentage of connected pores through which fluid can flow.

Porosity and permeability (discussed later) of rocks are affected by syndepositional and post-depositional processes. For example, dolomite can be primary or secondary. Primary dolomites are formed in place in evaporitic environments such as those in the Delaware Basin in Ochoan time. Basin water becomes rich in magnesium by the inflow of sea water and precipitation of carbonate and sulfate (Pettijohn, 1957). Primary dolomite is dense and has preserved depositional fossils and depositional features. Secondary dolomite is formed by magnesium-rich water moving through limestone, increasing porosity by altering the limestone and reducing the total rock volume by more than 10 percent. Limestones so altered do not have preserved depositional features such as cross-bedding, and fossils may not be evident.

According to Holt and Powers (1988), a complex post-depositional history of the Rustler Formation resulted from mechanical responses to stress and diagenetic reactions, that is, mechanical and chemical disequilibrium in the

unit. Discussion of the mechanisms that affect Rustler Formation rocks can be found in Holt and Powers (1988). Four constituents of the rocks (halite, anhydrite, gypsum, and carbonate) all react with each other in the system as cement or overgrowth material, replacing each other, recrystallizing, overgrowing, and filling fractures. These mechanisms can change rock volume, change porosity by filling fractures or vugs, and change permeability.

PERMEABILITY

Permeability (or intrinsic permeability, (k)) is a measure of the property of a rock that allows fluid to pass through it (that is, the pores are connected). Early hydrologists found that permeability is approximately proportional to the square of the mean grain diameter (d) or

$$k \propto d^2$$

or

$$k = Cd^2, \qquad \text{(A-1)}$$

where C is a constant of proportionality.

Permeability can also be expressed as

$$k = - \frac{q\nu}{g(dh/dl)} \qquad \text{(A-2)}$$

where k = intrinsic permeability
q = rate of flow-per unit area (Q/A)
ν = kinematic viscosity
g = acceleration due to gravity
dh/dl = hydraulic gradient.

The units are m^2.

Permeability is also often referred to in darcy units where

$$1 \text{ darcy} = \frac{[(1 \text{ cp})\ (1 \text{ cm/s})]/1 \text{ cm}}{1 \text{ atm/cm}} .$$

One darcy is equal to 9.87×10^{-13} m^2. (To obtain k in m^2 multiply darcies by 9.87×10^{-13}.)

HYDRAULIC CONDUCTIVITY

Hydraulic conductivity (K), which is sometimes called the coefficient of permeability, should not be confused with the term intrinsic permeability. Lohman (1972) defines hydraulic conductivity thus: "a medium has a hydraulic conductivity of unit length per unit time if it will transmit in unit time a unit volume of ground water at the prevailing viscosity through a cross section of unit area, measured at right angles to the direction of flow, under a hydraulic gradient of unit change in head through unit length of flow," or mathematically

$$K = - \frac{q}{dh/dl} \quad . \tag{A-3}$$

The units Lohman (1972) suggests are

$$K = - \frac{m^3}{m^2 \ sec(-m \ m^{-1})} = m/s \quad .$$

The minus sign indicates movement in the direction of decreasing head.

One darcy is approximately the same as a hydraulic conductivity of 10^{-5} m/s. Table A-1 is a convenient conversion chart that gives ranges of values of permeability and hydraulic conductivity.

Hydraulic conductivity values can vary in a formation because of measurement position or measurement direction. If position has no apparent effect on the value of hydraulic conductivity, the formation is said to be homogeneous, while if position has an effect, the formation is heterogenous. If direction has no effect on the value of hydraulic conductivity, the media is isotropic, and if an effect is measured, the formation is anisotropic.

TRANSMISSIVITY

Transmissivity (T) is a property of the confined liquid as well as of the aquifer and is defined as the rate at which water at the prevailing viscosity is passed through a given thickness (b) of aquifer under a hydraulic gradient (Lohman, 1972).

Mathematically,

$$T = Kb. \tag{A-4}$$

TABLE A-1. RELATIONSHIP OF PERMEABILITY AND HYDRAULIC CONDUCTIVITY

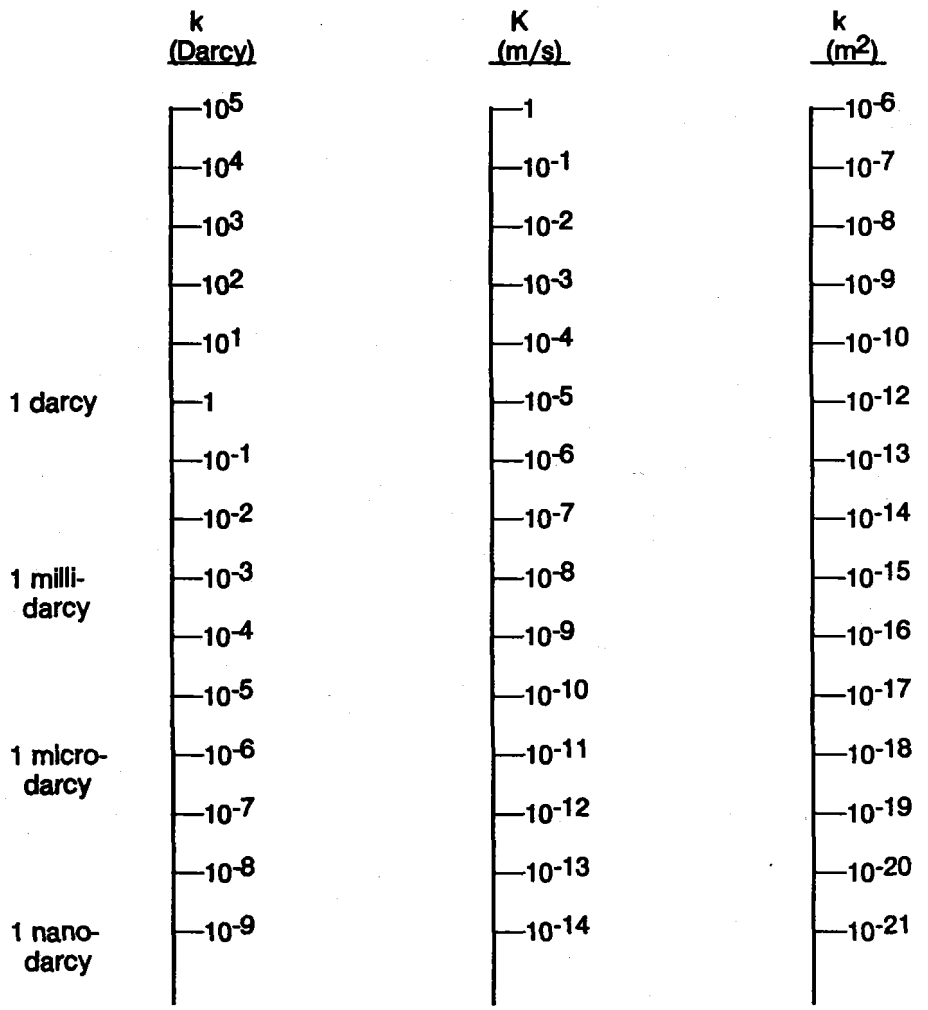

The units are m^2/s.

This property of the aquifer has also been called the coefficient of transmissibility, but transmissibility is a property of a liquid only. In modeling of ground-water flow, the term transmissibility may also have a different meaning.

SPECIFIC STORAGE, STORAGE COEFFICIENT, AND SPECIFIC YIELD

The specific storage (S_s) of an saturated aquifer is defined by Freeze and Cherry (1979) as the volume of water that is released by a unit volume of aquifer from storage under a unit decline in hydraulic head (a volume per volume per unit decline of head). The controlling mechanisms are the compressibilities of the aquifer and of the fluid. Mathematically

$$S_s = \rho g(\alpha + n\beta) \qquad \text{(A-5)}$$

where ρ = density of the fluid
α = compressibility of the aquifer
β = compressibility of the fluid
n = porosity
g = gravity constant.

The units are m^{-1}.

The storage coefficient (S) of a confined aquifer is the product of the thickness of the unit (b) and the specific storage (S_s). That is,

$$S = S_s b \tag{A-6}$$

and is defined by Lohman (1972) as the volume of water released by an aquifer per unit surface area per unit drop in hydraulic head and is dimensionless. Specific yield is the term used for the storage coefficient of an unconfined aquifer because very little water is lost through aquifer compression and fluid expansion as the hydraulic head declines.

DETERMINATION OF TRANSMISSIVITY AND STORATIVITY

Transmissivity of a hydrostratigraphic unit can be measured in the near field by the "slug" method or in the far field by pumping one well and measuring the aquifer response in one or more neighboring wells a known distance away. The slug method is the instantaneous injection or removal of a known quantity of water from a well, followed by a series of water-level measurements. The method gives a good estimate of transmissivity in units with a low transmissivity and where the well is fully penetrating and fully screened. The transmissivity can then be calculated using a simplified equation from Ferris and others (1962):

$$s' = \frac{114.6\ V}{Tt} \tag{A-7}$$

where s' = residual drawdown (residual head for injection)
V = volume of water removed or injected
t = time since injection
T = transmissivity.

T and S can be determined from pumping tests by using curve matching on a log-log plot, known as the Theis method. Another method or interpretation with a semilog plot is known as the Jacob method. These methods are explained in Lohman (1972), Ferris and others (1962), and Freeze and Cherry (1979). Storage can be calculated from this relationship (Freeze and Cherry 1979):

$$S = \frac{4U\ Tt}{r^2} \qquad \text{(A-8)}$$

where U = the independent variable of the well function, W(U)
r = radial distance from the well.

Both tests have advantages and disadvantages. The slug test is inexpensive while a pumping test is not. The slug test gives only a near-field T value and the pumping test gives a T value averaged over a large area. Curve matching is subjective, and a leaky aquifer will affect the results. Hydraulic conductivity can also be calculated from the results of either test using the equation

$$K = \frac{T}{b} \quad . \qquad \text{(A-9)}$$

FLUID DENSITY

The concept of fresh-water heads is used to describe the Los Medaños flow system. In the Los Medaños Study Area (the Study Area), the ground water contacts rocks made up partially or solely of evaporites. Because of the solubility of the rocks, the waters in some areas have high concentrations of dissolved solids. In regions with a large areal variation in densities, the chance of error becomes greater when determining flow direction if the heads are not density adjusted. Lusczynski (1961) defines fresh-water head in a well with variable density water

> ...as the water level in a well filled with freshwater from that [measuring] point to a level high enough to balance the existing pressure at the point [and the] environmental head is defined as the freshwater head reduced by an amount corresponding to the difference of salt mass in fresh water and that in the environmental water between that point and the top of the zone of saturation.

Using these definitions, the horizontal gradient is defined by the fresh-water head, and the vertical gradient is defined by the environmental head. Mercer (1983) used an equation derived from Lusczynski's (1961) work to calculate fresh-water heads for the Culebra Dolomite, Magenta Dolomite, and brine aquifer, and assumed the density measured for the hydrostratigraphic unit as the density of the column of water. The equation used by Mercer (1983) to get the increase (Zw) in fresh-water head is

$$Z_w = \frac{\rho s - \rho f}{\rho f} Z_s \qquad \text{(A-10)}$$

where Z_s = measured height of a column of water containing dissolved solids above a given point (Mercer [1983] used the center of the Culebra Dolomite)
ρ_s = density of the "brine"
ρ_f = fresh-water density.

FORMATION PRESSURE

The hydrostatic pressure exerted by a column of water on a point in the formation is calculated by the equation

$$p = p_o + \rho g(H - Z) \qquad \text{(A-11)}$$

where p_o = atmospheric pressure
ρ = water density
g = gravity (constant near surface of earth)
$H - Z$ = pressure head.

The density of a column of water in a well is seldom uniform throughout. If the pressure at a point in a well is not known but the fluid density is, the equation given above can be used to estimate the formation pressure. If fluid density measurements are made at different points in the well, the pressure can be estimated more closely by integrating the calculation down the well. If the formation pressure is measured using a transducer and the total head is known, the average density of the column of water can be calculated.

Ground-water flow and transport models may use environmental heads or formation pressures as inputs. As a rule, steady-state formation pressures have not been measured in the Study Area. A series of mid-formation pressure measurements in Culebra Dolomite wells were made to determine if estimating formation pressures using reported water densities was less accurate than using direct pressure measurements (Crawley, 1988, Tables 7, 8, and 9). Fifteen wells had an average absolute-head difference of less than 0.6 m (2 ft of head or 3 psi). The other eight wells had an average absolute-head difference of about 1.2 m (4 ft or 6 psi). Borehole uncertainty in many of the same wells was calculated by LaVenue and others (1988), yielding an average of about ±2 m for the area.

Formation pressures can be calculated using the latest water densities and observed elevations or by using the latest corrected head elevations from regional computer model input. Computer-generated regional models may use a discretization of grid blocks that will prohibit the modeler from setting up a finite-difference grid with wells located at the center of the grid block as was done by LaVenue and others (1988). Some blocks may have wells at the edge

of the block or may even have more than one well in each block. In one case, if a well is near an edge of a steeply dipping block, the formation elevation for that block's center must be estimated and the node pressure adjusted to the center of block. In the second case, the pressures can be adjusted and averaged to yield the block-center pressure.

The deep units in the area may not be important in a regional modeling study. A preliminary examination of northern Delaware Basin data from oil wells of less than 6000-ft depth shows that no wells drilled to rocks immediately below the Castile Formation have sufficient pressures to push available formation fluid to the surface; however, there may be sufficient pressure to force fluids to the Rustler Formation or the repository layer. Actually, the wells are somewhat underpressured. Deeper wells were reported (Lambert and Mercer, 1978, p. III-2 to III-3) to have pressures with calculated heads of greater than 1000 m (about ground level in the WIPP area) to about 2000 m. The names of the wells that produced these pressures were not listed, and the pressures have not been verified. Units deeper than the Delaware Mountain Group that are capable of producing large amounts of water are present in the Delaware Basin (Lambert in Lambert and Mercer, 1978), but whether the water-producing units have sufficient pressure to force water up to the repository horizon and then to the Culebra Dolomite Member of the Rustler Formation remains to be seen.

Commercial oil-production information companies provide data on all oil wells drilled in the northern Delaware Basin. These records should be examined to determine whether water from deep, high-pressure wells could reach the repository. Wire-line electric logs are also an indirect source of pressure data. Each log lists drilling-mud weights and the intervals at which the mud was used. Drilling mud balances the drilling fluid against the formation pore pressure so that fluid (or gas) from the formation does not go into the drill column and drilling fluid does not deeply invade permeable formations. A simple calculation can be used to estimate formation pressure (P_f):

$$P_f = (0.052)(M_w)(d_f). \qquad \text{(A-12)}$$

Mud weight of about 9 lb/gal is used in normally pressured rocks, 11 and 12 lb/gal mud weights is used in high-pressure zones, and muds greater than 12 lb/gal are used in abnormally high-pressured zones. A cursory examination of electric logs shows that most wells use a mud weight of from 9 to 10 lb/gal, with very few wells using a mud weight of from 11 to 12 lb/gal. No wells used mud weights greater than 12 lb/gal. Using 12 lb/gal mud to balance formation pressure in an 11,000-ft deep well would indicate a calculated pressure of 6864 psi. This pressure is equivalent to counterbalancing a column of salt water 14,921 ft high, which is about 4000 ft above the ground

surface in the WIPP area. A USGS well completion report and log on Badger Unit Federal #1 (Sec. 15, T22S, R31E) reports a drill stem test (DST) final shut-in pressure (FSIP) of 4252 psi at 14,039 ft below ground surface (middle Morrow Formation). When compared to a column of salt water, the column would rise 9243 ft in the well (about 4800 ft below ground surface), a distance that is below the repository horizon (2150 ft below the surface). However, a DST in the Brushy Canyon Formation at 6230 ft below ground surface had a FSIP of 2661 psi, enough pressure to support a column of salt water 5784 ft high (almost 400 ft above the Culebra in that area). Both DSTs, however, produced only extremely small amounts of fluid (oil or saltwater) or gas.

Fluid production will determine if a repository breach by these deep wells is important. Deep wells with adequate pressure to lift a column of salt water to repository level do not seem to have sufficient fluid to flush out the repository.

Ground water flows from a high to a low potential. To have a no-flow condition, the potential must be equal at all locations. Vertical flow between hydrostratigraphic units can only occur if the downward increase in pressure head is more or less than the downward change in elevation head. If the downward elevation head decreases faster than the downward decrease in pressure head, vertical flow is downward (Hubbert, 1940, 1953).

Conversely, if the downward elevation head decreases slower than the downward decrease in pressure, flow is upward. If the downward increase in pressure head equals the decrease in elevation head, the conditions are hydrostatic. As shown by Hubbert (1940), regional flow concentrates in high-transmissivity zones, and flow through low-transmissivity zones between the conductive zones is vertical. Studies by Belitz and Bredehoeft (1988) of anomalously underpressured hydrostratigraphic units showed that, because of fluid movement from high to low potential, subnormal pressuring occurs. They conclude the following:

> Generally, subnormal fluid pressures might be found in any subaerial, topographically tilted, structural basin capped by a thick sequence of low-permeability rocks (that is, shale or evaporites). The tilt can provide the topographic driving force for the fluid flow. The low-permeability cap can provide insulation from the elevation head of the water table, and the structure can provide the mechanism for reducing permeability in the basin deep that allows for better hydrologic connection to low-elevation outcrops than to high-elevation outcrops. The magnitude of the subpressure will be enhanced if the basin is asymmetric with the steeper limb located beneath the topographically elevated region.

The Delaware Basin in New Mexico fulfills the criteria established by their modeling because the units below the Castile Formation are generally underpressured. Davies (1989) demonstrated with a two-dimensional cross-sectional flow model that this condition also occurs in the Culebra Dolomite.

POTENTIOMETRIC SURFACES AND GROUND-WATER FLOW

The presentation and understanding of head data using potentiometric maps require a basic understanding of the concept of potential (Φ). Potential is defined as the amount of work required to move a unit mass of fluid from one state and position to another state and position (Hubbert, 1953).

In a well such as that shown in Figure A-1 where the reference elevation is sea level (0) and the reference pressure is atmospheric (p_o), the potential is stated as (from Hubbert, 1953)

$$\Phi = g(Z - Z_o) + (p - p_o)\, v \qquad \text{(A-13)}$$

where v is the volume per unit mass, or $v = \frac{1}{\rho}$

and if

$$Z_o = 0$$

and

$$p_o = 0$$

then

$$\Phi = gZ + p/\rho \ . \qquad \text{(A-14)}$$

The pressure at the point is

$$p = p_o + \rho g(H-Z)$$

and if

$$p_o = 0$$

then simplifying,

$$gh = gz + \frac{p}{\rho} \qquad \text{(A-15)}$$

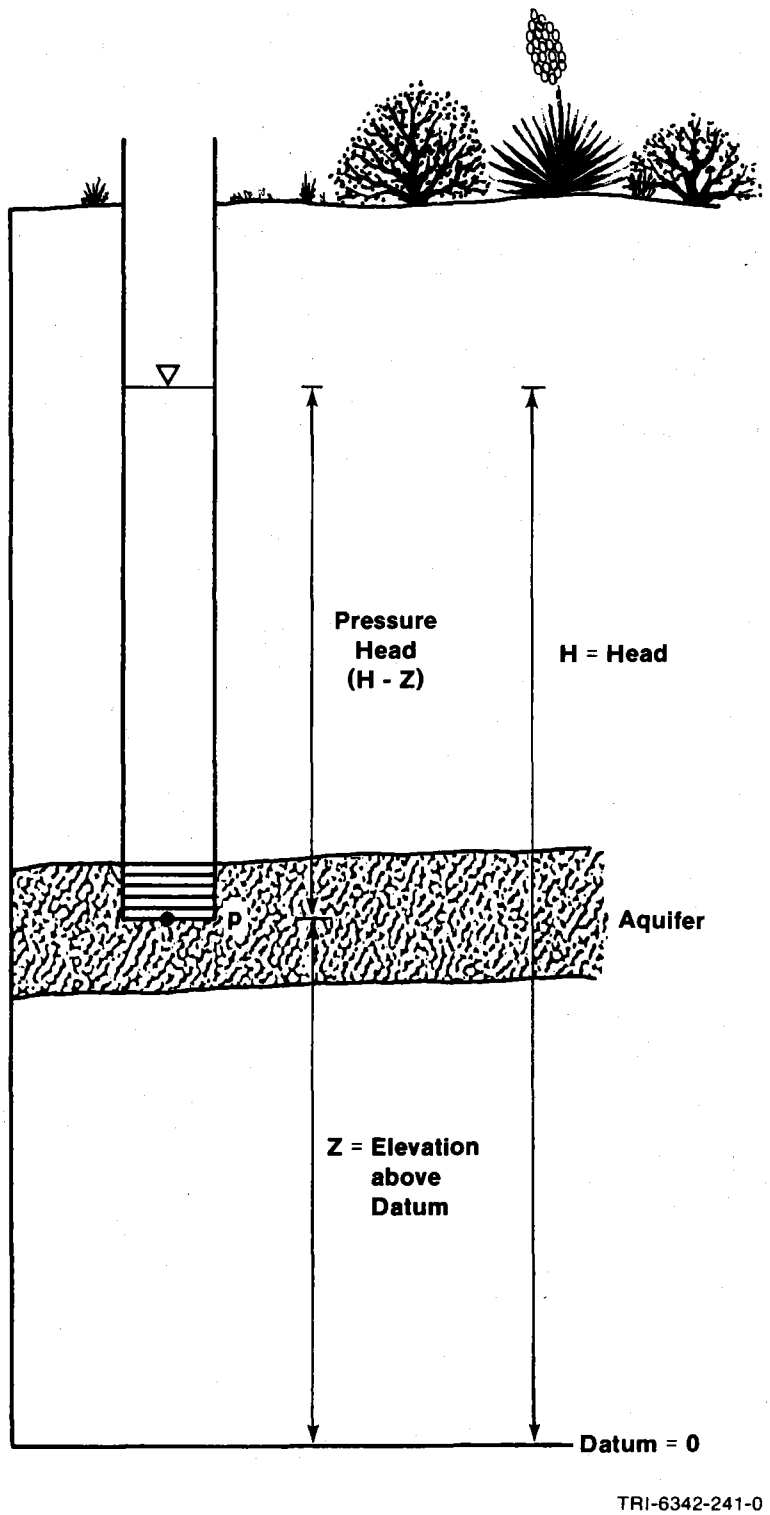

Figure A-1. Relationship of Pressure Head, Environmental Head, and Pressure.

or

$$\Phi = gh \quad . \qquad \text{(A-16)}$$

Because g is constant almost everywhere at or near the earth's surface, the potential and head are then correlative. Ground water moves from the higher potential (Φ) (head) to a lower Φ.

In all data presented here, sea level and atmospheric pressure are presented as reference states. All pressure data are presented as psig or gauge pressure (absolute pressure minus atmospheric pressure) or as psia (absolute pressure). Head means the elevation head plus the pressure head. Hydraulic head (head data or potentiometric data is defined as the elevation to which water from a hydrostratigraphic unit will rise in a properly completed, tightly cased well or a specially constructed standing pipe called a piezometer. Contour maps with lines connecting head values of the same elevations (equipotential lines) are called potentiometric maps. These maps can be used to determine horizontal and vertical flow direction and magnitude in a homogeneous, isotropic, hydrostratigraphic unit. When potentiometric maps are constructed, all head data incorporated in the map must be from the same hydrostratigraphic units. Sometimes maps are constructed using all the head data in a region without regard to hydrostratigraphic units (for example, Figure A-2, which is taken from Plate 1 in Hunter, 1985). These maps may be useful for characterizing horizontal flow patterns in a region but not for much else. The data are not adequate for vertical flow measurements and should be used with care. A potentiometric map of the composite heads is also useful for calculations of hydrostatic pressure for block-center values needed for model input.

Potentiometric lines and flow lines indicate boundary conditions, and potentiometric lines indicate gaining or losing streams. If a potentiometric line bends sharply when it crosses a stream with the flexure pointing downstream, the stream is losing water to the substrata; if the flexure points upstream, the stream is a gaining stream (that is, the stream is below the water table). Potentiometric lines that are normal to the stream indicate the stream elevation is at the water-table elevation. Flow lines normal to a boundary indicate a constant head boundary, while flow lines parallel to a boundary indicate no flow across the boundary. Figure A-2 shows that the Pecos River has potentiometric lines normal to the river and flow lines parallel to the river south of Carlsbad, thus indicating the stream is at equilibrium with the water table. At Malaga Bend, the potentiometric lines are bent more sharply, indicating a gaining region of river. At the northern and eastern boundaries of the Study Area, flow lines are normal to the

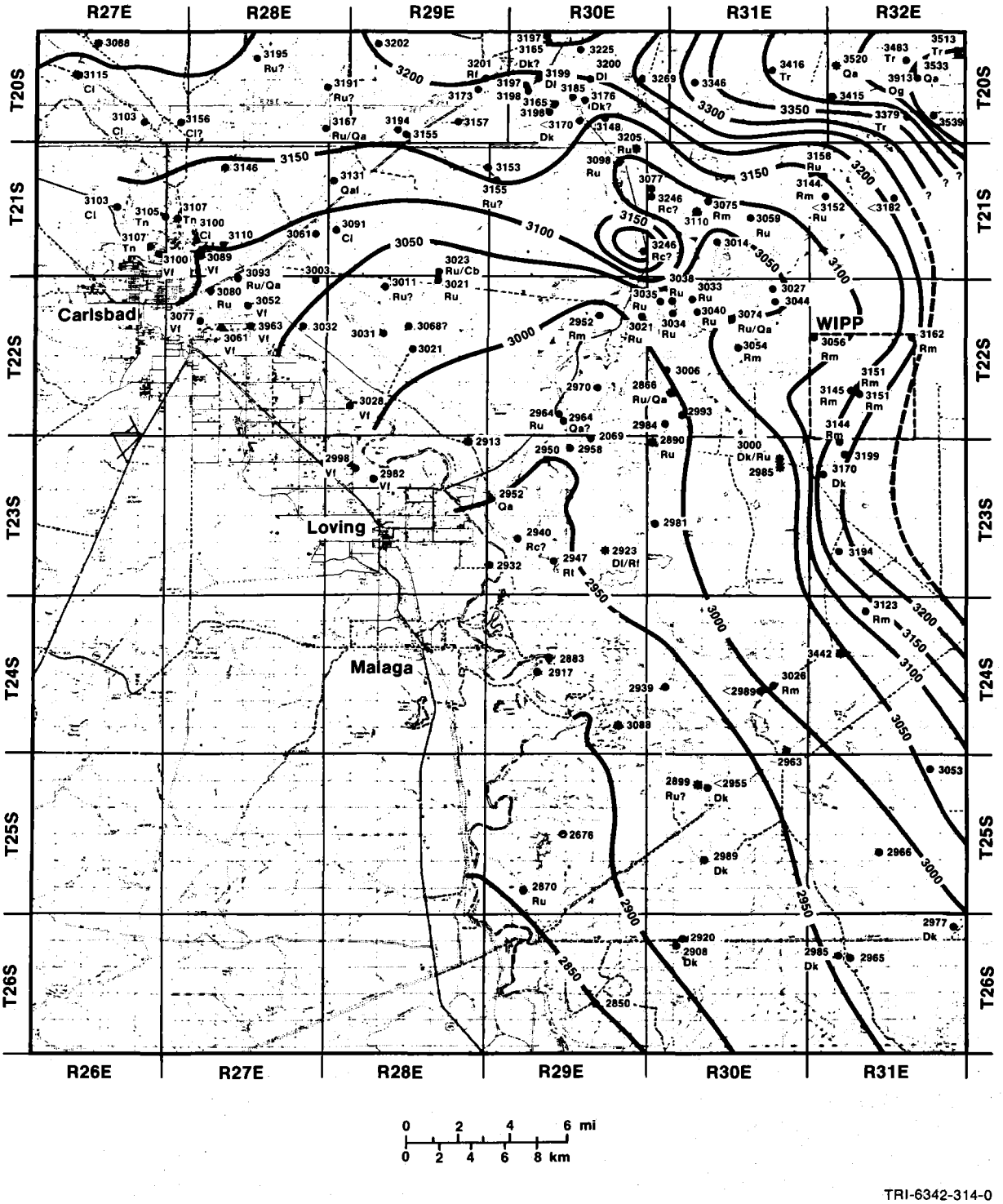

Figure A-2. Water Level Map of Study Area (contours in feet) (Hunter, 1985).

boundary, indicating areas of recharge. These assumptions are further discussed in the description of the conceptual hydrologic model in Chapter VI.

As stated above, potentiometric maps may be used for calculating horizontal flow, but several considerations must be taken into account: isotropy, homogeneity, and water density. The first consideration is the isotropy of the hydrostratigraphic unit. If a unit is isotropic, flow lines that indicate direction of flow are drawn orthogonally to the potentiometric lines, but if the unit is anisotropic, the flow lines are not orthogonal but are at an angle determined by the ratio of hydraulic conductivities normal and parallel to the hydrostratigraphic unit. Early modeling efforts (Barr and others, 1983) calculated, from tests at wells H-4, H-5, and H-6 (Figure A-3), an anisotropy ratio of 1:2.3 to 1:2.7 at an orientation roughly NE-SW. This ratio was then applied to all elements in the Study Area. Haug and others (1987) assumed the Study Area was isotropic and flow lines were orthogonal to the potentiometric-surface contour lines. As regional modeling continues, anisotropy, as determined by the heterogeneity of the rock layers and fracturing, may be determined as important.

If the hydraulic conductivity is independent of position in a hydrostratigraphic unit, the unit is homogeneous. This homogeneity occurs, however, only under ideal conditions. In hydrostratigraphic units such as the Culebra Dolomite Member of the Rustler Formation, hydraulic conductivity varies both vertically and horizontally. Vertically, variation within the unit is caused by the layering of dolomite with clay; horizontally, variation is caused by degrees of fracturing. Heterogeneity changing with distance from a given point in a continuous manner is termed a trend. Predicting trends in hydraulic conductivity necessitates understanding what conditions have affected the rocks. Trends can result from sedimentation rates or distances from the source of sediment. Other factors such as erosion, and degrees of dissolution of rocks can also show trends. In addition to the changes in layers and trending, hydraulic conductivity measured at one point must have absolutely no relationship with other measurements. If measurements are made both in fractured and intact dolomite, a large variation will likely be evident, even if the measurements are taken close together.

The third consideration, water-density changes in the Study Area, is one of the more bothersome problems in determining direction of ground-water flow. The equation Lusczynski (1961) used to calculate fresh-water heads assumes horizontal or nearly horizontal flow and no stratification of density in the column of water in the well bore caused by poor well completion or improper removal of foreign fluids.

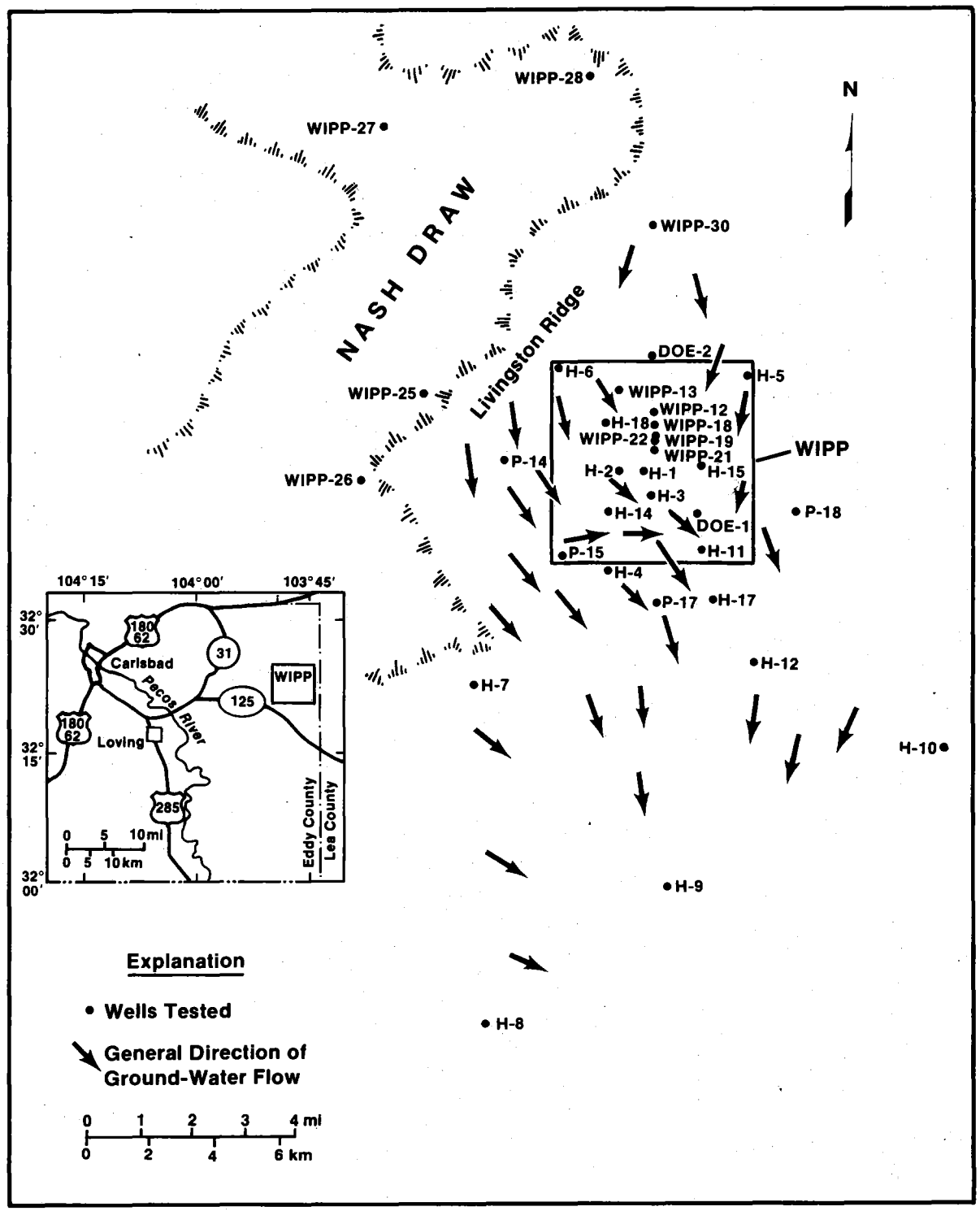

TRI-6342-313-0

Figure A-3. Results of the Variable Density Flow Analysis (Crawley, 1988).

Because the use of fresh-water head data assumes horizontal ground-water flow in areas of spatial variability of fluid density, Davies (1987) examined density-related gravity effects by expanding the gravity term in Darcy's equation and concluded that the relative magnitude, not the absolute magnitude, of the density-related error term determines whether the density-related gravity effects will be significant in any given situation. Davies (1987) examined ground-water flow in the Culebra Dolomite in the vicinity of the WIPP and found that in an area where the Culebra Dolomite is relatively flat-lying, density-related gravity effects are important. Davies (1987) showed in a comparison of fresh-water head simulations with variable density simulations that errors in flow direction up to 170 degrees and in velocity up to almost a factor of 10 could be produced. Davies' (1987) work provides a way for ground-water modelers to predict whether natural or man-made density variations should be considered when defining ground-water flow in a region.

The hydrostatic method reported by Jorgenson (1982) was used by Crawley (1988) for determining flow between wells in aquifers containing variable density water in the Culebra Dolomite Member. The method requires the hydrologist to first determine if hydrostatic conditions exist between three wells and then apply the "three-point" technique (a structural geology technique) to determine strike and dip, with the direction of dip as the direction of flow. The test for hydrostatic conditions assumes that the aquifer is confined and isotropic, that no intervening sources or sinks are between the wells, that structural dip does not reverse, and that flow is parallel to the upper and lower boundaries of the aquifer (Jorgenson and others, 1982). In other words, this technique is valid only if the wells occur on a monoclinal structure of consistent properties, which is not the case for some locations in the Culebra Dolomite. Comparing structure contour maps of the top and bottom of the Culebra Dolomite (Figure 2-20 in Jorgenson and others, 1982, and Figure 4.17 in Holt and Powers, 1988) to a map showing calculated flow directions (Figure A-3) from Crawley (1988) indicates that the flow lines between H-7 and H-8 may be suspect because the wells are on opposite sides of an anticlinal structure. Also, a strong synclinal structure with an associated anticline is present in the northeastern part of the WIPP, putting WIPP-30 and DOE-2 on one limb and H-5 on a different limb. Wells H-9 and H-8 are on opposite limbs of a synclinal structure. This method, therefore, should be used only for local flow estimates and not for regional scale estimates.

DARCY'S LAW

In middle of the nineteenth century, French engineer Henri Darcy studied flow through sand, which he determined was analogous to flow through a pipe. The results of his classical experiment gave the formulation of what is now called Darcy's Law. Darcy's Law, simply stated, says that a specific discharge (v_d

or sometimes called a Darcy flux or Darcy velocity) is directly proportional to the change in hydraulic head and inversely proportional to the distance between the head measurements, or mathematically

$$v_d = \frac{K(H_2 - H_1)}{L} \qquad \text{(A-17)}$$

where L = length the water has to travel
H_1 and H_2 = head measurements
K = hydraulic conductivity (m/s) of the medium (constant of proportionality).

The term $\frac{H_2 - H_1}{L}$ is the gradient, which can be replaced with I in the equation and which then becomes

$$v_d = KI. \qquad \text{(A-18)}$$

Because the discharge (Q) of a pipe is equal to the velocity of the fluid times the cross-sectional area of the pipe ($Q = v_d I$), Darcy's equation can be simply written as

$$Q = KIA. \qquad \text{(A-19)}$$

The equation is sometimes written Q = -KIA to show that the flow direction is toward the lower head.

THREE-DIMENSIONAL FLOW EQUATIONS

Flow of a gas and/or a fluid through fractures and pores in rocks and soil is generally the result of gravity and/or fluid pressure. Using Darcy's Law equation from above, the fluid movement can be expressed as

$$v_i = -K \frac{\partial h}{\partial x} \quad , \qquad \text{(A-20)}$$

where K = hydraulic conductivity with units of length per unit time (that is, the rate at which the fluid moves through a rock matrix)
h = fluid head or potential
v_i = specific discharge
$\partial h/\partial x$ = hydraulic gradient.

Again, the negative sign indicates movement in the direction of head loss.

The hydraulic conductivity (K) is directly proportional to the permeability of the matrix (k) and the density (ρ_f) of the fluid, and inversely proportional to the viscosity (μ) of the fluid. This relationship can be expressed as

$$K = \frac{\rho_f g k}{\mu} \qquad \text{(A-21)}$$

where g = acceleration due to gravity.

Consider a unit volume of a saturated, porous substance as shown in Figure A-4. The law of conservation of mass at steady state requires that fluid mass moving into the unit volume equal the mass of fluid out (Figure A-4) of the unit.

The flow in the x direction can be shown as the difference between the mass inflow and the outflow rate (Figure A-5). Or mathematically

$$\left[\rho v_x - \frac{\partial(\rho v_x)}{\partial x}\right] - \rho v_x = - \frac{\partial(\rho v_x)}{\partial x} \quad . \qquad \text{(A-22)}$$

Flows in the y and z directions are analogous. Combining the mass flow components in the x, y, and z directions

$$- \frac{\partial(\rho v_x)}{\partial x} - \frac{\partial(\rho v_y)}{\partial y} - \frac{\partial(\rho v_z)}{\partial z} = 0 \quad . \qquad \text{(A-23)}$$

If the fluid is incompressible, ρ (x,y,z) = constant, and the ρ's can be removed from Equation (A-22). If the fluid is slightly compressible, such as water, Freeze and Cherry (1979) show that $\rho \partial v_x/\partial x$ is much greater than terms of the form $v_x \partial \rho/\partial x$, both of which arise when the chain rule is used to expand Equation (4). Equation (4) then simplifies to

$$- \frac{\partial v_x}{\partial x} - \frac{\partial v_y}{\partial y} - \frac{\partial v_z}{\partial z} = 0 \quad . \qquad \text{(A-24)}$$

Substituting Darcy's equation (Equation A-19) for v_x, v_y, and v_z, we get

$$- \frac{\partial}{\partial x}\left[-K_x \frac{\partial h}{\partial x}\right] - \frac{\partial}{\partial y}\left[-K_y \frac{\partial h}{\partial y}\right] - \frac{\partial}{\partial z}\left[K_z \frac{\partial h}{\partial z}\right] = 0 \qquad \text{(A-25)}$$

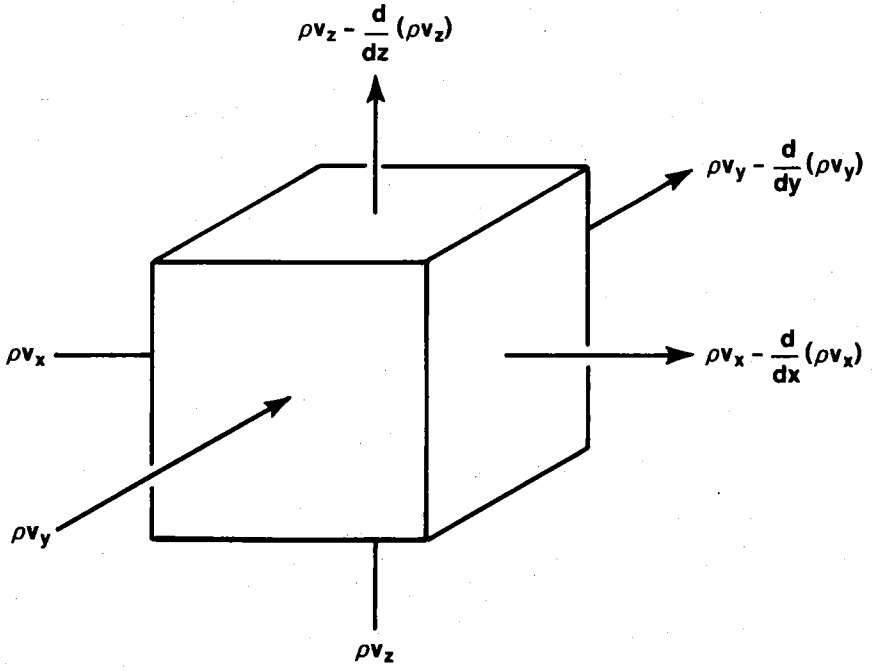

Figure A-4. Concept of Flow through a Control Volume of a Porous Medium (modified from Freeze and Cherry, 1979).

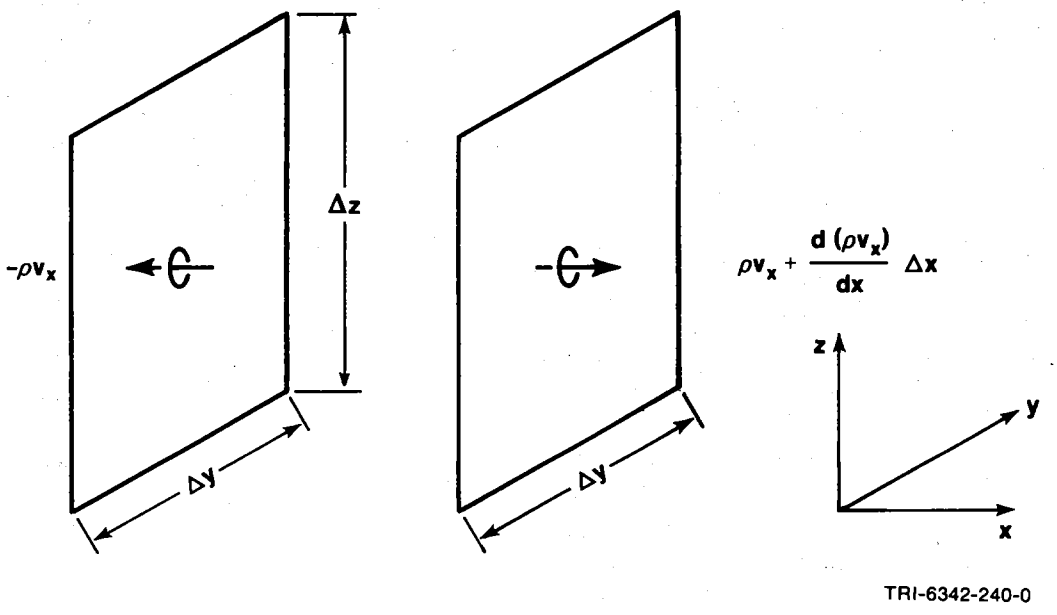

Figure A-5. Flow in the X-Axis Direction.

for flow through an anisotropic heterogeneous medium at steady state.

If

$$K_x = K_y = K_z,$$

then

$$\frac{\partial^2 h}{\partial x^2} + \frac{\partial^2 h}{\partial y^2} + \frac{\partial^2 h}{\partial z^2} = 0 \qquad \text{(A-26)}$$

for an isotropic medium at steady state.

In transient flow, the continuity equation (Equation A-22) is modified such that the outflow equals the inflow plus the water released from storage:

$$- \frac{\partial (\rho v_x)}{\partial x} - \frac{\partial (\rho v_y)}{\partial y} - \frac{\partial (\rho v_z)}{\partial z} = n' \frac{\partial \rho}{\partial t} + \frac{\rho \partial n'}{\partial t} \qquad \text{(A-27)}$$

where n' = the porosity of the porous rock matrix.

The change in storage of fluids in the porous matrix is the result of compaction of the aquifer and expansion of the water because of decreasing pressure. Compaction of the reservoir results in changes of porosity and can be expressed as $(1-n')\rho g\alpha$, where α is the vertical compressibility of the aquifer. Water in storage released by a change in density equals $\rho g n' \beta$, where β is the compressibility of the fluid. Because the storage is a result of the change in density (ρ) and the change in the porosity (n') as the head (h) changes, then

$$\frac{\partial}{\partial x}\left[K_x \frac{\partial h}{\partial x}\right] + \frac{\partial}{\partial y}\left[K_y \frac{\partial h}{\partial y}\right] + \frac{\partial}{\partial z}\left[K_z \frac{\partial h}{\partial z}\right] = S_s \frac{\partial h}{\partial t} \qquad \text{(A-28)}$$

for transient flow in an anisotropic heterogeneous medium,

and

$$\frac{\partial^2 h}{\partial x^2} + \frac{\partial^2 h}{\partial y^2} + \frac{\partial^2 h}{\partial z^2} = \frac{S_s}{K} \frac{\partial h}{\partial t} \qquad \text{(A-29)}$$

for transient flow in an isotropic homogeneous medium.

GROUND-WATER VELOCITY AND TRAVEL TIME

Often, the velocity or rate of movement of ground water and travel times of particles through a porous medium needs to be known. Velocity units are m/s, which are the same units for hydraulic conductivity but, as mentioned above in Lohman's (1972) definition, hydraulic conductivity is the volume rate across a cross-sectional area (Equation A-3). The derivation of the ground-water velocity equation can be found in many hydrology texts (Lohman, 1972; Freeze and Cherry, 1979; Driscoll, 1987). Ground-water velocity is a function of effective porosity, hydraulic conductivity, and hydraulic gradient, or mathematically

$$v = - \frac{K \, dh/dl}{n} \quad . \tag{A-30}$$

The units are m/s.

Ground-water travel time (TT) is the distance (D) divided by velocity or, $\frac{D}{v}$.

Then

$$TT = \frac{D}{v} = \frac{nD}{K \, dh/dl} \quad . \tag{A-31}$$

The units for travel time are seconds.

APPENDIX A REFERENCES

Barr, G. E., W. B. Miller, and D. D. Gonzalez. 1983. *Interior Report on the Modeling of the Regional Hydraulics of the Rustler Formation.* SAND83-0391. Albuquerque, NM: Sandia National Laboratories.

Belitz, K., and J. D. Bredehoeft. 1988. "Hydrodynamics of Denver Basin: Explanation of Subnormal Fluid Pressures." *American Association of Petroleum Geologists Bulletin* vol. 72, no. 11: 1334-1359.

Crawley, M. E. 1988. *Second Data Release Report for the Pressure-Density Survey Program,* Carlsbad, NM: IT Corporation/Westinghouse WID.

Davies, P. B. 1987. "Modeling Areal, Variable Density, Ground-Water Flow Using Equivalent Freshwater Head--Analysis of Potentially Significant Errors," *Proceedings of NWWA Converence on Solving Ground Water Problems with Models, February 10-12, 1987. Denver, CO.*

Davies, P. B. 1989. *Variable-Density Ground-Water Flow and Paleohydrology in the Waste Isolation Pilot Plant (WIPP) Region Southeastern New Mexico.* U.S. Geological Survey Open-File Report 88-490. Albuquerque, NM: U.S. Geological Survey/Water Resources Division.

Driscoll, F. G. 1987. *Groundwater and Wells.* Minnesota: Johnson Division.

Ferris, J. G., D. B. Knowles, R. H. Brown, and R. W. Stallman. 1962. *Theory of Aquifer Tests*, U.S. Geological Survey Water-Supply Paper 1536-E. Washington, DC: U.S. Geological Survey.

Freeze, R. A., and J. A. Cherry. 1979. *Groundwater.* New Jersey: Prentice-Hall, Inc.

Haug, A., V. A. Kelly, A. M. LaVenue, and J. F. Pickens. 1987. *Modeling of Groundwater Flow in the Culebra Dolomite at the Waste Isolation Pilot Plant (WIPP) Site: Interim Report,* SAND86-7167. Albuquerque, NM: Sandia National Laboratories.

Holt, R. M., and D. W. Powers. 1988. *Facies Variability and Post-Depositional Alteration Within the Rustler Formation in the Vicinity of the Waste Isolation Pilot Plant, Southeastern New Mexico,* DOE/WIPP-88-004. Carlsbad, NM: U.S. Department of Energy.

Hubbert, M. K. 1940. "The Theory of Groundwater Motion." *Journal of Geology* vol. 48, no. 8: 785-944.

Hubbert, M. K. 1953. "Entrapment of Petroleum Under Hydrodynamic Conditions," *American Association of Petroleum Geologist Bulletin* vol. 37, no. 8: 1954-2026.

Hunter, R. L. 1985. *A Regional Water Balance for the Waste Isolation Pilot Plant (WIPP) Site and Surrounding Area.* SAND84-2233. Albuquerque, NM: Sandia National Laboratories.

Jorgenson, D. G., T. Gogel, and D. C. Signor. 1982. "Determination of Flow in Aquifers Containing Variable-Density Water." *Ground-Water Monitoring Review*, Spring 1982: 40-45.

Lambert, S. J., and J. W. Mercer. 1978. *Hydrologic Investigation of the Los Medaños Area, Southeastern New Mexico, 1977.* SAND77-1401. Albuquerque, NM: Sandia National Laboratories.

LaVenue, A. M., A. Haug, and V. A. Kelley. 1988. *Numerical Simulation of Groundwater Flow in the Culebra Dolomite at the Waste Isolation Pilot Plant (WIPP) Site; Second Interim Report*, SAND88-7002. Albuquerque, NM: Sandia National Laboratories.

Lohman, S. W. 1972. *Ground-water Hydraulics*, U.S. Geological Survey Professional Paper No. 708. Washington, DC: U.S. Geological Survey.

Lusczynski, N. J. 1961. "Head and Flow of Ground Water of Variable Density," *Journal of Geophysical Research* vol. 66, no. 12: 4247-4256.

Mercer, J. W., 1983. *Geohydrology of the Proposed Waste Isolation Pilot Plant Site, Los Medaños Area, Southeastern New Mexico.* U.S. Geological Survey Water Resources Investigations Report 83-4016. Albuquerque, NM: U.S. Geological Survey.

Pettijohn, F. J. 1957. *Sedimentary Rocks.* New York: Harper and Row.

APPENDIX B:
PRELIMINARY GEOHYDROLOGIC DATA BASES

APPENDIX B:
PRELIMINARY GEOHYDROLOGIC DATA BASES

Appendix B is a compilation of geohydrologic data from various sources. Table B-1 is a stratigraphic information table compiled from tables in reports by Mercer (1983) and Richey (1989). The well names are from usage in previous reports because it did not seem appropriate to introduce yet another well naming system. The "FFG" designates far-field geologic data (Davies, 1989), the H-series wells were drilled specifically for hydrologic testing, and the remaining well designations (WIPP-, P-, ERDA, AEC, and so on) were geologic test holes and domestic and stock wells converted for the purpose of hydrologic testing (Mercer, 1983). The Transverse Mercator coordinates for the FFG wells were calculated from the original township, range, and section subdivisions used for public lands. The coordinates for the WIPP wells are from Gonzalez (1989). Table B-1 is a listing of the elevations of the tops of the Rustler Formation Members; Table B-2 is a listing of thicknesses of the Rustler Formation members; Table B-3 is a listing of the thicknesses and tops of the Supra-Rustler units and alluvium; Table B-4 is a listing of the Universal Transverse Mercator and state coordinates of the WIPP test wells; Table B-5 is a listing of aquifer test results conducted in the Supra-Rustler units; and Table B-6 is a listing of alluvial water-level data in the Los Medaños region.

TABLE B-1. ELEVATIONS (m) OF THE TOPS OF THE RUSTLER FORMATION MEMBERS (THE FORTY-NINER (RTOP), MAGENTA DOLOMITE (MTOP), TAMARISK (TAMTOP), CULEBRA DOLOMITE (CTOP), AND THE UNNAMED LOWER MEMBER (ULMTOP)) AND THE SALADO FORMATION (SATOP). UTMX AND UTMY ARE THE UNIVERSAL TRANSVERSE MERCATOR COORDINATES CONVERTED TO THE STUDY AREA COORDINATES

WIPPN	UTMX	UTMY	RTOP	MTOP	TAMTOP	CTOP	ULMTOP	SATOP
FFG_002	37502	54163	686.1	667.5	660.5	624.8	618.1	578.8
FFG_004	32293	51289	739.1	717.8	710.8	666.6	659.9	627.9
FFG_005	37627	51249	693.8	674.9	667.9	628.5	622.1	581.9
FFG_006	37929	51350	688.9	670.0	661.4	616.6	--	608.1
FFG_007	38029	50445	678.2	655.9	649.8	602.0	593.7	559.0
FFG_009	38230	50545	678.1	657.4	650.1	604.1	596.5	575.1
FFG_011	37929	50947	684.6	664.2	657.1	609.9	603.5	570.3
FFG_012	37526	50947	687.0	667.8	659.6	613.9	606.2	572.1
FFG_013	35520	50926	696.8	674.8	667.8	646.2	634.3	582.5
FFG_014	31496	50467	741.9	721.1	713.5	667.8	658.9	623.0
FFG_016	37574	48521	666.9	644.9	637.6	587.9	579.4	545.0
FFG_017	38765	49460	669.6	648.3	640.7	594.9	587.3	555.3
FFG_018	40907	48068	672.4	652.3	645.9	598.6	590.7	558.4
FFG_019	37991	46541	666.3	644.7	637.6	588.6	580.3	548.9
FFG_020	31943	47231	740.7	718.4	712.3	662.0	655.3	622.4
FFG_023	43329	45379	678.5	654.1	647.4	596.2	587.7	553.5
FFG_024	45740	45020	662.0	638.8	632.1	579.1	571.8	539.2
FFG_025	38809	46144	674.1	652.2	646.1	598.5	591.8	560.4
FFG_026	38393	46138	670.8	649.5	643.4	592.5	585.5	552.6
FFG_027	38091	45837	664.2	643.1	636.4	585.5	578.5	545.6
FFG_028	-5821	-7130	629.8	612.7	607.5	578.6	572.5	549.6
FFG_029	-963	-7495	616.0	599.2	594.0	563.5	558.1	537.9
FFG_030	-107	-9595	616.6	598.3	592.9	563.0	557.2	532.8
FFG_031	-3725	-9127	609.6	590.1	584.0	554.4	547.4	522.4
FFG_032	50519	-10341	611.9	592.1	586.0	549.4	546.1	519.0
FFG_033	-5393	-11158	607.2	588.3	582.8	549.2	542.2	518.8
FFG_034	1917	-10182	601.3	582.4	577.9	548.6	542.5	517.8
FFG_035	-99	-11890	590.3	572.6	566.5	533.9	530.9	504.9
FFG_036	-6088	-13742	602.6	582.2	576.7	541.4	535.6	510.3
FFG_037	-1337	-13151	592.9	571.8	566.9	534.0	528.8	502.9
FFG_038	2291	-13460	579.4	559.6	554.1	523.6	517.5	491.9
FFG_039	26739	52517	798.6	778.8	772.1	731.9	725.5	694.4
FFG_040	30312	49655	740.7	720.9	713.6	655.4	645.3	624.9
FFG_041	27076	50009	801.0	780.6	773.6	733.7	726.4	691.9
FFG_042	25534	50298	805.5	785.4	777.8	740.6	730.0	695.2
FFG_043	25095	48381	810.0	788.1	782.0	735.7	728.7	697.0
FFG_044	28706	48421	762.3	741.0	733.6	689.1	680.9	645.6
FFG_047	-7895	49334	633.4	613.9	607.5	561.1	556.0	526.1
FFG_048	-14374	49657	653.2	630.9	623.3	580.3	573.3	527.6
FFG_049	-13971	47645	641.9	620.9	614.8	567.5	559.6	526.7

Source: Modified from Richey, 1989

TABLE B-1. ELEVATIONS (m) OF THE TOPS OF THE RUSTLER FORMATION MEMBERS (THE FORTY-NINER (RTOP), MAGENTA DOLOMITE (MTOP), TAMARISK (TAMTOP), CULEBRA DOLOMITE (CTOP), AND THE UNNAMED LOWER MEMBER (ULMTOP)) AND THE SALADO FORMATION (SATOP). UTMX AND UTMY ARE THE UNIVERSAL TRANSVERSE MERCATOR COORDINATES CONVERTED TO THE STUDY AREA COORDINATES (continued)

WIPPN	UTMX	UTMY	RTOP	MTOP	TAMTOP	CTOP	ULMTOP	SATOP
FFG_050	-8810	45985	648.0	627.6	621.5	582.5	574.9	537.4
FFG_051	-9413	45985	648.9	627.3	622.1	573.9	566.3	530.9
FFG_052	-9011	45985	651.6	630.3	624.2	595.2	589.8	565.7
FFG_053	-9828	45362	642.8	623.3	615.4	563.0	555.6	510.5
FFG_054	-4174	44502	641.9	620.6	613.3	562.7	556.6	518.8
FFG_055	-3772	44804	641.6	621.1	612.6	565.7	557.8	521.2
FFG_056	-9514	45281	644.3	621.8	615.4	564.5	556.9	520.9
FFG_057	-9929	45663	645.6	625.2	617.6	564.8	558.1	524.6
FFG_058	-3269	44804	641.0	623.6	615.1	569.3	560.8	526.7
FFG_059	-2662	44821	643.4	623.6	617.5	569.7	564.8	529.7
FFG_060	-8408	45583	645.5	627.3	618.1	569.3	563.2	532.8
FFG_061	-8609	45583	645.9	626.0	619.9	570.6	565.1	532.5
FFG_062	-3571	53782	574.3	553.2	547.1	513.9	507.2	479.2
FFG_063	-2657	52958	534.7	513.7	508.5	470.7	465.8	438.4
FFG_064	-5962	52123	559.7	538.6	531.9	497.5	488.9	461.2
FFG_065	2108	50589	542.9	520.6	515.4	471.8	464.5	449.6
FFG_066	-716	50556	496.8	473.9	469.4	434.3	429.1	401.7
FFG_067	-2724	49739	537.1	516.4	511.2	470.0	464.0	435.9
FFG_068	907	48959	496.5	481.9	475.8	430.1	424.0	396.5
FFG_069	-2273	46133	524.3	502.4	496.3	447.5	441.4	407.9
FFG_070	-5719	45226	553.8	532.2	526.1	484.6	479.1	442.0
FFG_071	22118	-5185	811.1	790.7	784.3	755.0	748.3	700.2
FFG_072	30590	-9047	739.7	721.1	715.0	681.2	674.2	645.8
FFG_073	30771	-8425	717.8	699.5	690.6	659.3	652.2	623.3
FFG_074	30791	-8644	723.7	703.3	698.4	666.4	660.3	630.7
FFG_075	27431	-8373	773.3	756.0	749.2	717.9	712.1	683.4
FFG_076	24604	-9233	836.4	818.1	810.5	777.6	771.5	741.9
FFG_078	22074	-10057	874.4	855.2	847.0	814.7	807.7	776.9
FFG_079	24722	-10555	848.0	829.7	823.6	787.0	780.9	750.4
FFG_080	24639	-12885	827.5	808.3	800.4	765.6	758.3	727.5
FFG_081	30808	-11058	746.8	727.9	720.9	683.1	674.9	644.4
FFG_082	27835	54871	779.1	759.3	753.2	711.1	705.3	673.0
FFG_083	32701	-7103	693.0	674.7	668.6	638.1	632.0	604.6
FFG_084	31512	-8745	721.1	702.2	694.6	661.4	654.7	626.0
FFG_085	31082	-8371	714.2	695.6	687.4	655.4	649.0	620.9
FFG_086	30992	-8644	722.6	705.6	697.3	665.0	657.4	630.3
FFG_087	34750	-9515	698.0	680.0	671.4	636.7	630.0	601.3
FFG_088	37260	-10295	694.4	674.6	667.2	626.1	622.7	595.3
FFG_089	39133	-10627	675.8	656.0	649.6	613.9	606.6	576.7
FFG_091	33573	-12463	720.0	700.4	692.8	652.3	643.8	614.2
FFG_092	32746	-11160	734.9	716.6	706.5	670.9	662.3	633.7
FFG_093	31941	-11160	737.3	718.1	710.2	673.6	668.1	637.7

Source: Modified from Richey, 1989

TABLE B-1. ELEVATIONS (m) OF THE TOPS OF THE RUSTLER FORMATION MEMBERS (THE FORTY-NINER (RTOP), MAGENTA DOLOMITE (MTOP), TAMARISK (TAMTOP), CULEBRA DOLOMITE (CTOP), AND THE UNNAMED LOWER MEMBER (ULMTOP)) AND THE SALADO FORMATION (SATOP). UTMX AND UTMY ARE THE UNIVERSAL TRANSVERSE MERCATOR COORDINATES CONVERTED TO THE STUDY AREA COORDINATES (continued)

WIPPN	UTMX	UTMY	RTOP	MTOP	TAMTOP	CTOP	ULMTOP	SATOP
FFG_094	31519	-11561	740.6	720.2	713.2	674.2	666.6	637.0
FFG_095	36308	-5035	706.5	688.8	681.5	651.6	645.2	618.7
FFG_096	42392	-4401	689.5	671.2	665.1	635.5	629.4	605.0
FFG_097	41600	-6514	671.2	651.7	645.0	614.8	608.4	580.6
FFG_098	48846	-6043	645.5	625.4	619.9	587.9	581.8	555.9
FFG_099	48789	-8352	641.6	620.9	615.4	582.5	574.6	550.2
FFG_100	45568	-8989	624.9	603.9	598.1	564.8	558.7	530.4
FFG_101	48928	-11674	593.1	574.9	569.4	533.7	527.3	500.2
FFG_102	44600	-12024	613.9	593.5	587.4	549.0	542.9	512.4
FFG_103	40778	-11780	674.6	655.4	652.0	609.3	-	601.7
FFG_104	-9004	54153	572.5	551.1	545.0	508.1	502.1	474.3
FFG_105	19397	36021	926.9	909.6	901.3	867.5	861.4	812.9
FFG_106	17901	36981	954.7	939.7	931.8	902.6	894.6	840.7
FFG_107	18103	35872	945.2	923.0	916.9	887.9	878.8	836.1
FFG_108	20857	35617	933.6	918.4	912.3	878.7	869.6	836.1
FFG_109	23093	35559	917.2	898.9	892.8	862.3	856.2	831.8
FFG_110	23907	34104	887.0	865.7	859.6	832.1	824.5	798.6
FFG_111	26480	35620	896.7	871.7	867.1	836.6	830.6	806.2
FFG_112	25583	34098	879.3	861.0	854.9	824.5	816.8	784.8
FFG_113	25590	35632	893.4	875.1	869.0	838.5	830.9	802.2
FFG_114	19729	32759	924.2	905.6	898.3	870.5	863.2	828.8
FFG_115	18514	32663	913.8	895.5	889.4	857.4	848.3	803.5
FFG_116	17173	33851	929.3	911.0	904.9	871.4	865.3	795.2
FFG_117	17403	32849	935.7	911.3	902.2	868.7	856.5	810.8
FFG_119	14326	30912	-	-	937.9	870.9	864.8	828.2
FFG_120	15021	32024	944.3	923.0	913.8	874.2	865.1	819.3
FFG_121	14405	31693	946.4	928.1	922.0	882.4	873.3	830.6
FFG_122	14436	31268	944.9	926.6	920.5	876.3	868.7	813.8
FFG_123	16710	31873	928.1	900.6	894.5	867.1	861.0	815.3
FFG_124	18523	31859	900.4	865.3	857.7	837.9	830.9	785.5
FFG_125	17902	31220	912.2	890.9	883.2	851.2	-	842.1
FFG_126	19612	30369	904.5	886.2	880.1	852.7	846.6	813.0
FFG_127	18497	29286	909.5	891.2	885.1	860.7	851.6	824.1
FFG_128	15885	27657	948.0	926.6	917.5	887.0	877.6	852.6
FFG_129	15085	28813	923.8	899.4	893.3	858.3	852.2	815.6
FFG_130	14683	28007	954.0	929.6	920.5	897.6	888.5	854.9
FFG_132	16750	26831	956.5	935.1	929.0	898.6	890.9	852.8
FFG_133	16733	26029	959.5	938.1	932.0	901.6	895.5	837.6
FFG_134	15934	26170	963.8	944.0	935.5	904.4	896.8	861.7
FFG_135	17482	26741	937.3	917.5	910.8	880.9	875.1	844.0
FFG_136	19550	25173	934.3	919.1	911.5	882.5	876.4	844.4

Source: Modified from Richey, 1989

TABLE B-1. ELEVATIONS (m) OF THE TOPS OF THE RUSTLER FORMATION MEMBERS (THE FORTY-NINER (RTOP), MAGENTA DOLOMITE (MTOP), TAMARISK (TAMTOP), CULEBRA DOLOMITE (CTOP), AND THE UNNAMED LOWER MEMBER (ULMTOP)) AND THE SALADO FORMATION (SATOP). UTMX AND UTMY ARE THE UNIVERSAL TRANSVERSE MERCATOR COORDINATES CONVERTED TO THE STUDY AREA COORDINATES (continued)

WIPPN	UTMX	UTMY	RTOP	MTOP	TAMTOP	CTOP	ULMTOP	SATOP
FFG_137	20226	24632	946.8	927.9	919.3	892.8	884.6	853.2
FFG_138	21098	32834	897.4	880.6	874.5	844.1	834.9	798.3
FFG_139	20936	33485	907.7	889.7	882.4	855.6	847.9	810.1
FFG_140	23919	30886	849.1	829.2	823.1	792.7	785.0	750.0
FFG_141	22391	30877	873.1	854.2	845.7	820.1	812.5	782.9
FFG_142	25559	32430	849.3	829.4	821.8	795.9	788.3	757.8
FFG_143	26277	25049	855.8	839.3	831.7	804.0	-	797.3
FFG_144	10150	23591	-	-	903.5	894.3	883.7	825.1
FFG_145	9591	22895	-	-	905.3	893.1	887.0	830.6
FFG_146	10634	23949	-	-	912.9	906.8	897.7	826.0
FFG_147	5770	23951	-	897.9	893.7	882.7	875.4	816.3
FFG_148	10840	21956	-	-	907.7	900.1	894.9	832.1
FFG_149	10978	20481	-	-	912.2	910.7	903.1	842.1
FFG_152	3606	19654	-	-	-	-	893.1	836.7
FFG_155	6868	16427	-	914.1	905.6	901.3	894.0	830.9
FFG_156	5963	16646	-	-	-	906.5	895.5	837.6
FFG_157	9483	15216	-	915.3	907.1	904.1	-	898.6
FFG_158	10781	15199	-	937.2	931.1	928.1	918.0	856.8
FFG_159	19810	23864	956.2	936.7	928.8	898.6	891.6	859.6
FFG_160	20355	23433	950.1	929.7	924.2	895.2	886.1	855.6
FFG_161	17947	22831	957.4	936.1	930.0	901.0	894.9	856.8
FFG_162	17613	24368	955.9	933.3	925.4	891.9	884.6	857.7
FFG_163	18398	23613	955.3	933.9	927.8	897.4	888.2	856.2
FFG_164	12812	20361	-	-	955.9	937.6	928.5	854.7
FFG_165	12098	18833	-	-	935.7	912.8	902.2	838.8
FFG_166	19453	18968	954.3	936.0	928.4	900.0	891.8	858.3
FFG_167	19283	16609	936.7	922.1	914.4	887.0	877.9	836.7
FFG_168	14473	16344	967.5	944.6	933.9	906.5	898.9	843.1
FFG_169	14305	17828	980.2	957.3	949.1	919.2	909.2	861.3
FFG_170	11808	17823	933.6	922.9	916.8	903.7	893.0	839.1
FFG_171	12230	15481	-	931.5	924.2	922.1	909.3	848.0
FFG_172	13637	15861	-	937.2	933.0	915.3	906.1	851.9
FFG_173	20231	15700	934.8	914.1	906.5	876.9	867.8	831.5
FFG_177	1622	9585	-	-	-	889.1	880.0	812.6
FFG_179	3355	7103	-	-	886.6	875.1	816.8	
FFG_180	17759	13190	943.9	920.5	915.0	883.0	874.7	825.1
FFG_181	14299	14348	-	951.3	946.7	930.5	922.9	869.0
FFG_182	11813	14044	856.5	847.6	842.4	812.6	804.3	757.1
FFG_183	15448	12501	-	-	939.1	904.4	893.4	837.3
FFG_184	17835	11620	-	927.8	924.8	891.2	883.6	851.6
FFG_185	16137	11446	-	934.5	929.9	899.5	891.8	840.0

Source: Modified from Richey, 1989

TABLE B-1. ELEVATIONS (m) OF THE TOPS OF THE RUSTLER FORMATION MEMBERS (THE FORTY-NINER (RTOP), MAGENTA DOLOMITE (MTOP), TAMARISK (TAMTOP), CULEBRA DOLOMITE (CTOP), AND THE UNNAMED LOWER MEMBER (ULMTOP)) AND THE SALADO FORMATION (SATOP). UTMX AND UTMY ARE THE UNIVERSAL TRANSVERSE MERCATOR COORDINATES CONVERTED TO THE STUDY AREA COORDINATES (continued)

WIPPN	UTMX	UTMY	RTOP	MTOP	TAMTOP	CTOP	ULMTOP	SATOP
FFG_186	15287	11461	-	863.8	857.7	827.9	819.3	766.3
FFG_188	13219	9803	-	874.1	869.0	845.8	837.6	781.2
FFG_189	18676	9442	922.7	902.2	894.3	867.8	859.6	805.0
FFG_190	17956	8509	901.6	882.4	874.7	843.6	835.1	793.4
FFG_191	19608	6914	901.3	878.1	870.5	845.5	839.4	780.0
FFG_192	17672	8205	834.5	815.3	806.5	774.5	764.4	708.0
FFG_194	27989	14185	839.7	822.1	815.6	788.5	780.6	738.8
FFG_195	27212	13378	855.3	834.0	828.8	803.5	792.8	753.5
FFG_196	25587	14575	897.6	876.9	869.9	837.0	827.5	792.5
FFG_197	24883	14246	899.5	878.1	870.8	841.0	831.2	790.1
FFG_198	24078	14651	898.2	877.5	871.4	840.9	831.8	783.9
FFG_199	21899	14403	888.8	867.5	859.9	827.0	818.7	780.6
FFG_200	21544	14177	902.5	880.9	873.0	838.2	828.1	785.2
FFG_201	22425	11714	894.6	873.2	865.6	838.2	830.0	778.7
FFG_202	28963	12416	834.2	816.5	808.3	773.8	763.2	723.6
FFG_203	28414	12986	841.3	823.0	815.7	776.0	767.5	727.6
FFG_204	30061	10597	864.8	846.5	837.9	813.5	805.3	767.2
FFG_205	24005	11329	880.6	860.5	853.2	825.1	816.6	768.5
FFG_206	22442	10103	895.8	874.5	867.4	837.0	828.1	779.4
FFG_207	24047	9720	892.2	872.3	865.0	833.6	826.0	775.7
FFG_208	23263	8488	902.8	882.1	874.2	843.1	834.5	780.3
FFG_209	25651	9743	-	873.2	866.2	838.2	829.7	787.3
FFG_210	24470	8508	885.8	865.9	858.9	827.5	818.7	766.0
FFG_212	30082	8588	870.5	852.8	845.2	817.5	809.0	768.4
FFG_213	25186	6015	903.5	874.5	868.4	837.9	828.8	795.3
FFG_214	27709	5757	877.8	854.9	848.2	818.4	808.6	757.7
FFG_215	20847	4913	852.5	831.2	823.6	793.1	784.9	734.6
FFG_216	15124	4427	737.0	716.8	710.4	688.8	682.7	520.6
FFG_217	27965	5123	873.6	851.4	843.7	814.8	805.6	756.3
FFG_218	28506	4558	863.5	844.0	835.8	803.5	794.3	744.0
FFG_219	26920	2942	910.4	889.7	879.9	848.8	840.3	783.3
FFG_220	29328	3347	859.9	836.7	832.2	798.6	789.5	742.2
FFG_221	26299	1676	814.4	796.2	787.0	756.5	744.3	684.9
FFG_222	24519	-1534	770.6	749.8	741.6	713.3	705.0	604.5
FFG_224	39528	44633	677.0	655.7	648.1	597.8	590.1	558.1
FFG_225	39347	43742	683.7	662.4	656.3	603.5	598.0	566.3
FFG_226	38979	42513	683.2	661.0	654.0	601.8	594.8	561.9
FFG_228	36940	43689	673.7	651.7	643.2	588.3	580.7	549.3
FFG_229	36165	42487	701.6	679.4	672.0	614.7	607.1	572.1
FFG_230	35757	43265	688.6	665.1	658.1	601.1	595.0	558.4
FFG_231	34520	44066	704.0	681.8	674.2	619.9	613.8	578.2

Source: Modified from Richey, 1989

TABLE B-1. ELEVATIONS (m) OF THE TOPS OF THE RUSTLER FORMATION MEMBERS (THE FORTY-NINER (RTOP), MAGENTA DOLOMITE (MTOP), TAMARISK (TAMTOP), CULEBRA DOLOMITE (CTOP), AND THE UNNAMED LOWER MEMBER (ULMTOP)) AND THE SALADO FORMATION (SATOP). UTMX AND UTMY ARE THE UNIVERSAL TRANSVERSE MERCATOR COORDINATES CONVERTED TO THE STUDY AREA COORDINATES (continued)

WIPPN	UTMX	UTMY	RTOP	MTOP	TAMTOP	CTOP	ULMTOP	SATOP
FFG_232	34151	43242	717.8	695.6	688.2	631.5	625.8	586.1
FFG_233	34001	44133	709.3	685.8	678.8	624.0	617.9	581.9
FFG_234	32539	43630	745.8	722.7	715.0	660.2	653.5	616.3
FFG_235	33346	43242	722.4	698.6	691.3	635.5	628.5	595.9
FFG_236	30897	43597	768.4	746.4	738.5	682.7	677.2	641.9
FFG_237	34550	41656	735.3	712.1	704.8	646.2	634.4	600.8
FFG_238	36165	41682	716.6	691.0	685.5	628.5	621.5	584.3
FFG_239	38190	40910	703.1	679.1	673.3	620.5	613.5	570.5
FFG_240	37772	41708	695.2	671.2	664.5	609.9	602.6	568.8
FFG_241	38593	41312	688.9	666.3	659.0	605.1	598.1	562.7
FFG_242	33781	38816	799.8	783.1	776.7	732.2	724.2	681.3
FFG_243	38229	36885	763.8	743.1	735.5	668.4	659.3	615.1
FFG_244	37440	35249	798.4	780.8	773.1	721.3	715.2	689.3
FFG_245	44564	41777	597.1	573.0	566.9	510.8	503.5	470.6
FFG_246	46571	42198	601.7	578.5	573.0	516.0	508.1	473.1
FFG_247	49056	39436	589.1	563.8	558.0	501.3	493.7	460.1
FFG_248	49025	39838	594.7	571.2	566.0	506.6	498.3	464.5
FFG_249	45809	39796	593.7	569.7	564.2	505.3	498.3	464.2
FFG_250	40978	39336	674.1	651.5	644.5	587.5	580.5	545.5
FFG_251	49456	37819	568.7	544.9	538.5	477.3	470.0	432.2
FFG_252	42249	34911	708.6	683.9	677.8	619.6	612.6	567.5
FFG_253	44644	35354	660.5	639.2	632.5	566.7	561.5	521.9
FFG_254	45047	35354	651.0	630.0	623.9	562.0	554.7	517.8
FFG_255	46656	35775	609.9	587.7	580.1	514.5	506.3	467.3
FFG_256	705	42669	557.8	535.2	529.8	477.9	470.9	438.9
FFG_257	-4959	42605	600.4	579.4	573.6	523.3	517.2	484.0
FFG_258	-485	40243	615.0	594.9	587.6	546.2	536.4	497.7
FFG_259	-2193	39019	584.9	561.1	553.5	503.2	494.9	456.8
FFG_260	1834	38142	621.8	603.8	597.4	556.3	548.9	515.1
FFG_261	-962	37517	610.2	592.8	586.4	542.2	537.3	502.6
FFG_263	-7325	34126	553.4	526.6	521.1	456.5	448.5	406.8
FFG_264	34812	21540	777.6	760.5	753.2	703.8	696.2	653.5
FFG_265	36429	20766	775.4	755.9	749.8	686.1	677.3	634.6
FFG_266	40098	18407	758.9	736.7	730.9	665.4	656.8	609.6
FFG_267	42915	16425	736.4	713.5	708.3	641.3	632.7	582.7
FFG_268	46953	15266	716.0	690.7	684.6	613.6	606.3	563.3
FFG_269	-6015	16346	729.2	702.4	696.9	627.7	617.6	568.3
FFG_270	-1173	16377	791.8	774.5	769.3	730.3	721.1	689.4
FFG_271	461	16400	833.9	815.0	808.9	773.9	767.8	733.3
FFG_272	31537	25904	846.6	822.5	816.4	751.8	743.9	697.2
FFG_273	31985	22735	816.9	797.4	790.1	753.2	745.3	701.7

Source: Modified from Richey, 1989

TABLE B-1. ELEVATIONS (m) OF THE TOPS OF THE RUSTLER FORMATION MEMBERS (THE FORTY-NINER (RTOP), MAGENTA DOLOMITE (MTOP), TAMARISK (TAMTOP), CULEBRA DOLOMITE (CTOP), AND THE UNNAMED LOWER MEMBER (ULMTOP)) AND THE SALADO FORMATION (SATOP). UTMX AND UTMY ARE THE UNIVERSAL TRANSVERSE MERCATOR COORDINATES CONVERTED TO THE STUDY AREA COORDINATES (continued)

WIPPN	UTMX	UTMY	RTOP	MTOP	TAMTOP	CTOP	ULMTOP	SATOP
FFG_274	37533	29620	851.0	834.2	827.2	793.1	785.8	747.4
FFG_275	36326	30022	858.6	840.3	834.3	800.7	794.6	767.2
FFG_276	33107	29959	861.6	845.2	837.6	802.8	795.8	766.2
FFG_277	31898	29538	853.5	836.7	829.1	795.5	789.1	753.5
FFG_278	31917	27920	868.4	845.8	838.5	776.6	765.4	722.4
FFG_279	33107	28752	860.1	840.9	833.3	776.9	767.7	735.7
FFG_280	35516	28785	858.6	837.3	830.9	788.8	780.0	738.2
FFG_281	39149	27635	835.8	814.2	807.4	762.6	754.4	709.3
FFG_283	49093	34201	584.6	563.9	558.1	496.2	489.2	450.5
FFG_284	43531	33418	730.3	712.0	705.9	648.0	641.3	596.2
FFG_285	43187	32915	760.2	741.3	734.9	669.6	660.5	616.0
FFG_286	40316	31274	837.5	820.2	814.1	773.8	766.2	728.7
FFG_287	41086	31697	812.0	793.1	786.1	738.2	733.3	693.1
FFG_288	43489	32512	765.7	744.9	738.8	668.7	662.6	616.9
FFG_289	45939	30146	736.3	719.9	713.8	680.6	673.9	639.1
FFG_290	41920	28881	825.7	806.5	799.5	770.9	760.8	733.4
FFG_291	41987	24854	766.2	742.5	736.7	668.7	660.8	615.1
FFG_292	44784	26101	774.2	758.4	752.3	724.8	717.8	686.7
FFG_293	46012	24915	766.0	750.7	744.6	718.1	710.5	672.4
FFG_294	1582	32998	595.3	572.8	567.0	504.5	497.5	458.2
FFG_295	277	32570	582.8	560.2	554.7	489.5	480.0	438.9
FFG_297	-6017	33221	567.5	539.2	532.5	469.1	455.4	420.3
FFG_298	49946	31387	569.2	552.4	546.7	528.1	520.4	490.0
FFG_299	-7383	30874	594.4	569.1	564.2	497.8	489.8	441.4
FFG_300	-384	29019	543.7	520.6	515.4	480.6	473.0	416.9
FFG_301	1199	26523	514.8	491.1	485.6	435.9	430.4	359.4
FFG_302	11152	32606	542.5	518.5	514.2	443.5	436.8	420.3
FFG_303	4762	33812	535.9	511.2	505.1	449.0	442.0	404.8
FFG_304	3597	31383	540.4	517.5	512.9	445.9	438.9	399.3
FFG_305	6692	30580	534.6	509.3	503.2	443.2	434.6	399.6
FFG_306	3978	30176	492.2	469.3	465.1	413.0	405.3	361.4
FFG_307	2792	30578	517.9	493.5	488.0	432.2	424.3	383.8
FFG_308	5978	28562	491.3	465.7	460.5	376.1	367.8	323.0
FFG_309	6793	27749	535.2	508.1	503.2	434.6	427.9	388.6
FFG_310	8009	26963	564.2	539.2	534.6	475.2	469.1	430.0
FFG_311	6401	26537	498.7	486.5	481.0	428.6	420.3	387.4
FFG_312	6390	24535	537.4	510.6	504.5	429.8	424.0	384.1
FFG_313	31828	33560	934.3	915.1	908.1	870.3	862.0	832.2
FFG_314	39941	29665	862.3	843.1	836.1	788.9	781.6	734.9
FFG_315	36793	23977	782.9	764.3	758.5	701.5	694.2	650.9
FFG_316	38010	22398	771.4	747.9	742.1	678.4	670.2	624.2

Source: Modified from Richey, 1989

TABLE B-1. ELEVATIONS (m) OF THE TOPS OF THE RUSTLER FORMATION MEMBERS (THE FORTY-NINER (RTOP), MAGENTA DOLOMITE (MTOP), TAMARISK (TAMTOP), CULEBRA DOLOMITE (CTOP), AND THE UNNAMED LOWER MEMBER (ULMTOP)) AND THE SALADO FORMATION (SATOP). UTMX AND UTMY ARE THE UNIVERSAL TRANSVERSE MERCATOR COORDINATES CONVERTED TO THE STUDY AREA COORDINATES (continued)

WIPPN	UTMX	UTMY	RTOP	MTOP	TAMTOP	CTOP	ULMTOP	SATOP
FFG_317	32005	20683	792.2	777.0	772.7	732.4	725.1	693.1
FFG_318	33248	18296	758.0	742.2	734.6	710.2	702.6	666.0
FFG_319	34432	19498	769.3	751.6	745.8	704.6	696.4	662.0
FFG_320	39378	17865	762.3	741.3	735.5	669.4	662.0	616.0
FFG_321	38795	16856	760.5	737.9	732.1	668.4	661.7	612.9
FFG_322	38493	16655	755.1	733.2	727.4	669.8	662.2	616.8
FFG_323	37691	16728	751.1	729.5	723.4	675.2	667.9	626.8
FFG_324	34455	17893	761.7	745.3	738.0	699.5	692.2	653.2
FFG_325	30817	15031	819.6	800.4	793.4	762.3	753.2	713.5
FFG_326	35279	15903	754.4	736.1	729.1	706.5	698.0	657.5
FFG_327	37008	15524	748.3	729.1	723.6	689.8	681.9	645.3
FFG_328	37990	16052	757.0	734.5	728.7	673.8	664.7	620.5
FFG_329	38896	15951	755.6	733.9	728.4	669.0	661.4	613.2
FFG_330	39735	15597	754.9	733.2	728.0	669.5	661.0	611.6
FFG_331	44828	23285	753.5	728.5	722.7	652.9	646.8	602.6
FFG_332	41714	23147	744.0	719.3	713.8	639.5	632.8	587.0
FFG_333	40454	21619	746.3	722.8	717.3	650.6	643.0	598.8
FFG_334	42062	20025	743.1	718.1	712.6	644.9	637.0	589.1
FFG_335	40475	20013	757.1	733.7	724.8	663.3	655.0	607.8
FFG_336	40882	18809	754.4	730.6	725.1	658.1	650.4	603.2
FFG_337	43293	18437	738.5	713.8	708.0	641.9	634.3	584.6
FFG_338	41706	16413	744.8	720.7	715.2	646.9	639.0	589.6
FFG_339	48134	16089	711.1	684.8	680.3	611.7	604.1	553.8
FFG_340	49768	15705	721.4	694.0	688.8	617.8	609.3	559.9
FFG_342	-5677	22815	747.6	726.9	720.2	682.7	676.3	651.6
FFG_344	-302	19563	713.4	692.7	685.1	659.1	650.9	622.6
FFG_345	50509	20530	775.5	752.1	746.6	678.6	671.3	628.6
FFG_347	-805	18859	766.0	744.7	736.7	699.5	692.8	655.3
FFG_348	-2802	17987	790.9	773.3	768.1	738.5	733.0	686.1
FFG_349	2058	16399	764.2	742.2	738.0	714.5	709.3	678.8
FFG_350	-2802	17584	808.9	789.1	783.0	745.2	739.7	712.3
FFG_351	-7522	13007	732.2	705.6	701.1	629.4	621.2	571.5
FFG_352	-7622	13108	731.5	705.6	699.5	629.4	621.8	573.1
FFG_353	-6114	13510	751.7	726.7	721.2	651.1	644.1	598.4
FFG_354	461	15897	817.8	800.8	795.3	762.0	756.0	722.4
FFG_361	1678	53799	1011.0	986.9	982.6	955.2	948.5	905.8
FFG_362	-1148	53387	-	-	956.4	919.3	911.0	841.5
FFG_363	-3571	53785	-	-	972.9	947.0	937.9	881.5
FFG_364	-5851	50825	-	-	942.7	918.3	-	909.8
FFG_366	-1231	52063	960.4	940.6	933.9	911.6	904.0	863.8
FFG_367	-213	51462	975.9	954.6	948.5	931.7	922.6	876.9

Source: Modified from Richey, 1989

TABLE B-1. ELEVATIONS (m) OF THE TOPS OF THE RUSTLER FORMATION MEMBERS (THE FORTY-NINER (RTOP), MAGENTA DOLOMITE (MTOP), TAMARISK (TAMTOP), CULEBRA DOLOMITE (CTOP), AND THE UNNAMED LOWER MEMBER (ULMTOP)) AND THE SALADO FORMATION (SATOP). UTMX AND UTMY ARE THE UNIVERSAL TRANSVERSE MERCATOR COORDINATES CONVERTED TO THE STUDY AREA COORDINATES (continued)

WIPPN	UTMX	UTMY	RTOP	MTOP	TAMTOP	CTOP	ULMTOP	SATOP
FFG_370	1298	50561	-	-	1012.9	968.7	962.6	919.3
FFG_371	1605	50589	1012.9	997.7	994.6	965.7	958.6	919.9
FFG_372	1	49865	-	-	1006.4	949.1	-	941.5
FFG_373	-3537	50536	-	-	945.0	909.0	-	902.0
FFG_374	-4337	49324	946.4	940.9	929.7	908.3	902.2	855.0
FFG_376	826	47453	-	-	984.8	947.6	939.7	896.4
FFG_381	9443	45009	-	-	1021.4	914.7	908.6	875.1
FFG_383	11348	52679	955.3	938.8	931.2	908.3	902.2	867.2
FFG_384	4484	53411	976.0	945.8	937.9	921.1	-	912.3
FFG_385	8154	48207	-	-	922.0	915.9	906.8	856.5
FFG_387	6183	46094	966.6	940.3	934.6	911.1	901.6	862.0
FFG_388	6135	46982	959.2	936.7	929.4	900.7	-	893.7
FFG_389	3724	45365	-	-	976.6	924.8	-	917.5
FFG_390	5479	45792	974.4	954.0	945.5	919.6	913.5	863.5
FFG_391	5479	45390	973.5	951.5	944.5	919.2	913.1	868.3
FFG_392	6883	45495	967.8	948.6	941.9	910.5	904.4	863.2
FFG_393	16568	52748	835.6	816.1	810.6	785.6	781.0	752.7
FFG_394	13348	52709	925.9	908.6	903.1	882.4	877.2	846.7
FFG_395	13369	51394	918.4	901.6	895.8	874.5	867.5	842.2
FFG_396	13514	46161	901.6	884.3	877.2	853.8	847.1	787.3
FFG_398	-1712	43049	825.7	805.6	798.5	771.7	-	767.2
FFG_399	-2618	43150	-	-	838.5	785.2	-	780.6
FFG_401	48181	42220	-	-	874.8	839.7	-	833.6
FFG_402	1118	41052	1002.5	979.4	972.0	947.1	-	936.7
FFG_403	-3305	39003	963.0	941.4	935.3	914.6	903.3	846.9
FFG_404	-5741	37784	925.7	901.6	897.4	873.3	-	867.2
FFG_407	-5741	36577	958.3	940.0	932.4	908.0	-	898.9
FFG_408	-7256	36083	-	913.2	908.6	907.1	901.0	827.8
FFG_409	50131	38732	-	-	970.5	943.1	-	932.4
FFG_411	-4901	34130	-	-	-	887.3	873.9	789.1
FFG_413	-1259	34997	-	-	-	915.1	906.2	835.2
FFG_418	6633	43773	-	-	983.3	930.3	-	923.0
FFG_419	5047	43411	997.0	976.6	969.0	942.8	-	936.7
FFG_420	4933	44111	992.7	973.5	964.3	936.9	-	927.8
FFG_421	3827	44175	983.6	960.1	955.0	923.3	913.8	879.4
FFG_422	4229	43763	976.6	958.3	946.1	923.2	-	915.6
FFG_426	2669	37354	-	-	962.0	926.9	919.3	856.5
FFG_432	17672	34666	931.8	924.1	918.0	884.5	876.9	837.3
FFG_433	-1160	33884	-	-	920.5	897.6	892.4	816.8
FFG_438	28900	32673	892.6	874.6	866.7	835.6	829.8	797.5
FFG_445	797	26523	-	-	-	920.2	911.6	827.2

Source: Modified from Richey, 1989

TABLE B-1. ELEVATIONS (m) OF THE TOPS OF THE RUSTLER FORMATION MEMBERS (THE FORTY-NINER (RTOP), MAGENTA DOLOMITE (MTOP), TAMARISK (TAMTOP), CULEBRA DOLOMITE (CTOP), AND THE UNNAMED LOWER MEMBER (ULMTOP)) AND THE SALADO FORMATION (SATOP). UTMX AND UTMY ARE THE UNIVERSAL TRANSVERSE MERCATOR COORDINATES CONVERTED TO THE STUDY AREA COORDINATES (continued)

WIPPN	UTMX	UTMY	RTOP	MTOP	TAMTOP	CTOP	ULMTOP	SATOP
FFG_453	28686	24250	-	-	862.2	782.3	772.9	726.5
FFG_455	28829	21443	837.6	817.5	810.4	770.2	761.4	723.9
FFG_456	27948	20225	829.0	812.5	805.2	776.6	769.9	730.9
FFG_457	24727	20188	885.1	868.1	861.3	831.2	822.6	784.5
FFG_458	25545	18193	888.2	872.6	862.3	833.3	825.1	785.5
FFG_459	29566	17415	816.6	799.5	791.9	761.4	752.3	717.2
FFG_462	25970	16984	884.1	865.8	857.5	828.6	820.7	781.3
FFG_463	22746	16141	913.5	893.1	886.4	854.4	843.7	811.4
FFG_464	25165	16179	900.4	880.0	872.3	843.4	833.6	787.6
FFG_465	24361	15762	902.8	883.0	875.3	844.9	835.1	783.9
FFG_467	4687	21983	506.2	488.2	483.3	430.9	423.0	380.3
FFG_468	4016	21669	493.5	465.5	460.0	377.7	373.1	322.2
FFG_470	7224	20903	509.6	484.9	480.1	408.1	402.6	360.0
FFG_471	2800	20865	525.8	500.5	495.0	426.1	420.6	372.4
FFG_472	3622	17618	564.2	538.3	532.8	501.7	495.6	439.3
FFG_473	11329	16072	491.6	468.2	463.6	390.4	383.7	339.5
FFG_474	38948	13946	750.7	729.4	723.3	677.5	671.7	634.9
FFG_475	38515	14343	749.7	728.9	723.8	686.3	677.7	637.8
FFG_476	31680	14648	821.8	805.0	797.4	760.2	751.7	711.4
FFG_477	36546	12317	774.5	760.8	751.7	726.7	718.8	679.7
FFG_478	38161	12332	755.6	739.7	733.6	702.6	694.0	655.3
FFG_479	37739	12717	752.5	736.4	730.0	706.8	698.9	661.1
FFG_480	38948	12739	754.4	732.5	726.4	688.0	681.3	641.6
FFG_481	40192	10360	731.8	715.7	709.0	681.6	674.5	635.2
FFG_482	37753	11512	761.4	744.3	738.6	711.7	703.8	665.4
FFG_483	36164	10280	785.1	767.8	761.4	741.2	732.7	690.9
FFG_484	36872	9504	772.2	753.6	748.1	725.9	720.7	672.2
FFG_485	36594	9100	779.4	762.6	756.8	730.3	723.0	682.8
FFG_486	37375	9504	766.3	749.5	743.4	716.0	708.4	668.7
FFG_487	37274	9605	763.9	746.5	740.4	715.4	706.9	669.4
FFG_488	38889	10039	748.0	731.2	726.6	698.3	692.5	648.9
FFG_489	39412	7924	764.6	748.4	742.3	717.3	708.8	663.1
FFG_490	32561	7809	855.6	838.8	832.7	806.8	801.3	765.7
FFG_491	31756	7809	855.9	836.4	830.3	799.8	793.1	752.6
FFG_492	35378	5451	817.5	798.6	792.5	765.6	757.1	720.5
FFG_493	36183	5853	803.6	785.3	779.8	752.4	743.2	709.7
FFG_494	36183	5451	811.3	792.1	786.0	754.0	747.0	713.2
FFG_495	37397	5479	799.4	783.0	777.2	749.8	743.1	696.4
FFG_496	49366	14498	715.4	688.6	684.3	616.0	604.2	555.4
FFG_497	41765	11991	721.5	701.1	695.6	649.9	642.2	601.7
FFG_498	42154	13191	737.0	714.1	708.4	645.6	637.6	589.2

Source: Modified from Richey, 1989

TABLE B-1. ELEVATIONS (m) OF THE TOPS OF THE RUSTLER FORMATION MEMBERS (THE FORTY-NINER (RTOP), MAGENTA DOLOMITE (MTOP), TAMARISK (TAMTOP), CULEBRA DOLOMITE (CTOP), AND THE UNNAMED LOWER MEMBER (ULMTOP)) AND THE SALADO FORMATION (SATOP). UTMX AND UTMY ARE THE UNIVERSAL TRANSVERSE MERCATOR COORDINATES CONVERTED TO THE STUDY AREA COORDINATES (continued)

WIPPN	UTMX	UTMY	RTOP	MTOP	TAMTOP	CTOP	ULMTOP	SATOP
FFG_499	49807	11276	715.4	689.5	684.6	612.4	603.2	549.9
FFG_500	42973	11607	726.0	704.7	698.6	643.4	635.2	582.8
FFG_501	42616	8767	731.5	710.1	704.0	673.0	665.6	625.4
FFG_502	45411	9612	724.8	702.9	697.4	638.2	630.9	567.2
FFG_503	45857	7598	705.4	684.0	679.4	624.0	616.3	573.7
FFG_504	43042	7176	723.6	706.0	699.9	674.3	667.6	618.8
FFG_505	40510	8446	754.7	739.5	734.3	702.3	696.2	650.5
FFG_506	41847	5952	749.2	730.9	725.4	700.1	690.6	649.5
FFG_507	49878	6851	712.8	692.4	688.4	607.0	599.4	549.1
FFG_508	476	13568	763.3	744.1	738.6	688.9	680.7	628.8
FFG_509	-4001	13944	767.8	745.2	739.1	668.1	662.3	616.3
FFG_510	-5504	14336	767.3	744.8	738.7	670.1	658.8	615.2
FFG_511	-7622	12705	728.2	702.3	696.5	629.1	619.4	570.6
FFG_512	-731	12361	748.3	720.8	714.8	643.7	634.6	576.7
FFG_513	476	12763	763.0	740.7	734.9	667.0	659.3	606.0
FFG_514	1723	9933	754.7	731.2	726.0	645.9	637.0	577.3
FFG_515	-3975	10317	722.6	697.9	692.8	617.2	610.8	556.2
FFG_516	-2368	9522	715.9	691.3	685.5	612.6	601.6	545.9
FFG_517	3696	12373	809.3	788.8	783.7	755.3	750.7	732.5
FFG_518	2511	11960	797.9	778.1	772.0	742.2	735.8	720.2
FFG_519	3718	11960	765.7	743.7	740.1	704.1	696.5	659.9
FFG_520	8121	12816	653.0	635.4	631.7	590.9	585.4	542.7
FFG_521	8422	12414	673.3	655.0	650.4	633.1	628.2	604.7
FFG_522	11764	12433	531.7	504.3	499.7	434.2	427.5	382.4
FFG_523	11011	8790	541.3	516.9	509.3	449.3	443.2	388.9
FFG_524	5723	10773	693.1	675.1	670.8	616.0	607.4	561.7
FFG_525	8951	11201	543.3	513.7	508.5	443.9	436.6	388.4
FFG_526	3368	-5441	-	-	973.5	950.7	943.1	911.1
FFG_527	10815	-9407	958.9	938.7	933.6	894.2	888.1	871.1
FFG_528	9764	-8766	951.6	934.2	926.0	896.1	891.5	864.1
FFG_530	3921	-11075	-	-	1000.3	965.9	957.7	930.2
FFG_531	9573	-10399	-	-	919.3	894.9	888.8	855.2
FFG_532	9985	-10723	-	915.6	907.1	879.7	873.0	838.5
FFG_534	10730	-10720	-	-	946.4	892.8	-	883.3
FFG_535	10076	-10399	939.7	919.9	912.8	882.1	875.7	850.4
FFG_536	10410	-11040	-	-	928.4	892.5	884.5	853.5
FFG_537	9985	-11025	-	-	904.6	879.9	872.6	840.6
FFG_543	5041	-12533	-	-	970.9	932.2	-	926.7
FFG_548	11426	54582	930.6	914.1	907.7	883.3	-	877.2
FFG_552	6649	251	-	-	-	732.7	-	722.0
FFG_562	24588	-7613	670.6	652.3	645.3	621.8	-	614.5

Source: Modified from Richey, 1989

TABLE B-1. ELEVATIONS (m) OF THE TOPS OF THE RUSTLER FORMATION MEMBERS (THE FORTY-NINER (RTOP), MAGENTA DOLOMITE (MTOP), TAMARISK (TAMTOP), CULEBRA DOLOMITE (CTOP), AND THE UNNAMED LOWER MEMBER (ULMTOP)) AND THE SALADO FORMATION (SATOP). UTMX AND UTMY ARE THE UNIVERSAL TRANSVERSE MERCATOR COORDINATES CONVERTED TO THE STUDY AREA COORDINATES (continued)

WIPPN	UTMX	UTMY	RTOP	MTOP	TAMTOP	CTOP	ULMTOP	SATOP
FFG_563	29045	-7145	582.5	564.8	557.5	537.4	-	528.2
FFG_568	29403	-12513	-	-	634.6	631.9	-	625.8
FFG_569	29403	-12110	689.2	670.6	663.2	632.8	-	624.2
FFG_584	17150	2854	773.2	767.7	764.3	742.7	736.6	690.9
FFG_585	20040	2881	-	-	730.9	686.7	678.4	643.4
FFG_600	19263	-3615	729.1	727.6	722.1	700.1	-	692.5
FFG_601	18061	-4454	645.6	623.0	615.7	580.0	-	572.7
FFG_602	28506	4558	-	-	1053.1	803.5	794.3	743.7
FFG_606	28595	-3081	723.0	703.5	695.9	673.7	667.6	603.2
FFG_607	5016	3491	743.1	723.3	718.4	681.3	671.8	624.3
FFG_608	153	4699	754.6	731.8	726.6	663.2	654.7	593.7
FFG_609	1784	1415	758.3	738.8	732.7	656.5	646.7	586.1
FFG_610	1847	-1406	746.7	722.4	713.2	649.2	640.1	588.3
FFG_611	5030	-572	731.8	707.4	703.2	644.0	635.5	579.4
FFG_612	5049	-1387	733.4	715.7	712.7	679.1	669.7	624.9
FFG_613	11146	-2928	728.5	713.5	705.9	677.9	668.7	621.8
FFG_618	9663	-7861	-	-	701.9	686.7	-	679.1
FFG_620	10478	-9092	759.8	738.5	-	-	-	731.2
FFG_621	10076	-9092	-	-	-	-	-	695.0
FFG_638	18080	-6082	591.7	573.1	567.3	536.8	-	530.1
FFG_639	16458	-6101	566.3	543.8	537.4	508.1	-	498.4
FFG_640	14819	-4906	649.1	630.8	623.1	597.8	586.6	519.5
FFG_643	20928	-7665	688.9	669.7	662.4	642.3	637.1	576.1
FFG_644	16087	-9341	723.5	706.4	701.2	677.2	-	670.5
FFG_648	20134	-10108	558.4	541.3	536.1	513.3	-	500.5
FFG_652	18777	-4731	878.7	859.8	853.7	822.9	815.9	786.4
FFG_653	17275	-5579	880.0	859.9	854.1	822.7	815.7	788.6
FFG_654	15938	-4880	899.5	880.0	874.8	845.8	839.1	812.3
FFG_655	15221	-4936	897.3	878.1	873.2	847.3	840.3	812.9
FFG_656	15535	-5181	894.3	876.9	870.8	845.2	838.5	808.9
FFG_657	13091	-4829	906.2	889.8	883.7	862.9	856.2	830.0
FFG_658	13913	-5408	898.2	881.8	874.4	849.4	842.7	816.2
FFG_659	12905	-6045	901.9	886.1	879.7	856.8	848.6	821.1
FFG_660	11471	-4853	919.2	901.5	896.9	873.4	866.4	845.1
FFG_662	18496	-7702	894.6	876.3	870.8	843.4	837.3	810.2
FFG_664	20235	-8901	888.2	868.4	862.0	836.4	830.9	794.9
FFG_666	15261	-9363	938.1	920.5	914.4	890.0	883.9	860.1
FFG_667	14441	-8146	923.3	905.6	899.5	875.7	869.3	845.8
FFG_668	11620	-9407	-	-	947.7	926.1	919.4	905.1
FFG_669	12454	-10601	-	-	934.2	912.9	905.8	890.6
FFG_670	13762	-10903	946.1	926.9	919.3	897.3	889.1	876.0

Source: Modified from Richey, 1989

TABLE B-1. ELEVATIONS (m) OF THE TOPS OF THE RUSTLER FORMATION MEMBERS (THE FORTY-NINER (RTOP), MAGENTA DOLOMITE (MTOP), TAMARISK (TAMTOP), CULEBRA DOLOMITE (CTOP), AND THE UNNAMED LOWER MEMBER (ULMTOP)) AND THE SALADO FORMATION (SATOP). UTMX AND UTMY ARE THE UNIVERSAL TRANSVERSE MERCATOR COORDINATES CONVERTED TO THE STUDY AREA COORDINATES (continued)

WIPPN	UTMX	UTMY	RTOP	MTOP	TAMTOP	CTOP	ULMTOP	SATOP
FFG_671	13642	-9786	-	-	917.7	900.0	891.2	873.5
FFG_672	14077	-11088	943.7	925.7	919.9	897.1	889.8	868.1
FFG_673	13359	-10601	-	-	914.7	894.2	887.5	870.5
FFG_674	14781	-11088	937.0	921.7	915.0	893.4	885.5	860.2
FFG_675	19329	-10108	896.0	877.7	871.6	851.5	844.2	819.2
FFG_676	18507	-10128	905.0	891.9	884.2	862.3	854.7	831.8
FFG_677	14781	-11289	932.4	917.8	910.5	889.7	883.3	857.1
FFG_679	14077	-11390	934.8	917.1	910.4	891.2	883.9	861.1
FFG_685	2773	32591	-	-	-	918.1	911.1	825.7
FFG_689	36610	4176	817.2	799.5	793.7	764.5	756.8	718.1
FFG_690	35522	2539	824.8	805.0	798.9	768.7	760.8	718.1
FFG_691	36509	3019	816.3	796.2	790.4	760.8	752.9	711.4
FFG_692	38253	2283	806.2	786.4	780.3	749.9	-	741.6
FFG_693	37339	1357	817.7	797.0	790.9	760.4	753.7	712.6
FFG_694	36236	630	810.1	789.4	783.3	750.4	743.1	680.3
FFG_695	36226	1834	814.1	794.9	788.8	756.5	749.2	702.6
FFG_696	36226	1897	815.9	797.0	790.6	758.3	751.6	703.1
FFG_697	35019	1432	818.1	799.2	793.7	760.2	754.1	699.9
FFG_698	31260	1755	861.4	841.6	835.5	802.0	795.3	734.9
FFG_699	33950	-703	811.1	792.8	786.7	755.6	749.5	691.0
FFG_700	33950	-1106	801.4	782.5	777.0	749.3	744.4	682.2
FFG_701	35361	-879	810.6	788.6	781.9	749.6	740.8	686.5
FFG_702	35763	-476	811.7	792.8	786.7	755.6	747.0	693.7
FFG_703	38277	271	817.2	798.9	791.6	761.7	753.8	716.9
FFG_704	35763	-1281	806.2	785.5	779.4	745.6	737.3	686.4
FFG_705	34370	-2114	735.5	715.6	709.6	679.7	671.8	610.8
FFG_706	34571	-2114	755.0	736.1	730.7	702.3	694.4	637.1
FFG_707	33950	-1810	741.0	720.3	714.2	686.8	677.0	616.7
FFG_708	33950	-1307	791.6	773.3	767.2	736.7	728.8	669.7
FFG_709	31017	-3467	681.5	664.5	658.7	632.8	-	625.8
FFG_710	33042	-3438	682.5	665.4	659.3	631.6	625.2	579.2
FFG_711	34283	-4225	694.4	675.2	668.2	634.6	626.1	570.6
FFG_712	35534	-3797	735.6	718.8	710.9	678.3	-	669.5
FFG_713	35101	-4199	672.5	655.8	648.1	620.7	-	613.7
FFG_714	35897	-2995	790.3	770.2	761.9	731.5	-	725.1
FFG_715	37111	-2969	799.7	783.0	774.8	741.8	-	735.1
FFG_716	48691	5227	697.9	680.8	676.6	604.9	597.3	553.1
FFG_717	43464	5166	722.5	703.3	698.1	672.2	665.2	621.9
FFG_718	43505	2757	723.5	706.7	700.9	664.7	656.1	612.8
FFG_719	47100	3599	696.7	679.4	674.2	626.0	618.7	571.2
FFG_720	49969	915	699.6	679.1	671.5	625.8	614.5	570.6

Source: Modified from Richey, 1989

TABLE B-1. ELEVATIONS (m) OF THE TOPS OF THE RUSTLER FORMATION MEMBERS (THE FORTY-NINER (RTOP), MAGENTA DOLOMITE (MTOP), TAMARISK (TAMTOP), CULEBRA DOLOMITE (CTOP), AND THE UNNAMED LOWER MEMBER (ULMTOP)) AND THE SALADO FORMATION (SATOP). UTMX AND UTMY ARE THE UNIVERSAL TRANSVERSE MERCATOR COORDINATES CONVERTED TO THE STUDY AREA COORDINATES (continued)

WIPPN	UTMX	UTMY	RTOP	MTOP	TAMTOP	CTOP	ULMTOP	SATOP
FFG_721	46316	1600	698.0	679.1	673.6	646.2	639.5	594.4
FFG_723	40729	-497	808.2	791.7	785.3	762.8	755.1	712.5
FFG_724	43131	341	738.9	719.1	713.6	686.5	678.0	633.8
FFG_725	45130	352	712.3	694.9	689.7	652.9	646.5	610.5
FFG_726	47179	-830	698.9	682.7	677.5	648.6	641.0	589.1
FFG_727	48786	-811	702.9	680.0	674.9	639.2	630.7	575.5
FFG_728	50012	-2401	696.4	677.8	673.3	646.7	638.2	590.4
FFG_729	46790	-2440	706.6	688.9	683.7	648.9	641.0	595.9
FFG_730	45179	-2460	724.8	705.6	701.3	673.6	665.3	622.7
FFG_731	45153	-1254	720.7	703.0	697.8	670.4	662.8	617.7
FFG_732	42339	-1695	739.5	720.6	713.2	686.4	-	678.2
FFG_733	40779	-4115	806.5	787.6	781.2	749.8	741.9	698.3
FFG_734	43596	-3679	758.6	741.9	737.0	707.4	699.2	654.1
FFG_735	48802	-2825	704.1	684.6	679.1	638.9	630.3	584.0
FFG_736	557	3455	758.7	739.1	732.4	676.4	667.8	615.4
FFG_737	-6352	2974	702.6	682.8	678.8	620.3	611.8	559.3
FFG_738	-6722	1767	713.8	697.0	692.5	662.0	654.4	610.2
FFG_739	-4699	1780	753.9	734.4	729.8	694.8	683.8	628.6
FFG_740	1003	299	754.7	736.7	730.6	662.6	653.2	609.0
FFG_741	-7026	-3139	721.2	702.9	697.7	658.7	651.1	602.3
FFG_742	-5859	-1103	774.5	753.7	748.6	700.7	690.7	646.5
FFG_743	-3444	-2242	757.2	740.4	735.2	686.1	675.2	630.7
FFG_744	-5030	-3502	739.7	722.9	717.8	677.2	670.8	630.0
FFG_745	-2183	-4277	730.3	708.9	705.9	657.7	650.4	598.3
FFG_746	2252	-3427	719.8	699.1	693.0	645.5	637.2	581.8
H-1	23691	27450	882.7	864.1	856.2	829.7	822.6	784.5
H-2C	22934	27425	890.3	872.6	864.1	839.7	833.0	796.7
H-3	24006	26658	880.3	862.9	855.3	828.5	821.8	783.1
H-4C	22675	24260	920.2	901.3	893.4	866.8	858.9	825.4
H-5C	27171	30565	845.8	828.7	821.4	794.9	787.3	751.6
H-6C	20880	30790	890.4	871.1	863.8	836.4	829.4	800.7
H-7C	18357	20395	937.6	928.4	921.4	891.9	880.6	877.8
H-8C	18927	9304	924.8	904.4	897.7	867.2	859.3	823.0
H-9C	24236	13996	899.4	878.7	869.2	840.9	831.8	797.0
H-10C	33247	18212	756.8	741.0	733.7	709.3	699.8	666.3
H-11	25617	24893	-	-	-	-	-	-
H-12	27294	21215	-	-	-	-	-	-
H-14	22612	26667	-	-	-	-	-	-
H-15	25586	23622	-	-	-	-	-	-
H-16	23640	27935	-	-	-	-	-	-
H-17	25989	23276	-	-	-	-	-	-

Source: Modified from Richey, 1989

TABLE B-1. ELEVATIONS (m) OF THE TOPS OF THE RUSTLER FORMATION MEMBERS (THE FORTY-NINER (RTOP), MAGENTA DOLOMITE (MTOP), TAMARISK (TAMTOP), CULEBRA DOLOMITE (CTOP), AND THE UNNAMED LOWER MEMBER (ULMTOP)) AND THE SALADO FORMATION (SATOP). UTMX AND UTMY ARE THE UNIVERSAL TRANSVERSE MERCATOR COORDINATES CONVERTED TO THE STUDY AREA COORDINATES (continued)

WIPPN	UTMX	UTMY	RTOP	MTOP	TAMTOP	CTOP	ULMTOP	SATOP
H-18	22535	28929	-	-	-	-	-	-
P-1	22610	26102	910.5	890.7	883.0	855.6	847.4	813.3
P-2	25586	27613	850.1	832.4	824.8	799.2	791.3	753.2
P-3	23070	27651	888.5	869.9	862.5	835.4	828.4	791.5
P-4	25207	26087	864.1	847.9	840.6	813.5	805.3	766.2
P-5	23957	29298	868.1	848.9	841.3	812.9	805.9	769.4
P-6	20862	26896	913.5	895.2	887.3	858.6	851.6	821.4
P-7	22576	24239	920.5	901.9	894.3	864.4	856.5	823.6
P-8	24098	24230	898.5	880.5	873.2	846.1	838.5	799.8
P-9	25636	24888	868.7	851.9	843.7	816.3	809.3	771.5
P-10	27345	26956	860.4	838.8	831.5	785.7	777.8	738.5
P-11	27287	29225	840.9	824.8	817.1	790.0	782.1	745.5
P-12	20725	29215	887.9	870.2	862.9	835.5	828.5	800.1
P-13	20810	30842	889.5	870.2	862.9	835.5	828.5	799.8
P-14	19354	27737	906.1	886.0	878.7	849.4	842.7	814.7
P-15	20895	24556	938.5	919.3	911.1	883.0	876.3	843.7
P-16	22975	23075	915.0	896.7	889.1	858.9	851.9	814.4
P-17	24200	23222	900.4	883.3	875.7	846.7	839.1	798.9
P-18	28638	26115	868.4	845.2	837.3	782.7	773.9	728.2
P-19	27958	28173	849.5	832.4	824.8	785.8	776.6	740.0
P-20	28812	29533	845.3	827.3	819.0	792.5	784.6	746.8
P-21	27172	30610	845.8	829.3	822.0	795.5	787.9	751.6
ERDA-6	28497	34774	915.6	897.6	889.7	862.6	855.0	830.6
ERDA-9	23968	27721	878.1	860.4	853.1	827.5	820.5	783.6
ERDA-10	16955	16286	-	915.9	910.2	882.4	873.9	836.1
AEC-7	31388	35150	911.9	890.3	882.4	848.5	840.6	811.6
AEC-8	27793	32198	875.4	858.7	851.7	822.7	814.8	776.4
WIPP-11	24090	32237	842.1	822.6	815.6	786.9	779.9	754.3
WIPP-12	23980	29287	866.9	848.0	840.4	811.4	803.8	767.2
WIPP-13	22923	30004	880.2	865.9	860.1	824.1	817.1	780.5
WIPP-15	328	20348	-	-	-	-	-	996.4
WIPP-16	12651	42789	681.2	668.7	-	679.7	-	672.7
WIPP-18	24002	28942	866.6	848.6	841.3	813.8	807.1	770.5
WIPP-19	24018	28550	866.9	849.2	841.6	816.0	809.6	773.9
WIPP-21	24018	28112	870.8	853.1	846.1	819.3	812.0	776.9
WIPP-22	24018	28415	869.5	852.2	844.9	818.0	811.3	775.1
WIPP-25	16662	29800	908.6	887.3	879.3	843.1	835.4	807.1
WIPP-26	14277	26924	957.7	939.4	930.5	904.0	897.0	866.5
WIPP-27	14696	38836	921.7	914.7	909.2	879.3	871.4	841.5
WIPP-28	21536	40450	954.7	933.3	925.7	892.2	884.3	858.4
WIPP-29	7252	24463	-	-	907.4	903.7	894.6	863.8

Source: Modified from Richey, 1989

TABLE B-1. ELEVATIONS (m) OF THE TOPS OF THE RUSTLER FORMATION MEMBERS (THE FORTY-NINER (RTOP), MAGENTA DOLOMITE (MTOP), TAMARISK (TAMTOP), CULEBRA DOLOMITE (CTOP), AND THE UNNAMED LOWER MEMBER (ULMTOP)) AND THE SALADO FORMATION (SATOP). UTMX AND UTMY ARE THE UNIVERSAL TRANSVERSE MERCATOR COORDINATES CONVERTED TO THE STUDY AREA COORDINATES (concluded)

WIPPN	UTMX	UTMY	RTOP	MTOP	TAMTOP	CTOP	ULMTOP	SATOP
WIPP-30	23989	35463	908.0	888.5	881.2	852.6	845.6	816.6
WIPP-32	6180	24844	921.4	915.6	910.4	902.8	894.0	870.8
WIPP-33	19900	29782	891.6	876.0	870.3	845.3	836.7	812.6
WIPP-34	24604	30904	846.1	827.6	820.5	792.2	784.3	749.8
B-25	21966	26372	876.6	858.4	851.0	824.5	817.2	782.2
USGS-1	16733	15222						
ENGLE	25224	13217						
DOE-1	25474	26076						
CABIN-1	23462	23812						

Source: Modified from Richey, 1989

TABLE B-2. WELL NAMES AND THICKNESSES (m) OF THE SUPRA-RUSTLER (SURF) AND THE RUSTLER FORMATION MEMBERS (FORTY-NINER [FORTHM], MAGENTA [MAGTHM], TAMARISK [TAMTHM], CULEBRA [CULTHM], AND UNNAMED LOWER [ULMTHM]) IN THE LOS MEDAÑOS STUDY AREA

WIPPN	SURF	FORTHM	MAGTHM	TAMTHM	CULTHM	ULMTHM
FFG_002	404.2	18.6	7.0	35.7	6.7	39.3
FFG_004	329.2	21.3	7.0	44.2	6.7	32.0
FFG_005	395.9	18.9	7.0	39.4	6.4	40.2
FFG_006	402.6	18.9	8.6	44.8	8.5	-
FFG_007	415.7	22.3	6.1	47.8	8.3	34.7
FFG_009	416.7	20.7	7.3	46.0	7.6	21.4
FFG_011	408.1	20.4	7.1	47.2	6.4	33.2
FFG_012	405.1	19.2	8.2	45.7	7.7	34.1
FFG_013	383.4	22.0	7.0	21.6	11.9	51.8
FFG_014	326.7	20.8	7.6	45.7	8.9	35.9
FFG_016	432.8	22.0	7.3	49.7	8.5	34.4
FFG_017	431.3	21.3	7.6	45.8	7.6	32.0
FFG_018	444.1	20.1	6.4	47.3	7.9	32.3
FFG_019	444.7	21.6	7.1	49.0	8.3	31.4
FFG_020	350.8	22.3	6.1	50.3	6.7	32.9
FFG_023	431.3	24.4	6.7	51.2	8.5	34.2
FFG_024	462.6	23.2	6.7	53.0	7.3	32.6
FFG_025	443.5	21.9	6.1	47.6	6.7	31.4
FFG_026	445.2	21.3	6.1	50.9	7.0	32.9
FFG_027	453.2	21.1	6.7	50.9	7.0	32.9
FFG_028	554.1	17.1	5.2	28.9	6.1	22.9
FFG_029	529.4	16.8	5.2	30.5	5.4	20.2
FFG_030	537.7	18.3	5.4	29.9	5.8	24.4
FFG_031	558.7	19.5	6.1	29.6	7.0	25.0
FFG_032	546.6	19.8	6.1	36.6	3.3	27.1
FFG_033	536.4	18.9	5.5	33.6	7.0	23.4
FFG_034	538.0	18.9	4.5	29.3	6.1	24.7
FFG_035	530.8	17.7	6.1	32.6	3.0	26.0
FFG_036	545.0	20.4	5.5	35.3	5.8	25.3
FFG_037	536.4	21.1	4.9	32.9	5.2	25.9
FFG_038	538.9	19.8	5.5	30.5	6.1	25.6
FFG_039	247.5	19.8	6.7	40.2	6.4	31.1
FFG_040	336.5	19.8	7.3	58.2	10.1	20.4
FFG_041	264.3	20.4	7.0	39.9	7.3	34.5
FFG_042	264.0	20.1	7.6	37.2	10.6	34.8
FFG_043	257.1	21.9	6.1	46.3	7.0	31.7
FFG_044	318.2	21.3	7.4	44.5	8.2	35.3
FFG_047	479.4	19.5	6.4	46.4	5.1	29.9
FFG_048	452.9	22.3	7.6	43.0	7.0	45.7
FFG_049	477.3	21.0	6.1	47.3	7.9	32.9
FFG_050	484.5	20.4	6.1	39.0	7.6	37.5
FFG_051	482.2	21.6	5.2	48.2	7.6	35.4
FFG_052	480.4	21.3	6.1	29.0	5.4	24.1
FFG_053	494.7	19.5	7.9	52.4	7.4	45.1
FFG_054	508.3	21.3	7.3	50.6	6.1	37.8
FFG_055	503.5	20.5	8.5	46.9	7.9	36.6
FFG_056	492.3	22.5	6.4	50.9	7.6	36.0
FFG_057	489.2	20.4	7.6	52.8	6.7	33.5

TABLE B-2. WELL NAMES AND THICKNESSES (m) OF THE SUPRA-RUSTLER (SURF) AND THE RUSTLER FORMATION MEMBERS (FORTY-NINER [FORTHM], MAGENTA [MAGTHM], TAMARISK [TAMTHM], CULEBRA [CULTHM], AND UNNAMED LOWER [ULMTHM]) IN THE LOS MEDAÑOS STUDY AREA (continued)

WIPPN	SURF	FORTHM	MAGTHM	TAMTHM	CULTHM	ULMTHM
FFG_058	506.7	17.4	8.5	45.8	8.5	34.1
FFG_059	512.7	19.8	6.1	47.8	4.9	35.1
FFG_060	492.9	18.2	9.2	48.8	6.1	30.4
FFG_061	491.6	19.9	6.1	49.3	5.5	32.6
FFG_062	548.3	21.1	6.1	33.2	6.7	28.0
FFG_063	583.4	21.0	5.2	37.8	4.9	27.4
FFG_064	567.5	21.1	6.7	34.4	8.6	27.7
FFG_065	567.8	22.3	5.2	43.6	7.3	14.9
FFG_066	616.9	22.9	4.5	35.1	5.2	27.4
FFG_067	590.4	20.7	5.2	41.2	6.0	28.1
FFG_068	628.5	14.6	6.1	45.7	6.1	27.5
FFG_069	605.9	21.9	6.1	48.8	6.1	33.5
FFG_070	577.0	21.6	6.1	41.5	5.5	37.1
FFG_071	304.2	20.4	6.4	29.3	6.7	48.1
FFG_072	365.5	18.6	6.1	33.8	7.0	28.4
FFG_073	389.6	18.3	8.9	31.3	7.1	28.9
FFG_074	383.3	20.4	4.9	32.0	6.1	29.6
FFG_075	335.0	17.3	6.8	31.3	5.8	28.7
FFG_076	260.9	18.3	7.6	32.9	6.1	29.6
FFG_078	212.8	19.2	8.2	32.3	7.0	30.8
FFG_079	243.2	18.3	6.1	36.6	6.1	30.5
FFG_080	254.8	19.2	7.9	34.8	7.3	30.8
FFG_081	350.2	18.9	7.0	37.8	8.2	30.5
FFG_082	305.7	19.8	6.1	42.1	5.8	32.3
FFG_083	422.6	18.3	6.1	30.5	6.1	27.4
FFG_084	386.5	18.9	7.6	33.2	6.7	28.7
FFG_085	394.7	18.6	8.2	32.0	6.4	28.1
FFG_086	384.7	17.0	8.3	32.3	7.6	27.1
FFG_087	409.3	18.0	8.6	34.7	6.7	28.7
FFG_088	414.5	19.8	7.4	41.1	3.4	27.4
FFG_089	432.8	19.8	6.4	35.7	7.3	29.9
FFG_091	371.2	19.6	7.6	40.5	8.5	29.6
FFG_092	362.7	18.3	10.1	35.6	8.6	28.6
FFG_093	360.6	19.2	7.9	36.6	5.5	30.4
FFG_094	354.5	20.4	7.0	39.0	7.6	29.6
FFG_095	432.2	17.7	7.3	29.9	6.4	26.5
FFG_096	484.9	18.3	6.1	29.6	6.1	24.4
FFG_097	478.2	19.5	6.7	30.2	6.4	27.8
FFG_098	562.7	20.1	5.5	32.0	6.1	25.9
FFG_099	564.2	20.7	5.5	32.9	7.9	24.4
FFG_100	528.2	21.0	5.8	33.3	6.1	28.3
FFG_101	549.6	18.2	5.5	35.7	6.4	27.1
FFG_102	513.3	20.4	6.1	38.4	6.1	30.5
FFG_103	434.0	19.2	3.4	42.7	7.6	-
FFG_104	555.0	21.4	6.1	36.9	6.0	27.8
FFG_105	68.3	17.3	8.3	33.8	6.1	48.5
FFG_106	26.8	15.0	7.9	29.2	8.0	53.9
FFG_107	42.4	22.2	6.1	29.0	9.1	42.7

TABLE B-2. WELL NAMES AND THICKNESSES (m) OF THE SUPRA-RUSTLER (SURF) AND THE RUSTLER FORMATION MEMBERS (FORTY-NINER [FORTHM], MAGENTA [MAGTHM], TAMARISK [TAMTHM], CULEBRA [CULTHM], AND UNNAMED LOWER [ULMTHM]) IN THE LOS MEDAÑOS STUDY AREA (continued)

WIPPN	SURF	FORTHM	MAGTHM	TAMTHM	CULTHM	ULMTHM
FFG_108	82.3	15.2	6.1	33.6	9.1	33.5
FFG_109	121.9	18.3	6.1	30.5	6.1	24.4
FFG_110	158.5	21.3	6.1	27.5	7.6	25.9
FFG_111	165.5	25.0	4.6	30.5	6.0	24.4
FFG_112	176.8	18.3	6.1	30.4	7.7	32.0
FFG_113	161.5	18.3	6.1	30.5	7.6	28.7
FFG_114	90.5	18.6	7.3	27.8	7.3	34.4
FFG_115	56.7	18.3	6.1	32.0	9.1	44.8
FFG_116	42.7	18.3	6.1	33.5	6.1	70.1
FFG_117	30.5	24.4	9.1	33.5	12.2	45.7
FFG_119	12.2	-	-	67.0	6.1	36.6
FFG_120	12.2	21.3	9.2	39.6	9.1	45.8
FFG_121	12.2	18.3	6.1	39.6	9.1	42.7
FFG_122	9.1	18.3	6.1	44.2	7.6	54.9
FFG_123	33.5	27.5	6.1	27.4	6.1	45.7
FFG_124	76.8	35.1	7.6	19.8	7.0	45.4
FFG_125	64.0	21.3	7.7	32.0	9.1	-
FFG_126	109.7	18.3	6.1	27.4	6.1	33.6
FFG_127	109.7	18.3	6.1	24.4	9.1	27.5
FFG_128	46.3	21.4	9.1	30.5	9.4	25.0
FFG_129	38.1	24.4	6.1	35.0	6.1	36.6
FFG_130	25.9	24.4	9.1	22.9	9.1	33.6
FFG_132	45.7	21.4	6.1	30.4	7.7	38.1
FFG_133	33.5	21.4	6.1	30.4	6.1	57.9
FFG_134	24.4	19.8	8.5	31.1	7.6	35.1
FFG_135	65.2	19.8	6.7	29.9	5.8	31.1
FFG_136	73.2	15.2	7.6	29.0	6.1	32.0
FFG_137	60.6	18.9	8.6	26.5	8.2	31.4
FFG_138	126.5	16.8	6.1	30.4	9.2	36.6
FFG_139	115.8	18.0	7.3	26.8	7.7	37.8
FFG_140	193.5	19.9	6.1	30.4	7.7	35.0
FFG_141	157.3	18.9	8.5	25.6	7.6	29.6
FFG_142	193.5	19.9	7.6	25.9	7.6	30.5
FFG_143	196.9	16.5	7.6	27.7	6.7	-
FFG_144	1.5	-	-	9.2	10.6	58.6
FFG_145	-	-	-	12.2	6.1	56.4
FFG_146	-	-	-	6.1	9.1	71.7
FFG_147	10.4	-	4.2	11.0	7.3	59.1
FFG_148	-	-	-	7.6	5.2	62.8
FFG_149	4.3	-	-	1.5	7.6	61.0
FFG_152	12.2	-	-	-	-	56.4
FFG_155	4.0	-	8.5	4.3	7.3	63.1
FFG_156	1.8	-	-	-	11.0	57.9
FFG_157	10.7	-	8.2	3.0	5.5	-
FFG_158	4.6	-	6.1	3.0	10.1	61.2
FFG_159	45.1	19.5	7.9	30.2	7.0	32.0
FFG_160	52.4	20.4	5.5	29.0	9.1	30.5
FFG_161	30.5	21.3	6.1	29.0	6.1	38.1

TABLE B-2. WELL NAMES AND THICKNESSES (m) OF THE SUPRA-RUSTLER (SURF) AND THE RUSTLER FORMATION MEMBERS (FORTY-NINER [FORTHM], MAGENTA [MAGTHM], TAMARISK [TAMTHM], CULEBRA [CULTHM], AND UNNAMED LOWER [ULMTHM]) IN THE LOS MEDAÑOS STUDY AREA (continued)

WIPPN	SURF	FORTHM	MAGTHM	TAMTHM	CULTHM	ULMTHM
FFG_162	32.9	22.6	7.9	33.5	7.3	26.9
FFG_163	33.5	21.4	6.1	30.4	9.2	32.0
FFG_164	-	-	-	18.3	9.1	73.8
FFG_165	-	-	-	22.9	10.6	63.4
FFG_166	38.7	18.3	7.6	28.4	8.2	33.5
FFG_167	82.9	14.6	7.7	27.4	9.1	41.2
FFG_168	33.5	22.9	10.7	27.4	7.6	55.8
FFG_169	5.8	22.9	8.2	29.9	10.0	47.9
FFG_170	1.2	10.7	6.1	13.1	10.7	53.9
FFG_171	25.3	-	7.3	2.1	12.8	61.3
FFG_172	48.8	-	4.2	17.7	9.2	54.2
FFG_173	87.8	20.7	7.6	29.6	9.1	36.3
FFG_177	24.1	-	-	-	9.1	67.4
FFG_179	9.8	-	-	-	11.5	58.3
FFG_180	118.3	23.4	5.5	32.0	8.3	49.6
FFG_181	65.2	-	4.6	16.2	7.6	53.9
FFG_182	129.5	8.9	5.2	29.8	8.3	47.2
FFG_183	81.4	-	-	34.7	11.0	56.1
FFG_184	120.1	-	3.0	33.6	7.6	32.0
FFG_185	88.1	-	4.6	30.4	7.7	51.8
FFG_186	149.7	-	6.1	29.8	8.6	53.0
FFG_188	104.9	-	5.1	23.2	8.2	56.4
FFG_189	123.4	20.5	7.9	26.5	8.2	54.6
FFG_190	136.2	19.2	7.7	31.1	8.5	41.7
FFG_191	140.2	23.2	7.6	25.0	6.1	59.4
FFG_192	196.9	19.2	8.8	32.0	10.1	56.4
FFG_194	235.7	17.6	6.5	27.1	7.9	41.8
FFG_195	203.9	21.3	5.2	25.3	10.7	39.3
FFG_196	144.8	20.7	7.0	32.9	9.5	35.0
FFG_197	135.0	21.4	7.3	29.8	9.8	41.1
FFG_198	133.2	20.7	6.1	30.5	9.1	47.9
FFG_199	150.0	21.3	7.6	32.9	8.3	38.1
FFG_200	138.4	21.6	7.9	34.8	10.1	42.9
FFG_201	179.5	21.4	7.6	27.4	8.2	51.3
FFG_202	241.4	17.7	8.2	34.5	10.6	39.6
FFG_203	230.1	18.3	7.3	39.7	8.5	39.9
FFG_204	231.6	18.3	8.6	24.4	8.2	38.1
FFG_205	201.4	20.1	7.3	28.1	8.5	48.1
FFG_206	171.9	21.3	7.1	30.4	8.9	48.7
FFG_207	180.4	19.9	7.3	31.4	7.6	50.3
FFG_208	157.3	20.7	7.9	31.1	8.6	54.2
FFG_209	200.9	-	7.0	28.0	8.5	42.4
FFG_210	180.4	19.9	7.0	31.4	8.8	52.7
FFG_212	207.9	17.7	7.6	27.7	8.5	40.6
FFG_213	148.1	29.0	6.1	30.5	9.1	33.5
FFG_214	183.8	22.9	6.7	29.8	9.8	50.9
FFG_215	189.3	21.3	7.6	30.5	8.2	50.3
FFG_216	256.6	20.2	6.4	21.6	6.1	162.1

TABLE B-2. WELL NAMES AND THICKNESSES (m) OF THE SUPRA-RUSTLER (SURF) AND THE RUSTLER FORMATION MEMBERS (FORTY-NINER [FORTHM], MAGENTA [MAGTHM], TAMARISK [TAMTHM], CULEBRA [CULTHM], AND UNNAMED LOWER [ULMTHM]) IN THE LOS MEDAÑOS STUDY AREA (continued)

WIPPN	SURF	FORTHM	MAGTHM	TAMTHM	CULTHM	ULMTHM
FFG_217	184.1	22.2	7.7	28.9	9.2	49.3
FFG_218	189.6	19.5	8.2	32.3	9.2	50.3
FFG_219	125.9	20.7	9.8	31.1	8.5	57.0
FFG_220	191.1	23.2	4.5	33.6	9.1	47.3
FFG_221	213.4	18.2	9.2	30.5	12.2	59.4
FFG_222	249.3	20.8	8.2	28.3	8.3	100.5
FFG_224	456.6	21.3	7.6	50.3	7.7	32.0
FFG_225	454.6	21.3	6.1	52.8	5.5	31.7
FFG_226	467.1	22.2	7.0	52.2	7.0	32.9
FFG_228	459.9	22.0	8.5	54.9	7.6	31.4
FFG_229	444.4	22.2	7.4	57.3	7.6	35.0
FFG_230	445.9	23.5	7.0	57.0	6.1	36.6
FFG_231	416.1	22.2	7.6	54.3	6.1	35.6
FFG_232	406.3	22.2	7.4	56.7	5.7	39.7
FFG_233	405.4	23.5	7.0	54.8	6.1	36.0
FFG_234	367.0	23.1	7.7	54.8	6.7	37.2
FFG_235	394.7	23.8	7.3	55.8	7.0	32.6
FFG_236	332.8	22.0	7.9	55.8	5.5	35.3
FFG_237	402.5	23.2	7.3	58.6	11.8	33.6
FFG_238	436.2	25.6	5.5	57.0	7.0	37.2
FFG_239	474.0	24.0	5.8	52.8	7.0	43.0
FFG_240	467.0	24.0	6.7	54.6	7.3	33.8
FFG_241	476.4	22.6	7.3	53.9	7.0	35.4
FFG_242	315.2	16.7	6.4	44.5	8.0	42.9
FFG_243	389.9	20.7	7.6	67.1	9.1	44.2
FFG_244	321.6	17.6	7.7	51.8	6.1	25.9
FFG_245	573.6	24.1	6.1	56.1	7.3	32.9
FFG_246	560.2	23.2	5.5	57.0	7.9	35.0
FFG_247	556.3	25.3	5.8	56.7	7.6	33.6
FFG_248	555.3	23.5	5.2	59.4	8.3	33.8
FFG_249	575.5	24.0	5.5	58.9	7.0	34.1
FFG_250	485.7	22.6	7.0	57.0	7.0	35.0
FFG_251	570.3	23.8	6.4	61.2	7.3	37.8
FFG_252	425.5	24.7	6.1	58.2	7.0	45.1
FFG_253	448.1	21.3	6.7	65.8	5.2	39.6
FFG_254	460.6	21.0	6.1	61.9	7.3	36.9
FFG_255	512.7	22.2	7.6	65.6	8.2	39.0
FFG_256	578.2	22.6	5.4	51.9	7.0	32.0
FFG_257	536.8	21.0	5.8	50.3	6.1	33.2
FFG_258	505.4	20.1	7.3	41.4	9.8	38.7
FFG_259	554.7	23.8	7.6	50.3	8.3	38.1
FFG_260	489.2	18.0	6.4	41.1	7.4	33.8
FFG_261	495.9	17.4	6.4	44.2	4.9	34.7
FFG_263	562.2	26.8	5.5	64.6	8.0	41.7
FFG_264	343.5	17.1	7.3	49.4	7.6	42.7
FFG_265	355.4	19.5	6.1	63.7	8.8	42.7
FFG_266	372.5	22.2	5.8	65.5	8.6	47.2
FFG_267	384.0	22.9	5.2	67.0	8.6	50.0

TABLE B-2. WELL NAMES AND THICKNESSES (m) OF THE SUPRA-RUSTLER (SURF) AND THE RUSTLER FORMATION MEMBERS (FORTY-NINER [FORTHM], MAGENTA [MAGTHM], TAMARISK [TAMTHM], CULEBRA [CULTHM], AND UNNAMED LOWER [ULMTHM]) IN THE LOS MEDAÑOS STUDY AREA (continued)

WIPPN	SURF	FORTHM	MAGTHM	TAMTHM	CULTHM	ULMTHM
FFG_268	399.9	25.3	6.1	71.0	7.3	43.0
FFG_269	376.6	26.8	5.5	69.2	10.1	49.3
FFG_270	265.2	17.3	5.2	39.0	9.2	31.7
FFG_271	215.5	18.9	6.1	35.0	6.1	34.5
FFG_272	226.9	24.1	6.1	64.6	7.9	46.7
FFG_273	262.3	19.5	7.3	36.9	7.9	43.6
FFG_274	286.2	16.8	7.0	34.1	7.3	38.4
FFG_275	277.1	18.3	6.0	33.6	6.1	27.4
FFG_276	264.3	16.4	7.6	34.8	7.0	29.6
FFG_277	269.7	16.8	7.6	33.6	6.4	35.6
FFG_278	229.8	22.6	7.3	61.9	11.2	43.0
FFG_279	247.8	19.2	7.6	56.4	9.2	32.0
FFG_280	261.7	21.3	6.4	42.1	8.8	41.8
FFG_281	311.5	21.6	6.8	44.8	8.2	45.1
FFG_283	506.3	20.7	5.8	61.9	7.0	38.7
FFG_284	386.8	18.3	6.1	57.9	6.7	45.1
FFG_285	352.3	18.9	6.4	65.3	9.1	44.5
FFG_286	264.0	17.3	6.1	40.3	7.6	37.5
FFG_287	282.6	18.9	7.0	47.9	4.9	40.2
FFG_288	344.7	20.8	6.1	70.1	6.1	45.7
FFG_289	345.6	16.4	6.1	33.2	6.7	34.8
FFG_290	277.7	19.2	7.0	28.6	10.1	27.4
FFG_291	365.8	23.7	5.8	68.0	7.9	45.7
FFG_292	316.4	15.8	6.1	27.5	7.0	31.1
FFG_293	319.1	15.3	6.1	26.5	7.6	38.1
FFG_294	500.2	22.5	5.8	62.5	7.0	39.3
FFG_295	504.7	22.6	5.5	65.2	9.5	41.1
FFG_297	537.4	28.3	6.7	63.4	13.7	35.1
FFG_298	500.8	16.8	5.7	18.6	7.7	30.4
FFG_299	484.0	25.3	4.9	66.4	8.0	48.4
FFG_300	518.5	23.1	5.2	34.8	7.6	56.1
FFG_301	531.6	23.7	5.5	49.7	5.5	71.0
FFG_302	550.2	24.0	4.3	70.7	6.7	16.5
FFG_303	563.4	24.7	6.1	56.1	7.0	37.2
FFG_304	547.7	22.9	4.6	67.0	7.0	39.6
FFG_305	559.3	25.3	6.1	60.0	8.6	35.0
FFG_306	583.7	22.9	4.2	52.1	7.7	43.9
FFG_307	560.8	24.4	5.5	55.8	7.9	40.5
FFG_308	584.6	25.6	5.2	84.4	8.3	44.8
FFG_309	558.4	27.1	4.9	68.6	6.7	39.3
FFG_310	523.3	25.0	4.6	59.4	6.1	39.1
FFG_311	586.7	12.2	5.5	52.4	8.3	32.9
FFG_312	539.5	26.8	6.1	74.7	5.8	39.9
FFG_313	171.8	19.2	7.0	37.8	8.3	29.8
FFG_314	258.8	19.2	7.0	47.2	7.3	46.7
FFG_315	348.2	18.6	5.8	57.0	7.3	43.3
FFG_316	361.8	23.5	5.8	63.7	8.2	46.0
FFG_317	305.4	15.2	4.3	40.3	7.3	32.0

TABLE B-2. WELL NAMES AND THICKNESSES (m) OF THE SUPRA-RUSTLER (SURF) AND THE RUSTLER FORMATION MEMBERS (FORTY-NINER [FORTHM], MAGENTA [MAGTHM], TAMARISK [TAMTHM], CULEBRA [CULTHM], AND UNNAMED LOWER [ULMTHM]) IN THE LOS MEDAÑOS STUDY AREA (continued)

WIPPN	SURF	FORTHM	MAGTHM	TAMTHM	CULTHM	ULMTHM
FFG_318	365.5	15.8	7.6	24.4	7.6	36.6
FFG_319	351.4	17.7	5.8	41.2	8.2	34.4
FFG_320	367.3	21.0	5.8	66.1	7.4	46.0
FFG_321	364.2	22.6	5.8	63.7	6.7	48.8
FFG_322	369.6	21.9	5.8	57.6	7.6	45.4
FFG_323	369.3	21.6	6.1	48.2	7.3	41.1
FFG_324	360.3	16.4	7.3	38.5	7.3	39.0
FFG_325	260.3	19.2	7.0	31.1	9.1	39.7
FFG_326	363.3	18.3	7.0	22.6	8.5	40.5
FFG_327	353.9	19.2	5.5	33.8	7.9	36.6
FFG_328	364.4	22.5	5.8	54.9	9.1	44.2
FFG_329	364.8	21.7	5.5	59.4	7.6	48.2
FFG_330	360.7	21.7	5.2	58.5	8.5	49.4
FFG_331	350.2	25.0	5.8	69.8	6.1	44.2
FFG_332	380.7	24.7	5.5	74.3	6.7	45.8
FFG_333	384.2	23.5	5.5	66.7	7.6	44.2
FFG_334	382.8	25.0	5.5	67.7	7.9	47.9
FFG_335	372.5	23.4	8.9	61.5	8.3	47.2
FFG_336	369.7	23.8	5.5	67.0	7.7	47.2
FFG_337	385.9	24.7	5.8	66.1	7.6	49.7
FFG_338	378.7	24.1	5.5	68.3	7.9	49.4
FFG_339	396.8	26.3	4.5	68.6	7.6	50.3
FFG_340	385.6	27.4	5.2	71.0	8.5	49.4
FFG_342	308.5	20.7	6.7	37.5	6.4	24.7
FFG_344	327.2	20.7	7.6	26.0	8.2	28.3
FFG_345	297.7	23.4	5.5	68.0	7.3	42.7
FFG_347	273.7	21.3	8.0	37.2	6.7	37.5
FFG_348	244.8	17.6	5.2	29.6	5.5	46.9
FFG_349	270.6	22.0	4.2	23.5	5.2	30.5
FFG_350	232.6	19.8	6.1	37.8	5.5	27.4
FFG_351	370.6	26.6	4.5	71.7	8.2	49.7
FFG_352	371.6	25.9	6.1	70.1	7.6	48.7
FFG_353	344.1	25.0	5.5	70.1	7.0	45.7
FFG_354	233.2	17.0	5.5	33.3	6.0	33.6
FFG_361	1.5	24.1	4.3	27.4	6.7	42.7
FFG_362	54.3	-	-	37.1	8.3	69.5
FFG_363	36.6	-	-	25.9	9.1	56.4
FFG_364	50.9	-	-	24.4	8.5	-
FFG_366	50.0	19.8	6.7	22.3	7.6	40.2
FFG_367	30.5	21.3	6.1	16.8	9.1	45.7
FFG_370	-	-	-	44.2	6.1	43.3
FFG_371	-	15.2	3.1	28.9	7.1	38.7
FFG_372	-	-	-	57.3	7.6	-
FFG_373	53.1	-	-	36.0	7.0	-
FFG_374	48.8	5.5	11.2	21.4	6.1	47.2
FFG_376	25.6	-	-	37.2	7.9	43.3
FFG_381	-	-	-	106.7	6.1	33.5
FFG_383	90.8	16.5	7.6	22.9	6.1	35.0

TABLE B-2. WELL NAMES AND THICKNESSES (m) OF THE SUPRA-RUSTLER (SURF) AND THE RUSTLER FORMATION MEMBERS (FORTY-NINER [FORTHM], MAGENTA [MAGTHM], TAMARISK [TAMTHM], CULEBRA [CULTHM], AND UNNAMED LOWER [ULMTHM]) IN THE LOS MEDAÑOS STUDY AREA (continued)

WIPPN	SURF	FORTHM	MAGTHM	TAMTHM	CULTHM	ULMTHM
FFG_384	-	30.2	7.9	16.8	8.8	-
FFG_385	68.6	-	-	6.1	9.1	50.3
FFG_387	53.3	26.3	5.7	23.5	9.5	39.6
FFG_388	60.4	22.5	7.3	28.7	7.0	-
FFG_389	31.4	-	-	51.8	7.3	-
FFG_390	48.2	20.4	8.5	25.9	6.1	50.0
FFG_391	51.8	22.0	7.0	25.3	6.1	44.8
FFG_392	51.8	19.2	6.7	31.4	6.1	41.2
FFG_393	226.0	19.5	5.5	25.0	4.6	28.3
FFG_394	124.4	17.3	5.5	20.7	5.2	30.5
FFG_395	140.8	16.8	5.8	21.3	7.0	25.3
FFG_396	188.4	17.3	7.1	23.4	6.7	59.8
FFG_398	185.9	20.1	7.1	26.8	4.5	-
FFG_399	163.1	-	-	53.3	4.6	-
FFG_401	97.5	-	-	35.1	6.1	-
FFG_402	20.6	23.1	7.4	24.9	10.4	-
FFG_403	32.2	21.6	6.1	20.7	11.3	56.4
FFG_404	50.9	24.1	4.2	24.1	6.1	-
FFG_407	11.6	18.3	7.6	24.4	9.1	-
FFG_408	51.8	-	4.6	1.5	6.1	73.2
FFG_409	-	-	-	27.4	10.7	-
FFG_411	70.4	-	-	-	13.4	84.8
FFG_413	53.6	-	-	-	8.9	71.0
FFG_418	50.6	-	-	53.0	7.3	-
FFG_419	55.5	20.4	7.6	26.2	6.1	-
FFG_420	52.4	19.2	9.2	27.4	9.1	-
FFG_421	63.4	23.5	5.1	31.7	9.5	34.4
FFG_422	77.7	18.3	12.2	22.9	7.6	-
FFG_426	34.1	-	-	35.1	7.6	62.8
FFG_432	46.6	7.7	6.1	33.5	7.6	39.6
FFG_433	47.5	-	-	22.9	5.2	75.6
FFG_438	189.6	18.0	7.9	31.1	5.8	32.3
FFG_445	40.5	-	-	-	8.6	84.4
FFG_453	187.3	-	-	79.9	9.4	46.4
FFG_455	223.7	20.1	7.1	40.2	8.8	37.5
FFG_456	234.4	16.5	7.3	28.6	6.7	39.0
FFG_457	138.4	17.0	6.8	30.1	8.6	38.1
FFG_458	137.6	15.6	10.3	29.0	8.2	39.6
FFG_459	253.9	17.1	7.6	30.5	9.1	35.1
FFG_462	148.0	18.3	8.3	28.9	7.9	39.4
FFG_463	107.6	20.4	6.7	32.0	10.7	32.3
FFG_464	135.0	20.4	7.7	28.9	9.8	46.0
FFG_465	128.6	19.8	7.7	30.4	9.8	51.2
FFG_467	519.5	18.0	4.9	52.4	7.9	42.7
FFG_468	571.2	28.0	5.5	82.3	4.6	50.9
FFG_470	557.5	24.7	4.8	72.0	5.5	42.6
FFG_471	510.8	25.3	5.5	68.9	5.5	48.2
FFG_472	468.2	25.9	5.5	31.1	6.1	56.3

TABLE B-2. WELL NAMES AND THICKNESSES (m) OF THE SUPRA-RUSTLER (SURF) AND THE RUSTLER FORMATION MEMBERS (FORTY-NINER [FORTHM], MAGENTA [MAGTHM], TAMARISK [TAMTHM], CULEBRA [CULTHM], AND UNNAMED LOWER [ULMTHM]) IN THE LOS MEDAÑOS STUDY AREA (continued)

WIPPN	SURF	FORTHM	MAGTHM	TAMTHM	CULTHM	ULMTHM
FFG_473	569.1	23.4	4.6	73.2	6.7	44.2
FFG_474	349.9	21.3	6.1	45.8	5.8	36.8
FFG_475	354.0	20.8	5.1	37.5	8.6	39.9
FFG_476	268.3	16.8	7.6	37.2	8.5	40.3
FFG_477	328.3	13.7	9.1	25.0	7.9	39.1
FFG_478	349.2	15.9	6.1	31.0	8.6	38.7
FFG_479	353.9	16.1	6.4	23.2	7.9	37.8
FFG_480	341.7	21.9	6.1	38.4	6.7	39.7
FFG_481	359.1	16.1	6.7	27.4	7.1	39.3
FFG_482	342.0	17.1	5.7	26.9	7.9	38.4
FFG_483	309.1	17.3	6.4	20.2	8.5	41.8
FFG_484	323.4	18.6	5.5	22.2	5.2	48.5
FFG_485	317.1	16.8	5.8	26.5	7.3	40.2
FFG_486	331.3	16.8	6.1	27.4	7.6	39.7
FFG_487	333.1	17.4	6.1	25.0	8.5	37.5
FFG_488	340.6	16.8	4.6	28.3	5.8	43.6
FFG_489	322.0	16.2	6.1	25.0	8.5	45.7
FFG_490	217.0	16.8	6.1	25.9	5.5	35.6
FFG_491	221.6	19.5	6.1	30.5	6.7	40.5
FFG_492	249.9	18.9	6.1	26.9	8.5	36.6
FFG_493	265.6	18.3	5.5	27.4	9.2	33.5
FFG_494	258.2	19.2	6.1	32.0	7.0	33.8
FFG_495	272.9	16.4	5.8	27.4	6.7	46.7
FFG_496	392.9	26.8	4.3	68.3	11.8	48.8
FFG_497	369.1	20.4	5.5	45.7	7.7	40.5
FFG_498	367.9	22.9	5.7	62.8	8.0	48.4
FFG_499	376.1	25.9	4.9	72.2	9.2	53.3
FFG_500	365.5	21.3	6.1	55.2	8.2	52.4
FFG_501	344.1	21.4	6.1	31.0	7.4	40.2
FFG_502	367.6	21.9	5.5	59.2	7.3	63.7
FFG_503	358.7	21.4	4.6	55.4	7.7	42.6
FFG_504	346.9	17.6	6.1	25.6	6.7	48.8
FFG_505	323.1	15.2	5.2	32.0	6.1	45.7
FFG_506	320.6	18.3	5.5	25.3	9.5	41.1
FFG_507	339.1	20.4	4.0	81.4	7.6	50.3
FFG_508	288.6	19.2	5.5	49.7	8.2	51.9
FFG_509	298.7	22.6	6.1	71.0	5.8	46.0
FFG_510	313.2	22.5	6.1	68.6	11.3	43.6
FFG_511	374.6	25.9	5.8	67.4	9.7	48.8
FFG_512	325.2	27.5	6.0	71.1	9.1	57.9
FFG_513	298.0	22.3	5.8	67.9	7.7	53.3
FFG_514	305.4	23.5	5.2	80.1	8.9	59.7
FFG_515	359.7	24.7	5.1	75.6	6.4	54.6
FFG_516	359.1	24.6	5.8	72.9	11.0	55.7
FFG_517	243.8	20.5	5.1	28.4	4.6	18.2
FFG_518	238.4	19.8	6.1	29.8	6.4	15.6
FFG_519	268.2	22.0	3.6	36.0	7.6	36.6
FFG_520	377.8	17.6	3.7	40.8	5.5	42.7

TABLE B-2. WELL NAMES AND THICKNESSES (m) OF THE SUPRA-RUSTLER (SURF) AND THE RUSTLER FORMATION MEMBERS (FORTY-NINER [FORTHM], MAGENTA [MAGTHM], TAMARISK [TAMTHM], CULEBRA [CULTHM], AND UNNAMED LOWER [ULMTHM]) IN THE LOS MEDAÑOS STUDY AREA (continued)

WIPPN	SURF	FORTHM	MAGTHM	TAMTHM	CULTHM	ULMTHM
FFG_521	355.4	18.3	4.6	17.3	4.9	23.5
FFG_522	523.5	27.4	4.6	65.5	6.7	45.1
FFG_523	500.5	24.4	7.6	60.0	6.1	54.3
FFG_524	331.0	18.0	4.3	54.8	8.6	45.7
FFG_525	503.7	29.6	5.2	64.6	7.3	48.2
FFG_526	60.4	-	-	22.8	7.6	32.0
FFG_527	72.8	20.2	5.1	39.4	6.1	17.0
FFG_528	71.9	17.4	8.2	29.9	4.6	27.4
FFG_530	16.2	-	-	34.4	8.2	27.5
FFG_531	78.9	-	-	24.4	6.1	33.6
FFG_532	74.7	-	8.5	27.4	6.7	34.5
FFG_534	74.7	-	-	53.6	9.5	-
FFG_535	56.2	19.8	7.1	30.7	6.4	25.3
FFG_536	67.7	-	-	35.9	8.0	31.0
FFG_537	80.8	-	-	24.7	7.3	32.0
FFG_543	27.0	-	-	38.7	5.5	-
FFG_548	116.7	16.5	6.4	24.4	6.1	-
FFG_552	190.2	-	-	-	10.7	-
FFG_562	310.9	18.3	7.0	23.5	7.3	-
FFG_563	387.4	17.7	7.3	20.1	9.2	-
FFG_568	322.5	-	-	2.7	6.1	-
FFG_569	263.0	18.6	7.4	30.4	8.6	-
FFG_584	233.6	5.5	3.4	21.6	6.1	45.7
FFG_585	294.1	-	-	44.2	8.3	35.0
FFG_600	274.3	1.5	5.5	22.0	7.6	-
FFG_601	338.3	22.6	7.3	35.7	7.3	-
FFG_602	-	-	-	249.6	9.2	50.6
FFG_606	289.9	19.5	7.6	22.2	6.1	64.4
FFG_607	258.2	19.8	4.9	37.1	9.5	47.5
FFG_608	264.0	22.8	5.2	63.4	8.5	61.0
FFG_609	267.0	19.5	6.1	76.2	9.8	60.6
FFG_610	276.5	24.3	9.2	64.0	9.1	51.8
FFG_611	277.4	24.4	4.2	59.2	8.5	56.1
FFG_612	243.7	17.7	3.0	33.6	9.4	44.8
FFG_613	217.4	15.0	7.6	28.0	9.2	46.9
FFG_618	195.1	-	-	15.2	7.6	-
FFG_620	150.1	21.3	7.3	-	-	-
FFG_621	210.9	-	-	-	-	-
FFG_638	383.7	18.6	5.8	30.5	6.7	-
FFG_639	395.2	22.5	6.4	29.3	9.7	-
FFG_640	317.1	18.3	7.7	25.3	11.2	67.1
FFG_643	286.5	19.2	7.3	20.1	5.2	61.0
FFG_644	213.2	17.1	5.2	24.0	6.7	-
FFG_648	402.3	17.1	5.2	22.8	12.8	-
FFG_652	227.7	18.9	6.1	30.8	7.0	29.5
FFG_653	216.1	20.1	5.8	31.4	7.0	27.1
FFG_654	199.0	19.5	5.2	29.0	6.7	26.8
FFG_655	195.7	19.2	4.9	25.9	7.0	27.4

TABLE B-2. WELL NAMES AND THICKNESSES (m) OF THE SUPRA-RUSTLER (SURF) AND THE RUSTLER FORMATION MEMBERS (FORTY-NINER [FORTHM], MAGENTA [MAGTHM], TAMARISK [TAMTHM], CULEBRA [CULTHM], AND UNNAMED LOWER [ULMTHM]) IN THE LOS MEDAÑOS STUDY AREA (continued)

WIPPN	SURF	FORTHM	MAGTHM	TAMTHM	CULTHM	ULMTHM
FFG_656	197.5	17.4	6.1	25.6	6.7	29.6
FFG_657	177.1	16.4	6.1	20.8	6.7	26.2
FFG_658	189.9	16.4	7.4	25.0	6.7	26.5
FFG_659	170.7	15.8	6.4	22.9	8.2	27.5
FFG_660	151.9	17.7	4.6	23.5	7.0	21.3
FFG_662	191.1	18.3	5.5	27.4	6.1	27.1
FFG_664	196.3	19.8	6.4	25.6	5.5	36.0
FFG_666	125.0	17.6	6.1	24.4	6.1	23.8
FFG_667	135.9	17.7	6.1	23.8	6.4	23.5
FFG_668	95.6	-	-	21.6	6.7	14.3
FFG_669	102.1	-	-	21.3	7.1	15.2
FFG_670	103.0	19.2	7.6	22.0	8.2	13.1
FFG_671	127.2	-	-	17.7	8.8	17.7
FFG_672	114.3	18.0	5.8	22.8	7.3	21.7
FFG_673	122.5	-	-	20.5	6.7	17.0
FFG_674	127.7	15.3	6.7	21.6	7.9	25.3
FFG_675	182.4	18.3	6.1	20.1	7.3	25.0
FFG_676	179.5	13.1	7.7	21.9	7.6	22.9
FFG_677	132.0	14.6	7.3	20.8	6.4	26.2
FFG_679	125.9	17.7	6.7	19.2	7.3	22.8
FFG_685	85.4	-	-	-	7.0	85.4
FFG_689	242.0	17.7	5.8	29.2	7.7	38.7
FFG_690	227.4	19.8	6.1	30.2	7.9	42.7
FFG_691	236.2	20.1	5.8	29.6	7.9	41.5
FFG_692	251.5	19.8	6.1	30.4	8.3	-
FFG_693	232.9	20.7	6.1	30.5	6.7	41.1
FFG_694	232.3	20.7	6.1	32.9	7.3	62.8
FFG_695	234.4	19.2	6.1	32.3	7.3	46.6
FFG_696	234.7	18.9	6.4	32.3	6.7	48.5
FFG_697	227.7	18.9	5.5	33.5	6.1	54.2
FFG_698	178.3	19.8	6.1	33.5	6.7	60.4
FFG_699	218.5	18.3	6.1	31.1	6.1	58.5
FFG_700	225.7	18.9	5.5	27.7	4.9	62.2
FFG_701	221.5	22.0	6.7	32.3	8.8	54.3
FFG_702	224.9	18.9	6.1	31.1	8.6	53.3
FFG_703	229.8	18.3	7.3	29.9	7.9	36.9
FFG_704	226.5	20.7	6.1	33.8	8.3	50.9
FFG_705	288.3	19.9	6.0	29.9	7.9	61.0
FFG_706	270.7	18.9	5.4	28.4	7.9	57.3
FFG_707	278.3	20.7	6.1	27.4	9.8	60.3
FFG_708	235.0	18.3	6.1	30.5	7.9	59.1
FFG_709	327.1	17.0	5.8	25.9	7.0	-
FFG_710	324.9	17.1	6.1	27.7	6.4	46.0
FFG_711	318.5	19.2	7.0	33.6	8.5	55.5
FFG_712	282.4	16.8	7.9	32.6	8.8	-
FFG_713	338.8	16.7	7.7	27.4	7.0	-
FFG_714	233.8	20.1	8.3	30.4	6.4	-
FFG_715	225.6	16.7	8.2	33.0	6.7	-

TABLE B-2. WELL NAMES AND THICKNESSES (m) OF THE SUPRA-RUSTLER (SURF) AND THE RUSTLER FORMATION MEMBERS (FORTY-NINER [FORTHM], MAGENTA [MAGTHM], TAMARISK [TAMTHM], CULEBRA [CULTHM], AND UNNAMED LOWER [ULMTHM]) IN THE LOS MEDAÑOS STUDY AREA (continued)

WIPPN	SURF	FORTHM	MAGTHM	TAMTHM	CULTHM	ULMTHM
FFG_716	362.7	17.1	4.2	71.7	7.6	44.2
FFG_717	333.6	19.2	5.2	25.9	7.0	43.3
FFG_718	321.4	16.8	5.8	36.2	8.6	43.3
FFG_719	343.7	17.3	5.2	48.2	7.3	47.5
FFG_720	320.3	20.5	7.6	45.7	11.3	43.9
FFG_721	328.9	18.9	5.5	27.4	6.7	45.1
FFG_723	246.1	16.5	6.4	22.5	7.7	42.6
FFG_724	305.3	19.8	5.5	27.1	8.5	44.2
FFG_725	317.3	17.4	5.2	36.8	6.4	36.0
FFG_726	319.7	16.2	5.2	28.9	7.6	51.9
FFG_727	317.9	22.9	5.1	35.7	8.5	55.2
FFG_728	315.8	18.6	4.5	26.6	8.5	47.8
FFG_729	307.8	17.7	5.2	34.8	7.9	45.1
FFG_730	294.1	19.2	4.3	27.7	8.3	42.6
FFG_731	301.6	17.7	5.2	27.4	7.6	45.1
FFG_732	300.8	18.9	7.4	26.8	8.2	-
FFG_733	221.9	18.9	6.4	31.4	7.9	43.6
FFG_734	270.4	16.7	4.9	29.6	8.2	45.1
FFG_735	312.4	19.5	5.5	40.2	8.6	46.3
FFG_736	266.9	19.6	6.7	56.0	8.6	52.4
FFG_737	337.9	19.8	4.0	58.5	8.5	52.5
FFG_738	304.5	16.8	4.5	30.5	7.6	44.2
FFG_739	261.2	19.5	4.6	35.0	11.0	55.2
FFG_740	260.9	18.0	6.1	68.0	9.4	44.2
FFG_741	293.5	18.3	5.2	39.0	7.6	48.8
FFG_742	249.3	20.8	5.1	47.9	10.0	44.2
FFG_743	256.0	16.8	5.2	49.1	10.9	44.5
FFG_744	272.8	16.8	5.1	40.6	6.4	40.8
FFG_745	276.1	21.4	3.0	48.2	7.3	52.1
FFG_746	287.7	20.7	6.1	47.5	8.3	55.4
H-1	153.0	18.6	7.9	26.5	7.1	38.1
H-2	139.3	17.7	8.5	24.4	6.7	36.3
H-3	153.0	17.4	7.6	26.8	6.7	38.7
H-4	96.0	18.9	7.9	26.6	7.9	33.5
H-5	223.1	17.1	7.3	26.5	7.6	35.7
H-6	130.1	19.3	7.3	27.4	7.0	28.7
H-7	26.5	9.2	7.0	29.5	11.3	2.8
H-8	121.6	20.4	6.7	30.5	7.9	36.3
H-9	138.7	20.7	9.5	28.3	9.1	34.8
H-10	367.0	15.8	7.3	24.4	9.5	33.5
H-11	241	-	-	-	7.6	-
H-12	251.0	-	-	-	8.2	-
H-14	166.1	-	7.3	-	7.9	-
H-15	262.4	-	-	-	6.7	-
H-16	213.9	-	7.9	-	6.7	-
H-17	215.2	-	-	-	7.6	-
H-18	210.0	-	-	-	7.3	-
P-1	109.1	19.8	7.7	27.4	8.2	34.1

TABLE B-2. WELL NAMES AND THICKNESSES (m) OF THE SUPRA-RUSTLER (SURF) AND THE RUSTLER FORMATION MEMBERS (FORTY-NINER [FORTHM], MAGENTA [MAGTHM], TAMARISK [TAMTHM], CULEBRA [CULTHM], AND UNNAMED LOWER [ULMTHM]) IN THE LOS MEDAÑOS STUDY AREA (concluded)

WIPPN	SURF	FORTHM	MAGTHM	TAMTHM	CULTHM	ULMTHM
P-2	210.3	17.7	7.6	25.6	7.9	38.1
P-3	142.6	18.6	7.4	27.1	7.0	36.9
P-4	185.6	16.2	7.3	27.1	8.2	39.1
P-5	189.9	19.2	7.6	28.4	7.0	36.5
P-6	108.8	18.3	7.9	28.7	7.0	30.2
P-7	95.1	18.6	7.6	29.9	7.9	32.9
P-8	119.2	18.0	7.3	27.1	7.6	38.7
P-9	171.3	16.8	8.2	27.4	7.0	37.8
P-10	209.1	21.6	7.3	45.8	7.9	39.3
P-11	227.1	16.1	7.7	27.1	7.9	36.6
P-12	140.5	17.7	7.3	27.4	7.0	28.4
P-13	130.1	19.3	7.3	27.4	7.0	28.7
P-14	118.0	20.1	7.3	29.3	6.7	28.0
P-15	70.4	19.2	8.2	28.1	6.7	32.6
P-16	96.3	18.3	7.6	30.2	7.0	37.5
P-17	116.4	17.1	7.6	29.0	7.6	40.2
P-18	191.4	23.2	7.9	54.6	8.8	45.7
P-19	231.0	17.1	7.6	39.0	9.2	36.6
P-20	237.7	18.0	8.3	26.5	7.9	37.8
P-21	223.7	16.5	7.3	26.5	7.6	36.3
ERDA-6	163.4	18.0	7.9	27.1	7.6	24.4
ERDA-9	164.0	17.7	7.3	25.6	7.0	36.9
ERDA-10	111.6	-	5.7	27.8	8.5	37.8
AEC-7	201.8	21.6	7.9	33.9	7.9	29.0
AEC-8	201.2	16.7	7.0	29.0	7.9	38.4
WIPP-11	202.1	19.5	7.0	28.7	7.0	25.6
WIPP-12	191.4	18.9	7.6	29.0	7.6	36.6
WIPP-13	157.6	14.3	5.8	36.0	7.0	36.6
WIPP-15	-	-	-	-	-	-
WIPP-16	349.9	12.5	3.1	.	7.0	-
WIPP-18	186.8	18.0	7.3	27.5	6.7	36.6
WIPP-19	179.5	17.7	7.6	25.6	6.4	35.7
WIPP-21	170.7	17.7	7.0	26.8	7.3	35.1
WIPP-22	174.7	17.3	7.3	26.9	6.7	36.2
WIPP-25	70.7	21.3	8.0	36.2	7.7	28.3
WIPP-26	3.0	18.3	8.9	26.5	7.0	30.5
WIPP-27	46.6	7.0	5.5	29.9	7.9	29.9
WIPP-28	65.5	21.4	7.6	33.5	7.9	25.9
WIPP-29	-	-	-	3.7	9.1	30.8
WIPP-30	136.9	19.5	7.3	28.6	7.0	29.0
WIPP-32	-	5.8	5.2	7.6	8.8	23.2
WIPP-33	121.3	15.6	5.7	25.0	8.6	24.1
WIPP-34	200.3	18.5	7.1	28.3	7.9	34.5
B-25	162.5	18.2	7.4	26.5	7.3	35.0
USGS-1	-	-	-	-	-	-
ENGLE	200.9	-	-	-	6.7	-
DOE-1	250.2	-	-	-	6.7	-
CABIN-1	153.3	-	-	-	7.9	-

TABLE B-3. DATA BASE FOR SUPRA-RUSTLER FORMATION UNITS (ALLUVIUM THICKNESS [ALLUVM], TOP OF DEWEY LAKE RED BEDS [DLTOPM], DEWEY LAKE THICKNESS [DLTHKM] IN METERS]. UTMX AND UTMY ARE THE UNIVERSAL TRANSVERSE MERCATOR COORDINATES

OBS	TN	RNG	SEC	UTMX	UTMY	ALLUVM	DLTOPM	DLTHKM
1	20	29	25	590555	3601690	0.0	1010.4	25.6
2	20	29	28	586752	3600672	0.0	996.7	117.9
3	20	29	32	593958	3598805	66.4	921.1	14.0
4	20	29	36	600006	3599298	7.3	1027.4	53.3
5	20	30	32	595208	3599627	17.6	1007.6	34.1
6	20	30	35	607676	3598841	11.5	1025.0	217.0
7	20	31	30	603243	3600398	46.6	1043.3	141.7
8	20	32	10	616468	3606754	114.6	931.4	132.5
9	21	27	13	636745	3594033	10.0	954.0	27.4
10	21	27	35	636184	3590214	0.0	954.0	14.9
11	21	27	36	639526	3589243	0.0	945.1	4.5
12	21	28	2	588017	3597286	49.0	962.5	136.8
13	21	28	5	583564	3596707	30.4	950.0	43.8
14	21	28	12	590847	3595289	0.0	1023.2	21.0
15	21	28	15	586424	3593240	8.2	986.9	24.0
16	21	28	20	583988	3592021	17.3	959.2	33.5
17	21	28	27	587665	3590039	0.0	970.1	15.2
18	21	28	29	583988	3590814	0.0	969.8	11.5
19	21	28	29	583610	3590146	0.0	968.3	2.1
20	21	28	33	584828	3588367	0.0	957.6	70.4
21	21	28	35	588569	3588322	32.0	933.9	15.5
22	21	28	35	589481	3589846	0.0	968.6	18.5
23	21	28	35	588369	3589536	10.3	959.8	4.5
24	21	29	3	596362	3598010	14.6	1019.2	35.9
25	21	29	4	594776	3597648	16.4	1036.0	39.0
26	21	29	6	592332	3597631	0.0	1057.6	246.5
27	21	29	18	591979	3593600	39.6	964.0	0.0
28	21	29	19	592398	3591591	15.2	-15.2	21.3
29	21	29	22	596801	3592441	0.0	1048.5	85.9
30	21	29	34	596430	3589626	0.0	1044.2	55.4
31	21	30	5	602380	3597026	0.0	1031.1	45.1
32	21	30	21	604425	3593073	24.0	944.2	22.5
33	21	30	26	607832	3590109	42.3	941.2	93.8
34	21	30	35	607401	3588903	7.3	966.8	24.0
35	21	31	18	611265	3594687	3.6	1016.5	61.8
36	21	31	33	613718	3589700	0.0	1044.8	136.8
37	21	31	35	618226	3589011	21.6	1057.3	141.7
38	21	32	1	628708	3596750	311.5	838.8	155.1
39	21	32	2	627501	3596750	314.5	834.8	155.7
40	21	32	2	626669	3597926	292.6	840.9	167.3
41	21	32	4	623730	3598370	230.1	883.3	175.2
42	21	32	10	625894	3595919	240.1	912.8	195.9
43	21	32	31	621117	3589387	34.1	1079.6	167.6
44	21	32	31	621117	3589387	34.1	1079.6	167.6

TABLE B-3. DATA BASE FOR SUPRA-RUSTLER FORMATION UNITS (ALLUVIUM THICKNESS [ALLUVM], TOP OF DEWEY LAKE RED BEDS [DLTOPM], DEWEY LAKE THICKNESS [DLTHKM] IN METERS]. UTMX AND UTMY ARE THE UNIVERSAL TRANSVERSE MERCATOR COORDINATES (continued)

OBS	TN	RNG	SEC	UTMX	UTMY	ALLUVM	DLTOPM	DLTHKM
45	22	28	2	588569	3588121	10.0	957.9	37.4
46	22	28	22	586813	3582740	0.0	943.3	32.9
47	22	28	25	590526	3580760	0.0	965.6	40.5
48	22	28	27	586796	3581108	0.0	936.9	19.8
49	22	30	1	609459	3587000	-3.0	1020.1	93.2
50	22	30	2	608244	3586901	43.8	923.8	0.9
51	22	30	11	608252	3586095	75.8	898.8	0.9
52	22	30	13	609629	3584019	12.1	1000.6	109.1
53	22	30	15	606391	3584037	3.0	976.2	67.6
54	22	30	24	610454	3583452	2.4	1025.9	138.0
55	22	30	24	609083	3581974	12.8	1011.3	105.1
56	22	30	27	606666	3581659	0.0	1001.5	56.6
57	22	30	27	606666	3581659	20.4	983.8	39.0
58	22	30	29	604006	3581161	0.0	960.7	3.0
59	22	30	36	609954	3578869	8.8	1005.2	57.3
60	22	31	1	618629	3586910	36.8	1045.4	153.0
61	22	31	6	610665	3587721	0.0	1029.0	117.6
62	22	31	9	613819	3586474	49.0	995.1	153.0
63	22	31	9	614333	3585141	46.9	999.4	153.3
64	22	31	11	617522	3586435	50.2	1026.2	150.8
65	22	31	14	618541	3583770	79.5	1003.4	158.1
66	22	31	15	616315	3584158	57.6	1001.5	156.9
67	22	31	15	616900	3584802	68.5	1000.3	154.5
68	22	31	15	616901	3584847	68.5	1000.9	155.1
69	22	31	17	613686	3583535	44.5	1013.4	145.3
70	22	31	17	613709	3583524	47.2	1011.0	144.1
71	22	31	17	612652	3584241	20.1	1017.7	137.4
72	22	31	18	610609	3585027	11.5	1008.8	118.5
73	22	31	18	610539	3585079	11.5	1007.9	118.5
74	22	31	20	613532	3583327	13.7	1025.3	148.7
75	22	31	20	612799	3581888	12.4	1018.6	130.1
76	22	31	20	613697	3581958	15.5	1026.5	148.4
77	22	31	20	613731	3583179	42.0	1011.3	144.7
78	22	31	20	613747	3582787	29.2	1017.1	150.2
79	22	31	20	613747	3582349	22.2	1019.2	148.4
80	22	31	20	613747	3582652	24.3	1019.8	150.2
81	22	31	20	611695	3580609	13.7	1025.3	148.7
82	22	31	23	618474	3582021	66.1	1026.8	161.5
83	22	31	23	617016	3583462	68.2	999.7	158.8
84	22	31	23	617687	3582410	70.7	1009.8	160.3
85	22	31	26	617074	3581193	46.0	1023.5	163.0
86	22	31	26	618367	3580352	26.5	1033.2	164.8
87	22	31	28	615315	3581850	49.9	1010.4	160.3
88	22	31	28	614936	3580324	30.1	1019.5	155.4

TABLE B-3. DATA BASE FOR SUPRA-RUSTLER FORMATION UNITS (ALLUVIUM THICKNESS [ALLUVM], TOP OF DEWEY LAKE RED BEDS [DLTOPM], DEWEY LAKE THICKNESS [DLTHKM] IN METERS). UTMX AND UTMY ARE THE UNIVERSAL TRANSVERSE MERCATOR COORDINATES (continued)

OBS	TN	RNG	SEC	UTMX	UTMY	ALLUVM	DLTOPM	DLTHKM
89	22	31	29	613420	3581687	10.6	1025.0	142.3
90	22	31	29	612663	3581662	11.5	1018.0	127.7
91	22	31	29	613735	3580895	6.7	1026.5	146.3
92	22	31	29	612339	3580339	12.1	1007.3	96.9
93	22	31	30	610591	3581133	5.4	1016.8	103.3
94	22	31	31	610624	3578793	9.7	999.1	60.6
95	22	31	33	615365	3579125	20.1	1019.8	151.1
96	22	32	14	627262	3583857	105.1	1028.7	180.1
97	22	32	17	622836	3584196	120.0	1001.8	144.4
98	22	32	18	621627	3583775	103.6	1018.3	166.1
99	22	32	19	621646	3582157	67.3	1033.2	162.1
100	22	32	25	628878	3581872	163.0	984.2	147.8
101	22	32	36	629713	3580287	178.3	963.4	167.6
102	23	29	28	595692	3570883	0.0	908.3	1.8
103	23	30	1	610081	3577672	0.0	1006.1	56.6
104	23	30	14	608086	3574632	17.3	946.7	9.1
105	23	30	24	609182	3573205	38.1	957.6	0.9
106	23	30	24	609182	3573205	8.2	987.5	30.4
107	23	30	34	606684	3570523	46.0	981.4	65.5
108	23	31	2	618415	3578487	15.5	1033.8	171.6
109	23	31	4	613827	3578467	11.8	1005.8	107.2
110	23	31	4	613929	3577459	14.0	1002.7	102.4
111	23	31	5	612404	3578497	8.8	1007.3	87.1
112	23	31	5	612305	3578476	13.7	1001.8	81.3
113	23	31	5	612704	3577312	9.7	1001.5	86.5
114	23	31	11	618558	3575680	55.4	1005.8	168.5
115	23	31	14	617677	3574462	71.0	990.9	164.5
116	23	31	21	615274	3572430	97.8	927.8	40.2
117	23	31	23	618192	3572457	101.4	950.0	131.9
118	23	31	26	618192	3571652	54.8	994.8	173.1
119	23	31	26	618091	3571652	47.8	999.7	173.4
120	23	31	27	615699	3571221	17.0	1016.2	130.4
121	23	31	29	613285	3571206	106.0	915.6	0.0
122	23	31	32	612475	3570378	0.0	1021.0	109.7
123	23	31	36	618940	3569255	58.8	1011.6	171.2
124	23	32	3	626522	3578211	189.8	942.7	158.4
125	23	32	9	624541	3575777	174.0	950.0	169.7
126	23	32	11	627739	3576635	188.9	944.2	172.2
127	23	32	15	626158	3575003	189.8	940.9	165.2
128	23	32	18	621734	3574920	140.5	957.0	165.2
129	23	32	20	622977	3572600	199.0	924.4	166.4
130	23	32	20	622976	3572449	200.5	923.2	166.4
131	23	32	21	624563	3573759	187.1	937.8	163.3
132	23	32	24	629928	3572946	208.7	922.0	164.2

TABLE B-3. DATA BASE FOR SUPRA-RUSTLER FORMATION UNITS (ALLUVIUM THICKNESS [ALLUVM], TOP OF DEWEY LAKE RED BEDS [DLTOPM], DEWEY LAKE THICKNESS [DLTHKM] IN METERS]. UTMX AND UTMY ARE THE UNIVERSAL TRANSVERSE MERCATOR COORDINATES (continued)

OBS	TN	RNG	SEC	UTMX	UTMY	ALLUVM	DLTOPM	DLTHKM
133	23	32	24	629827	3572644	209.3	922.0	163.0
134	23	32	25	629946	3571133	193.8	929.9	170.9
135	23	32	25	629107	3572102	196.5	934.2	170.6
136	23	32	25	629107	3572102	198.1	927.2	169.4
137	23	32	26	627420	3570965	201.7	910.1	167.0
138	23	32	26	628323	3571395	198.4	928.4	169.1
139	23	32	28	624184	3572130	190.5	933.3	169.1
140	23	32	31	620546	3569268	98.7	981.1	161.5
141	23	32	34	626737	3569761	189.2	914.1	164.5
142	23	32	35	627842	3569787	191.7	923.8	167.0
143	23	32	35	627521	3570060	188.3	932.9	172.5
144	23	32	35	627018	3570160	198.1	915.9	165.2
145	23	32	35	628122	3570289	197.5	924.1	164.5
146	23	32	35	627719	3570289	192.6	929.9	172.2
147	23	32	36	628625	3570188	194.7	918.6	170.6
148	23	32	36	629464	3569834	179.2	937.2	181.3
149	24	29	27	596315	3560963	0.0	888.1	133.8
150	24	30	23	607685	3562746	98.7	939.0	37.7
151	24	30	23	608656	3563541	46.6	999.7	74.9
152	24	30	25	609337	3561151	110.6	930.8	33.2
153	24	30	29	604032	3561080	0.0	993.9	133.5
154	24	31	1	619350	3568028	57.3	1019.2	177.0
155	24	31	2	617729	3568422	69.1	991.2	183.4
156	24	31	3	616941	3567615	27.7	1036.3	175.2
157	24	31	4	614612	3568483	19.8	1017.7	114.3
158	24	31	4	614511	3568385	14.3	1022.6	114.3
159	24	31	4	615316	3568812	10.6	1033.5	133.8
160	24	31	4	613965	3568233	7.3	1030.8	131.3
161	24	31	6	611273	3568414	38.7	1002.1	99.6
162	24	31	6	611273	3568414	38.1	1002.7	100.2
163	24	31	7	612154	3565951	0.0	1074.1	178.3
164	24	31	7	612154	3565951	43.8	1030.2	135.6
165	24	31	11	618143	3567223	60.0	1011.3	170.0
166	24	31	17	613758	3565566	39.9	1041.8	161.5
167	24	31	18	612171	3564340	33.5	1034.1	138.6
168	24	31	20	612992	3562725	45.1	1014.9	112.4
169	24	31	20	613776	3563957	24.0	1048.5	156.9
170	24	31	21	615380	3563980	40.8	1033.2	166.7
171	24	31	21	614199	3562745	28.9	1037.2	151.4
172	24	31	24	619811	3562825	45.1	1033.5	162.4
173	24	31	28	615418	3561157	40.2	1020.1	134.4
174	24	31	35	617438	3559994	53.9	1007.6	130.4
175	24	32	1	629485	3567808	190.5	909.8	166.7
176	24	32	2	628244	3568580	165.8	937.8	187.4

TABLE B-3. DATA BASE FOR SUPRA-RUSTLER FORMATION UNITS (ALLUVIUM THICKNESS [ALLUVM], TOP OF DEWEY LAKE RED BEDS [DLTOPM], DEWEY LAKE THICKNESS [DLTHKM] IN METERS]. UTMX AND UTMY ARE THE UNIVERSAL TRANSVERSE MERCATOR COORDINATES (concluded)

OBS	TN	RNG	SEC	UTMX	UTMY	ALLUVM	DLTOPM	DLTHKM
177	24	32	2	627444	3568551	185.0	918.9	171.9
178	24	32	6	621409	3568885	104.8	985.1	163.3
179	24	32	10	626275	3566554	173.7	929.0	154.2
180	24	32	11	628292	3566167	191.1	914.1	168.2
181	24	32	15	626701	3564948	150.5	940.9	184.7
182	24	32	15	625893	3564517	142.0	952.2	167.0
183	24	32	15	626299	3564546	149.3	951.5	170.6
184	24	32	15	626683	3564546	173.7	922.3	165.2
185	24	32	22	626323	3563337	145.9	950.3	170.6
186	24	32	22	626299	3564143	148.4	946.1	171.9
187	24	32	23	628316	3564175	151.7	943.9	176.4
188	24	32	23	627104	3563741	154.5	943.0	176.1
189	24	32	33	625107	3559688	88.3	978.4	161.5
190	25	29	8	594349	3556099	0.0	888.1	6.4
191	25	29	14	598396	3554904	0.0	945.1	162.4
192	25	29	15	596378	3554488	0.0	926.5	89.3
193	25	32	9	625251	3556373	76.2	0.0	160.9
194	25	32	10	625526	3557677	76.5	980.5	157.5
195	25	32	10	626238	3557256	74.9	978.1	161.8
196	25	32	10	625526	3557677	106.3	944.8	128.0
197	25	32	10	625553	3556776	108.8	945.4	130.1
198	25	32	10	626263	3557002	59.1	994.8	174.0
199	25	32	10	625955	3556876	85.9	-85.9	153.3
200	25	32	10	625928	3557677	88.3	968.6	149.3
201	25	32	10	625928	3557275	0.0	0.0	231.9
202	25	32	10	625526	3557275	97.5	957.6	138.9
203	25	32	15	626364	3555694	112.7	934.8	117.6
204	25	32	31	620746	3550770	174.6	833.9	152.4

TABLE B-4. UNIVERSAL TRANSVERSE MERCATOR (UTM), AND STATE (STATE) COORDINATES FOR THE WIPP TEST HOLES

WELL NAME	UTM-X	UTM-Y	STATE-X	STATE-Y
WASTE SHAFT	613,579	3,582,079	666,919.9	499,287.2
EXHAUST SHAFT	613,717	3,582,080	667,370.4	499,287.2
AIR-INTAKE SHAFT	613,159	3,582,200	666,270.0	499,687.1
C&SH SHAFT	613,574	3,582,202	666,894.9	499,687.2
AEC-7	621,126	3,589,381	691,829	523,133
AEC-8	617,525	3,586,442	679,951	513,567
CABIN BABY	613,191	3,578,049	665,559	486,111
DOE-1	615,203	3,580,333	672,206	493,563
DOE-2	613,683	3,585,294	667,317	509,876
ENGLE (est.)	615,106	3,567,466	671,622	451,337
ERDA-6	618,220	3,589,008	682,279	521,970
ERDA-9	613,696	3,581,958	667,303	498,888
ERDA-10	606,685	3,570,515	644,058	461,520
H-1	613,423	3,581,684	666,400	497,991
H-2A	612,663	3,581,641	663,898	497,913
H-2B1	612,651	3,581,651	663,860	497,943
H-2B2	612,661	3,581,648	663,890	497,934
H-2C	612,666	3,581,668	663,907	498,002
H-3B1	613,729	3,580,895	667,377	495,440
H-3B2	613,701	3,580,906	667,283	495,476
H-3B3	613,705	3,580,876	667,298	495,376
H-3D	613,721	3,580,890	667,350	495,421
H-4A	612,407	3,578,469	662,993	486,962
H-4B	612,380	3,578,483	662,906	487,554
H-4C	612,406	3,578,499	662,991	487,607
H-5A	616,888	3,584,776	677,828	508,111
H-5B	616,872	3,584,801	677,777	508,194
H-5C	616,903	3,584,802	677,878	508,198
H-6A	610,580	3,584,982	657,132	508,881
H-6B	610,594	3,585,008	657,180	508,969
H-6C	610,610	3,584,983	657,232	508,884
H-7A	608,102	3,574,670	648,790	475,132
H-7B	608,124	3,574,648	648,862	475,061
H-7B2	608,111	3,574,612	648,812	474,967
H-7C	608,095	3,574,640	648,766	475,035
H-8A	618,658	3,563,566	650,392	438,678
H-8B	608,683	3,563,556	650,473	438,646
H-8C	608,664	3,563,537	650,409	438,581
H-9A	613,958	3,568,260	667,879	453,977
H-9B	613,989	3,568,261	667,979	453,978
H-9C	613,974	3,568,234	667,929	453,890
H-10A	622,949	3,572,457	697,463	467,561
H-10B	622,975	3,572,473	697,549	467,613
H-10C	622,976	3,572,443	697,550	467,513
H-11B1	618,346	3,579,130	672,647	489,617

Source: Modified from Gonzalez, 1989

TABLE B-4. UNIVERSAL TRANSVERSE MERCATOR (UTM), AND STATE (STATE) COORDINATES FOR THE WIPP TEST HOLES (continued)

WELL NAME	UTM-X	UTM-Y	STATE-X	STATE-Y
H-11B2	615,348	3,579,107	672,653	489,542
H-11B3	615,367	3,579,127	672,716	489,608
H-11B4	615,313	3,579,131	672,523	489,622
H-12	617,023	3,575,452	678,079	477,535
H-14	612,641	3,580,354	662,815	493,697
H-15	615,315	3,581,859	672,606	498,572
H-16	613,369	3,582,212	666,231.8	499,726.1
H-17	615,718	3,577,513	673,837	484,304
H-18	612,264	3,583,166	662,621	502,926
P-1	612,338	3,580,341	662,804	493,651
P-2	615,316	3,581,848	672,609	498,536
P-3	612,799	3,581,898	664,351	498,747
P-4	614,935	3,580,319	671,327	493,521
P-5	613,685	3,583,535	667,290	504,103
P-6	610,609	3,581,084	657,144	496,090
P-7	612,308	3,578,478	662,669	487,090
P-8	613,830	3,578,467	667,664	487,471
P-9	615,356	3,579,125	672,678	489,599
P-10	617,087	3,581,203	678,410	496,383
P-11	617,016	3,583,457	678,217	503,781
P-12	610,456	3,583,452	656,692	503,896
P-13	610,531	3,585,029	656,973	509,039
P-14	609,084	3,581,976	652,159	499,082
P-15	610,624	3,578,793	657,148	488,610
P-16	612,695	3,577,321	663,914	483,737
P-17	613,926	3,577,466	667,955	484,185
P-18	618,367	3,580,350	682,589	493,556
P-19	617,681	3,582,418	680,377	500,362
P-20	618,532	3,583,768	683,197	504,767
P-21	616,898	3,584,849	677,862	508,351
WIPP-11	613,791	3,586,475	667,700	513,751
WIPP-12	613,710	3,583,524	667,371	504,068
WIPP-13	612,644	3,584,247	663,885	506,464
WIPP-14	613,080	3,585,103	665,336	509,260
WIPP-15 (approx)	649,871	3,575,041	785,854	475,695
WIPP-16	603,987	3,597,048	632,738	548,644
WIPP-18	613,735	3,583,179	667,446	502,935
WIPP-19	613,739	3,582,782	667,453	501,632
WIPP-21	613,743	3,582,319	667,459.4	500,071.3
WIPP-22	613,739	3,582,653	667,453.8	501,165.7
WIPP-25	606,385	3,584,028	643,343	505,868
WIPP-26	604,014	3,581,162	635,509	496,516
WIPP-27	604,426	3,593,079	637,103	535,612
WIPP-28	611,266	3,594,680	659,579	540,722
WIPP-29	596,981	3,578,694	612,378	488,559
WIPP-30	613,721	3,589,701	667,536	524,337

Source: Modified from Gonzalez, 1989

TABLE B-4. UNIVERSAL TRANSVERSE MERCATOR (UTM), AND STATE (STATE) COORDINATES FOR THE WIPP TEST HOLES (concluded)

WELL NAME	UTM-X	UTM-Y	STATE-X	STATE-Y
WIPP-31	617,318	3,598,952	679,527	554,620
WIPP-32	595,904	3,579,081	608,848	489,850
WIPP-33	609,630	3,584,019	653,981	505,790
WIPP-34	614,334	3,585,142	669,449	509,375
WIPP-35	613,614	3,586,322	667,122	513,251

Source: Modified from Gonzalez, 1989

TABLE B-5. RESULTS OF AQUIFER TESTING PROGRAM

Well #	Well Location (T.R.S.¼.¼.¼)	Test Date (mm/dd/yy)	Pumping Rate (gpm)	Transmissivity ft^2/day	Depth to Water (ft)	Hydraulic Conductivity (ft/day)	Porosity	Storage Coefficient	Unit
AQUIFER TESTS									
1	19.30.33.31	12/19,21/78	3.5	35	20.66	1.59	0.15		Forty-niner
2	20.30.15.31	12/28,29/78	14.7	470	2.90	26.11	.20		Quaternary playa lake
3	20.30.23.11	12/29,30/78	3.8	12	72.99	1.2	.30		Dewey Lake (?)
4	20.32.17.13	12/19,22/78	10	350	9.66	6.63	.20		Quaternary playa lake
5	20.32.22.33	12/19/78	10	5	29.77	.5	.30		Triassic (undiff.)
6	21.29.25.423a	01/11,12/79	4.5	20	67.5	--			Culebra(?)
7	21.29.25.423b	01/11,12/79		7				9.6×10^{-6}	Culebra(?)
8	21.31.3.22	01/5,7/79	6.8	35	140.81	1.12	.30		Triassic (undiff.)
9	23.29.18.14	01/4,5/79	12	185	7.10	6.6	.20		Quaternary alluvium
10	20.33	01/18/79	17.6	135	23.0	12.29	.12		Culebra
11	28.41	12/15,18/78	11	40	40.96	5	.12		Tamarisk
		01/9,10/79	10		41.05	5			

			Slug Volume (gal)	Transmissivity (ft_2/day)	Depth to Water (ft)	Hydraulic Conductivity (ft/day)	Porosity	Storage Coefficient	Unit
SLUG TESTS									
12	19.30. 5.32	03/14/79	10	14	141.31	0.646	0.2	1×10^{-2}	Quaternary valley fill
13	24.133	03/07/79	1st test: 6 gal. brine 2nd test: 6 1/2 gal. fresh	251	52.13	25.1	.15	1×10^{-10}	Dewey Lake(?)
14	35.23	03/14/79	10	9.4	79.65	1.045	.30	1×10^{-2}	Dewey Lake(?)
15	20.29.25.33	03/08/79	10	330	87.27	3.90	.15	1×10^{-14}	Forty-niner
16	20.30.28.4	03/08/79	6.5	0.6	171.24	.0032	.30	1×10^{-2}	Dewey Lake(?)
17	29.31	03/13/79	10	3.0	134.63	.3775	.30	1×10^{-10}	Dewey Lake(?)
18	20.31. 2.34	03/12/79	10	.97	136.55	.060	.30	1×10^{-6}	Triassic (undiff.)
19	27.24	03/08/79	10	.44	114.43	.04	.30	1×10^{-4}	Triassic (undiff.)
20	23.29.26.12	03/06/79	10	.13	107.75	.02	.30	1×10^{-8}	Dewey Lake(?), Forty-niner

Source: Modified from Geohydrology Associates, Inc., 1979, Tables 1 and 2 and Appendix

TABLE B-6. WATER LEVELS OF WELLS IN THE ALLUVIAL AQUIFERS IN THE LOS MEDAÑOS STUDY AREA

Well Name			Location	Well Depth		Well Altitude		Water Elevation		Depth to Water	
				(ft)	(m)	(ft)	(m)	(ft)	(m)	(ft)	(m)
001	EDDY	ALVM	20.30.03.223	0	0.000	3175	967.74	3169	965.91	6.00	1.829
004	EDDY	ALVM	21.28.18.130	0	0.000	3150	960.12	3131	954.33	18.90	5.761
009	EDDY	ALVM	22.29.33.240	65	19.812	3020	920.50	2964	903.43	56.20	17.130
011	EDDY	ALVM	23.28.20.144	250	76.200	3060	932.69	3004	915.62	56.10	17.099
017	LEA	ALVM	20.32.01.322	30	9.144	3510	1069.85	3488	1063.14	21.80	6.645
018	LEA	ALVM	20.32.30.142	0	0.000	3530	1075.94	3520	1072.90	9.90	3.018
021	LEA	ALVM	24.32.10.344	60	18.288	3589	1093.93	3569	1087.83	19.93	6.075
022	LEA	ALVM	24.33.10.113	36	10.973	3595	1095.76	3570	1088.14	24.60	7.498
025	LEA	ALVM	26.33.03.444	180	54.864	3315	1010.41	3212	979.02	102.80	31.333
038	LEA	ALVM	25.33.03.233	122	37.186	3219	981.15	3111	948.23	108.04	32.931
067	EDDY	ALVM	22.28.04.131	0	0.000	~3140	957.1	3087	940.9	53.05	16.170
068	EDDY	ALVM	22.28.30.443	200	60.960	3042	927.20	3017	919.58	24.95	7.605
081	EDDY	ALVM	23.28.05.111	210	64.008	3040	926.6	2991	911.6	49.13	14.975
083	EDDY	ALVM	23.28.11.114	100	30.480	2990	911.35	2976	907.08	14.34	4.371
084	EDDY	ALVM	23.28.14.241	80	24.384	2980	908.3	2932	893.8	47.56	14.496
085	EDDY	ALVM	23.28.18.333	287	87.478	3083	939.70	3006	916.23	77.44	23.604
086	EDDY	ALVM	23.28.20.144	250	76.200	3060	932.69	2990	911.35	69.50	21.184
087	EDDY	ALVM	23.28.23.133	148	45.110	3020	920.50	2960	902.21	60.04	18.300
088	EDDY	ALVM	23.28.24.134	96	29.261	2991	911.66	2948	898.55	42.90	13.076
089	EDDY	ALVM	23.28.25.213	80	24.384	2980	908.30	2942	896.72	38.10	11.613
090	EDDY	ALVM	23.28.31.231	93	28.346	3124	952.20	3064	933.91	60.34	18.392
091	EDDY	ALVM	23.28.33.141	225	68.580	3095	943.36	3077	937.87	18.48	5.633
092	EDDY	ALVM	23.28.36.244	75	22.860	2960	902.21	2925	891.54	35.49	10.817
093	EDDY	ALVM	23.30.06.424	30	9.144	2978	907.69	2978	907.69	0.00	0.000
102	EDDY	ALVM	24.28.11.442	200	60.960	2978	907.69	2941	896.42	37.19	11.336
104	EDDY	ALVM	24.28.16.331	161	49.073	3048	929.03	3010	917.45	37.50	11.430
105	EDDY	ALVM	24.28.17.142	0	0.000	3058	932.08	3031	923.85	27.42	8.358
106	EDDY	ALVM	24.28.25.123	100	30.480	2925	891.54	2923	890.93	1.90	0.579
107	EDDY	ALVM	24.28.26.231	126	38.405	2940	896.1	2912	887.7	27.57	8.403

Source: Modified from Richey and others, 1985

TABLE B-6. WATER LEVELS OF WELLS IN THE ALLUVIAL AQUIFERS IN THE LOS MEDAÑOS STUDY AREA (concluded)

Well Name			Location	Well Depth		Well Altitude		Water Elevation		Depth to Water	
				(ft)	(m)	(ft)	(m)	(ft)	(m)	(ft)	(m)
108	EDDY	ALVM	24.31.17.131	0	0.000	3516	1071.68	3450	1051.56	65.97	20.108
118	EDDY	ALVM	25.28.03.222	0	0.000	2985	909.83	2952	899.77	32.97	10.049
125	EDDY	ALVM	26.30.05.334	770	234.696	3091	942.14	2920	890.02	171.35	52.227
135	EDDY	ALVM	22.28.15.334A	86	26.213	3095	943.36	3020	920.50	75.40	22.982
136	EDDY	ALVM	25.30.07.111	386	117.653	3170	966.22	2907	886.05	263.30	80.254
137	EDDY	ALVM	25.30.12.113	460	140.208	3375	1028.70	2984	909.52	391.30	119.268
141	LEA	ALVM	20.32.24.333	67	20.422	3555	1083.56	3517	1071.98	37.67	11.482
142	LEA	ALVM	20.32.27.144	30	9.144	3545	1080.52	3521	1073.20	23.67	7.215
143	LEA	ALVM	20.32.36.214	60	18.288	3585	1092.71	3538	1078.38	46.60	14.204
144	LEA	ALVM	20.33.21.111	49	14.935	3536	1077.77	3499	1066.50	36.90	11.247
145	LEA	ALVM	20.34.34.432	96	29.261	3770	1149.10	3680	1121.66	89.50	27.280
146	EDDY	ALVM	21.31.02.221	35	10.668	3570	1088.14	3540	1078.99	29.80	9.083
147	LEA	ALVM	21.33.02.420	94	28.651	3770	1149.10	3690	1124.71	79.58	24.256
148	LEA	ALVM	21.33.18.114	150	45.720	3890	1185.67	3749	1142.70	140.75	42.901
149	LEA	ALVM	21.33.25.421	67	20.422	3670	1118.62	3613	1101.24	56.58	17.246

Source: Modified from Richey and others, 1985

APPENDIX B REFERENCES

Davies, P. B. 1989. *Variable-Density Ground-Water Flow and Paleohydrology in the Waste Isolation Pilot Plant (WIPP) Region Southeastern New Mexico.* U.S. Geological Survey Open-File Report 88-490. Albuquerque, NM: U.S. Geological Survey/Water Resources Division.

Geohydrology Associates, Inc. 1979. *Water Resources Study of the Carlsbad Potash Area, New Mexico.* Denver, CO: Bureau of Land Management.

Gonzalez, M. M. 1989. *Compilation and Comparisons of Test-Hole Location Surveys in the Vicinity of the Waste Isolation Pilot Plant Site.* SAND88-1065. Albuquerque, NM: Sandia National Laboratories.

Mercer, J. W. 1983. *Geohydrology of the Proposed Waste Isolation Pilot Plant Site, Los Medaños Area, Southeastern New Mexico.* U.S. Geological Survey Water Resources Investigations Report 83-4016. Albuquerque, NM: U.S. Geological Survey.

Richey, S.F. 1989. *Geologic and Hydrologic Data for the Rustler Formation Near the Waste Isolation Pilot Plant, Southeastern New Mexico.* U.S. Geological Survey Open-File Report 89-32. Washington, DC: U.S. Geological Survey.

Richey, S.F., J.G. Wells, and K.T. Stephens. 1985. *Geohydrology of the Delaware Basin and Vicinity, Texas and New Mexico.* U.S. Geological Survey Water Resources Investigations Report 84-4077. Washington, DC: U.S. Geological Survey.

GLOSSARY

accessible environment - The accessible environment means (1) the atmosphere, (2) land surfaces, (3) surface waters, (4) oceans, and (5) all of the lithosphere that is beyond the controlled area *(40 CFR 191.12[k])*.

algal - Composed of photosynthetic, almost exclusively aquatic plants that range in size from simple unicellular forms to giant kelps several meters long.

algorithm - A procedure for solving a mathematical problem in a finite number of steps that frequently involves repetition of an operation.

anhydrite - A mineral consisting of anhydrous calcium sulfate ($CaSO_4$). It is gypsum without water, and is denser, harder, and less soluble.

anisotropic - Pertaining to any material property, such as hydraulic conductivity, that varies with direction.

anticline - A fold of rocks, generally convex upward, whose core contains stratigraphically older rocks.

aquifer - A body of rock that is sufficiently permeable to conduct ground water and to yield significant quantities of ground water to wells and springs.

aquitard - A confining bed that retards but does not prevent the flow of water to or from an adjacent aquifer.

argillaceous - Containing clay-sized particles or clay minerals.

basin - A depression in the Earth's crust in which sediments have accumulated.

Bell Canyon Formation - A sequence of rock strata that form the topmost formation of the Delaware Mountain Group (Early Permian).

biogenic - Produced directly by the physiological activities of organisms, either plant or animal.

borehole - (1) A manmade hole in the wall, floor, or ceiling of a subsurface room used for verifying geology, making observations, or emplacing canisters of remote-handled transuranic (RH-TRU) waste. (2) A hole drilled from the

surface for purposes of geologic or hydrologic testing, or to explore for resources; sometimes referred to as a drillhole.

breccia - A rock consisting of very angular, coarse fragments held together by a mineral cement or a fine-grained matrix (as sand or clay).

breccia pipe - A vertically cylindrical feature filled with collapse debris. It is formed when relatively fresh water from a deep-seated aquifer moves upward through fractures, dissolving evaporites and causing collapse of the surrounding rock material.

brine aquifer - The Rustler-Salado residuum, a zone of residual material, left after dissolution of the original salt at the interface of the Rustler and Salado Formations, that is highly permeable and contains much brine.

brine pocket - Hydraulically isolated, stagnant pocket of pressurized fluid in the Castile Formation; also referred to as "brine occurrence" or "brine reservoir."

brine reservoir - See brine pocket.

caliche - A calcareous material commonly found in layers on the surface of or within stony soils of arid or semi-arid regions. It occurs as gravels, sands, silts, and clays cemented together by calcium carbonate (lime) or as crusts at the surface of the soil.

Capitan Reef - A fossilized limestone reef of the Permian Period that surrounds most of the Delaware Basin.

Castile Formation - A stratigraphic unit of evaporite rocks (interbedded halite and anhydrite) of the Permian Period that immediately underlies the Salado Formation (in which the WIPP disposal level is being built).

cementation - The process by which coarse clastic sediments become consolidated into hard, compact rocks, usually through deposition or precipitation of minerals in the spaces among the individual grains of the sediment.

Cenozoic - An era of geologic time from the beginning of the Tertiary Period (about 66 million years ago) to the present.

cherty - Containing chert, a hard, extremely dense or compact, microcrystalline or cryptocrystalline sedimentary rock.

clastic - Rock or sediment composed principally of broken fragments that are derived from preexisting rocks or minerals.

claystone - An indurated clay having the texture and composition of shale but lacking the fine lamination and fissility.

compaction - Mechanical process by which the pore space in the waste is reduced prior to waste emplacement.

compliance evaluation or assessment - The process of assessing the regulatory compliance of a mined geologic waste repository.

compressibility - A measure of the ability of a substance to be reduced in volume by application of pressure; quantitatively, the reciprocal of the bulk modulus.

computer model - The appropriately coded analytical, quasi-analytical, or numerical solution technique used to solve a mathematical model.

conceptual model - The set of hypotheses and data that postulate the description and behavior of the disposal system (e.g., structural geometry, material properties, and all significant physical processes that affect behavior). For WIPP, the data pertinent for a conceptual model are stored in the secondary data base. Several secondary data bases exist because each scenario may have a slightly different conceptual model.

conductivity - A shortened form of hydraulic conductivity.

confined ground water - Groundwater under pressure significantly greater than atmospheric pressure. Its upper surface is the bottom of an impermeable bed or a bed of distinctly lower permeability than the material in which the water occurs.

conglomeratic - Having a sparse to liberal amount of pebbles or cobbles.

connate - Fluids or volatile materials trapped in sediments at the time the deposits were laid down.

controlled area - The controlled area means "(1) a surface location, to be identified by passive institutional controls, that encompasses no more that 100 km and extends horizontally no more than 5 km in any direction from the outer boundary of the original location of the radioactive wastes in a disposal system; and (2) the subsurface underlying such a surface location." *(40 CFR 191.12[g])*

Cretaceous - Last period of the Mesozoic Era, about 66 to 144 million years ago.

Culebra Dolomite Member - The lower of two layers of dolomite within the Rustler Formation that are locally water bearing.

Darcian - Pertaining to a formula derived by Darcy for the flow of fluids, with the assumption that the flow is laminar and that inertia can be neglected.

darcy - An English standard unit of permeability, defined by a medium for which a flow of 1 cm^3/s is obtained through a section of 1 cm^2, for a fluid viscosity of 1 cP and a pressure gradient of 1 atm/cm. One darcy is equal to 9.87×10^{-13} m^2.

Delaware Basin - The part of the Permian Basin in southeastern New Mexico and adjacent parts of Texas where a sea deposited large thicknesses of evaporites between approximately 260 and 250 million years ago. It is partially surrounded by the Capitan Reef.

Delaware Mountain Group - A set of three formations of the Permian Period that underlie the Castile Formation at the Los Medaños site.

depocenter - An area or site of maximum deposition.

depositional - The accumulation of loose rock material by an natural agent.

deterministic - An exact mathematical relationship between the dependent and independent variables in a system.

Dewey Lake Red Beds - A formation of the Permian Period that overlies the Rustler Formation and is composed of reddish-brown marine mudstones and siltstones interbedded with fine-grained sandstone.

diastrophism - All movement of the crust produced by tectonic processes, including the formation of ocean basins, continents, plateaus, and mountain ranges.

disconformable - Formations that exhibit parallel bedding but have between them a significant interval of erosion or non-deposition that indicates a break in the time sequence.

discordance - Lack of parallelism between adjacent rock units.

disposal - "Disposal means permanent isolation of spent nuclear fuel or radioactive waste from the accessible environment with no intent of recovery, whether or not such isolation permits the recovery of such fuel or waste. For example, disposal of waste in a mined geologic repository occurs when all of the shafts to the repository are backfilled and sealed." *(40 CFR 191.02[1])*

disposal system - Any combination of engineered and natural barriers that isolate spent nuclear fuel or radioactive waste after disposal (*40 CFR 191.12(a)*). The natural barriers extend to the accessible environment. The WIPP disposal system comprises the underground repository, shafts, and controlled area.

Dockum Group - A geologic sedimentary sequence of the Triassic Period that overlies the Dewey Lake Red Beds over part of the Los Medaños area.

dolomite - A carbonate sedimentary rock consisting of more than 50% of the mineral dolomite [$CaMg(CO_3)_2$].

drawdown - The lowering of water level in a well as a result of fluid withdrawal.

Eocene - An epoch of the early Tertiary Period (or Paleogene Period), subsequent to the Paleocene Epoch and preceding the Oligocene Epoch (about 37 to 58 million years ago).

equipotential - Points with the same hydraulic head elevations.

equipotentiometric - Pertaining to equal levels of water rise in wells.

evaporite - A sedimentary rock composed primarily of minerals produced by precipitation from a solution that has become concentrated by the evaporation of a solvent, especially salts deposited from a restricted or enclosed body of seawater or from the water of a salt lake. In addition to halite (NaCl), these salts include potassium, calcium, and magnesium chlorides and sulfates.

evapotranspiration - Loss of water from a land area through transpiration of plants and evaporation from the soil.

exploratory drilling - Drilling to an unexplored depth or in territory having unproven resources.

facies - An areally restricted part of a rock body that differs in mineralogic composition, grain size, or fossil content from nearby beds

deposited at the same time and that broadly corresponds to a certain environment or mode of deposition.

flowpath - The path traveled by a neutrally buoyant particle released into a groundwater-flow field.

fluvial - Of or pertaining to a river or rivers.

fossiliferous - Containing remains, traces, or imprints of plants or animals that have been preserved in the Earth's crust since some past geologic or prehistoric time.

fusulinids - A type of protozoan characterized by a multichambered elongate external shell that is composed of microgranular calcareous material and resembles the shape of a grain of wheat.

geochemistry - The study of the distribution and amounts of the chemical elements in minerals, ores, rocks, soils, water, and the atmosphere.

geohydrology - The study of the hydrologic or flow characteristics of subsurface waters.

geology - The study of the Earth, the materials of which it is made, the processes that act on these materials, the products formed, and the history of the planet and its life forms since its origin.

geomorphology - The study of the classification, description, nature, origin, and development of present landforms and their relationships to underlying structure, and of the history of geologic changes as recorded by these surface features.

geophysics - The study of the Earth by quantitative physical methods such as electric, gravity, magnetic, seismic, and thermal techniques.

glauberite - A brittle, light-colored, monoclinic mineral: $Na_2Ca(SO_4)_2$. It has a vitreous luster and saline taste and occurs in saline residues.

gradational - Gradual change in rock characteristics from one rock body to another.

grainstone - A carbonate sedimentary rock composed almost entirely of grains (either inorganic or organic particles) and virtually no mud.

Guadalupian - A North American geologic series, above the Leonardian Series and below the Ochoan Series, that corresponds to portions of the Early and Late Permian Period (about 253 to 263 million years ago).

gypsiferous - Containing gypsum, hydrous calcium sulfate ($CaSO_4 \cdot 2H_2O$), a mineral frequently associated with halite and anhydrite in evaporites.

halite - A dominant mineral in evaporites; salt, NaCl.

headward erosion - The lengthening and cutting upstream of a young valley or gully above the original source of its stream.

Holocene - A geologic epoch of the Quaternary Period, subsequent to the Pleistocene Epoch (about 10,000 years ago) and continuing to the present.

horizon - In geology, an interface indicative of a particular position in a stratigraphic sequence. An underground level; for instance, the waste-emplacement horizon at the WIPP is the level about 650 m (2,150 ft) deep in the Salado Formation where openings are mined for waste disposal.

host rock - The geologic medium in which radioactive waste is emplaced.

hydraulic - Pertaining to a fluid in motion.

hydraulic conductivity - The measure of the rate of flow of water through a cross-sectional area under a unit hydraulic gradient.

hydraulic gradient - A quantity defined in the study of ground-water hydraulics that describes the rate of change of total hydraulic head per unit distance of flow in a given direction.

hydraulic head - The elevation to which water rises at a given point as a result of reservoir pressure.

hydrochemical - The diagnostic chemical character of ground water occurring in hydrologic systems.

hydrogeology - The study of subsurface waters and of related geologic aspects of surface waters.

hydrologic properties - Those properties of a rock that govern the entrance of water and the capacity to hold, transmit, and deliver water, such as porosity, effective porosity, specific retention, permeability, and the directions of maximum and minimum permeabilities.

hydrology - The study of global water, its properties, circulation, and distribution.

hydropad - A complex of hydro-wells closely spaced for testing on hydrostratigraphic units.

hydrostratigraphic - Pertaining to a body of rock having considerable lateral extent and composing a geologic framework for a reasonably distinct hydrologic system.

in situ - In the natural or original position; used to distinguish in-place experiments, rock properties, and so on, from those in the laboratory.

interbeds - Sedimentary beds that lie between or alternate with other beds having different characteristics.

interfinger - The disappearance of sedimentary bodies into laterally adjacent masses by splitting into many thin layers, each terminating independently.

intergranular - Between the grains or particles of a rock.

intertonguing - The lateral intergradation of different rock types through a vertical succession of thin, interlocking or overlapping, wedge-shaped layers.

isolith - A line on a map through points of equal aggregate thickness of a particular type of material within a formation.

isopach - A line drawn on a map through points of equal true thickness of a designated stratigraphic unit or group of stratigraphic units.

isopleth - A line on a map along which all points have the same numeric constant or equal value for a specified variable.

isotropic - Independent material properties that are constant regardless of direction of movement.

Jurassic - The second period of the Mesozoic Era, subsequent to the Triassic Period and preceding the Cretaceous Period (about 144 to 208 million years ago).

karst - A topography formed from solution of limestone, dolomite, or gypsum; characterized by sinkholes, caves, and underground drainage.

karstification - The formation of karst features by the solutional and mechanical action of water.

Laguna Grande de la Sal - The largest lake in the Los Medaños area, located southwest of the WIPP.

lamprophyre - A group of dark-colored, porphyritic, igneous rocks characterized by a high percentage of mafic (Mg, Fe) minerals (esp. biotite, hornblende, and pyroxene).

langbeinite - A colorless to reddish mineral [$K_2Mg_2(SO_4)_3$] used as a source of potassium in fertilizers and formed as a saline residue from evaporation.

lenticular - Having the cross-sectional shape of a lens, esp. of a double-convex lens. The term may be applied to a body of rock or a sedimentary structure.

Leonardian - A North American geologic series, above the Wolfcampian Series and below the Guadalupian Series, that corresponds to the Early Permian Period (about 263 to 268 million years ago).

limey - Containing calcium carbonate ($CaCO_3$).

lithologic - The descriptive characteristics of rock composition.

lithostatic pressure - Subsurface pressure caused by the weight of overlying rock or soil, about 14.9 MPa at the WIPP repository level.

Livingston Ridge - Topographic feature marking the eastern boundary of Nash Draw.

lognormal distribution - A frequency distribution whose logarithm follows a normal distribution.

Los Medaños - Literally "the dunes." The area in which the WIPP is located.

low - A general geologic term for such features as a structural basin, a syncline, a saddle, or a sag.

Malaga Bend - Prominent bend in the Pecos River, southwest of the WIPP.

Mescalero caliche - Informal name for mid-Pleistocene (approximately 510,000 years ago) caliche occurring in southeastern New Mexico.

Mesozoic - The era of geologic time from about 66 to 245 million years ago.

microcrystalline - Crystals too small to see with the naked eye.

microdarcy (μd) - A unit of measurement of fluid permeability, equivalent to 10^{-6} darcy or 9.87×10^{-19} m^2.

millidarcy (md) - Unit of measurement of fluid permeability, equivalent to 10^{-3} darcy or 9.87×10^{-16} m^2.

Miocene - An epoch of the early Tertiary Period, subsequent to the Oligocene Epoch and preceding the Pliocene Epoch (about 5 to 24 million years ago).

modeler - One who formulates a working hypothesis or precise simulation, by means of description, statistical data, or analogy, of a phenomenon or process that cannot be observed directly.

monocline - A local steepening in an otherwise uniformly gentle dip.

mudstone - A blocky or massive, fine-grained sedimentary rock in which the proportion of clay and silt are approximately equal.

multipad - See hydropad.

nanodarcy (nd) - A unit of measurement of fluid permeability, equivalent to 10^{-9} darcy or 9.87×10^{-22} m^2.

Nash Draw - A shallow, 5-mile-wide valley located to the west of the WIPP and open to the southwest.

Ochoan - A North American geologic series, above the Guadalupian Series and below the Lower Triassic Series, corresponding to the Late Permian Period (about 248 to 253 million years ago).

Ogallala Formation - A sequence of late Tertiary Period (Miocene and Pliocene Epochs) sandstones and conglomerates widely distributed in the American Great Plains.

Oligocene - An epoch of the early Tertiary Period, subsequent to the Eocene Epoch and preceding the Miocene Epoch (about 24 to 38 million years ago).

Ordovician - The second earliest period of the Paleozoic Era, subsequent to the Cambrian Period and preceding the Silurian Period (about 408 to 505 million years ago).

Paleocene - An epoch of the early Tertiary Period, subsequent to the Late Cretaceous Period and preceding the Eocene Epoch (about 58 to 66 million years ago).

paleosol - A buried soil horizon of the geologic past.

panel - A group of several underground rooms bounded by two pillars and connected by drifts. Within the WIPP, a panel usually consists of seven rooms connected by 10-m-wide drifts at each end.

pascal (Pa) - Unit of pressure produced by a force of 1 newton applied over an area of 1 m^2. One pound per square inch is equal to 6.895 x 10^3 Pa.

Pecos River - Major river in eastern New Mexico and western Texas.

Pennsylvanian - Second to the last Paleozoic period (about 286 to 320 million years ago).

perched groundwater - Unconfined groundwater separated from an underlying body of groundwater by an unsaturated zone. Its water table is a perched water table. Perched groundwater is held up by a perching bed whose permeability is so low that water percolating downward through it is not able to bring water in the underlying unsaturated zone above atmospheric pressure.

performance assessment - The process of assessing the compliance of a deep, geologic, waste repository with the containment requirements of *40 CFR 191*, Subpart B. Performance assessment is defined by Subpart B as "an analysis that (1) identifies the processes and events that might affect the disposal system, (2) examines the effects of these processes and events on the performance of the disposal system, and (3) estimates the cumulative releases of radionuclides, considering the associated uncertainties, caused by all significant processes and events. These estimates shall be incorporated into an overall probability distribution of cumulative release to the extent practicable." (*40 CFR 191.12(q)*)

permeability - A measurement of the ability of a rock or soil to allow fluid to pass through it.

Permian - The last period of the Paleozoic Era, subsequent to the Pennsylvanian Period (about 245 to 286 million years ago).

Permian Basin - A region in the south-central United States, where during the Permian Period (245 to 286 million years ago), there were many shallow subbasins in which vast beds of marine evaporites were deposited.

Phanerozoic - That part of geologic time represented by rocks in which the evidence of life is abundant, i.e., Cambrian Period (570 million years ago) and later time.

phreatic - Pertaining to a subsurface zone in which all the interstices are filled with water under pressure greater than that of the atmosphere.

phreatophyte - A plant that obtains its water supply from the phreatic zone or from the zone immediately above the water table (capillary fringe) and is characterized by a deep root system.

physico-chemical - Pertaining to physical chemistry.

playa - An intermittently dry, vegetation-free, flat area at the lowest part of an undrained desert basin, underlain by stratified clay, silt, or sand, and commonly by soluble salts.

Pleistocene - An epoch of the Quaternary Period, subsequent to the Pliocene Epoch of the Tertiary Period and preceding the Holocene Epoch (about 1.6 million years ago to 10,000 years ago); corresponds to the "Great Ice Age."

Pliocene - An epoch of the Tertiary Period, subsequent to the Miocene Epoch and preceding the Pleistocene Epoch (about 1.6 to 5 million years ago).

pluvial - Of a geologic episode, change, deposit, process, or feature resulting from the action or effects of rain.

polyhalite - An evaporite mineral: $K_2MgCa_2(SO_4)_4.2H_2O$; a hard, poorly soluble mineral.

porosity - The percentage of total rock volume occupied by voids.

porphyritic - Refers to the texture of an igneous rock in which larger crystals (phenocrysts) are set in a finer-grained groundmass.

post-depositional - Occurring after sediments have been laid down.

potash - Specifically K_2CO_3. Also loosely used for many potassium compounds, especially as used in agriculture or industry.

potential - A function or set of functions of position in space, from whose first derivatives a vector can be formed, such as that of a static field intensity.

potentiometric surface - An imaginary surface representing the total head of ground water and defined by the level to which water will rise in a well.

probabilistic - Using the probability of a given set of events from a family of outcomes.

Quahada Ridge - Topographic feature marking the western boundary of Nash Draw.

Quaternary - The second period of the Cenozoic Era, subsequent to the Tertiary Period, starting about 1.6 million years ago and continuing to the present.

radioactive waste - Solid, liquid, or gaseous material of negligible economic value that contains radionuclides in excess of threshold quantities.

radionuclide - A radioactive nuclide.

radiochemistry - The chemical study of irradiated and naturally occurring radioactive materials and their behavior.

recharge - The processes involved in the addition of water to the ground-water zone of saturation.

recrystallization - The formation, essentially in the solid state, of new crystalline mineral grains in a rock. The new grains are generally larger than the original grains and may have the same or a different mineralogical composition.

reentrant - A prominent, generally angular indentation in a land form.

repository - The portion of the WIPP repository/shaft system within the Salado Formation, including the access drifts, waste panels, and experimental areas, but excluding the shafts.

Rustler Formation - A sequence of Late Permian age clastic and evaporite sedimentary rocks that contains two dolomite members and overlies the Salado Formation.

sabka - A supratidal environment of sedimentation, formed under arid to semiarid conditions on restricted coastal plains just above normal high-tide level.

Salado Formation - A Permian age sequence of salt with minor amounts of clay and anhydrite. Host unit for the WIPP.

saturated - All the pores in a given volume of rock contain fluid.

scenario - A combination of naturally occurring or human-induced events and processes that represents realistic future changes to the repository, geologic, and geohydrologic systems that could effect the escape of radionuclides from the repository, and release to the accessible environment.

sedimentation - The action or process of forming or depositing rock particles in layers.

semiperched water table - The water table of a body of unconfined ground water separated by a low-permeability but saturated bed from a body of confined water whose hydrostatic level is below the water table.

shaft - A man-made hole, either vertical or steeply inclined, that connects the surface with the underground workings of a mine.

silicification - The introduction of, or replacement by, silica, generally resulting in the formation of fine-grained quartz, which may fill pores and replace existing minerals.

siltstone - A sedimentary rock composed of at least two-thirds silt-sized grains (1/256 to 1/16 mm); it tends to be flaggy, containing hard, durable, generally thin layers.

sinkhole - A hollow in a limestone region that communicates with a cavern or passage.

solute - The material dissolved in a solvent.

Standard - 40 CFR Part 191, *Environmental Standards for the Management and Disposal of Spent Nuclear Fuel, High-Level and Transuranic Radioactive Wastes; Final Rule.*

storativity - The volume of water released by an aquifer per unit surface area per unit drop in hydrologic head.

stratabound - A deposit confined to a single stratigraphic unit.

stratigraphy - The study of rock strata; concerned with the original succession and age relations of rock strata, their form, distribution,

lithologic composition, fossil content, and geophysical and geochemical properties.

supratidal - Pertaining to the shore area just above high-tide level.

sylvite - A white or colorless mineral (KCl), the principal ore mineral of potassium compounds, that occurs in beds as a saline residue from evaporation.

syncline - A fold having stratigraphically younger rock material in its center; it is usually concave upward.

syndepositional - Forming contemporaneously with deposition.

Tamarisk Member - A sequence of anhydrite, claystone, and siltstone within the Late Permian Rustler Formation of southeastern New Mexico.

tectonic - The forces involved in, or the resulting structures and features of, movements of the Earth's crust.

tight - Pertaining to a rock that has all interstices filled with fine grains or with matrix material so that porosity and permeability are almost non-existent.

topographic - The configuration of a land surface, including its relief and the position of its natural and man-made features.

transgressive - The spread or extension of the sea over land areas, and the consequent evidence of such an advance (such as strata deposited unconformably on older rocks).

transmissivity - The rate at which water of the prevailing viscosity is transmitted through a unit width of the aquifer under a hydraulic gradient.

transuranic radioactive waste (TRU waste) - Waste that, without regard to source or form, is contaminated with more than 100 nCi of alpha-emitting transuranic isotopes with half-lives greater than 20 yr, per gram of waste, except for (1) HLW; (2) wastes that the DOE has determined, with the concurrence of the EPA Administrator, do not need the degree of isolation required by *40 CFR 191*; or (3) wastes that the NRC Commission has approved for disposal on a case-by-case basis in accordance with *10 CFR 61*. Heads of DOE field organizations can determine that other alpha-contaminated wastes, peculiar to a specific site, must be managed as TRU waste.

Triassic - The first period of the Mesozoic Era, subsequent to the Permian Period and preceding the Jurassic Period (about 208 to 245 million years ago).

turbidity current - A density current in water, air, or other fluid, caused by different amounts of matter in suspension; specifically a bottom-flowing current laden with suspended sediment moving swiftly (under the influence of gravity) down a subsqueous slope and spreading horizontally on the floor of a body of water.

unconfined - Not confined under pressure beneath relatively impermeable rocks.

unconformably - Not conformable, i.e., a break in deposition of sedimentary material.

unconformity - A substantial break or gap in the geologic record in which a rock unit is overlain by another that is not normally next in stratigraphic succession.

unconsolidated - Material that is loosely arranged or whose particles are not cemented together.

unsaturated - Refers to a rock or soil in which the pores are not completely full of water.

Uranium-234/Uranium-238 activity ratio - Comparison of the radioactivities of U-234 and U-238; the change in this ratio is directly related to the passage of time because the two isotopes have very different half-lives, allowing the calculation in years of the age of a substance.

vadose - Refers to subsurface water under pressure that is less than that of the atmosphere, usually found below the land surface but above the water table.

varve - A sedimentary bed or lamina or sequence of lamina deposited cyclically in a body of still water.

water table - In saturated rock, the surface of the water that is at atmospheric pressure.

Wolfcampian - A North American geologic series, above the Virgilian Series and below the Leonardian Series, that corresponds to the Early Permian Period (about 268 to 286 million years ago).

NOMENCLATURE

CFR - Code of Federal Regulations

cm - centimeter

DOE - The U.S. Department Of Energy, established in 1978 as a successor to ERDA and the AEC.

DST - drill-stem test

EPA - Environmental Protection Agency of the U.S. Government

ERDA - Energy Research and Development Administration

fm - formation

ft - foot

40 CFR 191 - Code of Federal Regulations, Title 40, Part 191

g - grams

gal - gallon

kg - kilogram(s)

km - kilometer(s)

ℓ - liter

lb - pound

m - meter(s)

M - Molar (molarity): Concentration of a solution expressed as moles of solute per liter of solution.

mg/ℓ - milligrams per liter

mi - mile(s)

μd - microdarcy

md - millidarcy

MPa - megapascal (10^6 Pa)

NM - New Mexico

Pa - pascal

SNL - Sandia National Laboratories

TRU - TRansUranic

U - uranium

WIPP - Waste Isolation Pilot Plant

yr - year

Distribution

FEDERAL AGENCIES

U. S. Department of Energy (6)
Office of Environmental Restoration
and Waste Management
Attn: Leo P. Duffy, EM-1
Jill E. Lytle, EM-30
Mark Duff, EM-34
Steve Schneider, EM-34
Clyde Frank, EM-50
Lynn Tyler, EM-50
Washington, DC 20585

U.S. Department of Energy (5)
WIPP Task Force
Attn: Mark Frei (2)
G. H. Daly
Sandi Fucigna
Jay Rhoderick
12800 Middlebrook Rd.
Suite 400
Germantown, MD 20874

U.S. Department of Energy (4)
Office of Environment, Safety and
Health
Attn: Raymond P. Berube, EH-20
Carol Borgstrum, EH-25
Ray Pelletier, EH-231
Kathleen Taimi, EH-232
Washington, DC 20585

U. S. Department of Energy (6)
Albuquerque Operations Office
Attn: Bruce G. Twining
J. E. Bickel
K. A. Griffith
D. Krenz
G. Runkle
C. Soden
P.O. Box 5400
Albuquerque, NM 87185-5400

U. S. Department of Energy (10)
WIPP Project Office (Carlsbad)
Attn: A. Hunt (4)
M. McFadden
V. Daub (4)
K. Hunter
P.O. Box 3090
Carlsbad, NM 88221-3090

U. S. Department of Energy, (5)
Office of Civilian Radioactive Waste
Management
Attn: Deputy Director, RW-2
Associate Director, RW-10
Office of Program
Administration and
Resources Management
Associate Director, RW-20
Office of Facilities
Siting and
Development
Associate Director, RW-30
Office of Systems
Integration and
Regulations
Associate Director, RW-40
Office of External
Relations and Policy
Office of Geologic Repositories
Forrestal Building
Washington, DC 20585

U. S. Department of Energy
Attn: National Atomic Museum Library
Albuquerque Operations Office
P.O. Box 5400
Albuquerque, NM 87185

U. S. Department of Energy
Research & Waste Management Division
Attn: Director
P.O. Box E
Oak Ridge, TN 37831

U. S. Department of Energy (2)
Idaho Operations Office
Fuel Processing and Waste
Management Division
785 DOE Place
Idaho Falls, ID 83402

U.S. Department of Energy
Savannah River Operations Office
Defense Waste Processing
Facility Project Office
Attn: W. D. Pearson
P.O. Box A
Aiken, SC 29802

U.S. Department of Energy (2)
Richland Operations Office
Nuclear Fuel Cycle & Production
Division
Attn: R. E. Gerton
825 Jadwin Ave.
P.O. Box 500
Richland, WA 99352

U.S. Department of Energy (3)
Nevada Operations Office
Attn: J. R. Boland
D. Livingston
P. K. Fitzsimmons
2753 S. Highland Drive
Las Vegas, NV 87183-8518

U.S. Department of Energy (2)
Technical Information Center
P.O. Box 62
Oak Ridge, TN 37831

U.S. Department of Energy (2)
Chicago Operations Office
Attn: J. C. Haugen
David Dashavsky
9800 South Cass Avenue
Argonne, IL 60439

U.S. Department of Energy
Los Alamos Area Office
528 35th Street
Los Alamos, NM 87544

U.S. Department of Energy (3)
Rocky Flats Area Office
Attn: W. C. Rask
Gary Huffman
Tom Lukow
P.O. Box 928
Golden, CO 80402-0928

U.S. Department of Energy
Dayton Area Office
Attn: R. Grandfield
P.O. Box 66
Miamisburg, OH 45343-0066

U.S. Department of Energy
Attn: Edward Young
Room E-178
GAO/RCED/GTN
Washington, DC 20545

U.S. Environmental Protection
Agency (2)
Office of Radiation Protection
Programs (ANR-460)
Attn: Richard Guimond (2)
Washington, D.C. 20460

U.S. Nuclear Regulatory Commission
(4)
Division of Waste Management
Attn: Joseph Bunting, HLEN 4H3 OWFN
Ron Ballard, HLGP 4H3 OWFN
Jacob Philip, WMB
NRC Library
Mail Stop 623SS
Washington, DC 20555

U.S. Nuclear Regulatory Commission
(4)
Advisory Committee on Nuclear Waste
Attn: Dade Moeller
Martin J. Steindler
Paul W. Pomeroy
William J. Hinze
7920 Norfolk Avenue
Bethesda, MD 20814

Defense Nuclear Facilities Safety
Board
Attn: Dermot Winters
600 E. Street NW
Suite 675
Washington, DC 20004

Nuclear Waste Technical Review Board (2)
Attn: Don U. Deere
1111 18th Street NW #801
Washington, DC 20006

Katherine Yuracko
Energy and Science Division
Office of Management and Budget
725 17th Street NW
Washington, DC 20503

U.S. Geological Survey
Branch of Regional Geology
Attn: R. Snyder
MS913, Box 25046
Denver Federal Center
Denver, CO 80225

U.S. Geological Survey
Conservation Division
Attn: W. Melton
P.O. Box 1857
Roswell, NM 88201

U.S. Geological Survey (2)
Water Resources Division
Attn: Cathy Peters
Suite 200
4501 Indian School, NE
Albuquerque, NM 87110

STATE AGENCIES

Bureau of Land Management
101 E. Mermod
Carlsbad, NM 88220

Bureau of Land Management
New Mexico State Office
P.O. Box 1449
Santa Fe, NM 87507

Environmental Evaluation Group (5)
Attn: Robert Neill
Suite F-2
7007 Wyoming Blvd., N.E.
Albuquerque, NM 87109

New Mexico Bureau of Mines and Mineral Resources (2)
Attn: F. E. Kottlowski, Director
J. Hawley
Socorro, NM 87801

NM Department of Energy & Minerals
Attn: Kasey LaPlante, Librarian
P.O. Box 2770
Santa Fe, NM 87501

Bob Forrest
Mayor, City of Carlsbad
P.O. Box 1569
Carlsbad, NM 88221

Chuck Bernard
Executive Director
Carlsbad Department of Development
P.O. Box 1090
Carlsbad, NM 88221

Robert M. Hawk (2)
Chairman, Hazardous and Radioactive Materials Committee
Room 334
State Capitol
Sante Fe, NM 87503

Kirkland Jones (2)
Deputy Director
New Mexico Environmental Improvement Division
P.O. Box 968
1190 St. Francis Drive
Santa Fe, NM 87503-0968

ADVISORY COMMITTEE ON NUCLEAR FACILITY SAFETY

John F. Ahearne
Executive Director, Sigma Xi
99 Alexander Drive
Research Triangle Park, NC 27709

James E. Martin
109 Observatory Road
Ann Arbor, MI 48109

Dr. Gerald Tape
Assoc. Universities
1717 Massachusetts Ave. NW
Suite 603
Washington, DC 20036

DOE BLUE RIBBON PANEL

Thomas Bahr, Director
New Mexico State University
New Mexico Waste Resources Research
Institute
Box 3167
Las Cruces, NM 88001

Robert Bishop
Nuclear Management Resources Council
1776 I Street, NW
Suite 300
Washington, DC 20006-2496

Arthur Kubo
BDM Corporation
7915 Jones Branch Drive
McLean, VA 22102

Leonard Slosky
Slosky & Associates
Bank Western Tower
Suite 1400
1675 Broadway
Denver, CO 80202

Newal Squyres, Esq.
Eberle and Berlin
P.O. Box 1368
Boise, ID 83702

WIPP PANEL OF NATIONAL RESEARCH COUNCIL'S BOARD ON RADIOACTIVE WASTE MANAGEMENT

Charles Fairhurst, Chairman
Department of Civil and
Mineral Engineering
University of Minnesota
500 Pillsbury Dr. SE
Minneapolis, MN 55455

John O. Blomeke
Route 3
Sandy Shore Drive
Lenoir City, TN 37771

John D. Bredehoeft
Western Region Hydrologist
Water Resources Division
U.S. Geological Survey (M/S 439)
345 Middlefield Road
Menlo Park, CA 94025

Karl P. Cohen
928 N. California Avenue
Palo Alto, CA 94303

Fred M. Ernsberger
1325 NW 10th Avenue
Gainesville, FL 32601

Rodney C. Ewing
Department of Geology
University of New Mexico
200 Yale, NE
Albuquerque, NM 87131

B. John Garrick
Pickard, Lowe & Garrick, Inc.
2260 University Drive
Newport Beach, CA 92660

Leonard F. Konikow
U.S. Geological Survey
431 National Center
Reston, VA 22092

Jeremiah O'Driscoll
505 Valley Hill Drive
Atlanta, GA 30350

Christopher Whipple
Clement International Corp.
160 Spear St.
Suite 1380
San Francisco, CA 94105-1535

National Research Council (3)
Board on Radioactive
Waste Management
Attn: Peter B. Myers, Staff Director
(2)
Dr. Geraldine J. Grube
2101 Constitution Avenue
Washington, DC 20418

PERFORMANCE ASSESSMENT PEER REVIEW PANEL

G. Ross Heath
College of Ocean
and Fishery Sciences
583 Henderson Hall
University of Washington
Seattle, WA 98195

Thomas H. Pigford
Department of Nuclear Engineering
4153 Etcheverry Hall
University of California
Berkeley, CA 94720

Thomas A. Cotton
JK Research Associates, Inc.
4429 Butterworth Place, NW
Washington, DC 20016

Robert J. Budnitz
President, Future Resources
Associates, Inc.
2000 Center Street
Suite 418
Berkeley, CA 94704

C. John Mann
Department of Geology
245 Natural History Bldg.
1301 West Green Street
University of Illinois
Urbana, IL 61801

Frank W. Schwartz
Department of Geology and Mineralogy
Ohio State University
Scott Hall
1090 Carmack Rd.
Columbus, OH 43210

FUTURES SOCIETIES EXPERT PANEL

Theodore S. Glickman
Resources for the Future
1616 P St., NW
Washington, DC 20036

Norman Rosenberg
Resources for the Future
1616 P St., NW
Washington, DC 20036

Max Singer
The Potomac Organization, Inc.
5400 Greystone St.
Chevy Chase, MD 20815

Maris Vinovskis
Institute for Social Research
Room 4086
University of Michigan
426 Thompson St
Ann Arbor, MI 48109-1045

Gregory Benford
University of California, Irvine
Department of Physics
Irvine, CA 92717

Craig Kirkwood
College of Business Administration
Arizona State University
Tempe, AZ 85287

Harry Otway
Health, Safety, and Envir. Div.
Mail Stop K-491
Los Alamos National Laboratory
Los Alamos, NM 87545

Martin J. Pasqualetti
Department of Geography
Arizona State University
Tempe, AZ 85287-3806

Michael Baram
Bracken and Baram
33 Mount Vernon St.
Boston, MA 02108

Wendell Bell
Department of Sociology
Yale University
1965 Yale Station
New Haven, CT 06520

Bernard L. Cohen
Department of Physics
University of Pittsburgh
Pittsburgh, PA 15260

Ted Gordon
The Futures Group
80 Glastonbury Blvd.
Glastonbury, CT 06033

Duane Chapman
5025 S. Building, Room S5119
The World Bank
1818 H Street NW
Washington, DC 20433

Victor Ferkiss
Georgetown University
37th and O Sts. NW
Washington, DC 20057

Dan Reicher
Senior Attorney
Natural Resources Defense Council
1350 New York Ave. NW, #300
Washington, DC 20005

Theodore Taylor
P.O. Box 39
3383 Weatherby Rd.
West Clarksville, NY 14786

NATIONAL LABORATORIES

Argonne National Labs
Attn: A. Smith, D. Tomasko
9700 South Cass, Bldg. 201
Argonne, IL 60439

Battelle Pacific Northwest
Laboratories (6)
Attn: D. J. Bradley
J. Relyea
R. E. Westerman
S. Bates
H. C. Burkholder
L. Pederson
Battelle Boulevard
Richland, WA 99352

Lawrence Livermore National
Laboratory
Attn: G. Mackanic
P.O. Box 808, MS L-192
Livermore, CA 94550

Los Alamos National Laboratory
Attn: B. Erdal, CNC-11
P.O. Box 1663
Los Alamos, NM 87544

Los Alamos National Laboratories (3)
HSE-8
Attn: M. Enoris
L. Soholt
J. Wenzel
P.O. Box 1663
Los Alamos, NM 87544

Los Alamos National Laboratories (2)
HSE-7
Attn: A. Drypolcher
S. Kosciewiscz
P.O. Box 1663
Los Alamos, NM 87544

Oak Ridge National Laboratory
ORGDP
Attn: J.E. Myrick
P.O. Box 2003
Oak Ridge TN 37831

Oak Ridge National Labs
Martin Marietta Systems, Inc.
Attn: J. Setaro
P.O. Box 2008, Bldg. 3047
Oak Ridge, TN 37831-6019

Oak Ridge National Laboratory (2)
Attn: R. E. Blanko
E. Bondietti
Box 2008
Oak Ridge, TN 37831

Savannah River Laboratory (6)
Attn: N. Bibler
E. L. Albenisius
M. J. Plodinec
G. G. Wicks
C. Jantzen
J. A. Stone
Aiken, SC 29801

Savannah River Plant (2)
Attn: Richard G. Baxter
Building 704-S
K. W. Wierzbicki
Building 703-H
Aiken, SC 29808-0001

CORPORATIONS/MEMBERS OF THE PUBLIC

Arthur D. Little, Inc.
Attn: Charles R. Hadlock
Acorn Park
Cambridge, MA 02140-2390

Benchmark Environmental Corp.
Attn: John Hart
4501 Indian School Rd., NE
Suite 105
Albuquerque, NM 87110

Deuel and Associates, Inc.
Attn: R. W. Prindle
208 Jefferson, NE
Albuquerque, NM 87109

Disposal Safety, Inc.
Attn: Benjamin Ross
Suite 600
1629 K Street NW
Washington, DC 20006

Ecodynamics Research Associates (3)
Attn: P. J. Roache
P. Knupp
R. Blaine
P.O. Box 8172
Albuquerque, NM 87198

E G & G Idaho (3)
1955 Fremont Street
Attn: C. Atwood
C. Hertzler
T. I. Clements
Idaho Falls, ID 83415

In-Situ, Inc. (2)
Attn: S. C. Way
C. McKee
209 Grand Avenue
Laramie, WY 82070

INTERA Technologies, Inc. (3)
Attn: G. E. Grisak
J. F. Pickens
A. Haug
Suite #300
6850 Austin Center Blvd.
Austin, TX 78731

INTERA Technologies, Inc.
Attn: Wayne Stensrud
P.O. Box 2123
Carlsbad, NM 88221

IT Corporation (3)
Attn: R. F. McKinney (2)
P. Drez
Regional Office - Suite 700
5301 Central Avenue, NE
Albuquerque, NM 87108

IT Corporation
R. J. Eastmond
825 Jadwin Ave.
Richland, WA 99352

IT Corporation (2)
Attn: D. E. Deal
P.O. Box 2078
Carlsbad, NM 88221

Pacific Northwest Laboratory
Attn: Bill Kennedy
Battelle Blvd.
P.O. Box 999
Richland, WA 99352

RE/SPEC, Inc. (2)
Attn: W. Coons
P. F. Gnirk
P.O. Box 14984
Albuquerque NM 87191

RE/SPEC, Inc. (7)
Attn: L. L. Van Sambeek
D. B. Blankenship
G. Callahan
T. Pfeifle
J. L. Ratigan
P.O. Box 725
Rapid City, SD 57709

Reynolds Elect/Engr. Co., Inc.
Building 790, Warehouse Row
Attn: E. W. Kendall
P.O. Box 98521
Las Vegas, NV 89193-8521

Rockwell International (3)
Atomics International Division
Rockwell Hanford Operations
Attn: J. Nelson (HWVP)
P. Salter
W. W. Schultz
P.O. Box 800
Richland, WA 99352

Science Applications
International Corporation
Attn: Howard R. Pratt,
Senior Vice President
10260 Campus Point Drive
San Diego, CA 92121

Science Applications
International Corporation
Attn: Michael B. Gross
Ass't. Vice President
Suite 1250
160 Spear Street
San Francisco, CA 94105

Science Applications
International Corporation
Attn: George Dymmel
101 Convention Center Dr.
Las Vegas, NV 89109

Southwest Research Institute
Center for Nuclear Waste Regulatory
Analysis (4)
Attn: P. K. Nair (4)
6220 Culebra Road
San Antonio, Texas 78228-0510

Systems, Science, and Software (2)
Attn: E. Peterson
P. Lagus
Box 1620
La Jolla, CA 92038

TASC
Attn: Steven G. Oston
55 Walkers Brook Drive
Reading, MA 01867

Tech. Reps., Inc. (2)
Attn: Janet Chapman
5000 Marble NE
Suite 222
Albuquerque, NM 87110

Westinghouse Electric Corporation (7)
Attn: Library
L. Trego
W. P. Poirier
L. Fitch
V. F. Likar
R. Cook
R. F. Kehrman
P.O. Box 2078
Carlsbad, NM 88221

Westinghouse Hanford Company
Attn: Don Wood
P.O. Box 1970
Richland, WA 99352

Westinghouse/Hanford
Attn. K. Owens
2401 Stevens Road
Richland, WA 99352

Weston Corporation
Attn: David Lechel
5301 Central Avenue, NE
Albuquerque, NM 87108

Western Water Consultants
Attn: D. Fritz
P.O. Box 3042
Sheridan, WY 82801

Western Water Consultants
Attn: P. A. Rechard
P.O. Box 4128
Laramie, WY 82071

Neville Cook
Rock Mechanics Engineering
Mine Engineering Dept.
University of California
Berkeley, CA 94720

Dennis W. Powers
Star Route Box 87
Anthony, TX 79821

UNIVERSITIES

University of Arizona
Attn: J. G. McCray
Department of Nuclear Engineering
Tucson, AZ 85721

University of New Mexico (2)
Geology Department
Attn: D. G. Brookins
Library
Albuquerque, NM 87131

Pennsylvania State University
Materials Research Laboratory
Attn: Della Roy
University Park, PA 16802

Texas A&M University
Center of Tectonophysics
College Station, TX 77840

University of California
Mechanical, Aerospace, and
Nuclear Engineering Department (2)
Attn: W. Kastenberg
D. Browne
5532 Boelter Hall
Los Angeles, CA 90024

University of Wyoming
Department of Civil Engineering
Attn: V. R. Hasfurther
Laramie, WY 82071

University of Wyoming
Department of Geology
Attn: J. I. Drever
Laramie, WY 82071

University of Wyoming
Department of Mathematics
Attn: R. E. Ewing
Laramie, WY 82071

LIBRARIES

Thomas Brannigan Library
Attn: Don Dresp, Head Librarian
106 W. Hadley St.
Las Cruces, NM 88001

Hobbs Public Library
Attn: Marcia Lewis, Librarian
509 N. Ship Street
Hobbs, NM 88248

New Mexico State Library
Attn: Ingrid Vollenhofer
P.O. Box 1629
Santa Fe, NM 87503

New Mexico Tech
Martin Speere Memorial Library
Campus Street
Socorro, NM 87810

New Mexico Junior College
Pannell Library
Attn: Ruth Hill
Lovington Highway
Hobbs, NM 88240

Carlsbad Municipal Library
WIPP Public Reading Room
Attn: Lee Hubbard, Head Librarian
101 S. Halagueno St.
Carlsbad, NM 88220

University of New Mexico
General Library
Government Publications Department
Albuquerque, NM 87131

NEA/PSAC USER'S GROUP

Timo K. Vieno
Technical Research Centre of Finland (VTT)
Nuclear Engineering Laboratory
P.O. Box 169
SF-00181 Helsinki
FINLAND

Alexander Nies (PSAC Chairman)
Gesellschaft für Strahlen- und Institut für Tieflagerung
Abteilung für Endlagersicherheit
Theodor-Heuss-Strasse 4
D-3300 Braunscheweig
FEDERAL REPUBLIC OF GERMANY

Eduard Hofer
Gesellschaft für Reaktorsicherheit (GRS) MBH
Forschungsgelände
D-8046 Garching
FEDERAL REPUBLIC OF GERMANY

Takashi Sasahara
Environmental Assessment Laboratory
Department of Environmental Safety Research
Nuclear Safety Research Center,
Tokai Research Establishment, JAERI
Tokai-mura, Naka-gun
Ibaraki-ken
JAPAN

Alejandro Alonso
Cátedra de Tecnología Nuclear
E.T.S. de Ingenieros Industriales
José Gutiérrez Abascal, 2
E-28006 Madrid
SPAIN

Pedro Prado
CIEMAT
Instituto de Tecnología Nuclear
Avenida Complutense, 22
E-28040 Madrid
SPAIN

Miguel Angel Cuñado
ENRESA
Emilio Vargas, 7
E-28043 Madrid
SPAIN

Francisco Javier Elorza
ENRESA
Emilio Vargas, 7
E-28043 Madrid
SPAIN

Nils A. Kjellbert
Swedish Nuclear Fuel and Waste Management Company (SKB)
Box 5864
S-102 48 Stockholm
SWEDEN

Björn Cronhjort
Swedish National Board for Spent Nuclear Fuel (SKN)
Sehlsedtsgatan 9
S-115 28 Stockholm
SWEDEN

Richard A. Klos
Paul-Scherrer Institute (PSI)
CH-5232 Villingen PSI
SWITZERLAND

Charles McCombia
NAGRA
Parkstrasse 23
CH-5401 Baden
SWITZERLAND

Brian G. J. Thompson
Department of the Environment
Her Majesty's Inspectorate of Pollution
Room A5.33, Romney House
43 Marsham Street
London SW1P 2PY
UNITED KINGDOM

Trevor J. Sumerling
INTERA/ECL
Chiltern House
45 Station Road
Henley-on-Thames
Oxfordshire RG9 1AT
UNITED KINGDOM

Richard Codell
U.S. Nuclear Regulatory Commission
Mail Stop 4-H-3
Washington, D.C. 20555

Norm A. Eisenberg
Division of High Level Waste Management
Office of Nuclear Material Safety and Safeguards
Mail Stop 4-H-3
Washington, D.C. 20555

Paul W. Eslinger
Battelle Pacific Northwest Laboratories (PNL)
P.O. Box 999, MS K2-32
Richland, WA 99352

Budhi Sagar
Center for Nuclear Waste Regulatory Analyses (CNWRA)
Southwest Research Institute
Post Office Drawer 28510
6220 Culebra Road
San Antonio, TX 78284

Andrea Saltelli
Commission of the European Communities
Joint Resarch Centre od Ispra
I-21020 Ispra (Varese)
ITALY

Shaheed Hossain
Division of Nuclear Fuel Cycle and Waste Management
International Atomic Energy Agency
Wagramerstrasse 5
P.O. Box 100
A-1400 Vienna
AUSTRIA

Daniel A. Galson
Division of Radiation Protection and Waste Management
38, Boulevard Suchet
F-75016 Paris
FRANCE

FOREIGN ADDRESSES

Studiecentrum Voor Kernenergie
Centre D'Energie Nucleaire
Attn: A. Bonne
SCK/CEN
Boeretang 200
B-2400 Mol
BELGIUM

Atomic Energy of Canada, Ltd. (4)
Whiteshell Research Estab.
Attn: Peter Haywood
John Tait
Michael E. Stephens
Bruce W. Goodwin
Pinewa, Manitoba, CANADA
ROE 1L0

D. K. Mukerjee
Ontario Hydro Research Lab
800 Kipling Avenue
Toronto, Ontario, CANADA
M8Z 5S4

Ghislain de Marsily
Lab. Géologie Appliqué
Tour 26, 5 étage
4 Place Jussieu
F-75252 Paris Cedex 05, FRANCE

Jean-Pierre Olivier
OECD Nuclear Energy Agency (2)
38, Boulevard Suchet
F-75016 Paris, FRANCE

D. Alexandre, Deputy Director
ANDRA
31 Rue de la Federation
75015 Paris, FRANCE

Claude Sombret
Centre D'Etudes Nucleaires
De La Vallee Rhone
CEN/VALRHO
S.D.H.A. BP 171
30205 Bagnols-Sur-Ceze
FRANCE

Bundesministerium fur Forschung und Technologie
Postfach 200 706
5300 Bonn 2
FEDERAL REPUBLIC OF GERMANY

Bundesanstalt fur Geowissenschaften und Rohstoffe
Attn: Michael Langer
Postfach 510 153
3000 Hannover 51
FEDERAL REPUBLIC OF GERMANY

Hahn-Mietner-Institut fur Kernforschung
Attn: Werner Lutze
Glienicker Strasse 100
100 Berlin 39
FEDERAL REPUBLIC OF GERMANY

Institut fur Tieflagerung (4)
Attn: K. Kuhn
Theodor-Heuss-Strasse 4
D-3300 Braunschweig
FEDERAL REPUPLIC OF GERMANY

Kernforschung Karlsruhe
Attn: K. D. Closs
Postfach 3640
7500 Karlsruhe
FEDERAL REPUBLIC OF GERMANY

Physikalisch-Technische Bundesanstalt
Attn: Peter Brenneke
Postfach 33 45
D-3300 Braunschweig
FEDERAL REPUBLIC OF GERMANY

D. R. Knowles
British Nuclear Fuels, plc
Risley, Warrington, Cheshire WA3 6AS
1002607 GREAT BRITAIN

Shingo Tashiro
Japan Atomic Energy Research Institute
Tokai-Mura, Ibaraki-Ken
319-11 JAPAN

Netherlands Energy Research Foundation
ECN (2)
Attn: Tuen Deboer, Mgr.
L. H. Vons
3 Westerduinweg
P.O. Box 1
1755 ZG Petten, THE NETHERLANDS

Johan Andersson
Statens Kärnkraftinspektion
SKI
Box 27106
S-102 52 Stockholm, SWEDEN

Fred Karlsson
Svensk Karnbransleforsorjning AB
SKB
Box 5864
S-102 48 Stockholm, SWEDEN

INTERNAL

1 A. Narath
20 O. E. Jones
1511 D. K. Gartling
1520 L. W. Davison
1521 J. G. Arguello
1521 H. S. Morgan
3151 S. M. Wayland
3200 N. R. Ortiz
3223 P. Davis
6000 D. L. Hartley
6232 W. R. Wawersik
6233 J. C. Eichelberger
6233 J. L. Krumhansl
6300 R. W. Lynch
6310 T. O. Hunter
6311 A. L. Stevens
6312 G. E. Barr
6312 F. W. Bingham
6313 T. Blejwas
6315 P. C. Kaplan
6315 L. E. Shephard
6315 M. D. Siegel
6316 R. P. Sandoval
6317 S. Sinnock
6320 J. E. Stiegler
6340 W. D. Weart
6340 S. Y. Pickering
6341 J. M. Covan
6341 D. P. Garber
6341 R. D. Klett
6341 R. C. Lincoln
6341 Sandia WIPP Central Files (100)
6342 D. R. Anderson
6342 B. L. Baker
6342 S. G. Bertram-Howery
6342 K. Brinster (25)
6342 J. Bean
6342 A. Schreyer
6342 R. McCurley
6342 D. Morrison
6342 J. Rath
6342 D. Rudeen
6342 A. Gilkey
6342 L. S. Gomez
6342 R. Guzowski
6342 H. Iuzzolino
6342 M. G. Marietta
6342 A. C. Peterson
6342 R. P. Rechard
6342 D. W. Scott
6342 P. N. Swift
6342 J. Sandha
6342 W. Beyeler
6342 J. Schreiber
6342 K. M. Trauth
6343 T. M. Schultheis
6344 R. L. Beauheim
6344 P. B. Davies
6344 E. Gorham
6344 S. J. Finley
6344 A. M. LaVenue
6344 C. F. Novak
6344 S. W. Webb
6345 R. Beraun
6345 L. Brush
6345 B. M. Butcher
6345 A. R. Lappin
6345 M. A. Molecke
6346 B. L. Ehgartner
6346 D. E. Munson
6346 E. J. Nowak
6346 J. R. Tillerson
6346 T. M. Torres
6350 R. L. Hunter
6400 D. J. McCloskey
6415 J. Campbell
6415 R. M. Cranwell
6415 J. C. Helton
6415 R. L. Iman
6415 M. Tierney
6416 E. Bonano
6416 M.S.Y. Chu
9300 J. E. Powell
9310 J. D. Plimpton
9320 M. J. Navratil
9325 R. L. Rutter
9325 J. T. McIlmoyle
9330 J. O. Kennedy
9333 O. Burchett
9333 J. W. Mercer
9334 P. D. Seward
8524 J. A. Wackerly
3141 S. A. Landenberger (5)
3151 G. L. Esch (3)
3154-1 C. L. Ward (8) for DOE/OSTI

*U.S. GOVERNMENT PRINTING OFFICE 1991-0-573-038/44005

ERRATA
For The Report

"Preliminary Geohydrologic Conceptual Model of the Los Medanos Region Near the Waste Isolation Pilot Plant for the Purpose of Performance Assessment"

SAND89-7147 by K. F. Brinster

Enclosed are 14 modified geologic maps with pages numbered to replace the respective geologic maps presented in the report "Preliminary Geohydrologic Conceptual Model of the Los Medanos Region Near the Waste Isolation Pilot Plant for the Purpose of Performance Assessment" (SAND89-7147) by K. F. Brinster. Thirteen of the maps are unchanged east of Nash Draw at or near the Waste Isolation Pilot Plant but are changed west of the draw. This is because of an inadvertent inclusion of data from Townships 34 and 35 far to the east of the study area into Township 28 and part of Township 29 west of Nash Draw. The mistake was discovered shortly after release of the report and has been corrected for the data set presented in Volume 3 of the Preliminary Comparison report (SAND91-0893/3). The extraneous data in the western part of the region have never been included in any PA work, but the corrected maps are being sent out for the sake of completeness. A potentiometric map of the Lower Dockum was inserted in place of the Lower Dockum structure map (Figure II-29) and is replaced in this set of maps. Also note, the contours on the adjusted Culebra potentiometric surface map (Figure IV-17) were mislabeled and each contour should be 4 meters less than indicated on the map. (The map is not included in the replacement set.)

The original and corrected maps were constructed using data from USGS reports by Mercer (1983) and Richey (1989). The USGS reports and a report by Holt and Powers (1988) are the only reports available with geologic data that can be referenced for performance assessment use. The USGS data and the Holt and Powers data were compiled from geophysical logs, and the USGS data were chosen because well name, datum altitude, and depths to tops of Rustler Formation members were included. Well name and depths to tops were also in the Holt and Powers report, but some well reference elevations were taken from the kelly bushing on the floor of the drill rig which varies in height above ground for various rigs. The data from the Holt and Powers report will be included once a standard datum altitude is established for each well. A preliminary comparison of the USGS and Holt and Powers data sets indicates that thicknesses of the Rustler members vary only slightly.

The maps are only for visualizing the data, considering the large number of data points on a page-sized surface. The exact locations of the wells are available in tables in the reference data report (SAND91-0893/3) and the elevations of the tops and thicknesses of the members are available in Brinster (1991). The outside ticmarks and township/range marks are plotted on the modified maps at exact UTM coordinates which was not the case for the original maps. All the data are available as ASCII files on 3.5 and 5.25 floppy disks. Complete titles of the above mentioned reports can be found in Brinster (1991).

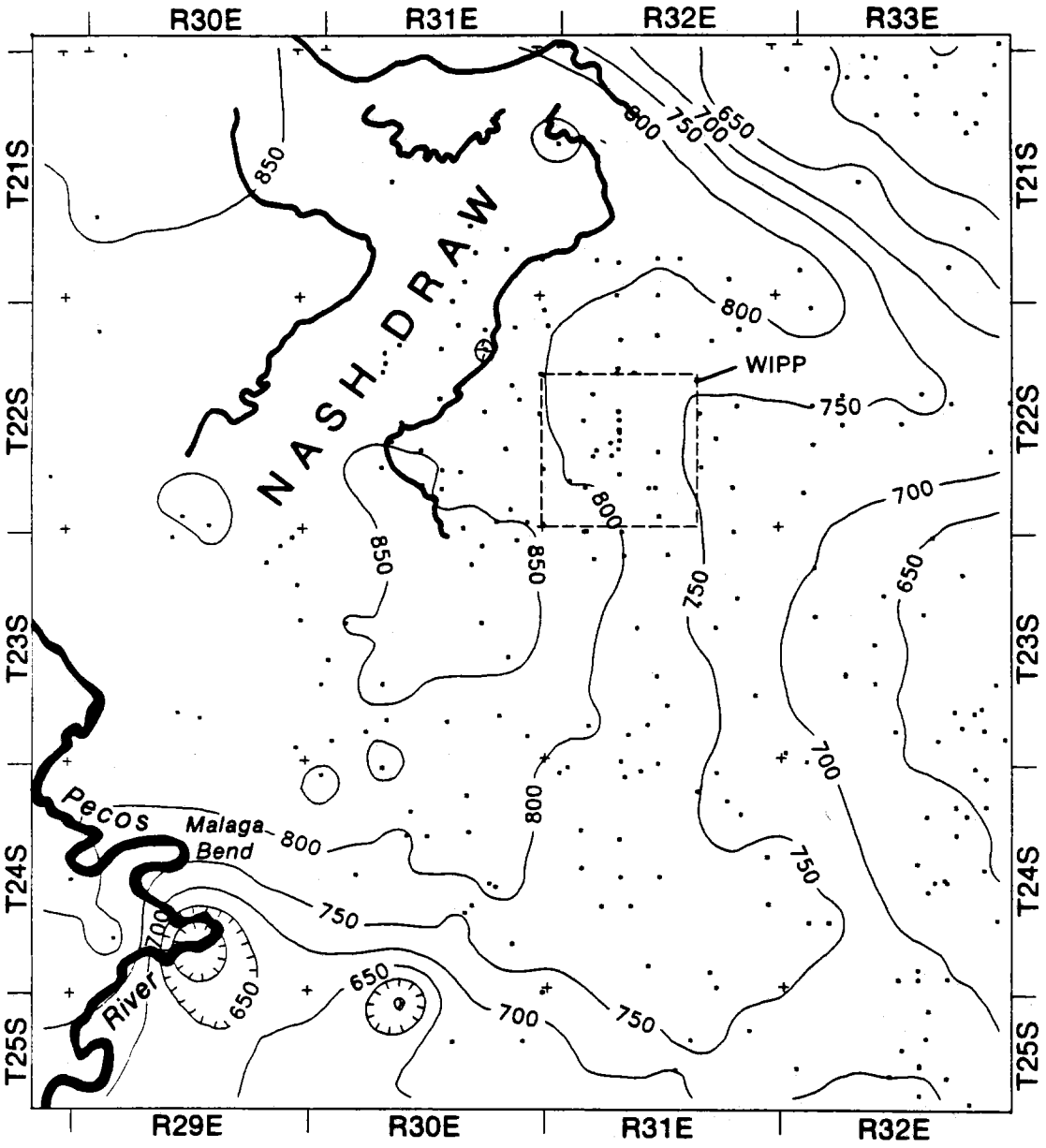

Figure II-9. Structure Contours on Top of the Salado Formation.

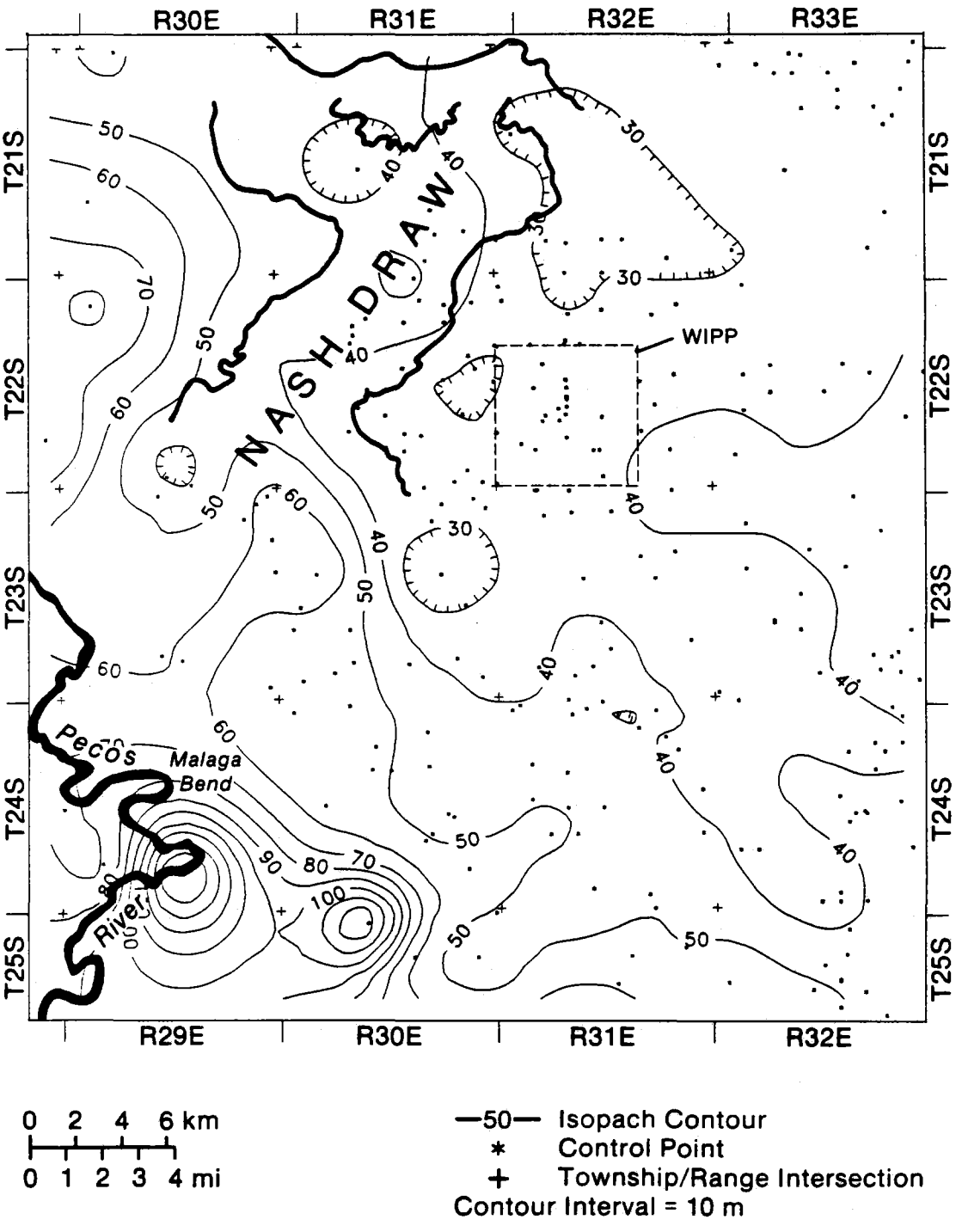

Figure II-15. Isopach Map of the Unnamed Lower Member.

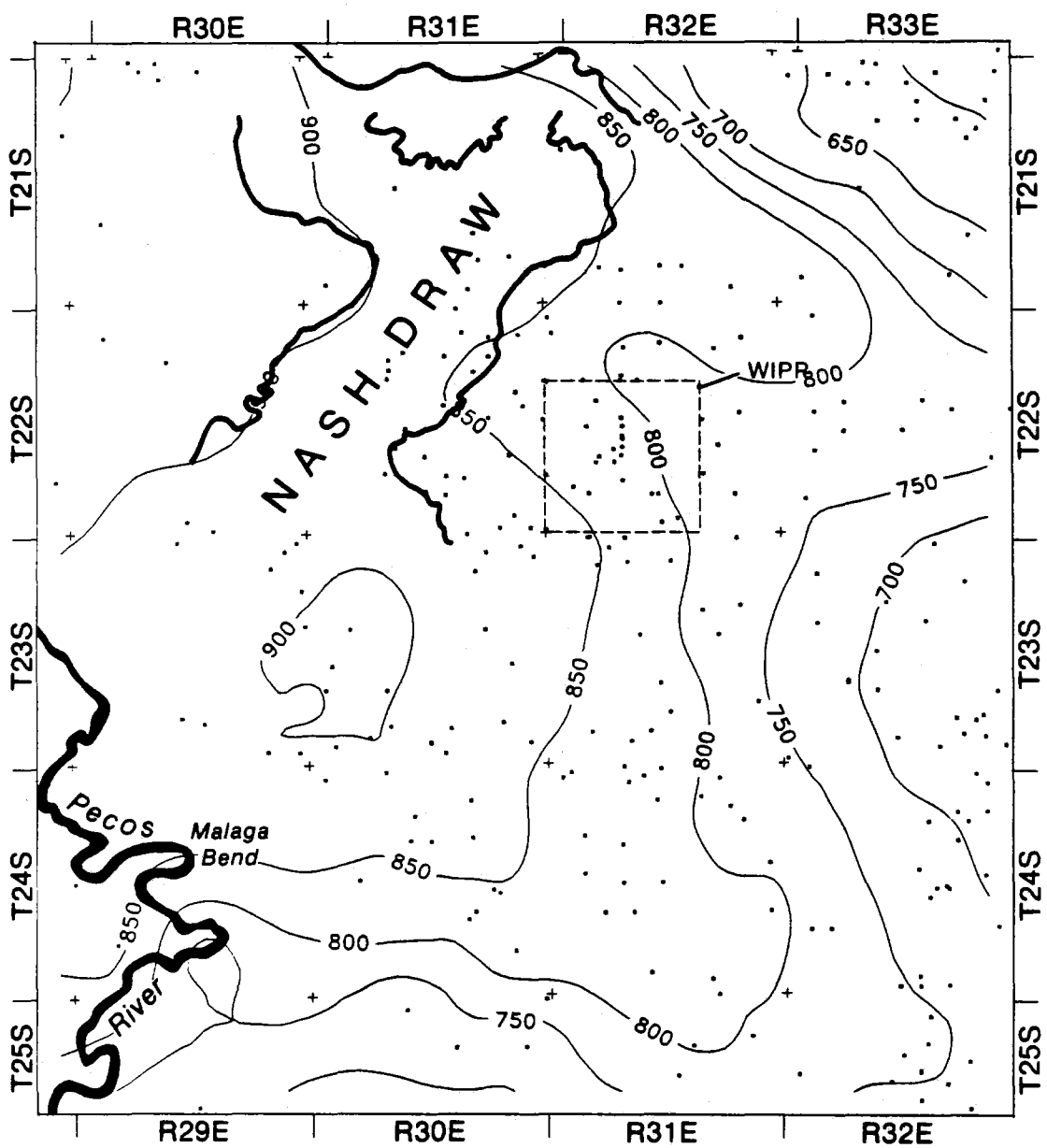

Figure II-17. Structure Contours on Top of the Unnamed Lower Member.

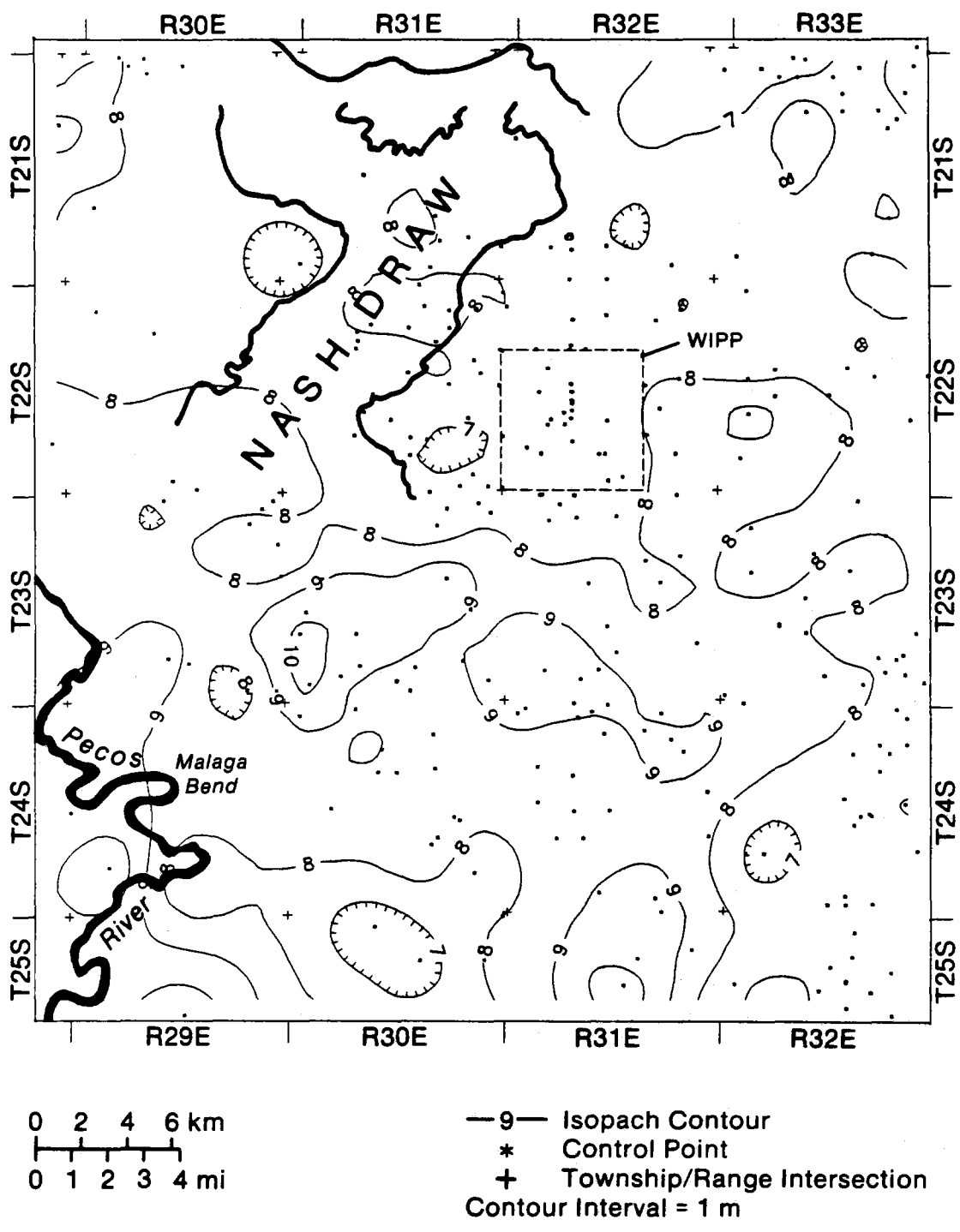

Figure II-18. Isopach Map of the Culebra Dolomite Member.

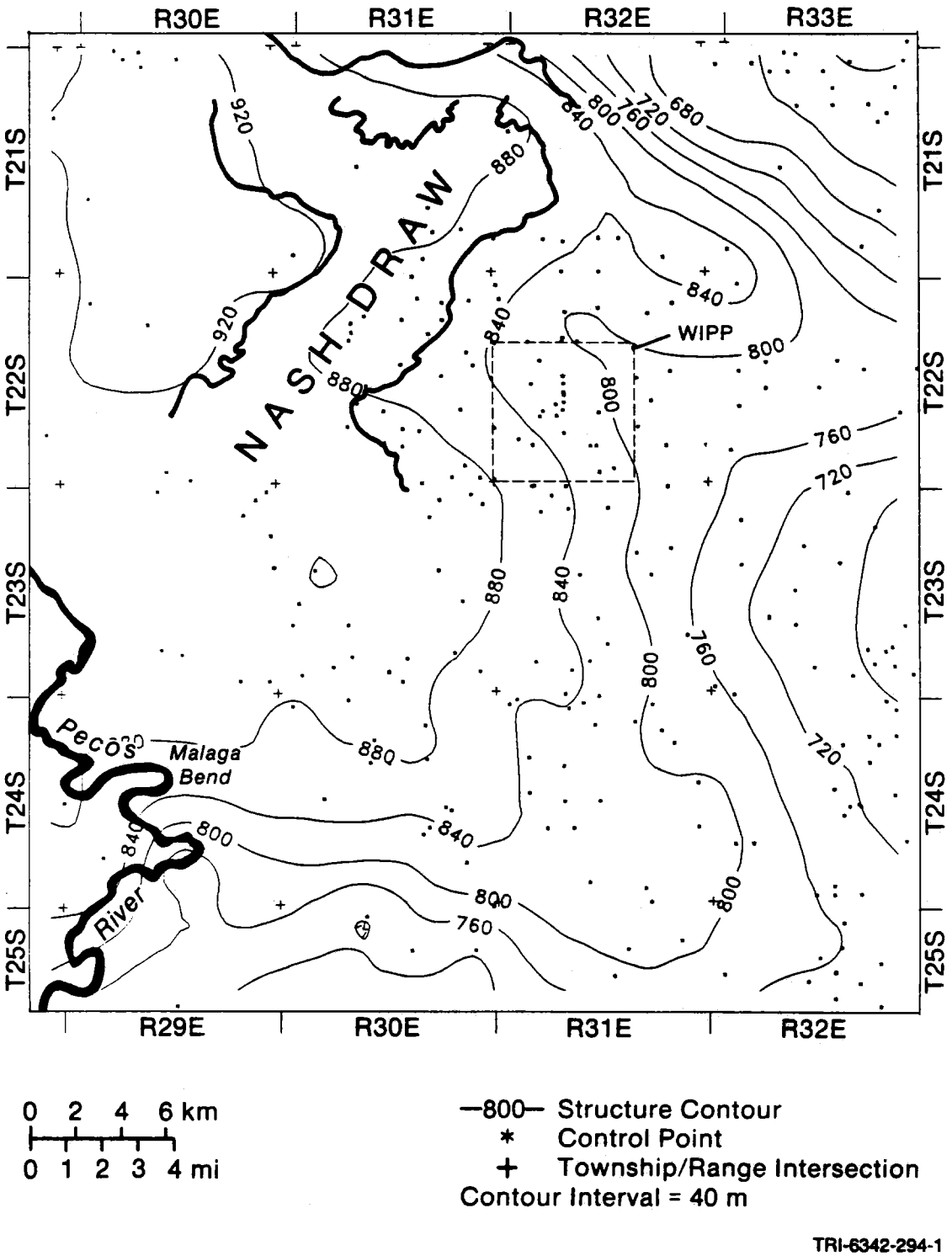

Figure II-19. Structure Contours on Top of the Culebra Dolomite Member.

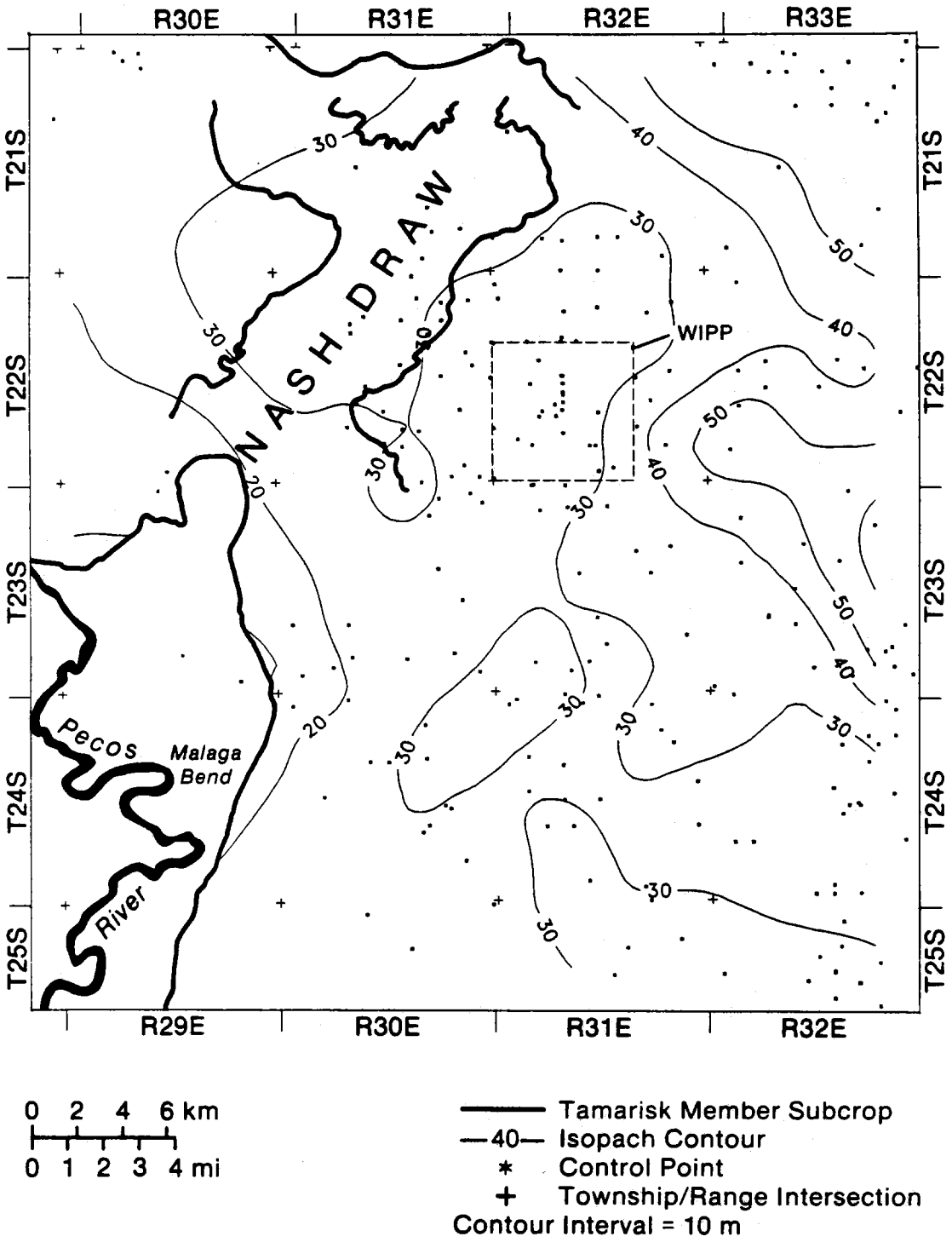

Figure II-20. Isopach Map of the Tamarisk Member.

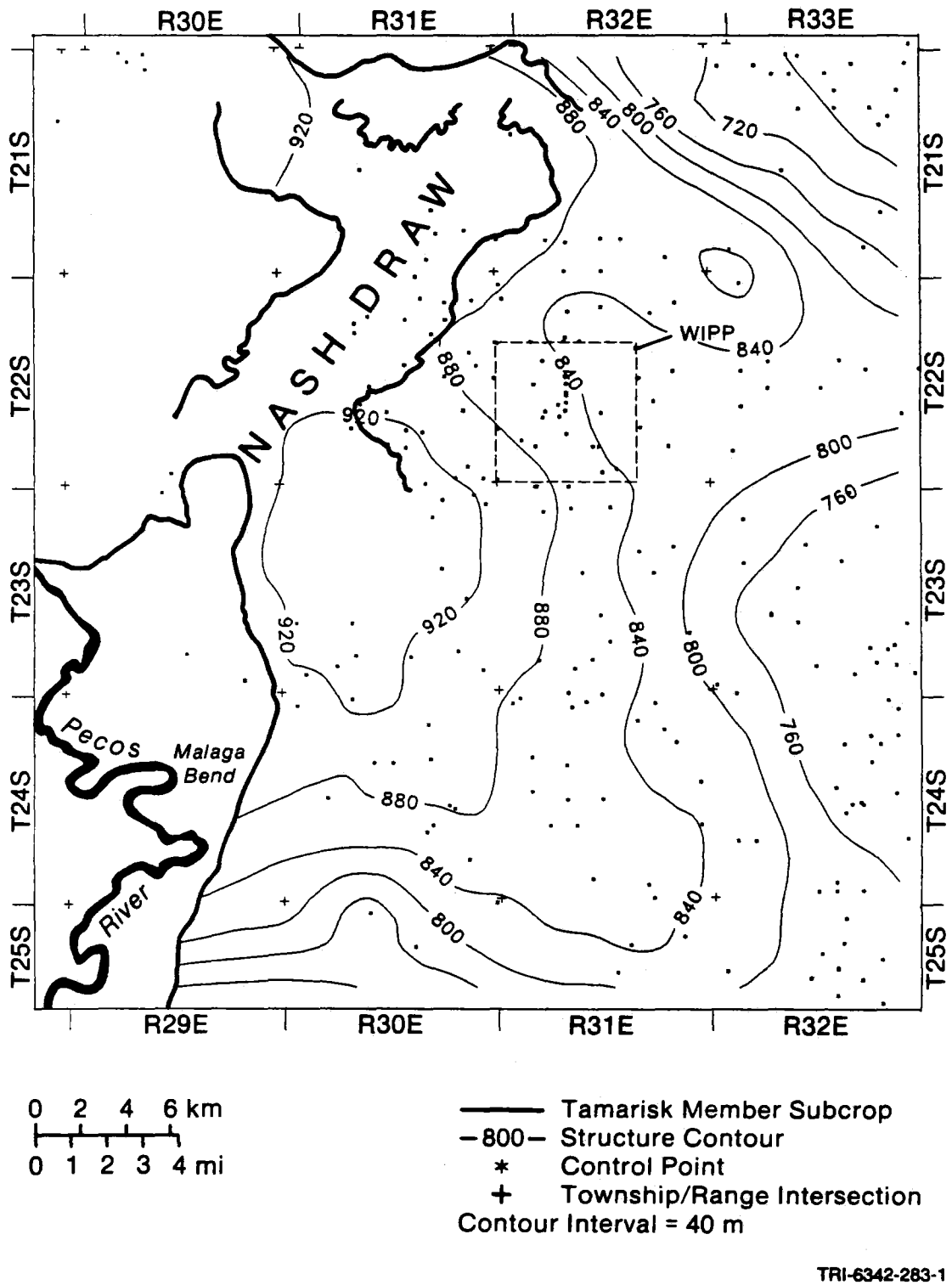

Figure II-22. Structure Contours on Top of the Tamarisk Member.

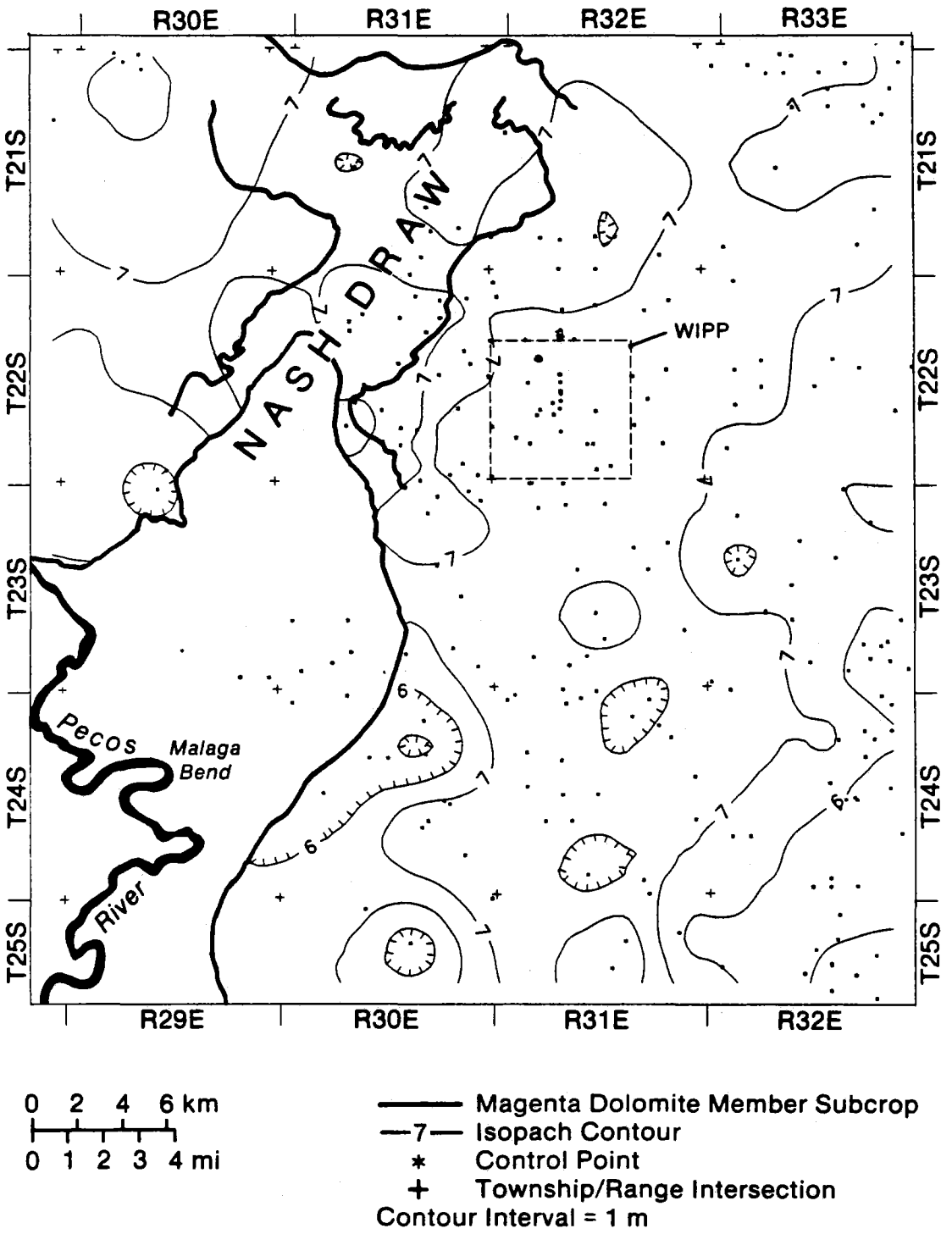

Figure II-23. Isopach Map of the Magenta Member.

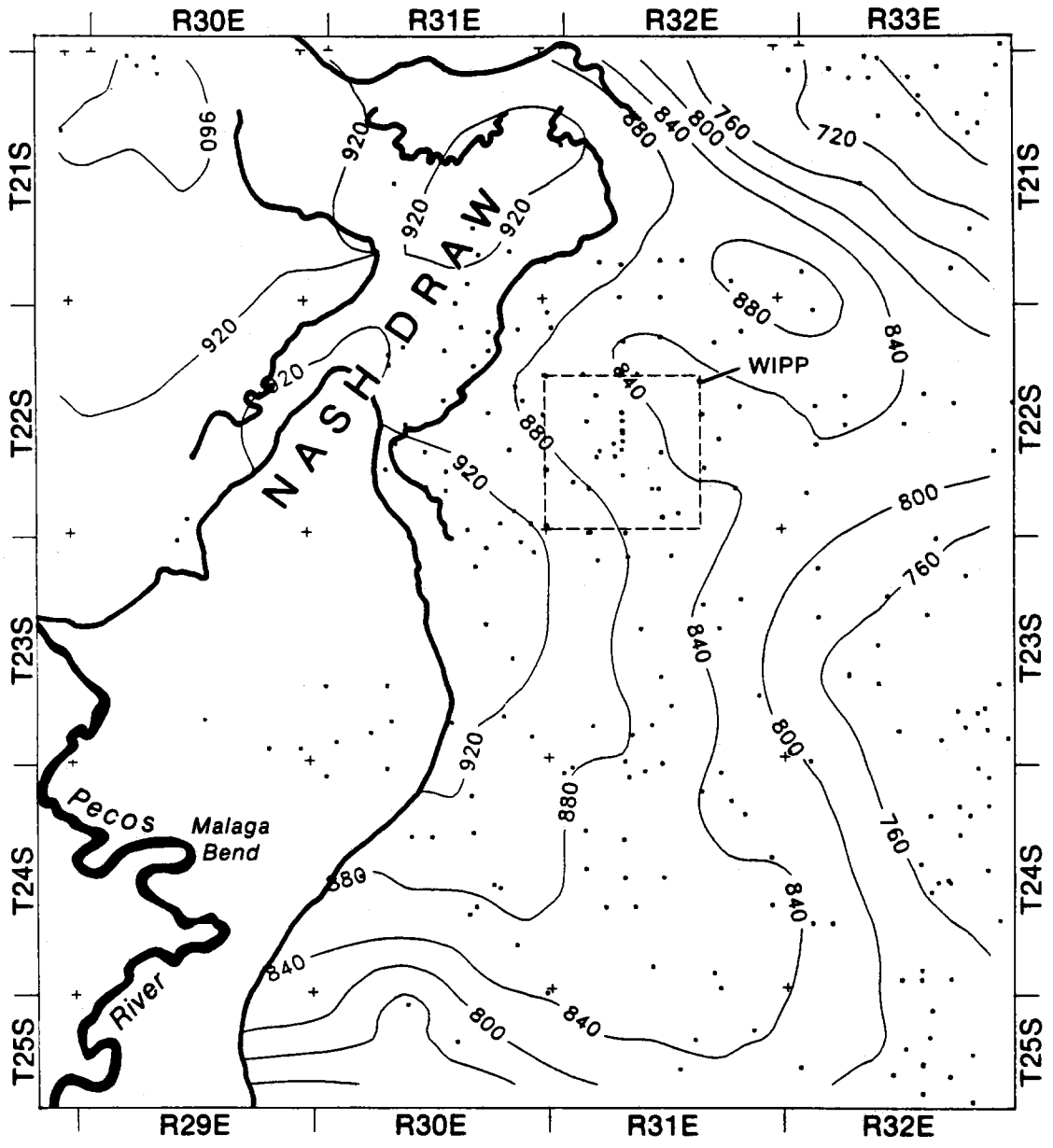

Figure II-24. Structure Contours on Top of the Magenta Member.

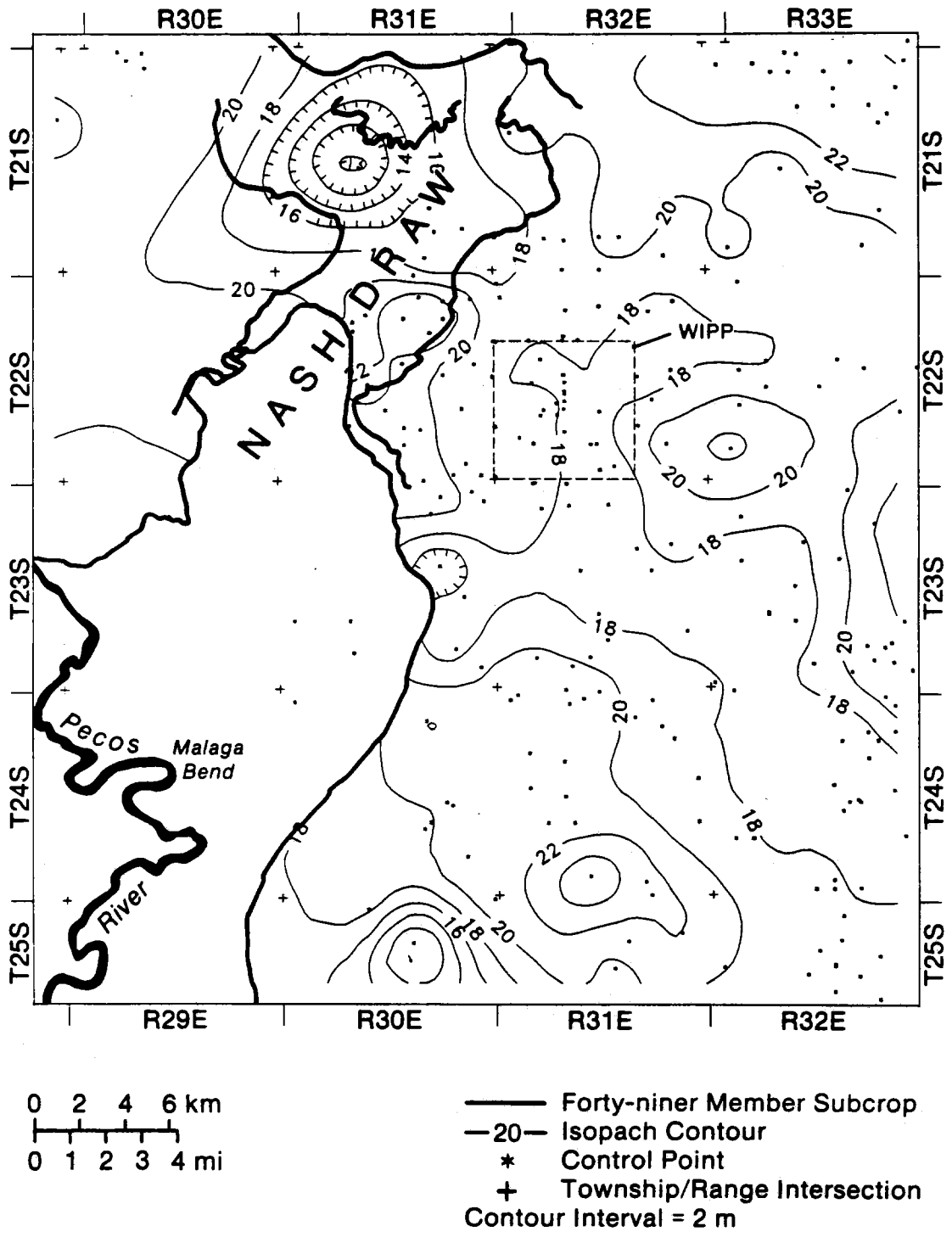

Figure II-25. Isopach Map of the Forty-niner Member.

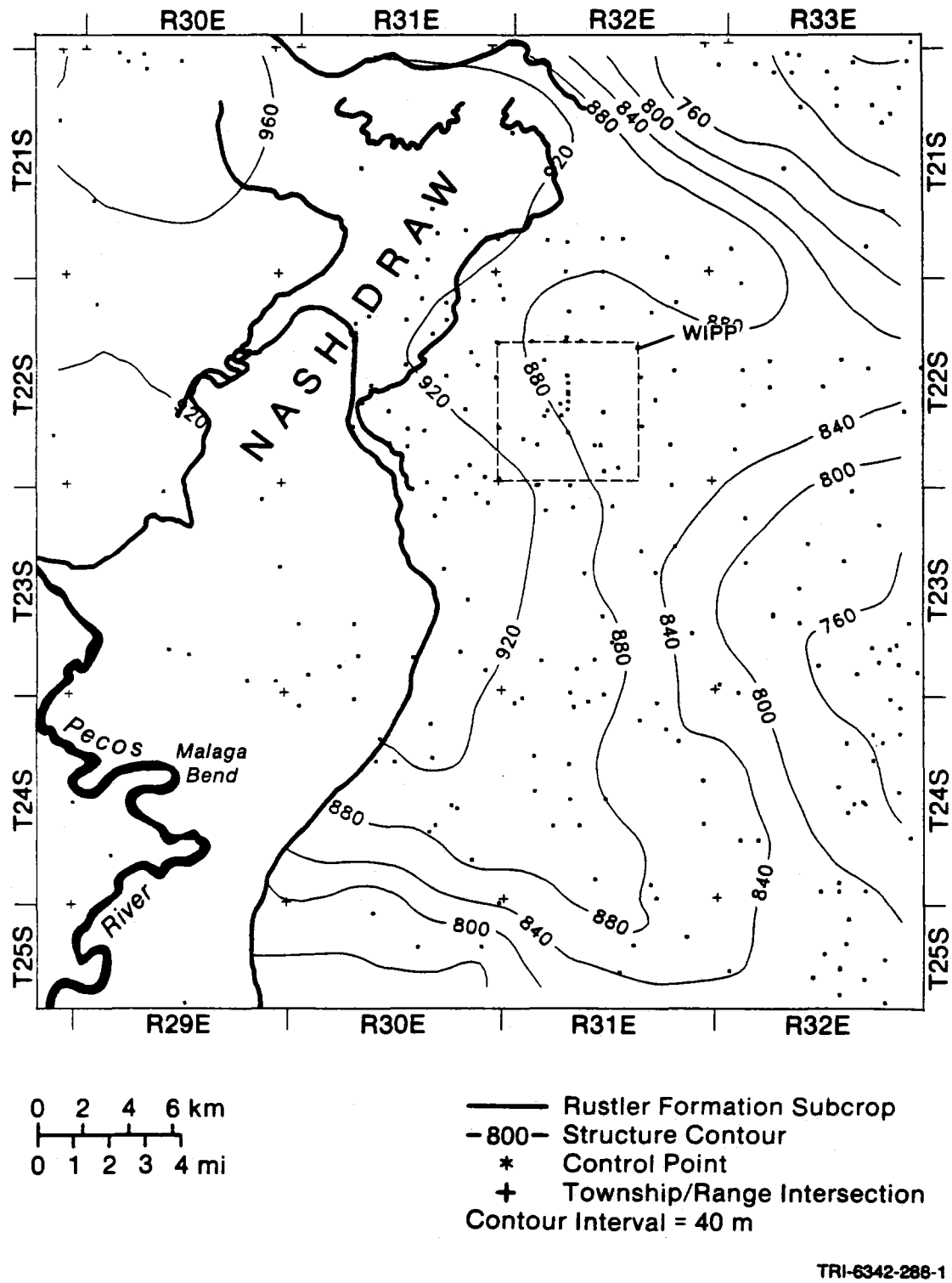

Figure II-26. Structure Contours on Top of the Forty-niner Member.

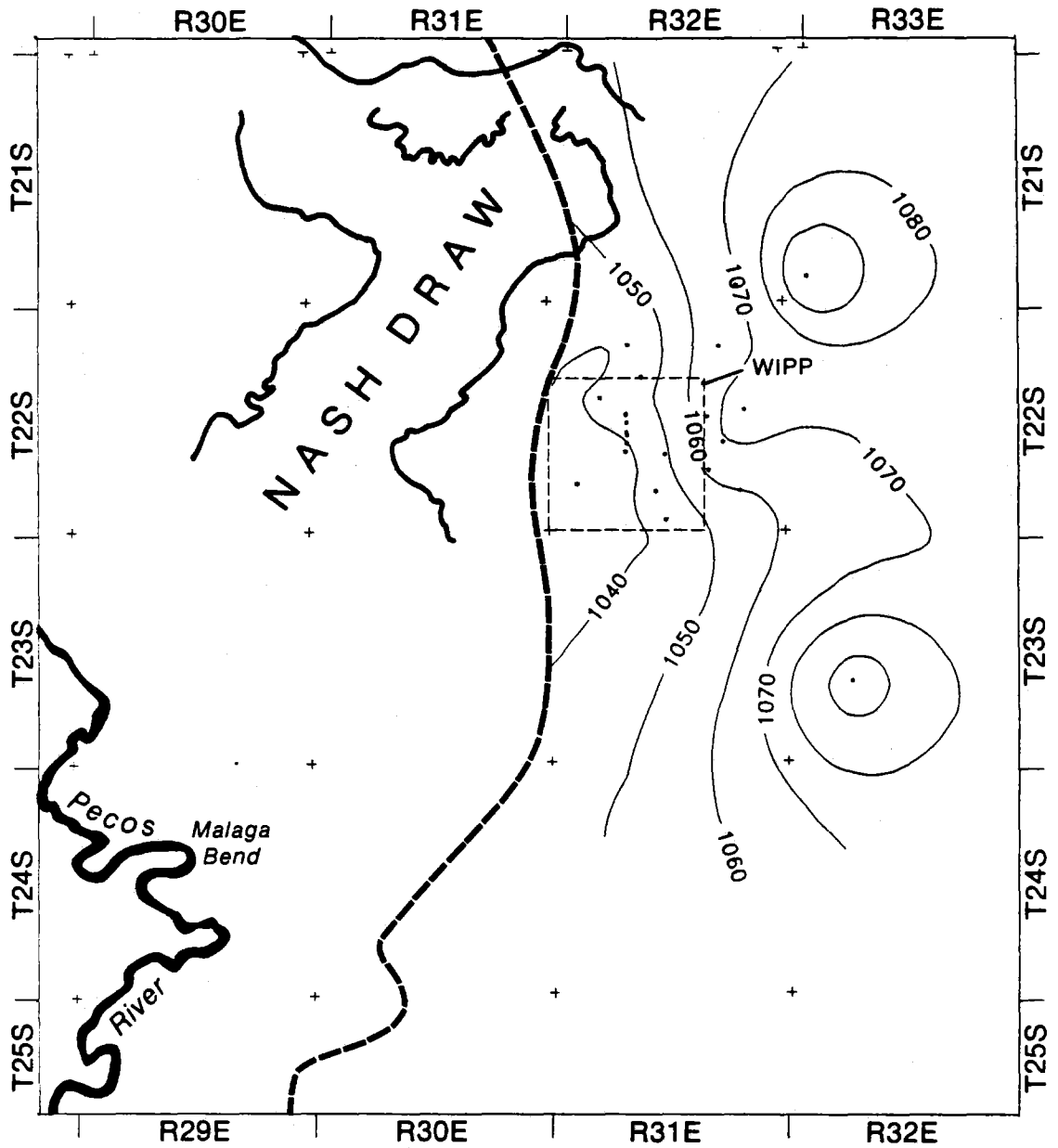

Figure II-29. Structure Contours on Top of Lower Dockum Group (modified from Cooper and Glanzman, 1971).

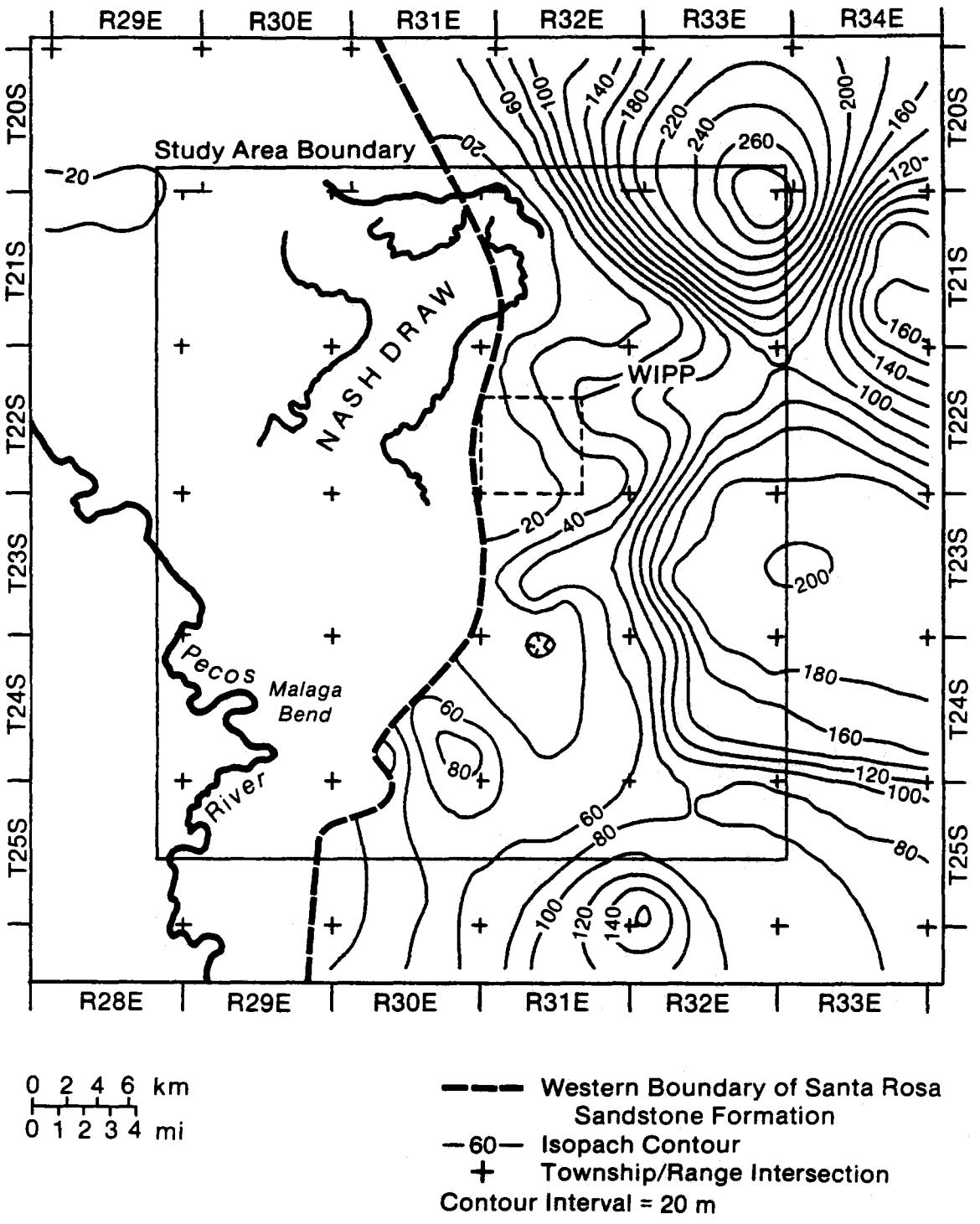

Figure II-30. Isopach Map of Lower Dockum Group in the Study Area.

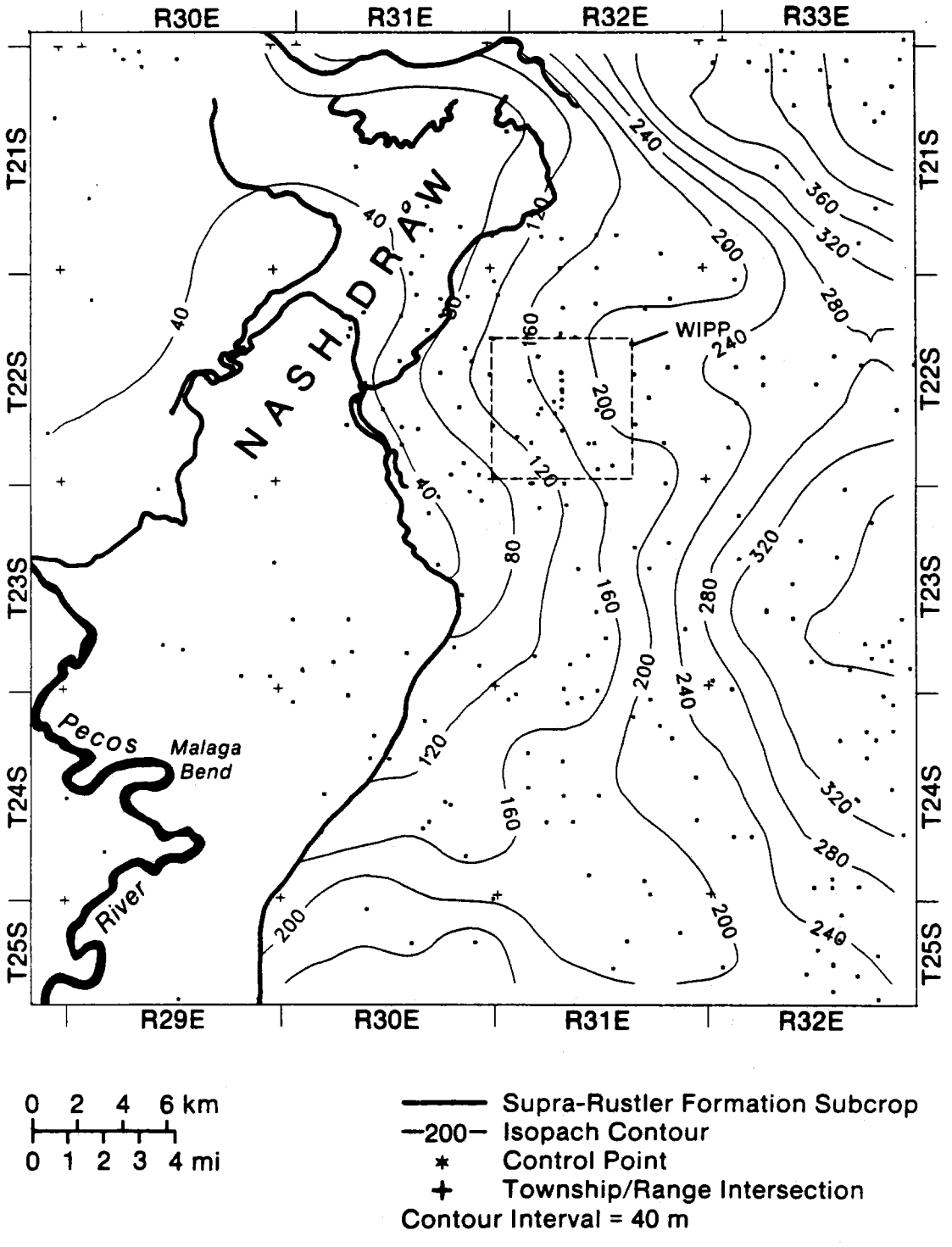

Figure II-31. Isopach Map of the Supra-Rustler Rocks.